Sinteza, karakterizacija i biološko djelovanje harmicina, harmikina i harmicena

Poje, Goran

Doctoral thesis / Disertacija

2022

Degree Grantor / Ustanova koja je dodijelila akademski / stručni stupanj: **University of Zagreb, Faculty of Pharmacy and Biochemistry / Sveučilište u Zagrebu, Farmaceutsko-biokemijski fakultet**

Permanent link / Trajna poveznica: https://urn.nsk.hr/urn:nbn:hr:163:725337

Sveučilište u Zagrebu

Farmaceutsko-biokemijski fakultet

Goran Poje

SINTEZA, KARAKTERIZACIJA I BIOLOŠKO DJELOVANJE HARMICINA, HARMIKINA I HARMICENA

DOKTORSKI RAD

Zagreb, 2022.

Sveučilište u Zagrebu

Farmaceutsko-biokemijski fakultet

Goran Poje

SINTEZA, KARAKTERIZACIJA I BIOLOŠKO DJELOVANJE HARMICINA, HARMIKINA I HARMICENA

DOKTORSKI RAD

Mentor: prof. dr. sc. Zrinka Rajić

Zagreb, 2022.

Sveučilište u Zagrebu

Faculty of Pharmacy and Biochemistry

Goran Poje

SYNTHESIS, CHARACTERIZATION AND BIOLOGICAL ACTIVITY OF HARMICINES, HARMIQUINS AND HARMICENES

DOCTORAL DISSERTATION

Supervisor: Professor Zrinka Rajić, PhD

Zagreb, 2022

Doktorski rad predan je na ocjenu Fakultetskom vijeću Farmaceutsko-biokemijskog fakulteta Sveučilišta u Zagrebu radi stjecanja akademskog stupnja doktora znanosti u znanstvenom području biomedicine i zdravstva, polje farmacija, grana farmacija.

Rad je izrađen u Zavodu za farmaceutsku kemiju Farmaceutsko-biokemijskog fakulteta Sveučilišta u Zagrebu, u okviru doktorskog studija „Farmaceutsko-biokemijske znanosti“. Rad je financiran projektom Hrvatske zaklade za znanost „Derivati harmina kao potencijalni antimalarici“ (HRZZ- UIP-2017-05-5160).

Zahvale

Mentorici prof. dr. sc. Zrinki Rajić na pruženoj prilici, prenesenom znanju, savjetima te stručnom vodstvu tijekom izrade ovog doktorskog rada.

Izv. prof. dr. sc. Ivani Perković na pomoći i savjetima, posebno u počecima rada u laboratoriju.

Marini Marinović, mag. appl. chem. na nesebičnim savjetima, pomoći i prijateljstvu. Hvala na svim šalama i gomili smijeha koji su dane kada „reakcije ne idu“, a spojevi „ne izlaze čisti“ nakon treće kolone učinili boljima. Hvala i dr. sc. Kristini Pavić na savjetima, pomoći i ugodnom društvu u labosu.

Ostalim članovima Zavoda za farmaceutsku kemiju na ugodnoj atmosferi i druženju. Hvala gđi Ljiljani Jurkin što je uvijek bila spremna pomoći.

Dr. sc. Maji Beus na uvođenju u rad sa staničnim kulturama.

Hvala asistentima Zavoda za farmaceutsku tehnologiju, a posebno dr. sc. Lauri Nižić Nodilo i Mirni Perkušić, mag. pharm., na svoj pomoći pri radu sa staničnim kulturama i ugodnoj atmosferi tijekom boravka u njihovom znanstvenom laboratoriju.

Dr. sc. Marijeti Kralj i dr. sc. Lidiji Uzelac na pomoći prilikom ispitivanja unutarstanične lokalizacije spojeva.

Danijeli Ranogajec, mag. pharm., Marku Duševiću, mag. pharm., Ivani Vilenici, mag. pharm., Tini Šutalo, mag. pharm. te studentu Natanu Koraj koji su radeći svoje diplomske radove ili radove za Rektorovu nagradu pomogli u izradi dijela ovog rada.

Asistentskoj ekipi FBF-a na korisnim raspravama i zajedničkim druženjima.

Mojoj obitelji na bezuvjetnoj ljubavi, razumijevanju i podršci!

SAŽETAK

Rak i malarija su smrtonosne bolesti koje predstavljaju značajan globalni javnozdravstveni problem. Učinkovitost postojećih citostatika i antimalarika opada uslijed pojave rezistencije, zbog čega je potrebno kontinuirano istraživati nove potencijalne lijekove. Popularan pristup u razvoju novih lijekova je molekulska hibridizacija, odnosno kovalentno povezivanje dva bioaktivna spoja s ciljem poboljšanja njihovog djelovanja. U okviru ovog doktorskog rada sintetizirani su hibridni spojevi harmina, β-karbolinskog alkaloida s izraženim antimalarijskim i protutumorskim djelovanjem, i: 1) derivata cimetne kiseline (harmicini), 2) klorokina (harmikini), 3) ferocena (harmiceni). U pripravi harmicina korištena je bakrom(I) katalizirana azid-alkin cikloadicija, odnosno klik-reakcija koja je rezultirala harmicinima triazolskog tipa. Harmikini i harmiceni pripravljeni su korištenjem klik-reakcije te reakcije povezivanja amina i karboksilnih kiselina, dajući harmikine i harmicene triazolskog i amidnog tipa. Za potrebe klik-reakcija sintetizirani su odgovarajući alkini i azidi β-karbolina, derivata cimetne kiseline, 7-klorkinolina te ferocena, dok su amini i karboksilna kiselina harmina te karboksilna kiselina i amini 7-klorkinolina pripravljeni za potrebe reakcija povezivanja. Novi spojevi karakterizirani su uobičajenim analitičkim i spektroskopskim metodama te je ispitano njihovo antiproliferativno i antimalarijsko djelovanje *in vitro*. U seriji harmicina najjače antiproliferativno djelovanje ostvarili su triazoli **49a-e**, dok su u seriji harmikina najcitotoksičniji bili triazoli **54** i **57**. Najsnažnije antiproliferativno djelovanje među harmicenima prema svim ispitivanim staničnim linijama pokazao je amid **82**, dok su harmiceni triazolskog tipa **67**, odnosno **66** i **69** pokazali značajno i selektivno djelovanje prema MCF-7 i HCT116. Najbolje antimalarijsko djelovanje na eritrocitnu fazu životnog ciklusa svih ispitanih sojeva *P. falciparum*, u nanomolarnim koncentracijama, pokazali su harmikini. Spoj **63** ispoljio je 5,5 puta snažniji učinak u odnosu na klorokin (CQ) (IC_{50} = 2 ± 0,3 nM), dok je spoj **65** bio najučinkovitiji prema sojevima plazmodija rezistentnima na postojeće antimalarike. Temeljem dobivenih rezultata može se zaključiti da harmikini predstavljaju spojeve uzore za razvoj novih potencijalnih antimalarika, dok je harmicine i harmicene potrebno razvijati kao potencijalne protutumorske lijekove.

Ključne riječi: harmin, derivati cimetne kiseline, klorokin, ferocen, hibridni spojevi, klik-reakcija, reakcija povezivanja, antimalarijsko djelovanje, antiproliferativno djelovanje

SUMMARY

Introduction

Cancer and malaria are etiologically and pathophysiologically distinct diseases that belong to different therapeutic areas. Cancer is characterized by uncontrolled growth and spread of abnormal cells. Malaria, on the other hand, is a tropical infectious disease caused by parasites of the genus *Plasmodium* and transmitted by the bite of an infected female *Anopheles* mosquito. However, both cancer and malaria have high incidence rates and are major causes of death worldwide. Successful treatment of these diseases is hampered by the emergence of resistance to existing drugs. Therefore, there is a great need for the development of new and effective cytostatic and antimalarial agents. A useful concept for drug design and development is molecular hybridization, which is the covalent linking of two bioactive moieties, either directly or through a spacer, to form a single molecule with improved properties. The advantages of hybrid compounds include increased efficacy due to synergistic effect, reduced risk of resistance development, improved solubility and pharmacokinetics, and reduced side effects and drug-drug interactions. In this thesis, synthesis, characterization, and biological activity of three novel classes of hybrid compounds are reported. Harmine, a naturally occurring β-carboline alkaloid with pronounced antimalarial and anticancer properties, was covalently linked with moieties exhibiting significant biological activities, namely cinnamic acid derivatives (CADs), chloroquine (CQ) and ferrocene, resulting in harmicines, harmiquins and harmicenes, respectively. CADs showed remarkable anticancer and antimalarial activities *in vitro* and *in vivo*. CQ is a well-known antimalarial agent used for the prevention and treatment of malaria. Its repurposing for cancer therapy has been extensively studied. Ferrocene is an organometallic that has been hybridized with other molecules, resulting in compounds with enhanced biological activities such as antimalarial and anticancer.

Materials and Methods

The hybrid compounds were prepared either by a Cu(I)-catalyzed azide-alkyne cycloaddition (CuAAC) leading to the introduction of a triazole ring or by a coupling reaction resulting in the formation of an amide bond. To prepare the title hybrids, required building blocks, *i.e.* alkynes, azides, carboxylic acids, and amines, were synthesized.

β-Carboline-based alkynes, azides and amines at the C-1, C-3, and O-6 positions were prepared in a multistep reaction pathway, starting from tryptamine or its analogues. Pictet-Spengler condensation of 1) tryptamine with 2,2-dimethoxyacetaldehyde, 2) tryptophan methyl

ester with acetaldehyde dimethyl acetal, 3) 5-methoxytryptamine with acetaldehyde dimethyl acetal, followed by oxidation of tetrahydro-β-carboline intermediates **1**, **8** and **16**, afforded the corresponding β-carbolines substituted at positions C-1 (**2**), C-3 (**9**), and O-6 (**17**), respectively. The acetal group at C-1 was hydrolyzed in a CH_3COOH/H_2O mixture, and the aldehyde **3** obtained was reduced with $LiAlH_4$ to give the alcohol **5**. The ester group at C-3 was reduced to give alcohol **10** by applying similar reaction conditions. Alcohols **5** and **10** were converted to azides **6** and **11** by the means of 2-azido-1,3-dimethylimidazolinium hexafluorophosphate (ADMP) and 1,8-diazabicyclo[5.4.0]undec-7-ene (DBU), respectively. Reduction of the azides with H_2/Pd/C gave amines **7** and **12**. In addition, the alcohol at C-3 was N-alkylated with propargyl bromide in the presence of Cs_2CO_3 to give alkyne **13** and oxidized in the presence of MnO_2 to give aldehyde **14**. Aldehydes **3** and **14** were homologated to alkynes **4** and **15**, respectively, with Bestman-Ohira reagent in the presence of K_2CO_3.

The ether group at position O-6 was hydrolyzed in a CH_3COOH/HBr mixture to give phenol **18**, which was alkylated either with propargyl bromide in the presence of Cs_2CO_3 to give alkyne **19** or with $BocNH(CH_2)_2Br$ in the presence of the same base and tetrabutylammonium hydrogen sulfate (TBAHS) to give Boc-protected amine **20**. Removal of the Boc-protecting group in 4 M HCl gave amine **21**, which was converted to azide **22** by the means of ISA × HCl in the presence of K_2CO_3 and $CuSO_4 \times 5H_2O$.

The synthesis of alkyne, azide, carboxylic acid, and amine at position N-9 was carried out starting from commercially available harmine, while the key intermediates at O-7 position were prepared from harmol **23**, obtained by hydrolysis of harmine in a CH_3COOH/HBr mixture. Alkylation of harmine/harmol with propargyl bromide in the presence of a base (NaH or Cs_2CO_3) gave alkynes **24** and **28**, while their alkylation with $BocNH(CH_2)_2Br$ in the presence of Cs_2CO_3 resulted with Boc-protected amines **25** and **29**. The latter were converted to amines (**26**, **30**) and azides (**27**, **31**) as described previously. The harmine-based carboxylic acid **33** was prepared in a two-step procedure. The first step involved the Michael addition between harmine and methyl acrylate. The ester **32** obtained was subsequently hydrolyzed with $LiOH \times H_2O$ to the corresponding acid.

CAD-based alkynes **34** were obtained in one reaction step by reacting the corresponding CADs with propargyl bromide in the presence of K_2CO_3. In contrast, the synthesis of the CAD-based azides **37** was carried out in several steps. First, the CADs were converted to the corresponding esters **35**, followed by reduction to alcohols **36** by $LiAlH_4$. The alcohols were efficiently converted to azides by ADMP in the presence of DBU.

The synthesis of the CQ-based azide **38** was straightforward and was carried out by nucleophilic substitution of 4,7-dichloroquinoline with NaN_3, whereas the preparation of azide **40** required a two-step procedure. The first step was the reaction of 4,7-dichloroquinoline with aminoethanol in the presence of triethylamine (TEA). The alcohol **39** obtained was successfully converted to an azide using ADMP and DBU. CQ-based alkyne **42** was prepared by treating 4,7-dichloroquinoline with glacial acetic acid followed by alkylation of the obtained phenol **41** with propargyl bromide and Cs_2CO_3. CQ-based carboxylic acid **43** and amines **44**, **45** were prepared by nucleophilic substitution of 4,7-dichloroquinoline with 1) glycine, 2) ethylenediamine, and 3) 1,4-diaminobutane, respectively. Finally, azidomethylferrocene **46** was prepared from ferrocenemethanol in reaction with ADMP and DBU.

The progress of the chemical reactions was monitored by thin-layer chromatography (TLC). The products were purified by column chromatography/re-crystallisation. The structures of the new compounds were confirmed by ^{1}H and ^{13}C NMR, IR and MS. All chemicals were obtained from commercial sources.

Furthermore, we investigated the antiproliferative activity of the prepared compounds *in vitro* against a panel of human tumour cell lines, as well as the antimalarial activity against the erythrocytic and hepatic stages of the *Plasmodium* life cycle. For antiproliferative screening, we chose four human tumour cell lines: breast cancer cell line (MCF-7), hepatocellular (HepG2), colorectal (HCT116) and colon carcinoma (SW620). In addition, we included a non-cancer cell line (human embryonic kidney cells, Hek293T) to evaluate the selectivity of the hybrids. Cell growth rate was determined using the 3-(4,5-dimethylthiazol-2-yl)-2,5-diphenyltetrazolium bromide (MTT) assay in comparison with untreated cells. The commonly used anticancer drug 5-fluorouracil (5-FU) and harmine were used as positive controls. We also investigated the intracellular localization of the harmicine **49c** and harmicene **69** based on their intrinsic fluorescence properties. Antimalarial activity against the erythrocytic stage was evaluated on two *P. falciparum* laboratory strains: 3D7 (CQ-sensitive) and Dd2 (CQ-resistant), using the histidine-rich protein 2 assay (HRP-2), with CQ as a positive control. In addition, some of the harmiquins were tested against two multidrug-resistant *P. falciparum* strains (K1 and 7G8). The potential mechanism of action of the harmiquins was examined using the heme polymerization inhibition activity (HPIA) assay. Antimalarial activity against the hepatic stage of the *Plasmodium* life cycle was evaluated on hepatocellular carcinoma cells (Huh7) infected with *P. berghei* using a bioluminescence assay, with primaquine (PQ) as a positive control.

Results

Harmicines **47**-**50** were prepared by CuAAC using different reagents and reaction conditions. For the synthesis of harmicines at C-1 (**47**) and C-3 (**48**), CAD -based alkynes **34** and β-carboline-based azides **6** and **11** were used, respectively. CuAAC was carried out using sodium ascorbate and $CuSO_4 \times 5H_2O$ as the source of Cu(I) ions in a 1:1 mixture of *t*-BuOH and H_2O. The reactions proceeded smoothly at r.t. and gave hybrids in moderate yields. In contrast, the starting compounds for the synthesis of harmicines at O-6 (**49**) and N-9 (**50**) were β-carboline-based alkynes **13** or **19** and cinnamyl azides **37**. In this case, the reaction was carried out in methanol with Cu(II) acetate at r.t. The hybrids were obtained in good yields.

Harmiquins and harmicenes were prepared by both CuAAC and coupling reactions. CQ-based alkyne **42** and β-carboline-based azides **6** and **11** served as building blocks for the synthesis of TT harmiquins at C-1 (**51**) and C-3 (**52**), respectively. In contrast, the starting compounds for the synthesis of TT harmiquins at O-6 (**53**, **56**), O-7 (**54**, **57**), and N-9 (**55**, **58**) were CQ-based azides **38** or **40** and β-carboline-based alkynes **19**, **24** and **28**. In both cases, the CuAAC reactions using the Cu(II) acetate precatalyst in methanol proceeded smoothly at r.t. and led to TT-harmiquins **51**-**58** in good yields. AT harmiquins were prepared by reacting either CQ-based carboxylic acid **43** and β-carboline-based amines **7**, **12**, **21**, **26**, **30** (compounds **59**-**63**) or CQ-based amines **44**, **45** and β-carboline-based carboxylic acid **33** (compounds **64** and **65**). Different coupling reagents were used depending on the reactants. Harmiquins **59**-**63** were prepared with T3P/TEA in DMF, while HATU and DIEA in DCM were used for the synthesis of harmiquins **64** and **65**. The coupling reaction proceeded at r.t. and gave AT harmiquins in poor to moderate yields. The TT harmicenes **66**-**70** were prepared by reaction of azidomethylferrocene **46** with β-carboline-based alkynes **4**, **15**, **19**, **24**, **28**, while their counterparts **71**-**75** were obtained by reaction of ethynylferrocene with β-carboline-based azides **6**, **11**, **22**, **27**, **31** in good yields. On the other hand, AT harmiquins **76**-**79** and **80**-**83** were prepared by the reaction of ferrocenecarboxylic acid or ferroceneacetic acid and β-carboline-based amines **7**, **12**, **26**, **30** in poor to moderate yields.

In general, the harmicines and harmiquins were consistent with Lipinski, Veber, and Gelovani rules for prospective small molecule drugs. Only a few compounds (**48c**, **56**-**58** and **65**) showed minimal aberration. Thus, acceptable oral activity of the compounds could be predicted.

Among harmicines, the O-6-substituted derivatives **48** exhibited the strongest antiproliferative activity, especially against MCF-7 and HCT116 cell lines. These compounds

poorly affected Hek293T cells, showing selective cytotoxic activity. In contrast, the C-1-, C-3- and N-9-substituted harmicines were inactive, except for compounds **48c** and **50c** bearing *m*-Br substituent on the phenyl ring. Among the harmicenes, the most active compounds were the O-6-substituted triazole **73** and the O-7-substituted amide **82** (IC_{50} < 10 μM). Triazoles substituted at C-1, O-7, and N-9 (**66**, **69**, and **70**, respectively) showed selectivity toward HCT116, whereas the C-1-substituted amide **76** was selective toward MCF-7. We also examined the intracellular distribution of harmicines and harmicenes in MCF-7 cells based on their fluorescence properties. Harmicine **49c** showed punctate staining within the cytoplasm but not in the nucleus. On the other hand, harmicene **69** showed bright staining within the cytoplasm while nuclei also fluoresced, suggesting that compound did enter the nucleus. The harmiquins showed strong but mostly nonselective antiproliferative activity. The O-7-substituted triazoles **54** and **57** affected all cell lines studied at low micromolar concentrations (IC_{50} < 10 μM). On the other hand, the C-1-substituted triazole **51** showed moderate but selective activity against the HCT116 cell line.

Among the harmine hybrids, harmiquins showed the strongest activity against the erythrocytic stage of *P. falciparum* strains, followed by harmicenes and harmicines. Harmiquins displayed remarkable activity against both CQ-sensitive and CQ-resistant *P. falciparum* strains. The most active compound, harmiquine **63**, displayed a single-digit nanomolar IC_{50} value against *Pf*3D7 (IC_{50} = 2.0 ± 0.3 nM). Importantly, it also showed significantly higher activity than CQ against the resistant *Plasmodium* strains and had a very high selectivity index (10500). Interestingly, harmiquine **65** showed stronger activity against the resistant *P. falciparum* strains compared to *Pf*3D7. The HPIA assay results did not fully correlate with the antiplasmodial activities obtained, suggesting that other mechanisms are involved in the antimalarial activity of harmiquins, probably the inhibition of *Pf*Hsp90. Harmicenes showed moderate antimalarial activity, better than the parent molecule harmine but weaker than CQ. Among the TT harmicenes, the O-6- and O-7-substituted derivatives showed the strongest antimalarial activity, with the exception of compound **69**, which was found to be inactive. On the other hand, in the series of AT harmicenes, the O-7- and N-9-substituted derivatives were the most active, with IC_{50} values in the submicromolar range. Among harmicines, the O-6-substituted derivatives (**49**) showed moderate antimalarial activity, while their C-1-, C-3-, and N-9-substituted counterparts were inactive. Harmiquins and harmicenes exhibited good activity against *P. berghei* hepatic stages. The most active compounds were **53** (IC_{50} = 0,548 ± 0,051 μM) and **80** (IC_{50} < 1 μM).

Conclusion

This work presents design, synthesis and results of the biological evaluation of three novel classes of hybrid compounds, harmicines, harmiquins and harmicenes. We have shown that harmine's antimalarial and/or antitumour properties can be improved by applying the molecular hybridization approach. Among the hybrid compounds prepared, harmiquins exerted the strongest antimalarial activity. Although the antimalarial activity of harmicines and harmicenes was weaker, some of these compounds showed pronounced and selective antiproliferative activity against MCF-7 and HCT116 cells. Based on the obtained results, it can be concluded that harmiquins represent novel antimalarial hits, while further studies including harmicines and harmicenes should focus on their anticancer properties.

Keywords: harmine, cinnamic acid derivatives, chloroquine, ferrocene, hybrid compounds, “click” reaction, coupling reaction, antimalarial activity, anticancer activity

SADRŽAJ

1. UVOD 1
1.1. TUMOR 2
1.2. MALARIJA 3
1.3. HIBRIDNI SPOJEVI 5
1.4. ALKALOIDI β-KARBOLINSKOG TIPA 7
1.4.1. Priprava β-karbolina 9
1.4.2. Harmin 10
1.4.2.1. Protutumorsko djelovanje harmina 10
1.4.2.2. Antimalarijsko djelovanje harmina 12
1.4.3. Protutumorsko djelovanje derivata β-karbolina 12
1.4.3.1. Derivati β-karbolina koji djeluju na DNA 12
1.4.3.2. Derivati β-karbolina koji inhibiraju kinaze 19
1.4.3.3. Derivati β-karbolina koji djeluju na tubulin 21
1.4.3.4. Inhibitori histonskih deacetilaza 22
1.4.3.5. Derivati koji izazivaju feroptozu 24
1.4.3.6. Različito 24
1.4.3.7. SAR protutumorskog djelovanja derivata β-karbolina 26
1.4.4. Antimalarijsko djelovanje derivata β-karbolina 27
1.5. CIMETNA KISELINA I NJENI DERIVATI 33
1.5.1. Cimetna kiselina i njeni derivati u prirodi 33
1.5.2. Priprava cimetne kiseline i derivata 33
1.5.3. Biološko djelovanje cimetne kiseline i DCK-a 34
1.5.3.1. Antimalarijsko djelovanje 34
1.5.3.2. Protutumorsko djelovanje 37
1.6. KLOROKIN 39
1.6.1. Fizikalno-kemijska svojstva klorokina 39
1.6.2. Sinteza klorokina 40
1.6.3. Antimalarijsko djelovanje klorokina 41
1.6.4. Protutumorsko djelovanje klorokina 43
1.6.5. Ostala djelovanja klorokina 44
1.6.6. SAR derivata klorokina 45
1.6.7. Derivati klorokina s antimalarijskim djelovanjem 47

1.7. FEROCEN 51
1.7.1. Struktura i svojstva ferocena 51
1.7.2. Sinteza ferocena 51
1.7.3. Ferokin 52
1.7.3.1. Derivati ferokina 54
1.7.4. Ferocifeni 55
1.7.4.1. Derivati ferocifena 57
1.7.5. Ostali derivati ferocena s protutumorskim djelovanjem 57
1.8. TRIAZOL 59
1.8.1. Reakcije klik-kemije 60
2. OBRAZLOŽENJE TEME 62
3. MATERIJALI I METODE 64
3.1. MATERIJALI I INSTRUMENTI 65
3.2. SINTEZE 68
3.2.1. Sinteza 1-(dimetoksimetil)-2,3,4,9-tetrahidro-1*H*-pirido[3,4-*b*]indola (**1**) 68
3.2.2. Sinteza 1-(dimetoksimetil)-9*H*-pirido[3,4-*b*]indola (**2**) 68
3.2.3. Sinteza 9*H*-pirido[3,4-*b*]indol-1-karbaldehida (**3**) 68
3.2.4. Sinteza (9*H*-pirido[3,4-*b*]indol-1-il)metanola (**5**) 69
3.2.5. Sinteza metil-1-metil-2,3,4,9-tetrahidro-1*H*-pirido[3,4-*b*]indol-3-karboksilata (**8**) 69
3.2.6. Sinteza etil-1-metil-9*H*-pirido[3,4-*b*]indol-3-karboksilata (**9**) 70
3.2.7. Sinteza (1-metil-9*H*-pirido[3,4-*b*]indol-3-il)metanola (**10**) 70
3.2.8. Sinteza azida β-karbolina **6** i **11**. Opća metoda 70
3.2.9. Sinteza amina β-karbolina **7** i **12**. Opća metoda 72
3.2.10. Sinteza 1-metil-9*H*-pirido[3,4-*b*]indol-3-karbaldehida (**14**) 73
3.2.11. Sinteza β-karbolinskih alkina **4** i **15**. Opća metoda 73
3.2.12. Sinteza 6-metoksi-1-metil-2,3,4,9-tetrahidro-1*H*-pirido[3,4-*b*]indol-2-ijevog trifluoracetata (**16**) 74
3.2.13. Sinteza 6-metoksi-1-metil-9*H*-pirido[3,4-*b*]indola (**17**) 75
3.2.14. Sinteza 1-metil-9*H*-pirido[3,4-*b*]indol-6-ola (**18**) 75
3.2.15. Sinteza *tert*-butil-(2-((1-metil-9*H*-pirido[3,4-*b*]indol-6-il)oksi)etil)karbamata (**20**) 75
3.2.16. Sinteza 1-metil-9*H*-pirido[3,4-*b*]indol-7-ola (**23**) 76
3.2.17. Sinteza alkina β-karbolina **13**, **19** i **24**. Opća metoda 76
3.2.18. Sinteza Boc-zaštićenih amina β-karbolina **25** i **29**. Opća metoda 78

3.2.19. Sinteza amina β-karbolina **21**, **26** i **30**. Opća metoda 79
3.2.20. Sinteza azida β-karbolina **22**, **27** i **31**. Opća metoda.....80
3.2.21. Sinteza 7-metoksi-1-metil-9-(prop-2-in-1-il)-9*H*-pirido[3,4-*b*] indola (**28**).....81
3.2.22. Sinteza metil-3-(7-metoksi-1-metil-9*H*-pirido[3,4-*b*]indol-9-il) propanoata (**32**).....81
3.2.23. Sinteza 3-(7-metoksi-1-metil-9*H*-pirido[3,4-*b*]indol-9-il)propanske kiseline (**33**).....82
3.2.24. Sinteza propargilnih estera DCK-a (**34a-e**). Opća metoda.....82
3.2.25. Sinteza etilnih estera derivata cimetne kiseline (**35a-e**). Opća metoda.....83
3.2.26. Sinteza cimetnih alkohola (**36a-e**). Opća metoda 84
3.2.27. Sinteza azida DCK-a (**37a-e**). Opća metoda 86
3.2.28. Sinteza 4-azido-7-klorkinolina (**38**) 87
3.2.29. Sinteza 2-((7-klorkinolin-4-il)amino)etan-1-ola (**39**).....87
3.2.30. Sinteza *N*-(2-azidoetil)-7-klorkinolin-4-amina (**40**).....87
3.2.31. Sinteza 7-klorkinolin-4-ola (**41**).....88
3.2.32. Sinteza 7-klor-4-(prop-2-in-1-iloksi)kinolina (**42**).....88
3.2.33. Sinteza (7-klorkinolin-4-il)glicina (**43**).....88
3.2.34. Sinteza amina 7-klorkinolina **44** i **45**. Opća metoda 89
3.2.35. Sinteza azidometilferocena (**46**).....89
3.2.36. Sinteza harmicina **47a-e**. Opća metoda.....90
3.2.37. Sinteza harmicina **48a-e**. Opća metoda.....93
3.2.38. Sinteza harmicina **49a-e**. Opća metoda.....97
3.2.39. Sinteza harmicina **50a,c-e** 100
3.2.40. Sinteza harmikina triazolskog tipa **51-58**. Opća metoda.....103
3.2.41. Sinteza harmikina amidnog tipa **59-63**. Opća metoda 108
3.2.42. Sinteza harmikina amidnog tipa **64**, **65**. Opća metoda.....111
3.2.43. Sinteza harmicena triazolskog tipa **66-70**. Opća metoda 112
3.2.44. Sinteza harmicena triazolskog tipa **71-75**. Opća metoda 115
3.2.45. Sinteza harmicena amidnog tipa **76-79**. Opća metoda.....118
3.2.46. Sinteza harmicena amidnog tipa **80-83**. Opća metoda.....121
3.3. ISPITIVANJA BIOLOŠKOG DJELOVANJA.....124
3.3.1. ANTIPROLIFERATIVNO DJELOVANJE 124
3.3.1.1. Ispitivanje unutarstanične lokalizacije spojeva 125
3.3.2. ISPITIVANJE ANTIMALARIJSKOG DJELOVANJA 126

3.3.2.1. Ispitivanje djelovanje hibrida na eritrocitnu fazu životnog ciklusa plazmodija 126
3.3.2.2. Ispitivanje inhibicije polimerizacije hemozoina 126
3.3.2.3. Ispitivanje učinka hibrida na hepatocitnu fazu životnog ciklusa plazmodija 127
4. REZULTATI I RASPRAVA 128
4.1. SINTEZE 129
4.1.1. Sinteza C-1 alkina, azida i amina β-karbolina 132
4.1.2. Sinteza C-3 alkina, azida i amina β-karbolina 137
4.1.3. Sinteza O-6 alkina, azida i amina β-karbolina 141
4.1.4. Sinteza O-7 i N-9 derivata β-karbolinskog prstena 145
4.1.5. Sinteza alkina i azida DCK-a 147
4.1.6. Sinteza azida, alkina, karboksilne kiseline i amina 7-klorkinolina 149
4.1.7. Sinteza azida ferocena 150
4.1.8. Sinteza harmicina **47-50** 151
4.1.9. Sinteza harmikina **51-65** 162
4.1.10. Sinteza harmicena **66-83** 173
4.2. FIZIKALNO-KEMIJSKA SVOJSTVA HIBRIDNIH DERIVATA HARMINA POŽELJNA ZA LJEKOVITE TVARI 185
4.3. BIOLOŠKO DJELOVANJE HARMICINA, HARMIKINA I HARMICENA 189
4.3.1. ANTIPROLIFERATIVNO DJELOVANJE 189
4.3.2. ANTIMALARIJSKO DJELOVANJE 195
4.3.2.1. Djelovanje na eritrocitnu fazu životnog ciklusa plazmodija 195
4.3.2.1.1. Harmikini 195
4.3.2.1.2. Harmiceni i harmicini 199
4.3.2.1.3. Selektivnost antimalarijskog djelovanja hibridnih derivata β-karbolina 202
4.3.2.2. Djelovanje na hepatocitnu fazu životnog ciklusa plazmodija 204
5. ZAKLJUČCI 208
6. LITERATURA 211
7. ŽIVOTOPIS 234
PRILOG A
PRILOG B
TEMELJNA DOKUMENTACIJSKA KARTICA

KRATICE

5-FU	5-fluorouracil
A-549	humana stanična linija adenokarcinoma alveolarnog bazalnog epitela
ACN	acetonitril
ADMET	apsorpcija, distribucija, metabolizam, eliminacija i toksičnost
ADMP	2-azido-1,3-dimetilimidazolinijev heksafluorofosfat
ATP	adenozin-trifosfat
ATR	prigušena totalna refleksija (engl. *attenuated total reflection*)
Bax	X protein povezan s Bcl-2
BIU87	humana stanična linija karcinoma mokraćnog mjehura
B-16	stanična linija mišjeg melanoma
B16F10	stanična linija mišjeg melanoma
BJeLR	stanična linija genetički modificiranih fibroblasta
Boc	*tert*-butiloksikarbonil
BXPC-3	humana stanična linija adenokarcinoma gušterače
Calu-1	humana stanična linija karcinoma pluća nemalih stanica
CCRF-CEM	humana stanična linija limfoblastične leukemije
CDK	kinaza ovisna o ciklinima
CFPAC-1	humana stanična linija duktalnog adenokarcinoma gušterače
CQ	klorokin
CQOS	sojevi plazmodija osjetljivi na klorokin
CQRS	sojevi plazmodija otporni na klorokin
CuAAC	bakrom(I) katalizirana alkin-azid cikloadicija
CYP	citokrom P450 enzim
DBU	1,8-diazabiciklo(5.4.0)undek-7-en
DCK	derivat cimetne kiseline
DIEA	*N*,*N*-diizopropiletilamin
DMF	*N*,*N*-dimetilformamid

DMEM	Dulbeccov modificirani Eagleov medij
DMSO	dimetilsulfoksid
DNA	deoksiribonukleinska kiselina
DU-145	humana stanična linija karcinoma prostate
EDTA	etilendiamintetraoctena kiselina
ESI	ionizacija elektroraspršenjem
FBS	fetalni goveđi serum
FP	falcipain (cistein proteaza)
FQ	ferokin
H520	humana stanična linija karcinoma skvamoznih stanica pluća
HAR	harmin
HATU	1-[*bis*(dimetilamino)metilen]-1*H*-1,2,3- triazolo[4,5-*b*]-piridinijev-3-oksid heksafluorofosfat
HCT116	humana stanična linija kolorektalnog karcinoma
HDAC	histonske deacetilaze
Hek293T	humana stanična linija epitelnih stanica bubrega embrija
HeLa	humana stanična linija karcinoma grlića maternice
HepG2	humana stanična linija hepatocelularnog karcinoma
HFF-1	stanična linija fibroblasta ljudskog prepucija
HGC-27	humana stanična linija karcinoma želuca
HPLC	tekućinska kromatografija visoke djelotvornosti
Hsp	protein toplinskog šoka (engl. *heat shock protein*)
HT-29	humana stanična linija kolorektalnog karcinoma
IC_{50}	koncentracija spoja koja inhibira rast stanica za 50 %
IR	infracrveno elektromagnetsko zračenje
K562	humana stanična linija mijeloične leukemije
L1210	stanična linija mišje limfocitne leukemije
LoVo	humana stanična linija adenokarcinoma kolona
MCF-7	humana stanična linija adenokarcinoma dojke
MDA-MB-231	humana stanična linija adenokarcinoma dojke
MGC-803	humana stanična linija adenokarcinoma želuca

MKN-28	humana stanična linija adenokarcinoma želuca
MS	masena spektrometrija
MTT	3-(4,5-dimetiltiazol-2-il)-2,5-difeniltetrazolijev bromid
MW	mikrovalno zračenje
NF-κB	nuklearni faktor kappa B
NMP	*N*-metil-2-pirolidinon
NMR	nuklearna magnetska rezonancija
NPP	novi putovi propusnosti
P-388	stanična linija mišjeg limfoma pre-B stanica
PANC-1	humana stanična linija duktalnog adenokarcinoma gušterače
PARP1	poli[ADP-riboza]polimeraza-1
PC-3	humana stanična linija adenokarcinoma prostate
*Pf*3D7	soj *P. falciparum* osjetljiv na klorokin
*Pf*7G8	soj *P. falciparum* otporan na klorokin i pirimetamin
*Pf*CRT	transporter odgovoran za rezistenciju na klorokin
*Pf*Dd2	soj *P. falciparum* otporan na klorokin
*Pf*Hsp	protein toplinskog šoka vrste *P. falciparum*
*Pf*K1	soj *P. falciparum* otporan na klorokin, pirimetamin i sulfadoksin
*Pf*W2	soj *P. falciparum* otporan na klorokin
Ph	fenil
PQ	primakin
q.s.	količina koja je dovoljna (lat. *quantum satis*)
RI	indeks rezistencije
RKV	reaktivne kisikove vrste
RPMI-8226	humana stanična linija multiplog mijeloma
RT112	humana stanična linija karcinoma mokraćnog mjehura
RT4	humana stanična linija karcinoma mokraćnog mjehura
SAHA	suberoilanilid hidroksamska kiselina (vorinostat)
SAR	odnos strukture i djelovanja (engl. *structure-activity relationship*)
SI	indeks selektivnosti

s.t.	sobna temperatura
SW-1990	humana stanična linija adenokarcinoma gušterače
SW620	humana stanična linija adenokarcinoma debelog crijeva
SW780	humana stanična linija karcinoma mokraćnog mjehura
T3P	anhidrid propanfosfonske kiseline
T98G	humana stanična linija glioblastoma
TBAHS	tetrabutilamonijev hidrogensulfat
t-Bu	*tert*-butil
TEA	trietilamin
TFA	trifluoroctena kiselina
THF	tetrahidrofuran
TLC	tankoslojna kromatografija
TLR	*Toll-like* receptor
TMS	tetrametilsilan
TNF-α	faktor nekroze tumora alfa
TPC-1	humana stanična linija papilarnog karcinoma štitnjače
TrxR	tioreduksin reduktaza
t_t	temperatura taljenja
UV	ultraljubičasto zračenje
WHO	Svjetska zdravstvena organizacija (engl. *World Health Organization*)

1. UVOD

1.1. TUMOR

Tumor je svaka nenormalna proliferacija stanica u tijelu (1). Uzrokuju ga karcinogeni iz okoliša, hrane i duhanskog dima, virusi (npr. Epstein-Barrov virus) te bakterije (npr. *Helicobacter pylori*). Također, može biti uzrokovan radioterapijom i kemoterapijom, a bitnu ulogu u nastanku ove bolesti imaju i nasljedni faktori. Nabrojani čimbenici dovode do mutacija gena što rezultira deaktivacijom tumor supresorskih gena i aktivacijom protoonkogena. Posljedice genskih defekata su: abnormalni signalni putevi, neosjetljivost na signale koji inhibiraju rast stanice, nepravilnosti u regulaciji staničnog ciklusa, neograničen broj dioba, odnosno besmrtnost, prevladavanje programirane stanične smrti (apoptoza), sposobnost tvorbe novih krvnih žila (angiogeneza), invazija okolnog tkiva i udaljenih dijelova tijela (metastaziranje). Zbog svega navedenog tumorske stanice narušavaju normalno funkcioniranje tkiva i organa, odnosno organizma u cjelini (1, 2).

Postoje dvije vrste tumora: dobroćudni (benigni), koji ostaje lokaliziran na mjestu nastanka, i zloćudni (maligni), poznat kao rak, koji ima tendenciju širenja u ostale dijelove tijela zbog čega je izrazito opasan. Karcinom je vrsta raka koja zahvaća epitelne stanice te čini 90 % svih vrsta raka (1). Najčešće vrste tumora u žena su karcinom dojke, cerviksa i štitinjače, dok muškaraci najčešće obolijevaju od karcinoma prostatate, želuca i jetre. Oba spola jednako pogađaju kolorektalni karcinom i karcinom pluća (3). Tumor se može liječiti kirurškim odstranjivanjem, radioterapijom i/ili kemoterapijom (2).

Rak je drugi vodeći uzrok smrti u svijetu zbog čega predstavlja globalni javnozdravstveni problem. Prema podacima Svjetske zdravstvene organizacije (engl. *World Health Organization*, WHO), u 2020. godini uzrokovao je oko 10 milijuna smrti u svijetu (3). Iako je kemoterapija posljednjih desetljeća značajno napredovala, njenu učinkovitost narušava razvoj rezistencije tumorskih stanica prema postojećim citostaticima (4). Osim toga, neselektivnost, odnosno toksičnost postojećih citostatika uzrokuje ozbiljne nuspojave koje narušavaju kvalitetu života bolesnika i smanjuju adherenciju (5). Slijedom svega navedenoga, razvoj novih, sigurnijih i učinkovitijih protutumorskih lijekova od iznimne je važnosti.

1.2. MALARIJA

Malarija je zarazna bolest koju uzrokuju paraziti iz roda *Plasmodium*, a prenose ženke komarca iz roda *Anopheles*. Široko je rasprostranjena u tropskim i suptropskim područjima (6). Najčešće pogađa dojenčad, djecu do 5 godina starosti, trudnice i putnike (7, 8). U 2020. godini zabilježeno je 241 milijun slučajeva malarije, od čega je 627 tisuća rezultiralo smrtnim ishodom (9).

Postoji više od 120 vrsta plazmodija, ali samo njih 5 uzrokuje malariju u čovjeka: *P. falciparum, P. vivax, P. ovale, P. malariae* i *P. knowlesi.* Od navedenih, najsmrtonosniji je *P. falciparum* (6). Plazmodij ima dvije faze životnog ciklusa: spolnu, koja se odvija u komarcu, i nespolnu, koja se odvija u čovjeku (Slika 1). Nespolna faza započinje ubodom zaraženog komarca, pri čemu dolazi do prijenosa sporozoita plazmodija iz sline komarca u ljudsku krv. Iz periferne krvi sporozoit prvo dospijeva u jetru gdje sazrijeva u shizont (hepatocitna ili egzoeritrocitna faza). *P. vivax* i *P. ovale* mogu u hepatocitima tvoriti hipnozoite, dormantne oblike, koji se mogu aktivirati mjesecima ili godinama nakon primarne infekcije te izazvati simptome bolesti. Prsnućem shizonta oslobađa se veliki broj merozoita koji inficiraju eritrocite. Merozoiti se u eritrocitima hrane hemoglobinom, rastu i sazrijevaju u shizont. Zreli shizonti razaraju eritrocit oslobađajući veliki broj merozoita, koji napadaju nove eritrocite te se nespolni ciklus ponavlja (tzv. shizogonija u krvi). Prilikom svakoga pucanja eritrocita kod bolesnika se javlja malarični napad. Neki paraziti tijekom shizogonije u krvi prelaze u spolne gametocite koji prilikom sljedećeg uboda dospijevaju u želudac komarca, gdje započinju spolni dio životnog ciklusa (10).

Prema simptomima razlikujemo nekompliciranu i tešku malariju. Kod nekomplicirane malarije javljaju se nespecifični simptomi poput groznice, glavobolje, mučnine, abdominalne boli, povraćanja i dijaree (11). Ukoliko se pravovremeno ne dijagnosticira i ne liječi, bolest može uznapredovati u teži oblik, pa čak uzrokovati i smrt. Teška malarija uključuje cerebralnu malariju, plućni edem, respiratorni distres, šok, metaboličku acidozu, zatajenje bubrežne ili jetrene funkcije (8).

Od 2000. do 2015. godine bio je vidljiv opadajući trend zabilježenih slučajeva malarije u svijetu, kao i malarijom uzrokovanih smrti (9, 12). Tome je pridonijelo korištenje artemizininske kombinirane terapije, zaštitnih mreža tretiranih insekticidima i brzi dijagnostički testovi. Unatoč tome, od malarije i dalje umire približno 1700 ljudi dnevno. Zabrinjavajuća je činjenica da posljednjih godina napredak u suzbijanju malarije stagnira (12). Jedan od glavnih

razloga je pojava rezistentnih sojeva plazmodija. Rezistencija na klorokin (CQ) te križna rezistencija na 4-aminokinolinske antimalarike poznata je već neko vrijeme (13). Ranih 2000-ih zabilježeni su prvi slučajevi rezistencije na artemizinin i njegove derivate na području Kambodže. Međutim, nedavno je rezistencija na artemizinine primijećena i u Africi, kontinentu s više od 90 % svih slučajeva malarije (14). S druge strane, kontrola ove bolesti u budućnosti je neizvjesna. Globalizacija svijeta i procesi migracija te klimatske promjene mogle bi rezultirati pojavom malarije u krajevima u kojim je ona odavno iskorijenjenja (15). S obzirom na prethodno, razvoj novih, učinkovitih lijekova otpornih na rezistenciju i dalje ostaje jedan od ključnih segmenata u borbi protiv ove bolesti. Veliki napredak dogodio se u listopadu 2021. godine kada je WHO preporučio široku upotrebu cjepiva RTS,S (Mosquirix) za prevenciju malarije u djece (16).

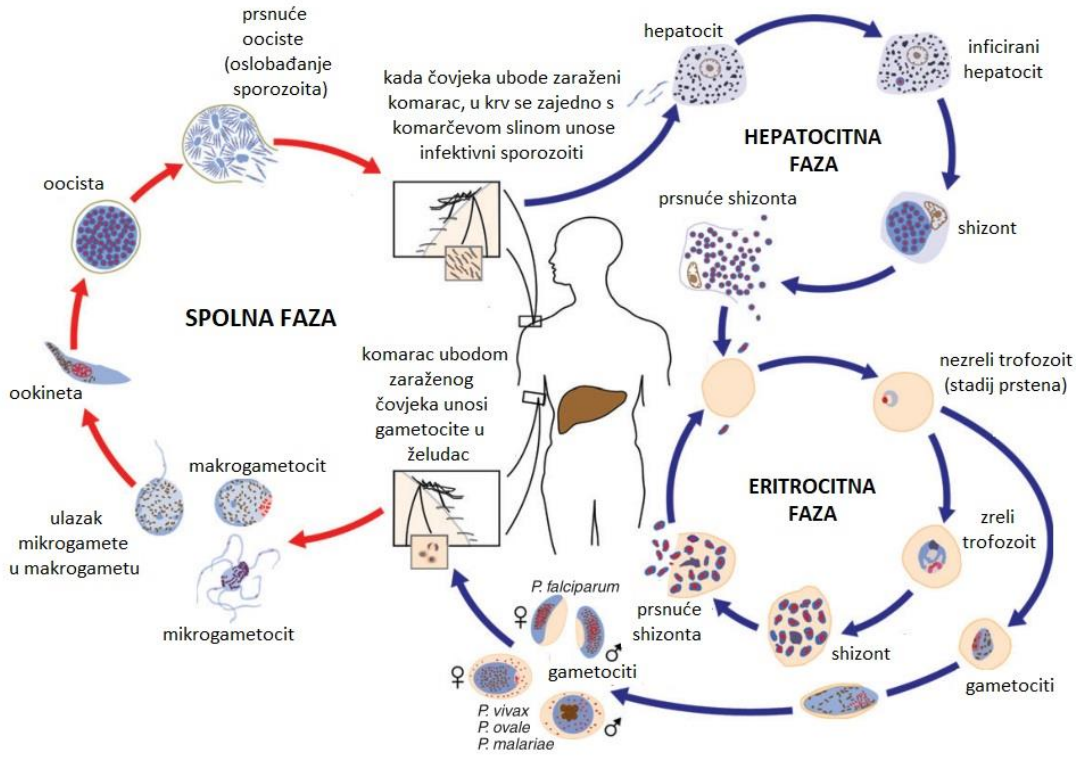

Slika 1. Životni ciklus plazmodija (prilagođeno prema (17))

1.3. HIBRIDNI SPOJEVI

Popularan pristup u dizajniranju i razvoju novih lijekova je molekulska hibridizacija koja podrazumijeva kovalentno povezivanje dviju bioaktivnih molekula ili farmakofora u jedinstveni kemijski entitet, odnosno hibridni spoj (18). S obzirom na način povezivanja, razlikuju se tri vrste hibrida: 1) hibridi povezani metabolički nestabilnom poveznicom (Slika 2a), 2) hibridi povezani metabolički stabilnom poveznicom (Slika 2b) i 3) kondenzirani hibridi koji ne sadrže poveznicu (Slika 2c) (19).

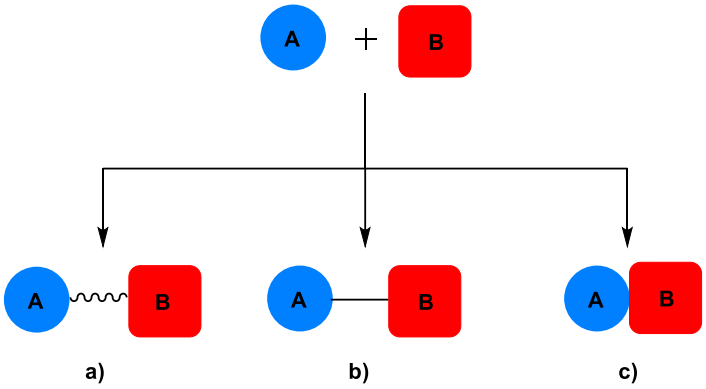

Slika 2. Vrste hibridnih molekula

Hibridi pokazuju poboljšana svojstva u odnosu na zasebne molekule. Budući da sadrže dva farmakofora u strukturi, ostvaruju sinergistički učinak i pokazuju jače biološko djelovanje od zasebnih molekula (18). Walsh i suradnici pripravili su hibride artemizinina i kinina koji su ostvarili bolje antimalarijsko djelovanje od zasebnih molekula ili njihove smjese u omjeru 1:1 (20). Priprava hibridnih spojeva od posebnog je značaja ako se žele pripraviti molekule otporne prema razvoju rezistencije. Farmakofori u hibridu se uzajamno „štite“ zbog čega je vjerojatnost razvoja rezistencije mala. Štoviše, racionalnim dizajniranjem hibridnih spojeva moguće je povratiti učinkovitost koju je određeni lijek izgubio zbog razvoja rezistencije (18). Poznato je da CQ ne djeluje na rezistentne sojeve plazmodija zato što ti sojevi u membrani digestivne vakuole sadrže transporter odgovoran za rezistenciju na CQ (*Pf*CRT). Ovaj transporter izbacuje CQ iz digestivne vakuole, čime onemogućava njegovo nakupljanje i antimalarijsko djelovanje (21). Peyton i suradnici pripravili su hibride CQ-a i različitih molekula za koje je poznato da inhibiraju *Pf*CRT. Hibridi su jednako snažno djelovali na sojeve osjetljive na CQ (CQOS) i rezistentne sojeve (CQRS) (22). Nadalje, pripravom hibridnih spojeva moguće je povećati

selektivnost djelovanja (npr. estramustin), povećati topljivost (npr. hibridi paklitaksela i hidrofilnijih molekula) i poboljšati farmakokinetička svojstva molekula (18, 19).

1.4. ALKALOIDI β-KARBOLINSKOG TIPA

β-Karbolini su velika skupina alkaloida i srodnih sintetskih spojeva, čija struktura se temelji na tricikličkom pirido[3,4-*b*]indolnom prstenu. Prefiks β u nazivu označava položaj atoma dušika u piridinskom prstenu. S obzirom na zasićenost piridinskog prstena razlikuju se potpuno zasićeni tetrahidro-β-karbolini, djelomično zasićeni dihidro-β-karbolini te potpuno nezasićeni β-karbolini (Slika 3) (23, 24). Svojstva β-karbolina uvelike određuju dva različita dušikova atoma u strukturi: piridinski dušik bazičnijeg karaktera i kiseliji indolski dušik. Ovisno o pH i otapalu, β-karbolini postoje u četiri oblika: kation, neutralni oblik, zwitterion i anion (25).

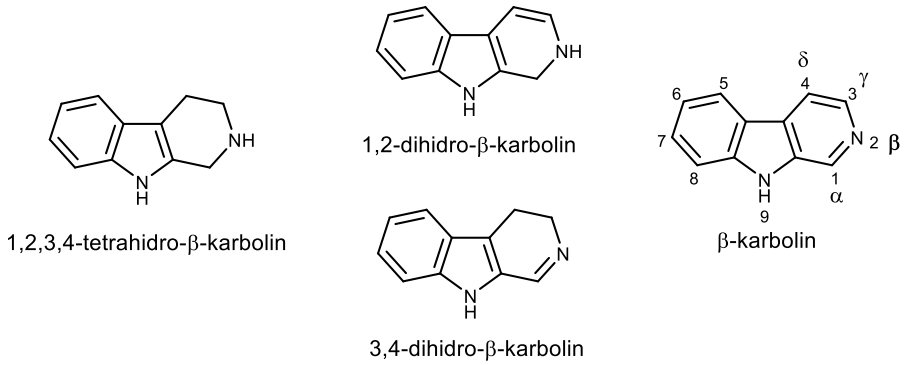

Slika 3. Strukturna raznolikost β-karbolina

Prirodni β-karbolini. β-karbolinski alkaloidi široko su rasprostranjeni u prirodi. Mogu se pronaći u biljkama iz porodica Rutaceae, Simaroubaceae, Amaranthaceae, Caryophyllaceae, Rubiaceae i Zygophyllaceae, morskim organizmima kao što su meki koralji, spužve, žarnjaci, mikroorganizmima, kukcima, prehrambenim proizvodima, alkoholnim pićima, duhanskom dimu te ljudskim tkivima i tjelesnim tekućinama (24). Posjeduju široki spektar bioloških djelovanja, uključujući antioksidativno (26), protuupalno (27), protutumorsko (28), antimikrobno (29), antivirusno (30), antiparazitsko (31), sedativno (32), hipnotičko (33), antikonvulzivno (34). Na Slici 4 prikazani su odabrani primjeri prirodnih β-karbolina. Eudistomin K izoliran je iz mješćićnice *Ritterella sigillinoides* podrijetlom iz Novog Zelanda. Karakterističan je po tome što u strukturi sadrži oksatiazepinski prsten. Antiproliferativno djelovanje eudistomina K ispitano je na nekoliko tumorskih staničnih linija. Otkriveno je da spoj snažno djeluje na mišji limfom pre-B stanica (P388) (IC_{50} = 0,01 μM) (35). Manzamini su izolirani iz određenih vrsta morskih spužvi s područja Indonezije. Strukturno su kompleksniji:

sadrže β-karbolinski dio povezan sa složenim alicikličkim sustavom. Manzamini ispoljavaju protutumorsko, antimalarijsko, tuberkulostatsko i antileishmanijsko djelovanje (36). Pinolin je β-karbolinski alkaloid prisutan u epifizi koji pokazuje antioksidativno djelovanje usporedivo s melatoninom (37). Reserpin je izoliran iz korijena biljke *Rauwolfia serpentina*, a koristi se za liječenje hipertenzije (38).

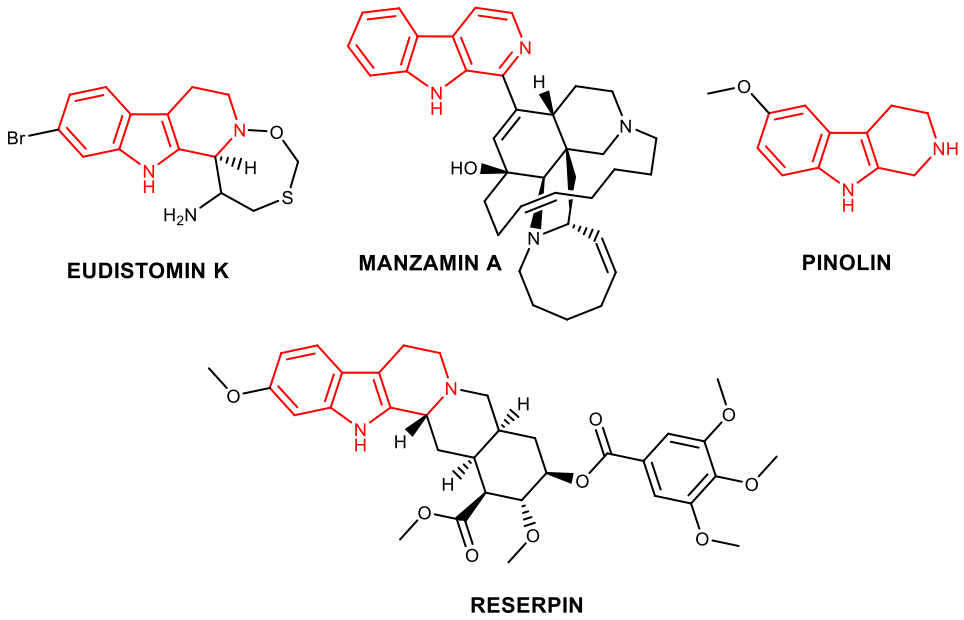

Slika 4. Primjeri prirodnih β-karbolina

Sintetski β-karbolini. Sintetizirani su brojni derivati koji u svojoj strukturi sadrže β-karbolinski motiv te je ispitano njihovo biološko djelovanje. Na Slici 5 prikazani su odabrani sintetski β-karbolini. Tadalafil je reverzibilni inhibitor forsfodiesteraze 5 zbog čega djeluje kao vazodilatator. Koristi se u liječenju erektilne disfunkcije, benigne hipertrofije prostate i plućne hipertenzije (39). Cipargamin je antimalarik koji spada u skupinu spiroindola. Mehanizam djelovanja cipargamina temelji se na inhibiciji plazmodijske Na^+-ATPaze (*Pf*ATP4), čime je narušena homeostaza Na^+ u parazitu. Trenutno se nalazi u drugoj fazi kliničkih ispitivanja (40).

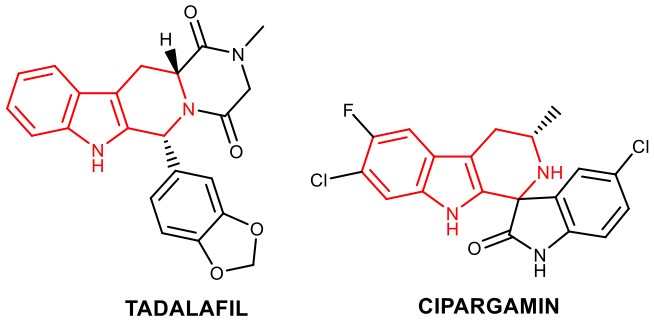

Slika 5. Primjeri sintetskih β-karbolina

1.4.1. Priprava β-karbolina

Za pripravu β-karbolina najčešće se koristi Pictet-Spenglerova reakcija koju su 1911. godine otkrili Amé Pictet i Theodor Spengler (41, 42). Pictet-Spenglerovom reakcijom derivata triptamina i aldehida uz kiseli katalizator dobiva se tetrahidro-β-karbolin, koji se naknadno oksidira u željeni β-karbolin (42). Detaljan mehanizam Pictet-Spenglerove reakcije prikazan je na Shemi 1. U prvom koraku amino skupina indoletilamina nukleofilno se adira na karbonilnu skupinu čime nastaje karbinolamin. Slijedi protoniranje hidroksilne skupine, eliminacija vode i nastajanje imina. Protoniranje imina daje iminijev ion koji reagira s elektronima bogatim indolskim prstenom zatvarajući šesteročlani heterociklički prsten. S obzirom na Baldwinova pravila, riječ je o 6-*endo-trig* ciklizaciji. Gubitkom protona ponovno nastaje aromatski indolski prsten kao konačni produkt (43).

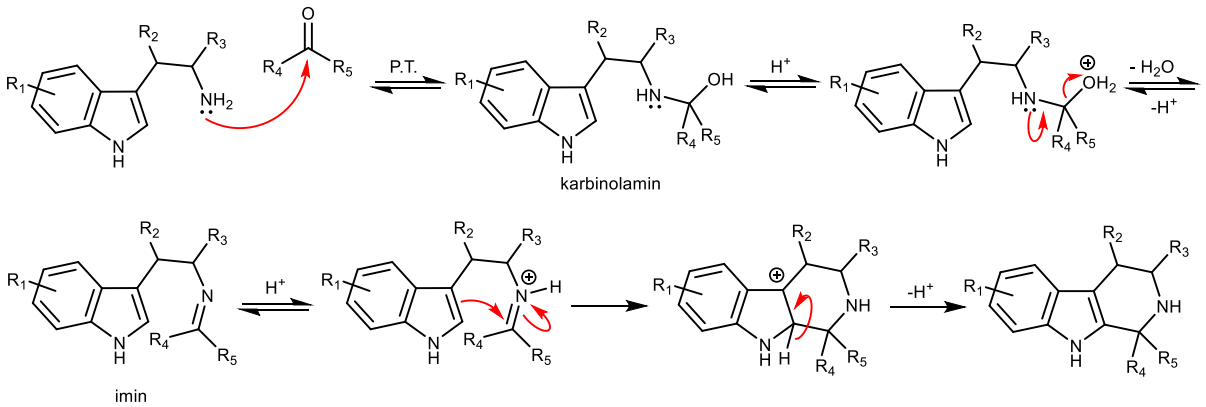

Shema 1. Mehanizam Pictet-Spenglerove reakcije, P.T. – transfer protona

1.4.2. Harmin

Harmin je trivijalno ime za 7-metoksi-1-metil-9*H*-pirido[3,4-*b*]indol, jedan od najbolje proučenih β-karbolinskih alkaloida. Prvotno je izoliran iz sjemenki sirijske rutvice (*Peganum harmala,* Zygophyllaceae), višegodišnje biljke koja raste u središnjoj Aziji, sjevernoj Africi i Bliskom Istoku. Sirijska rutvica koristila se u tradicionalnoj medicini kao abortiv, emenagog, diuretik, antipiretik, halucinogen i laktagog, dok se ekstrakt sjemenki u sjevernom dijelu Kine koristio za liječenje malarije i karcinoma probavnog trakta (44, 45). Osim harmina, u biljci su pronađeni i drugi β-karbolinski alkaloidi poput harmalina, harmalola i tetrahidroharmina poznati kao harmala alkaloidi (Slika 6) (45). Harmin, poput ostalih β-karbolina, ispoljava brojne biološke učinke (46). U nastavku teksta detaljnije je opisano njegovo protutumorsko i antimalarijsko djelovanje.

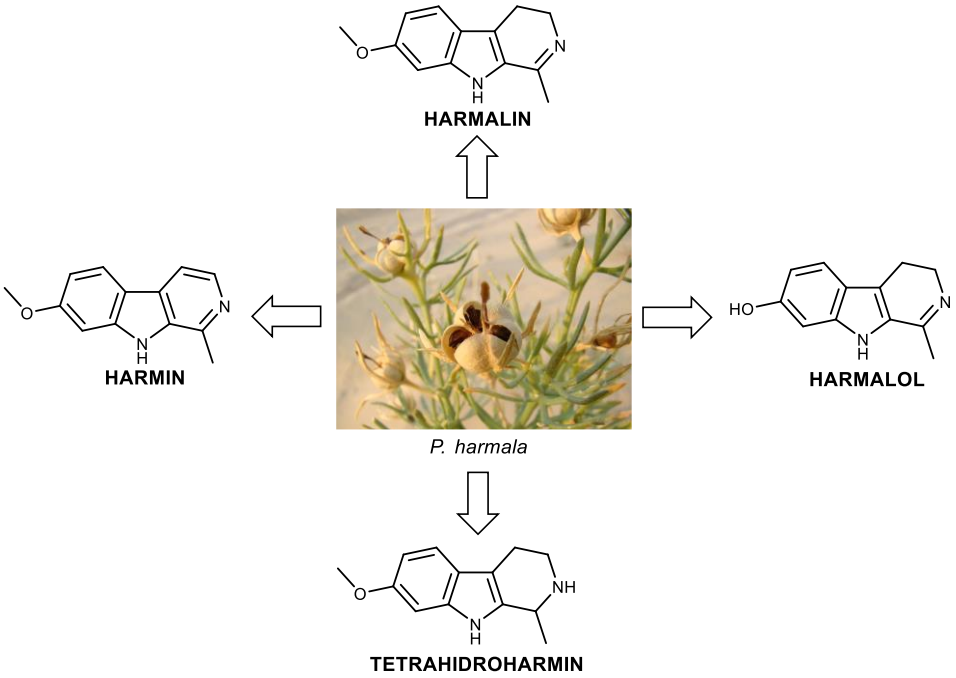

Slika 6. *P. harmala* i harmala alkaloidi (prilagođeno prema (47))

1.4.2.1. Protutumorsko djelovanje harmina

Protutumorsko djelovanje harmina ispitano je na nizu staničnih linija (Tablica 1). Vidljivo je da harmin ostvaruje protutumorski učinak različitim mehanizmima, izravno ili pomažući djelovanje poznatih citostatika (npr. gemcitabin i temozolomid).

Mota i suradnici istražili su protutumorsko djelovanje harmina *in vitro, in vivo* i *in silico* metodama. Ispitivanjem antiproliferativnog djelovanja na humanim tumorskim staničnim linijama (MCF-7 i karcinom grlića maternice, HeLa) i normalnim (netumorskim) mišjim fibroblastima došli su do zaključka da harmin djeluje na tumorske stanice citotoksično i selektivno. U MCF-7 stanicama uzrokovao je smanjenje mitohondrijskog membranskog potencijala i apoptozu ovisnu o Bax, a neovisnu o p53. Inhibicijom fosforilacije pRb i smanjenjem ekspresije kinaze ovisne o ciklinima (CDK) 2, ciklina A i ciklina B1 uzrokovao je zaustavljanje ciklusa u G2/M fazi. Biofizikalnim metodama i molekulskim simulacijama potvrdili su interkalaciju harmina u molekulu deoksiribonukleinske kiseline (DNA). Nadalje, pokazali su da harmin inhibira popravak DNA ovisan o poli[ADP-riboza] polimerazi-1 (PARP1). *In vivo* protutumorsko djelovanje istraženo je na miševima koji nose Ehrlichov ascitični tumor te je pokazano da harmin smanjuje stopu rasta i veličinu tumora, povećava omjer nevijabilnih i vijabilnih tumorskih stanica te produljuje životni vijek miševa (54).

Tablica 1. Protutumorski učinak harmina na različitim tumorskim staničnim linijama

Stanične linije	**Učinak**	**Literaturni izvor**
adenokarcinom dojke (MCF-7 i MDA-MB-231)	supresija stanične proliferacije i migracije, izazivanje apoptoze *in vitro*, inhibicija rasta tumora *in vivo*, značajno smanjena ekspresija TAZ, p-Erk, p-Akt i Bcl-2, a povećana ekspresija Bax	Ding i suradnici (48)
adenokarcinom želuca (MGC-803)	inhibicija Akt/mTOR/p70S6K signaliziranja, izazivanje apoptoze i autofagije	He i suradnici (49)
adenokarcinom gušterače (PANC-1, CFPAC-1, SW-1990, BXPC-3)	zaustavljanje proliferacije tumorskih stanica, pojačavanje citotoksičnog učinka gemcitabina, inhibicija AKT/mTOR signalnog puta (u kombinaciji s gemcitabinom)	Zhang i suradnici (50)
adenokarcinom štitnjače (TPC-1)	zaustavljanje proliferacije tumorskih stanica, izazivanje apoptoze reguliranjem omjera Bcl-2/Bax, inhibiranje sposobnosti stvaranja kolonija stanica, inhibicija migracije i invazije tumorskih stanica	Li i suradnici (51)
karcinom mokraćnog mjehura (RT112, RT4, SW780, BIU87 i 5637)	inhibicija proliferacije i migracije tumorskih stanica, izazivanje apoptoze ovisne o kaspazama, zaustavljanje signalnog puta povezanog s VEGFR2	Zhang i suradnici (52)
glioblastom (T98G)	sinergističko djelovanje s temozolomidom, inhibicija migracije, invazije i adhezije tumorskih stanica, smanjena ekspresija metaloproteinaza 2 i 9	Jalili i suradnici (53)

1.4.2.2. Antimalarijsko djelovanje harmina

Pillai i suradnici pokazali su da se harmin selektivno i s visokim afinitetom veže za ATP-vezno mjesto u proteinu toplinskog šoka 90 *P. falciparum* (*Pf*Hsp90). Predložili su da je inhibicija *Pf*Hsp90 jedan od mogućih mehanizama antimalarijskog djelovanja harmina je (55, 56). Hsp su visoko očuvani proteini prisutni u svim oblicima života, od prokariota do viših eukariota (npr. biljaka i sisavaca). Djeluju kao šaperoni, odnosno pomažu pravilno smatanje proteina, čime su uključeni u mnoge stanične procese poput ekspresije gena, unutarstaničnog transporta proteina, reguliranja staničnog ciklusa i diferencijacije. Hsp90 jedan je od važnijih proteina u ovoj porodici. Na N-kraju sadrži vezno mjesto za adenozin-trifosfat (ATP), koje je bitno za ATP-azno djelovanje (55, 57). *Pf*Hsp90 ima nekoliko bitnih uloga: omogućava otpornost plazmodija na stres uzrokovan toplinskim šokom prilikom promjene domaćina, neophodan je za razvoj plazmodija tijekom eritrocitne faze, a novija istraživanja ukazuju na njegovu ulogu u razvoju rezistencije plazmodija na postojeće lijekove (57–59). *Pf*Hsp90 je dobra meta za razvoj novih antimalarika iz nekoliko razloga. Prvo, postoje razlike u veznom mjestu za ATP između *Pf*Hsp i humanog Hsp što omogućava selektivno djelovanje (59). Drugo, usporedbom veznog mjesta za ATP *Pf*Hsp90 između izolata *P. falciparum* iz geografski različitih područja zaključeno je da postoji visoka očuvanost što ukazuje na malu vjerojatnost razvoja rezistencije spram ove mete (55). Nadalje, nakon tretmana *P. falciparum* s inhibitorom Hsp90 PU-H17 uočen je gubitak *Pf*CRT. Kombinacija CQ i harmina djelovala je na sojeve plazmodija otporne na CQ (CQRS) što govori u prilog tome da harmin inhibicijom *Pf*Hsp90 može interferirati s mehanizmima u plazmodiju odgovornim za rezistenciju (56).

1.4.3. Protutumorsko djelovanje derivata β-karbolina

Postoji veliki broj pripravljenih derivata β-karbolina kojima je ispitano protutumorsko djelovanje. U nastavku je dan pregled tih derivata s obzirom na potencijalni mehanizam djelovanja.

1.4.3.1. Derivati β-karbolina koji djeluju na DNA

Interkalirajući agensi

Brojne studije ukazuju na sposobnost interkalacije β-karbolina u dvostruku uzvojnicu DNA čime interferiraju s procesom replikacije DNA i djelovanjem enzima uključenih u taj

proces. Kamal i suradnici sintetizirali su C-1- i C-3-supstituirane konjugate β-karbolina i benzimidazola te su ispitali njihovu citotoksičnost na humanim tumorskim staničnim linijama. Konjugat koji je imao 4-metoksifenilni prsten u položaju C-1 i 6-metoksi-supstituirani benzimidazol u položaju C-3 (Slika 7a) pokazao je najbolje djelovanje na stanice multiplog mijeloma (RPMI-8226) i limfoblastične leukemije (CCRF-CEM) s IC_{50} vrijednostima 0,36, odnosno 0,88 μM. Biofizikalnim eksperimentima (spektroskopija, fotocijepanje DNA, inhibicija topoizomeraze I) i molekulskim modeliranjem pokazano je da ovi spojevi mogu interkalirati u DNA (60).

Yang i suradnici sintetizirali su seriju C-3-supstituiranih derivata β-karbolina. Primijetili su da uvođenje alkildiaminskog bočnog lanca (Slika 7b) povećava fleksibilnost molekule i sposobnost interkaliranja u DNA (61).

Nagula i suradnici sintetizirali su derivate β-karbolina supstituirane piridinom u položaju C-3. Sintetiziranim spojevima ispitan je afinitet vezanja za DNA te je uočeno da spoj prikazan na Slici 7c ima veći afinitet vezanja za DNA od doksorubicina. Studije molekularnog modeliranja otkrile su postojanje π-π interakcija između planarnog β-karbolinskog dijela molekule i parova baza u DNA ukazujući na interkalaciju u DNA kao vjerojatni mehanizam djelovanja ovih spojeva.

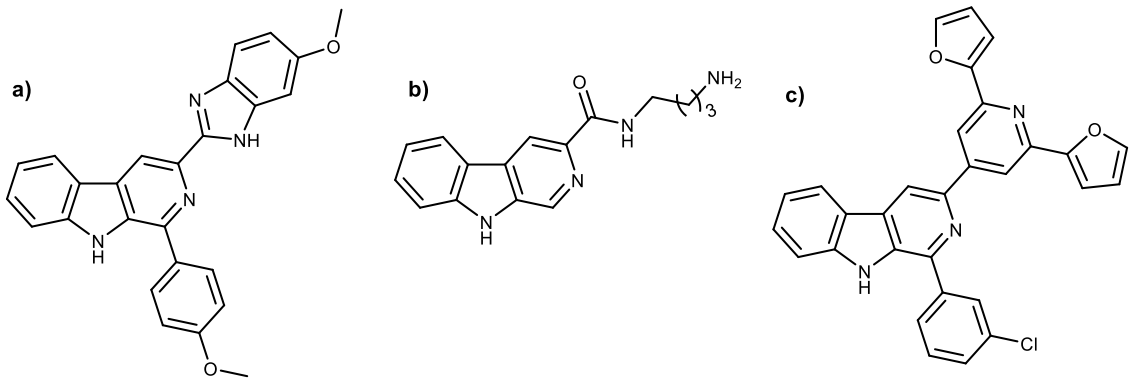

Slika 7. Derivati β-karbolina koji djeluju kao interkalirajući agensi

Nadalje, hibridima β-karbolina i kalkona *in vitro* je ispitana citotoksičnost na nizu humanih tumorskih staničnih linija. Većina hibrida pokazala je dobro djelovanje protiv staničnih linija mišjeg melanoma (B-16) i adenokarcinoma alveolarnog bazalnog epitela (A-549). Hibrid koji je u položaju C-1 imao fenilni prsten supstituiran fluorom i metoksi skupinom, a fenilni prsten kalkonskog dijela molekule supstituiran metoksi skupinom pokazao je snažno i selektivno djelovanje na A-549 (Slika 8a). Na temelju fluorescencijske titracije, mjerenja

viskoznosti DNA, molekulskog uklapanja i dinamike zaključeno je da ova serija spojeva ima sposobnost interkaliranja u DNA (62).

Peng i suradnici izvijestili su o sintezi i *in vitro* citotoksičnom djelovanju konjugata β-karbolina i estera aminokiselina. Zaključili su da uvođenje kationskih aminokiselina kao što su lizin i arginin značajno pojačava citotoksični učinak spojeva u usporedbi s nenabijenim aminokiselinama. Spojevi prikazani na Slici 8b snažno su djelovali na HeLa, MCF-7 i staničnu liniju hepatocelularnog karcinoma (HepG2) (IC_{50} vrijednosti u rasponu 1–7 μM) te je uočeno da interkaliraju u DNA (63).

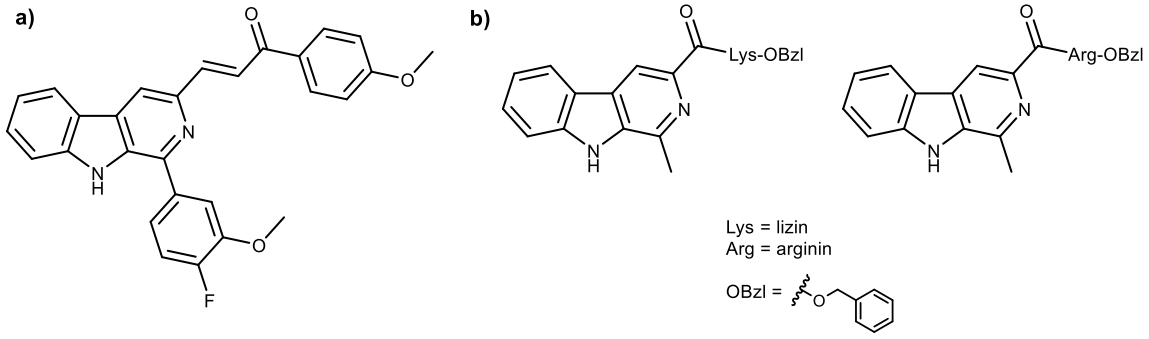

Slika 8. Hibridi β-karbolina i: a) kalkona, b) aminokiselina

Song i suradnici pripravili su seriju bivalentnih β-karbolina s poveznicom između dva indolska atoma dušika duljine 3–10 metilenskih jedinica. Sintetiziranim spojevima ispitano je citotoksično djelovanje protiv različitih humanih tumorskih staničnih linija. SAR studija otkrila je važnost supstituenta u položaju C-1 za djelovanje: uvođenjem odgovarajućeg supstituenta u ovaj položaj uvelike se može poboljšati protutumorsko djelovanje molekula. Također, pokazano je da je optimalna duljina lanca 4–6 metilenskih jedinica. Dalje, odabranim molekulama ispitano je protutumorsko djelovanje *in vivo* na miševima uz ciklofosfamid kao referentni lijek. Spoj prikazan na Slici 9a je u dozi od 40 mg/kg najučinkovitije inhibirao rast tumora *in vivo* (64).

Chen i suradnici pripravili su hibride β-karbolina i tripeptida (Slika 9b) te su ispitali njihovo antiproliferativno djelovanje na nekoliko tumorskih staničnih linija. Rezultati *in vitro* ispitivanja pokazali su njihovo umjereno antiproliferativno djelovanje, dok su neki derivati u *in vivo* ispitivanjima ostvarili učinak usporediv s adriamicinom (pozitivna kontrola). Na temelju eksperimenata (UV apsorpcija, fluorescencijska spektroskopija, mjerenje viskoznosti)

zaključeno je da ovi spojevi djeluju interkaliranjem u DNA. Smatra se da interkaliranje omogućavaju planarni policiklički farmakofori: β-karbolinski prsten i Trp-Trp motiv (24).

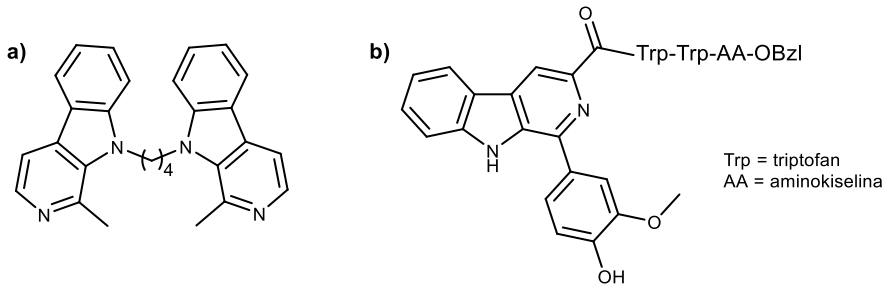

Slika 9. a) Bivalentni β-karbolni, b) hibridi β-karbolina i tripeptida

Agensi koji se vežu u utor DNA

Klik-reakcijom sintetizirana je serija derivata koji su supstituirani triazolom u položaju C-3 te je ispitan njihov citotoksični učinak na tumorske stanične linije. Spoj prikazan na Slici 10a pokazao se najučinkovitijim protiv stanica kolorektalnog adenokarcinoma (HT-29) (IC_{50} = 3,67 μM). Studije molekulske dinamike pokazale su da se ova serija spojeva veže u manji utor DNA. Daljnji eksperimenti (cirkularni dikroizam, fluorescencijska titracija, viskozimetrijska titracija) potvrdile su prethodnu teoriju te ukazale na jake elektrostatske sile između DNA i ovih spojeva (65).

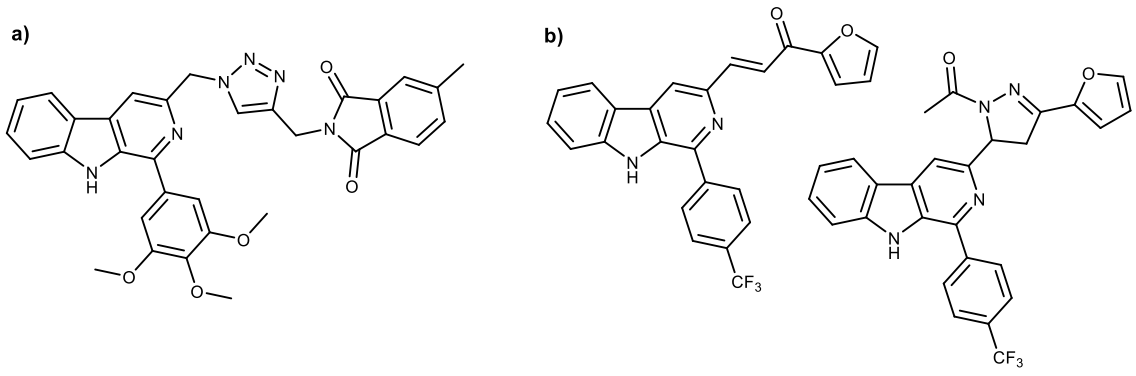

Slika 10. a) Derivati β-karbolina i triazola, b) kombileksini

Kamal i suradnici pripravili su derivate β-karbolina koji sadrže supstituirani fenil u položaju C-1 i kalkon/(*N*-acetil)-pirazol u položaju C-3. Derivatima je ispitano antiproliferativno djelovanje na A-549, DU-145, MCF-7, HeLa, ACHN i HEK-293 uz

doksorubicin i harmin kao pozitivne kontrole. Općenito, spojevi su pokazali dobru do umjerenu aktivnost, dok su spojevi prikazani na Slici 10b bili najučinkovitiji. Hoechstovim bojanjem, fragmentacijom DNA i analizom s aneksinom V-FITC, potvrđeno je da ovi spojevi uzrokuju apopotozu. S druge strane, molekulskim uklapanjem (engl. *docking*) utvrđeno je da ovi spojevi mogu inhibirati topoizomerazu I (66). Nadalje, pripravili su hibride C-1-supstituiranih β-karbolina i *trans*-cinamida u položaju C-3 β-karbolinskog prstena (Slika 11). Hibridi su pokazali izrazito snažno i selektivno djelovanje u niskim nanomolarnim koncentracijama. Nađeno je da ovi spojevi učinak ostvaruju induciranjem apoptoze i inhibicijom topoizomeraze I. Pokazali su da se spojevi interkaliraju u DNA na mjestu vezanja topoizomeraze te da se cinamidni dio veže u manji utor DNA π-π interakcijama (67).

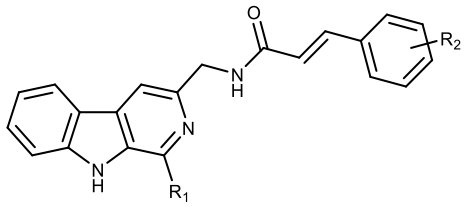

Slika 11. Hibrid C-1-supstituiranog β-karbolina i *trans*-cinamida

Inhibitori topoizomeraze

Hibridi β-karbolina i bisindola dizajnirani su s ciljem vezanja za DNA i inhibicije topoizomeraze. Svim spojevima ispitano je antiproliferativno djelovanje na različitim humanim tumorskim staničnim linijama. Spojevi su pokazali umjereno do dobro djelovanje s IC_{50} vrijednostima u rasponu od 1,80 do 44,20 μM. Najučinkovitiji spojevi (Slika 12) snažno su djelovali na karcinom prostate (DU-145) u niskim mikromolarnim koncentracijama. SAR analiza otkrila je da supstituenti na fenilnom i indolskom prstenu utječu na djelovanje. Spoj s 4-fluor-supstituiranim fenilnim prstenom u položaju C-1 pokazao je najjače djelovanje na DU-145, a slijedio ga je spoj s 4-metil-supstituiranim fenilnim prstenom. Utvrđeno je da zamjena metilne skupine metoksi skupinom dovodi do smanjenja antiproliferativnog djelovanja. Najučinkovitijim spojevima ispitan je mehanizam djelovanja. Uočeno je da ovi spojevi dovode do cijepanja pBR322 plazmidne DNA kada se ozrače UV svjetlom. Raznim biofizikalnim eksperimentima (Annexin V-FITC, Hoechstovo bojenje, analiza DNA fragmentacije) utvrđena je sposobnost uzrokovanja apoptoze tumorskih stanica. Molekulskim uklapanjem pokazano je

da spojevi tvore ternarni kompleks s DNA i topoizomerazom I uzrokujući inhibiciju enzima (68).

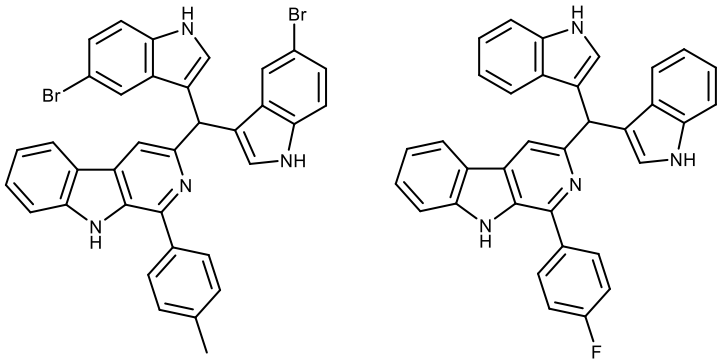

Slika 12. Hibridi β-karbolina i bisindola

Kamal i suradnici sintetizirali su hibride β-karbolina i podofilotoksina kao potencijalne inhibitore topoizomeraze II. Pripravljenim spojevima ispitana je citotoksičnost *in vitro* na različitim humanim tumorskim stanicama (A-549, DU-145, MDA-MB-231, HT-29 i HeLa). Općenito, spojevi su pokazali visoku citotoksičnost i selektivnost u usporedbi s doksorubicinom, etopozidom i podofilotoksinom protiv DU-145 s IC_{50} vrijednošću u niskim mikromolarnim vrijednostima. Najbolje djelovanje na ovu staničnu liniju pokazali su spojevi prikazani na Slici 13. Mehanizam djelovanja spojeva određen je analizom staničnog ciklusa, ispitivanjem inhibicije enzima i molekulskim uklapanjem. Uočeno je da ovi spojevi imaju afinitet vezanja za DNA te sposobnost inhibicije topoizomeraze II (69).

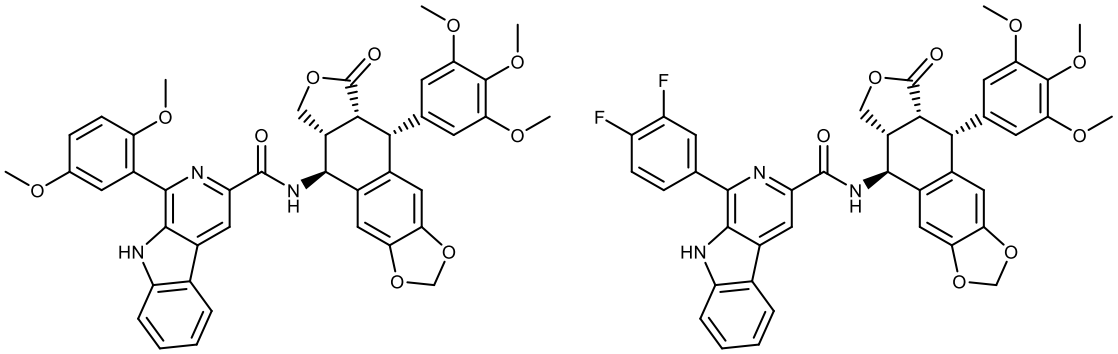

Slika 13. Hibridi β-karbolina i podofilotoksina

Ista istraživačka skupina sintetizirala je derivate β-karbolina koji sadrže ditiokarbamatnu funkcionalnu skupinu te su ispitali njihovo djelovanje na humanim tumorskim staničnim linijama. Spojevi prikazani na Slici 14a pokazali su snažno djelovanje na DU-145 te im je u

daljnjim eksperimentima ispitan mehanizam djelovanja. Nađeno je da se vežu za DNA s velikim afinitetom te inhibiraju topoizomerazu II, što dovodi do apoptoze stanice (70).

Macdonald i suradnici sintetizirali su hibride β-karbolina i aminokiselina te su *in vitro* ispitali njihov učinak na humanim tumorskim staničnim linijama i sposobnost inhibicije topoizomeraze II. Za spojeve prikazane na Slici 14b utvrđeno je da inhibiraju proliferaciju tumorskih stanica i topoizomerazu II (71).

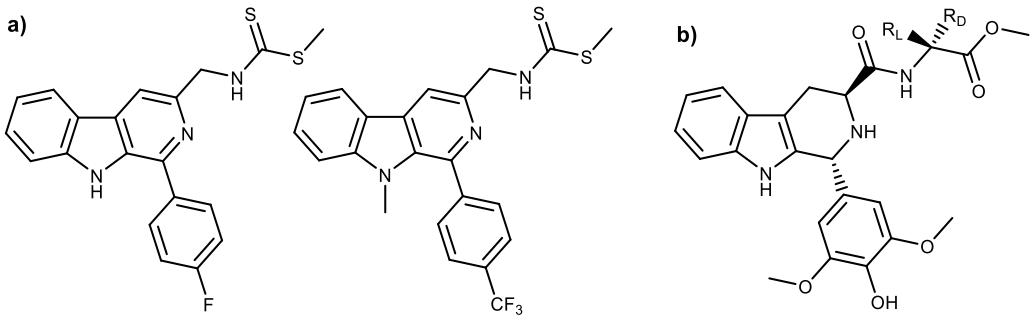

Slika 14. a) Ditiokarbamati, b) hibridi β-karbolina i aminokiselina

Cijepanje DNA

Al-Allaf i suradnici pripravili su komplekse harmina i paladija te su ispitali njihovo djelovanje na P388, mišju limfocitnu leukemiju (L1210) i mijeloičnu leukemiju (K562). Spoj prikazan na Slici 15a pokazao je značajan citotoksični učinak u usporedbi s lijekovima koji sadrže platinu poput cisplatina i karboplatina, s vrijednošću IC_{50} u rasponu 0,364–0,385 μM (72).

Toshima i suradnici pripravili su hibride β-karbolina i ugljikohidrata. Uočili su da hibrid koji sadrži 2,6-dideoksi šećer (Slika 15b) cijepa DNA u položaju gvanina kada je ozračen UV zračenjem duge valne duljine. Uvođenjem dideoksi šećera u strukturu smanjuje hidrofilnost molekule što pridonosi boljem vezanju u utor DNA te poboljšava sposobnost cijepanja DNA (73).

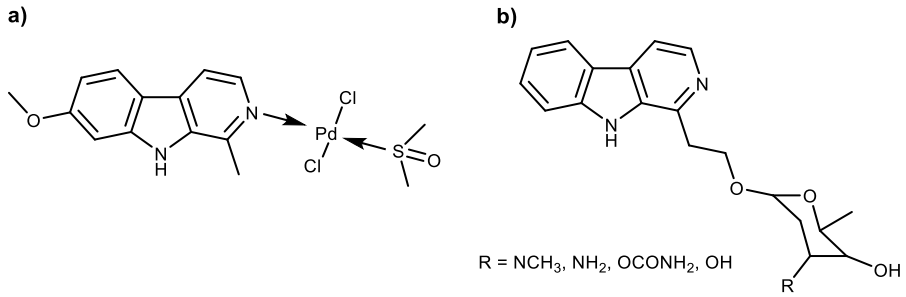

Slika 15. a) Kompleks harmina s paladijem, b) hibrid β-karbolina i ugljikohidrata

1.4.3.2. Derivati β-karbolina koji inhibiraju kinaze

Proteinske kinaze su enzimi koji fosforiliraju specifične aminokiseline u proteinu posredstvom kofaktora, odnosno ATP-a (2). Fosforilacijom aminokiselina uzrokuju konformacijsku promjenu proteina što mijenja njegovu aktivnost. Proteinske kinaze imaju važnu ulogu u reguliranju različitih staničnih funkcija poput rasta, proliferacije, popravka DNA, pokretljivosti stanice i apoptoze. Budući da je u tumorskim stanicama uočena pojačana ekspresija proteinskih kinaza, svrsishodno je razvijati inhibitore ovih enzima kao potencijalne protutumorske lijekove (2, 24). Brojni inhibitori proteinskih kinaza poput gefitiniba, erlotiniba, afatiniba, imatiniba, sorafeniba, sunitiniba registrirani su citostatici (2).

Bauerin C, prirodni produkt alge *Dichotrix baueriana*, ispoljava antiproliferativno i antivirusno djelovanje, dok njegovi 1-okso-derivati djeluju kao inhibitori kinaza. Bracher i suradnici pripravili su seriju 7,8-diklor-1-okso-β-karbolina temeljenih na strukturi bauerina C. Utvrđeno je da derivati snažno i selektivno inhibiraju onkogene PIM kinaze u usporedbi s drugim humanim kinazama. Spoj prikazan na Slici 16a ostvario je najjače djelovanje na PIM1 i PIM3 kinaze s IC_{50} vrijednostima 60, odnosno 90 nM. Selektivnost derivata objašnjena je posebnim načinom njihovog vezanja za zglobno mjesto enzima. Analiza kokristala otkrila je da ovi spojevi, za razliku od ostalih inhibitora koji oponašaju vezanje ATP-a, stvaraju halogenske veze s aminokiselinskim ostacima iz okosnice enzima (74).

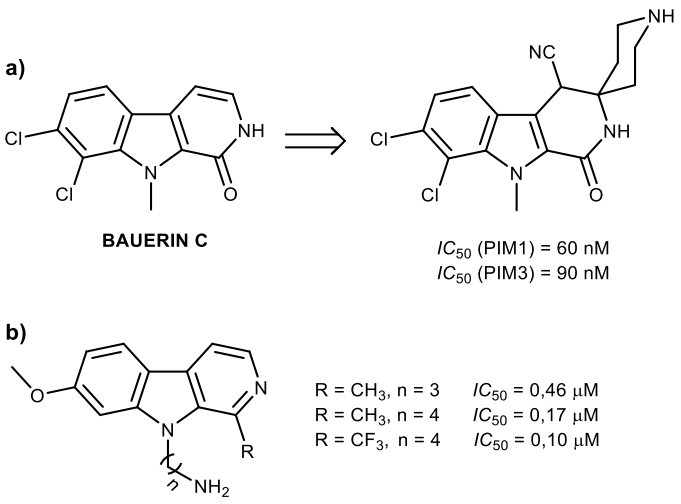

Slika 16. a) Inhibitor PIM kinaza, b) inhibitori haspin kinaza

Haspin kinaze su atipične eukariotske proteinske kinaze koje se vežu za kromosom i fosforiliraju treonin 3 u histonu 3 tijekom mitoze. Prekomjerna ekspresija ili izostanak ekspresije haspin kinaza rezultiraju disfunkcionalnom mitozom. Istraživanja su pokazala da inhibitori haspin kinaza imaju protutumorski učinak (75). Pretraživanjem visokog kapaciteta (engl. *high throughput screening*) nađeno je da harmin i harmol umjereno inhibiraju haspin kinaze. Cuny i suradnici pripravili su derivate harmina te ispitali njihovo inhibitorno djelovanje spram haspin kinaza. Spojevi prikazani na Slici 16b pokazali su snažno inhibitorno djelovanje s IC_{50} vrijednostima u submikormolarnim koncentracijama (76).

B-Raf je serin-treonin kinaza koja posreduje u prenošenju signala između Ras i MEK u MAPK signalnom putu. Primijećeno je da neke vrste tumorskih stanica sadrže mutirani gen za ovu kinazu. Njegovom ekspresijom nastaje modificirani B-Raf koji je zaključan u aktivnoj konformaciji zbog čega vrši kontinuirano unutarstanično signaliziranje. Posljedica je povećana proliferacija, preživljavanje i pokretljivost tumorskih stanica (77). Lu i suradnici dizajnirali su seriju 1-karboksamid-6-sulfonamid-supstituiranih β-karbolina kao potencijalnih B-Raf inhibitora. Svi sintetizirani spojevi pokazali su dobro inhibitorno djelovanje s vrijednostima IC_{50} u rasponu 1,62–91,55 μM. Derivat koji je sadržavao dvije dimetilaminopropilne skupine ostvario je najsnažnije djelovanje (IC_{50} = 1,62 μM). Uočeno je da zamjena obje dimetilaminopropilne skupine s dietilaminopropilnim skupinama rezultira smanjenjem učinka (IC_{50} = 2,81 mM). Studijama molekulskog uklapanja pokazano je da se najučinkovitiji derivat veže za enzim na sličan način kao referentni lijek sorafenib i spoj PLX4032 (Slika 17). Temeljem toga autori su predložili da se u dizajniranju novih inhibitora B-Rafa β-karbolinska jezgra može upotrijebiti kao dio molekule koji se veže za zglobnu regiju enzima (78).

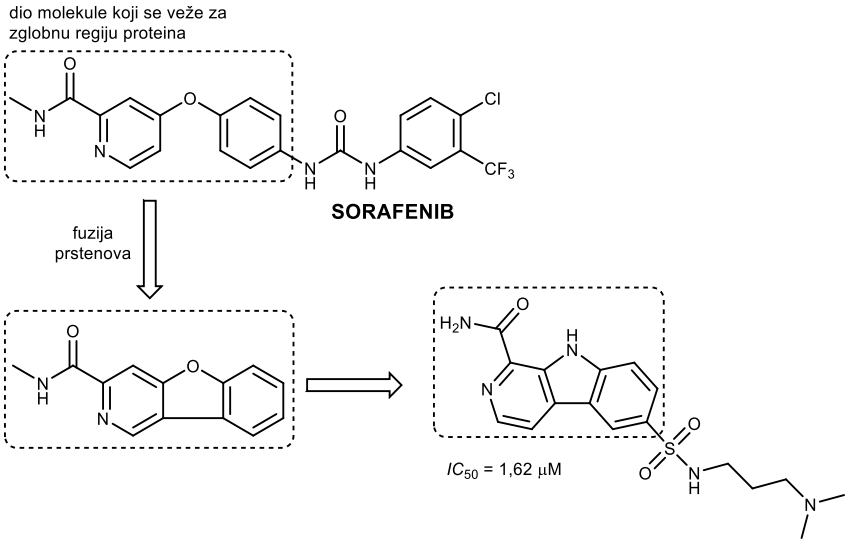

Slika 17. Korištenje β-karbolinske jezgre u dizajniranju B-Raf inhibitora

CDK su heterodimerni proteini koji reguliraju napredovanje staničnog ciklusa. Uočeno je da je funkcija CDK u tumorskim stanicama poremećena zbog čega mogu poslužiti kao mete za razvoj lijekova. Inhibitori CDK natječu se s kompleksom ATP-Mg^{2+} za ATP-vezno mjesto u CDK. Sintetizirani su harmin i C-1-supstituirani β-karbolini te je ispitano njihovo protutumorsko djelovanje. Derivat koji sadrži 5-metilimidazol-4-ilni supstituent u položaju C-1 (Slika 18) pokazao je najsnažnije djelovanje, pri 50 μM koncentraciji inhibirao je CDK5 94 %, a CDK2 89 % (24).

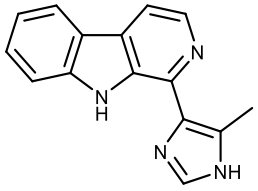

Slika 18. Inhibitor kinaza ovisnih o ciklinima

1.4.3.3. Derivati β-karbolina koji djeluju na tubulin

Tubulin je globularni protein koji u stanici polimerizira u mikrotubule. Tubulin, odnosno mikrotubuli imaju mnoge funkcije u stanici, između ostalih sudjeluju u diobi stanice. Prije diobe mikrotubuli depolimeriziraju u tubulin koji ponovno polimerizira i tvori diobeno vreteno. Neki protutumorski lijekovi interferiraju s ovim procesom: vežu se na tubulin i sprječavaju polimerizaciju ili stabiliziraju mikrotubule i spriječavaju depolimerizaciju (2).

Shen i suradnici pripravili su C-1-supstituirane derivate 1,2,3,4-tetrahidro-β-karbolina i 3,4-dihidro-β-karbolina (Slika 19a) te su ispitali njihovo protutumorsko djelovanje na nizu tumorskih staničnih linija. Spojevi su pokazali značajno protutumorsko djelovanje: 3,4-dihidro-β-karbolin ostvario najsnažnije djelovanje (IC_{50} < 0,001 μg/mL na svim ispitivanim linijama), dok je 1,2,3,4-tetrahidro-β-karbolin snažno djelovao na P-388 (IC_{50} = 0,07 μg/mL). Pretpostavljeni mehanizam djelovanja ovih derivata je spriječavanje stvaranja diobenog vretena i segregacije kromosoma (79).

Kulkarni i suradnici pripravili su hibride tetrahidro-β-karbolina/dihidro-β-karbolina/β-karbolina i kumarina (Slika 19b) te su ispitali njihovu citotoksičnost na 60 različitih tumorskih linija. Većina hibrida pokazala je dobro djelovanje. Uočeno je da najbolje djelovanje ostvaruju β-karbolini, potom tetrahidro-β-karbolini, dok su dihidro-β-karbolini djelovali slabije. U seriji β-karbolina najbolje djelovanje ostvarili su derivati kojima je kumarinski prsten u položaju O-6 bio supstituiran klorom ili metoksi skupinom. Molekulskim uklapanjem pokazano je da se spojevi vežu za tubulin i motorni protein KSP (80).

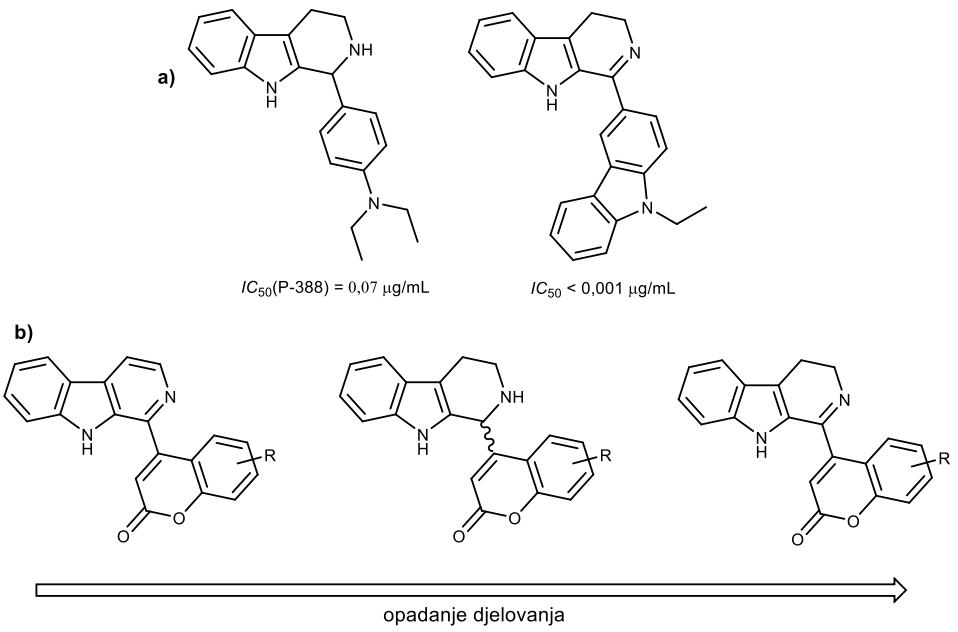

Slika 19. Derivati β-karbolina koji djeluju na tubulin

1.4.3.4. Inhibitori histonskih deacetilaza

Općenito, inhibitori histonskih deacetilaza (engl. *histone deacetylase*, HDAC) kompleksiraju cink u aktivnom mjestu HDAC čime inhibiraju njegovo djelovanje. Građeni su od tri dijela: skupina koja kompleksira cink, površinska vezujuća skupina i poveznica (81).

Ling i suradnici sintetizirali su dvije serije derivata β-karbolina supstituiranih hidroksamskom kiselinom u položaju C-3 te su ispitali njihovo antiproliferativno djelovanje na tri linije ljudskog kolorektalnog karcinom (HCT116, SW620, LoVo) i sposobnost inhibicije HDAC. Hidroksamska kiselina djelovala je kao cink-kompleksirajuća skupina, β-karbolinski prsten predstavljao je površinsku vezujuću skupinu, a ugljikovodični lanac je bio poveznica. U prvoj seriji poveznica između β-karbolinskog prstena i ugljikovodičnog lanca bio je amid, a strukturna raznolikost postignuta je variranjem supstituenata u položaju C-1 i duljine poveznice (Slika 20a). Utvrđeno je da derivati koji su bili supstituirani *p*-metoksifenilnom skupinom u položaju C-1 imaju usporedljiv ili bolji učinak u odnosu na suberoilanilidhidroksamsku kiselinu (SAHA, vorinostat). S druge strane, derivati koji su u tom položaju imali metilnu skupinu ili su bili nesupstituirani, pokazali su slabije antiproliferativno djelovanje. Dalje, spojevima je *in vitro* ispitano inhibitorno djelovanje na HDAC enzime. Spojevi koji su sadržavali poveznicu s jednom ili dvije metilenske jedinice pokazale su slabiju inhibiciju enzima u odnosu na spojeve koji su sadržavali više od 3 ili 4 metilenske jedinice.

Na temelju ovih rezultata sintetizirana je druga serija spojeva u kojoj je zadržan *p*-metoksifenilni supstituent u položaju C-1, amid zamijenjen ureom, dok je strukturna raznolikost postignuta variranjem supstituenta u položaju N-9 i duljine poveznice (Slika 20b). Antiproliferativno djelovanje ovih spojeva bilo je blago jače od spojeva prve serije. SAR analizom nađeno je da derivati s poveznicom duljine 3 ili 4 metilenske jedinice pokazuju najbolje djelovanje, dok supstituent u položaju N-9 ima mali utjecaj na antiproliferativni učinak. U ispitivanju inhibitornog djelovanja spojeva na HDAC enzime otkriveno je da djeluju usporedivo ili snažnije od SAHA-e. Zanimljivo je da su neki spojevi mnogo snažnije inhibirali proliferaciju stanica nego HDAC enzime zbog čega su autori zaključili da uz, inhibiciju HDAC, postoje i drugi mehanizmi djelovanja spojeva (82).

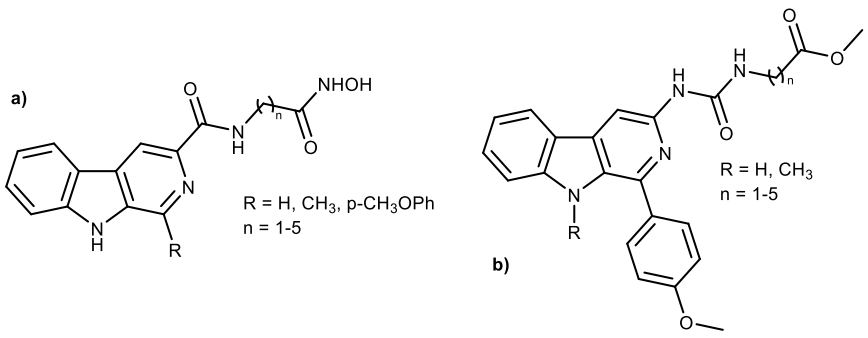

Slika 20. Derivati β-karbolina koji djeluju kao inhibitori HDAC

1.4.3.5. Derivati koji izazivaju feroptozu

Feroptoza je programirana stanična smrt ovisna o željezu koju karakterizira nakupljanje lipidnih peroksida. RSL3, derivat β-karbolina (Slika 21), inducirao je feroptozu u genetički modificiranim fibroblastima (BJeLR) (IC_{50} = 2 μM) i Calu-1 stanicama (IC_{50} = 20 μM). Nađeno je da je za djelovanje ovog derivata bitna kloracetamidna skupina. Daljnja istraživanja pokazala su da RSL3 izaziva apoptozu inhibicijom glutation-reduktaze, zbog čega dolazi do lipidne peroksidacije (83).

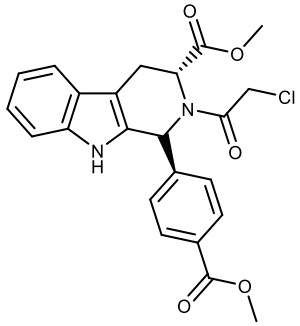

Slika 21. RSL3

1.4.3.6. Različito

Zjawiony i suradnici pripravili su hibride N-9-supstituiranih β-karbolina i hidantoina. Hibridi su pokazali dobro antiproliferativno djelovanje *in vitro*. Derivati prikazani na Slici 22 snažno su djelovali na MCF-7, MDA-MB-231 i A549. Derivat supstituiran *p*-CN-benzilnom skupinom u položaju N-9 djelovao je 83 puta jače na MCF-7 od 5-fluorouracila (5-FU) te je pokazao visoku selektivnost prema tumorskim stanicama. Uočeno je da supstituenti bogati elektronima u položaju N-9 doprinose citotoksičnom učinku, dok ga elektron-odvlačeće skupine smanjuju (84).

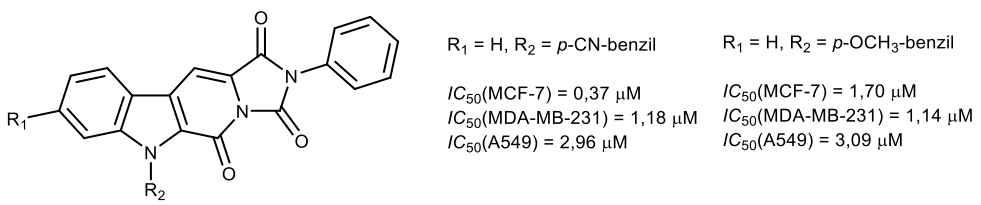

Slika 22. Hibridi β-karbolina i hidantoina

Na Slici 23 prikazani su triazolski derivati β-karbolina. Povezivanje C-1 položaja β-karbolina i C-4 položaja triazola arilnom/alkilnom/eterskom poveznicom rezultiralo je derivatima s umjerenim djelovanjem (Slika 23a). Na Slici 23b prikazani su hibridi građeni od β-karbolina, triazola i supstituiranih arila uz kalkonsku poveznicu kojima je ispitano djelovanje na MCF-7 i MDA-MB-231. SAR analiza pokazala je da priroda arilnog supstituenta i duljina poveznice značajno utječu na djelovanje. Derivat s trimetoskifenilom i poveznicom od 4 ugljikova atoma pokazao je snažno i selektivno djelovanje na MDA-MB-231, dok je derivat s *p*-fluorfenilom i kraćom poveznicom (3 ugljikova atoma) bio selektivan prema MCF-7. Policiklički hibridi građeni od tetrahidro-β-karbolina i triazola (Slika 23c) pokazali su dobro djelovanje na MCF-7 i mišji melanom (B16F10). Pokazano je da se ovi derivati vežu za manji utor molekule DNA, induciraju apoptozu, zaustavljaju stanični ciklus, inhibiraju migraciju stanica i stvaranje kolonija stanica (85).

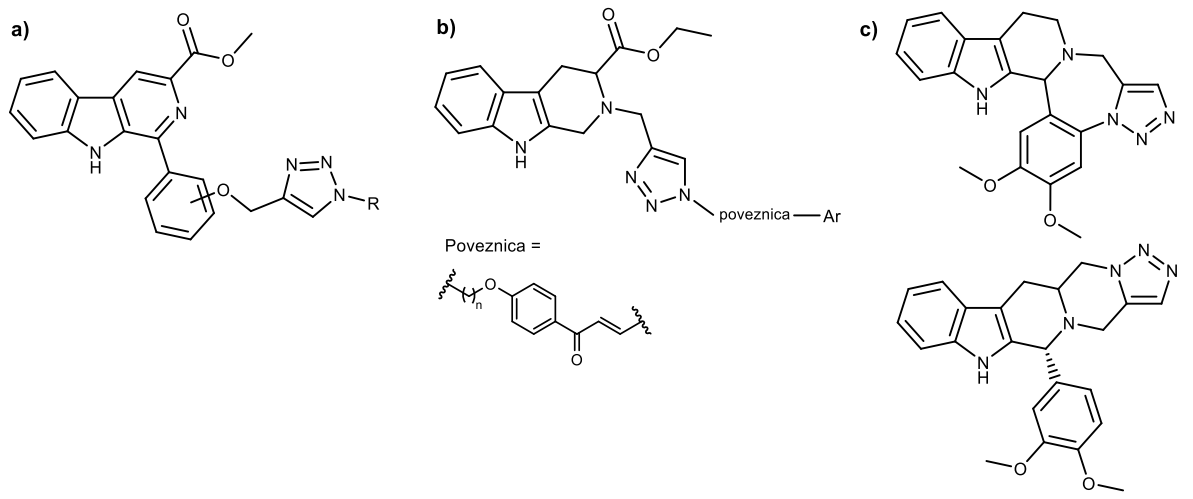

Slika 23. Triazolski derivati β-karbolina

Konakahara i suradnici sintetizirali su β-karboline supstituirane aminobenzilnom skupinom u položaju C-3. Sintetiziranim spojevima ispitali su protutumorsko djelovanje na HeLa i sarkom 180. Utvrđeno je da je većina hibrida ostvaruje dobro djelovanje s IC_{50} vrijednostima u rasponu 0,032–16 μM. Spojevi prikazani na Slici 24 pokazali su najbolje djelovanje protiv HeLa sa submikormolarnim IC_{50} vrijednostima. Na temelju fragmentacije DNA, Hoechst bojanja te rezultata protočne citometrije zaključeno je da spojevi zaustavljaju stanični ciklus u G2/M fazi (86).

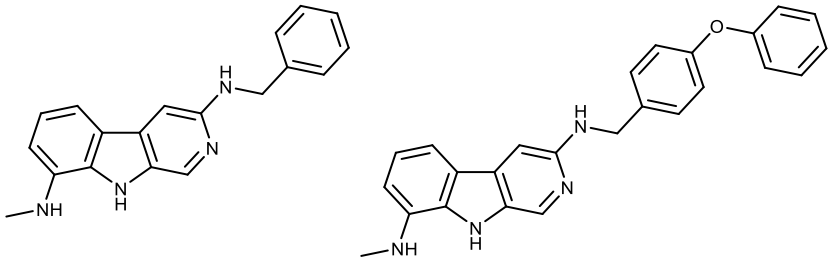

Slika 24. Derivati β-karbolina koji utječu na stanični ciklus

1.4.3.7. SAR protutumorskog djelovanja derivata β-karbolina

Veliki broj pripravljenih derivata β-karbolina omogućio je analizu utjecaja položaja i vrste supstituenta na β-karbolinskom prstenu na protutumorsko djelovanje. Rezultati SAR analize sažeto su prikazani na Slici 25.

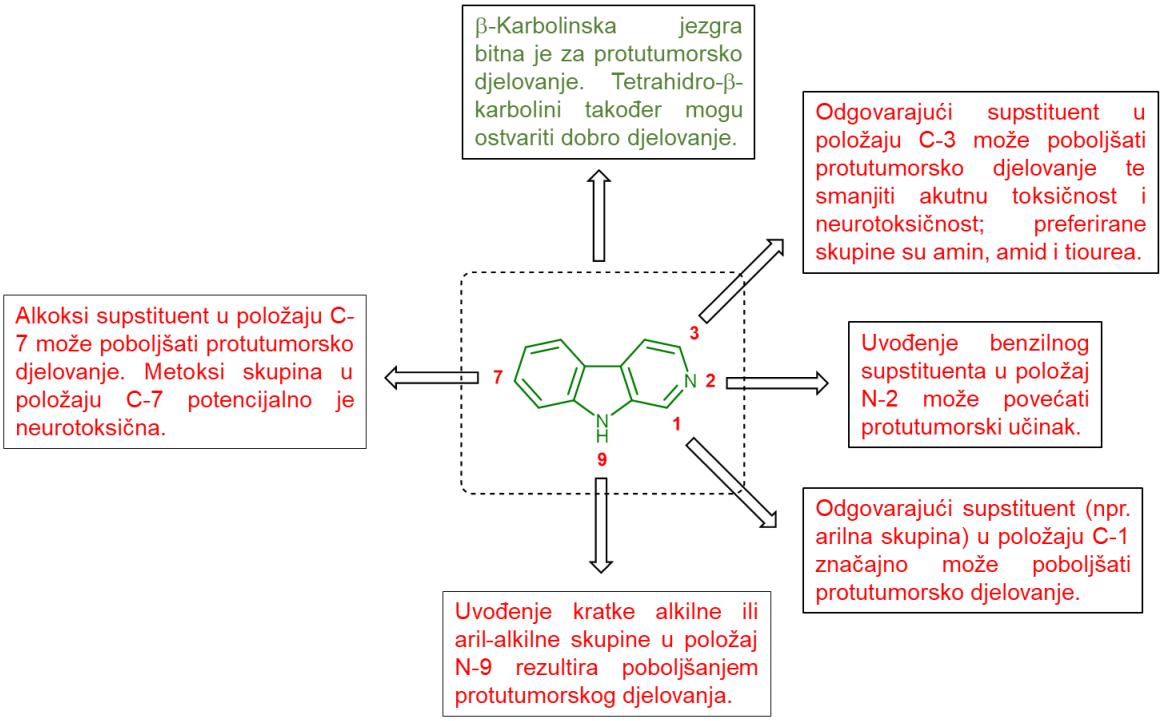

Slika 25. SAR analiza derivata β-karbolina (87)

1.4.4. Antimalarijsko djelovanje derivata β-karbolina

Coldham i suradnici pripravili su derivate β-karbolina supstituirane različitim aminima u položaju C-1 te su ispitali njihovo antimalarijsko djelovanje (Slika 26a). Derivati supstituirani *N*-alkiliranim propan-1,3-diaminom pokazali su dobro djelovanje, dok je derivat supstituiran etanolaminom bio manje učinkovit. Između derivata supstituiranih cikličkim aminima najučinkovitiji je bio onaj koji je sadržavao 1-(piperidin-4-il)azepan (IC_{50} = 0,35 μM). Derivati supstituirani piperazinom djelovali su snažnije od derivata s piperidinom i morfolinom (88).

Ista istraživačka skupina pripravila je seriju srodnih 1-amino-β-karbolina koji su bili supstituirani halogenom (F ili Br) u položaju C-7. Uočeno je da uvođenje halogena u položaj C-6 doprinosi antimalarijskom djelovanju. U seriji kloriranih derivata najbolje djelovanje pokazao je spoj koji u položaju C-1 sadrži diaminoalkilni lanac identičan onom u CQ, dok je u seriji fluoriranih derivata najučinkovitiji bio derivat supstituiran u položaju C-1 s nerazgranatim, za jednu metilensku jedinicu skraćenim diaminoalkilnim lancem (Slika 26b) (89).

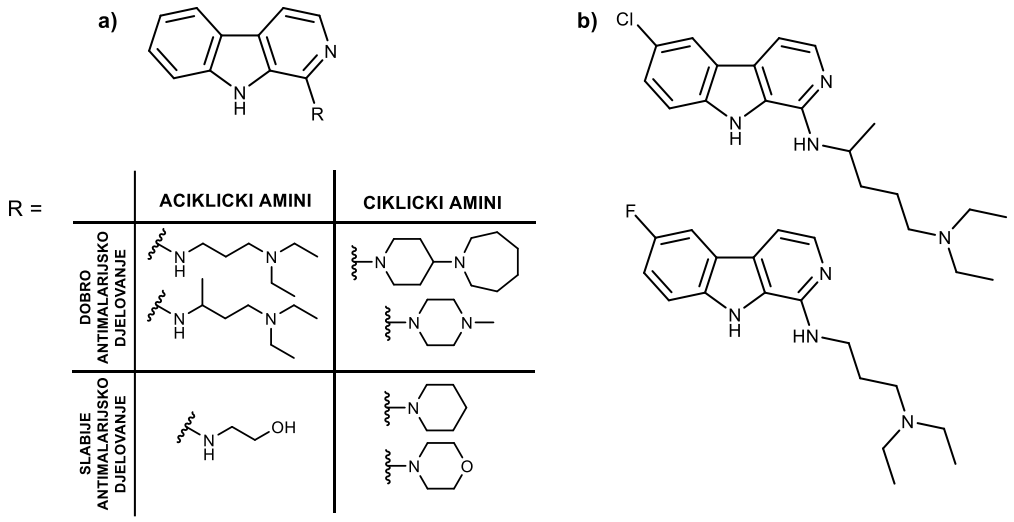

Slika 26. a) 1-amino-β-karbolini, b) C-6-halogenirani 1-amino-β-karbolini

Alkiliranjem položaja N-2 pripravljene su kvarterne amonijeve soli β-karbolina (Slika 27a) koje su pokazale značajno antimalarijsko djelovanje. Derivat supstituiran metilnom skupinom pokazao je najsnažnije djelovanje (IC_{50} = 0,194 μM). Uočeno je da zamjena metilne skupine dužim alkilnim, alilnim ili aromatskim skupinama rezultira opadanjem antimalarijskog djelovanja i porastom citotoksičnosti (90).

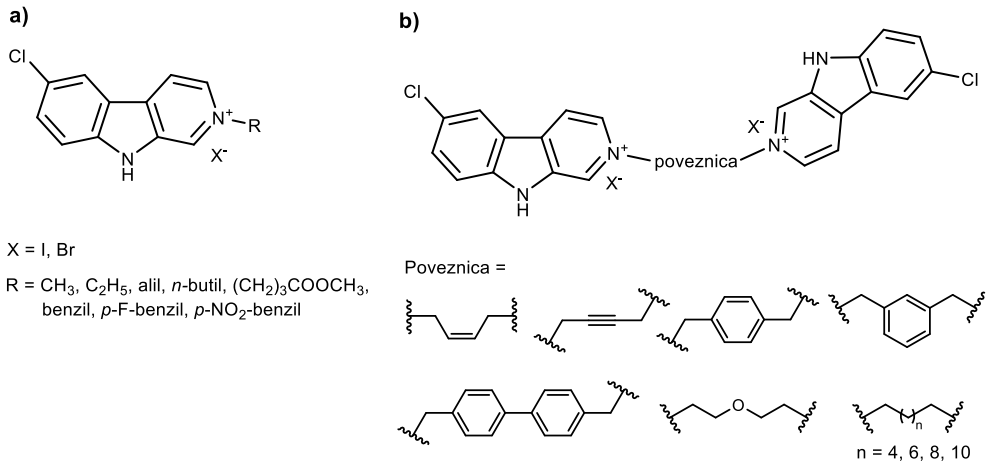

Slika 27. a) Monomerne i b) dimerne kvarterne amonijeve soli β-karbolina

Gademann i suradnici pripravili su seriju dimernih kvarternih amonijevih soli β-karbolina (Slika 27b) koje su djelovale snažnije od analognih monomera. Najbolje antimalarijsko djelovanje pokazali su derivati s dugačkom alifatskom (fleksibilnom) poveznicom (IC_{50} vrijednosti < 0,1 μM). S druge strane, porastom duljine poveznice dolazi do povećanja citotoksičnosti i smanjenja selektivnosti. Nađeno je da derivati koji sadrže poveznicu duljine pet, odnosno šest ugljikovih atoma imaju optimalan odnos između antimalarijskog djelovanja i citotoksičnosti (91).

Pripravljeni su N-2-supstituirani derivati eudistomina N i eudistomina O. Eudistomini su β-karbolini supstituirani bromom u položaju C-6, odnosno C-8 (Slika 28). Između derivata eudistomina N najbolje antimalarijsko djelovanje ostvarili su oni koji su u položaju N-2 sadržavali metilnu (IC_{50} = 18 nM), odnosno etilnu (IC_{50} = 32 nM) skupinu. Ovi derivati nisu bili citotoksični zbog čega su pokazali visoke indekse selektivnosti. Derivati eudistomina O djelovali su slabije (IC_{50} vrijednosti u rasponu 0,502–6,738 μM) (90).

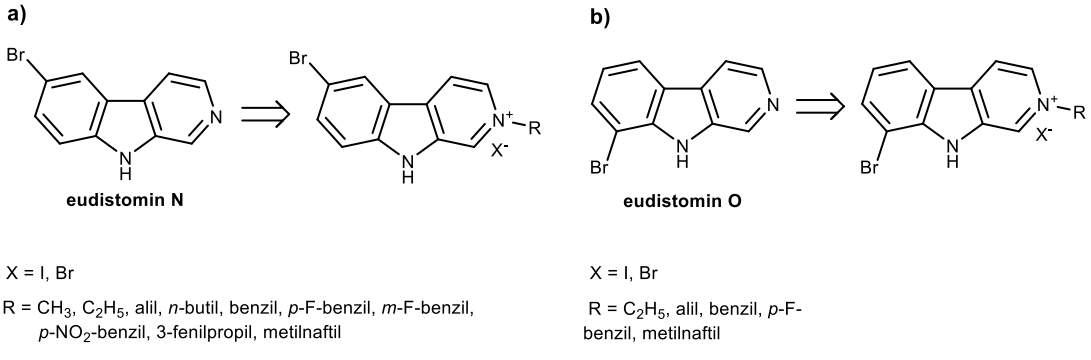

Slika 28. N-2-supstituirani derivati: a) eudistomina N i b) eudistomina O

Liew i suradnici pripravili su derivate β-karbolina, 3,4-dihidro-β-karbolina i 1,2,3,4-tetrahidro-β-karbolina supstituirane indolom u položaju C-1 (Slika 29). Derivati β-karbolina koji su sadržavali metoksi, odnosno hidroksilne skupine ($R_1 = R_3 = OCH_3$, $R_2 = H$, odnosno $R_1 = R_3 = OH$, $R_2 = H$) pokazali su dobro antimalarijsko djelovanje. S druge strane, nesupstituirani derivat β-karbolina te derivati β-karbolina koji su u položaju C-3 bili supstituirani karboksilnom kiselinom ili esterom ($R_1 = R_3 = H$, $R_2 = COOH$, odnosno $R_1 = R_3 = H$, $R_2 = COOCH_3$) djelovali su slabije. Tetrahidro-β-karbolin supstituiran metoksi skupinama ($R_1 = R_3 = OCH_3$, $R_2 = H$) djelovao je usporedljivo, a nesusptituirani tetrahidro-β-karbolin snažnije od analogno supstituiranih β-karbolina. Derivati dihidro-β-karbolini djelovali su najslabije u ovoj seriji spojeva (92).

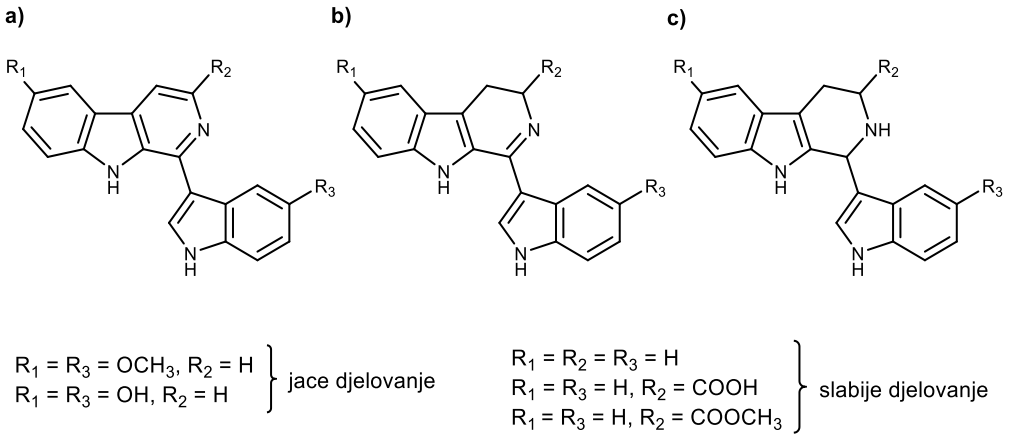

Slika 29. Derivati indola i: a) β-karbolina, b) 3,4-dihidro-β-karbolina, c) 1,2,3,4-tetrahidro-β-karbolina

Batra i suradnici pripravili su fuzionirane derivate β-karbolina i 1,4-oksazepina Između ostalih derivata, spoj prikazan na Slici 30 pokazao je najsnažnije antimalarijsko djelovanje koje je ipak bilo slabije u odnosu na CQ (93).

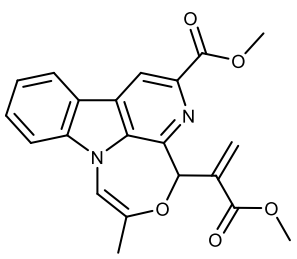

Slika 30. Derivat β-karbolina i 1,4-oksazepina

Anderson i suradnici pripravili su tetrahidro-β-karbolinske i β-karbolinske derivate harmina (42). U seriji spojeva najučinkovitijim se pokazao 6-klortetrahidro-β-karbolinski derivat (Slika 31) koji je ostvario dobro antimalarijsko djelovanje, nije bio toksičan prema ljudskim stanicama te je, poput harmina, pokazao sposobnost inhibicije *Pf*Hsp90. U nastavku istraživanja ovaj derivat poslužio je kao spoj uzor. Alkiliranjem indolskog dušika, odnosno uvođenjem arilnih supstituenata u položaj C-1 pripravljena je nova serija spojeva. Nealkilirani derivat supstituiran *m*-metilfenilom u položaju C-1 pokazao je dva reda veličine snažnije djelovanje u odnosu na spoj uzor (94).

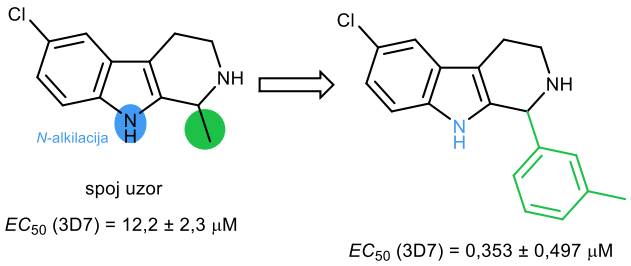

Slika 31. Derivati β-karbolina supstituirani u položajima C-1 i C-6

Saha i suradnici pripravili su konjugate β-karbolina i tiouree/gvanidina. Dva gvanidina (Slika 32a) pokazali su dobro djelovanje na CQOS i CQRS *P. falciparum* s IC_{50} vrijednostima u rasponu 0,6–1 μM. Studije molekulskog uklapanja pokazale su da se ovi spojevi mogu vezati za dihidrofolat reduktazu i FP3 (95).

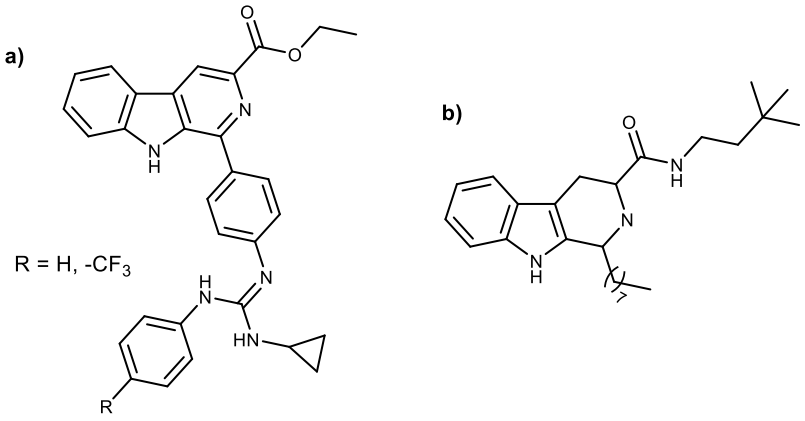

Slika 32. a) Konjugati β-karbolina i gvanidina, b) derivati β-karbolina amidnog tipa

Zagórska i suradnici pripravili su seriju tetrahidro-β-karbolina koji sadrže aromatski i/ili alkilni lanac u položaju C-1 te amidnu skupinu u položaju C-3. Općenito, derivati su pokazali

umjereno antimalarijsko djelovanje. Važno je istaći da su derivati snažnije djelovali na CQRS od CQOS. Spoj prikazan na Slici 32b pokazao je najsnažnije djelovanje, visoku selektivnost i nisku toksičnost (96).

Rajić i suradnici pripravili su harmicine, hibridne spojeve harmina i derivata cimetne kiseline, koji u strukturi poveznice sadrže triazol u položajima O-7 i N-9 (Slika 33). Pripravljenim spojevima ispitali su antimalarijsko djelovanje *in vitro* na eritrocitnu fazu dva soja *P. falciparum* (*Pf*3D7, CQOS, i *Pf*Dd2, CQRS), hepatocitnu fazu *P. berghei* i citotoksičnost na HepG2. Većina spojeva pokazala je značajno djelovanje protiv obje faze životnog ciklusa plazmodija, snažnije od roditeljske molekule harmina. Harmicini supstituirani u položaju O-7 pokazali su najsnažnije djelovanje protiv eritrocitnog stadija oba soja *P. falciparum*, dok su O-7,N-9-*bis*-harmicini bili najučinkovitiji protiv hepatocitne faze *P. berghei*. Za *bis*-harmicine molekulskom dinamikom utvrđeno je vezanje za ATP-vezno mjesto *Pf*Hsp90. N-9-supstituirani harmicini bili su najmanje, a O-7-supstituirani harmicini najviše citotoksični prema HepG2 (97).

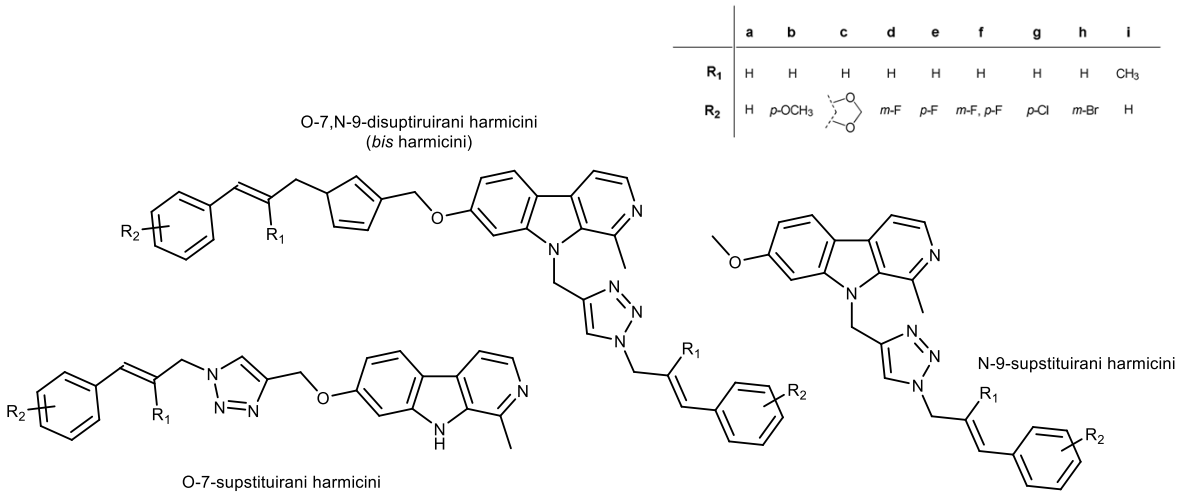

Slika 33. Harmicini triazolskog tipa

Ista istraživačka skupina pripravila je analognu seriju spojeva u kojima je triazol zamijenjen amdinom skupinom (Slika 34). Ovi derivati pokazali su dobro djelovanje na eritroctinu fazu *P. falciparum* (IC_{50} vrijednosti u niskim submikromolarnim koncentracijama), dok su na hepatocitnu fazu *P. berghei* djelovali slabije. Nadalje, ispitivanje citotoksičnosti na HepG2 pokazalo je povoljne indekse selektivnosti. Molekulskom dinamikom pokazano je da se i ovi harmicini vežu za ATP-vezno mjesto *Pf*Hsp90 (98).

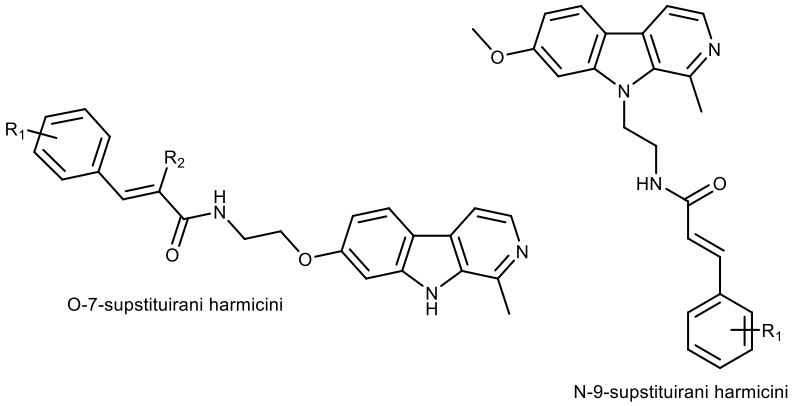

Slika 34. Harmicini amidnog tipa

1.5. CIMETNA KISELINA I NJENI DERIVATI

1.5.1. Cimetna kiselina i njeni derivati u prirodi

Cimetna kiselina (3-fenilprop-2-enska ili fenilakrilna kiselina) (Slika 35) i njeni derivati (DCK-i) prirodni su produkti nastali sekundarnim metabolizmom biljaka (99). Široko su rasprostranjeni u biljnom svijetu, uglavnom kao stabilniji *trans* izomeri. Primjerice, *trans*-cimetna kiselina prisutna je u kori kineskog cimeta (*Cinnamomum cassia*) i drugih biljaka iz roda Cinnamomum prema kojem je dobila trivijalno ime (100). U biljkama cimetna kiselina nastaje deaminacijom L-fenilalanina uz enzim fenilalanin-amonij-liazu. Djelovanjem enzima citokrom P450 (CYP) cimetna kiselina se prevodi u fenolne derivate (*p*-kumarinska, kavena, ferulična i sinapinska kiselina). Također, motiv cimetne kiseline prisutan je u brojnim sekundarnim metabolitima fenilpropanoidnog biosintetskog puta (99, 101). Cimetna kiselina i njeni derivati imaju široki spektar djelovanja u biljaka, od zaštite od mikroba do privlačenja oprašivača (100).

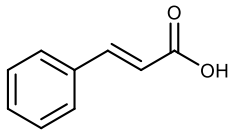

Slika 35. Struktura cimetne kiseline

1.5.2. Priprava cimetne kiseline i derivata

Cimetna kiselina i DCK-i upotrebljavaju se u proizvodnji mirisa, okusa, boja i lijekova. Za industrijske potrebe ne izoliraju se iz prirodnih izvora, nego se pripravljaju sintetskim putem. Postoje brojne metode za pripravu cimetne kiseline i DCK-a, a najčešće se koristi Perkinova reakcija (Shema 2) (102). Ova metoda podrazumijeva kondenzaciju aromatskog aldehida i anhidrida alifatske karboksilne kiseline u prisutnosti slabe baze, npr. natrijevog acetata (43, 102).

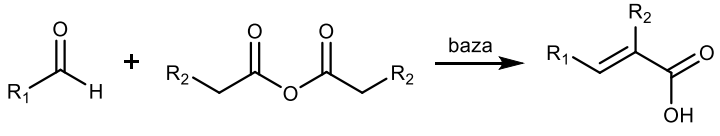

Shema 2. Sinteza cimetne kiseline i DCK-a Perkinovom reakcijom

1.5.3. Biološko djelovanje cimetne kiseline i DCK-a

Cimetna kiselina i DCK-i posjeduju brojna biološka djelovanja poput antioksidativnog (103), protutumorskog (101), antimikrobnog (99), protuvirusnog (104), antituberkulotskog (105), antimalarijskog (100), neuroprotektivnog (106), protuupalnog (107) i antidijabetičkog (108). U nastavku teksta detaljnije je prikazano njihovo antimalarijsko i protutumorsko djelovanje.

1.5.3.1. Antimalarijsko djelovanje

Tijekom eritrocitne faze plazmodij primarno osigurava energiju potrebnu za rast i razvoj procesom glikolize. Uočeno je da eritrociti zaraženi plazmodijem čak 100 puta brže metaboliziraju glukozu u odnosu na zdrave crvene krvne stanice, pri čemu stvaraju veliku količinu laktata, nusprodukta ovog metaboličkog puta. Kako bi parazit održao potrebnu količinu energije, pH i osmotski tlak neophodan je kontinuirani unos glukoze te izlučivanje laktata. Potonji se iz plazmodija izlučuje posredstvom transportera za prijenos monokarboksilata (109). Na temelju spoznaje da DCK-i inhibiraju prijenos monokarboksilata kroz staničnu i mitohondrijsku membranu, Kanaani i Ginsburg pretpostavili su da je mehanizam antimalarijskog djelovanja DCK-a inhibicija prijenosa laktata. Međutim, uočili su da DCK-i inhibiraju transport gukoze, glicina i sorbitola snažnije nego laktata. Zaključili su da DCK-i, osim transporta laktata, inhibiraju i nove putove propusnosti (NPP) koje plazmodij inducira u membrani eritrocita kako bi omogućio dostavu tvari potrebnih za razvoj. Također, uočeno je da DCK-i smanjuju količinu ATP-a i proliferaciju parazita (100, 110).

U literaturi postoje brojni primjeri uspješne hibridizacije DCK-a s drugim bioaktivnim molekulama, koji su rezultirali poboljšanim antimalarijskim djelovanjem. Gomes i suradnici pripravili su dvije serije hibrida 4-amino-7-klorkinolina i različitih DCK-a. U prvoj seriji klorkinolinski i cimetni strukturni motivi bili su izravno povezani (Slika 36a), dok su derivati druge serije sadržavali dipeptidnu poveznicu (Slika 36b). Spojevima je ispitano antimalarijsko djelovanje *in vitro* na eritrocitnu fazu *P. falciparum* te sposobnost inhibicije polimerizacije hemozoina i proteaza falcipain-2 i -3. Hibridi prve serije su nešto snažnije inhibirali falcipain proteaze, ali su bili nedjelotvorni protiv *P. falciparum* (IC_{50} > 10 μM) i nisu inhibirali polimerizaciju hemozoina. S druge strane, hibridi druge serije pokazali su umjereno anitmalarijsko djelovanje (0,8 < IC_{50} < 10 μM), koje nije bilo u korelaciji s njihovom

sposobnošću inhibicije polimerizacije hemozoina. Zamjena L-aminokiselina D-aminokiselinama u poveznici rezultirala je jačim antimalarijskim djelovanjem (111).

Na temelju prethodnih podataka i *in silico* studija, isti autori su dizajnirali i sintetizirali novu generaciju hibrida u kojima je dipeptidna poveznica zamijenjena hidrofobnijom i fleksibilnijom (Slika 36c). Pronađeno je da spojevi koji u poveznici između amino i amidne skupine imaju četiri metilenske jedinice (n = 4) pokazuju snažno djelovanje *in vitro* protiv CQRS *P. falciparum* ($11 < IC_{50} < 111$ nM). Antimalarijsko djelovanje hibrida nove generacije nije bilo u potpunoj korelaciji sa sposobnošću inhibicije falcipain proteaza i polimerizacije hemozoina što sugerira da hibridi imaju dodatni mehanizam djelovanja. Budući da hibridi sadrže cimetnu kiselinu kao strukturni motiv, autori su pretpostavili da bi dodatni mehanizam djelovanja bio inhibicija NPP (112).

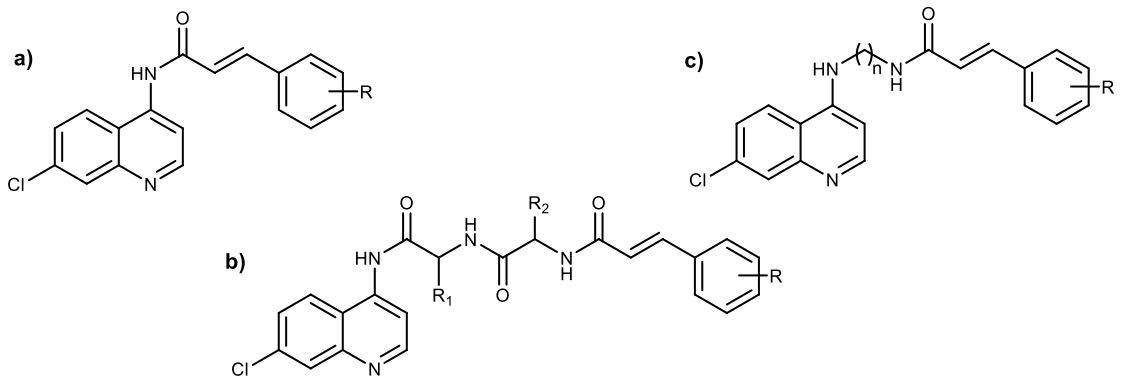

Slika 36. Hibridni spojevi DCK-a i 4-amino-7-klorkinolina

Ista istraživačka skupina naknadno je pripravila analoge spojeva prikazanih na Slici 36c. Nakon provedene SAR analize zaključeno je da se učinak spojeva značajno smanjuje ili čak izostaje ako se: 1) 4-amino-7-klorkinolinska jezgra zamijeni drugim heteroaromatskim ili nearomatskim prstenom, 2) amidna veza zamijeni esterskom, 3) broj metilenskih jedinica razlikuje od 4, 4) fenilni prsten cimetnog dijela molekule disupstituira, i 5) supstituent na fenilnom prstenu ne nalazi u *p*-položaju. Također, uočeno je da ovi hibridi ostvaruju dvostruko djelovanje: učinkoviti su protiv eritrocitne i hepatocitne faze životnog ciklusa plazmodija (112).

Gomes i suradnici pripravili su hibride DCK-a i mepakrina (kinakrina), jednog od najstarijih sintetskih antimalarika, te su ispitali njihovo antimalarijsko djelovanje *in vitro* na eritrocitnu fazu dva soja *P. falciparum* (CQOS i CQRS) i hepatocitnu fazu *P. berghei*. Hibridi čiji je akridinski prsten bio supstituiran ($R_1 = OCH_3$, $R_2 = Cl$) (Slika 37) pokazali su jače djelovanje od nesupstituiranih analoga ($R_1 = R_2 = H$). Supstituirani hibridi pokazali su 2 do 4

puta snažnije djelovanje od primakina (PQ) protiv hepatocitne faze, protiv soja 3D7 *P. falciparum* djelovali su usporedivo s CQ, dok im je učinak protiv soja Dd2 bio 2 do 4 puta snažniji od CQ. Neki od hibrida bili su manje citotoksični, ali učinkovitiji protiv plazmodija u odnosu na roditeljsku molekulu mepakrin.(113).

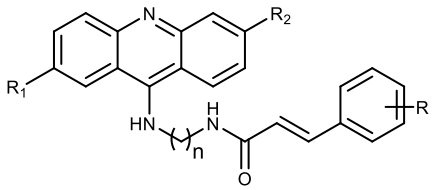

Slika 37. Hibridni spojevi DCK-a i mepakrina

U literaturi su opisani i brojni primjeri povezivanja derivata cimetnih kiselina sa strukturnim motivima koje ne pronalazimo u postojećim antimalaricima. Primjerice, Schlitzer i suradnici pripravili su konjugate derivata cimetne kiseline prikazane na Slici 38a te su ispitali njihovo djelovanje na CQRS Dd2. Uočili su da antimalarijsko djelovanje uvelike ovisi o vrsti supstituenta u fenilnom prstenu cimetnog dijela molekule. Derivat supstituiran *p*-propoksi skupinom ispoljio je najsnažnije djelovanje (IC_{50} = 0,2 μM) (114). Gassama i suradnici pripravili su konjugate DCK-a i 1-(*R*)-feniletilalanina (Slika 38b). Spoj koji sadrži 3,4-dihidroksi supstituirani fenilni prsten ostvario je najbolje djelovanje na 3D7, usporedivo s CQ-om (115).

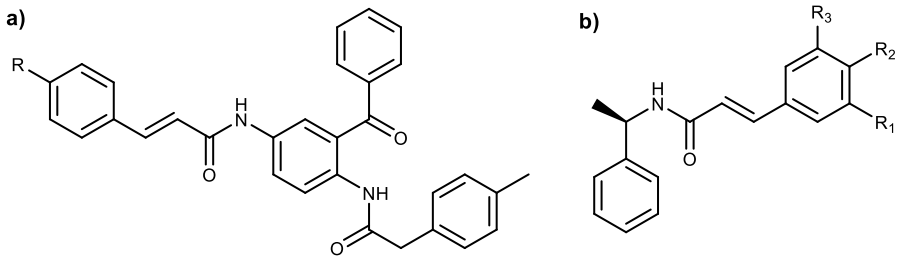

Slika 38. Različiti konjugati DCK-a

1.5.3.2. Protutumorsko djelovanje

Protutumorsko djelovanje cimetne kiseline i DCK-a detaljno je opisano u preglednom radu De i suradnika. Cimetne kiseline i DCK-i ostvaruju protutumorski učinak različitim mehanizmima djelovanja, poput izazivanja apoptoze, zaustavljanja staničnog ciklusa u S fazi, narušavanja staničnog citoskeleta, aktivacije kaspaza, generiranja reaktivnih kisikovih vrsta (RKV) te inhibicije histonskih deacetilaza. Jedan od mogućih mehanizama citostatskog djelovanja cimetne kiseline i DCK je stvaranje adukata Michaelovom adicijom. Ovi spojevi u strukturi sadrže α,β-nezasićenu karboksilnu skupinu, koja djeluje kao Michaelov akceptor zbog čega može reagirati s tiolnim skupinama glutationa i cisteina. Ne postoji izravan dokaz da ovi spojevi ostvaruju protutumorsko djelovanje Michaelovom adicijom, ali je na nekoliko primjera uočeno da redukcijom dvostruke veze dolazi do smanjenja citostatskog djelovanja (101).

Gomes i suradnici ispitali su antiproliferativno djelovanje hibrida 4-amino-7-klorkinolina i DCK-a (Slika 36c) na tumorskim staničnim linijama karcinoma želuca (MKN-28), kolorektalnog adenokarcinom (Caco-2) i MCF-7. Svi hibridi pokazali su dobro djelovanje na ispitivane tumorske stanične linije u niskim mikromolarnim koncentracijama, dok su bili netoksični prema fibroblastima ljudskog prepucija (HFF-1, netumorska stanična linija). Učinak spojeva bio je uvelike smanjen ili je izostao ako je aminokinolinska jezgra bila zamijenjena drugim aromatskim, heteroaromatskim ili nearomatskim prstenovima, a povećao se s duljinom alkilne poveznice. Promjene u molekuli, odnosno uklanjanje atoma klora u kinolinskom prstenu ili zamjena amida esterom, rezultirale su gubitkom selektivnosti (116).

Ista istraživačka skupina ispitala je djelovanje hibrida mepakrina i DCK-a (Slika 37), odnosno analoga DCK-a u kojima je cimetni dio zamijenjen drugim acilnim motivima. Spojevi su bili značajno selektivniji od roditeljske molekule, mepakrina, prema MKN-28, Caco-2 i MCF-7 u odnosu na HFF-1. Jedan od spojeva (R_1 = OMe, R_2 = Cl, R = *p*-F) istaknuo se selektivnim djelovanjem na MKN-28. Proučena je lokalizacija ovoga spoja u jezgri te predloženo da se veže za DNA (117).

Zorc i suradnici pripravili su hibride primakina i DCK-a amidnog (Slika 39a) i acilsemikarbazidnog tipa (Slika 39b). Općenito, hibridi su pokazali dobro antiproliferativno djelovanje *in vitro* protiv šest humanih tumorskih staničnih linija. Posebno su bili učinkoviti protiv MCF-7 (0,03 μM < GI_{50} < 16 μM). Acilsemikarbazid supstituiran *p*-CF_3 skupinom u fenilnom prstenu cimetnog dijela molekule bio najučinkovitiji. Zamjena *p*-CF_3 skupine *m*-CF_3 ili priprava disupstituiranog analoga rezultirala je smanjenjem antiproliferativnog djelovanja. Nadalje, proučen je mehanizam djelovanja tri najaktivnija acilsemikarbazida (R = *p*-CF_3, *p*-F i

p-OCH_3) na MCF-7. Nađeno je da ti acilsemikarbazidi induciraju apoptozu cijepanjem PARP i aktivacijom kaspaze-9. Također, uočeno je da uzrokuju morfološke promjene na MCF-7 stanicama koje su tipične za apoptozu (118).

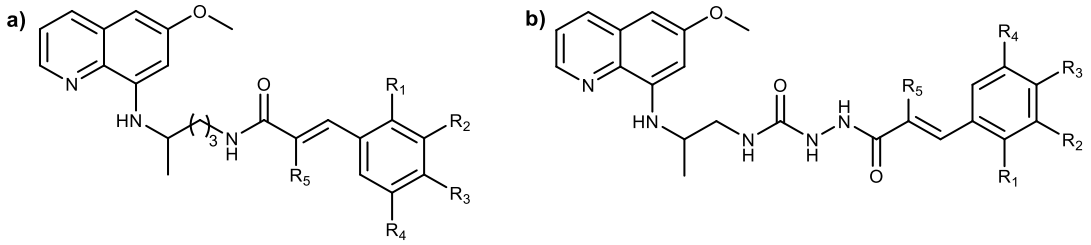

Slika 39. Hibridni spojevi primakina i DCK

Yu i suradnici pripravili su *mono* (Slika 40a) i *bis* hibride (Slika 40b) artemizinina i DCK-a te su ispitali njihovo antiproliferativno djelovanje *in vitro* protiv humanih tumorskih staničnih linija jedne netumorske linije (stanična linija hepatocita fetusa, L-02). Jedan od *bis* derivata (R_1 = R_4 =R_5 = H, R_2 = R_3 = OCH_3) pokazao je snažno i selektivno antiproliferativno djelovanje protiv A549 (GI_{50} = 0,20 μM). Nađeno je da spoj povećava količinu unutarstaničnih Fe^{2+} iona i oksidativni stres, zbog čega uzrokuje apoptozu (119).

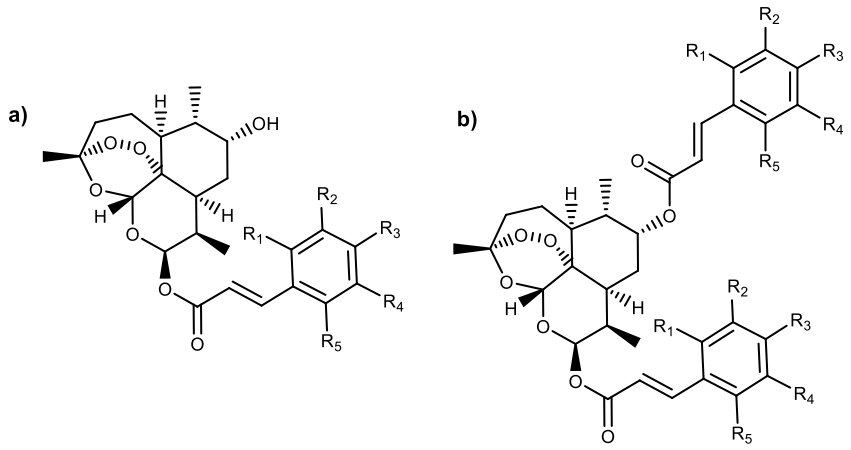

Slika 40. Hibridni spojevi artemizinina i DCK-a

1.6. KLOROKIN

CQ je antimalarik iz skupine 4-aminokinolina. Prvi ga je sintetizirao Hans Andersag (tvrtka Bayer) 1934. godine, a u kliničku primjenu uveden je 1947. godine (120). Iako je od otkrića CQ-a prošlo otprilike 90 godina, još uvijek se nalazi na listi esencijalnih lijekova WHO-a (121).

1.6.1. Fizikalno-kemijska svojstva klorokina

CQ je međunarodno nezaštićeno ime (engl. *International Nonproprietary Name*) N^4-(7-klorkinolin-4-il)-N^1,N^1-dietilpentan-1,4-diamina (Slika 41).

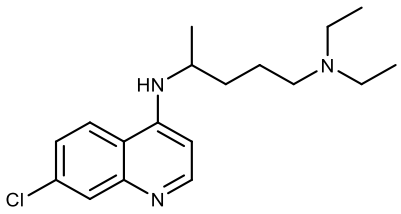

Slika 41. Struktura CQ

Molekulska formula CQ-a je $C_{18}H_{26}ClN_3$, a relativna molekulska masa 319,88. Na sobnoj temperaturi CQ je kristalinični prah bijele do blago žute boje. Talište CQ-a iznosi 87–89,5 °C. Slabo je topljiv u vodi, a dobro u kloroformu, dietil-eteru i razrijeđenim kiselinama (122). Iako CQ ima kiralni ugljikov atom, upotrebljava se kao racemat. Na tržištu je dostupan u obliku soli s fosfornom i sulfatnom kiselinom (123).

CQ je dibazična tvar s pK_a vrijednostima 10,2 (tercijarni amin postraničnog lanca) i 8,1 (kinolinski dušik) (Shema 3). Pri pH 7,4 (pH krvne plazme) 18 % CQ-a je u monoprotoniranom obliku, koji je topljiv u lipidima te može prolaziti kroz staničnu membranu (124).

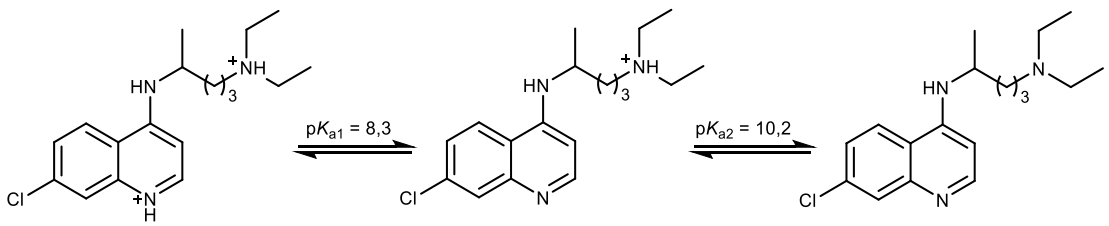

Shema 3. Disocijacijske konstante CQ-a

1.6.2. Sinteza klorokina

CQ se pripravlja reakcijom 4,7-diklorkinolina i 4-dietilamino-1-metilbutilamina na 180 °C tijekom 7 sati (Shema 4) (125).

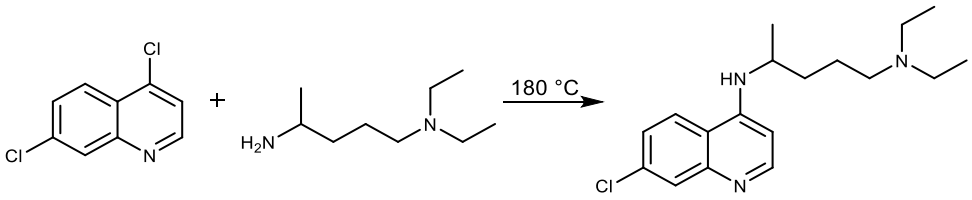

Shema 4. Sinteza CQ-a

Za sintezu CQ-a potrebno je pripraviti odgovarajuće prekursore. 4,7-Diklorkinolin pripravlja se iz *m*-kloranilina u nekoliko reakcijskih koraka. U Metodi 1 (Shema 5) sinteza započinje nukleofilnom adicijom amino skupine *m*-kloranilina na karbonilnu skupinu dietilnog estera oksaloctene kiseline u prisustvu octene kiseline. Eliminacijom molekule vode nastaje imin, koji zagrijavanjem na 250 °C heterociklizira u etilni ester 7-klor-4-hidroksikinolin-2-karboksilne kiseline. Hidrolizom estera u lužnatom mediju nastaje 7-klor-4-hidroksikinolin-2-karboksilna kiselina koja zagrijavanjem na 250 °C dekarboksilira u 7-klor-4-hidroksikinolin. Potonji međuprodukt reagira s $POCl_3$ dajući 4,7-diklorkinolin (125, 126).

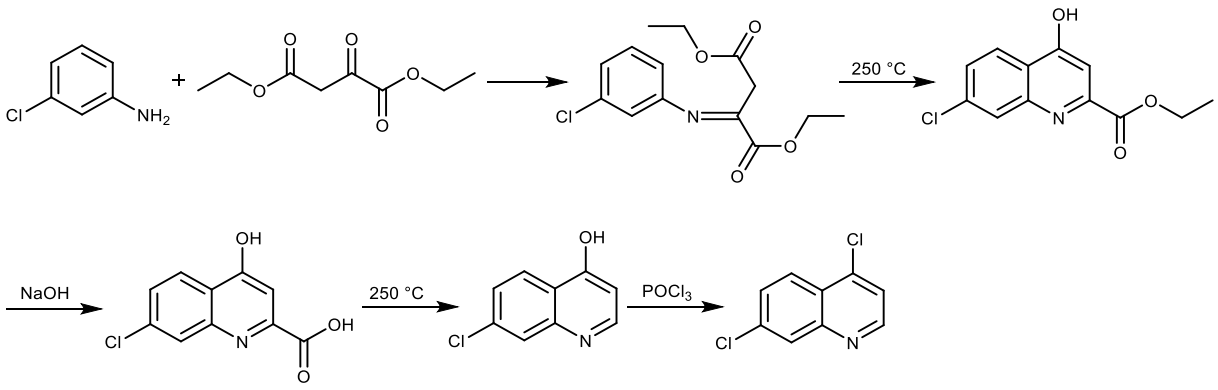

Shema 5. Sinteza 4,7-diklorkinolina prema Metodi 1

Metoda 2 analogna je prethodnoj, samo što u prvom koraku *m*-kloranilin reagira s esterom etoksimetilenmalonske kiseline (125, 127). U Metodi 3 (Shema 6) 4,7-diklorkinolin se pripravlja u tri reakcijska koraka jer sinteza kreće iz etilnog estera formiloctene kiseline te nema koraka hidrolize estera i dekarboksilacije (125, 128).

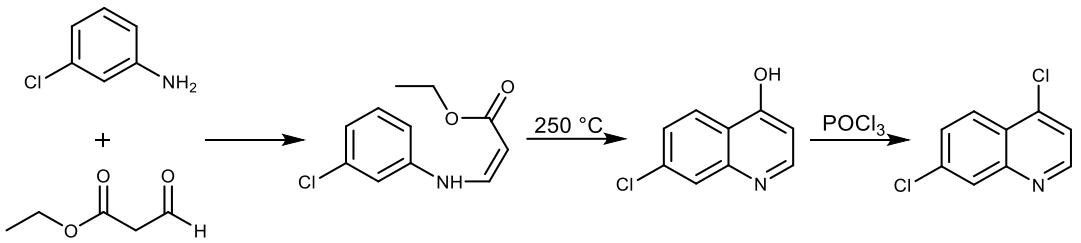

Shema 6. Sinteza 4,7-diklorkinolina prema Metodi 3

Drugi prekursor potreban za sintezu CQ-a je 4-dietilamino-1-metilbutilamin. Pripravlja se reakcijom etilnog estera acetooctene kiseline i 2-dietilaminoetilklorida (Shema 7). Nakon hidrolize u kiselom mediju i spontane dekarboksilacije nastaje 1-dietilamino-4-pentanon. Reduktivnom aminacijom korištenjem vodika i amonijaka uz Raney nikal (katalizator) nastaje 4-dietilamino-1-metilbutilamin (125).

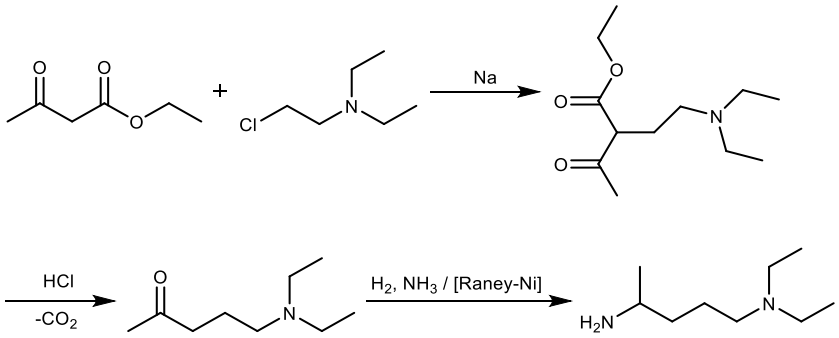

Shema 7. Sinteza 4-dietilamino-1-metilbutilamina

1.6.3. Antimalarijsko djelovanje klorokina

CQ se prvenstveno upotrebljava kao antimalarik. Nakon otkrića 1934. godine dugi niz godina bio je lijek prvog izbora za prevenciju i liječenje malarije. Široka upotreba dovela je do razvoja rezistencije te je danas *P. falciparum*, glavni uzročnik malarije, rezistentan na CQ u brojnim endemskim područjima. Unatoč tome, CQ je ostao lijek izbora za prevenciju i liječenje nekompliciranе malarije uzrokovane vrstama *P. vivax*, *P. ovale*, *P. malarie* i *P. knowlesi* u područjima gdje nije zabilježena rezistencija (129). CQ učinkovito djeluje na eritrocitnu fazu životnog ciklusa plazmodija, dok je nedjelotvoran na hepatocitnu i gametocitnu fazu, te hipnozoite koje stvaraju *P. vivax* i *P. ovale.* Za radikalno liječenje infekcija uzrokovanih ovim vrstama plazmodija kombinira se s 8-aminokinolinskim antimalarikom (primakinom ili tafenokinom) (130).

Antimalarijsko djelovanje CQ-a temelji se na inhibiciji polimerizacije hema u hemozoin. Tijekom eritrocitne faze plazmodij unutar digestivne vakuole razgrađuje hemoglobin u globin i slobodni hem (Fe^{2+}). Globin se dalje razgrađuje cistein proteazom i egzopeptidazama u manje peptide i aminokiseline koje parazit koristi za sintezu proteina. S druge strane, hem je toksičan za parazita jer uzrokuje razaranje membrane, lipidnu peroksidaciju te oksidaciju proteina i DNA. Parazit ima razvijen sustav detoksifikacije kojim prevodi toksičan i topljiv hem u netoksični i netopljivi hemozoin. Struktura hemozoina je kompleksna: sačinjavaju ga dimeri hema povezani međumolekulskim vodikovim vezama. Svaki dimer predstavlja koordinacijski kompleks: karboksilna skupina propionatnog lanca jednog monomera koordinira Fe^{2+} u porfirinskom prstenu drugog monomera (131). CQ inhibicijom polimerizacije hema u hemozoin uzrokuje nakupljanje toksičnog hema što dovodi do smrti parazita. Točan mehanizam inhibicije polimerizacije hema u hemozoin i dalje je predmet istraživanja. Ranije studije govore u prilog tome da CQ u prehrambenoj vakuoli plazmodija s hemom tvori kompleks koji interferira s lipidima i proteinima bitnim za proces polimerizacije. Također, upućuju na mogućnost da se kompleks CQ-a i hema veže na kraj rastućeg polimera hemozoina te uzrokuje terminaciju daljnje polimerizacije. Novije studije ukazuju na izravno vezanje CQ-a za rastući kraj polimera (132).

Osim sposobnosti vezanja za hem/hemozoin, za djelovanje CQ bitno je njegovo nakupljanje unutar prehrambene vakuole. Mnoge molekule, iako imaju sposobnost vezanja za hem/hemozoin, ne nakupljaju se u prehrambenoj vakuoli zbog čega ne ispoljavaju antimalarijski učinak. Ionizabilni kinolinski dušik i postranična amino skupina omogućavaju nakupljanje CQ u prehrambenoj vakuoli plazmodija principom pH klopke. U citoplazmi plazmodija (pH = 7,4) CQ je prisutan u monoprotoniranom i diprotoniranom obliku. Monoprotonirani oblik može pasivno difundirati kroz membranu prehrambene vakuole. Kada se CQ nađe u kiselom mediju prehrambene vakuole (pH = 5,0–5,2) u cijelosti je diprotoniran zbog čega više ne može pasivno difundirati kroz membranu i ostaje zarobljen unutar organela. Na ovaj način osigurava se visoka koncentracija CQ na mjestu djelovanja (132).

CQ se uglavnom dobro podnosi u terapijskim dozama. Najčešće nuspojave su glavobolja, mučnina, povraćanje, dijarea, abdominalni bolovi i osip. Visoke doze i dugotrajna terapija CQ-om mogu izazvati ozbiljnije nuspojave poput retinopatije, miopatije, kardiomiopatije, hipoglikemije, ototoksičnosti. Između ostalih, najčešće se javlja retinopatija koja može dovesti do ireverzibilnog oštećenja mrežnice i gubitka vida te je kod produljene primjene CQ-a uputno periodično raditi preglede oka (129). Smatra se da CQ nema štetne učinke na fetus. Dozvoljena je njegova upotreba u trudnica, dojilja i djece (133).

Doziranje i režim primjene CQ-a ovise o vrsti indikacije i tjelesnoj masi pacijenata. U prevenciji malarije odrasli koriste 300 mg CQ-a, što odgovara 500 mg CQ difosfata, tjedno za prevenciju malarije. Preporuča se korištenje lijeka 1-2 tjedna prije putovanja, tijekom boravka u rizičnim područjima te 4 tjedna nakon povratka iz tih područja. U liječenju malarije odrasli koriste početnu dozu od 600 mg CQ-a (1000 mg CQ disfosfata) te dozu od 300 mg CQ-a (500 mg difosfata) 6-8, 24, odnosno 48 sati nakon početne doze. Primjena u djece smatra se sigurnom te se primjenjuje u dozi od 5 mg/kg tjedno za prevenciju, dok liječenje započinje s početnom dozom od 10 mg/kg te se nastavlja s 5 mg/kg 6, 24, odnosno 36 sati nakon početne doze (134).

1.6.4. Protutumorsko djelovanje klorokina

Mnogi lijekovi protiv malarije, a naročito oni iz skupine seskviterpenskih laktona (artemizinini) i kinolina (CQ i hidroksiklorokin), pokazuju antitumorsko djelovanje i/ili djeluju radiosenzitirajuće i kemosenzitirajuće, odnosno povećavaju osjetljivost tumora na zračenje ili citostatike i/ili inhibiraju razvoj rezistencije te u konačnici povećavaju protutumorski učinak (135).

CQ ostvaruje protutumorski učinak izravnim djelovanjem na tumorske stanice, ali djeluje i na njihov mikrookoliš. Inhibicija autofagije jedan je od najistraženijih mehanizama izravnog protutumorskog djelovanja CQ (136). Autofagija je proces kojim stanica uništava i razgrađuje stare ili nefunkcionalne stanične komponente stvarajući nukleotide, aminokiseline i masne kiseline koje kasnije može ponovno koristiti za metaboličke potrebe. Autofagija predstavlja esencijalni unutarstanični proces koji omogućava preživljavanje stanice u stresnim uvjetima (npr. hipoksija, gladovanje, oštećenje organela) (137). Može imati protumorski i protutumorski učinak. U ranoj karcinogenezi autofagija ima protutumorski učinak jer štiti stanicu od nefunkcionalnih staničnih komponenti (npr. oštećenih mitohondrija) i održava staničnu homeostazu. Štoviše, nekoliko proteina uključenih u autofagiju (npr. Beclin-1, UVRAG i Bif-1) izravno inhibiraju stvaranje tumora, dok sam proces autofagije uništava proteine koji promoviraju rast tumora (npr. P62/SQSTM1). S druge strane, u kasnijim stadijima karcinogeneze autofagija pomaže rast tumora jer mu osigurava energiju i hranjive tvari (138, 139). CQ inhibira proces autofagije tako što se nakuplja u lizosomima principom pH klopke i podiže pH vrijednost čime inhibira lizosomske enzime. Također, onemogućava fuziju autofagosoma i lizosoma te razgrađuje autolizosome. Inhibicija autofagije CQ-om od značaja je u slučaju kada autofagija ima protumorski učinak. Takav učinak čest je tijekom kemoterapije/radioterapije, kada autofagija pomaže preživljavanje tumorskih stanica.

Kombinacija CQ-a i postojećih citostatika ili radioterapije senzibilizira tumorske stanice čime se postiže bolji terapijski ishod i smanjuje vjerojatnost preživljavanja tumorskih stanica i razvoja rezistencije (138).

Također, nađeno je da CQ inhibira TLR-9/NF-κB signalni put, signaliziranje posredovanao CXCL12/CXCR4 te stabilizira protein p53. Inhibicijom TLR-9/NF-kB signalnog puta smanjuje ekspresiju metaloproteinaza matriksa 2 i 3 te mRNA ciklooksigenaze 2, čimbenika bitnih za progresiju i migraciju tumora (140). Antagonističkim djelovanjem na CXCR4 receptore ili njihovom internalizacijom s površine stanične membrane onemogućava vezanje CXCL12, zbog čega negativno djeluje na kemotaksiju i adheziju stanica te izlučivanje faktora rasta (141). CQ stabilizira protein p53 i aktivira apoptozu ovisnu o p53 (142).

U tumorskom mikrookolišu CQ normalizira vaskulaturu tumora i modulira imunološki odgovor. Tumorska vaskulatura bitna je zbog opskrbe tumora kisikom i hranjivim tvarima te omogućava metastaziranje. Iako je prvi terapijski pristup podrazumijevao uništavanje tumorske vaskulature, novija istraživanja otkrivaju pozitivne učinke normalizacije abnormalne tumorske vaskulature poput smanjenja hipoksije, intravazije i metastaziranja te poboljšane dostave citostatika. CQ smanjuje gustoću vaskulature, poboljšava slaganje stanica i tijesne veze čime doprinosi normalizaciji vaskulature (143). Također, CQ djeluje na fibroblaste povezane s tumorom (CAF) čime utječe na stvaranje i remodeliranje matriksa te uzajamno djelovanje CAF i tumorskih stanica (138, 144).

Na temelju prethodnih protutumorskih učinaka, CQ je ispravnije smatrati senzibilizirajućim agensom u kemoterapiji i radioterapiji, koji pojačava učinak antitumorskih lijekova i smanjuje pojavu rezistencije, nego antitumorskim lijekom.

1.6.5. Ostala djelovanja klorokina

CQ pokazuje protuupalno i imunomodulatorno djelovanje zbog čega je odobren za liječenje reumatoidnog artritisa i sistemskog eritematoznog lupusa. Također, primjenjuje se *off-label* za liječenje drugih upalnih i autoimunih bolesti kao što su Sjögrenov sindrom, kronični ulcerozni stomatitis i porfirija *cutanea tarda* (145). Mehanizmi protuupalnog i imunomodulatornog djelovanja CQ-a nisu u potpunosti razjašnjeni. Otkriveno je da se CQ na već opisan način (pH klopka) nakuplja u lizosomima i podiže pH vrijednost unutar organela čime narušava njihovu funkciju. U lizosomima antigen-prezentirajućih stanica interferira s obradom antigena, zbog čega je onemogućena prezentacija antigena i aktivacija autoimunog odgovora (129). Također, nađeno je da u makrofagima inhibira signalizaciju ovisnu o kalciju,

TLR-7 i metabolizam željeza, čime inhibira stvaranje interleukina 1 i 6 te faktora nekroze tumora-α (TNF-α) (136).

Tijekom zadnja dva desetljeća, brojne studije ukazuju na antivirusno djelovanje CQ-a. Pojavom virusa SARS-CoV-2, uzročnika pandemije COVID-19, ispitivanja antivirusnog djelovanja CQ-a su se intenzivirala. U početku pandemije CQ i njegov derivat hidroksiklorokin su se s manje ili više uspjeha koristili u terapiji težih oblika bolesti, sami ili u kombinaciji s nekim antimikrobnim ili antivirusnim lijekom (133). Kasnije su iskustva upotrebe CQ i hidroksiklorokina u kliničkoj praksi i randomizirana klinička ispitivanja opovrgnula učinkovitost ovih lijekova u terapiji COVID-19 (146).

1.6.6. SAR derivata klorokina

Kako bi se identificirali dijelovi u strukturi kinolina bitni za antimalarijsko djelovanje, pripravljeni su i farmakološki ispitani brojni derivati.

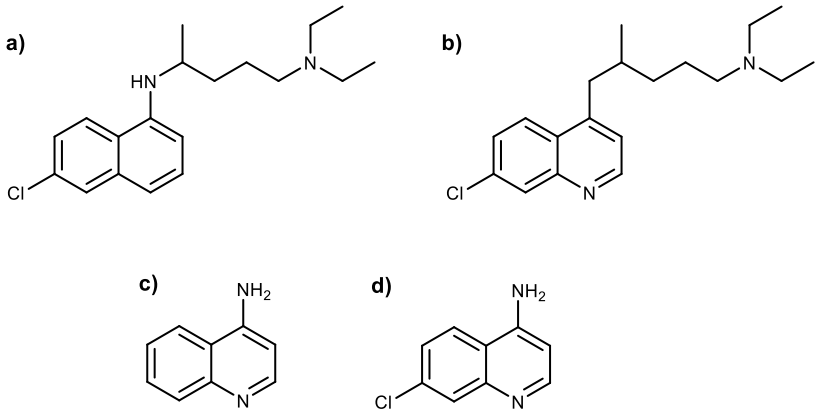

Slika 42. Derivati CQ-a

Vannerstrom i suradnici pripravili su derivate CQ-a u kojima su kinolinski dušik i aminoskupinu u položaju 4 zamijenili ugljikovim atomima te su proučili njihovu sposobnost vezanja za β-hematin, sintetski oblik hemozoina, koji se *in vitro* može prirediti iz hemina u kiseloj sredini. Derivat koji nije sadržavao kinolinski dušik (Slika 42a) nije se vezao za hematin u otopini, dok je derivat bez 4-amino skupine (Slika 42b) imao 6,4 puta manji afinitet za hematin od CQ. Autori su zaključili da je kinolinski prsten neophodan za vezanje na hematin, dok 4-aminoskupina utječe na elektronsku gustoću kinolinskog prsten, a posljedično i na sposobnost vezanja za hematin. Oba derivata nisu djelovala na *P. falciparum in vitro* što je

objašnjeno smanjenim nakupljanjem lijeka u prehrambenoj vakuoli plazmodija. Također, vidljivo je da tercijarna amino skupina u postraničnom lancu nema utjecaja na sposobnost vezanja na hematin (147).

4-Aminokinolin (Slika 42c) se vezao za hematin u otopini, ali nije inhibirao polimerizaciju β-hematina niti pokazao antimalarijsko djelovanje *in vitro*. Njegov analog supstituiran klorom u položaju 7 inhibirao je polimerizaciju β-hematina (Slika 42d), ali je *in vitro* djelovao 120 puta slabije od CQ (132). Na temelju prethodnog, Egan i suradnici zaključili su da je 4-aminokinolinska jezgra bitna za vezanje na hem, 4-amino-7-klorkinolin za inhibiciju polimerizacije β-hematina, dok je za antimalarijsko djelovanje *in vitro* bitan i postranični lanac s amino skupinom koji omogućava nakupljanje lijeka u prehrambenoj vakuoli plazmodija (148).

Kaschula i suradnici istražili su značaj klora u položaju 7 kinolinskog prstena. Atom klora su zamijenili različitim atomima, odnosno atomskim skupinama koje imaju elektron-donirajući ili elektron-odvlačeći učinak. Uočeno je da zamjena klora u tom položaju mijenja p*K*a vrijednosti amino skupina u molekuli što ima utjecaj na nakupljanje molekula u prehrambenoj vakuoli plazmodija, a time i na antimalarijsko djelovanje (149). Nsumiwa i suradnici pokazali su da se derivati koji u položaju 7 kinolinskog prstena imaju elektron-odvlačeću skupinu (npr. Cl, NO_2, CN) dobro vežu za hem i snažno inhibiraju polimerizacije hemozoina. Nasuprot tome, derivati s elektron-donirajućim supstituentima su pokazali slabi afinitet za vezanje za hem te su slabo ili uopće nisu inhibirali inhibiciju polimerizacije hemozoina (148). Ray i suradnici su na temelju ADMET predikcija pripravili 20 derivata CQ. Derivati u kojima je klor zamijenjen drugim skupinama (npr. OCF_3, OPh) pokazali su slabije antimalarijsko djelovanje (150). Prethodna istraživanja ukazuju na važnost klora u položaju 7 kinolinskog prstena te ne iznenađuje činjenica da postoji relativno mali broj derivata CQ-a temeljenih na promjeni supstituenta u tom položaju.

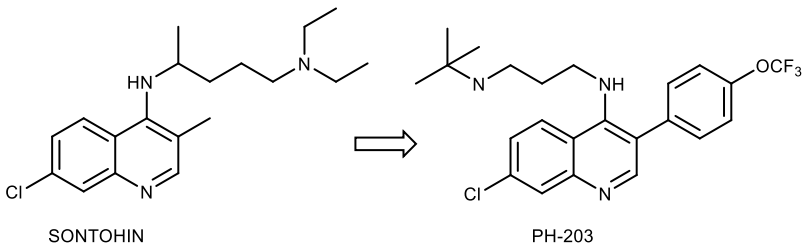

Slika 43. Sontohin i PH-203

Sontohin (Slika 43) je derivat CQ susptituiran metilnom skupinom u položaju 3 kinolinskog prstena. Razvijen je nekoliko godina nakon otkrića CQ, ali je dugi niz godina bio zapostavljen. Pou i suradnici uočili su da ovaj derivat CQ u *in vitro* ispitivanjima pokazuje značajno djelovanje na CQRS. Kako bi pojačali antimalarijsko djelovanje, a smanjili toksičnost, pripravili su farmacine, derivate sontohina koji sadrže alkilne ili arilne supstituente u položaju C-3 kinolinskog prstena. Farmacin PH-203 supstituiran *p*-OCF_3-fenilnom skupinom s manjom modifikacijom postraničnog lanca (Slika 43) pokazao je bolje djelovanje u odnosu na CQ te snažno djelovanje na multirezistentne sojeve u u niskim nanomolarnim vrijednostima (IC_{50} vrijednosti u rasponu 0,9–1,3 nM) (151). SAR derivata CQ-a sažeto je prikazan na Slici 44 (132).

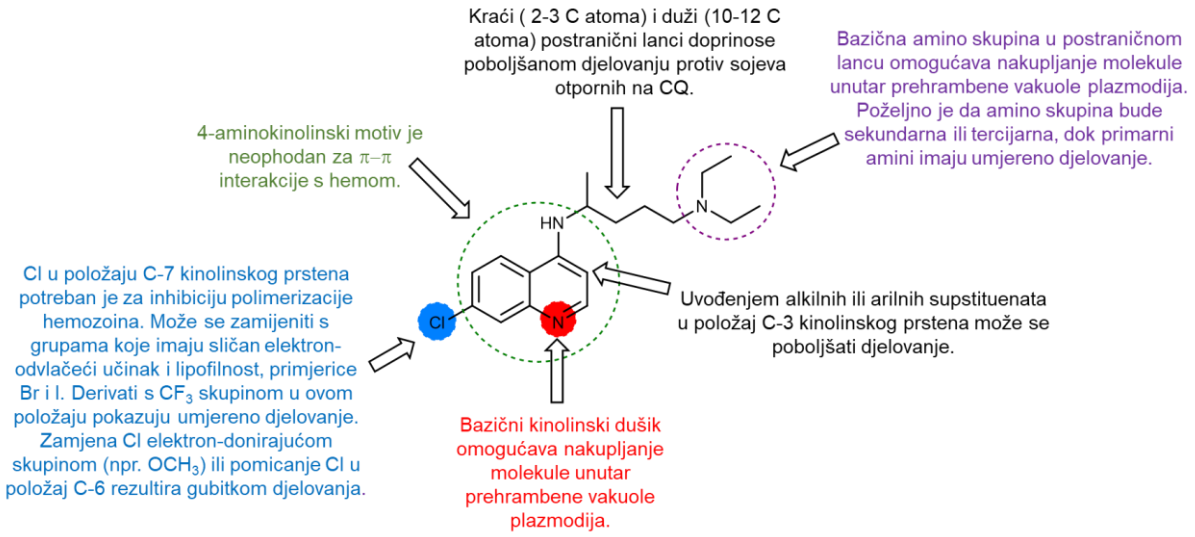

Slika 44. SAR CQ-a i njegovih derivata

1.6.7. Derivati klorokina s antimalarijskim djelovanjem

Iako je zbog razvoja rezistencije učinkovitost CQ-a u liječenju malarije narušena, njegove pozitivne karakteristike poput relativno jednostavne priprave, niske cijene, brzog i dugog djelovanja i dobrog sigurnosnog profila i dalje ga čine veoma dragocjenom molekulom u području farmaceutske kemije. S ciljem poboljšanja svojstava (posebno u vidu nadvladavanja rezistencije), farmaceutski kemičari su korištenjem različitih pristupa modificirali njegovu strukturu. Najveći broj derivata CQ pripravljen je modifikacijom postraničnog lanca (120). U nastavku teksta dan je prikaz derivata CQ koji u postraničnom lancu sadrže triazol.

Kumar i suradnici pripravili su hibride 4-aminokinolina i ferocenilkalkona korištenjem triazola kao poveznice te su ispitali njihovo antimalarijsko djelovanje. Derivati koji su u strukturi poveznice sadržavali fleksibilni alifatski motiv (aminoetanol ili aminopropanol) pokazali su bolje djelovanje od derivata s cikličkim motivima (piperazin ili aminofenol). Spoj prikazan na Slici 45 ostvario je najsnažnije djelovanje protiv W2 soja *P. falciparum* (IC_{50} = 0,37 μM), dok je bio slabo citotoksičan na HeLa stanice (152).

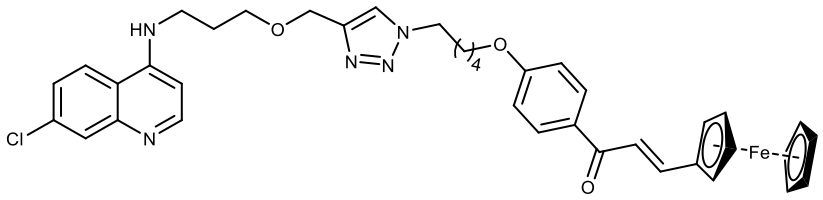

Slika 45. Hibrid 4-aminokinolina i ferocenilkalkona

Oliveira i suradnici pripravili su triazolske derivate 7-klorkinolina. Sintetiziranim spojevima ispitano je antimalarijsko djelovanje na W2 soj *P. falciparum* te citotoksičnost prema HepG2A16 staničnoj liniji. Spojevi su pokazali slabi citotoksični učinak (IC_{50} > 100 μM). 5 od 27 spojeva pokazalo je umjereno antimalarijsko djelovanje (IC_{50} vrijednosti u rasponu 9,6–40,9 μM) (Slika 46) (153).

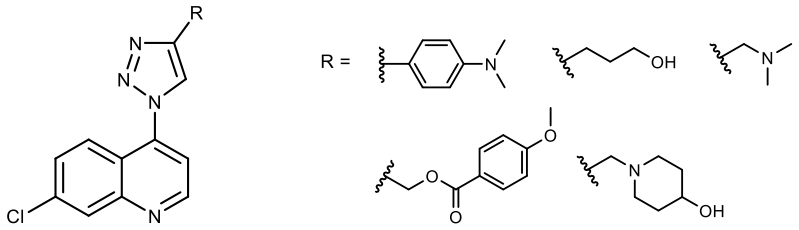

Slika 46. Hibridi 7-klorkinolina i različito supstituiranih triazola

Rawat i suradnici pripravili su hibride 4-amino-7-klorkinolina i triazola (Slika 47a) te 4-aminokinolina i 1,3,5-triazina povezanih triazolom (Slika 47b). Hibridi 4-aminokinolina i triazola supstituirani alifatskim lancima s hidroksilnom skupinom pokazali su umjereno antimalarijsko djelovanje. Uvođenje arilnih skupina rezultiralo je poboljšanjem djelovanja. Derivati koji su sadržavali fenilni prsten supstituiran halogenom djelovali su u niskim mikromolarnim koncentracijama, dok su derivati s fenilnim prstenom supstituiranim s *p*-$COCH_3$ skupinom pokazali najsnažniji učinak (IC_{50} vrijednosti u submikromolarnom području). U seriji hibrida 4-aminokinolina i 1,3,5-triazina uočeno je da zamjena halogena na

triazinskom prstenu bazičnim skupinama poput piperidina, morfolina i dimetilamina dovodi do poboljšanja antimalarijskog djelovanja što je u skladu s poznatom činjenicom da je za antimalarijsko djelovanje bitan bazični postranični lanac. U ovoj seriji najučinkovitiji je bio derivat supstituiran dimetilanilino (R_1) i dimetilamino (R_2) skupinama (IC_{50}(*Pf*D6) = 0,58 μM, IC_{50}(*Pf*W2) = 0,73 μM). Spojevi su bili slabo citotoksični prema Vero stanicama što ukazuje na selektivnost djelovanja (154).

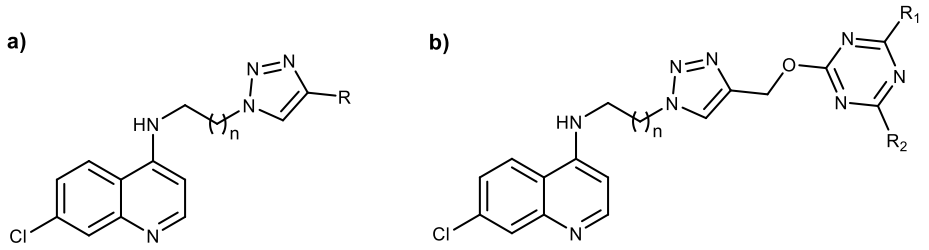

Slika 47. a) Hibridi 4-amino-7-klorkinolina i triazola, b) hibridi 4-amino-7-klorkinolina i triazina povezanih triazolom

Chibale i suradnici pripravili su hibride kinolina i kalkona (Slika 48a), odnosno dienona (Slika 48b), s triazolskom poveznicom. Hibridi kinolina i kalkona pokazali su dobro antimalarijsko djelovanje. Najsnažnije je djelovao derivat supstituiran metoksi skupinama u položajima 2' i 4' fenilnog prstena kalkonskog dijela molekule (IC_{50}(*Pf*D10) = 0,04 μM, IC_{50}(*Pf*Dd2) = 0,07 μM, IC_{50}(*Pf*W2) = 0,09 μM). Hibridi kinolina i dienona umjereno su djelovali na D10 i Dd2 sojeve *P. falciparum*, dok su na W2 soj djelovali slabo (155).

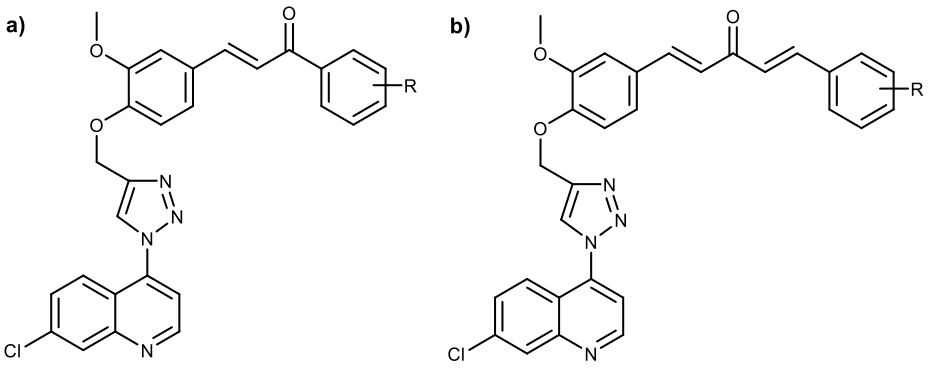

Slika 48. Hibridi 7-klorkinolina i: a) kalkona, b) dienona

Boechat i suradnici pripravili su hibride kinolina i triazola s različitim supstituentima u položaju 4 triazolskog prstena (Slika 49). Između ostalih derivata, spoj supstituiran aldehidnom

skupinom pokazao je najsnažnije antimalarijsko djelovanje na W2 soj *P. falciparum* (IC_{50} = 1,4 ± 0,2 μM) i slabo citotoksično djelovanje što ukazuje na selektivnost djelovanja (SI = 351). Derivati s hidroksilnim skupinama, metilnim esteromi i fluorom bili su neaktivni (156).

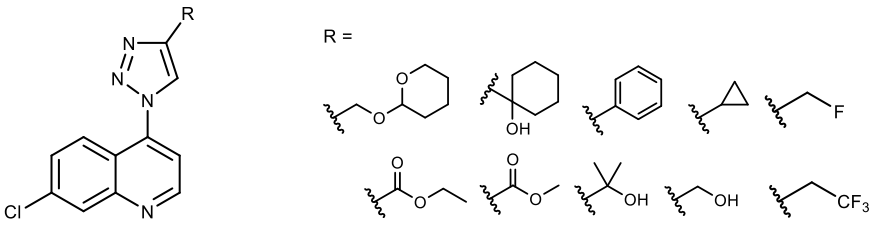

Slika 49. Hibridi 7-klorkinolina i triazola supstituiranih u položaju C-4

Hoda i suradnici dizajnirali su hibride kinolina i različito supstituiranih fenila povezanih triazolom kao potencijalne inhibitore falcipain-2 (FP-2), cisteinskih proteaza koje plazmodij koristi za razgradnju hemoglobina (Slika 50). Derivati su inhibirali FP-2 u mikromolarnim koncentracijama i negativno utjecali na razvoj parazita. Također, uzrokovali su morfološke promjene parazita poput E-64, poznatog inhibitora FP2. Autori predlažu daljnje istraživanje FP-2 inhibitora kao potencijalnih antimalarika (157).

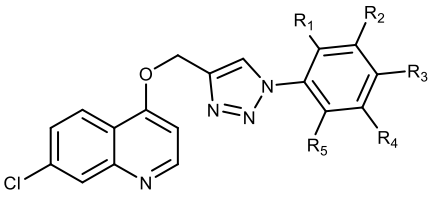

Slika 50. Hibridi 7-klorkinolina i supstituiranih fenila povezanih triazolom

1.7. FEROCEN

1.7.1. Struktura i svojstva ferocena

Ferocen pripada skupini organometalnih spojeva. Otkrili su ga Kealy i Pauson 1951. godine kada su reakcijom ciklopentadienilmagnezijevog bromida i $FeCl_2$ umjesto očekivanog fulvalena ($C_{10}H_8$) dobili narančasto obojeni spoj molekulske formule $C_{10}H_{10}Fe$ (158). Godinu dana nakon otkrića, ferocen je strukturno okarateriziran kao „sendvič“ kompleks građen od dva paralelna ciklopentadienilna aniona ($C_5H_{10}^-$) između kojih se nalazi Fe^{2+} ion (Slika 51) (159). Svaki ciklopentadienilini prsten ima 6 π elektrona te se prema Hückelovom pravilu smatra aromatskim sustavom (160, 161).

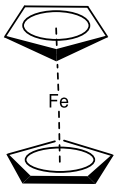

Slika 51. Struktura ferocena

Ferocen je stabilan u vodi i na zraku, dobro topljiv u organskim otapalima, a slabo u vodi. Na temperaturi višoj od 100 °C sublimira. Podložan je reakcijama elektrofilne supstitucije (161, 162).

1.7.2. Sinteza ferocena

U literaturi je opisano više različitih načina sinteze ferocena. Ovdje je prikazana metoda kojom se ferocen pripravlja iz ciklopentadiena.

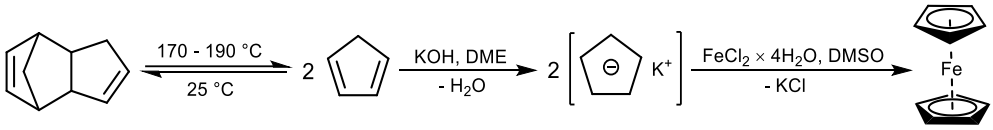

Shema 8. Sinteza ferocena

Ciklopentadien Diels-Alderovom reakcijom brzo dimerizira u diciklopentadien zbog čega je nepostojan u monomernom obliku (163). Priređuje se neposredno prije korištenja

frakcijskom destilacijom diciklopentadiena, pri čemu dolazi do cijepanja dimera i destilacije nastalih monomera. Miješanjem ciklopentadiena i kalijevog hidroksida u 1,2-dimetoksietanu dobiju se ciklopentadienilni anioni, koji u reakciji s $FeCl_2$ u DMSO-u daju ferocen (Shema 8) (164).

1.7.3. Ferokin

Zbog niske toksičnosti, biokemijske stabilnosti, lipofilnosti i povoljnih elektrokemijskih svojstava brojni farmaceutski kemičari iskoristili su ferocen u dizajniranju novih bioaktivnih molekula (165). Najpoznatiji derivati ferocena u farmaceutskoj kemiji su antimalarik ferokin (FQ) i ferocifeni, spojevi s protutumorskim djelovanjem.

FQ je derivat CQ koji između dvije amino skupine u postraničnom lancu sadrži ferocenski prsten (Shema 9). Prvi su ga pripravili Biot i suradnici sa Sveučilišta u Lillu 1994. godine (166). Sinteza FQ kreće iz [(dimetilamino)metil]ferocena, koji se metalira pomoću *n*-butillitija. Dobiveni međuprodukt kondenzira s DMF-om dajući 2-[(*N*,*N*-dimetilamino)metil]ferocenkarboksaldehid. Reakcijom aldehida i hidroksilamina hidroklorida nastaje oksim koji se pomoću $LiAlH_4$ reducira u amin. Kondenzacijom amina i 4,7-diklorkinolina u prisustvu *N*-metil-2-pirolidinona (NMP) nastaje FQ (166).

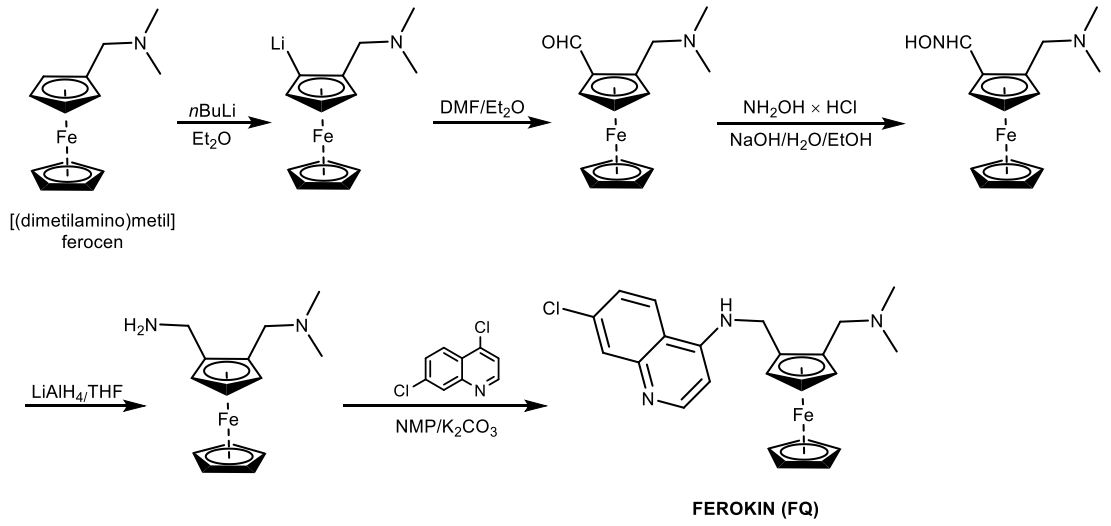

Shema 9. Sinteza ferokina

S obzirom da u strukturi sadrži 1,2-disupstituirani nesimetrični ferocenski motiv, FQ karakterizira planarna kiralnost. Delhaes i suradnici pokazali su da racemat ima nešto bolje

antimalarijsko djelovanje od čistih entantiomera zbog čega se FQ uglavnom koristi kao racemična smjesa (167).

FQ je u *in vitro* i *in vivo* ispitivanjima pokazao snažno antimalarijsko djelovanje. Od posebnog je značaja njegova učinkovitost protiv rezistentnih spojeva plazmodija (168). Antimalarijsko djelovanje FQ posljedica je dva različita mehanizma djelovanja: inhibicije polimerizacije hemozoina i generiranja hidroksilnih radikala. Sposobnost FQ da inhibira polimerizaciju hemozoina posljedica je strukturne sličnosti s CQ, odnosno prisutnosti amino skupina i kinolinskog prstena u strukturi (169). Ipak, zbog razlike u fizikalno-kemijskim svojstvima FQ bolje interferira s procesom polimerizacije hemozoina od CQ. U FQ je prisutna intramolekularna vodikova veza između sekundarne i tercijarne amino skupine (Slika 52) zbog čegaje smanjena bazičnost ovih skupina (pK_{a1} = 6,99 pK_{a2} = 8,19) u odnosu na CQ (pK_{a1} = 8,3, pK_{a2} = 10,2). Pri fiziološkom pH FQ je uglavnom neprotoniran ili monoprotoniran, dok je CQ uglavnom diprotoniran. S obzirom da su neprotonirani i monoprotonirani oblici hidrofobniji, FQ brže prolazi kroz membranu prehrambene vaukuole. Veća lipofilnost FQ (log $D_{7,4}$ = 2,95) u odnosu na CQ (log $D_{7,4}$ = 0,85) dodatno doprinosi boljem prolasku kroz membrane što doprinosi i nakupljanju FQ unutar prehrambene vakuole (170, 171).

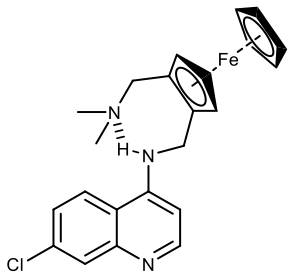

Slika 52. Intramolekulska vodikova veza u FQ

Za drugi mehanizam djelovanja FQ bitna je ferocenilna skupina koja u oksidirajućim uvjetima unutar prehrambene vakuole plazmodija generira hidroksilne radikale prema sljedećoj jednadžbi:

$$FQ + H_2O_2 \rightarrow FQ^+ + OH^- + \cdot OH$$

Hidroksilni radikali uzrokuju lipidnu peroksidaciju čime razaraju membranu prehrambene vakuole. Također, oksidiraju glutation, molekulu koja je uključena u proces detoksikacije hema. Uloga generiranja hidroksilnih radikala posebno je značajna u *in vivo* uvjetima (168).

Za snažno antimalarijsko djelovanje FQ bitna je njegova lokalizacija unutar prehrambene vakuole. Novija istraživanja pokazuju da se FQ pretežno lokalizira na granici lipidnog i vodenog sloja, odnosno uz membranu. Lipofilni ferocenski dio stupa u interakciju s lipidima membrane , dok je kinolinski dio izložen vodenom sloju. Kinolinski dio nekovalentno veže hem i zadržava ga u vodenom sloju onemogućavajući njegovu polimerizaciju. Smještaj FQ blizu lipida membrane dodatno doprinosi njegovoj sposobnosti lipidne peroksidacije. Konačno, zadržavanje uz membrane onemogućava interakciju FQ s *Pf*CRT, efluks i razvoj rezistencije (170, 172).

1.7.3.1. Derivati ferokina

Obećavajuće antimalarijsko djelovanje ferokina u *in vitro* i *in vivo* ispitivanjima potaknulo je nekoliko istraživačkih skupina na pripravu njegovih derivata.

Hidroksiferokini. Biot i suradnici sintetizirali su hidroksiferokine (Slika 53a) koji pokazuju analogiju s hidroksiklorokinom. Iako su ovi spojevi *in vitro* inhibirali *P. falciparum* snažnije od CQ, njihovo djelovanje bilo je slabije od FQ. Hidroksiferokini su pokazali i selektivno antiviralno djelovanje prema SARS-CoV te bi njihova upotreba bila od posebne koristi u područjima gdje malarija koegzistira sa spomenutom virusnom infekcijom (173).

Trioksaferokini. Na temelju trioksakina, hibridnih molekula 1,2,4-trioksana i 4-aminokinolina, Robert i suradnici dizajnirali su trioksaferokine koji u poveznici sadrže ferocenski prsten. Trioksaferokini su snažno djelovali na rezistentne sojeve u niskim nanomolarnim koncentracijama (16-43 nM). Slika 53b prikazuje najdjelotvorniji trioksaferokin u *in vitro* ispitivanjima. U nastvaku istraživanja njegov učinak ispitan je *in vivo* na mišu inficiranim s *P. vinckei petteri*. Rezultati su potvrdili učinkovitost trioksaferokina i njihovu sposobnost smanjenja parazitemije ispod detektabilne razine. Međutim, potpuno izlječenje bez recidiva nije zabilježeno u dozama manjim od 25 mg/kg/danu. Kako bi se smanjila doza, potrebno je prema ovom strukturnom predlošku sintetizirati i ispitati novu generaciju molekula (174).

Ferocenofani. Orvig i suradnici pripravili su ferocenofane u čijoj strukturi terminalni dušikov atom klorokinskog dijela molekule premošćuje dva ciklopentadienilna prstena ferocena (Slika 53c). U svrhu usporedbe i SAR analize pripravljeni su i analozi ferocenofana: monosupstituirani derivati te derivati bez ferocenskog dijela. Svi spojevi ispitani su na CQOS i CQRS *P. falciparum*. Najsnažnije djelovanje pokazali su monosupstituirani derivati.

Međutim, uočeno je da ferocenofani snažnije djeluju na QCRS u odnosu na CQOS. Provedena je analiza povezanosti kemijsko-fizikalnih svojstava i antimalarijskog djelovanja. Potvrđen je utjecaj intramolekulske vodikove veze na antimalarijsko djelovanje, ali je veći značaj pripisan odgovarajućem omjeru hidrofilnosti i lipofilnosti molekula. Štoviše, smatra se da su odgovarajuća konformacija, kompaktnost te povoljan omjer lipofilnosti i hidrofilnosti omogućili ferocenofanima nadvladavanje rezistencije (175).

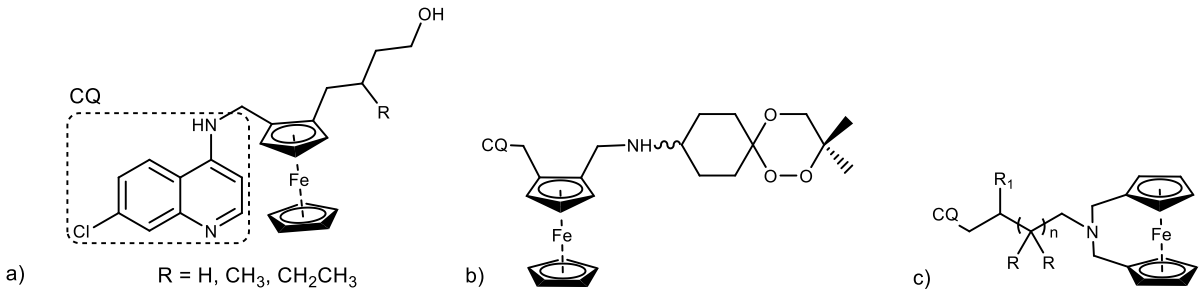

Slika 53. Derivati ferokina

1.7.4. Ferocifeni

Ferocifeni su derivati tamoksifena (TAM), protutumorskog lijeka koji se koristi za liječenje karcinoma dojke ovisnog o estrogenu (Slika 54). TAM se u organizmu oksidira u hidroksitamoksifen (OH-TAM) koji se kompetitivno veže za estrogenski receptor α (Erα). Na ovaj način OH-TAM interferira s vezanjem estradiola, prirodnog liganda Erα, ometajući transkripciju DNA, što dovodi do smrti tumorske stanice (176). Zamjenom fenilnog prstena ferocenskim u strukturi TAM-a i njegovog metabolita dobiveni su ferocifen (Fc-TAM) i hidroksiferocifen (Fc-OH-TAM) (Slika 54) (171).

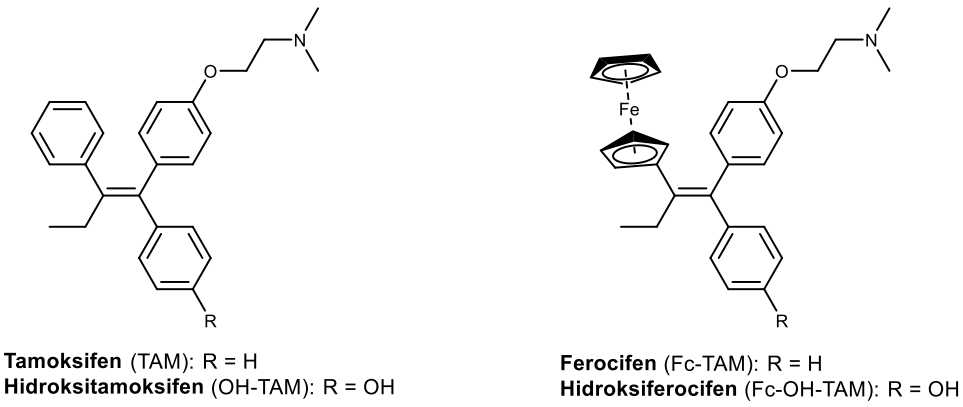

Slika 54. Strukture tamoksifena, hidroksitamoksifena i njihovih ferocenskih analoga

Poput, TAM i OH-TAM, Fc-TAM i OH-Fc-TAM snažno djeluju na stanice karcinoma dojke ovisnog o estrogenu. Ovo djelovanje, poput roditeljskih molekula, ostvaruju kompetitivnim vezanjem za Erα. Međutim, uočeno je da Fc-TAM-a i OH-Fc-TAM, za razliku od TAM i OH-TAM, djeluju i na stanice karcinoma dojke neovisnog o hormonima, koji čini 1/3 svih karcinoma dojke. Prethodno se objašnjava prisutnošću ferocenskog prstena u strukturi (171). Fc-TAM-a i OH-Fc-TAM, analogno FQ, mogu stvarati fericenijeve hidroksilne radikale koji su pogubni za tumorske stanice (177, 178). Štoviše, uočeno je da gubitkom 2 elektrona i 2 protona stvaraju kinon metide. U ovom procesu ferocenski prsten djeluje kao donor elektrona (Shema 10). Kinon metidi imaju svojstva Michaelovog akceptora zbog čega mogu reagirati s endogenim nukleofilima poput glutationa i nukleobaza (Shema 10) (179). Značajno je što ferocifeni djeluju selektivno: ostvaruju 110-200 puta jači antiproliferativni učinak na tumorske stanice nego na zdrave stanice (astrocite i melanocite) (180, 181). Proveden je pokus s kinon metidima i modelnim molekulama koji su sadržavale selenolne i tiolne skupine oponašajući enzime koji u aktivnom mjestu sadrže selenolne (npr. tioredoksin reduktaza, TrxR), odnosno tiolne skupine (npr. glutation reduktaza). Uočeno je da kinon metidi reagiraju sa silanolnom, ali ne i tiolnom skupinom. Ovakvo selektivno djelovanje veoma je važno jer je TrxR prekomjerno eksprimirana u tumorskim stanicama (182). Također, ferocifeni mogu inducirati staničnu smrt neovisno o apopotozi, primjerice induciranjem senescencije (183).

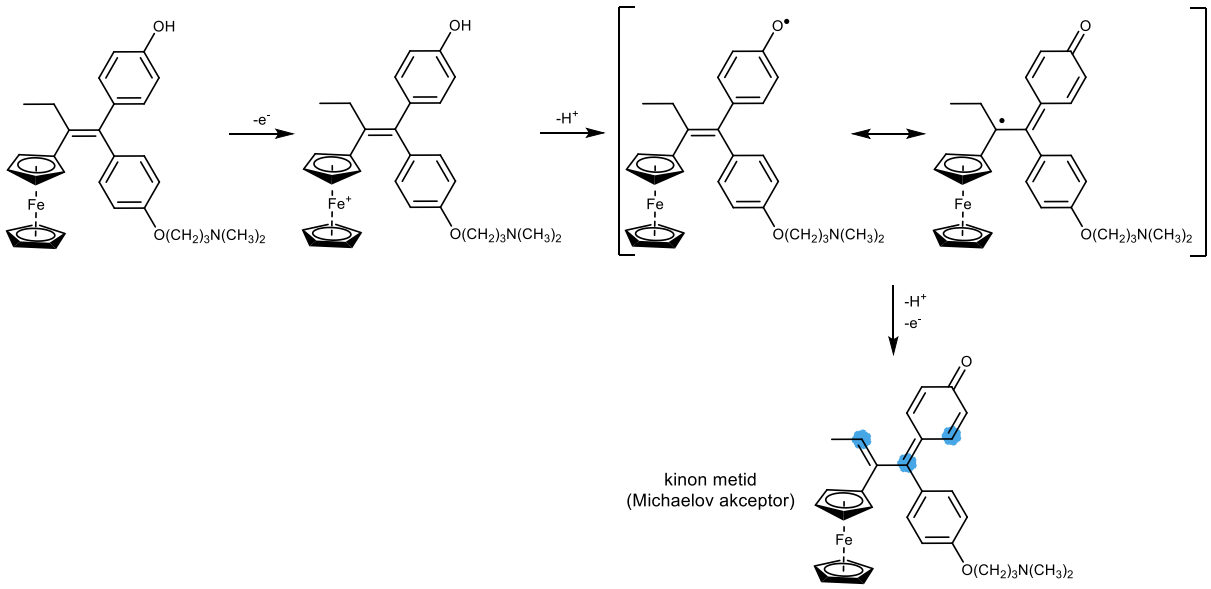

Shema 10. Stvaranje kinon metida (plavom bojom su označena mjesta koja mogu reagirati s endogenim nukleofilima)

1.7.4.1. Derivati ferocifena

Derivatizacijom ferocifena pripravljeni su ferocenofanski suberamidi. Ferocenofanski strukturni motiv (Slika 55) od velikog je značaja u bioorganometalnoj kemiji jer zbog rigidne strukture omogućava optimalno vezanje molekule za aktivno mjesto enzima. Jaouen i suradnici modificirali su strukturu poznatog citostatika vorinostata (suberoilanilidhidroksamske kiseline, SAHA-e) i njegovih derivata (karboksilne kiseline i amida) uvođenjem ferocena, odnosno ferocenofanskog motiva (Slika 55). Antitumorsko djelovanje sintetiziranih spojeva ispitano je na dvije linije adenokarcinoma dojke: MCF-7 i MDA-MB-231. SAR analizom nađeno je: 1) uvođenje ferocena/ferocenofanskog motiva u molekulu pojačalo je antitumorsko djelovanje, 2) fleksibilni derivati (u strukturi sadrže ferocen) pokazali su selektivnost prema MDA-MB-231, 3) rigidni derivati (u strukturi sadrže ferocenofanski motiv) bili su selektivni prema MCF-7. Utvrđeno je da obje serije derivata tvore fericenijeve ione koji generiraju RKV što dovodi do antiproliferativnog učinka. Djelovanje ostvaruju i drugim mehanizmima: aktivacijom tumorsupresorskih gena što dovodi do apoptoze te oštećenjem molekule DNA (184, 185).

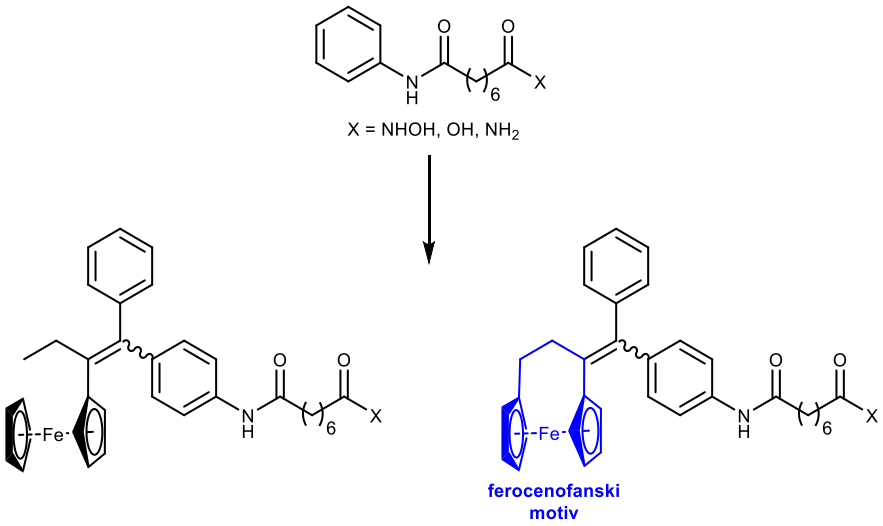

Slika 55. Derivati ferocena i suberamida

1.7.5. Ostali derivati ferocena s protutumorskim djelovanjem

Ferocifeni i ferocenofanski suberamidi nisu jedini primjeri uspješnog uvođenja ferocena u strukturu bioaktivnih molekula i poboljšanja njihovih djelovanja. Uvođenjem ferocena u strukturu nilutamida, steroida (npr. testosterona, dihidrotestosterona, androsterona, estrona, pregnenolona), retinoida, kurkuminoida, novobiocina, kolhicina, paklitaksela, docetaksela,

plinabulina, klotrimazola, kinolina i artemizinina rezultiralo je snažnijim antiproliferativnim djelovanjem derivata u odnosu na roditeljske molekule. U nekim slučajevima došlo je do promjene mehanizma djelovanja, što je od velikog značaja u borbi protiv rezistencije. S druge strane, u nekim slučajevima je uvođenje ferocena u strukturu molekula rezultiralo smanjenjem njihove citotoksičnosti. Primjerice, uvođenje ferocena u strukturu iludina dovelo je do smanjenja toksičnosti i povećanja selektivnosti. Nadalje, zamjena arilnog dijela molekule u hibridima tetrahidro-β-karbolina i kalkona dovela je do smanjenja antiproliferativnog djelovanja, ali povećanja selektivnosti derivata prema MCF-7. Zamjena arilnog dijela molekule ferocenom u hibridima naftalimida i kalkona nije rezultirala poboljšanim protutumorskim djelovanjem, dok je analogna zamjena u hibridima naftalimida i pirazolina dovela do gubitka djelovanja (185).

1.8. TRIAZOL

Triazol je heterociklički prsten iz skupine azola građen od tri atoma dušika i dva atoma ugljika. S obzirom na razmještaj atoma dušika razlikuju se 1,2,3-triazol i 1,2,4-triazol. Svaki od prethodnih postoji u tri tautomerna oblika (Slika 56). Od šest tautomera, četiri (istaknuti pravokutnikom) su aromatski – atomi koji sačinjavaju prsten su sp^2 hibridizirani te je 6 elektrona delokalizirano u π sustavu molekulskih orbitala (186).

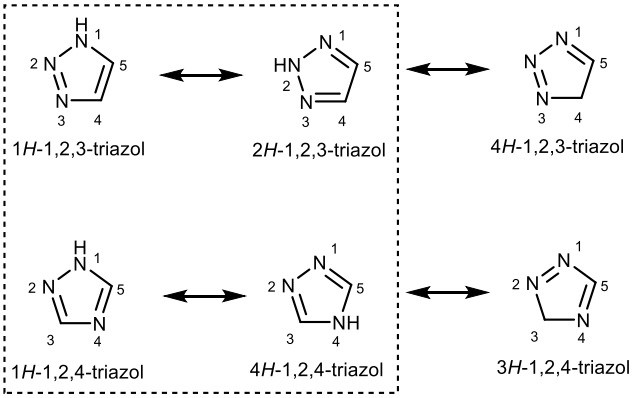

Slika 56. Tautomerni oblici triazola

1*H*-1,2,3-triazol (dalje u tekstu triazol) od velike je važnosti u farmaceutskoj kemiji iz nekoliko razloga:

i. pokazuje brojna biološka djelovanja poput protuupalnog, antiagregacijskog, antimikrobnog, antituberkulotskog, protutumorskog, antivirusnog, antiparazitskog (186),
ii. stabilan je prema oksidaciji, redukciji i hidrolizi u kiselim i bazičnim uvjetima (187),
iii. relativno jednostavno i učinkovito može se pripraviti reakcijom klik-kemije (187),
iv. djeluje kao bioizoster amidne veze (188) (Slika 57),
v. s biološkim metama može stvarati vodikove veze i dipol-dipol interakcije.

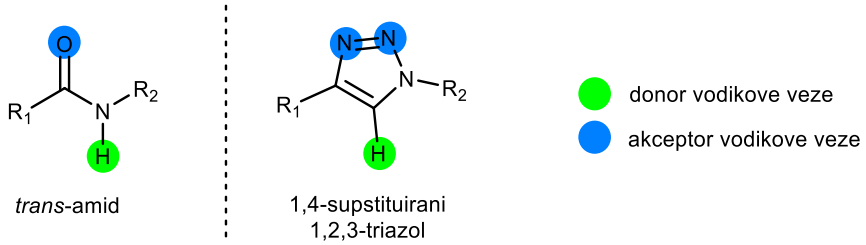

Slika 57. Triazol – bioizoster amida

1.8.1. Reakcije klik-kemije

Pojam „klik“ kemija uveo je K. B. Sharpless 2001. godine opisujući reakcije koje su visokog iskorištenja, širokog spektra primjene, stereospecifične, jednostavne izvedbe, provedive u lako uklonjivim ili bezopasnim otapalima te daju produkte koje je moguće izolirati bez kromatografskih postupaka (189). Tipičan primjer reakcije klik-kemije je bakrom(I) katalizirana azid-alkin cikloadicija (CuAAC).

Ova rekacija razvijena je iz Huisgenove 1,3-dipolarne cikloadicije. Klasična Huisgenova reakcija je dugotrajna, zahtijeva povišenu temperaturu i rezultira smjesom dvaju regioizomera zbog čega se ne može smatrati reakcijom klik-kemije. Korištenje bakra kao katalizatora ubrzalo je reakciju 10^7 do 10^8 puta te omogućilo stereospecifičnu sintezu 1,4-disupstituiranih izomera. S druge strane, ako se kao katalizator koristi rutenij dolazi do selektivnog nastanka 1,5-disupstituiranih triazola (Shema 11) (187).

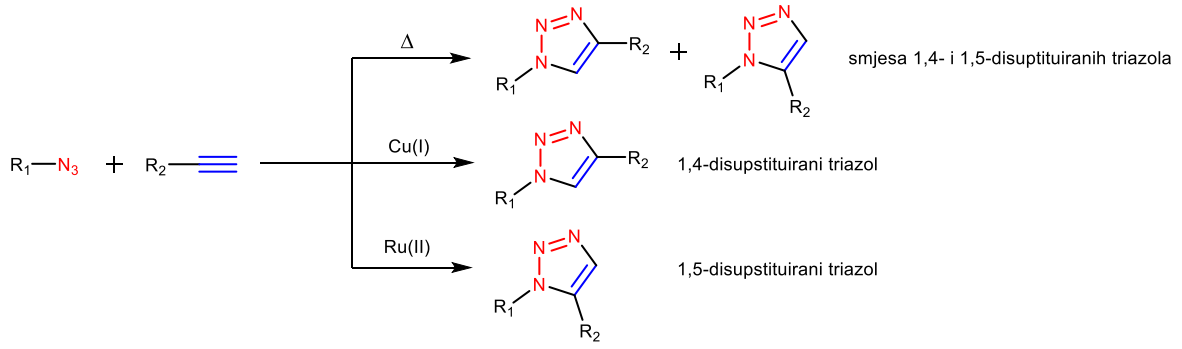

Shema 11. Huisgenova 1,3-dipolarna cikloadicija i reakcije klik-kemije katalizirane Cu i Ru

Pretpostavljeni mehanizam CuAAC detaljno je prikazan na Shemi 12. U prvom koraku Cu^+ koordinira π-elektrone trostruke C≡C veze terminalnog alkina dajući kompleks bakra i

alkina (A). Koordinacijom Cu^+ na trostruku vezu smanjuje se pK_a terminalnog protona alkina, što omogućuje deprotonaciju i nastanak bakrovog acetilida (B). Kompleks bakrovog acetilida koordinira azid, pri čemu nastaje intermedijar (C). Njegovom pregradnjom nastaje šesteročlani prsten (D), u koji je uključen i bakar. Ovaj korak ima računski dobivenu energijsku barijeru 18,7 kcal mol^{-1} , što je znatno manje od 23,7 kcal mol^{-1}, koliko iznosi teorijska barijera nekatalizirane reakcije. Energijska barijera za nastajanje triazolila (E) (triazola supstituiranog bakrom) je niska; 3,2 kcal mol^{-1}. Protoniranjem triazolila E oslobađa se bakar i nastaje produkt, 1,4-supstituirani 1,2,3-triazol (190).

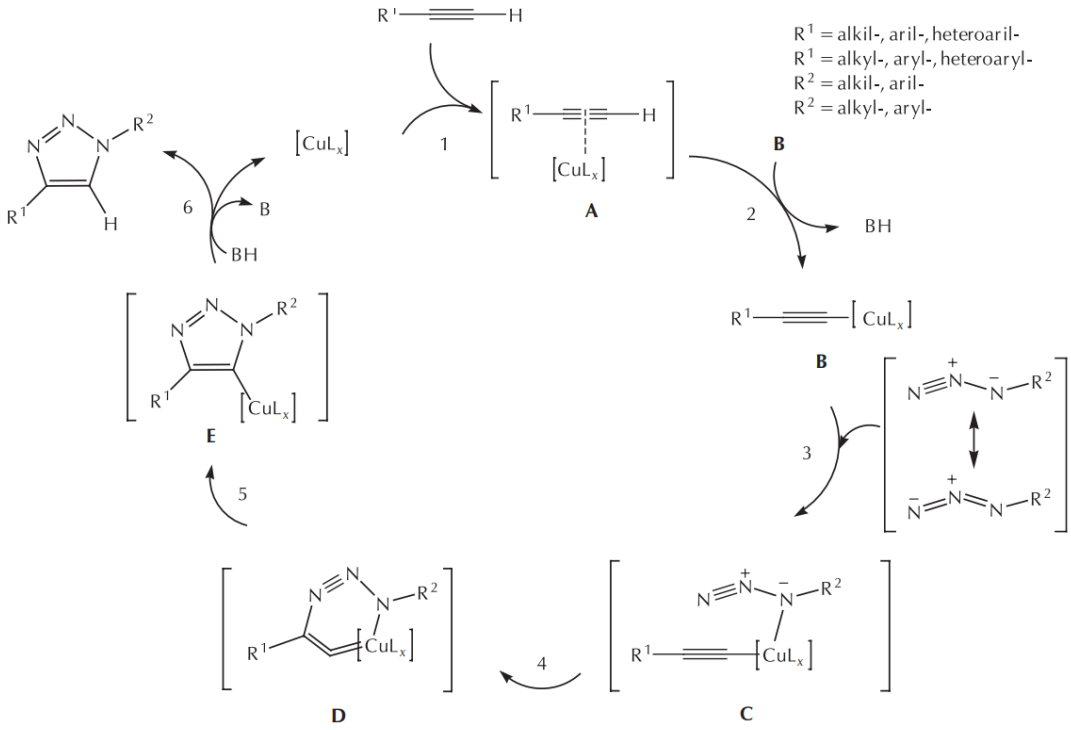

Shema 12. Mehanizam CuAAC (190)

Cu(I) se u reakcijsku smjesu uvodi izravno ili se priprema *in situ*. Izravna primjena Cu(I) uključuje korištenje Cu(I) soli (npr. CuBr i CuI) ili kompleksa (npr. $[Cu(CH_3CN)_4]PF_6$ i $[Cu(PPh_3)_3]Br$). S druge strane, *in situ* priprema katalizatora zahtijeva dodatak prekatalizatora i odgovarajućeg redukcijskog sredstva (npr. $CuSO_4 \times 5H_2O$ i natrijev askorbat). Moguće je kao prekatalizator koristiti bakrenu žicu (Cu(0)) uz dodatak odgovarajućeg oksidansa (190).

2. OBRAZLOŽENJE TEME

Rak i malarija su smrtonosne bolesti zbog čega predstavljaju globalni javnozdravstveni problem. Prema podacima WHO, 2020. godini zabilježeno je gotovo 20 milijuna novih slučajeva raka i 10 milijuna rakom uzrokovanih smrti (3), dok je u istoj godini zabilježen 241 milijun slučajeva malarije, od čega je 627 tisuća rezultiralo smrtnim ishodom (9). Uspješnost terapije ovih bolesti narušena je pojavom rezistencije na postojeće lijekove zbog čega je kontinuiran razvoj novih i učinkovitih lijekova, s novim mehanizmom djelovanja, od velike važnosti.

S obzirom da su rak i malarija etiološki i patofiziološki potpuno različite bolesti, teško je za očekivati da bi se mogle liječiti istim lijekom. Ipak, antimalarici, posebno oni iz skupina kinolina i artemizinina, pokazuju dobro protutumorsko djelovanje. S druge strane, neki citostatici, npr. inhibitori histonskih deacetilaza, ispoljavaju antimalarijsko djelovanje. Štoviše, znanstvena literatura obiluje izvješćima o prirodnim i sintetskim spojevima s antimalarijskim i protutumorskim djelovanjem (135, 191). Primjerice, harmin, β-karbolinski alkaloid sa širokim spektrom farmakoloških djelovanja, pokazao je u *in vitro* i *in vivo* studijama obećavajuće protutumorsko i antimalarijsko djelovanje (46).

U ovom doktorskom radu su korištenjem molekulske hibridizacije pripravljeni hibridi harmina, odnosno strukturno sličnih β-karbolina i: 1) DCK-a (harmicini), 2) CQ-a (harmikini) i 3) ferocena (harmiceni). Navedene molekule odabrane su kao partner harminu u hibridima zbog toga što pokazuju dvostruko djelovanje: protutumorsko i antimalarijsko. Cilj molekulske hibridizacije harmina i derivata cimetne kiseline/CQ-a/ferocena je priprava molekula koje djeluju na različite mete zbog čega ostvaruju snažnije protutumorsko i/ili antimalarijsko djelovanje te su otpornije prema razvoju rezistencije.

Kako bi se dobio uvid u SAR, strukturna raznolikost hibrida postignuta je: 1) povezivanjem harmina s tri različite bioaktivne molekule, 2) variranjem mjesta supstitucije na β-karbolinskom prstenu, 3) korištenjem dvaju različitih poveznica. Kao poveznice u hibridima korištene su amidna skupina te triazol, bioizoster amida, dajući u svakoj seriji spojeva podseriju amidnog (AT), odnosno triazolskog tipa (TT). Jedino su u seriji harmicina pripravljeni samo hibridi TT jer su njihovi analozi AT već opisani u literaturi (98).

Budući da polazne molekule (harmin, DCK-i, CQ i derivati ferocena) posjeduju i antimalarijsko i citostatsko djelovanje, pripravljenim hibridima ispitana su oba djelovanja.

3. MATERIJALI I METODE

3.1. MATERIJALI I INSTRUMENTI

Tijek reakcija i čistoća produkata praćeni su tankoslojnom kromatografijom (TLC). Za TLC su upotrijebljene silikagel ploče 60 F_{254} (Merck, Njemačka) te diklormetan/metanol (97:3, 95:5, 90:10, 85:15, 80:10, 80:20, 75:25), cikloheksan/etil-acetat/metanol (30:10:5, 10:10:5, 300:100:75, 10:10:1), cikloheksan/etil-acetat (9:1, 2:1), etil-acetat/metanol (100:5) i aceton/diklormetan (9:1, 3:2, 1:1) kao pokretne faze. Analizirani spojevi detektirani su UV (λ = 254 i 366 nm) i parama joda. Za kromatografiju na koloni kao nepokretna faza korišten je silikagel veličine čestica 0,063–0,200 mm (Merck) uz iste pokretne faze kao u TLC-u. Pročišćavanje derivata dobivenih klik-reakcijom provedeno je kromatografijom na koloni uz dodatak sloja Al_2O_3 kako bi se uklonile zaostale bakrove soli. Iskorištenja reakcija nisu optimirana.

CEM Discover mikrovalni reaktor (CEM Corporation, SAD) korišten je u sintezi uz pomoć mikrovalova (P = 150 W). ^{1}H i ^{13}C NMR spektri snimljeni su na NMR spektrometru Bruker Avance III HD (Bruker, SAD) kod 400 ili 600 MHz za ^{1}H i kod 75, 101 ili 151 MHz za ^{13}C jezgru. Uzorci su mjereni u DMSO-d_6 otopinama na 20 °C u NMR cjevčicama promjera 5 mm. Kemijski pomaci izraženi su u ppm u odnosu na tetrametilsilan (TMS) kao unutarnji standard u ^{1}H, odnosno signal DMSO-a u ^{13}C spektru (39,52 ppm). Konstante sprege (J) izražene su u Hz. IR spektri snimljeni su na Paragon 500 (Perkin Elmer, UK) i Fourier-Transform Infrared Attenuated Total Reflection UATR Two spectrometer (PerkinElmer) u području valnih brojeva od 4000 do 450 cm^{-1}. Spektri masa snimljeni su na HPLC-MS/MS instrumentu (HPLC, Agilent Technologies 1200; MS, Agilent Technologies 6420 Triple Quad, SAD). Kao tehnika ionizacije korištena je ionizacija elektroraspršenjem (ESI) u pozitivnom i/ili negativnom modu. Tališta (t_t) su određena na Stuart SMP3 instrumentu za određivanje tališta (Barloworld Scientific, UK) u otvorenim kapilarama i nisu korigirana. Za mjerenje apsorbancije u MTT testu korišten je VICTOR3 Multilabel Plate Reader (Perkin Elmer).

Harmin, 2,2-dimetoksiacetaldehid, octena kiselina, 1,8-diazabiciklo[5.4.0]undek-7-en (DBU), 10 %-tni paladij na aktivnom ugljenu (Pd/C), acetaldehid-dimetil-acetal, Li_2CO_3, tetrabutilamonijev hidrogensulfat (TBAHS), LiOH × H_2O, MnO_2, 1,4-diaminobutan, anhidrid propanfosfonske kiseline (T3P), ferocen-metanol, etinilferocen, ferocenoctena kiselina, ferocenkarboksilna kiselina, *tert*-butanol, 4,7-diklorkinolin, $CuSO_4$ × 5H_2O, 2-aminoetanol, glicin i fenol nabavljeni su od tvrtke Sigma-Aldrich (SAD). Od iste tvrtke nabavljene su cimetna kiselina, *m*-fluorcimetna kiselina, *m*-bromcimetna kiselina, *p*-klorcimetna kiselina, *p*-

metoksicimetna kiselina kao trans stereoizomeri (≥ 99 %). Bromovodična kiselina, $LiAlH_4$, natrijev azid i 1,2-diaminoetan nabavljeni su od tvrtke Merck. Triptamin, metilni ester triptofana, 5-metoksitriptamin, trifluoroctena kiselina (TFA), dimetil-(1-diazo-2-oksopropil)fosfonat (Bestmann Ohirin reagens), 2-azido-1,3-dimetilimidazolinijev heksafluorofosfat (ADMP), propargil-bromid, cezijev karbonat, *N*,*N*-dimetilformamid (DMF), *tert*-butil-*N*-(2-brometil)karbamat, metil-akrilat, 1-[*bis*(dimetilamino)metilen]-1*H*-1,2,3-triazolo[4,5-*b*]piridinijev-3-oksid heksafluorofosfat (HATU) i *N*,*N*-diizopropiletilamin (DIEA) nabavljeni su od tvrtke Tokyo Chemical Industry (Japan). Acetonitril (ACN), aceton, cikloheksan, metanol, etil-acetat, klorovodična kiselina, toluen i dietil-eter nabavljeni su od tvrtke Honeywell (SAD). Natrijev askorbat nabavljen je od tvrtke Acros Organics (Belgija), a bakrov(II) acetat i trietilamin (TEA) od tvrtke Alfa Aesar (SAD). Diklormetan je nabavljen od tvrtke Fisher Chemical (SAD), kalijev permanganat od tvrtke Grammol (Hrvatska), kalijev karbonat od tvrtke Kemika (Hrvatska), a tionil-klorid od tvrtke Fluka (SAD). U reakcijama organske sinteze korištena su bezvodna otapala. Bezvodni ACN i metanol nabavljeni su od tvrtke Sigma-Aldrich, bezvodni etanol od tvrtke Acros Organics, bezvodni tetrahidrofuran (THF) od tvrtke Merck, a bezvodni dietil-eter od tvrtke J.T. Baker (SAD). Sve kemikalije bile su *p. a.* čistoće.

Bezvodni toluen dobiven je sljedećim postupkom: toluen je ekstrahiran vodom, osušen nad bezvodnim kalcijevim kloridom, destiliran i čuvan nad elementarnim natrijem. Bezvodni DMF priređen je na sljedeći način: smjesa 1 L DMF-a i 100 mL bezvodnog toluena destilirana je, pri čemu prvo destilira azeotropna smjesa toluena i vode, a zatim čisti DMF. DMF je čuvan nad aktiviranim molekulskim sitima. Bezvodni diklormetan dobiven je na prema sljedećem postupku: diklormetan je ekstrahiran vodom, sušen iznad kalcijevog klorida, predestiliran te čuvan nad aktiviranim molekulskim sitima.

Spojevi **1-3**, **14**, **17**, **23-26**, **28-30**, **32**, **33**, **35a-e**, **36a-e**, **37a-e**, **38**, **41** i **43-45** pripravljeni su prema ranije objavljenim propisima (42, 97, 98, 192–198), dok su spojevi **8**, **9**, **16** i **39** pripravljeni prema modificiranim ranije objavljenim propisima (42, 199). Spojevi **4**, **5**, **10** i **18** opisani su u literaturi (193, 200, 201), ali su pripravljeni novim metodama.

U reakcijama pretvorbe amina u azide korišten je imidazol-1-sulfonilazid hidroklorid (ISA × HCl) koji je pripravljen prema ranije objavljenom propisu (202). Ukratko, u suspenziju natrijevog azida (0,960 g, 14,767 mmol) u bezvodnom ACN-u (10 mL) dodan je SO_2Cl_2 (1,2 mL, 14,767 mmol) pri 0 °C. Reakcijska smjesa miješana je 24 h na s.t., nakon čega je dodan imidazol (2,011 g, 29,534 mmol) pri 0 °C te je nastavljeno miješanje tijekom 18 h na s.t. Reakcija smjesa razrijeđena je etil-acetatom (20 mL) te isprana zasićenom vodenom otopinom

$NaHCO_3$ (2 × 30 mL) i zasićenom vodenom otopinom NaCl (2 × 30 mL). Organski sloj je sušen nad bezvodnim Na_2SO_4 i profiltriran. Filtratu je dokapavana 1 M HCl u etil-acetatu pri 0 °C do prestanka taloženja. Nastali talog je odsisan i ispran etil-acetatom (2 × 10 mL).

Za ispitivanje antiproliferativnog djelovanja korištene su stanične linije iz Američke zbirke staničnih kultura. Dulbeccov modificirani Eagleov medij (DMEM), fetalni goveđi serum (FBS), penicilin (1×10^7 U/L)/streptomicin (1×10^4 mg/L) i tripsin-EDTA nabavljeni su od tvrtke Capricorn Scientific (Njemačka). Dimetilsulfoksid (DMSO) nabavljen je od tvrtke ITW Reagents (SAD), 3-(4,5-dimetiltiazol-2-il)-2,5-difeniltetrazolijev bromid (MTT) od tvrtke Thermo Fisher Scientific (SAD), a propan-2-ol od tvrtke Honeywell.

3.2. SINTEZE

3.2.1. Sinteza 1-(dimetoksimetil)-2,3,4,9-tetrahidro-1*H*-pirido[3,4-*b*]indola (1)

Suspenziji triptamina (1 g, 6,242 mmol, 1 ekv.) u diklormetanu (10 mL) uz miješanje su dodani 2,2-dimetoksiacetaldehid (1,13 mL, 7,49 mmol, 1,2 ekv.) i otopina TFA (0,669 mL, 8,739 mmol, 1,4 ekv.) u diklormetanu (2 mL). Reakcijska smjesa miješana je 18 h na s.t., nakon čega je razrijeđena diklormetanom (40 mL) te je dodana zasićena vodena otopina $NaHCO_3$ (30 mL). Vodeni sloj je zakiseljen 10 %-tnom otopinom HCl do pH ≈ 7,5 te je ekstrahiran diklormetanom (3 × 50 mL). Organski slojevi su skupljeni, sušeni nad bezvodnim Na_2SO_4, profiltrirani, a otapalo upareno pod sniženim tlakom. Dobiveni sirovi produkt **1** (žuto ulje) bez pročišćavanja je upotrijebljen u sljedećem reakcijskom koraku.

Iskorištenje: 1,352 g (88 %).

3.2.2. Sinteza 1-(dimetoksimetil)-9*H*-pirido[3,4-*b*]indola (2)

Otopini spoja **1** (1,352 g, 5,489 mmol, 1 ekv.) u bezvodnom THF-u (10 mL) uz miješanje je dodan $KMnO_4$ (3,470 g, 21,956 mmol, 4 ekv.). Reakcijska smjesa miješana je na s.t. 48 h, nakon čega je razrijeđena metanolom (5 mL) te profiltrirana kroz sloj Celita. Otapalo je iz filtrata uklonjeno uparavanjem pod sniženim tlakom, a ostatak nakon uparavanja otopljen u diklormetanu (50 mL) te ispran vodom (2 × 25 mL). Organski sloj je sušen nad bezvodnim Na_2SO_4, profiltriran te je otapalo upareno pod sniženim tlakom. Dobiveni sirovi produkt (smeđe ulje) bez pročišćavanja je upotrijebljen u sljedećem reakcijskom koraku.

Iskorištenje: 0,944 g (71 %).

3.2.3. Sinteza 9*H*-pirido[3,4-*b*]indol-1-karbaldehida (3)

Smjesa spoja **2** (0,944 g, 3,896 mmol), ledene octene kiseline (4,922 mL) i vode (7,383 mL) refluksirana je 1 h na 100 °C. Reakcijska smjesa je zalužena 5 %-tnom otopinom NaOH do pH 8-9 te ekstrahirana diklormetanom (3 × 50 mL). Organski slojevi su skupljeni, sušeni nad bezvodnim Na_2SO_4, profiltrirani te je otapalo upareno pod sniženim tlakom. Sirovi produkt

pročišćen je kromatografijom na koloni uz pokretnu fazu cikloheksan/etil-acetat/metanol 30:10:5 i rastrljavanjem u dietil-eteru.

Iskorištenje: 0,619 g (81 %).

3.2.4. Sinteza (9*H*-pirido[3,4-*b*]indol-1-il)metanola (5)

Suspenziji spoja **3** (0,550 g, 2,803 mmol, 1 ekv.) u bezvodnom THF-u (10 mL) dodan je $LiAlH_4$ (0,160 g, 4,205 mmol, 1,5 ekv.) te je reakcijska smjesa miješana 0,5 h na s.t. Zatim je dodana voda (20 mL) te je smjesa zalužena 5 %-tnom otopinom NaOH do pH 8-9 i ekstrahirana etil-acetatom (3 × 50 mL). Organski slojevi su skupljeni, sušeni nad bezvodnim Na_2SO_4, profiltrirani te je otapalo upareno pod sniženim tlakom. Sirovi produkt pročišćen je rastrljavanjem u dietil-eteru.

Iskorištenje: 0,505 g (91 %).

3.2.5. Sinteza metil-1-metil-2,3,4,9-tetrahidro-1*H*-pirido[3,4-*b*]indol-3-karboksilata (8)

Suspenziji hidroklorida metilnog estera triptofana (1 g, 3,926 mmol, 1 ekv.) u diklormetanu (10 mL) uz miješanje su dodani acetaldehid-dimetil-acetal (0,525 mL, 4,711 mmol, 1,2 ekv.) i otopina TFA (0,600 mL, 7,852 mmol, 2 ekv.) u vodi (2 mL). Reakcijska smjesa miješana je 18 h na s.t., nakon čega je razrijeđena diklormetanom (40 mL) te je dodana zasićena vodena otopina $NaHCO_3$ (30 mL). Vodeni sloj je zakiseljen 10 %-tnom HCl do pH ≈ 7,5 te je ekstrahiran diklormetanom (3 × 50 mL). Organski slojevi su skupljeni, sušeni nad bezvodnim Na_2SO_4, profiltrirani te je otapalo upareno pod sniženim tlakom. Dobiveni sirovi produkt (žuta smola) upotrijebljen je u sljedećem reakcijskom koraku bez pročišćavanja.

Iskorištenje: 0,782 g (82 %)

3.2.6. Sinteza etil-1-metil-9*H*-pirido[3,4-*b*]indol-3-karboksilata (9)

Suspenzija spoja **8** (0,2 g, 0,819 mmol) i 10 %-tnog Pd/C (0,038 g) u bezvodnom etanolu (4 mL) miješana je 0,33 h na 150 °C u mikrovalnom reaktoru. Zatim je reakcijska smjesa profiltrirana kroz sloj Celita, a otapalo uklonjeno iz filtrata uparavanjem pod sniženim tlakom. Sirovi produkt pročišćen je rastrljavanjem u smjesi dietil-etera i petroletera.

Iskorištenje: 0,148 g (71 %).

3.2.7. Sinteza (1-metil-9*H*-pirido[3,4-*b*]indol-3-il)metanola (10)

U otopinu spoja **9** (0,5 g, 1,966 mmol, 1 ekv.) u bezvodnom THF-u (10 mL) dodan je $LiAlH_4$ (0,112 g, 2,949 mmol, 1,5 ekv.) te je reakcijska smjesa miješana 0,5 h na s.t. Zatim je dodana voda (20 mL) te je smjesa zalužena 5 %-tnom otopinom NaOH do pH 8-9 i ekstrahirana etil-acetatom (3 × 50 mL). Organski slojevi su skupljeni, sušeni nad bezvodnim Na_2SO_4, profiltrirani te je otapalo upareno pod sniženim tlakom. Nakon rastrljavanja u dietil-eteru dobiven je prljavo-bijeli talog koji je upotrijebljen u sljedećim reakcijskim koracima bez pročišćavanja.

Iskorištenje: 0,376 g (90 %).

3.2.8. Sinteza azida β-karbolina 6 i 11. Opća metoda

Otopini alkohola **5** ili **10** (2,5 mmol, 1 ekv.) u bezvodnom THF-u (10 mL) pri 0 °C dodani su ADMP (1,711 g, 6 mmol, 2,4 ekv.) i DBU (1,122 mL, 7,5 mmol, 3 ekv.). Reakcijska smjesa miješana je 1 h na 0 °C, nakon čega je dodana zasićena vodena otopina NH_4Cl (20 mL) te je smjesa ekstrahirana diklormetanom (2 × 30 mL). Organski slojevi su skupljeni i isprani zasićenom vodenom otopinom NaCl (2 × 60 mL), sušeni nad bezvodnim Na_2SO_4, profiltrirani te je otapalo upareno pod sniženim tlakom. Sirovi produkt pročišćen je kromatografijom na koloni uz pokretnu fazu cikloheksan/etil-acetat/metanol 10:10:5.

1-(Azidometil)-9*H*-pirido[3,4-*b*]indola (6)

Količina reaktanta: 0,496 g alkohola **5**.

Iskorištenje: 0,407 g (73 %).

Ulje.

IR (ATR, ν/cm^{-1}) 3663, 3451, 3288, 3059, 2937, 2855, 2105, 1730, 1631, 1566, 1493, 1428, 1371, 1321, 1248, 1118, 1052, 971, 938, 873, 824, 751, 718, 620, 579, 432.

^{1}H NMR (DMSO-d_6) δ 11,78 (s, 1H), 8,36 (d, 1H, J = 5,2 Hz), 8,29–8,23 (m, 1H), 8,13 (d, 1H, J = 5,2 Hz), 7,64 (dt, 1H, J = 8,3, 0,9 Hz), 7,60–7,57 (m, 1H), 7,29–7,26 (m, 1H), 4,89 (s, 2H).

^{13}C NMR (DMSO-d_6) δ 140,58, 139,19, 137,75, 133,86, 128,50, 128,44, 121,87, 120,74, 119,57, 114,77, 112,02, 51,59.

ESI-MS: raspad.

3-(Azidometil)-1-metil-9*H*-pirido[3,4-*b*]indol (11)

Količina reaktanta: 0,531 g alkohola **10**.

Iskorištenje: 0,451 g (76 %).

Ulje.

IR (ATR, ν/cm^{-1}) 3671, 3451, 3239, 3051, 2937, 2863, 2447, 2325, 2104, 1689, 1631, 1566, 1509, 1452, 1403, 1354, 1264, 1085, 1036, 971, 848, 759, 718, 644, 579, 431.

^{1}H NMR (DMSO-d_6) δ 11,66 (s, 1H), 8,20 (d,1H, J = 7,9 Hz), 8,00 (s, 1H), 7,62–7,60 (m, 1H), 7,57–7,53 (m, 1H), 7,26–7,23 (m, 1H), 4,57 (s, 2H), 2,78 (s, 3H).

^{13}C NMR (DMSO-d_6) δ 143,23, 142,12, 140,74, 133,94, 128,02, 127,56, 121,74, 121,01, 119,39, 112,07, 111,72, 55,30, 20,41.

ESI-MS: raspad.

3.2.9. Sinteza amina β-karbolina 7 i 12. Opća metoda

U otopinu spoja **6** ili **11** (1 mmol) u bezvodnom metanolu (5 mL) dodan je 10 %-tni Pd/C te je reakcijska smjesa miješana 3 h na s.t. u atmosferi vodika. Reakcijska smjesa profiltrirana je kroz sloj Celita, a otapalo uklonjeno iz filtrata uparavanjem pod sniženim tlakom. Sirovi produkt pročišćen je prekristalizacijom iz smjese dietil-etera i petroletera.

(9*H*-pirido[3,4-*b*]indol-1-il)metanamin (7)

Količina reaktanta: 0,223 g azida **6**, 0,045 g 10 %-tnog Pd/C.

Iskorištenje: 0,112 g (57 %).

t_t = 201–205 °C (raspad).

IR (ATR, ν/cm^{-1}) 3347, 3282, 3120, 3051, 2955, 2856, 2776, 1625, 1600, 1562, 1501, 1477, 1460, 1430, 1355, 1327, 1316, 1240, 1212, 1163, 1127, 1108, 1071, 960, 896, 848, 829, 772, 747, 671, 595, 564, 516.

^{1}H NMR (DMSO-d_6) δ 8,26 (d, 1H, J = 5,2 Hz), 8,21 (dt, 1H, J = 7,8, 1,0 Hz), 7,97 (d, 1H, J = 5,2 Hz), 7,63–7,62 (m, 1H), 7,55–7,52 (m, 1H), 7,24–7,22 (m, 1H), 4,19 (s, 2H).

^{13}C NMR (DMSO-d_6) δ 146,51, 140,35, 137,18, 133,23, 127,82, 127,42, 121,60, 120,88, 119,15, 113,19, 112,01, 44,59.

ESI-MS: *m/z* 196,0 $(M-1)^-$.

(1-Metil-9*H*-pirido[3,4-*b*]indol-3-il)metanamin (12)

Količina reaktanta: 0,237 g azida **11**, 0,047 g 10 %-tnog Pd/C.

Iskorištenje: 0,129 g (61 %).

t_t = 176–178,5 °C.

IR (ATR, ν/cm^{-1}) 3338, 3239, 3130, 3057, 2978, 2940, 2914, 2882, 2850, 2783, 2737, 2690, 2637, 1626, 1606, 1566, 1503, 1453, 1401, 1374, 1344, 1317, 1284, 1250, 1176, 1147, 1103, 1083, 1009, 970, 945, 891, 838, 813, 775, 734, 643, 588, 545.

^{1}H NMR (DMSO-d_6) δ 11,42 (s, 1H), 8,14 (d, 1H, J = 7,6 Hz), 7,91 (s, 1H), 7,57–7,47 (m, 2H), 7,20 (t, 1H, J = 6,9 Hz), 3,89 (s, 2H), 2,73 (s, 3H).

^{13}C NMR (DMSO-d_6) δ 151,13, 140,89, 140,74, 133,29, 127,76, 127,62, 121,53, 121,19, 118,98, 111,89, 109,01, 47,59, 20,38.

ESI-MS: *m/z* 210,0 $(M-1)^-$.

3.2.10. Sinteza 1-metil-9*H*-pirido[3,4-*b*]indol-3-karbaldehida (14)

Otopini spoja **10** (0,2 g, 0,942 mmol, 1 ekv.) u bezvodnom diklormetanu (7 mL) dodan je MnO_2 (0,82 g, 9,43 mmol, 10 ekv.) te je reakcijska smjesa miješana 72 h na s.t. Zatim je reakcijska smjesa profiltrirana kroz sloj Celita, a otapalo uklonjeno iz filtrata uparavanjem pod sniženim tlakom. Sirovi produkt je pročišćen kromatografijom na koloni uz pokretnu fazu cikloheksan/etil-acetat/metanol 10:10:5 te rastrljavanjem u dietil-eteru.

Iskorištenje: 0,133 g (67 %).

3.2.11. Sinteza β-karbolinskih alkina 4 i 15. Opća metoda

Suspenziji spoja **3** ili **14** (0,5 mmol, 1 ekv.) i kalijevog karbonata (0,138 g, 1 mmol, 2 ekv.) u bezvodnom metanolu (7,7 mL) dodana je 10 %-tna otopina Bestmann-Ohirinog reagensa u ACN-u (0,901 mL, 0,6 mmol, 1,2 ekv.). Reakcijska smjesa miješana je u atmosferi argona 2-24 h na s.t., nakon čega je otapalo upareno pod sniženim tlakom. Ostatku nakon uparavanja (smeđa smola) uz ultrasoniciranje je dokapavana 5 %-tna otopina $NaHCO_3$ do prestanka stvaranja taloga koji je odsisan. Sirovi produkt pročišćen je Metodom A ili Metodom B.

Metoda A. Kromatografija na koloni uz pokretnu fazu diklormetan/metanol 90:10.

Metoda B. Kromatografija na koloni uz pokretnu fazu cikloheksan/etil-acetat/metanol 10:10:5 i prekristalizacija iz smjese acetona i vode.

1-Etinil-9*H*-pirido[3,4-*b*]indol (4)

Količina reaktanta: 0,098 g aldehida **3**.

Trajanje reakcije: 2 h.

Pročišćavanje: Metoda A.

Iskorištenje: 0,071 g (74 %).

3-Etinil-1-metil-9*H*-pirido[3,4-*b*]indola (15)

Količina reaktanta: 0,105 g aldehida **14**.

Trajanje reakcije: 24 h.

Pročišćavanje: Metoda B.

Iskorištenje: 0,063 g (61 %).

t_t = 230–235 °C (raspad).

IR (ATR, ν/cm^{-1}) 3306, 3143, 2104, 1622, 1597, 1563, 1499, 1446, 1375, 1338, 1315, 1247, 1178, 1146, 1014, 961, 899, 877, 776, 740, 654, 625, 587, 504, 457.

^{1}H NMR (DMSO-d_6) δ 11,83 (s, 1H), 8,25–8,22 (m, 1H), 8,21 (s, 1H), 7,62–7,59 (m, 1H), 7,57–7,53 (m, 1H), 7,27–7,23 (m, 1H), 4,03 (s, 1H), 2,74 (s, 3H).

^{13}C NMR (DMSO-d_6) δ 142,83, 140,70, 134,06, 129,54, 128,30, 127,01, 122,05, 120,72, 119,78, 117,22, 112,15, 84,85, 76,72, 20,33.

ESI-MS: *m/z* 207,6 $(M+1)^+$.

3.2.12. Sinteza 6-metoksi-1-metil-2,3,4,9-tetrahidro-1*H*-pirido[3,4-*b*]indol-2-ijevog trifluoracetata (16)

Otopini 5-metoksitriptamina (0,200 g, 1,051 mmol, 1 ekv.) u ACN-u (4,5 mL) dodani su acetaldehid-dimetil-acetal (0,234 mL, 2,102 mmol, 2 ekv.) i TFA (0,161 mL, 2,102 mmol, 2 ekv.). Reakcijska smjesa miješana je 0,17 h na 110 °C u mikrovalnom reaktoru, nakon čega je dodan dietil-eter (15 mL). Nastali talog je odsisan, ispran dietil-eterom (2 × 5 mL) i upotrijebljen u sljedećem reakcijskom koraku bez pročišćavanja.

Iskorištenje: 0,237 g (68 %).

3.2.13. Sinteza 6-metoksi-1-metil-9*H*-pirido[3,4-*b*]indola (17)

Suspenzija spoja **16** (0,200 g, 0,602 mmol, 1 ekv.), Li_2CO_3 (0,089 g, 1,204 mmol, 2 ekv.) i 10 %-tnog Pd/C (0,023 g) u bezvodnom etanolu (4 mL) miješana je 0,33 h na 150 °C u mikrovalnom reaktoru. Potom je reakcijska smjesa profiltrirana kroz sloj Celita, a otapalo uklonjeno iz filtrata uparavanjem pod sniženim tlakom. Ostatak nakon uparavanja rastrljan je u 20 %-tnoj vodenoj otopini NaCl. Nastali svijetlo žuti talog je odsisan i prekristaliziran iz dietil-etera.

Iskorištenje: 0,121 g (95 %).

3.2.14. Sinteza 1-metil-9*H*-pirido[3,4-*b*]indol-6-ola (18)

Smjesa spoja **17** (0,100 g, 0,471 mmol), 47 %-tne bromovodične kiseline (2 mL) i ledene octene kiseline (2,5 mL) miješana je 0,5 h na 140 °C u mikrovalnom reaktoru. Zatim je reakcijska smjesa zalužena 5 M otopinom NaOH do pH 9 i ekstrahirana etil-acetatom (5 × 40 mL). Organski slojevi su skupljeni, sušeni nad bezvodnim Na_2SO_4, profiltrirani, a otapalo upareno pod sniženim tlakom. Sirovi produkt pročišćen je kromatografijom na koloni uz pokretnu fazu diklormetan/metanol 75:25 i rastrljavanjem u dietil-eteru.

Iskorištenje: 0,080 g (86 %).

3.2.15. Sinteza *tert*-butil-(2-((1-metil-9*H*-pirido[3,4-*b*]indol-6-il)oksi)etil)karbamata (20)

U suspenziju spoja **18** (0,3 g, 1,513 mmol, 1 ekv.) u bezvodnom DMF-u (5 mL) dodani su cezijev karbonat (1,380 g, 4,236 mmol, 2,8 ekv.), TBAHS (0,411 g, 1,210 mmol, 0,8 ekv.) i $BocNH(CH_2)_2Br$ (1,356 g, 6,052 mmol, 4 ekv.). Reakcijska smjesa miješana je 18 h na s.t. u atmosferi argona, nakon čega je razrijeđena vodom (50 mL) i ekstrahirana etil-acetatom (3 × 50 mL). Organski slojevi su skupljeni, isprani vodom (2 × 150 mL), sušeni nad bezvodnim Na_2SO_4, profiltrirani, a otapalo je uklonjeno iz filtrata uparavanjem pod sniženim tlakom. Sirovi produkt pročišćen je kromatografijom na koloni uz pokretnu fazu diklormetan/metanol 80:10 i rastrljavanjem u smjesi dietil-etera i petroletera.

Iskorištenje: 0,325 g (63 %).

Ulje.

^{1}H NMR (DMSO-d_6) δ 11,42 (s, 1H), 8,16 (d, 1H, J = 5,3 Hz), 7,92 (d, 1H, J = 5,3 Hz), 7,77 (d, 1H, J = 1,7 Hz), 7,51 (d, 1H, J = 8,8 Hz), 7,18 (dd, 1H, J = 8,8, 2,3 Hz), 7,06 (t, 1H, J = 5,0 Hz), 4,05 (t, 2H, J = 5,8 Hz), 3,39–3,34 (m, 2H), 2,75 (s, 3H), 1,40 (s, 9H).

^{13}C NMR (DMSO-d_6) δ 155,73, 152,39, 142,04, 136,57, 135,41, 135,03, 126,88, 121,35, 118,42, 112,78, 112,75, 104,68, 77,76, 67,19, 39,61, 28,24, 20,23.

ESI-MS: *m/z* 342,4 $(M+1)^+$.

3.2.16. Sinteza 1-metil-9*H*-pirido[3,4-*b*]indol-7-ola (23)

Smjesa harmina (0,250 g, 1,178 mmol), ledene octene kiseline (3 mL) i 47 %-tne bromovodične kiseline (1,5 mL) miješana je 0,5 h na 140 °C u mikrovalnom reaktoru. Zatim je reakcijska smjesa zalužena 5 %-tnom otopinom NaOH do pH 8-9 i ekstrahirana etil-acetatom (5 × 40 mL). Organski slojevi su skupljeni, sušeni nad bezvodnim Na_2SO_4, profiltrirani, a otapalo je uklonjeno iz filtrata uparavanjem pod sniženim tlakom. Sirovi produkt pročišćen je kromatografijom na koloni uz pokretnu fazu diklormetan/metanol 85:15 i rastrljavanjem u dietil-eteru.

Iskorištenje: 0,215 g (92 %).

3.2.17. Sinteza alkina β-karbolina 13, 19 i 24. Opća metoda

Otopini alkohola **10**, odnosno fenola **18** ili **23** (1 mmol, 1 ekv.) u bezvodnom DMF-u (5 mL) dodani su cezijev karbonat (0,456 g, 1,4 mmol, 1,4 ekv.) i 80 %-tna otopina propargil-bromida u toluenu (0,134 mL, 1,2 mmol, 1,2 ekv.) te je reakcijska smjesa miješana 3-5 h na s.t. u atmosferi argona. Zatim je reakcijska smjesa razrijeđena vodom (50 mL) te je ekstrahirana etil-acetatom (3 × 50 mL). Organski slojevi su skupljeni, isprani vodom (2 × 150 mL), sušeni nad bezvodnim Na_2SO_4, profiltrirani te je otapalo upareno pod sniženim tlakom. Sirovi produkt pročišćen je kromatografijom na koloni uz pokretnu fazu diklormetan/metanol i rastrljavanjem u smjesi dietil-etera i petroletera.

(1-Metil-9-(prop-2-in-1-il)-9*H*-pirido[3,4-*b*]indol-3-il)metanol (13)

Količina reaktanta: 0,212 g alkohola **10**.

Trajanje reakcije: 5 h.

Pokretna faza: diklormetan/metanol 95:5.

Iskorištenje: 0,180 g (72 %).

t_t = 225–230 °C (raspad).

IR (ATR, ν/cm^{-1}) 3154, 2929, 2823, 2109, 1621, 1561, 1475, 1453, 1360, 1333, 1283, 1206, 1139, 1063, 1040, 965, 933, 877, 744, 724, 641, 578.

^{1}H NMR (DMSO-d_6) δ 8,25 (d, 1H, J = 7,8 Hz), 8,03 (s, 1H), 7,78 (d, 1H, J = 8,3 Hz), 7,63–7,58 (m, 1H), 7,29 (t, 1H, J = 7,4 Hz), 5,45 (d, 2H, J = 2,4 Hz), 5,35 (t, 1H, J = 5,8 Hz), 4,68 (d, 2H, J = 5,8 Hz), 3,35 (t, 1H, J = 2,4 Hz), 3,04 (s, 3H).

^{13}C NMR (DMSO-d_6) δ 150,83, 141,27, 140,52, 133,22, 129,53, 128,23, 121,52, 121,05, 120,04, 110,37, 109,11, 75,50, 64,34, 34,19, 22,45.

ESI-MS: *m/z* 251,1 $(M+1)^+$.

1-Metil-6-(prop-2-in-1-iloksi)-9*H*-pirido[3,4-*b*]indol (19)

Količina reaktanta: 0,198 g fenola **18**.

Trajanje reakcije: 3 h.

Pokretna faza: diklormetan/metanol 97:3, 95:5.

Iskorištenje: 0,120 g (51 %).

t_t = 175,5–177,5 °C.

IR (ATR, ν/cm^{-1}) 3292, 3122, 3054, 2950, 2860, 2766, 2716, 2366, 2330, 2128, 2058, 1866, 1764, 1736, 1606, 1570, 1506, 1476, 1448, 1412, 1380, 1334, 1292, 1260, 1200, 1120, 1068, 1030, 986, 944, 914, 886, 818, 758, 646, 524.

^{1}H NMR (DMSO-d_6) δ 11,42 (s, 1H), 8,17 (d, 1H, J = 5,4 Hz), 7,88 (d, 1H, J = 5,3 Hz), 7,81 (d, 1H, J = 2,5 Hz), 7,53 (d, 1H, J = 8,9 Hz), 7,23 (dd, 1H, J = 8,8, 2,5 Hz), 4,88 (d, 2H, J = 2,4 Hz), 3,56 (t, 1H, J = 2,4 Hz), 2,75 (s, 3H).

^{13}C NMR (DMSO-d_6) δ 151,09, 142,26, 137,03, 135,67, 135,12, 126,63, 121,27, 118,34, 112,72, 112,62, 105,62, 78,04, 56,26, 20,40.

ESI-MS: *m/z* 237,1 $(M+1)^+$.

1-Metil-7-(prop-2-in-1-iloksi)-9*H*-pirido[3,4-*b*]indol (24)

Količina reaktanta: 0,198 g fenola **23**.

Trajanje reakcije: 3 h.

Pokretna faza: diklormetan/metanol 97:3, 95:5.

Iskorištenje: 0,137 g (58 %)

3.2.18. Sinteza Boc-zaštićenih amina β-karbolina 25 i 29. Opća metoda

U suspenziju harmola **23** ili harmina (1 mmol, 1 ekv.) u bezvodnom DMF-u (3 mL) dodani su cezijev karbonat (0,456 g, 1,4 mmol, 1,4 ekv.) i $BocNH(CH_2)_2Br$ (0,538 g, 2,4 mmol, 2,4 ekv.) te je reakcijska smjesa miješana 18 h na 90 °C u atmosferi argona. Zatim je reakcijska smjesa razrijeđena vodom (30 mL) i ekstrahirana etil-acetatom (3 × 40 mL). Organski slojevi su skupljeni, isprani vodom (2 × 100 mL), sušeni nad bezvodnim Na_2SO_4, profiltrirani, a otapalo uklonjeno iz filtrata uparavanjem pod sniženim tlakom. Sirovi produkt pročišćen je kromatografijom na koloni uz pokretnu fazu diklormetan/metanol 80:10 i rastrljavanjem u smjesi dietil-etera i petroletera.

***Tert*-butil-(2-((1-metil-9*H*-pirido[3,4-*b*]indol-7-il)oksi)etil)karbamat (25)**

Količina reaktanta: 0,198 g fenola **23**.

Iskorištenje: 0,239 g (70 %).

***Tert*-butil-(2-(7-metoksi-1-metil-9*H*-pirido[3,4-*b*]indol-9-il)etil)karbamat (29)**

Količina reaktanta: 0,212 g harmina.

Iskorištenje: 0,125 g (59 %).

3.2.19. Sinteza amina β-karbolina 21, 26 i 30. Opća metoda

Otopini spoja **20**, **25** ili **29** (1 mmol, 1 ekv.) u metanolu (6 mL) dodana je 4 M otopina HCl u MeOH (2,5 mL, 10 mmol, 10 ekv.) te je reakcijska smjesa miješana 18 h na 50 °C, nakon čega je otapalo upareno pod sniženim tlakom. Ostatku nakon uparavanja dodana je voda (20 mL) te je smjesa zalužena 5 %-tnim NaOH do pH 9-10 i ekstrahirana etil-acetatom (5 × 50 mL). Organski slojevi su skupljeni, sušeni nad bezvodnim Na_2SO_4, profiltrirani, a otapalo je uklonjeno iz filtrata uparavanjem pod sniženim tlakom. Ostatak nakon uparavanja rastrljan je u dietil-eteru.

2-((1-Metil-9*H*-pirido[3,4-*b*]indol-6-il)oksi)etan-1-amin (21)

Količina reaktanta: 0,341 g spoja **20**.

Iskorištenje: 0,166 g (69 %).

t_t = 170,5–172 °C.

IR (ATR, ν/cm^{-1}) 3645, 3359, 3241, 3065, 2925, 2869, 1605, 1581, 1566, 1500, 1478, 1458, 1401, 1288, 1234, 1211, 1126, 1071, 1059, 992, 905, 884, 847, 825, 816, 741, 703, 632.

^{1}H NMR (DMSO-d_6) δ 11,36 (s, 1H), 8,15 (d, 1H, J = 5,3 Hz), 7,90 (d, 1H, J = 5,3 Hz), 7,74 (d, 1H, J = 2,3 Hz), 7,50 (d, 1H, J = 8,8 Hz), 7,19 (dd, 1H, J = 8,8, 2,5 Hz), 4,02 (t, 2H, J = 5,8 Hz), 2,94 (t, 2H, J = 5,7 Hz), 2,74 (s, 3H).

^{13}C NMR (DMSO-d_6) δ 152,47, 141,87, 136,70, 135,19, 134,93, 126,54, 121,29, 117,98, 112,34, 112,18, 104,86, 71,06, 40,87, 19,97.

ESI-MS: m/z 242,2 $(M+1)^+$.

2-((1-Metil-9*H*-pirido[3,4-*b*]indol-7-il)oksi)etan-1-amin (26)

Količina reaktanta: 0,341 g spoja **26**.

Iskorištenje: 0,225 g (88 %).

2-(7-Metoksi-1-metil-9*H*-pirido[3,4-*b*]indol-9-il)etan-1-amin (30)

Količina reaktanta: 0,355 g spoja **30**.

Iskorištenje: 0,125 g (59 %).

3.2.20. Sinteza azida β-karbolina 22, 27 i 31. Opća metoda

Suspenziji amina **21**, **26** ili **30** (1 mmol, 1 ekv.), kalijevog karbonata (0,346 g, 2,5 mmol, 2,5 ekv.) i $CuSO_4 \times 5H_2O$ (*q.s.*, vrh špatule) u bezvodnom metanolu (5 mL) dodan je ISA × HCl (0,252 g, 1,2 mmol, 1,2 ekv.) te je reakcijska smjesa miješana 2–18 h na s.t. Zatim je otapalo upareno pod sniženim tlakom, a ostatku nakon uparavanja je dodana voda (20 mL) te je ekstrahirano etil-acetatom (2 × 30 mL). Organski slojevi su skupljeni, sušeni nad bezvodnim Na_2SO_4, profiltrirani, a otapalo uklonjeno iz filtrata uparavanjen pod sniženim tlakom. Sirovi produkt pročišćen je kromatografijom na koloni uz pokretnu fazu cikloheksan/etil-acetat/metanol 10:10:5.

6-(2-Azidoetoksi)-1-metil-9*H*-pirido[3,4-*b*]indol (22)

Količina reaktanta: 0,241 g amina **21**.

Trajanje reakcije: 2 h.

Iskorištenje: 0,246 g (92 %).

7-(2-Azidoetoksi)-1-metil-9*H*-pirido[3,4-*b*]indol (27)

Količina reaktanta: 0,241 g amina **26**.

Trajanje reakcije: 18 h.

Iskorištenje: 0,211 g (79 %).

Ulje.

^{1}H NMR (DMSO-d_6) δ 11,44 (s, 1H), 8,16 (d, 1H, J = 5,3 Hz), 8,08 (d, 1H, J = 8,6 Hz), 7,82 (d, 1H, J = 5,2 Hz), 7,04 (d, 1H, J = 2,2 Hz), 6,87 (dd, 1H, J = 8,6, 2,2 Hz), 4,30 (t, 2H, J = 4,8 Hz), 3,72 (t, 2H, J = 4,8 Hz), 2,73 (s, 3H).

^{13}C NMR (DMSO-d_6) δ 158,70, 141,77, 141,35, 137,78, 134,60, 127,12, 122,75, 115,26, 111,99, 109,14, 95,62, 67,14, 49,64, 20,33.

ESI-MS: raspad.

9-(2-Azidoetil)-7-metoksi-1-metil-9*H*-pirido[3,4-*b*]indol (31)

Količina reaktanta: 0,255 g amina **30**.

Trajanje reakcije: 3 h.

Iskorištenje: 0,149 g (53 %).

3.2.21. Sinteza 7-metoksi-1-metil-9-(prop-2-in-1-il)-9*H*-pirido[3,4-*b*]indola (28)

Otopini harmina (0,250 g, 1,179 mmol, 1 ekv.) u bezvodnom DMF-u (5 mL) dodani su natrijev hidrid (0,075 g, 1,886 mmol, 1,6 ekv.) i 80 %-tna otopina propargil-bromida u toluenu (0,394 mL, 3,537 mmol, 3 ekv.) te je reakcijska smjesa miješana 3 h na s.t. u atmosferi argona. Zatim je reakcijska smjesa razrijeđena vodom (50 mL) te je ekstrahirana etil-acetatom (3 × 50 mL). Organski slojevi su skupljeni, isprani vodom (2 × 150 mL), sušeni nad bezvodnim Na_2SO_4, profiltrirani te upareni pod sniženim tlakom. Sirovi produkt pročišćen je kromatografijom na koloni uz pokretnu fazu diklormetan/metanol 95:5 i rastrljavanjem u smjesi dietil-etera i petroletera.

Iskorištenje: 0,168 g (57 %).

3.2.22. Sinteza metil-3-(7-metoksi-1-metil-9*H*-pirido[3,4-*b*]indol-9-il)propanoata (32)

Suspenziji harmina (0,250 g, 1,178 mmol, 1 ekv.) u ACN-u (5 mL) dodan je DBU (0,324 mL, 2,120 mmol, 1,8 ekv.) te je reakcijska smjesa miješana 0,5 h na s.t. Zatim je dodan metil-akrilat (0,267 mL, 2,945 mmol, 2,5 ekv.), nakon čega je miješanje reakcijske smjese nastavljeno tijekom 48 h na 60 °C uz zaštitu od svjetlosti. Otapalo je upareno, a sirovi produkt je pročišćen kromatografijom na koloni uz pokretnu fazu diklormetan/metanol 80:10 i rastrljavanjem u dietil-eteru.

Iskorištenje: 0,214 g (61 %).

3.2.23. Sinteza 3-(7-metoksi-1-metil-9*H*-pirido[3,4-*b*]indol-9-il)propanske kiseline (33)

Suspenziji spoja **32** (0,214 g, 0,718 mmol, 1 ekv.) u metanolu (2 mL) uz miješanje je dokapana otopina LiOH × H_2O (0,06 g, 1,436 mmol, 2 ekv.) u smjesi vode (2 mL) i metanola (2 mL). Reakcijska smjesa je miješana 1 h na s.t., nakon čega je otapalo upareno pod sniženim tlakom. Ostatak nakon uparavanja je otopljen u vodi (20 mL) te je vodeni sloj zakiseljen 10 %-tnom HCl do pH 5,5. Nastali talog je odsisan i ispran dietil-eterom (2 × 10 mL).

Iskorištenje: 0,180 g (88 %).

3.2.24. Sinteza propargilnih estera DCK-a (34a-e). Opća metoda

Suspenziji odgovarajućeg DCK-a (3,375 mmol, 1 ekv.) i kalijevog karbonata (0,653 g, 4,725 mmol, 1,4 ekv.) u bezvodnom DMF-u (5 mL) dokapana je 80 %-tna otopina propargil-bromida u toluenu (0,601 mL, 5,4 mmol, 1,6 ekv.) te je reakcijska smjesa miješana 48 h na s.t. Zatim je reakcijska smjesa razrijeđena vodom (50 mL) i ekstrahirana etil-acetatom (3 × 50 mL). Organski slojevi su skupljeni, isprani vodom (2 × 150 mL), sušeni nad bezvodnim Na_2SO_4, profiltrirani, a otapalo uklonjeno iz filtrata uparavanjem pod sniženim tlakom. Sirovi produkt pročišćen je kromatografijom na koloni uz pokretnu fazu cikloheksan/etil-acetat/metanol 10:10:5.

Prop-2-in-1-il cinamat (34a)

Količina reaktanta: 0,500 g *trans*-cimetne kiseline.

Iskorištenje: 0,584 g (93 %).

Prop-2-in-1-il *(E)*-3-(3-fluorfenil)akrilat (34b)

Količina reaktanta: 0,561 g *m*-fluorcimetne kiseline.

Iskorištenje: 0,648 g (94 %).

Prop-2-in-1-il *(E)*-3-(3-bromfenil)akrilat (34c)

Količina reaktanta: 0,766 g *m*-bromcimetne kiseline.

Iskorištenje: 0,779 g (87 %).

t_t 79,0–81,0 °C.

IR (ATR, υ/cm^{-1}) 3416, 3279, 3060, 3042, 2940, 2132, 1716, 1637, 1561, 1479, 1419, 1360, 1295, 1201, 1169, 1073, 991, 965, 851, 780, 754, 696, 665, 632, 554.

^{1}H NMR (DMSO-d_6) δ 8,02 (t, 1H, J =1,8 Hz), 7,78 (dt, 1H, J = 7,7, 1,4 Hz), 7,69 (d, 1H, J = 16,1 Hz), 7,64–7,62 (m, 1H), 7,39 (t, 1H, J = 7,9 Hz), 6,79 (d, 1H, J = 16,1 Hz), 4,84 (d, 2H, J = 2,4 Hz), 3,59 (t, 1H, J = 2,5 Hz).

^{13}C NMR (DMSO-d_6) δ 165,21, 143,81, 136,38, 133,17, 130,99, 130,97, 127,45, 122,32, 118,90, 77,80, 51,93.

ESI-MS: raspad.

Prop-2-in-1-il *(E)*-3-(4-klorfenil)akrilat (34d)

Količina reaktanta: 0,616 g *p*-klorcimetne kiseline.

Iskorištenje: 0,700 g (94 %).

Prop-2-in-1-il *(E)*-3-(4-metoksifenil)akrilat (34e)

Količina reaktanta: 0,601 g *p*-metoksicimetne kiseline.

Iskorištenje: 0,540 g (74 %).

3.2.25. Sinteza etilnih estera derivata cimetne kiseline (35a-e). Opća metoda

Suspenzija cimetne kiseline ili odgovarajućeg DCK-a (6,749 mmol, 1 ekv.) i tionil-klorida (2,461 mL, 33,745 mmol, 5 ekv.) u bezvodnom toluenu (10 mL) miješana je 1 h na s.t. u prisutnosti katalitičke količine bezvodnog DMF-a. Otapalo je upareno pod sniženim tlakom, a ostatak je naparen dva puta bezvodnim toulenom i korišten u sljedećem reakcijskom koraku bez pročišćavanja.

Otopina odgovarajućeg kiselinskog klorida u bezvodnom diklormetanu (10 mL) dokapana je u otopinu TEA (0,941 mL, 6,749 mmol, 1 ekv.) u bezvodnom etanolu (5 mL) te je reakcijska smjesa miješana 3 h na s.t. Zatim je otapalo upareno pod sniženim tlakom, a ostatak otopljen u etil-acetatu (30 mL) i ispran vodom (2 × 30 mL). Organski sloj je sušen nad bezvodnim Na_2SO_4, profiltriran, a otapalo uklonjeno iz filtrata uparavanjem pod sniženim tlakom.

Etil-cinamat (35a)

Količina reaktanta: 1 g cimetne kiseline.

Iskorištenje: 1,022 g (86 %).

Etil-(*E*)-3-(3-fluorfenil)prop-2-enoat (35b)

Količina reaktanta: 1,121 g *m*-fluorcimetne kiseline.

Iskorištenje: 0,721 g (55 %).

Etil-(*E*)-3-(3-bromfenil)prop-2-enoat (35c)

Količina reaktanta: 1,532 g *m*-bromcimetne kiseline.

Iskorištenje: 1,549 g (90 %).

Etil-(*E*)-3-(4-klorfenil)prop-2-enoat (35d)

Količina reaktanta: 1,232 g *p*-klorcimetne kiseline.

Iskorištenje: 1,294 g (91 %).

Etil-(*E*)-3-(4-metoksifenil)prop-2-enoat (35e)

Količina reaktanta: 1,203 g *p*-metoksicimetne kiseline.

Iskorištenje: 1,045 g (75 %).

3.2.26. Sinteza cimetnih alkohola (36a-e). Opća metoda

Otopini odgovarajućeg estera DCK-a **35a-e** (3,752 mmol, 1 ekv.) u bezvodnom dietil-eteru (1 mL) pri –5 °C dodan je $LiAlH_4$ (0,142 g, 3,752 mmol, 1 ekv.) u malim obrocima. Reakcijska smjesa miješana je 1,5 h na < 0 °C u atmosferi argona, nakon čega je dodana voda (20 mL). Smjesa je zakiseljena s nekoliko kapi 10 %-tne klorovodične kiseline do prestanka pjenjenja.

Potom je dodan dietil-eter (10 mL) te je smjesa isprana 1 %-tnom klorovodičnom kiselinom (2 × 20 mL) i vodom (2 × 20 mL). Organski sloj je sušen nad bezvodnim Na_2SO_4, profiltriran, a otapalo je uklonjeno iz filtrata uparavanjem pod sniženim tlakom. Sirovi produkt pročišćen je kromatografijom na koloni uz pokretnu fazu cikloheksan/etil-acetat 2:1 te je dobiven uljasti produkt.

(*E*)-3-fenilprop-2-en-1-ol (36a)

Količina reaktanta: 0,661 g estera **35a**.

Iskorištenje: 0,226 g (45 %).

(*E*)-3-(3-fluorfenil)prop-2-en-1-ol (36b)

Količina reaktanta: 0,729 g estera **35b**.

Iskorištenje: 0,188 g (33 %).

(*E*)-3-(3-bromfenil)prop-2-en-1-ol (36c)

Količina reaktanta: 0,957 g estera **35c**.

Iskorištenje: 0,384 g (48 %).

(*E*)-3-(4-klorfenil)prop-2-en-1-ol (36d)

Količina reaktanta: 0,790 g estera **35d**.

Iskorištenje: 0,291 g (46 %).

(*E*)-3-(4-metoksifenil)prop-2-en-1-ol (36e)

Količina reaktanta: 0,774 g estera **35e**.

Iskorištenje: 0,308 g (50 %).

3.2.27. Sinteza azida DCK-a (37a-e). Opća metoda

Otopini odgovarajućeg alkohola **36a-e** (1,491 mmol, 1 ekv.) u bezvodnom THF-u (5 mL) pri 0 °C dodani su ADMP (0,510 g, 1,789 mmol, 1,2 ekv.) i DBU (0,289 mL, 1,938 mmol, 1,3 ekv.). Reakcijska smjesa miješana je 0,5 h na 0 °C, nakon čega je dodana zasićena otopina NH_4Cl (20 mL) te je smjesa ekstrahirana diklormetanom (2 × 20 mL). Organski slojevi su skupljeni i isprani zasićenom vodenom otopinom NaCl (2 × 40 mL), sušeni nad bezvodnim Na_2SO_4, profiltrirani, a otapalo je uklonjeno iz filtrata uparavanjem pod sniženim tlakom. Sirovi produkt je pročišćen kromatografijom na koloni uz pokretnu fazu cikloheksan/etil-acetat 9:1.

(*E*)-(3-azidoprop-1-en-1-il)benzen (37a)

Količina reaktanta: 0,200 g alkohola **36a**.

Iskorištenje: 0,136 g (57 %).

(*E*)-1-(3-azidoprop-1-en-1-il)-3-fluorbenzen (37b)

Količina reaktanta: 0,227 g alkohola **36b**.

Iskorištenje: 0,180 g (68 %).

(*E*)-1-(3-azidoprop-1-en-1-il)-3-brombenzen (37c)

Količina reaktanta: 0,318 g alkohola **36c**.

Iskorištenje: 0,195 g (55 %).

(*E*)-1-(3-azidoprop-1-en-1-il)-4-klorbenzen (37d)

Količina reaktanata: 0,251 g alkohola **36d**.

Iskorištenje: 0,202 g (70 %).

(*E*)-1-(3-azidoprop-1-en-1-il)-4-metoksibenzen (37e)

Količina reaktanata: 0,245 g alkohola **36e**.

Iskorištenje: 0,212 g (75 %).

3.2.28. Sinteza 4-azido-7-klorkinolina (38)

Otopini 4,7-diklorkinolina (0,5 g, 2,525 mmol, 1 ekv.) u bezvodnom DMF-u (3 mL) dodan je NaN_3 (0,492 g, 7,575 mmol, 3 ekv.) te je reakcijska smjesa miješana 18 h na 65 °C. Zatim je reakcijska smjesa razrijeđena diklormetanom (30 mL), isprana vodom (3 × 30 mL), a otapalo upareno pod sniženim tlakom. Sirovi produkt pročišćen je rastrljavanjem u dietil-eteru.
Iskorištenje: 0,191 g (37 %).

3.2.29. Sinteza 2-((7-klorkinolin-4-il)amino)etan-1-ola (39)

Smjesa 4,7-diklorkinolina (0,198 g, 1 mmol, 1 ekv.), etanolamina (0,121 mL, 2 mmol, 2 ekv.) i TEA (0,209 mL, 1,5 mmol, 1,5 ekv.) miješana je 2 h na 120 °C. Nakon toga je u reakcijsku smjesu dodan led te je smjesa hlađena 1 sat na 4 °C. Nastali talog je odsisan te ispran vodom (2 × 10 mL) i dietil-eterom (2 × 10 mL). Sirovi produkt pročišćen je prekristalizacijom iz metanola.

Iskorištenje: 0,143 g (64 %).

3.2.30. Sinteza *N*-(2-azidoetil)-7-klorkinolin-4-amina (40)

U otopinu spoja **39** (0,143 g, 0,642 mmol, 1 ekv.) u bezvodnom THF-u (3 mL) pri 0 °C dodani su ADMP (0,263 g, 0,924 mmol, 1,4 ekv.) i DBU (0,150 mL, 1,002 mmol, 1,6 ekv.). Reakcijska smjesa miješana je 1,5 h na 0 °C, nakon čega je dodana zasićena otopina amonijevog klorida (20 mL). Smjesa je ekstrahirana diklormetanom (2 × 30 mL). Organski slojevi su skupljeni, isprani zasićenom vodenom otopinom natrijevog klorida (2 × 30 mL), sušeni nad bezvodnim Na_2SO_4, profiltrirani, otapalo uklonjeno iz filtrata uparavanjem pod sniženim tlakom. Sirovi produkt pročišćen je kromatografijom na koloni uz pokretnu fazu cikloheksan/etil-acetat/metanol 10:10:5 i rastrljavanjem u smjesi dietil-etera i petroletera.

Iskorištenje: 0,092 g (58 %).

3.2.31. Sinteza 7-klorkinolin-4-ola (41)

Smjesa 4,7-diklorkinolina (1 g, 5,049 mmol) i ledene octene kiseline (1,9 mL) refluksirana je 1 h na 125 °C, nakon čega je dodan dietil-eter (10 mL), a nastali talog je odsisan te ispran vodom (2 × 10 mL) i dietil-eterom (2 × 10 mL). Dobiveni sirovi produkt **41** (bijeli prah) je korišten u sljedećem reakcijskom koraku bez pročišćavanja.
Iskorištenje: 0,186 g (36 %).

3.2.32. Sinteza 7-klor-4-(prop-2-in-1-iloksi)kinolina (42)

Otopini spoja **41** (0,2 g, 1,114 mmol, 1 ekv.) u bezvodnom DMF-u (4 mL) dodani su cezijev karbonat (0,508 g, 1,56 mmol, 1,4 ekv.) i 80 %-tna otopina propargil-bromida u toluenu (0,143 mL, 1,337 mmol, 1,2 ekv.) te je reakcijska smjesa miješana 1 h na s.t. u atmosferi argona. Zatim je dodana voda (40 mL) te je smjesa ekstrahirana etil-acetatom (3 × 40 mL). Organski slojevi su skupljeni, isprani vodom (2 × 120 mL), sušeni nad bezvodnim Na_2SO_4, profiltrirani, a otapalo uklonjeno iz filtrata uparavanjem pod sniženim tlakom. Sirovi produkt pročišćen je rastrljavanjem u dietil-eteru.

Iskorištenje: 0,172 g (71 %).

3.2.33. Sinteza (7-klorkinolin-4-il)glicina (43)

Smjesa 4,7-diklorkinolina (1 g, 5,049 mmol, 1 ekv.), glicina (0,758 g, 10,098 mmol, 2 ekv.) i fenola (2,737 g, 29,082 mmol, 5,8 ekv.) refluksirana je 18 h na 125 °C, nakon čega je dodan dodatni obrok glicina (0,379 g, 5,049 mmol, 1 ekv.) te je refluksiranje nastavljeno tijekom 3 h. Zatim je dodan etil-acetat (20 mL), a nastali talog je odsisan, ispran etil-acetatom (20 mL) i otopljen u 10 %-tnom $NaHCO_3$ uz zagrijavanje. Vodena otopina je isprana toluenom (2 × 50 mL) te je zakiseljena 10 %-tnom otopinom HCl do pH 5,7. Nastali bijeli talog je odsisan, ispran vodom (2 × 5 mL) i dietil-eterom (2 × 5 mL).

Iskorištenje: 0,595 g (50 %).

3.2.34. Sinteza amina 7-klorkinolina 44 i 45. Opća metoda

Smjesa 4,7-diklorkinolina (0,4 g, 2,02 mmol, 1 ekv.) i odgovarajućeg diamina (20,197 mmol, 10 ekv.) miješana je 1 h na 95 °C u mikrovalnom reaktoru. Reakcijska smjesa je razrijeđena diklormetanom (50 mL) te isprana 5 %-tnim NaOH (3 × 50 mL). Organski sloj je sušen nad bezvodnim Na_2SO_4, profiltriran, a otapalo uklonjeno iz filtrata uparavanjem pod sniženim tlakom. Sirovi produkt je rastrljan u smjesi dietil-etera i petroletera.

N^1-(7-Klorkinolin-4-il)etan-1,2-diamin (44)

Količina reaktanta: 1,49 mL diaminoetana.

Iskorištenje: 0,335 g (75 %).

N^1-(7-Klorkinolin-4-il)butan-1,4-diamin (45)

Količina reaktanta: 2,03 mL 1,4-diaminobutana.

Iskorištenje: 0,388 g (77 %).

3.2.35. Sinteza azidometilferocena (46)

U otopinu ferocen-metanola (0,2 g, 0,926 mmol, 1 ekv.) u bezvodnom THF-u (7 mL) pri 0 °C dodani su ADMP (0,660 g, 2,316 mmol, 2,5 ekv.) i DBU (0,374 mL, 2,5 mmol, 2,7 ekv.). Reakcijska smjesa miješana je 2 h na 0 °C, nakon čega je dodana zasićena vodena otopina NH_4Cl (20 mL) te je smjesa ekstrahirana diklormetanom (2 × 30 mL). Organski slojevi su skupljeni i isprani zasićenom vodenom otopinom NaCl (2 × 60 mL), sušeni nad bezvodnim Na_2SO_4, profiltrirani, a otapalo uklonjeno iz filtrata uparavanjem pod sniženim tlakom. Sirovi produkt je pročišćen kromatografijom na koloni uz pokretnu fazu cikloheksan/etil-acetat/metanol 10:10:5.
Iskorištenje: 0,160 g (72 %).

3.2.36. Sinteza harmicina 47a-e. Opća metoda

Otopini azida **6** (0,04 g, 0,179 mmol, 1 ekv.) i odgovarajućeg alkina **34a-e** (0,197 mmol, 1,1 ekv.) u *tert*-butanolu (2,5 mL) dodana je otopina natrijevog askorbata (0,04 g, 0,2 mmol) u vodi (2,5 mL) i 1 M otopina $CuSO_4 \times 5H_2O$ (0,02 mL, 0,02 mmol). Reakcijska smjesa miješana je 0,5 h na s.t., nakon čega je razrijeđena ledenom vodom (5 mL), a nastali talog je odsisan. Sirovi produkt pročišćen je Metodom A ili Metodom B.

Metoda A. Kromatografija na koloni uz pokretnu fazu diklormetan/metanol 95:5 i rastrljavanje u dietil-eteru.

Metoda B. Kromatografija na koloni uz pokretnu fazu diklormetan/metanol 95:5 i prekristalizacija iz etanola.

(1-((9*H*-pirido[3,4-*b*]indol-1-il)metil)-1*H*-1,2,3-triazol-4-il)metil cinamat (47a)

Količina reaktanta: 0,037 g alkina **34a**.

Pročišćavanje: Metoda A.

Iskorištenje: 0,036 g (49 %).

t_t 181,5–183,5 °C.

IR (ATR, ν/cm^{-1}) 3220, 3168, 3093, 3059, 3029, 2994, 2961, 2898, 2877, 2798, 2776, 1713, 1637, 1567, 1505, 1452, 1432, 1402, 1370, 1346, 1325, 1307, 1281, 1243, 1203, 1167, 1066, 1038, 1003, 972, 859, 820, 804, 764, 739, 707, 682, 641, 605, 593, 573, 547, 525, 483.

^{1}H NMR (600 MHz, DMSO-d_6) δ/ppm: 11,98 (s, 1H), 8,32 (s, 1H), 8,30 (d, 1H, J = 5,2 Hz), 8,27 (d, 1H, J = 7,9 Hz), 8,13 (d, 1H, J = 5,2 Hz), 7,73–7,66 (m, 4H), 7,62–7,58 (m, 1H), 7,44–7,38 (m, 3H), 7,31–7,26 (m, 1H), 6,66 (d, 1H, J = 16,0 Hz), 6,11 (s, 2H), 5,28 (s, 2H).

^{13}C NMR (DMSO-d_6) δ 165,93, 145,03, 141,79, 140,70, 137,98, 137,88, 133,92, 133,84, 130,57, 128,91, 128,74, 128,57, 128,42, 125,73, 121,92, 120,74, 119,66, 117,65, 114,87, 112,07, 57,29, 51,21.

ESI-MS: *m/z* 410,1 $(M+1)^+$.

(1-((9*H*-pirido[3,4-*b*]indol-1-il)metil)-1*H*-1,2,3-triazol-4-il)metil (*E*)-3-(3-fluorfenil)akrilat (47b)

Količina reaktanta: 0,040 g alkina **34b**.

Pročišćavanje: Metoda A.

Iskorištenje: 0,043 g (56 %).

t_t 185,5–187,5 °C.

IR (ATR, ν/cm^{-1}) 3311, 3230, 3198, 3147, 3105, 3063, 3019, 2998, 2973, 1715, 1639, 1585, 1569, 1502, 1485, 1472, 1449, 1429, 1403, 1390, 1349, 1323, 1272, 1234, 1190, 1168, 1147, 1122, 1075, 1060, 1035, 983, 954, 939, 874, 858, 837, 819, 780, 728, 671, 643, 605, 582, 562, 534, 521.

^{1}H NMR (DMSO-d_6) δ 11,98 (s, 1H), 8,32 (s, 1H), 8,30 (d, 1H, J = 5,2 Hz), 8,27 (d, 1H, J = 7,9 Hz), 8,13 (d, 1H, J = 5,2 Hz), 7,69–7,63 (m, 3H), 7,61–7,59 (m, 1H), 7,56 (dt, 1H, J = 7,8, 1,2 Hz), 7,47–7,43 (m, 1H), 7,30–7,24 (m, 2H), 6,75 (d, 1H, J = 16,1 Hz), 6,11 (s, 2H), 5,28 (s, 2H).

^{13}C NMR (DMSO-d_6) δ 165,75, 162,40 (d, J = 243,8 Hz), 143,66, 141,71, 140,71, 137,99, 137,89, 136,49 (d, J = 8,1 Hz), 133,85, 130,87 (d, J = 8,4 Hz), 128,75, 128,59, 125,78, 124,94 (d, J = 2,5 Hz), 121,94, 120,75, 119,68, 119,30, 117,26 (d, J = 21,4 Hz), 114,89, 114,58 (d, J = 22,1 Hz), 112,08, 57,40, 51,22.

ESI-MS: m/z 428,1 $(M+1)^+$.

(1-((9*H*-pirido[3,4-*b*]indol-1-il)metil)-1*H*-1,2,3-triazol-4-il)metil (*E*)-3-(3-bromfenil)akrilat (47c)

Količina reaktanta: 0,052 g alkina **34c**.

Pročišćavanje: Metoda B.

Iskorištenje: 0,032 g (37 %).

t_t 184,0–186,0 °C.

IR (ATR, ν/cm^{-1}) 3311, 3223, 3194, 3147, 3102, 3060, 2997, 2971, 1715, 1640, 1607, 1564, 1501, 1472, 1457, 1428, 1404, 1389, 1347, 1308, 1276, 1234, 1189, 1168, 1122, 1090, 1060, 1036, 984, 860, 830, 812, 777, 735, 670, 643, 605, 578, 542.

^{1}H NMR (DMSO-d_6) δ 11,97 (s, 1H), 8,32 (s, 1H), 8,30 (d, 1H, J = 5,2 Hz), 8,26 (d, 1H, J = 7,8 Hz), 8,13 (d, 1H, J = 5,2 Hz), 7,98 (t, 1H, J = 1,8 Hz), 7,73 (dt, 1H, J = 7,8, 1,3 Hz), 7,69–7,57 (m, 4H), 7,36 (t, 1H, J = 7,9 Hz), 7,31–7,27 (m, 1H), 6,75 (d, 1H, J = 16,0 Hz), 6,11 (s, 2H), 5,28 (s, 2H).

^{13}C NMR (DMSO-d_6) δ 165,68, 143,33, 141,71, 140,69, 137,97, 137,87, 136,45, 133,83, 133,03, 130,93, 128,74, 128,57, 127,32, 125,74, 122,28, 121,92, 120,73, 119,66, 119,37, 114,87, 112,07, 57,40, 51,21.

ESI-MS: *m/z* 488,0 $(M+1)^+$, 489,9 $(M+1)^+$.

(1-((9*H*-pirido[3,4-*b*]indol-1-il)metil)-1*H*-1,2,3-triazol-4-il)metil (*E*)-3-(4-klorfenil)akrilat (47d)

Količina reaktanta: 0,043 g alkina **34d**.

Pročišćavanje: Metoda A.

Iskorištenje: 0,02 g (25 %).

t_t 201,0–203,5 °C.

IR (ATR, ν/cm^{-1}) 3227, 3192, 3096, 3061, 2993, 2965, 2926, 2894, 2872, 1713, 1642, 1594, 1568, 1503, 1490, 1468, 1453, 1431, 1404, 1370, 1346, 1308, 1271, 1242, 1201, 1171, 1148, 1087, 1068, 1038, 1012, 972, 868, 818, 775, 737, 695, 683, 669, 637, 593, 560, 547, 529, 491, 455.

^{1}H NMR (DMSO-d_6) δ 11,97 (s, 1H), 8,31 (s, 1H), 8,30 (d, 1H, J = 5,3 Hz), 8,27 (d, 1H, J = 7,9 Hz), 8,13 (d, 1H, J = 5,2 Hz), 7,77–7,74 (m, 2H), 7,70–7,64 (m, 2H), 7,62–7,58 (m, 1H), 7,50–7,45 (m, 2H), 7,31–7,26 (m, 1H), 6,69 (d, 1H, J = 16,1 Hz), 6,11 (s, 2H), 5,28 (s, 2H).

^{13}C NMR (DMSO-d_6) δ 165,79, 143,60, 141,74, 140,69, 137,97, 137,87, 135,08, 133,83, 132,91, 130,15, 128,94, 128,74, 128,57, 125,73, 121,92, 120,73, 119,66, 118,49, 114,87, 112,07, 57,35, 51,21.

ESI-MS: *m/z* 444,0 $(M+1)^+$.

(1-((9*H*-pirido[3,4-*b*]indol-1-il)metil)-1*H*-1,2,3-triazol-4-il)metil (*E*)-3-(4-metoksifenil)akrilat (47e)

Količina reaktanta: 0,043 g alkina **34e**.

Pročišćavanje: Metoda A.

Iskorištenje: 0,032 g (41 %).

t_t 155,0–157,5 °C.

IR (ATR, ν/cm^{-1}) 3223, 3170, 3131, 3094, 3082, 2996, 2965, 2934, 2900, 2837, 1712, 1636, 1607, 1573, 1513, 1455, 1429, 1402, 1375, 1322, 1308, 1287, 1258, 1240, 1202, 1163, 1065, 1037, 1002, 971, 867, 852, 824, 774, 734, 592, 547, 527, 513.

^{1}H NMR (DMSO-d_6) δ 11,98 (s, 1H), 8,32–8,29 (m, 2H), 8,27 (d, 1H, J = 7,9 Hz), 8,12 (d, 1H, J = 5,2 Hz), 7,69–7,59 (m, 5H), 7,28 (t, 1H, J = 7,5 Hz), 6,96 (d, 2H, J = 8,4 Hz), 6,50 (d, 1H, J = 16,0 Hz), 6,11 (s, 2H), 5,25 (s, 2H), 3,79 (s, 3H).

^{13}C NMR (DMSO-d_6) δ 166,22, 161,24, 144,85, 141,92, 140,71, 138,01, 137,88, 133,85, 130,26, 128,74, 128,58, 126,56, 125,70, 121,94, 120,75, 119,67, 114,88, 114,38, 112,09, 57,11, 55,34, 51,21.

ESI-MS: *m/z* 440,1 $(M+1)^+$.

3.2.37. Sinteza harmicina 48a-e. Opća metoda

Otopini azida **11** (0,04 g, 0,169 mmol, 1 ekv.) i odgovarajućeg alkina **34a-e** (0,186 mmol, 1,1 ekv.) u *tert*-butanolu (2,5 mL) dodana je otopina natrijevog askorbata (0,04 g, 0,2 mmol) u vodi (2,5 mL) i 1 M otopina $CuSO_4 \times 5H_2O$ (0,02 mL, 0,02 mmol). Reakcijska smjesa miješana je 0,5 h na s.t., nakon čega je razrijeđena ledenom vodom (5 mL), a nastali talog je odsisan. Sirovi produkt pročišćen je kromatografijom na koloni uz pokretnu fazu diklormetan/metanol 95:5 i rastrljavanjem u dietil-eteru.

(1-((1-Metil-9*H*-pirido[3,4-*b*]indol-3-il)metil)-1*H*-1,2,3-triazol-4-il)metil cinamat (48a)

Količina reaktanta: 0,035 g alkina **34a**.

Iskorištenje: 0,026 g (36 %).

t_t 194,5–195,5 °C.

IR (ATR, ν/cm^{-1}) 3220, 3194, 3175, 3145, 3101, 3060, 3030, 2989, 2945, 1712, 1694, 1644, 1626, 1605, 1565, 1503, 1451, 1392, 1376, 1356, 1329, 1312, 1271, 1254, 1223, 1202, 1170, 1116, 1059, 1037, 1002, 972, 934, 898, 859, 843, 827, 804, 765, 752, 738, 708, 681, 642, 611, 587, 524, 480.

^{1}H NMR (DMSO-d_6) δ 11,67 (s, 1H), 8,26 (s, 1H), 8,17 (d, 1H, J = 7,9 Hz), 7,99 (s, 1H), 7,72–7,70 (m, 2H), 7,67 (d, 1H, J = 16,0 Hz), 7,60 (dt, 1H, J = 8,2, 1,0 Hz), 7,55–7,53 (m, 1H), 7,44–7,39 (m, 3H), 7,24–7,21 (m, 1H), 6,65 (d, 1H, J = 16,1 Hz), 5,77 (s, 2H), 5,27 (s, 2H), 2,75 (s, 3H).

^{13}C NMR (DMSO-d_6) δ 165,94, 145,02, 142,54, 142,16, 141,92, 140,78, 134,00, 133,93, 130,58, 128,91, 128,42, 128,10, 127,60, 125,13, 121,72, 120,91, 119,46, 117,66, 112,10, 112,05, 57,34, 55,25, 20,40.

ESI-MS: *m/z* 424,0 $(M+1)^+$.

(1-((1-Metil-9*H*-pirido[3,4-*b*]indol-3-il)metil)-1*H*-1,2,3-triazol-4-il)metil (*E*)-3-(3-fluorfenil)akrilat (48b)

Količina reaktanta: 0,038 g alkina **34b**.

Iskorištenje: 0,045 g (60 %).

t_t 197,0–198,5 °C.

IR (ATR, ν/cm^{-1}) 3223, 3198, 3166, 3104, 3067, 3043, 3012, 2970, 2895, 1707, 1627, 1608, 1583, 1568, 1506, 1483, 1449, 1387, 1355, 1320, 1271, 1252, 1213, 1151, 1115, 1084, 1057, 1036, 1008, 980, 942, 911, 898, 864, 832, 788, 766, 738, 693, 675, 649, 609, 586, 555, 537, 520, 480.

^{1}H NMR (DMSO-d_6) δ 11,67 (s, 1H), 8,26 (s, 1H), 8,18 (d, 1H, J = 7,9 Hz), 8,00 (s, 1H), 7,67 (d, 1H, J = 16,1 Hz), 7,65–7,62 (m, 1H), 7,61–7,59 (m, 1H), 7,56–7,53 (m, 2H), 7,46–7,43 (m, 1H), 7,27–7,22 (m, 2H), 6,74 (d, 1H, J = 16,0 Hz), 5,77 (s, 2H), 5,28 (s, 2H), 2,75 (s, 3H).

^{13}C NMR (DMSO-d_6) δ 165,73, 162,39 (d, J = 243,8 Hz), 143,61, 142,52, 142,16, 141,83, 140,77, 136,47 (d, J = 8,1 Hz), 134,00, 130,84 (d, J = 8,4 Hz), 128,09, 127,60, 125,14, 124,91 (d, J = 2,5 Hz), 121,71, 120,90, 119,44, 119,29, 117,23 (d, J = 21,3 Hz), 114,56 (d, J = 22,1 Hz), 112,09, 112,06, 57,43, 55,25, 20,40.

ESI-MS: *m/z* 442,1 $(M+1)^+$.

HPLC čistoća 97,6 %.

(1-((1-Metil-9*H*-pirido[3,4-*b*]indol-3-il)metil)-1*H*-1,2,3-triazol-4-il)metil (*E*)-3-(3-bromfenil)akrilat (48c)

Količina reaktanta: 0,049 g alkina **34c**.

Iskorištenje: 0,045 g (53 %).

t_t 204,5–205,5 °C.

IR (ATR, ν/cm^{-1}) 3347, 3281, 3170, 3080, 3054, 3023, 2970, 2950, 1708, 1684, 1638, 1592, 1569, 1498, 1474, 1455, 1423, 1383, 1354, 1341, 1313, 1290, 1272, 1247, 1231, 1188, 1146, 1110, 1073, 1053, 1032, 1009, 980, 928, 899, 872, 829, 791, 766, 731, 697, 666, 649, 623, 586, 563, 549, 527.

^{1}H NMR (DMSO-d_6) δ 11,67 (s, 1H), 8,26 (s, 1H), 8,17 (d, 1H, J = 7,9 Hz), 7,99 (s, 1H), 7,97 (t, 1H, J = 1,8 Hz), 7,75–7,71 (m, 1H), 7,64 (d, 1H, J = 16,0 Hz), 7,62–7,58 (m, 2H), 7,56–7,52 (m, 1H), 7,36 (t, 1H, J = 7,9 Hz), 7,25–7,21 (m, 1H), 6,74 (d, 1H, J = 16,1 Hz), 5,77 (s, 2H), 5,28 (s, 2H), 2,75 (s, 3H).

^{13}C NMR (DMSO-d_6) δ 165,67, 143,31, 142,52, 142,14, 141,84, 140,77, 136,44, 133,99, 133,01, 130,91, 128,08, 127,59, 127,29, 125,11, 122,27, 121,70, 120,90, 119,43, 119,38, 112,08, 112,03, 57,44, 55,24, 20,39.

ESI-MS: *m/z* 501,9 $(M+1)^+$, 503,9 $(M+1)^+$.

HPLC čistoća 97,4 %.

(1-((1-Metil-9*H*-pirido[3,4-*b*]indol-3-il)metil)-1*H*-1,2,3-triazol-4-il)metil (*E*)-3-(4-klorfenil)akrilat (48d)

Količina reaktanta: 0,041 g alkina **34d**.

Iskorištenje: 0,044 g (57 %).

t_t 209,0–211,0 °C.

IR (ATR, ν/cm^{-1}) 3250, 3157, 3103, 3086, 3067, 3052, 1703, 1633, 1592, 1566, 1493, 1475, 1456, 1428, 1408, 1388, 1356, 1305, 1278, 1251, 1222, 1204, 1182, 1160, 1117, 1089, 1058,

1036, 1004, 964, 899, 865, 840, 823, 805, 753, 739, 719, 702, 646, 605, 586, 550, 524, 501, 456.

^{1}H NMR (DMSO-d_6) δ 11,67 (s, 1H), 8,26 (s, 1H), 8,18 (d, 1H, J = 7,9 Hz), 8,00 (s, 1H), 7,76–7,73 (m, 2H), 7,66 (d, 1H, J = 16,0 Hz), 7,60 (dt, 1H, J = 8,3, 1,0 Hz), 7,56–7,53 (m, 1H), 7,48–7,45 (m, 2H), 7,24–7,22 (m, 1H), 6,68 (d, 1H, J = 16,1 Hz), 5,77 (s, 2H), 5,28 (s, 2H), 2,75 (s, 3H).

^{13}C NMR (DMSO-d_6) δ 165,80, 143,60, 142,53, 142,17, 141,88, 140,78, 135,09, 134,01, 132,92, 130,15, 128,94, 128,11, 127,61, 125,13, 121,72, 120,91, 119,46, 118,51, 112,10, 112,07, 57,40, 55,26, 20,41.

ESI-MS: *m/z* 458,0 $(M+1)^+$.

HPLC čistoća 98,3 %.

(1-((1-Metil-9*H*-pirido[3,4-*b*]indol-3-il)metil)-1*H*-1,2,3-triazol-4-il)metil (*E*)-3-(4-metoksifenil)akrilat (48e)

Količina reaktanta: 0,040 g alkina **34e**.

Iskorištenje: 0,048 g (62 %).

t_t 240,5–243,0 °C.

IR (ATR, ν/cm^{-1}) 3236, 3201, 3165, 3103, 3068, 3036, 3007, 2965, 2940, 2911, 2839, 1699, 1626, 1601, 1574, 1514, 1456, 1426, 1389, 1357, 1307, 1290, 1252, 1223, 1207, 1179, 1155, 1115, 1056, 1023, 1009, 992, 971, 937, 898, 868, 830, 810, 776, 751, 735, 710, 693, 663, 652, 637, 608, 586, 555, 521.

^{1}H NMR (DMSO-d_6) δ 11,67 (s, 1H), 8,25 (s, 1H), 8,18 (d, 1H, J = 7,9 Hz), 7,99 (s, 1H), 7,68–7,64 (m, 2H), 7,64–7,59 (m, 2H), 7,55–7,53 (m, 1H), 7,24–7,22 (m, 1H), 6,97–6,94 (m, 2H), 6,49 (d, 1H, J = 16,0 Hz), 5,77 (s, 2H), 5,25 (s, 2H), 3,79 (s, 3H), 2,75 (s, 3H).

^{13}C NMR (DMSO-d_6) δ 166,19, 161,20, 144,80, 142,53, 142,14, 142,03, 140,76, 133,99, 130,22, 128,08, 127,59, 126,54, 125,05, 121,70, 120,90, 119,44, 114,88, 114,35, 112,08, 112,04, 57,14, 55,32, 55,23, 20,39.

ESI-MS: *m/z* 454,1 $(M+1)^+$.

HPLC čistoća 98,6 %.

3.2.38. Sinteza harmicina 49a-e. Opća metoda

Otopini alkina **19** (0,050 g, 0,212 mmol, 1 ekv.) i odgovarajućeg cimetnog azida **37a-e** (0,254 mmol, 1,2 ekv.) u metanolu (5 mL) dodana je katalitička količina bakrovog(II) acetata. Reakcijska smjesa miješana je 24 h na s.t., nakon čega je otapalo upareno pod sniženim tlakom. Sirovi produkt pročišćen je kromatografijom na koloni i rastrljavanjem u smjesi dietil-etera i petroletera.

6-((1-Cinamil-1*H*-1,2,3-triazol-4-il)metoksi)-1-metil-9*H*-pirido[3,4-*b*]indol (49a)

Količina reaktanta: 0,040 g azida **37a**.

Pokretna faza: diklormetan/metanol 80:10.

Iskorištenje: 0,059 g (70 %).

t_t 205,0–206,5 °C.

IR (ATR, ν/cm^{-1}) 3136, 3120, 3030, 2945, 2856, 2760, 2693, 2676, 1632, 1604, 1579, 1565, 1504, 1481, 1460, 1412, 1389, 1361, 1335, 1289, 1237, 1202, 1123, 1054, 1034, 1002, 967, 888, 858, 817, 780, 755, 725, 705, 694, 625, 584, 520, 502.

^{1}H NMR (DMSO-d_6) δ 11,39 (s, 1H), 8,30 (s, 1H), 8,16 (d, 1H, J = 5,3 Hz), 7,91–7,89 (m, 2H), 7,51 (d, 1H, J = 8,8 Hz), 7,45–7,22 (m, 6H), 6,65–6,49 (m, 2H), 5,26 (s, 2H), 5,21 (d, 2H, J = 6,3 Hz), 2,74 (s, 3H).

^{13}C NMR (DMSO-d_6) δ 151,94, 143,26, 142,22, 136,98, 135,70, 135,42, 135,10, 133,62, 128,68, 128,14, 126,70, 126,56, 124,43, 123,72, 121,36, 118,35, 112,76, 112,69, 105,12, 61,89, 51,34, 20,42.

ESI-MS: *m/z* 396,3 (M+1)$^+$.

***l*)-6-((1-(3-(3-fluorfenil)alil)-1*H*-1,2,3-triazol-4-il)metoksi)-1-metil-9*H*-pirido[3,4-*b*]indol (49b)**

Količina reaktanta: 0,045 g azida **37b**.

Pokretna faza: cikloheksan/etil-acetat/metanol 10:10:5, diklormetan/metanol 90:10

Iskorištenje: 0,039 g (44 %).

t_t 145,0–147,0 °C.

IR (ATR, ν/cm^{-1}) 3357, 3293, 3166, 3071, 3052, 2975, 2937, 2900, 2866, 1601, 1583, 1568, 1493, 1473, 1459, 1404, 1379, 1365, 1330, 1286, 1262, 1207, 1149, 1120, 1067, 1054, 1039, 976, 938, 884, 847, 812, 792, 776, 752, 736, 715, 675, 641, 620, 593, 561, 528, 493, 456.

^{1}H NMR (DMSO-d_6) δ 11,41 (s, 1H), 8,31 (s, 1H), 8,17 (d, 1H, J = 5,4 Hz), 7,91–7,89 (m, 2H), 7,52 (d, 1H, J = 8,8 Hz), 7,39–7,32 (m, 2H), 7,27–7,23 (m, 2H), 7,13–7,08 (m, 1H), 6,64–6,62 (m, 2H), 5,26 (s, 2H), 5,23–5,21 (m, 2H), 2,75 (s, 3H).

^{13}C NMR (DMSO-d_6) δ 162,49 (d, J = 243,3 Hz), 151,97, 143,26, 142,16, 138,36 (d, J = 7,9 Hz), 136,80, 135,48, 135,07, 132,34, 130,58 (d, J = 8,5 Hz), 126,78, 125,50, 124,47, 123,00 (d, J = 1,7 Hz), 121,34, 118,42, 114,81 (d, J = 21,3 Hz), 112,80 (d, J = 17,4 Hz), 112,77, 112,67, 105,11, 61,89, 51,16, 20,32.

ESI-MS: *m/z* 414,2 (M+1)$^{+}$.

(*E*)-6-((1-(3-(3-bromfenil)alil)-1*H*-1,2,3-triazol-4-il)metoksi)-1-metil-9*H*-pirido[3,4-*b*]indol (49c)

Količina reaktanta: 0,060 g azida **37c**.

Pokretna faza: cikloheksan/etil-acetat/metanol 300:100:75.

Iskorištenje: 0,051 g (50 %).

t_t 181,5–183,0 °C.

IR (ATR, ν/cm^{-1}) 3252, 3198, 3151, 3089, 3064, 3039, 3015, 2965, 2945, 2916, 2892, 1601, 1584, 1566, 1495, 1475, 1422, 1400, 1373, 1350, 1337, 1289, 1256, 1233, 1217, 1199, 1129, 1095, 1066, 1052, 1033, 1008, 977, 944, 882, 857, 807, 782, 738, 707, 674, 620, 589, 563, 542, 479.

^{1}H NMR (DMSO-d_6) δ 11,40 (s, 1H), 8,31 (s, 1H), 8,16 (d, 1H, J = 5,4 Hz), 7,92–7,89 (m, 2H), 7,71 (t, 1H, J = 2,0 Hz), 7,51 (d, 1H, J = 8,8 Hz), 7,48–7,43 (m, 2H), 7,30 (t, 1H, J = 7,8 Hz), 7,24 (dd, 1H, J = 8,8, 2,5 Hz), 6,68–6,58 (m, 2H), 5,26 (s, 2H), 5,21 (d, 2H, J = 4,6 Hz), 2,74 (s, 3H).

^{13}C NMR (DMSO-d_6) δ 151,98, 143,28, 142,20, 138,30, 136,89, 135,46, 135,09, 132,03, 130,77, 129,05, 126,75, 125,67, 124,47, 122,17, 121,36, 118,40, 112,78, 112,71, 105,10, 61,91, 51,20, 20,37.

ESI-MS: *m/z* 474,2 (M+1)$^{+}$, 476,2 (M+1)$^{+}$.

(*E*)-6-((1-(3-(4-klorfenil)alil)-1*H*-1,2,3-triazol-4-il)metoksi)-1-metil-9*H*-pirido[3,4-*b*]indol (49d)

Količina reaktanta: 0,049 g azida **37d**.

Pokretna faza: cikloheksan/etil-acetat/metanol 10:10:5.

Iskorištenje: 0,046 g (51 %).

t_t 195,0–196,5 °C.

IR (ATR, ν/cm^{-1}) 3208, 3136, 3089, 3069, 2969, 2923, 2893, 2870, 2802, 1602, 1582, 1567, 1494, 1480, 1459, 1405, 1385, 1340, 1289, 1257, 1237, 1207, 1163, 1127, 1094, 1054, 1033, 1015, 987, 971, 950, 884, 857, 843, 818, 742, 702, 687, 662, 623, 583, 563, 533, 487.

^{1}H NMR (DMSO-d_6) δ 11,39 (s, 1H), 8,30 (s, 1H), 8,16 (d, 1H, J = 5,4 Hz), 7,91–7,89 (m, 2H), 7,51 (d, 1H, J = 8,8 Hz), 7,47–7,44 (m, 2H), 7,39–7,36 (m, 2H), 7,23 (dd, 1H, J = 8,9, 2,5 Hz), 6,62–6,51 (m, 2H), 5,26 (s, 2H), 5,21 (d, 2H, J = 5,1 Hz), 2,74 (s, 3H).

^{13}C NMR (DMSO-d_6) δ 151,93, 143,27, 142,22, 136,98, 135,44, 135,10, 134,68, 132,51, 132,23, 128,65, 128,28, 126,71, 124,77, 124,48, 121,36, 118,38, 112,76, 112,69, 105,15, 61,89, 51,23, 20,41.

ESI-MS: *m/z* 430,4 $(M+1)^+$.

(*E*)-6-((1-(3-(4-metoksifenil)alil)-1*H*-1,2,3-triazol-4-il)metoksi)-1-metil-9*H*-pirido[3,4-*b*]indol (49e)

Količina reaktanta: 0,048 g azida **37e**.

Pokretna faza: cikloheksan/etil-acetat/metanol 10:10:5.

Iskorištenje: 0,069 g (77 %).

t_t 200,0–203,0 °C.

IR (ATR, ν/cm^{-1}) 3208, 3138, 3069, 2953, 2929, 2894, 2873, 2836, 2802, 1743, 1607, 1582, 1567, 1513, 1498, 1480, 1460, 1441, 1405, 1386, 1337, 1289, 1257, 1238, 1207, 1175, 1127, 1109, 1054, 1032, 1015, 987, 968, 884, 856, 819, 760, 741, 703, 666, 624, 582, 563, 529, 498, 477.

^{1}H NMR (DMSO- d_6) δ 11,39 (s, 1H), 8,28 (s, 1H), 8,16 (d, 1H, J = 5,4 Hz), 7,92–7,89 (m, 2H), 7,51 (d, 1H, J = 8,8 Hz), 7,37 (d, 2H, J = 8,2 Hz), 7,23 (d, 1H, J = 8,9 Hz), 6,88 (d, 2H, J

= 8,2 Hz), 6,58 (d, 1H, *J* = 15,8 Hz), 6,39–6,32 (m, 1H), 5,25 (s, 2H), 5,16 (d, 2H, *J* = 6,5 Hz), 3,75 (s, 3H), 2,74 (s, 3H).

^{13}C NMR (DMSO-d_6) δ 159,22, 151,94, 143,23, 142,21, 136,98, 135,42, 135,09, 133,36, 128,30, 127,89, 126,70, 124,31, 121,36, 121,11, 118,34, 114,06, 112,75, 112,68, 105,12, 61,89, 55,11, 51,46, 20,41.

ESI-MS: *m/z* 426,3 $(M+1)^+$.

3.2.39. Sinteza harmicina 50a,c-e

Otopini alkina **13** (0,040 g, 0,160 mmol, 1 ekv.) i odgovarajućeg cimetnog azida **37a,c-e** (0,176 mmol, 1,1 ekv.) u metanolu (5 mL) dodana je katalitička količina bakrovog(II) acetata. Reakcijska smjesa miješana je 24 h na s.t., nakon čega je otapalo upareno pod sniženim tlakom. Sirovi produkt pročišćen je kromatografijom na koloni i rastrljavanjem u smjesi dietil-etera i petroletera.

(9-((1-Cinamil-1*H*-1,2,3-triazol-4-il)metil)-1-metil-9*H*-pirido[3,4-*b*]indol-3-il)metanol (50a)

Količina reaktanta: 0,028 g azida **37a**.

Pokretna faza: cikloheksan/etil-acetat/metanol 30:10:5.

Iskorištenje: 0,032 g (49 %).

t_t 197,0–200,0 °C.

IR (ATR, ν/cm^{-1}) 3113, 3060, 2966, 2917, 2859, 1657, 1619, 1560, 1512, 1445, 1402, 1362, 1337, 1290, 1252, 1220, 1190, 1156, 1136, 1122, 1062, 1043, 962, 934, 860, 842, 813, 780, 748, 691, 638, 620, 577, 530, 511, 477, 463.

^{1}H NMR (DMSO-d_6) δ 8,23 (d, 1H, *J* = 7,7 Hz), 8,02 (s, 1H), 7,98 (s, 1H), 7,82 (d, 1H, *J* = 8,3 Hz), 7,59–7,55 (m, 1H), 7,40–7,24 (m, 6H), 6,51 (d, 1H, *J* = 15,9 Hz), 6,47–6,35 (m, 1H), 5,90 (s, 2H), 5,33 (t, 1H, *J* = 5,7 Hz), 5,07 (d, 2H, *J* = 6,0 Hz), 4,67 (d, 2H, *J* = 5,7 Hz), 3,05 (s, 3H).

^{13}C NMR (DMSO-d_6) δ 150,27, 144,17, 141,35, 140,55, 135,63, 133,45, 133,41, 129,10, 128,66, 128,10, 128,06, 126,51, 123,66, 122,72, 121,41, 120,99, 119,71, 110,61, 109,07, 64,35, 51,27, 39,73, 23,15.

ESI-MS: *m/z* 410,3 $(M+1)^+$.

(*E*)-(9-((1-(3-(3-bromfenil)alil)-1*H*-1,2,3-triazol-4-il)metil)-1-metil-9*H*-pirido[3,4-*b*]indol-3-il)metanol (50c)

Količina reaktanta: 0,042 g azida **37c**.

Pokretna faza: diklormetan/metanol 95:5.

Iskorištenje: 0,031 g (39 %).

t_t 164,5–167,5 °C.

IR (ATR, ν/cm^{-1}) 3117, 3060, 2959, 2922, 2861, 1619, 1592, 1560, 1471, 1460, 1445, 1380, 1358, 1336, 1290, 1252, 1222, 1199, 1154, 1120, 1095, 1062, 1044, 995, 965, 934, 875, 861, 829, 786, 747, 719, 685, 668, 636, 621, 577, 534, 492, 463.

^{1}H NMR (DMSO-d_6) δ 8,23 (d, 1H, J = 7,7 Hz), 8,02 (s, 1H), 7,97 (s, 1H), 7,82 (d, 1H, J = 8,3 Hz), 7,70 (t, 1H, J = 2,2 Hz), 7,57 (t, 1H, J = 8,0 Hz), 7,47–7,42 (m, 2H), 7,30–7,24 (m, 2H), 6,67–6,60 (m, 2H), 5,93 (s, 2H), 5,32 (t, 1H, J = 5,7 Hz), 5,07 (d, 2H, J = 5,1 Hz), 4,67 (d, 2H, J = 5,6 Hz), 3,08 (s, 3H).

^{13}C NMR (DMSO-d_6) δ 150,26, 144,16, 141,34, 140,54, 138,20, 133,45, 131,73, 130,74, 130,69, 129,09, 129,00, 128,04, 125,64, 125,56, 122,78, 122,12, 121,40, 120,99, 119,71, 110,60, 109,06, 64,34, 51,11, 39,72, 23,13.

ESI-MS: *m/z* 488,1 $(M+1)^+$, 490,1 $(M+1)^+$.

(*E*)-(9-((1-(3-(4-klorfenil)alil)-1*H*-1,2,3-triazol-4-il)metil)-1-metil-9*H*-pirido[3,4-*b*]indol-3-il)metanol (50d)

Količina reaktanta: 0,034 g azida **37d**.

Pokretna faza: etil-acetat/metanol 100:5.

Iskorištenje: 0,029 g (41 %).

t_t 183,0–186,5 °C.

IR (ATR, ν/cm^{-1}) 3111, 3064, 2971, 2918, 2858, 2822, 1727, 1658, 1619, 1592, 1559, 1489, 1471, 1447, 1405, 1361, 1336, 1292, 1254, 1221, 1192, 1158, 1121, 1085, 1041, 1014, 964, 938, 861, 837, 819, 799, 779, 748, 719, 685, 637, 577, 537, 502, 462.

^{1}H NMR (DMSO-d_6) δ 8,23 (d, 1H, J = 7,8 Hz), 8,02 (s, 1H), 7,97 (s, 1H), 7,82 (d, 1H, J = 8,3 Hz), 7,57 (t, 1H, J = 7,5 Hz), 7,43–7,35 (m, 4H), 7,27 (t, 1H, J = 7,4 Hz), 6,52–6,41 (m, 2H), 5,90 (s, 2H), 5,32 (t, 1H, J = 5,7 Hz), 5,07 (d, 2H, J = 5,1 Hz), 4,67 (d, 2H, J = 5,7 Hz), 3,05 (s, 3H).

^{13}C NMR (DMSO-d_6) δ 150,27, 144,18, 141,35, 140,55, 134,61, 133,44, 132,47, 132,05, 129,10, 128,64, 128,24, 128,06, 124,71, 122,76, 121,41, 120,99, 119,72, 110,60, 109,06, 64,35, 51,17, 39,73, 23,15.

ESI-MS: m/z 444,2 $(M+1)^+$.

(*E*)-(9-((1-(3-(4-metoksifenil)alil)-1*H*-1,2,3-triazol-4-il)metil)-1-metil-9*H*-pirido[3,4-*b*]indol-3-il)metanol (50e)

Količina reaktanta: 0,033 g azida **37e**.

Pokretna faza: diklormetan/metanol 95:5.

Iskorištenje: 0,030 g (43 %).

t_t 202,0–205,0 °C.

IR (ATR, ν/cm^{-1}) 3180, 3119, 3067, 3024, 3002, 2945, 2923, 2869, 1622, 1563, 1488, 1462, 1441, 1379, 1364, 1333, 1298, 1254, 1222, 1203, 1160, 1135, 1122, 1067, 1037, 1003, 965, 915, 857, 771, 745, 696, 636, 582, 533, 509, 471, 454.

^{1}H NMR (DMSO-d_6) δ 8,23 (d, 1H, J = 7,8 Hz), 8,02 (s, 1H), 7,96 (s, 1H), 7,82 (d, 1H, J = 8,3 Hz), 7,57 (t, 1H, J = 7,5 Hz), 7,34–7,30 (m, 2H), 7,26 (t, 1H, J = 7,5 Hz), 6,89–6,85 (m, 2H), 6,47 (d, 1H, J = 15,8 Hz), 6,25 (dt, 1H, J = 15,8, 6,5 Hz), 5,90 (s, 2H), 5,33 (t, 1H, J = 5,7 Hz), 5,03 (d, 2H, J = 7,2 Hz), 4,67 (d, 2H, J = 5,7 Hz), 3,74 (s, 3H), 3,05 (s, 3H).

^{13}C NMR (DMSO-d_6) δ 159,20, 150,26, 144,14, 141,35, 140,56, 133,45, 133,19, 129,09, 128,24, 128,05, 127,86, 122,61, 121,40, 121,05, 120,98, 119,71, 114,06, 110,60, 109,07, 64,35, 55,11, 51,41, 39,73, 23,15.

ESI-MS: m/z 440,3 $(M+1)^+$.

3.2.40. Sinteza harmikina triazolskog tipa 51-58. Opća metoda

Otopini alkina (0,230 mmol, 1 ekv.) i odgovarajućeg azida (0,253 mmol, 1,1 ekv.) u metanolu (5 mL) dodana je katalitička količina bakrovog(II) acetata te je reakcijska smjesa miješana 24 h na s.t. Otapalo je upareno pod sniženim tlakom, a ostatak je pročišćen kromatografijom na koloni uz pokretnu fazu diklormetan/metanol ili cikloheksan/etil-acetat/metanol i rastrljavanjem u smjesi dietil-etera i petroletera.

1-((4-(((7-Klorkinolin-4-il)oksi)metil)-1*H*-1,2,3-triazol-1-il)metil)-9*H*-pirido[3,4-*b*]indol (51)

Količina reaktanata: 0,050 g alkina **42**, 0,056 g azida **6**.

Pokretna faza: cikloheksan/etil-acetat/metanol 10:10:5.

Iskorištenje: 0,046 g (45 %).

t_t 170–172 °C.

IR (ATR, ν/cm^{-1}) 3235, 3058, 1619, 1604, 1566, 1541, 1488, 1454, 1432, 1374, 1322, 1299, 1228, 1136, 1100, 1054, 945, 856, 806, 755, 724, 656, 587, 541, 493, 478.

^{1}H NMR (DMSO-d_6) δ 11,93 (s, 1H), 8,30 (s, 1H), 8,28–8,24 (m, 2H), 8,19 (d, 1H, J = 7,8 Hz), 8,14 (d, 1H, J = 8,6 Hz), 8,11 (d, 1H, J = 5,1 Hz), 8,00 (d, 1H, J = 1,9 Hz), 7,65 (dt, 1H, J = 8,2, 0,9 Hz), 7,60–7,58 (m, 1H), 7,38 (dd, 1H, J = 8,6, 1,9 Hz), 7,29–7,27 (m, 1H), 6,13 (d, 1H, J = 7,8 Hz), 6,06 (s, 2H), 5,55 (s, 2H).

^{13}C NMR (DMSO-d_6) δ 175,78, 145,22, 141,86, 140,68, 140,57, 137,85, 137,84, 136,92, 133,82, 128,72, 128,56, 127,86, 125,26, 124,62, 123,75, 121,91, 120,72, 119,65, 116,69, 114,85, 112,05, 109,78, 51,25, 46,88.

ESI-MS: m/z 441,0 $(M+1)^+$.

3-((4-(((7-Klorkinolin-4-il)oksi)metil)-1*H*-1,2,3-triazol-1-il)metil)-1-metil-9*H*-pirido[3,4-*b*]indol (52)

Količina reaktanata: 0,050 g alkina **42**, 0,060 g azida **11**.

Pokretna faza: diklormetan/metanol 90:10.

Iskorištenje: 0,042 g (40 %).

t_t 172–174,5 °C.

IR (ATR, ν/cm^{-1}) 3617, 3130, 3057, 2888, 2787, 1623, 1603, 1568, 1507, 1486, 1468, 1446, 1398, 1376, 1357, 1340, 1254, 1224, 1140, 1103, 1058, 1055, 1027, 971, 860, 812, 800, 749, 646, 589, 543, 479.

^{1}H NMR (DMSO-d_6) δ 11,66 (s, 1H), 8,25 (s, 1H), 8,19 (d, 1H, J = 7,8 Hz), 8,14 (d, 1H, J = 8,6 Hz), 8,11 (d, 1H, J = 7,9 Hz), 8,00 (d, 1H, J = 1,8 Hz), 7,90 (s, 1H), 7,59 (d, 1H, J = 8,16 Hz), 7,56–7,52 (m, 1H), 7,38 (dd, 1H, J = 8,6, 1,8 Hz), 7,27–7,22 (m, 1H), 6,13 (d, 1H, J = 7,8 Hz), 5,73 (s, 2H), 5,55 (s, 2H), 2,71 (s, 3H).

^{13}C NMR (DMSO-d_6) δ 175,79, 145,24, 142,44, 142,14, 141,95, 140,75, 140,55, 136,90, 133,95, 128,09, 127,87, 127,55, 125,28, 124,08, 123,73, 121,62, 120,87, 119,43, 116,65, 112,09, 111,81, 109,77, 55,19, 46,97, 20,34.

ESI-MS: *m/z* 455,4 $(M+1)^+$.

6-((1-(7-Klorkinolin-4-il)-1*H*-1,2,3-triazol-4-il)metoksi)-1-metil-9*H*-pirido[3,4-*b*]indol (53)

Količina reaktanata: 0,054 g alkina **19**; 0,052 g azida **38**.

Pokretna faza: cikloheksan/etil-acetat/metanol 10:10:5.

Iskorištenje: 0,043 g (42 %).

t_t 281,5–283 °C.

IR (ATR, ν/cm^{-1}) 3247, 3076, 3030, 2901, 1588, 1567, 1497, 1477, 1458, 1441, 1414, 1372, 1350, 1265, 1253, 1208, 1174, 1116, 1076, 1039, 1030, 1008, 987, 968, 878, 849, 829, 816, 803, 770, 736, 700, 672, 655, 621, 543, 500.

^{1}H NMR (DMSO-d_6) δ 11,42 (s, 1H), 9,17 (d, 1H, J = 4,6 Hz), 9,01 (s, 1H), 8,30 (d, 1H, J = 2,2 Hz), 8,18 (d, 1H, J = 5,3 Hz), 8,00–7,98 (m, 2H), 7,93 (d, 1H, J = 5,3 Hz), 7,89 (d, 1H, J = 4,6 Hz), 7,75 (dd, 1H, J = 9,1, 2,2 Hz), 7,55 (d, 1H, J = 8,8 Hz), 7,31 (dd, 1H, J = 8,8, 2,5 Hz), 5,42 (s, 2H), 2,75 (s, 3H).

^{13}C NMR (DMSO-d_6) δ 152,38, 151,88, 149,38, 143,96, 142,25, 140,38, 137,00, 135,56, 135,36, 135,10, 128,98, 128,14, 126,85, 126,69, 125,35, 121,39, 120,34, 118,44, 117,15, 112,82, 112,69, 105,40, 61,80, 20,40.

ESI-MS: *m/z* 441,4 $(M+1)^+$.

7-((1-(7-Klorkinolin-4-il)-1*H*-1,2,3-triazol-4-il)metoksi)-1-metil-9*H*-pirido[3,4-*b*]indol (54)

Količina reaktanata: 0,054 g alkina **24**, 0,052 g azida **38**.

Pokretna faza: diklormetan/metanol 95:5.

Iskorištenje: 0,051 g (50 %).

t_t 236–239,5 °C.

IR (ATR, ν/cm^{-1}) 3049, 1629, 1610, 1564, 1505, 1486, 1440, 1321, 1295, 1278, 1253, 1233, 1215, 1106, 1071, 1036, 996, 953, 920, 872, 822, 812, 801, 767, 629, 572.

^{1}H NMR (DMSO-d_6) δ 11,51 (s, 1H), 9,17 (d, 1H, J = 4,7 Hz), 9,02 (s, 1H), 8,30 (d, 1H, J = 2,1 Hz), 8,17 (d, 1H, J = 5,3 Hz), 8,11 (d, 1H, J = 8,6 Hz), 8,01 (d, 1H, J = 9,1 Hz), 7,90 (d, 1H, J = 4,7 Hz), 7,83 (d, 1H, J = 5,3 Hz), 7,79 (dd, 1H, J = 9,1, 2,2 Hz), 7,27 (d, 1H, J = 2,2 Hz), 6,99 (dd, 1H, J = 8,6, 2,2 Hz), 5,47 (s, 2H), 2,74 (s, 3H).

^{13}C NMR (DMSO-d_6) δ 158,72, 152,39, 149,39, 143,72, 141,79, 141,37, 140,36, 137,74, 135,39, 134,62, 129,03, 128,17, 127,14, 127,00, 125,35, 122,73, 120,34, 117,17, 115,31, 111,99, 109,45, 96,03, 61,29, 20,32.

ESI-MS: m/z 441,3 $(M+1)^+$.

9-((1-(7-Klorkinolin-4-il)-1*H*-1,2,3-triazol-4-il)metil)-7-metoksi-1-metil-9*H*-pirido[3,4-*b*]indol (55)

Količina reaktanata: 0,058 g alkina **28**; 0,052 g azida **38**.

Pokretna faza: cikloheksan/etil-acetat/metanol 10:10:5, diklormetan/metanol 95:5.

Iskorištenje: 0,040 g (38 %).

t_t 235–237 °C.

IR (ATR, ν/cm^{-1}) 3143, 1621, 1561, 1499, 1442, 1406, 1372, 1345, 1255, 1223, 1194, 1171, 1138, 1115, 1036, 931, 925, 876, 813, 722, 623, 554.

^{1}H NMR (DMSO-d_6) δ 9,09 (d, 1H, J = 4,7 Hz), 8,83 (s, 1H), 8,26 (d, 1H, J = 2,2 Hz), 8,20 (d, 1H, J = 5,2 Hz), 8,11 (d, 1H, J = 8,6 Hz), 7,95–7,88 (m, 2H), 7,78 (d, 1H, J = 4,7 Hz), 7,74 (dd, 1H, J = 9,1, 2,2 Hz), 7,42 (d, 1H, J = 2,2 Hz), 6,90 (dd, 1H, J = 8,6, 2,1 Hz), 6,05 (s, 2H), 3,92 (s, 3H), 3,13 (s, 3H).

^{13}C NMR (DMSO-d_6) δ 160,62, 152,29, 149,31, 144,79, 142,74, 141,17, 140,22, 138,15, 135,28, 134,75, 128,91, 128,62, 128,10, 125,34, 122,40, 120,31, 117,20, 114,51, 112,29, 109,48, 94,13, 55,66, 23,31.

ESI-MS: *m/z* 455,3 $(M+1)^+$.

7-Klor-*N*-(2-(4-(((1-metil-9*H*-pirido[3,4-*b*]indol-6-il)oksi)metil)-1*H*-1,2,3-triazol-1-il)etil)kinolin-4-amin (56)

Količina reaktanata: 0,054 g alkina **19**; 0,063 g azida **40**.

Pokretna faza: diklormetan/metanol 75:25.

Iskorištenje: 0,048 g (43 %).

t_t 272–273 °C.

IR (ATR, ν/cm^{-1}) 3201, 1608, 1583, 1544, 1498, 1456, 1429, 1383, 1365, 1352, 1330, 1248, 1207, 1170, 1061, 1139, 1050, 1026, 990, 909, 872, 845, 808, 765, 624, 492.

^{1}H NMR (DMSO-d_6) δ 11,43 (s, 1H), 8,41 (d, 1H, J = 5,4 Hz), 8,32 (s, 1H), 8,20 (d, 1H, J = 9,1 Hz), 8,16 (d, 1H, J = 5,3 Hz), 7,92–7,85 (m, 2H), 7,81 (d, 1H, J = 2,2 Hz), 7,54 (t, 1H, J = 5,8 Hz), 7,50 (d, 1H, J = 8,8 Hz), 7,44 (dd, 1H, J = 9,0, 2,3 Hz), 7,20 (dd, 1H, J = 8,8, 2,5 Hz), 6,57 (d, 1H, J = 5,5 Hz), 5,21 (s, 2H), 4,70 (t, 2H, J = 6,1 Hz), 3,82 (q, 2H, J = 5,9 Hz), 2,75 (s, 3H).

^{13}C NMR (DMSO-d_6) δ 151,99, 151,87, 149,76, 148,95, 142,97, 142,22, 136,93, 135,43, 135,09, 133,53, 127,47, 126,70, 124,96, 124,35, 124,00, 121,35, 118,28, 117,47, 112,76, 112,66, 105,00, 98,90, 61,91, 47,86, 42,46, 20,41.

ESI-MS: *m/z* 484,1 $(M+1)^+$.

7-Klor-*N*-(2-(4-(((1-metil-9*H*-pirido[3,4-*b*]indol-7-il)oksi)metil)-1*H*-1,2,3-triazol-1-il)etil)kinolin-4-amin (57)

Količina reaktanata: 0,054 g alkina **24**, 0,063 g azida **40**.

Pokretna faza: cikloheksan/etil-acetat/metanol 10:10:5.

Iskorištenje: 0,060 g (54 %).

t_t 238–241 °C.

IR (ATR, ν/cm^{-1}) 3340, 3158, 3065, 2957, 1638, 1584, 1543, 1485, 1450, 1428, 1371, 1338, 1251, 1235, 1155, 1110, 1056, 874, 851, 813, 800, 761, 648, 858, 531.

^{1}H NMR (DMSO-d_6) δ 11,48 (s, 1H), 8,41 (d, 1H, J = 5,4 Hz), 8,32 (s, 1H), 8,19–8,15 (m, 2H), 8,05 (d, 1H, J = 8,6 Hz), 7,82–7,80 (m, 2H), 7,54 (t, 1H, J = 5,2 Hz), 7,45 (dd, 1H, J = 9,0, 2,3 Hz), 7,17 (d, 1H, J = 2,2 Hz), 6,88 (dd, 1H, J = 8,7, 2,3 Hz), 6,57 (d, 1H, J = 5,5 Hz), 5,25 (s, 2H), 4,70 (t, 2H, J = 5,8 Hz), 3,82 (q, 2H, J = 6,0 Hz), 2,73 (s, 3H).

^{13}C NMR (DMSO-d_6) δ 158,79, 151,77, 149,82, 148,82, 142,70, 141,82, 141,30, 137,65, 134,59, 133,60, 127,38, 127,18, 125,08, 124,40, 124,00, 122,64, 117,44, 115,10, 111,98, 109,42, 98,91, 95,82, 61,45, 47,90, 42,43, 20,29.

ESI-MS: *m/z* 482,1 $(M-1)^-$.

7-Klor-*N*-(2-(4-((7-metoksi-1-metil-9*H*-pirido[3,4-*b*]indol-9-il)metil)-1*H*-1,2,3-triazol-1-il)etil)kinolin-4-amin (58)

Količina reaktanata: 0,058 g alkina **28**, 0,063 g azida **40**.

Pokretna faza: diklormetan/metanol 85:15, 80:20.

Iskorištenje: 0,076 g (66 %).

t_t 244–245,5 °C.

IR (ATR, ν/cm^{-1}) 2957, 1619, 1578, 1495, 1441, 1428, 1403, 1369, 1355, 1324, 1252, 1224, 1193, 1171, 1082, 973, 926, 910, 875, 814, 764, 732, 641, 593, 462.

^{1}H NMR (DMSO-d_6) δ 8,31 (d, 1H, J = 5,4 Hz), 8,17 (d, 1H, J = 5,2 Hz), 8,08 (d, 1H, J = 8,6 Hz), 8,05 (d, 1H, J = 9,1 Hz), 7,98 (s, 1H), 7,87 (d, 1H, J = 5,2 Hz), 7,79 (d, 1H, J = 2,2 Hz), 7,44–7,37 (m, 2H), 7,26 (d, 1H, J = 2,1 Hz), 6,87 (dd, 1H, J = 8,6, 2,1 Hz), 6,45 (d, 1H, J = 5,5 Hz), 5,83 (s, 2H), 4,57 (t, 2H, J = 6,0 Hz), 3,83 (s, 3H), 3,70 (q, 2H, J = 5,9 Hz,), 2,98 (s, 3H).

^{13}C NMR (DMSO-d_6) δ 160,52, 151,63, 149,73, 148,74, 143,88, 142,65, 141,07, 137,98, 134,60, 133,56, 128,49, 127,34, 124,35, 123,78, 123,47, 122,34, 117,33, 114,39, 112,23, 109,36, 98,77, 93,95, 55,53, 47,86, 42,34, 23,11.

ESI-MS: *m/z* 496,1 $(M-1)^-$.

Elementarna analiza za $C_{27}H_{24}ClN_7O$: C, 65,12; H, 4,86; N, 19,69; nađeno: C, 64,87; H, 4,92; N, 19,93.

3.2.41. Sinteza harmikina amidnog tipa (59-63). Opća metoda

Suspenzija karboksilne kiseline **43** (0,050 g, 0,211 mmol, 1,1 ekv.), odgovarajućeg amina (0,192 mmol, 1 ekv.) i TEA (0,059 mL, 0,422 mmol, 2,2 ekv.) u bezvodnom DMF-u (2 mL) miješana je 0,17 h na s.t., nakon čega je postupno dokapana 50 % otopina T3P u etil-acetatu (0,126 mL, 0,211 mmol, 1,1 ekv.). Reakcijska smjesa miješana je 18 h na s.t., nakon čega je uz ultrasoniciranje dokapavana 5 % NaOH do prestanka taloženja. Nastali prljavo-bijeli talog je odsisan i pročišćen kromatografijom na koloni uz pokretnu fazu diklormetan/metanol 85:15 i rastrljavanjem u dietil-eteru.

_N_-((9_H_-pirido[3,4-_b_]indol-1-il)metil)-2-((7-klorkinolin-4-il)amino)acetamid (59)

Količina reaktanta: 0,038 g amina **7**.

Iskorištenje: 0,034 g (42 %).

t_t 244–247 °C.

IR (ATR, ν/cm^{-1}) 3267, 1651, 1627, 1585, 1451, 1431, 1323, 1284, 1235, 1151, 1126, 1082, 1023, 986, 902, 871, 853, 742, 578, 563, 519.

^{1}H NMR (DMSO-d_6) δ 11,54 (s, 1H), 8,79 (t, 1H, J = 5,5 Hz), 8,34 (d, 1H, J = 5,4 Hz), 8,28–8,25 (m, 2H), 8,22 (d, 1H, J = 7,9 Hz), 8,03 (d, 1H, J = 5,2 Hz), 7,83 (t, 1H, J = 6,5 Hz), 7,81 (d, 1H, J = 2,3 Hz), 7,59 (d, 1H, J = 8,2 Hz), 7,56–7,53 (m, 1H), 7,50 (dd, 1H, J = 9,0, 2,3 Hz), 7,26–7,23 (m, 1H), 6,40 (d, 1H, J = 5,4 Hz), 4,81 (d, 2H, J = 5,4 Hz), 4,07 (d, 2H, J = 6,0 Hz).

^{13}C NMR (DMSO-d_6) δ 169,38, 151,63, 150,35, 148,74, 141,33, 140,40, 137,30, 133,56, 133,36, 128,14, 127,74, 127,36, 124,41, 124,23, 121,76, 120,83, 119,42, 117,56, 113,89, 112,03, 99,44, 45,81, 41,48.

ESI-MS: m/z 416,1 $(M+1)^+$.

2-((7-Klorkinolin-4-il)amino)-_N_-((1-metil-9_H_-pirido[3,4-_b_]indol-3-il)metil)acetamid (60)

Količina reaktanta: 0,041 g amina **12**.

Iskorištenje: 0,023 g (28 %).

t_t 274,5–277 °C.

IR (ATR, ν/cm^{-1}) 3616, 3285, 1662, 1629, 1587, 1502, 1453, 1431, 1375, 1328, 1234, 1150, 1083, 1014, 901, 851, 801, 737.

^{1}H NMR (DMSO-d_6) δ 11,48 (s, 1H), 8,71 (t, 1H, J = 5,9 Hz), 8,44 (d, 1H, J = 5,4 Hz), 8,29 (d, 1H, J = 9,0 Hz), 8,05 (d, 1H, J = 7,8 Hz), 7,90–7,79 (m, 2H), 7,71 (s, 1H), 7,60–7,46 (m, 3H), 7,26–7,19 (m, 1H), 6,47 (d, 1H, J = 5,4 Hz), 4,52 (d, 2H, J = 5,8 Hz), 4,07 (d, 2H, J = 6,0 Hz), 2,70 (s, 3H).

^{13}C NMR (DMSO-d_6) δ 168,98, 151,79, 150,26, 148,97, 146,08, 141,11, 140,73, 133,51, 133,45, 127,82, 127,65, 127,46, 124,32, 121,46, 120,94, 119,13, 117,63, 111,95, 109,34, 99,28, 46,01, 44,21, 20,24.

ESI-MS: *m/z* 430,1 $(M+1)^+$.

2-((7-Klorkinolin-4-il)amino)-*N*-(2-((1-metil-9*H*-pirido[3,4-*b*]indol-6-il)oksi)etil)acetamid (61)

Količina reaktanta: 0,046 g amina **21**.

Iskorištenje: 0,023 g (26 %).

t_t 304–307 °C.

IR (ATR, ν/cm^{-1}) 3525, 3369, 3219, 3145, 3054, 2874, 1679, 1581, 1530, 1505, 1485, 1452, 1372, 1334, 1287, 1240, 1213, 1116, 1075, 990, 877, 854, 810, 793, 629, 614, 488, 467.

^{1}H NMR (DMSO-d_6) δ 11,41 (s, 1H), 8,41 (t, 1H, J = 5,7 Hz), 8,29 (d, 1H, J = 5,4 Hz), 8,27 (d, 1H, J = 9,1 Hz), 8,15 (d, 1H, J = 5,3 Hz), 7,88 (d, 1H, J = 5,3 Hz), 7,82 (t, 1H, J = 6,4 Hz), 7,81 (d, 1H, J = 2,3 Hz), 7,73 (d, 1H, J = 2,5 Hz), 7,52–7,48 (m, 2H), 7,15 (dd, 1H, J = 8,8, 2,5 Hz), 6,31 (d, 1H, J = 5,4 Hz), 4,10 (t, 2H, J = 5,6 Hz), 3,98 (d, 2H, J = 5,9 Hz), 3,54 (q, 2H, J = 5,6 Hz), 2,74 (s, 3H).

^{13}C NMR (DMSO-d_6) δ 169,14, 152,30, 151,54, 150,39, 148,64, 142,18, 136,88, 135,36, 135,08, 133,57, 127,24, 126,70, 124,36, 124,26, 121,37, 118,23, 117,52, 112,73, 112,69, 104,77, 99,15, 66,99, 45,80, 38,50, 20,39.

ESI-MS: *m/z* 460,0 $(M+1)^+$.

2-((7-Klorkinolin-4-il)amino)-*N*-(2-((1-metil-9*H*-pirido[3,4-*b*]indol-7-il)oksi)etil)acetamid (62)

Količina reaktanta: 0,046 g amina **26**.

Iskorištenje: 0,026 g (30 %).

t_t 275–277,5 °C.

IR (ATR, ν/cm^{-1}) 3641, 3284, 3093, 1659, 1631, 1612, 1587, 1487, 1431, 1376, 1328, 1274, 1232, 1178, 1148, 1109, 1056, 974, 903, 878, 852, 801, 569.

^{1}H NMR (DMSO-d_6) δ 11,54 (s, 1H), 8,46 (t, 1H, J = 5,7 Hz), 8,30–8,28 (m, 2H), 8,16 (d, 1H, J = 5,3 Hz), 8,06 (d, 1H, J = 8,6 Hz), 7,92 (t, 1H, J = 6,1 Hz), 7,82 (d, 1H, J = 5,3 Hz), 7,81 (d, 1H, J = 2,3 Hz), 7,50 (dd, 1H, J = 9,0, 2,3 Hz), 7,02 (d, 1H, J = 2,2 Hz), 6,83 (dd, 1H, J = 8,6, 2,2 Hz), 6,32 (d, 1H, J = 5,5 Hz), 4,12 (t, 2H, J = 5,6 Hz), 3,99 (d, 2H, J = 5,9 Hz), 3,55 (q, 2H, J = 5,6 Hz), 2,74 (s, 3H).

^{13}C NMR (DMSO-d_6) δ 169,16, 159,20, 151,28, 150,57, 148,37, 141,96, 141,23, 137,51, 134,57, 133,69, 127,28, 127,01, 124,42, 124,35, 122,68, 117,48, 114,98, 112,00, 109,35, 99,13, 95,41, 66,42, 45,78, 38,38, 20,27.

ESI-MS: m/z 460,1 $(M+1)^+$.

2-((7-Klorkinolin-4-il)amino)-*N*-(2-(7-metoksi-1-metil-9*H*-pirido[3,4-*b*]indol-9-il)etil)acetamid (63)

Količina reaktanta: 0,049 g amina **30**.

Iskorištenje: 0,032 g (35 %).

t_t 252,5–255 °C.

IR (ATR, ν/cm^{-1}) 3268, 3063, 1656, 1625, 1582, 1445, 1408, 1375, 1343, 1280, 1251, 1198, 1174, 1140, 1081, 1047, 1025, 976, 809, 639, 597, 569.

^{1}H NMR (DMSO-d_6) δ 8,37 (t, 1H, J = 6,0 Hz), 8,31 (d, 1H, J = 5,3 Hz), 8,24 (d, 1H, J = 9,0 Hz), 8,16 (d, 1H, J = 5,2 Hz), 8,10 (d, 1H, J = 8,6 Hz), 7,87 (d, 1H, J = 5,1 Hz), 7,81 (d, 1H, J = 2,3 Hz), 7,74 (t, 1H, J = 6,1 Hz), 7,49 (dd, 1H, J = 9,0, 2,3 Hz), 7,28 (d, 1H, J = 2,2 Hz), 6,89 (dd, 1H, J = 8,6, 2,2 Hz), 6,07 (d, 1H, J = 5,4 Hz), 4,58 (t, 2H, J = 7,1 Hz), 3,90 (s, 3H), 3,85 (d, 2H, J = 6,0 Hz), 3,52 (q, 2H, J = 6,8 Hz), 2,96 (s, 3H).

^{13}C NMR (DMSO-d_6) δ 169,63, 160,57, 151,91, 150,13, 148,95, 142,90, 140,62, 137,87, 134,64, 133,50, 128,43, 127,53, 124,36, 124,22, 122,48, 117,56, 114,31, 112,30, 109,25, 98,97, 93,63, 55,57, 45,97, 43,29, 38,84, 23,14.

ESI-MS: *m/z* 474,1 $(M+1)^+$.

3.2.42. Sinteza harmikina amidnog tipa 64, 65. Opća metoda

Otopina karboksilne kiseline **33** (0,050 g, 0,176 mmol, 1,1 ekv.), DIEA (0,061 mL, 0,352 mmol, 2,2 ekv.) i HATU (0,067 g, 0,176 mmol, 1,1 ekv.) u diklormetanu (4 mL) miješana je 0,33 h na s.t., nakon čega je dodan odgovarajući amin **44** ili **45** (0,160 mmol, 1 ekv.). Reakcijska smjesa miješana je 18 h na s.t. Potom je nastali talog odsisan, a sirovi produkt pročišćen kromatografijom na koloni uz pokretnu fazu diklormetan/metanol 75:25 i rastrljavanjem u dietil-eteru.

N-(2-((7-Klorkinolin-4-il)amino)etil)-3-(7-metoksi-1-metil-9*H*-pirido[3,4-*b*]indol-9-il)propanamid (64)

Količina reaktanta: 0,035 g amina **44**.

Iskorištenje: 0,027 g (35 %).

t_t 224–227 °C.

IR (ATR, ν/cm^{-1}) 3226, 3060, 2967, 1645, 1624, 1582, 1547, 1503, 1449, 1409, 1342, 1300, 1284, 1267, 1231, 1167, 1140, 1120, 1083, 1042, 1017, 976, 946, 872, 853, 827, 814, 801, 764, 636, 595, 567, 546, 474.

^{1}H NMR (DMSO-d_6) δ 8,40 (d, 1H, J = 5,4 Hz), 8,23 (t, 1H, J = 5,8 Hz), 8,20–8,12 (m, 2H), 8,05 (d, 1H, J = 8,6 Hz), 7,85 (d, 1H, J = 5,1 Hz), 7,79 (d, 1H, J = 2,2 Hz), 7,44 (dd, 1H, J = 9,0, 2,3 Hz), 7,31 (t, 1H, J = 5,5 Hz), 7,22 (d, 1H, J = 2,2 Hz), 6,85 (dd, 1H, J = 8,6, 2,2 Hz), 6,47 (d, 1H, J = 5,5 Hz), 4,82 (t, 2H, J = 7,2 Hz), 3,90 (s, 3H), 3,27 (q, 2H, J = 6,3 Hz), 3,17 (q, 2H, J = 5,9 Hz), 2,97 (s, 3H), 2,63 (t, 2H, J = 7,2 Hz).

^{13}C NMR (DMSO-d_6) δ 170,35, 160,43, 151,89, 149,97, 149,07, 142,51, 140,75, 137,90, 134,49, 133,40, 128,56, 127,52, 124,10, 123,94, 122,29, 117,42, 114,32, 112,21, 109,20, 98,57, 93,88, 55,52, 41,76, 40,87, 37,23, 36,34, 23,11.

ESI-MS: *m/z* 488,1 $(M+1)^+$.

***N*-(4-((7-Klorkinolin-4-il)amino)butil)-3-(7-metoksi-1-metil-9*H*-pirido[3,4-*b*]indol-9-il)propanamid (65)**

Količina reaktanta: 0,040 g amina **45**.

Iskorištenje: 0,036 g (43 %).

t_t 230–233 °C.

IR (ATR, ν/cm^{-1}) 3306, 2936, 1642, 1624, 1577, 1499, 1448, 1408, 1366, 1330, 1305, 1227, 1205, 1166, 1187, 1119, 1046, 883, 849, 810, 546.

^{1}H NMR (DMSO-d_6) δ 8,39 (d, 1H, J = 5,6 Hz), 8,31 (d, 1H, J = 9,0 Hz), 8,16 (d, 1H, J = 5,2 Hz), 8,06 (d, 1H, J = 8,6 Hz), 7,96 (t, 1H, J = 5,6 Hz), 7,86 (d, 1H, J = 5,2 Hz), 7,79 (d, 1H, J = 2,3 Hz), 7,54–7,40 (m, 2H), 7,20 (d, 1H, J = 2,2 Hz), 6,85 (dd, 1H, J = 8,6, 2,1 Hz), 6,43 (d, 1H, J = 5,6 Hz), 4,79 (t, 2H, J = 7,1 Hz), 3,90 (s, 3H), 3,23–3,13 (m, 2H), 3,04 (q, 2H, J = 6,5 Hz), 2,97 (s, 3H), 2,60 (t, 2H, J = 7,0 Hz), 1,53–1,43 (m, 2H), 1,36 (q, 2H, J = 7,2 Hz).

^{13}C NMR (DMSO-d_6) δ 169,59, 160,42, 151,10, 150,48, 148,19, 142,54, 140,71, 137,75, 134,48, 133,71, 128,57, 126,73, 124,28, 124,17, 122,26, 117,27, 114,26, 112,22, 109,21, 98,57, 93,91, 55,50, 42,01, 40,96, 38,17, 36,37, 26,49, 24,98, 23,04.

ESI-MS: m/z 516,4 $(M+1)^+$.

3.2.43. Sinteza harmicena triazolskog tipa 66-70. Opća metoda

Otopini odgovarajućeg alkina **4**, **15**, **19**, **24** ili **28** (0,169 mmol, 1,1 ekv) i azida **46** (0,045 g, 0,186 mmol, 1,1 ekv.) u bezvodnom DMF-u (2 mL) dodane su otopina natrijevog askorbata (0,04 g, 0,202 mmol) u vodi (1 mL) i 1 M vodena otopina $CuSO_4 \times 5H_2O$ (0,02 mL, 0,02 mmol). Reakcijska smjesa miješana je 18 h na s.t., nakon čega je dodana ledena voda (5 mL), a nastali talog je odsisan. Sirovi produkt pročišćen je kromatografijom na koloni uz pokretnu fazu cikloheksan/etil-acetat /metanol 10:10:5 ili diklormetan/metanol 97:3 i rastrljavanjem u smjesi dietil-etera i petroletera.

1-(1-(Ferocenilmetil)-1*H*-1,2,3-triazol-4-il)-9*H*-pirido[3,4-*b*]indol (66)

Količina reaktanta: 0,032 g alkina **4**.

Iskorištenje: 0,037 g (51 %).

t_t 229–230 °C.

IR (ATR, ν/cm^{-1}) 3385, 3172, 3105, 3065, 2991, 1625, 1576, 1489, 1452, 1437, 1419, 1351, 1314, 1282, 1254, 1239, 1152, 1103, 1000, 829, 807, 749, 629, 591, 548, 499, 479.

^{1}H NMR (DMSO-d_6) δ 11,53 (s, 1H), 8,78 (s, 1H), 8,38 (d, 1H, J = 5,2 Hz), 8,26–8,24 (m, 1H), 8,11 (d, 1H, J = 5,1 Hz), 7,91–7,90 (m, 1H), 7,57–7,54 (m, 1H), 7,27–7,25 (m, 1H), 5,49 (s, 2H), 4,46 (t, 2H, J = 1,9 Hz), 4,24 (s, 5H), 4,22 (t, 2H, J = 1,9 Hz).

^{13}C NMR (DMSO-d_6) δ 147,60, 141,15, 137,83, 133,68, 131,74, 129,05, 128,18, 122,94, 121,47, 120,40, 119,51, 114,11, 113,23, 82,36, 68,74, 68,69, 68,48, 49,33.

ESI-MS: m/z 434,1 $(M+1)^+$.

3-(1-(Ferocenilmetil)-1*H*-1,2,3-triazol-4-il)-1-metil-9*H*-pirido[3,4-*b*]indol (67)

Količina reaktanta: 0,035 g alkina **15**.

Iskorištenje: 0,034 g (45 %).

t_t 183–186 °C.

IR (ATR, ν/cm^{-1}) 3361, 2920, 2851, 1734, 1626, 1574, 1496, 1455, 1431, 1373, 1338, 1303, 1277, 1234, 1172, 1104, 1049, 1024, 1000, 924, 889, 818, 788, 775, 704, 631, 558, 584, 503, 478.

^{1}H NMR (DMSO-d_6) δ 11,69 (s, 1H), 8,58 (s, 1H), 8,41 (s, 1H), 8,29 (d, 1H, J = 7,9 Hz), 7,60 (d, 1H, J = 8,1 Hz), 7,54 (t, 1H, J = 7,6 Hz), 7,24 (t, 1H, J = 7,4 Hz), 5,39 (s, 2H), 4,45 (t, 2H, J = 1,9 Hz), 4,23 (s, 5H), 4,21 (t, 2H, J = 1,9 Hz), 2,80 (s, 3H).

^{13}C NMR (DMSO-d_6) δ 148,61, 141,93, 140,82, 138,95, 133,96, 128,02, 127,73, 121,97, 121,27, 121,25, 119,36, 112,01, 108,31, 82,45, 68,86, 68,68, 68,44, 49,05, 20,48.

ESI-MS: m/z 447,9 $(M+1)^+$.

6-((1-(Ferocenilmetil)-1*H*-1,2,3-triazol-4-il)metoksi)-1-metil-9*H*-pirido[3,4-*b*]indol (68)

Količina reaktanta: 0,040 g alkina **19**.

Iskorištenje: 0,055 g (68 %).

t_t 244,5–248 °C.

IR (ATR, ν/cm^{-1}) 3631, 3137, 3081, 2950, 1637, 1603, 1583, 1567, 1499, 1480, 1451, 1411, 1283, 1211, 1107, 1069, 1054, 1040, 1027, 849, 821, 765, 620, 504.

^{1}H NMR (DMSO-d_6) δ 11,37 (s, 1H), 8,24 (s, 1H), 8,16 (d, 1H, J = 5,3 Hz), 7,89–7,88 (m, 2H), 7,49 (d, 1H, J = 8,8 Hz), 7,21 (dd, 1H, J = 8,9, 2,5 Hz), 5,32 (s, 2H), 5,21 (s, 2H), 4,32 (t, 2H, J = 1,8 Hz), 4,16–4,14 (m, 7H), 2,73 (s, 3H).

^{13}C NMR (DMSO-d_6) δ 151,88, 142,95, 142,19, 136,96, 135,42, 135,08, 126,69, 124,09, 121,34, 118,39, 112,73, 112,67, 105,20, 82,49, 68,62, 68,59, 68,31, 61,88, 48,92, 20,40.

ESI-MS: m/z 478,1 $(M+1)^+$.

7-((1-(Ferocenilmetil)-1*H*-1,2,3-triazol-4-il)metoksi)-1-metil-9*H*-pirido[3,4-*b*]indol (69)

Količina reaktanta: 0,040 g alkina **24**.

Iskorištenje: 0,048 g (60 %).

t_t 242–244 °C.

IR (ATR, ν/cm^{-1}) 3344, 3072, 2869, 2785, 1738, 1626, 1567, 1488, 1444, 1377, 1325, 1305, 1290, 1278, 1177, 1142, 1110, 1058, 1142, 1011, 965, 828, 813, 781, 661, 639, 598, 572, 505, 480.

^{1}H NMR (DMSO-d_6) δ 11,45 (s, 1H), 8,23 (s, 1H), 8,15 (d, 1H, J = 5,2 Hz), 8,05 (d, 1H, J = 8,6 Hz), 7,80 (d, 1H, J = 5,3 Hz), 7,16 (d, 1H, J = 2,2 Hz), 6,89 (dd, 1H, J = 8,7, 2,3 Hz), 5,33 (s, 2H), 5,25 (s, 2H), 4,34 (t, 2H, J = 1,9 Hz), 4,18–4,16 (m, 7H), 2,72 (s, 3H).

^{13}C NMR (DMSO-d_6) δ 158,74, 142,71, 141,76, 141,33, 137,74, 134,58, 127,13, 124,15, 122,63, 115,11, 111,95, 109,46, 95,86, 82,41, 68,66, 68,64, 68,36, 61,45, 48,98, 20,32.

ESI-MS: m/z 478,1 $(M+1)^+$.

9-((1-(Ferocenilmetil)-1*H*-1,2,3-triazol-4-il)metil)-7-metoksi-1-metil-9*H*-pirido[3,4-*b*]indol (70)

Količina reaktanta: 0,042 g alkina **28**.

Iskorištenje: 0,025 g (30 %).

t_t 187–190 °C.

IR (ATR, ν/cm^{-1}) 3135, 3090, 2929, 1709, 1623, 1564, 1499, 1449, 1408, 1325, 1252, 1227, 1193, 1174, 1106, 1042, 1000, 913, 815, 764, 732, 638, 596, 550, 481.

^{1}H NMR (DMSO-d_6) δ 8,16 (d, 1H, J = 5,2 Hz), 8,07 (d, 1H, J = 8,5 Hz), 7,98 (s, 1H), 7,86 (d, 1H, J = 5,2 Hz), 7,32 (d, 1H, J = 2,2 Hz), 6,87 (dd, 1H, J = 8,5, 2,2 Hz), 5,86 (s, 2H), 5,21 (s, 2H), 4,23 (t, 2H, J = 1,8 Hz), 4,12 (t, 2H, J = 1,8 Hz), 4,06 (s, 5H), 3,88 (s, 3H), 3,03 (s, 3H).

^{13}C NMR (DMSO-d_6) δ 160,55, 143,81, 142,67, 141,13, 138,05, 134,66, 128,54, 122,55, 122,38, 114,46, 112,26, 109,46, 94,05, 82,59, 68,54, 68,44, 68,21, 55,62, 48,77, 23,24.

ESI-MS: m/z 492,1 $(M+1)^+$.

3.2.44. Sinteza harmicena triazolskog tipa 71-75. Opća metoda

Otopini odgovarajućeg azida **6**, **11**, **22**, **27** ili **31** (0,209 mmol, 1,1 ekv.) i etinilferocena (0,040 g, 0,190 mmol, 1 ekv.) u bezvodnom DMF-u (2 mL) dodana je otopina natrijevog askorbata (0,04 g, 0,202 mmol) u vodi (1 mL) i 1 M vodena otopina $CuSO_4 \times 5H_2O$ (0,02 mL, 0,02 mmol). Reakcijska smjesa miješana je 18 h na s.t., nakon čega je željeni produkt izoliran Metodom A ili Metodom B.

Metoda A. U reakcijsku smjesu dodana je ledena voda (5 mL) te je nastali talog odsisan. Sirovi produkt pročišćen je kromatografijom na koloni uz pokretnu fazu cikloheksan/etil-acetat/metanol 10:10:5 i rastrljavanjem u smjesi dietil-etera i petroletera**.**

Metoda B. U reakcijsku smjesu je dodana voda (20 mL) te je dobivena otopina ekstrahirana etil-acetatom (2 × 30 mL). Organski slojevi su skupljeni, sušeni nad bezvodnim Na_2SO_4, profiltrirani, a otapalo uklonjeno iz filtrata uparavanjem pod sniženim tlakom. Sirovi produkt je pročišćen kromatografijom na koloni i rastrljavanjem u smjesi dietil-etera i petroletera.

1-((4-Ferocenil-1*H*-1,2,3-triazol-1-il)metil)-9*H*-pirido[3,4-*b*]indol (71)

Količina reaktanta: 0,047 g azida **7**.

Pročišćavanje: Metoda A.

Iskorištenje: 0,064 g (78 %).

t_t 252–255,5 °C.

IR (ATR, ν/cm^{-1}) 3249, 3138, 3094, 2987, 2953, 1625, 1585, 1567, 1497, 1455, 1430, 1389, 1321, 1236, 1212, 1189, 1094, 1058, 998, 875, 816, 794, 750, 730, 622, 592, 500.

^{1}H NMR (DMSO-d_6) δ 11,95 (s, 1H), 8,31 (d, 1H, J = 5,2 Hz), 8,28–8,26 (m, 2H), 8,13 (d, 1H, J = 5,1 Hz), 7,70–7,68 (m, 1H), 7,61–7,59 (m, 1H), 7,30–7,27 (m, 1H), 6,08 (s, 2H), 4,73 (t, 2H, J = 1,9 Hz), 4,28 (t, 2H, J = 1,8 Hz), 4,03 (s, 5H).

^{13}C NMR (DMSO-d_6) δ 145,22, 140,71, 138,17, 137,86, 133,85, 128,71, 128,54, 121,91, 121,57, 120,76, 119,64, 114,82, 112,09, 76,04, 69,23, 68,21, 66,34, 51,24.

ESI-MS: m/z 434,9 $(M+1)^+$.

3-((4-Ferocenil-1*H*-1,2,3-triazol-1-il)metil)-1-metil-9*H*-pirido[3,4-*b*]indol (72)

Količina reaktanta: 0,050 g azida **11**.

Pročišćavanje: Metoda B, pokretna faza: cikloheksan/etil-acetat/metanol 10:10:1.

Iskorištenje: 0,053 g (62 %).

t_t 242,5–244 °C.

IR (ATR, ν/cm^{-1}) 3148, 3101, 2993, 2891, 1737, 1627, 1566, 1506, 1456, 1443, 1351, 1328, 1251, 1219, 1086, 1057, 1019, 1000, 874, 815, 729, 680, 587, 506, 487.

^{1}H NMR (DMSO-d_6) δ 11,66 (s, 1H), 8,23 (s, 1H), 8,16 (d, 1H, J = 7,9 Hz), 7,90 (s, 1H), 7,60–7,59 (m, 1H), 7,55–7,52 (m, 1H), 7,24–7,21 (m, 1H), 5,76 (s, 2H), 4,74 (t, 2H, J = 1,9 Hz), 4,29 (t, 2H, J = 1,9 Hz), 4,03 (s, 5H), 2,76 (s, 3H).

^{13}C NMR (DMSO-d_6) δ 145,37, 142,95, 142,05, 140,77, 133,94, 128,08, 127,63, 121,64, 121,06, 120,91, 119,44, 112,09, 111,42, 76,09, 69,26, 68,21, 66,32, 55,10, 20,38.

ESI-MS: m/z 448,9 $(M+1)^+$.

6-(2-(4-Ferocenil-1*H*-1,2,3-triazol-1-il)etoksi)-1-metil-9*H*-pirido[3,4-*b*]indol (73)

Količina reaktanta: 0,056 g azida **22**.

Pročišćavanje: Metoda B; pokretna faza: cikloheksan/etil-acetat/metanol 10:10:5.

Iskorištenje: 0,034 g (37 %).

t_t 201,5–204,0 °C.

IR (ATR, ν/cm^{-1}) 3133, 2949, 2872, 1583, 1568, 1497, 1458, 1286,1210, 1105, 1041, 988, 878, 818, 705, 621, 504.

^{1}H NMR (DMSO-d_6) δ 11,39 (s, 1H), 8,29 (s, 1H), 8,15 (d, 1H, J = 5,3 Hz), 7,87 (d, 1H, J = 5,3 Hz), 7,78 (d, 1H, J = 2,5 Hz), 7,48 (d, 1H, J = 8,8 Hz), 7,16 (dd, 1H, J = 8,8, 2,5 Hz), 4,82 (t, 2H, J = 5,1 Hz), 4,73 (t, 2H, J = 1,9 Hz), 4,53 (t, 2H, J = 5,2 Hz), 4,30 (t, 2H, J = 1,8 Hz), 4,01 (s, 5H), 2,72 (s, 3H).

^{13}C NMR (DMSO-d_6) δ 151,85, 145,24, 142,24, 136,98, 135,52, 135,10, 126,63, 121,35, 121,28, 118,14, 112,77, 112,64, 105,13, 76,05, 69,22, 68,21, 67,14, 66,34, 49,24, 20,40.

ESI-MS: *m/z* 477,9 $(M+1)^+$.

7-(2-(4-Ferocenil-1*H*-1,2,3-triazol-1-il)etoksi)-1-metil-9*H*-pirido[3,4-*b*]indol (74)

Količina reaktanta: 0,056 g azida **27**.

Pročišćavanje: Metoda A.

Iskorištenje: 0,070 g (77 %).

t_t 228,0–229,5 °C.

IR (ATR, ν/cm^{-1}) 3125, 3077, 2959, 2850, 2772, 1623, 1566, 1443, 1426, 1301, 1278, 1240, 1185, 1108, 1053, 1042, 977, 874, 822, 810, 743, 720, 693, 638, 587, 570, 522, 513, 495, 483.

^{1}H NMR (DMSO-d_6) δ 11,44 (s, 1H), 8,30 (s, 1H), 8,14 (d, 1H, J = 5,3 Hz), 8,05 (d, 1H, J = 8,6 Hz), 7,79 (d, 1H, J = 5,3 Hz), 7,03 (d, 1H, J = 2,2 Hz), 6,85 (dd, 1H, J = 8,6, 2,2 Hz), 4,83 (t, 2H, J = 5,1 Hz), 4,73 (t, 2H, J = 1,9 Hz), 4,55 (t, 2H, J = 5,1 Hz), 4,30 (t, 2H, J = 1,8 Hz), 4,01 (s, 5H), 2,72 (s, 3H).

^{13}C NMR (DMSO-d_6) δ 158,62, 145,25, 141,72, 141,35, 137,76, 134,59, 127,07, 122,71, 121,34, 115,33, 111,98, 109,17, 95,73, 76,01, 69,23, 68,22, 66,57, 66,35, 49,09, 20,36.

ESI-MS: *m/z* 477,9 $(M+1)^+$.

9-(2-(4-Ferocenil-1*H*-1,2,3-triazol-1-il)etil)-7-metoksi-1-metil-9*H*-pirido[3,4-*b*]indol (75)

Količina reaktanta: 0,059 g azida **31**.

Pročišćavanje: Metoda A.

Iskorištenje: 0,059 g (63 %).

t_t 218,0–220,0 °C.

IR (ATR, ν/cm^{-1}) 2968, 1621, 1565, 1445, 1404, 1339, 1253, 1222, 1158, 1182, 1136, 1096, 1041, 1021, 970, 929, 877, 821, 807, 641, 590, 545, 501, 475.

^{1}H NMR (DMSO-d_6) δ 8,17 (d, 1H, J = 5,2 Hz), 8,04 (d, 1H, J = 8,5 Hz), 7,88 (d, 1H, J = 5,2 Hz), 7,80 (s, 1H), 6,84–6,78 (m, 2H), 5,08 (t, 2H, J = 5,6 Hz), 4,88 (t, 2H, J = 5,6 Hz), 4,49 (t, 2H, J = 1,9 Hz), 4,22 (t, 2H, J = 1,9 Hz), 3,86–3,85 (m, 8H), 2,90 (s, 3H).

^{13}C NMR (DMSO-d_6) δ 160,51, 145,15, 142,76, 140,67, 138,12, 134,68, 128,73, 122,23, 121,79, 114,10, 112,26, 109,81, 92,93, 75,78, 68,09, 68,06, 66,26, 55,37, 49,71, 44,47, 23,18.

ESI-MS: m/z 491,9 $(M+1)^+$.

3.2.45. Sinteza harmicena amidnog tipa 76-79. Opća metoda

Otopina ferocenkarboksilne kiseline (0,050 g, 0,217 mmol, 1,1 ekv.), DIEA (0,075 mL, 0,434 mmol, 2,2 ekv.) i HATU (0,083 g, 0,217 mmol, 1,1 ekv.) u bezvodnom diklormetanu (4 mL) miješana je 0,33 h na s.t., nakon čega je dodan odgovarajući amin **7**, **12**, **26** ili **30** (0,197 mmol, 1 ekv.). Reakcijska smjesa miješana je 18 h na s.t. Željeni produkt izoliran je Metodom A ili Metodom B.

Metoda A. Otapalo je upareno pod sniženim tlakom, a ostatak nakon uparavanja je otopljen u etil-acetatu (20 mL) te ispran zasićenom vodenom otopinom NaCl (2 × 20 mL) i vodom (1 × 20 mL). Organski sloj je sušen nad bezvodnim Na_2SO_4, filtriran, a otpalo upareno pod sniženim tlakom. Sirovi produkt pročišćen je kromatografijom na koloni uz pokretnu fazu aceton/diklormetan i rastrljavanjem u smjesi dietil-etera i petroletera.

Metoda B. Nastali talog je odsisan, a sirovi produkt pročišćen kromatografijom na koloni uz pokretnu fazu aceton/diklormetan 9:1 i rastrljavanjem u smjesi dietil-etera i petroletera.

***N*-((9*H*-pirido[3,4-*b*]indol-1-il)metil)ferocenkarboksamid (76)**

Količina reaktanta: 0,039 g amina **7**.

Pročišćavanje: Metoda A; pokretna faza: aceton/diklormetan 1:1.

Iskorištenje: 0,039 g (48 %).

t_t 210–213 °C.

IR (ATR, ν/cm^{-1}) 3623, 3467, 3085, 3050, 2962, 2928, 1711, 1649, 1622, 1531, 1503, 1444, 1408, 1375, 1340, 1300, 1249, 1229, 1195, 138, 1123, 1106, 1041, 1017, 914, 819, 801, 634, 598, 558.

^{1}H NMR (DMSO-d_6) δ 11,49 (s, 1H), 8,58 (t, 1H, J = 6,0 Hz), 8,31 (d, 1H, J = 5,2 Hz), 8,23 (d, 1H, J = 7,8 Hz), 8,05 (d, 1H, J = 5,2 Hz), 7,68 (d, 1H, J = 8,2 Hz), 7,56 (t, 1H, J = 7,6 Hz), 7,25 (t, 1H, J = 7,5 Hz), 4,88–4,87 (m, 4H), 4,35 (t, 2H, J = 1,9 Hz), 4,07 (s, 5H).

^{13}C NMR (DMSO-d_6) δ 169,83, 142,64, 140,17, 137,35, 133,55, 128,10, 127,74, 121,74, 120,93, 119,37, 113,86, 111,99, 76,11, 70,10, 69,31, 68,30, 41,73.

ESI-MS: m/z 410,0 $(M+1)^+$.

_N_-((1-metil-9_H_-pirido[3,4-_b_]indol-3-il)metil)ferocenkarboksamid (77)

Količina reaktanta: 0,042 g amina **12**.

Pročišćavanje: Metoda A; pokretna faza: aceton/diklormetan 1:1.

Iskorištenje: 0,033 g (39 %).

t_t 240,5–243 °C.

IR (ATR, ν/cm^{-1}) 3324, 3226, 1634, 1574, 1532, 1498, 1447, 1380, 1348, 1297, 1248, 1104, 1026, 901, 814, 755, 738, 629, 528, 482.

^{1}H NMR (DMSO-d_6) δ 11,51 (s, 1H), 8,47 (t, 1H, J = 6,1 Hz), 8,12 (d, 1H, J = 7,9 Hz), 7,89 (s, 1H), 7,57 (d, 1H, J = 8,2 Hz), 7,52–7,48 (m, 1H), 7,21–7,17 (m, 1H), 4,90 (t, 2H, J = 1,9 Hz), 4,60 (d, 2H, J = 6,0 Hz), 4,37 (t, 2H, J = 1,9 Hz), 4,20 (s, 5H), 2,78 (s, 3H).

^{13}C NMR (DMSO-d_6) δ 168,94, 147,17, 141,14, 140,76, 133,49, 127,78, 127,66, 121,35, 120,95, 119,16, 111,98, 109,47, 76,73, 69,96, 69,25, 68,28, 44,31, 20,27.

ESI-MS: m/z 424,0 $(M+1)^+$.

_N_-(2-((1-metil-9_H_-pirido[3,4-_b_]indol-7-il)oksi)etil)ferocenkarboksamid (78)

Količina reaktanta: 0,048 g amina **26**.

Pročišćavanje: Metoda B.

Iskorištenje: 0,038 g (42 %).

t_t 243–245,5 °C.

IR (ATR, ν/cm^{-1}) 3216, 1716, 1622, 1551, 1451, 1422, 1376, 1312, 1278, 1236, 1217, 1105, 960, 842, 801, 741, 641, 605, 505,476.

^{1}H NMR (DMSO-d_6) δ 11,41 (s, 1H), 8,14 (d, 1H, J = 5,3 Hz,), 8,07–8,05 (m, 2H), 7,79 (d, 1H, J = 5,3 Hz), 7,07 (d, 1H, J = 2,4 Hz), 6,90 (dd, 1H, J = 8,7, 2,2 Hz), 4,83 (t, 2H, J = 2,0 Hz), 4,35 (t, 2H, J = 1,9 Hz), 4,23 (t, 2H, J = 5,7 Hz), 4,13 (s, 5H), 3,63 (q, 2H, J = 5,7 Hz), 2,71 (s, 3H).

^{13}C NMR (DMSO-d_6) δ 169,36, 159,31, 141,89, 141,28, 137,74, 134,55, 127,17, 122,69, 114,98, 111,93, 109,22, 95,38, 76,31, 70,01, 69,40, 68,22, 66,40, 38,49, 20,33.

ESI-MS: *m/z* 454,0 $(M+1)^+$.

_N_-(2-(7-metoksi-1-metil-9_H_-pirido[3,4-_b_]indol-9-il)etil)ferocenkarboksamid (79)

Količina reaktanta: 0,050 g amina **30**.

Pročišćavanje: Metoda A; pokretna faza: aceton/diklormetan 3:2.

Iskorištenje: 0,046 g (50 %).

t_t 225–227 °C.

IR (ATR, ν/cm^{-1}) 3623, 3467, 3085, 3050, 2962, 2928, 1711, 1649, 1622, 1531, 1503, 1444, 1408, 1375, 1340, 1300, 1249, 1229, 1195, 1177, 1138, 1123, 1107, 1041, 1016, 914, 819, 801, 634, 598, 558.

^{1}H NMR (DMSO-d_6) δ 8,17 (d, 1H, J = 5,1 Hz), 8,10–8,07 (m, 2H), 7,88 (d, 1H, J = 5,1 Hz), 7,32 (d, 1H, J = 2,2 Hz), 6,88 (dd, 1H, J = 8,5, 2,1 Hz), 4,69 (t, 2H, J = 1,9 Hz), 4,66 (t, 2H, J = 7,1 Hz), 4,34 (t, 2H, J = 1,9 Hz), 4,07 (s, 5H), 3,91 (s, 3H), 3,60 (q, 2H, J = 6,7 Hz), 3,04 (s, 3H).

^{13}C NMR (DMSO-d_6) δ 169,75, 160,52, 143,00, 140,66, 137,82, 134,67, 128,43, 122,39, 114,28, 112,26, 109,20, 93,78, 76,40, 69,93, 69,32, 68,08, 55,50, 43,56, 39,10, 23,14.

ESI-MS: *m/z* 468,1 $(M+1)^+$.

3.2.46. Sinteza harmicena amidnog tipa 80-83. Opća metoda

Otopina ferocenoctene kiseline (0,050 g, 0,205 mmol, 1,1 ekv.), DIEA (0,071 mL, 0,410 mmol, 2,2 ekv.) i HATU (0,078 g, 0,205 mmol, 1,1 ekv.) u bezvodnom diklormetanu (4 mL) miješana je 0,33 h na s.t., nakon čega je dodan odgovarajući amin **7**, **12**, **26** ili **30** (0,186 mmol, 1 ekv.). Reakcijska smjesa miješana je 18 h na s.t. Željeni produkt izoliran je Metodom A ili Metodom B.

Metoda A. Nastali talog je odsisan te prekristaliziran iz etanola.
Metoda B: Reakcijska smjesa je razrijeđena diklormetanom (15 mL) te isprana zasićenom vodenom otopinom NaCl (2 × 20 mL) i vodom (1 × 20 mL). Organski sloj je sušen nad bezvodnim Na_2SO_4, profiltriran, a otapalo uklonjeno iz filtrata uparavanjem pod sniženim tlakom. Sirovi produkt pročišćen je rastrljavanjem u smjesi dietil-etera i petroletera.

N-((9*H*-pirido[3,4-*b*]indol-1-il)metil)-2-ferocenilacetamid (80)

Količina reaktanta: 0,037 g amina **7**.

Pročišćavanje: Metoda A.

Iskorištenje: 0,027 g (34 %).

t_t 222,0–224,5 °C.

IR (ATR, ν/cm^{-1}) 3333, 3219, 3168, 3099, 2995, 2898, 1651, 1568, 1521, 1502, 1445, 1436, 1413, 1361, 1321, 1285, 1248, 1151, 1106, 1045, 1026, 999, 878, 820, 740, 677, 595, 564, 504.

^{1}H NMR (DMSO-d_6) δ 11,50 (s, 1H), 8,55 (t, 1H, J = 5,4 Hz), 8,29 (d, 1H, J = 5,2 Hz), 8,22 (d, 1H, J = 7,8 Hz), 8,04 (d, 1H, J = 5,2 Hz), 7,63 (d, 1H, J = 8,2 Hz), 7,55 (t, 1H, J = 7,6 Hz), 7,25 (t, 1H, J = 7,4 Hz), 4,76 (d, 2H, J = 5,4 Hz), 4,22 (t, 2H, J = 1,9 Hz), 4,05 (m, 7H), 3,26 (s, 2H).

^{13}C NMR (DMSO-d_6) δ 170,47, 141,60, 140,36, 137,36, 133,50, 128,12, 127,74, 121,73, 120,87, 119,39, 113,89, 112,05, 82,66, 68,58, 68,41, 67,11, 41,52, 36,33.

ESI-MS: m/z 424,1 $(M+1)^+$.

2-Ferocenil-*N*-((1-metil-9*H*-pirido[3,4-*b*]indol-3-il)metil)acetamid (81)

Količina reaktanta: 0,039 g amina **12**.

Pročišćavanje: Metoda A.

Iskorištenje: 0,032 g (39 %).

t_t 247,5–250,0 °C.

IR (ATR, ν/cm^{-1}) 3404, 3191, 3081, 2944, 1649, 1621, 1570, 1522, 1471, 1455, 1421, 1312, 1247, 1267, 1136, 1103, 1038, 1023, 997, 925, 826, 803, 753, 741, 693, 621, 584, 543, 500, 482.

^{1}H NMR (DMSO-d_6) δ 11,48 (s, 1H), 8,42 (t, 1H, J = 5,9 Hz), 8,10 (d, 1H, J = 7,8 Hz), 7,73 (s, 1H), 7,56 (d, 1H, J = 8,2 Hz), 7,52–7,50 (m, 1H), 7,21 (t, 1H, J = 7,4 Hz), 4,46 (d, 2H, J = 5,8 Hz), 4,27 (t, 2H, J = 1,9 Hz), 4,12 (s, 5H), 4,10 (t, 2H, J = 1,9 Hz), 3,24 (s, 2H), 2,73 (s, 3H).

^{13}C NMR (DMSO-d_6) δ 169,93, 146,33, 141,16, 140,71, 133,44, 127,78, 127,66, 121,49, 120,98, 119,11, 111,94, 109,54, 83,05, 68,63, 68,45, 67,15, 44,28, 36,72, 20,28.

ESI-MS: *m/z* 438,0 $(M+1)^+$.

2-Ferocenil-*N*-(2-((1-metil-9*H*-pirido[3,4-b]indol-7-il)oksi)etil)acetamid (82)

Količina reaktanta: 0,045 g amina **26**.

Pročišćavanje: Metoda B.

Iskorištenje: 0,050 g (58 %).

t_t 176,0–177,5 °C.

IR (ATR, ν/cm^{-1}) 3222, 3055, 2875, 1656, 1630, 1539, 1484, 1434, 1378, 1324, 1299, 1273, 1238, 1174, 1134, 1106, 1073, 1037, 1023, 1002, 961, 924, 871, 814, 776, 738, 661, 634, 590, 567, 484.

^{1}H NMR (DMSO-d_6) δ 11,40 (s, 1H), 8,19 (t, 1H, J = 5,5 Hz), 8,14 (d, 1H, J = 5,3 Hz), 8,05 (d, 1H, J = 8,6 Hz), 7,80 (d, 1H, J = 5,3 Hz), 7,02 (d, 1H, J = 2,2 Hz), 6,85 (dd, 1H, J = 8,6, 2,2 Hz), 4,20 (t, 2H, J = 1,9 Hz), 4,13 (t, 2H, J = 5,5 Hz), 4,11 (s, 5H), 4,05 (t, 2H, J = 1,9 Hz), 3,51 (q, 2H, J = 5,6 Hz), 3,16 (s, 2H), 2,72 (s, 3H).

^{13}C NMR (DMSO-d_6) δ 170,25, 159,17, 141,84, 141,29, 137,75, 134,56, 127,16, 122,63, 115,00, 111,93, 109,30, 95,40, 82,72, 68,50, 68,43, 67,08, 66,5, 38,40, 36,37, 20,35.

ESI-MS: *m/z* 468,1 $(M+1)^+$.

_N_-(2-(7-metoksi-1-metil-9_H_-pirido[3,4-_b_]indol-9-il)etil)-2-ferocenilacetamid (83)

Količina reaktanta: 0,047 g amina **30**.

Pročišćavanje: Metoda B.

Iskorištenje: 0,062 g (69 %).

t_t 170,5–172,0 °C.

IR (ATR, ν/cm^{-1}) 3341, 2931, 1655, 1624, 1566, 1503, 1451, 1439, 1410, 1347, 1330, 1300, 1251, 1195, 1172, 1141, 1104, 1048, 1024, 929, 835, 813, 794, 639, 567, 496, 482.

^{1}H NMR (DMSO-d_6) δ 8,17 (d, 1H, J = 5,1 Hz), 8,09 (d, 1H, J = 8,6 Hz), 8,01 (t, 1H, J = 6,0 Hz), 7,88 (d, 1H, J = 5,1 Hz), 7,27 (d, 1H, J = 2,2 Hz), 6,89 (dd, 1H, J = 8,6, 2,2 Hz), 4,57 (t, 2H, J = 7,1 Hz), 4,13 (t, 2H, J = 1,9 Hz), 4,11 (s, 5H), 4,05 (t, 2H, J = 1,8 Hz), 3,92 (s, 3H), 3,45 (q, 2H, J = 6,7 Hz), 3,07 (s, 2H), 2,95 (s, 3H).

^{13}C NMR (DMSO-d_6) δ 170,58, 160,52, 142,86, 140,61, 137,80, 134,64, 128,43, 122,40, 114,31, 112,25, 109,24, 93,64, 82,12, 68,72, 68,46, 67,21, 55,52, 43,37, 38,73, 36,65, 23,08.

ESI-MS: *m/z* 482,2 $(M+1)^+$.

3.3. ISPITIVANJA BIOLOŠKOG DJELOVANJA

3.3.1. ANTIPROLIFERATIVNO DJELOVANJE

Antiproliferativno djelovanje sintetiziranih spojeva ispitano je na sljedećim humanim tumorskim staničnim linijama: MCF-7, HepG2, HCT116 i SW620, te na jednoj ne-tumorskoj staničnoj liniji (Hek293T). Sve korištene stanične linije bile su adherentne te su uzgajane u monosloju i održavane u mediju koji sadrži 89 % DMEM-a, 10 % FBS-a i 1 % antibiotika (100 U/mL penicilin i 100 μg/mL streptomicin), na 37 °C pri 5 % CO_2, u atmosferi zasićenoj vlagom.

Inhibicija rasta tumorskih stanica uslijed izlaganja sintetiziranim spojevima ispitana je prema ranije opisanoj metodi (203). Stanice su nasađene na mikrotitarske ploče s 96 bunarića u koncentraciji 5000–7000 stanica/mL, ovisno o brzini diobe stanica. Nakon jednodnevne inkubacije na 37 °C pri 5 % CO_2 medij je uklonjen, a stanicama su dodane otopine ispitivanih spojeva (0,1 mL) različitih koncentracija. Otopine ispitivanih spojeva svježe su razrijeđene na dan provođenja pokusa. Stanice su inkubirane 72 h na 37 °C pri 5 % CO_2. Potom je medij uklonjen te su stanice inkubirane s otopinom 3-(4,5-dimetiltiazol-2-il)-2,5-difenil-tetrazolijevog bromida (MTT) u DMEM-u (0,5 mg/mL, 0,1 mL) tijekom 1 h. Po završetku inkubacije medij je uklonjen, a kristali formazana su otopljeni u propan-2-olu (0,1 mL). Intenzitet nastalog obojenja proporcionalan je broju metabolički aktivnih stanica, odnosno vijabilnosti stanica, a očitan je spektrofotometrijski na valnoj duljini 570 nm. Postotak preživljenja, odnosno vijabilnost stanica, određen je na temelju srednjih vrijednosti očitanih apsorbancija prema sljedećim izrazu:

$$vijabilnost\ (\%) = \frac{\bar{A}_{tretirane\ stanice}}{\bar{A}_{kontrola}} \times 100$$

Provedena su minimalno dva neovisna pokusa u triplikatu. IC_{50} vrijednosti izračunate su iz krivulje ovisnosti vijabilnosti stanica o koncentraciji ispitivanog spoja primjenom nelinearne regresijske analize. Rezultati su izraženi kao srednje vrijednosti IC_{50} s pripadajućim standardnim pogreškama.

3.3.1.1. Ispitivanje unutarstanične lokalizacije spojeva

Lokalizacija spojeva u stanici ispitana je na MCF-7 prema ranije objavljenoj metodi (203). Stanice su nasađene na okrugla pokrovna mikroskopska stakalca u ploči s 24 bunarića u koncentraciji 5×10^4 stanica/bunarić te su inkubirane pri 37 °C i 5 % CO_2 tijekom 24 h. Potom je medij uklonjen, a stanicama su dodane otopine ispitivanih spojeva (1 mL) koncentracije 10 μM. Nakon inkubacije koja je trajala 0,5 h medij je uklonjen, a pokrovna stakalca su isprana dva puta PBS-om, prebačena na predmetno stakalce i odmah analizirana. Lokalizacija spoja u stanici istražena je pomoću fluorescentnog mikroskopa (Olympus BX51), pri povećanju 400 ×, uz DAPI filter. Slike su snimljene korištenjem Olympus DP70 digitalne kamere.

3.3.2. ISPITIVANJE ANTIMALARIJSKOG DJELOVANJA

Ispitivanje antimalarijskog djelovanja sintetiziranih hibrida na eritrocitnu fazu životnog ciklusa plazmodija provedeno je na Institutu za tropsku medicinu, Sveučilište u Tübingenu, Njemačka, dok je djelovanje na hepatocitnu fazu ispitano na Institutu za molekularnu medicinu, Medicinski fakultet, Sveučilište u Lisabonu, Portugal.

3.3.2.1. Ispitivanje djelovanje hibrida na eritrocitnu fazu životnog ciklusa plazmodija

Djelovanje sintetiziranih hibrida na eritrocitnu fazu životnog ciklusa plazmodija ispitano je korištenjem HRP2 testa (engl. *histidine-rich protein 2*) prema ranije opisanoj metodi (204, 205). Ispitivanje je provedeno na dva soja *P. falciparum*: *Pf*3D7 (CQOS) i *Pf*Dd2 (CQRS, porijeklom iz Indokine). Antimalarijsko djelovanje odabranih harmikina ispitano je na dva dodatna soja: *Pf*K1 (soj otporan na CQ, pirimetamin i sulfadoksin, porijeklom iz Tajlanda) i *Pf*7G8 (soj otporan na CQ i pirimetamin, porijeklom iz Brazila). Ukratko, ispitivani spojevi naneseni su u serijskim razrijeđenjima na mikrotitarsku ploču s 96 bunarića, nakon čega je dodana stanična kultura plazmodija u stadiju prstena (hematokrit 1,5 %, parazitemija 0,05 %). Nakon trodnevne inkubacije na 37 °C, pri 5 % CO_2 i 5 % O_2, uzorci su analizirani HRP2-ELISA metodom. Ispitivanja su provedena u duplikatu, u najmanje dva neovisna eksperimenta. Koncentracija spoja koja inhibira rast stanica za 50 % *(*IC_{50}) određena je iz krivulje ovisnosti učinka o koncentraciji ispitivanog spoja primjenom nelinearne regresijske analize u programu R v2.6.1. Rezultati su izraženi kao srednje vrijednosti IC_{50} s pripadajućim standardnim pogreškama.

3.3.2.2. Ispitivanje inhibicije polimerizacije hemozoina

Ispitivanje sposobnosti spojeva da inhibiraju polimerizaciju hemozoina provedeno je prema ranije objavljenoj metodi (111). Na mikrotitarsku ploču s 96 bunarića nanesena je otopina hemin klorida u DMSO-u (5,2 mg/mL, 50 μL), nakon čega su u bunariće dodane otopine ispitivanih spojeva u DMSO-u (1 mM, 50 μL). Kao pozitivna kontrola korištena je otopina CQ difosfata u DMSO-u (1 mM, 50 μL), dok je kao negativna kontrola korišten DMSO (50 μL). Stvaranje β-hematina inicirano je dodatkom fosfatnog pufer pH = 4,4 (0,2 M, 100 μL). Uzorci su inkubirani pri 37 °C tijekom 48 h, nakon čega su ploče centrifugirane pri 1500 rcf

(Eppendorf Centrifuge 5804/5804R) tijekom 0,33 h. Supernatant je uklonjen, a talog ispran DMSO-om (3 × 200 μL) i ultračistom vodom (× 200 mL). Svako ispiranje taloga podrazumijevalo je centrifugiranje pri 1500 rcf i odstranjivanje supernatanta. Talog koji je zaostao nakon ispiranja otopljen je u 0,2 M NaOH (200 μL), a otopina razrijeđena s 0,1 M NaOH (omjer 1:6). Dobivenim otopinama izmjerena je apsorbancija pri 405 nm korištenjem uređaja Victor 3 (Perkin Elmer).

3.3.2.3. Ispitivanje učinka hibrida na hepatocitnu fazu životnog ciklusa plazmodija

Djelovanje sintetiziranih spojeva na hepatocitnu fazu *P. berghei* ispitano je korištenjem testa bioluminiscencije prema ranije opisanoj metodi (206, 207). Ukratko, humana stanična linija hepatocelularnog karcinoma (Huh7) nasađena je u mikrotitarsku ploču s 96 bunarića te inkubirana tijekom noći na 37 °C, pri 5 % CO_2. Idući dan stanični medij je zamijenjen otopinama ispitivanih spojeva odgovarajućih koncentracija, a mikrotitarske ploče su inkubirane tijekom 1 h na 37 °C, pri 5 % CO_2. Potom su stanične kulture u bunarićima tretirane sporozoitima *P. berghei* koji eksprimiraju luciferazu. Infektirane stanične kulture su centrifugirane te inkubirane tijekom 46 sati na 37 °C, pri 5 %. Kako bi se odredio učinak ispitivanih spojeva na vijabilnost parazita, stanične kulture su inkubirane bojom Alamar Blue, nakon čega je proveden test bioluminiscencije. IC_{50} je određena iz krivulje doza-učinak primjenom nelinearne regresijske analize u programu GraphPad Prism 6.0. Rezultati su izraženi kao srednje vrijednosti IC_{50} s pripadajućim standardnim pogreškama.

4. REZULTATI I RASPRAVA

4.1. SINTEZE

U ovom doktorskom radu opisana je priprava, karakterizacija i biološko djelovanje hibridnih spojeva harmina, odnosno β-karbolina i: a) DCK-a (harmicini), b) CQ-a (harmikini) i c) ferocena (harmiceni). U hibridima su kao poveznice između β-karbolinskog i cimetnog/klorokinskog/ferocenskog dijela molekule korišteni 1,2,3-triazol i amid te su dobiveni derivati triazolskog (TT), odnosno amidnog tipa (AT). Triazol je u molekulu hibrida uveden korištenjem CuAAC, poznatije kao klik-reakcije, dok je amid pripravljen reakcijom povezivanja (engl. *coupling reaction*) karboksilne kiseline i amina. Osim korištenja dvije vrste poveznica, strukturna raznolikost hibrida dodatno je ostvarena supstituiranjem β-karbolinskog prstena u 5 različitih položaja. Sintetizirani su (Slike 58-60):

i. harmicini TT **47a-e**, **48a-e**, **49a-e**, **50a,c-e**,
ii. harmikini TT **51-58**,
iii. harmikini AT **59-65**,
iv. harmiceni TT **66-75**,
v. harmiceni AT **76-83**.

Prije priprave harmicina, harmikina i harmicena, bilo je potrebno sintetizirati njihove prekursore, derivate β-karbolina, DCK-a, CQ-a i ferocena. Pripravljeni su sljedeći spojevi prekursori:

i. alkini β-karbolina **4**, **13**, **15**, **19**, **24** i **28**,
ii. azidi β-karbolina **6**, **11**, **22**, **27** i **31**,
iii. amini β-karbolina **7**, **12**, **21**, **26**, **30**,
iv. karboksilna kiselina harmina **33**,
v. alkini DCK-a **34a-e**,
vi. azidi DCK-a **37a-e**,
vii. alkin 7-klorkinolina **42**,
viii. azidi 7-klorkinolina **38** i **40**,
ix. karboksilna kiselina 7-klorkinolina **43**
x. amini 7-klorkinolina **44** i **45**
xi. azid ferocena **46**.

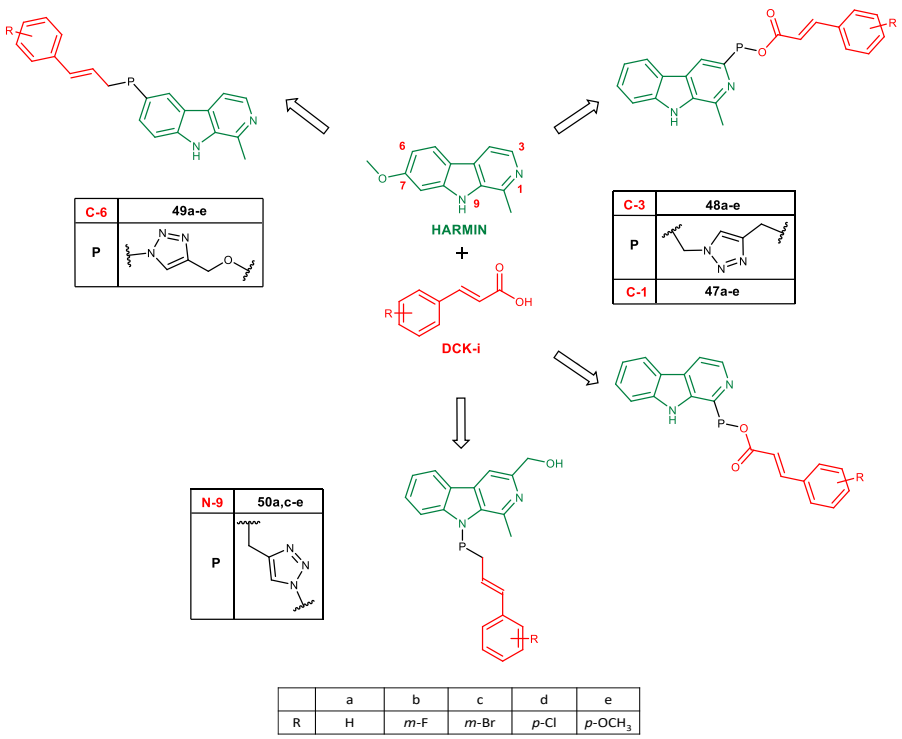

Slika 58. Harmicini, P – poveznica

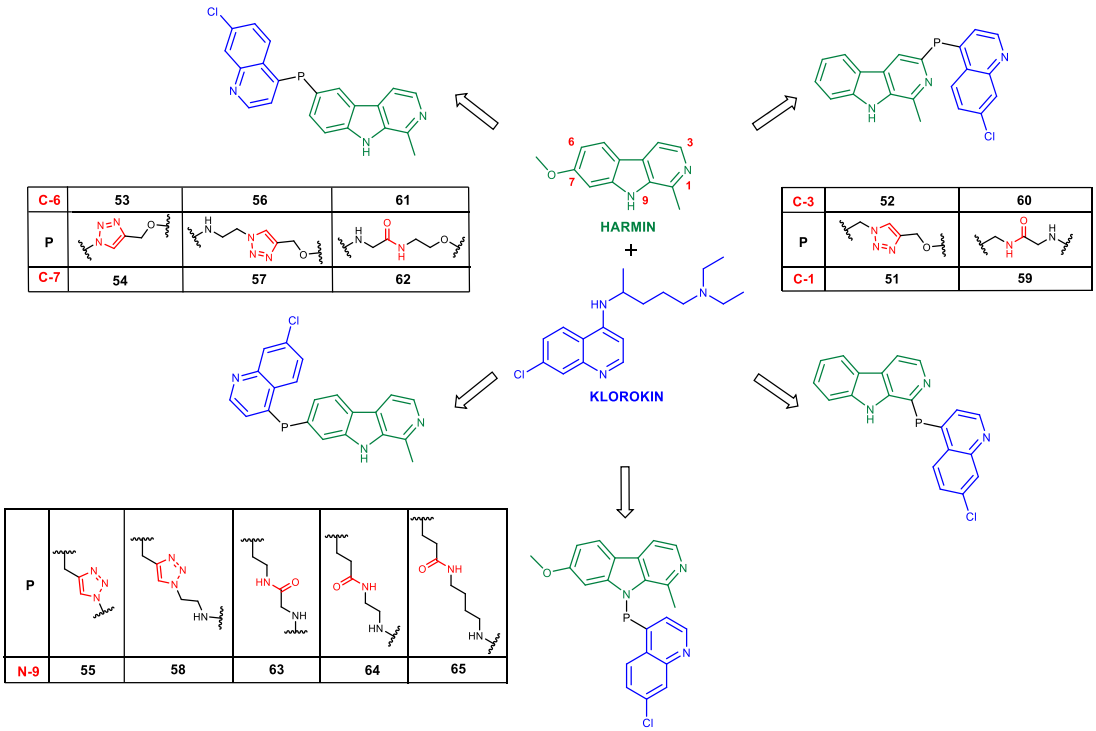

Slika 59. Harmikini, P – poveznica

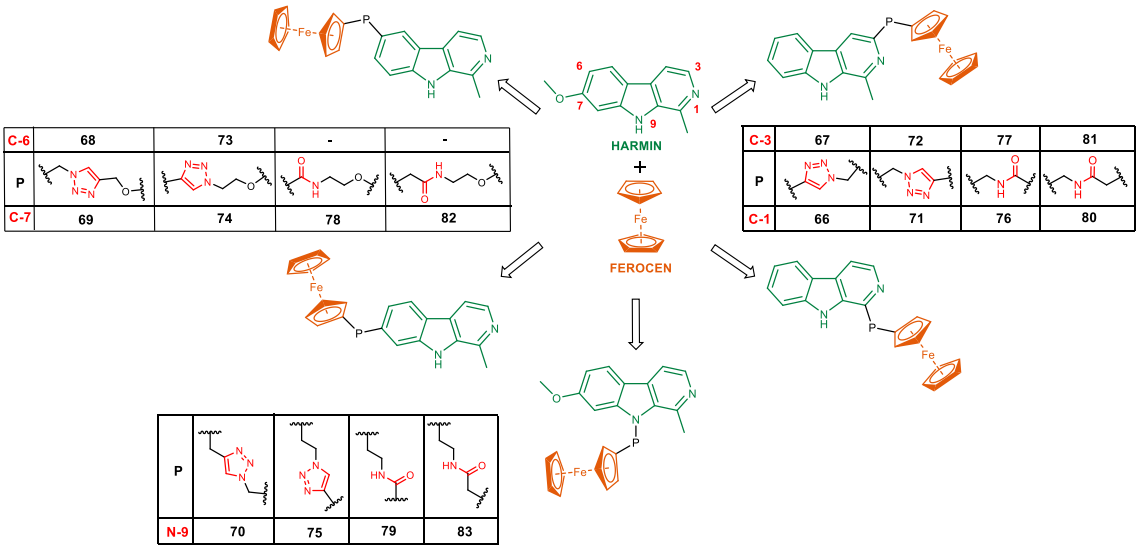

Slika 60. Harmiceni, P – poveznica

4.1.1. Sinteza C-1 alkina, azida i amina β-karbolina

Prvi korak u pripravi C-1, C-3 i O-6 alkina, azida i amina β-karbolina podrazumijevao je sintezu tetrahidro-β-karbolina Pictet-Spenglerovom reakcijom triptamina ili njegovog derivata i odgovarajućeg aldehida. U drugom koraku dobiveni tetrahidro-β-karbolini oksidirani su u β-karboline, nakon čega su modifikacijama supstituenata pripravljeni potrebni alkini, azidi i amini.

Sinteza C-1 alkina, azida i amina počinje Pictet-Spenglerovom reakcijom triptamina i 2,2-dimetoksiacetaldehida uz TFA pri čemu nastaje enantiomerna smjesa tetrahidro-β-karbolina **1** koja je pomoću $KMnO_4$ oksidirana u β-karbolin **2** (Shema 13) (192). MnO_2, nusprodukt koji nastaje redukcijom $KMnO_4$, uklonjen je filtracijom rekacijske smjese kroz sloj Celita. Acetalna skupina spoja **2** hidrolizirana je refluksiranjem u smjesi octene kiseline i vode (omjer 2:3) dajući aldehid **3** (192) koji je poslužio za pripravu alkina **4** i alkohola **5**.

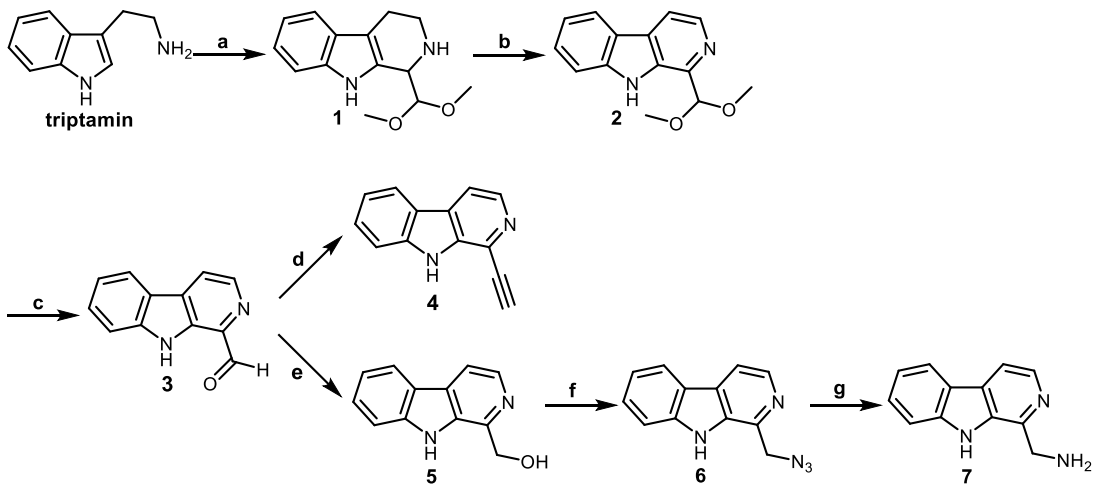

Shema 13. Sinteza C-1 međuprodukata β-karbolina
Reagensi i uvjeti: (a) $(CH_3O)_2CHCHO$, TFA, CH_2Cl_2, s.t., 18 h; (b) $KMnO_4$, THF, s.t, 48 h; (c) AcOH, H_2O, 100 °C, 1 h; (d) $CH_3COCN_2PO(OCH_3)_2$, K_2CO_3, MeOH, s.t., 2 h; (e) $LiAlH_4$, THF, s.t., 0,5 h; (f) ADMP, DBU, THF, 0 °C, 1 h; (g) H_2/Pd/C, MeOH, s.t., 3 h.

Alkin **4** je pripravljen na drugačiji način nego je opisano u literaturi (200), pretvorbom aldehida u alkin primjenom reakcije homologacije. Postoje različite metode homologacije za pripravu alkina iz aldehida (208). Metode isprobane za sintezu C-1 alkina prikazane su na Shemi 14.

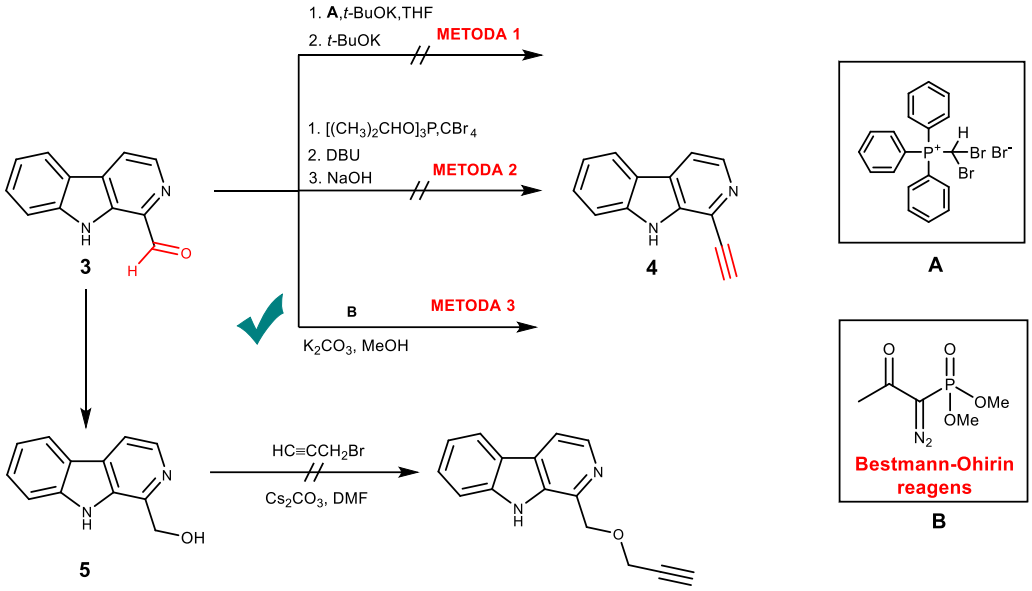

Shema 14. Optimiranje sinteze C-1 alkina β-karbolina

Metode 1 i 2 podrazumijevale su korištenje jakih baza (*t*-BuOK, DBU, NaOH) i zahtijevale složene postupke obrade reakcijske smjese (209, 210). Dodatno, Metoda 1 uključivala je pripravu reagensa A. Metoda 3 predstavlja Bestman-Ohirinu modifikaciju Seyferth-Gilbertove homologacije. Klasična Seyferth-Gilbertova homologacija je *one-pot* rekacija prevođenja adehida u alkin posredstvom dimetil(diazometil)fosfonata (DAMP). Ovaj reagens je nestabilan, zbog čega nije komercijalno dostupan, već ga je potrebno pripremiti neposredno prije reakcije. Bestmann i Ohira otkrili su da se DAMP može učinkovito zamijeniti stabilnim dimetil(1-diazo-2-oksopropil)fosfonatom (Bestmann-Ohirin reagens, BOR), koji se *in situ* deacilira i tvori anion DAMP-a potreban za odvijanje reakcije (208, 211). Detaljan mehanizam Bestman-Ohirine modifikacije Seyferth-Gilbertove homologacije prikazan je na Shemi 15.

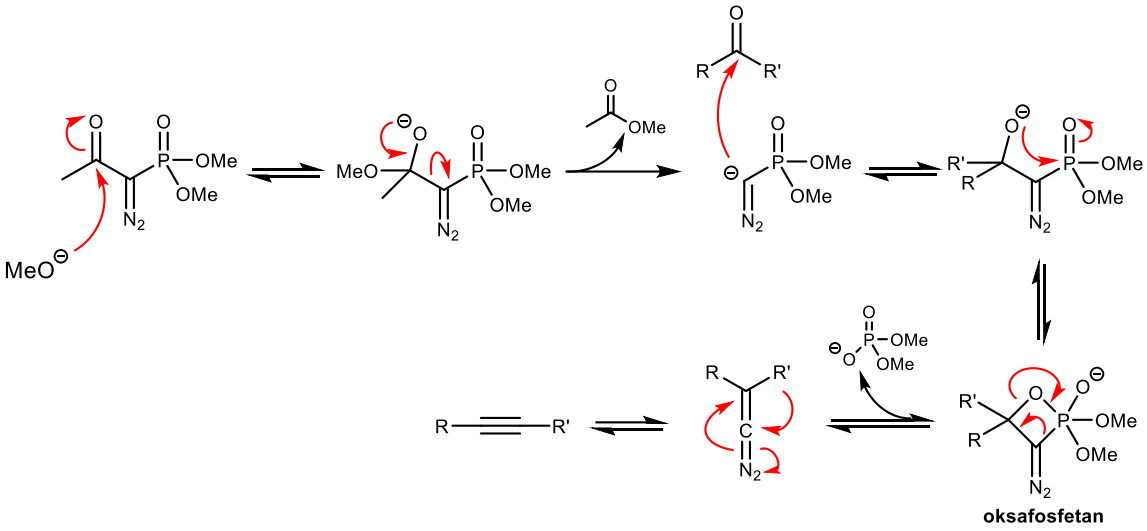

Shema 15. Mehanizam Seyferth-Gilbertove homologacije uz Bestmann-Ohirinu modifikaciju

Reakcijom K_2CO_3 i metanola nastaju metoksidni anioni koji se nukleofilno adiraju na karbonilnu skupinu BOR-a, nakon čega dolazi do deacilacije i nastanka aniona DAMP-a. Potonji reagira s karbonilnom skupinom aldehida ili ketona dajući α-diazoalkoksid. Nukleofilnim napadom kisikovog aniona na fosfor dolazi do generiranja oksafosfetana. Slijedi eliminacija dimetilfosfonata i nastajanje termički nestabilnog diazovinilnog međuprodukta. Gubitkom dušika nastaje vinilkarben koji 1,2-pregradnjom prelazi u alkin (43). Seyferth-Gilbertovom homologacijom modificiranoj prema Bestmann-Ohiri mogu se uspješno pripraviti odgovarajući alkini s dobrim do odličnim iskorištenjima. Nakon jednostavne obrade reakcijske smjese dobiju se alkini visoke čistoće. Štoviše, ova metoda ne zahtjeva korištenje jakih baza, niskih temperatura i odvijanje reakcije pod atmosferom inertnih plinova. Reakcija uspijeva s aromatskim, heteroaromatskim i alifatskim aldehidima (208). Ovom metodom uspješno je pripravljen alkin **4** u dobrom iskorištenju (75 %). Alternativna metoda sinteze C-1 alkina, koja podrazumijeva alkiliranje alkohola **5** uz propargil-bromid i cezijev karbonat (analogno pripravi O-6 i O-7 alkina β-karbolina), nije bila uspješna jer je kisik alkoholne skupine slabiji nukleofil od dušika amino skupine te se alkiliranje gotovo selektivno odvijalo u položaju N-9 β-karbolinskog prstena.

Alkohol **5**, dobiven redukcijom aldehida **3** uz $LiAlH_4$, preveden je reakcijom azidacije u azid **6** korištenjem ADMP-a i baze DBU (212). U ovoj reakciji ADMP je donor azidne skupine, dok DBU ima dvije uloge: aktivira ADMP i neutralizira nastalu heksafluorfosfornu kiselinu (213). Nusprodukti, 2-imidazolidinon i DBU × HPF_6, topljivi su u vodi te se ekstrakcijom lako uklanjaju iz reakcijske smjese (212). Azid **6** je redukcijom u atmosferi vodika uz 10 %-tni Pd/C (katalizator) preveden u amin **7**.

NMR spektroskopski podaci pripravljenih spojeva **1-5** odgovaraju literaturnim podacima. Strukture novosintetiziranih spojeva **6** i **7** potvrđene su uobičajenim metodama (IR, ^{1}H i ^{13}C NMR, MS).

Azid **6** se tijekom MS analize raspada te njegov MS spektar nije priložen. Njegova struktura potvrđena je analizom IR i NMR spektara. IR spektar azida **6** pokazuje karakterističnu vrpcu na 2105 cm^{-1} (N=N=N istezanje), dok su kemijski pomaci protona u ^{1}H, odnosno atoma ugljika u ^{13}C NMR spektrima u skladu s predloženom strukturom azida. U ^{1}H spektru amina **7** nisu vidljivi signali protona za NH, odnosno NH_2 skupinu jer su izmijenjeni s D_2O, ali su kemijski pomaci atoma ugljika u ^{13}C NMR spektru u skladu s predloženom strukturom. U IR spektru amina **7** nema karakteristične vrpce za N=N=N istezanje azidne skupine što potvrđuje uspješnu konverziju azida u amin. U MS spektru vidljiv je pseudomolekulski ion. Analitički, MS, IR te ^{1}H i ^{13}C NMR podaci za spojeve **6** i **7** dani su u Tablicama 2 i 3.

Tablica 2. Analitički, MS i IR podaci za C-1 derivate β-karbolinskog prstena – azid **6** i amin **7**

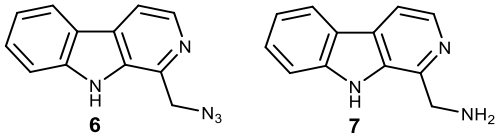

Spoj	Iskor. (%)	t_t (°C)	Molekulska formula M_r	MS (*m/z*)	IR (ATR, ν_{max}/cm^{-1})
6	73	ulje	$C_{12}H_9N_5$ 223,24	– [a]	3663, 3451, 3288, 3059, 2937, 2855, 2105, 1730, 1631, 1566, 1493, 1428, 1371, 1321, 1248, 1118, 1052, 971, 938, 873, 824, 751, 718, 620, 579, 432
7	71	201–205[a]	$C_{12}H_{11}N_3$ 197,24	196,0 $(M-1)^-$	3347, 3282, 3120, 3051, 2955, 2856, 2776, 1625, 1600, 1562, 1501, 1477, 1460, 1430, 1355, 1327, 1316, 1240, 1212, 1163, 1127, 1108, 1071, 960, 896, 848, 829, 772, 747, 671, 595, 564, 516

[a] raspad

Tablica 3. ^{1}H i ^{13}C NMR spektroskopski podaci za C-1 derivate β-karbolinskog prstena – azid **6** i amin **7**

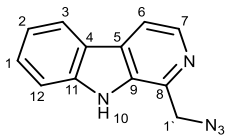

6

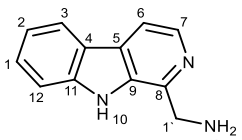

7

Spoj	^{1}H NMR (DMSO-d_6, δ ppm)	^{13}C NMR (DMSO-d_6, δ ppm)
6	11,78 (s, 1H, 10), 8,36 (d, 1H, 7, *J* = 5,2 Hz), 8,29–8,23 (m, 1H, 3), 8,13 (d, 1H, 6, *J* = 5,2 Hz), 7,64 (dt, 1H, 12, *J* = 8,3, 0,9 Hz), 7,60–7,57 (m, 1H, 1), 7,29–7,26 (m, 1H, 2), 4,89 (s, 2H, 1')	140,58 (8), 139,19 (11), 137,75 (7), 133,86 (9), 128,50 (5), 128,44 (1), 121,87 (3), 120,74 (4), 119,57 (2), 114,77 (6), 112,02 (12), 51,59 (1')
7	8,26 (d, 1H, 7, *J* = 5,2 Hz), 8,21 (dt, 1H, 3, *J* = 7,8, 1,0 Hz), 7,97 (d, 1H, 6, *J* = 5,2 Hz), 7,63–7,62 (m, 1H, 12), 7,55–7,52 (m, 1H, 1), 7,24–7,22 (m, 1H, 2), 4,19 (s, 2H, 1')	146,51 (8), 140,35 (11), 137,18 (7), 133,23 (9), 127,82 (1), 127,42 (5), 121,60 (3), 120,88 (4), 119,15 (2), 113,19 (6), 112,01 (12), 44,59 (1')

4.1.2. Sinteza C-3 alkina, azida i amina β-karbolina

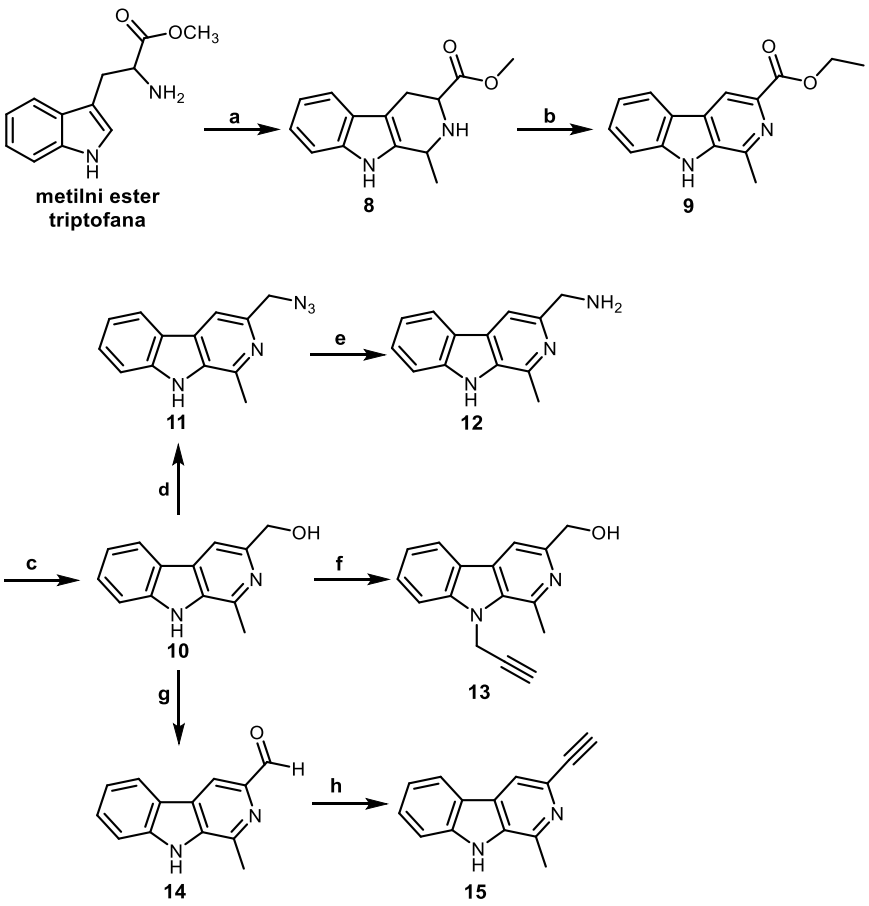

Shema 16. Sinteza C-3 alkina, azida i amina β-karbolina

Reagensi i uvjeti: (a) $(CH_3O)_2CHCH_3$, TFA, CH_2Cl_2, s.t., 18 h; (b) Pd/C, EtOH, MW, 150 °C, 0,33 h; (c) $LiAlH_4$, THF, s.t., 0,5 h; (d) ADMP, DBU, THF, 0 °C, 1 h; (e) H_2/Pd/C, MeOH, s.t., 3 h; (f) $HC{\equiv}CCH_2Br$, Cs_2CO_3, DMF, s.t., 5 h; (g) MnO_2, CH_2Cl_2, s.t., 72 h, (h) $CH_3COCN_2PO(OCH_3)_2$, K_2CO_3, MeOH, s.t., 24 h.

Sinteza C-3 alkina, azida i amina počinje reakcijom metilnog estera triptofana i acetaldehid-dimetil-acetala uz TFA pri čemu nastaje dijastereomerna smjesa tetrahidro-β-karbolina **8** (192) koja je oksidirana uz 10 %-tni Pd/C pomoću mikrovalova u β-karbolin **9** (Shema 16) (42). Provođenje reakcije pri visokoj temperaturi (150 °C), u velikom suvišku etanola, rezultiralo je transesterifikacijom metilnog u etilni ester, što nije opisano u literaturi, ali nije imalo utjecaj na daljnji tijek sinteze (42). Ester **9** reduciran je korištenjem $LiAlH_4$ u alkohol **10** koji je poslužio za sintezu: a) azida **11**, reakcijom azidacije uz ADMP i DBU, b) alkina **13**, alkiliranjem s propargil-bromidom u prisustvu Cs_2CO_3, c) aldehida **14**, oksidacijom uz MnO_2. Redukcijom azida **11** u atmosferi vodika uz Pd/C priređen je amin **12**, dok je reakcijom homologacije aldehid **14** preveden u alkin **15**.

NMR spektroskopski podaci pripravljenih spojeva **8**, **10** i **14** odgovaraju literaturnim podacima. ^{1}H i ^{13}C NMR spektroskopski podaci spoja **9** potvrđuju nastajanje etilnog estera. Strukture novosintetiziranih spojeva **11-13** i **15** potvrđene su uobičajenim metodama (IR, ^{1}H i ^{13}C NMR, MS). Analitički, MS, IR te ^{1}H i ^{13}C NMR podaci za spojeve **11-13** i **15** dani su u Tablicama 4 i 5.

Azid **11** se, poput azida **6**, raspada prilikom MS analize. Njegova struktura potvrđena je IR i NMR spektrima. U IR spektru azida **11** vidljiva je karakteristična vrpca na 2108 cm^{-1} (N=N=N istezanje), dok su kemijski pomaci protona u ^{1}H, odnosno atoma ugljika u ^{13}C NMR spektrima u skladu s predloženom strukturom azida. U ^{1}H spektru amina **7** nije vidljiv signal protona za NH_2 skupinu jer je izmijenjen s D_2O, ali su kemijski pomaci atoma ugljika u ^{13}C NMR spektru u skladu s predloženom strukturom. U IR spektru amina **7** nema karakteristične vrpce za N=N=N istezanje azidne skupine što potvrđuje uspješnu konverziju azida u amin. U IR spektrima alkina **13** i **15** vidljiva je karakteristična vrpca (C≡C istezanje) pri 2109 cm^{-1}, odnosno 2104 cm^{-1}, redom. Dodatno, u IR spektru alkina **15** vidljiva je oštra, slaba vrpca pri 3306 cm^{-1} (≡C-H istezanje), dok je u IR spektru alkina **13** ta vrpca spojena sa širokom, jakom vrpcom pri 3154 cm^{-1} (O-H istezanje). U ^{1}H NMR spektru alkina **13** signal protona iz OH skupine vidljiv je kao triplet (sprezanje sa susjednom metilenskom skupinom) i očekivano pomaknut ulijevo (5,35 ppm), dok je signal za proton ≡C-H vidljiv kao triplet (sprezanje s metilenskom skupinom udaljenom 1 C atom) na 3,35 ppm. U MS spektrima spojeva **12**, **13** i **15** vidljivi su pseudomolekulski ioni.

Tablica 4. Analitički, MS i IR podaci za C-3 derivate β-karbolinskog prstena (**11-13**, **15**)

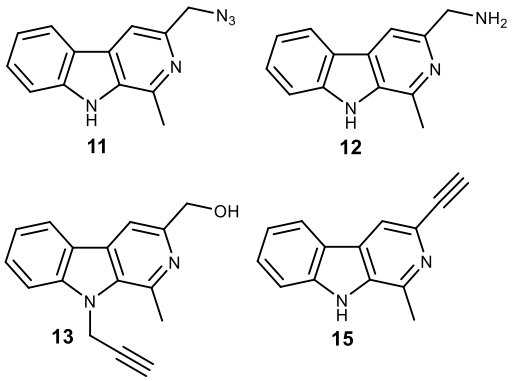

Spoj	Iskor. (%)	t_t (°C)	Molekulska formula M_r	MS (*m/z*)	IR (ATR, ν_{max}/cm^{-1})
11	76	ulje	$C_{13}H_{11}N_5$ 237,27	– [a]	3671, 3451, 3239, 3051, 2937, 2863, 2447, 2325, 2104, 1689, 1631, 1566, 1509, 1452, 1403, 1354, 1264, 1085, 1036, 971, 848, 759, 718, 644, 579, 431
12	61	176–178,5	$C_{13}H_{13}N_3$ 211,27	210,0 $(M-1)^-$	3338, 3239, 3130, 3057, 2978, 2940, 2914, 2882, 2850, 2783, 2737, 2690, 2637, 1626, 1606, 1566, 1503, 1453, 1401, 1374, 1344, 1317, 1284, 1250, 1176, 1147, 1103, 1083, 1009, 970, 945, 891, 838, 813, 775, 734, 643, 588, 545
13	72	225–230[a]	$C_{16}H_{14}N_2O$ 250,30	251,1 $(M+1)^+$	3154, 2929, 2823, 2109, 1621, 1561, 1475, 1453, 1360, 1333, 1283, 1206, 1139, 1063, 1040, 965, 933, 877, 744, 724, 641, 578
15	61	230–235 [a]	$C_{14}H_{10}N_2$ 206,25	207,6 $(M+1)^+$	3306, 3143, 2104, 1622, 1597, 1563, 1499, 1446, 1375, 1338, 1315, 1247, 1178, 1146, 1014, 961, 899, 877, 776, 740, 654, 625, 587, 504, 457

[a] raspad

Tablica 5. ^{1}H i ^{13}C NMR spektroskopski podaci za C-3 derivate β-karbolinskog prstena (**11**-**13**, **15**)

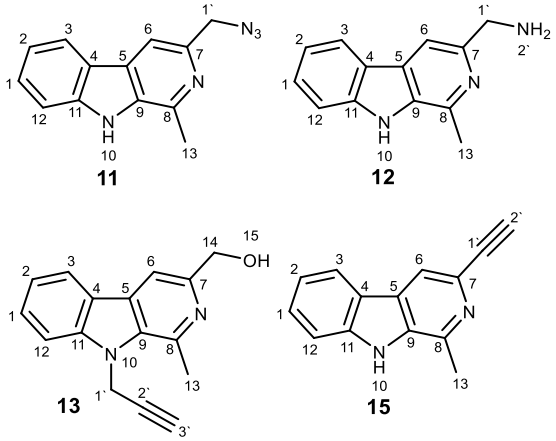

Spoj	^{1}H NMR (DMSO-d_6, δ ppm)	^{13}C NMR (DMSO-d_6, δ ppm)
11	11,66 (s, 1H, 10), 8,20 (d,1H, 3, *J* = 7,9 Hz), 8,00 (s, 1H, 6), 7,62–7,60 (m, 1H, 12), 7,57–7,53 (m, 1H, 1), 7,26–7,23 (m, 1H, 2), 4,57 (s, 2H, 1'), 2,78 (s, 3H, 13)	143,23 (7), 142,12 (11), 140,74 (8), 133,94 (9), 128,02 (1), 127,56 (5), 121,74 (3), 121,01 (4), 119,39 (2), 112,07 (12), 111,72 (6), 55,30 (1'), 20,41 (13)
12	11,42 (s, 1H, 10), 8,14 (d, 1H, 3, *J* = 7,6 Hz), 7,91 (s, 1H, 6), 7,57–7,47 (m, 2H, 1, 12), 7,20 (t, 1H, 2, *J* = 6,9 Hz), 3,89 (s, 2H, 1'), 2,73 (s, 3H, 13)	151,13 (7), 140,89 (11), 140,74 (8), 133,29 (9), 127,76 (5), 127,62 (1), 121,53 (3), 121,19 (4), 118,98 (2), 111,89 (12), 109,01 (6), 47,59 (1'), 20,38 (13)
13	8,25 (d, 1H, 3, *J* = 7,8 Hz), 8,03 (s, 1H, 6), 7,78 (d, 1H, 12, *J* = 8,3 Hz), 7,63–7,58 (m, 1H, 1), 7,29 (t, 1H, 2, *J* = 7,4 Hz), 5,45 (d, 2H, 1', *J* = 2,4 Hz), 5,35 (t, 1H, 15, *J* = 5,8 Hz), 4,68 (d, 2H, 14, *J* = 5,8 Hz), 3,35 (t, 1H, 3', *J* = 2,4 Hz), 3,04 (s, 3H, 13)	150,83 (8), 141,27 (7), 140,52 (9), 133,22 (11), 129,53 (4), 128,23 (1), 121,52 (3), 121,05 (5), 120,04 (2), 110,37 (12), 109,11 (6), 75,50 (2'), 64,34 (14), 34,19 (1'), 22,45 (13)
15	11,83 (s, 1H, 10), 8,25–8,22 (m, 1H, 3), 8,21 (s, 1H, 6), 7,62–7,59 (m, 1H, 12), 7,57–7,53 (m, 1H, 1), 7,27–7,23 (m, 1H, 2), 4,03 (s, 1H, 2'), 2,74 (s, 3H, 13)	142,83 (7), 140,70 (8), 134,06 (11), 129,54 (9), 128,30 (1), 127,01 (4), 122,05 (3), 120,72 (5), 119,78 (2), 117,22 (6), 112,15 (12), 84,85 (1'), 76,72 (2'), 20,33 (13)

4.1.3. Sinteza O-6 alkina, azida i amina β-karbolina

Sinteza O-6 alkina, azida i amina počinje reakcijom 5-metoksitriptamina i acetaldehid-dimetil-acetala uz TFA na 110 °C pri čemu nastaje trifluroctena sol tetrahidro-β-karbolina **16** (Shema 17). Reakcija se razlikuje u odnosu na literaturni propis prema korištenom otapalu (ACN umjesto 1,2-dikloretana). Spoj **16** oksidiran je uz 10 %-tni Pd/C i Li_2CO_3 na 150 °C u β-karbolin **17** (42). Li_2CO_3 *in situ* oslobađa spoj **16** iz oblika soli. Eterska skupina spoja **17** hidrolizirana je u smjesi octene i bromovodične kiseline na 140 °C u fenol **18**. Prehodne reakcije provedene su uz pomoć mikrovalova.

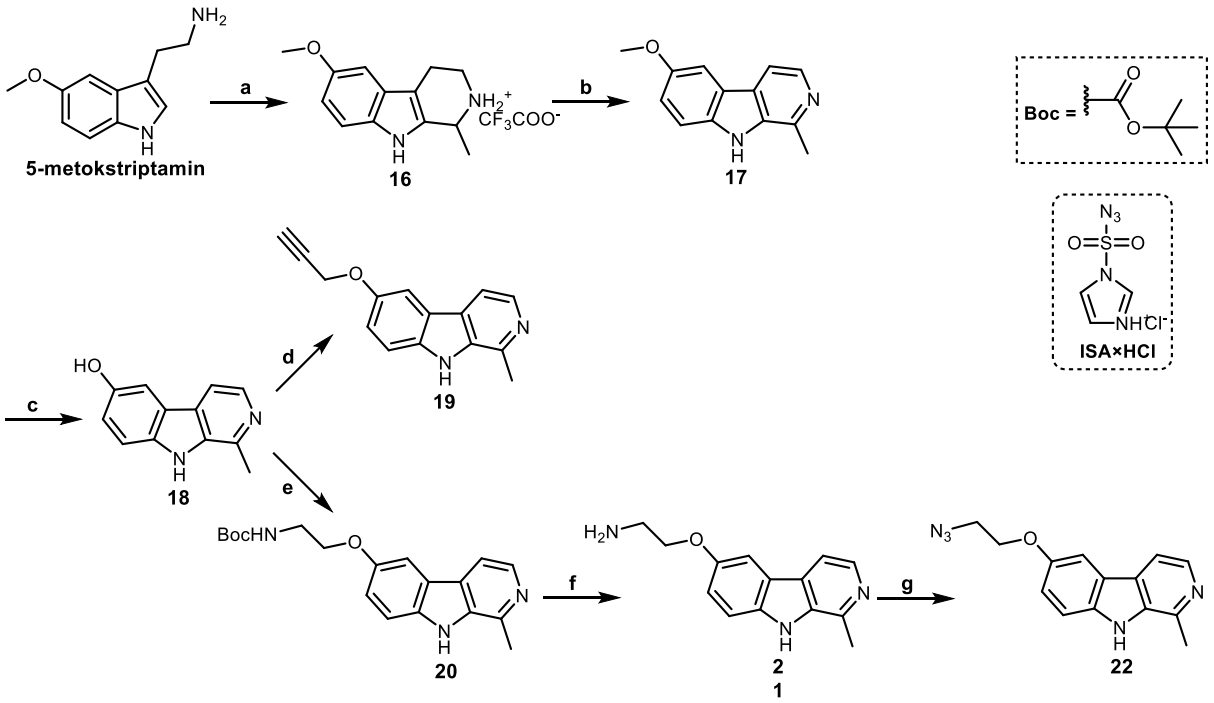

Shema 17. Sinteza O-6 alkina, azida i amina β-karbolina

Reagensi i uvjeti: (a) $(CH_3O)_2CHCH_3$, TFA, ACN, MW, 110 °C, 0,17 h; (b) Pd/C, Li_2CO_3, EtOH, MW, 150 °C, 0,33 h; (c) HBr/CH_3COOH, MW, 140 °C, 0,5 h; (d) $HC{\equiv}CCH_2Br$, Cs_2CO_3, DMF, s.t., 3 h; (e) $BocNH(CH_2)_2Br$, Cs_2CO_3, TBAHS, DMF, s.t., 18 h; (f) HCl/MeOH, 50 °C, 18 h; (g) ISA × HCl, K_2CO_3, $CuSO_4 \times 5H_2O$, MeOH, s.t., 2 h.

Fenol **18** alkiliran je prema S_N2 mehanizmu: 1) propargil-bromidom u prisustvu cezijevog karbonata u alkin **19**, 2) *tert*-butil-(2-bromoetil)karbamatom u prisustvu cezijevog karbonata i TBAHS u *tert*-butil(2-((1-metil-9*H*-pirido[3,4-*b*]indol-6-il)oksi)etil)karbamat **20**. TBAHS ima ulogu katalizatora faznog prijelaza, odnosno služi za prijenos karbonatnih iona u organsku fazu čime ubrzava reakciju alkiliranja. Uklanjanjem Boc zaštitne skupine u kiselim uvjetima, uz 4 M otopinu klorovodične kiseline u metanolu, na 50 °C, dobiven je amin **21**. Uklanjanje Boc-a

odvija se u dva koraka: 1) hidroliza *O*-*tert*-butilne skupine, 2) spontana dekarboksilacija nastale karbaminske kiseline. Amin **21** preveden je uz ISA × HCl, kalijev karbonat i $CuSO_4 \times 5H_2O$ u azid **22**. Diazo donor u reakciji je ISA × HCl, dok je Cu^{2+} katalizator. ISA × HCl može se relativno jednostavno i jeftino pripremiti reakcijom sulfuril-klorida s natrijevim azidom i imidazolom (202). Nestabilni 1*H*-imidazol-1-sulfonil azid preveden je dokapavanjem 1 M klorovodične kiseline u etil-acetatu u stabilnu hidrokloridnu sol.

NMR spektroskopski podaci spojeva **16**-**18** odgovaraju literaturnim podacima. Spojevi **19**-**22** su novi, do sada neopisani spojevi. Strukture spojeva **19**-**21** potvrđene su uobičajenim metodama (IR, MS, ^{1}H i ^{13}C NMR), dok je spoj **22** nestabilan te je njegova struktura potvrđena neizravno, prevođenjem u odgovarajući triazol.

U IR spektru alkina **19** vidljive su karakteristične vrpce na 2128 (C≡C istezanje) i 3292 cm^{-1} (≡C-H istezanje). U IR spektru amina **21** vidljiva je vrpca na 3359 cm^{-1} (N-H istezanje). Kemijski pomaci protona u ^{1}H, odnosno ugljika u ^{13}C NMR spektrima spojeva u skladu su s predloženim strukturama. U ^{1}H NMR spektru alkina **19** signal ≡C-H vidljiv je kao triplet (sprezanje s metilenskom skupinom) na 3,56 ppm. ^{1}H NMR spektar spoja **20** sadrži NH signal amida na 7,06 ppm te 1 signal (singlet, 9 protona) na 1,40 ppm koji odgovara *tert*-butilnoj skupini, dok je u ^{13}C NMR-u vidljiv signal karbonila na 155,73 ppm. U ^{1}H NMR-u amina **21** NH signal nije vidljiv zbog izmjene s D_2O, ali je struktura potvrđena MS analizom. Analitički, MS, IR te ^{1}H i ^{13}C NMR podaci za spojeve **19**-**21** dani su u Tablicama 6 i 7.

Tablica 6. Analitički, MS i IR podaci za O-6 derivate β-karbolinskog prstena (**19-21**)

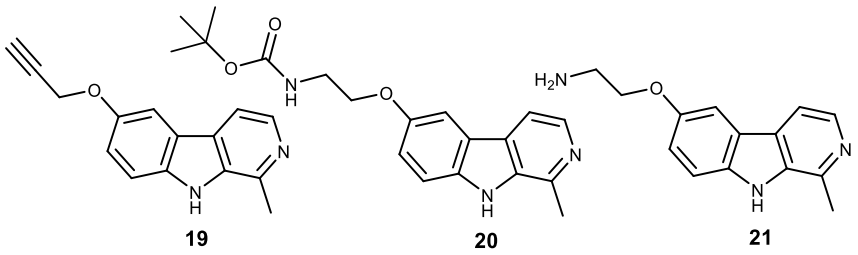

19 **20** **21**

Spoj	Iskor. (%)	t_t (°C)	Molekulska formula M_r	MS (*m/z*)	IR (ATR, ν_{max}/cm^{-1})
19	51	175,5-177,5	$C_{15}H_{12}N_2O$ 236,27	237,1 $(M+1)^+$	3292, 3122, 3054, 2950, 2860, 2766, 2716, 2366, 2330, 2128, 2058, 1866, 1764, 1736, 1606, 1570, 1506, 1476, 1448, 1412, 1380, 1334, 1292, 1260, 1200, 1120, 1068, 1030, 986, 944, 914, 886, 818, 758, 646, 524
20	56	Ulje	$C_{19}H_{23}N_3O_3$ 341,41	342,4 $(M+1)^+$	n.o.[a]
21	69	170,5-172	$C_{14}H_{15}N_3O$ 241,29	242,2 $(M+1)^+$	3645, 3359, 3241, 3065, 2925, 2869, 1605, 1581, 1566, 1500, 1478, 1458, 1401, 1288, 1234, 1211, 1126, 1071, 1059, 992, 905, 884, 847, 825, 816, 741, 703, 632

[a] n.o. – nije određeno

Tablica 7. ^{1}H i ^{13}C NMR spektroskopski podaci za O-6 derivate β-karbolinskog prstena (**19-21**)

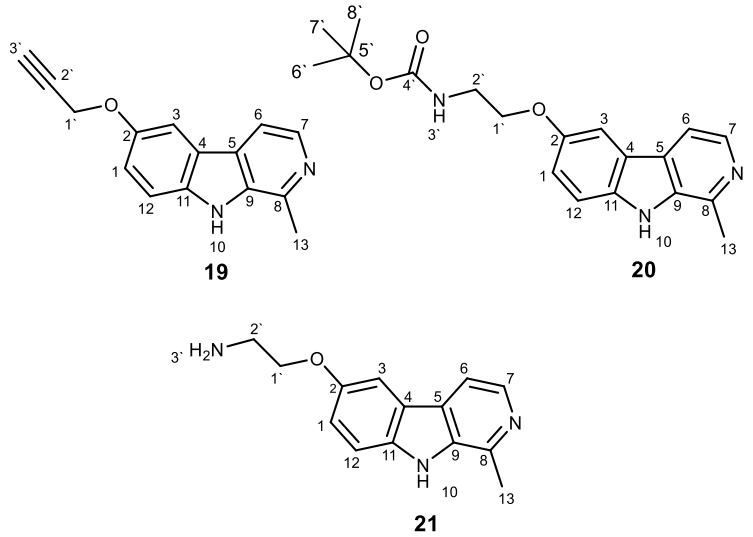

19 **20** **21**

Spoj	^{1}H NMR (DMSO-d_6, δ ppm)	^{13}C NMR (DMSO-d_6, δ ppm)
19	11,42 (s, 1H, 10), 8,17 (d, 1H, 7, *J* = 5,4 Hz), 7,88 (d, 1H, 6, *J* = 5,3 Hz), 7,81 (d, 1H, 3, *J* = 2,5 Hz), 7,53 (d, 1H, 12, *J* = 8,9 Hz), 7,23 (dd, 1H, 1, *J* = 8,8, 2,5 Hz), 4,88 (d, 2H, 1', *J* = 2,4 Hz), 3,56 (t, 1H, 3', *J* = 2,4 Hz), 2,75 (s, 3H, 13)	151,09 (2), 142,26 (8), 137,03 (7), 135,67 (11), 135,12 (9), 126,63 (4), 121,27 (5), 118,34 (1), 112,72 (6), 112,62 (12), 105,62 (3), 78,04 (2'), 56,26 (1'), 20,40 (13)
20	11,42 (s, 1H, 10), 8,16 (d, 1H, 7, *J* = 5,3 Hz), 7,92 (d, 1H, 6, *J* = 5,3 Hz), 7,77 (d, 1H, 3, *J* = 1,7 Hz), 7,51 (d, 1H, 12, *J* = 8,8 Hz), 7,18 (dd, 1H, 1, *J* = 8,8, 2,3 Hz), 7,06 (t, 1H, 3', *J* = 5,0 Hz), 4,05 (t, 2H, 1', *J* = 5,8 Hz), 3,39–3,34 (m, 2H, 2'), 2,75 (s, 3H, 13), 1,40 (s, 9H, 6', 7', 8')	155,73 (4'), 152,39 (2), 142,04 (8), 136,57 (7), 135,41 (11), 135,03 (9), 126,88 (4), 121,35 (5), 118,42 (1), 112,78 (6), 112,75 (12), 104,68 (3), 77,76 (5'), 67,19 (1'), 39,61 (2'), 28,24 (6', 7', 8'), 20,23 (13)
21	11,36 (s, 1H, 10), 8,15 (d, 1H, 7, *J* = 5,3 Hz), 7,90 (d, 1H, 6, *J* = 5,3 Hz), 7,74 (d, 1H, 3, *J* = 2,3 Hz), 7,50 (d, 1H, 12, *J* = 8,8 Hz), 7,19 (dd, 1H, 1, *J* = 8,8, 2,5 Hz), 4,02 (t, 2H, 1', *J* = 5,8 Hz), 2,94 (t, 2H, 2', *J* = 5,7 Hz), 2,74 (s, 3H, 13)	152,47 (2), 141,87 (8), 136,70 (7), 135,19 (11), 134,93 (9), 126,54 (4), 121,29 (5), 117,98 (6), 112,34 (1), 112,18 (12), 104,86 (3), 71,06 (1'), 40,87 (2'), 19,97 (13)

4.1.4. Sinteza O-7 i N-9 derivata β-karbolinskog prstena

O-7 i N-9 derivati β-karbolinskog prstena pripravljeni su iz komercijalno dostupnog harmina, odnosno iz harmola **23** (97, 98) (Shema 18). Harmol **23** dobiven je hidrolizom eterske skupine harmina u smjesi octene i bromovodične kiseline na 140 °C uz mikrovalno zračenje (97). Alkiliranjem harmina, odnosno harmola **23** propargil-bromidom u prisustvu cezijevog karbonata sintetizirani su alkini **24** i **28** (97). Analogno, alkiliranjem harmina/harmola *tert*-butil-(2-bromoetil)karbamatom u prisustvu cezijevog karbonata pripravljeni su *tert*-butil-(2-((1-metil-9*H*-pirido[3,4-*b*]indol-7-il)oksi)etil)karbamat **25** i *tert*-butil-(2-(7-metoksi-1-metil-9*H*-pirido[3,4-*b*]indol-9-il)etil)karbamat **29**. Uklanjanjem Boc zaštitne skupine u 4 M otopini klorovodične kiseline u metanolu na 50 °C dobiveni su amini **26** i **30** (98).

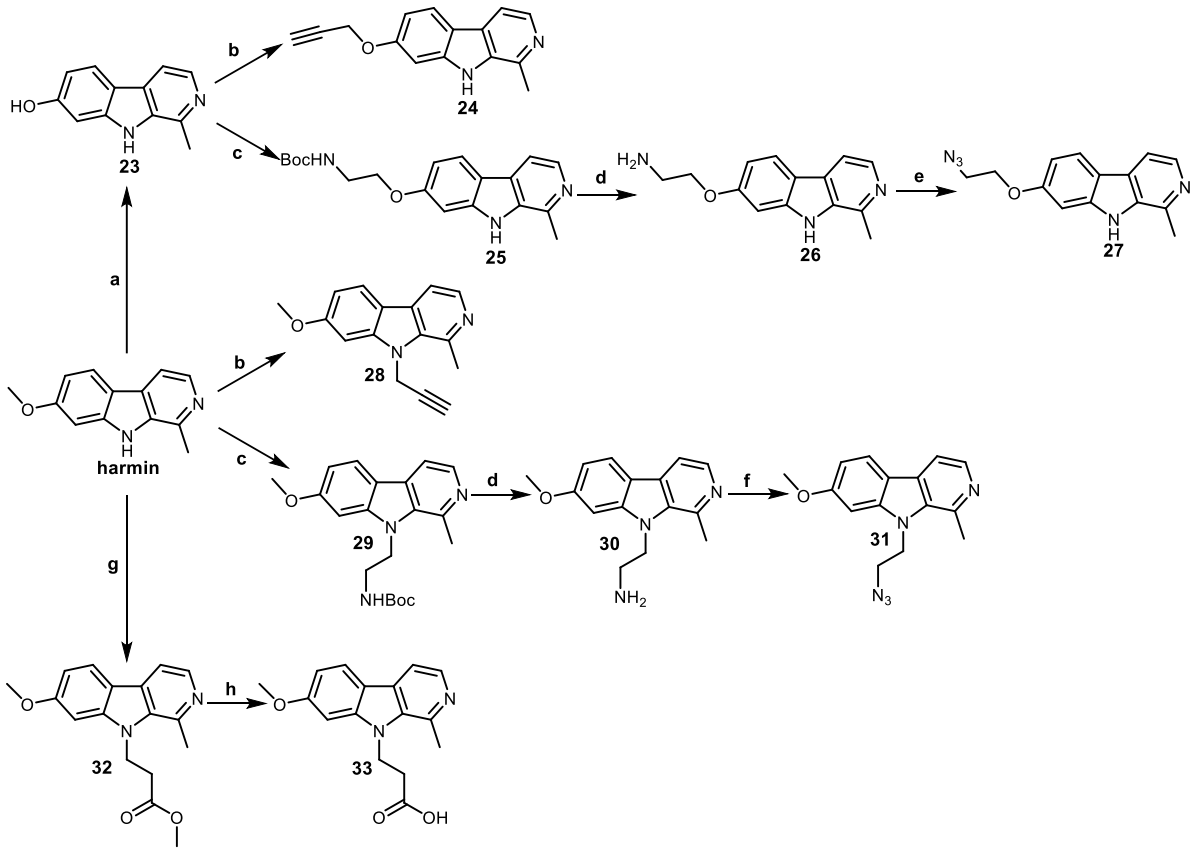

Shema 18. O-7 i N-9 derivata β-karbolinskog prstena

Reagensi i uvjeti: (a) HBr/CH_3COOH, MW, 140 °C, 0,5 h; (b) $HC{\equiv}CCH_2Br$, Cs_2CO_3, DMF, s.t., 3 h; (c) $BocNH(CH_2)_2Br$, Cs_2CO_3, DMF, 90 °C, 24 h; (d) HCl/MeOH, 50 °C, 18 h; (e) ISA × HCl, K_2CO_3, $CuSO_4 \times 5H_2O$, MeOH, s.t., 18 h; (f) ISA × HCl, K_2CO_3, $CuSO_4 \times 5H_2O$, MeOH, s.t., 3h; (g) $CH_2{=}CHCOOCH_3$, DBU, ACN, 60 °C, 48 h; (h) LiOH × H_2O, MeOH/H_2O, s.t., 1 h.

Amini **26** i **30** su pomoću ISA×HCl uz kalijev karbonat i $CuSO_4 \times 5H_2O$ prevedeni u azide **27** i **31** (202). Spojevi **27** i **31** su novi, do sada neopisani spojevi. Struktura spoja **27**

potvrđena je uobičajenim metodama (IR, ^{1}H i ^{13}C NMR), a odgovarajući podaci su dani u Tablici 8. Struktura spoja **31** potvrđena neizravno, prevođenjem u triazol.

Karboksilna kiselina **33** pripravljena je u dva koraka (194). Michaelovom adicijom harmina na metil-akrilat uz DBU u ACN-u na 60 °C pripravljen je ester **32**. Reakcija je provedena uz zaštitu od svjetlosti jer je metil-akrilat na svjetlosti nestabilan. Hidrolizom estera **32** uz LiOH × H_2O u smjesi metanola i vode dobivena je karboksilna kiselina **33**. NMR spektroskopski podaci spojeva **32** i **33** odgovaraju literaturnim podacima.

Tablica 8. Analitički, MS i IR podaci za azid **27**

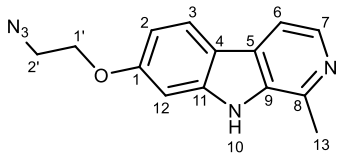

27

Spoj	**27**
Iskor. (%)	79
***t*$_t$ (°C)**	ulje
Molekulska formula	$C_{14}H_{13}N_5O$
***M*$_r$**	267,11
MS (*m/z*)	– [a]
IR (ATR, ν_{max}/cm^{-1})	n.o.[b]
^{1}H NMR (DMSO-*d*$_6$, *δ* ppm)	11,44 (s, 1H, 10), 8,16 (d, 1H, 7, *J* = 5,3 Hz), 8,08 (d, 1H, 3, *J* = 8,6 Hz), 7,82 (d, 1H, 6, *J* = 5,2 Hz), 7,04 (d, 1H, 12, *J* = 2,2 Hz), 6,87 (dd, 1H, 2, *J* = 8,6, 2,2 Hz), 4,30 (t, 2H, 1', *J* = 4,8 Hz), 3,72 (t, 2H, 2', *J* = 4,8 Hz), 2,73 (s, 3H, 13)
^{13}C NMR (DMSO-*d*$_6$, *δ* ppm)	158,70 (1), 141,77 (8), 141,35 (11), 137,78 (7), 134,60 (9), 127,12 (5), 122,75 (3), 115,26 (4), 111,99 (6), 109,14 (2), 95,62 (12), 67,14 (1'), 49,64 (2'), 20,33 (13)

[a] raspad; [b] n.o. – nije određeno.

4.1.5. Sinteza alkina i azida DCK-a

DCK-i su prevedeni u propargilne estere **34a-e** i azide **37a-e** (Shema 19). Propargilni esteri DCK-i pripravljeni su reakcijom cimetne kiseline ili njenih derivata i propargil-bromida uz kalijev karbonat. Propargilni esteri **34a-e**, osim derivata **34c**, su poznati spojevi. Njihovi NMR spektroskopski podaci odgovaraju literaturnim podacima, dok su analitički, IR i NMR spektroskopski podaci za novosintetizirani *m*-Br derivat (**34c**) dani u Tablici 9.

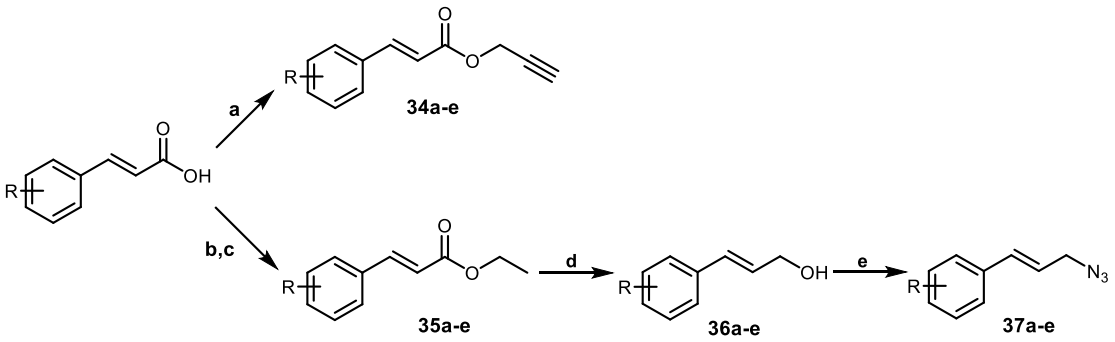

	a	b	c	d	e
R	H	*m*-F	*m*-Br	*p*-Cl	*p*-OCH_3

Shema 19. Sinteza alkina i azida DCK-a

Reagensi i uvjeti: (a) $HC{\equiv}CCH_2Br$, K_2CO_3, DMF, s.t., 48 h; (b) $SOCl_2$, DMF, toluen, s.t., 1 h; (c) EtOH/TEA/CH_2Cl_2, s.t., 3 h; (d) $LiAlH_4$, Et_2O, < 0 °C, 1,5 h; (e) ADMP, DBU, THF, 0 °C, 0,5 h.

Tablica 9. Analitički, MS, IR, ^{1}H i ^{13}C NMR podaci za alkin **34c**

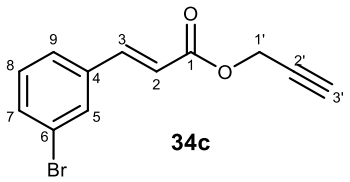

34c

Spoj	**34c**
Iskor. (%)	87
t_t (°C)	79–81
Molekulska formula	$C_{12}H_9BrO_2$
M_r	265,11
MS (*m/z*)	–[a]
IR (ATR) ν_{max} (cm^{-1})	3416, 3279, 3060, 3042, 2940, 2132, 1716, 1637, 1561, 1479, 1419, 1360, 1295, 1201, 1169, 1073, 991, 965, 851, 780, 754, 696, 665, 632, 554
^{1}H NMR (DMSO-d_6, δ ppm)	8,02 (t, 1H, 5, *J* = 1,8 Hz), 7,78 (dt, 1H, 9, *J* = 7,7, 1,4 Hz), 7,69 (d, 1H, 3, *J* = 16,1 Hz), 7,64–7,62 (m, 1H, 7), 7,39 (t, 1H, 8, *J* = 7,9 Hz), 6,79 (d, 1H, 2, *J* = 16,1 Hz), 4,84 (d, 2H, 1', *J* = 2,4 Hz), 3,59 (t, 1H, 3', *J* = 2,5 Hz)
^{13}C NMR (DMSO-d_6, δ ppm)	165,21 (1), 143,81 (3), 136,38 (4), 133,17 (5), 130,99 (7), 130,97 (8), 127,45 (9), 122,32 (6), 118,90 (2), 77,80 (2'), 51,93 (1')

[a] raspad

Azidi DCK-a **37a-e** pripravljeni su u tri reakcijska koraka (97). U prvom reakcijskom koraku DCK-i su uz tionil-klorid i katalitičku količinu DMF-a u bezvodnom toluenu prevedeni u kiselinske kloride koji su nakon uparavanja otopljeni u bezvodnom diklormetanu i dokapani u otopinu TEA u bezvodnom etanolu. Dobiveni etilni esteri **35a-e** reducirani su uz $LiAlH_4$ u bezvodnom eteru u alkohole **36a-e**. Reakcije redukcije provedene su pri temperaturi < –5 °C, uz dodavanje reducensa u obrocima, kako se ne bi reducirala α,β dvostruka veza. Alkoholi su uz reagens ADMP i bazu DBU prevedeni u odgovarajuće azide **37a-e**. NMR spektroskopski podaci pripravljenih azida odgovaraju literaturnim podacima.

4.1.6. Sinteza azida, alkina, karboksilne kiseline i amina 7-klorkinolina

Prekursori u sintezi harmikina, azidi **38** i **40**, alkin **42**, karboksilna kiselina **43** te amini **44** i **45**, pripravljeni su iz 4,7-diklorkinolina (Shema 20), a njihovi NMR spektroskopski podaci odgovaraju literaturi.

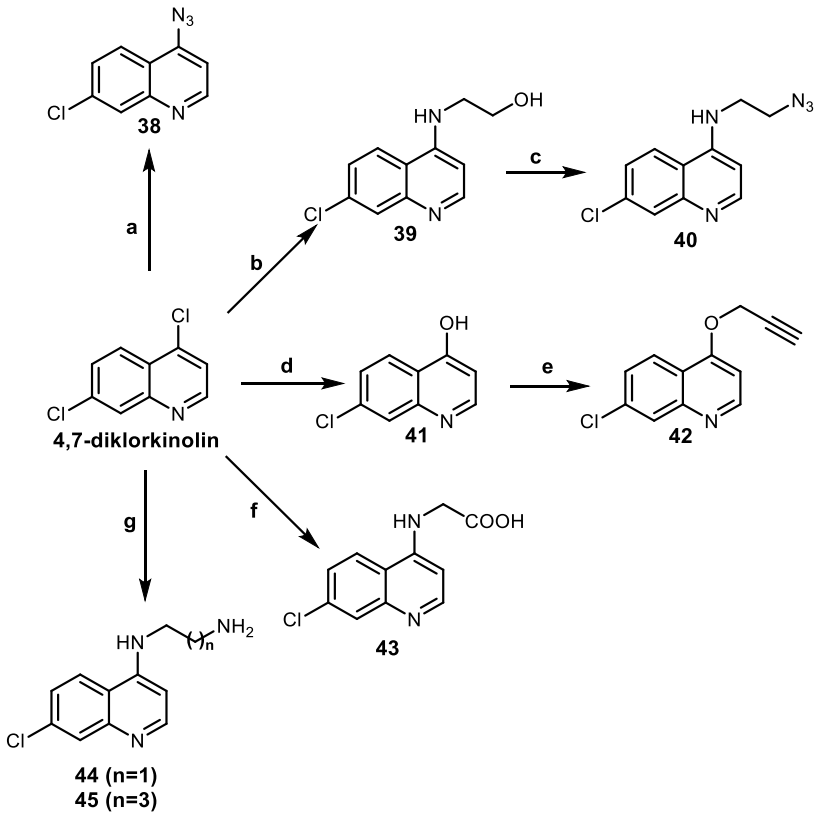

Shema 20. Sinteza klorkinolinskih alkina, azida, karboksilne kiseline i amina
Reagensi i uvjeti: (a) NaN_3, DMF, 65 °C, 18 h; (b) $H_2N(CH_2)_2OH$, TEA, 120 °C, 2 h; (c) ADMP, DBU, THF, 0 °C, 1,5 h; (d) AcOH, 125 °C, 1 h; (e) $HC{\equiv}CCH_2Br$, Cs_2CO_3, DMF, s.t., 1 h; (f) H_2NCH_2COOH, C_6H_5OH, 125 °C, 21 h; (g) $H_2NCH_2(CH_2)_nNH_2$, 95 °C, 1 h.

Azid **38** sintetiziran je u jednom reakcijskom koraku, reakcijom 4,7-diklorkinolina i natrijevog azida u bezvodnom DMF-u na 65 °C (195), dok je priprava azida **40** uključivala dva reakcijska koraka. Reakcijom 4,7-diklorkinolina i etanolamina u prisutstvu TEA na 120 °C dobiven je alkohol **39** (199) koji je uz ADMP i DBU na 0 °C preveden u azid **40** (97).

Alkin **42** pripravljen je na drugačiji način nego je opisano u literaturi, alkiliranjem 7-klorkinolin-4-ola **41** propargil bromidom u prisustvu cezijevog karbonata u bezvodnom DMF-u. Fenol **41** dobiven je reakcijom 4,7-diklorkinolina i AcOH na 125 °C (196). Karboksilna kiselina **43** pripravljena je reakcijom 4,7-diklorkinolina s glicinom u fenolu refluksiranjem na 125 °C (197). Amini **44** i **45** dobiveni su nukleofilnom supstitucijom 4,7-diklorkinolina s

alifatskim diaminima različite duljine ugljikovodičnog lanca na 95 °C uz mikrovalno zračenje. Reakcijom 4,7-diklorkinolina s diaminoetanom dobiven je amin **44**, dok je u reakciji s diaminobutanom pripravljen amin **45** (198).

4.1.7. Sinteza azida ferocena

Ferocenski prekursori (etinil-ferocen, ferocenkarboksilna kiselina i ferocenoctena kiselina), osim azidometilferocena, nabavljeni su iz komercijalnih izvora. Azidometilferocen je pripravljen reakcijom ferocenmetanola i ADMP uz DBU na 0 °C (Shema 21) (97). Pri praćenju tijeka kemijske reakcije i čistoće produkta korištena je identifikacija parama joda. ^{1}H i ^{13}C NMR azidometilferocena odgovaraju literaturnim podacima.

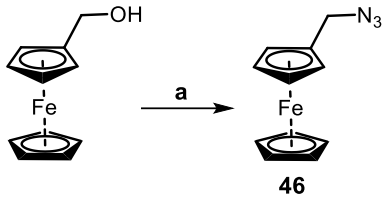

Shema 21. Sinteza ferocenskog azida
Reagensi i uvjeti: (a) ADMP, DBU, 0 °C, 2 h.

4.1.8. Sinteza harmicina 47-50

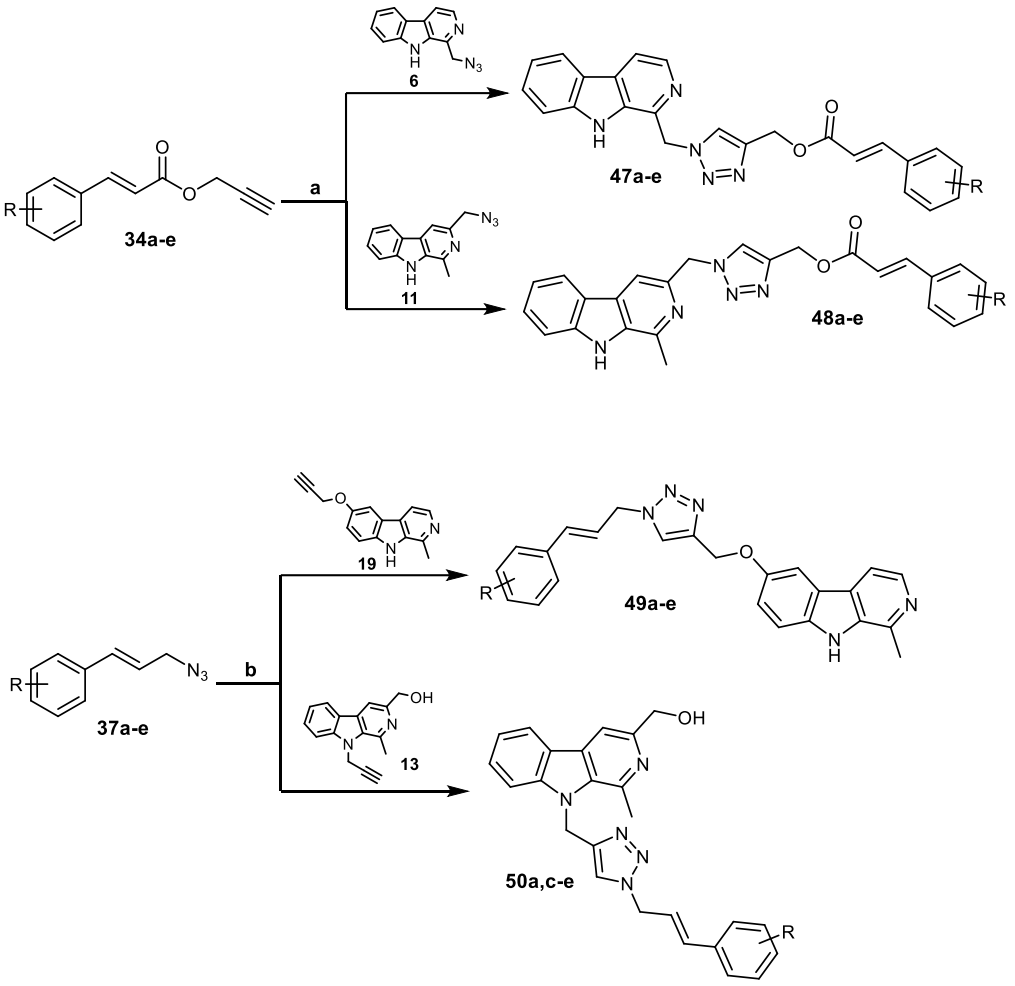

	a	b	c	d	e
R	H	*m*-F	*m*-Br	*p*-Cl	*p*-OCH_3

Shema 22. Sinteza harmicina **47-50**
Reagensi i uvjeti: (a) Na-askorbat, $CuSO_4 \times 5H_2O$, *t*-BuOH/H_2O (1:1), s.t., 0,5 h;
(b) $Cu(CH_3COO)_2$, MeOH, s.t., 24 h.

C-1 (**47**) i C-3 (**48**) harmicini pripravljeni su klik-reakcijom propargilnih estera **34** i azida **6**, odnosno **11** uz natrijev askorbat i $CuSO_4 \times 5H_2O$ u smjesi *tert*-butanola i vode (omjer 1:1) (Metoda 1). S druge strane, O-6 (**49**) i N-9 (**50**) harmicini pripravljeni su klik-reakcijom alkina **19**, odnosno **13** i azida **37** uz bakrov(II) acetat u metanolu (Metoda 2) (Shema 22). U obje metode Cu(I) ioni potrebni za odvijanje klik-reakcije generirani su *in situ*: u Metodi 1 redoks reakcijom Cu(II) iona (oksidans) i askorbata (reducens), a u Metodi 2 redoks reakcijom Cu(II) iona i metanola (reducens). Reducensi su dodani u suvišku kako bi se spriječila oksidacija Cu(I) u Cu(II) i nastanak nusprodukata. Klik-reakcije provedene su na s.t., uz različita reakcijska

vremena. Klik-reakcije provedene Metodom 1 završavale su unutar 0,5 h, dok su klik-reakcije provedene Metodom 2 trajale 24 h. Nakon završetka reakcije, produkti su izolirani na različite načine. U Metodi 1 produkt se nakon dodatka ledene vode taložio iz reakcijske smjese te je odisan, dok je u Metodi 2 sirovi produkt dobiven nakon uparavanja otapala pod sniženim tlakom. Svi harmiceni pročišćeni su kromatografijom na koloni s dodatkom sloja Al_2O_3 kako bi se uklonile zaostale bakrove soli. Jedino je spoj **47c** dodatno pročišćen prekristalizacijom iz etanola. Spoj (*E*)-(9-((1-(3-(3-fluorfenil)alil)-1*H*-1,2,3-triazol-4-il)metil)-1-metil-9*H*-pirido[3,4-*b*]indol-3-il)metanola **50b** nije uspješno izoliran jer se raspada prilikom pročišćavanja. Iskorištenja reakcija provedenih Metodom 2 (39–77 %) bila su nešto veća od iskorištenja reakcija provedenih Metodom 1 (25–62 %).

Pripravljeni su sljedeći spojevi:

- (1-((9*H*-pirido[3,4-*b*]indol-1-il)metil)-1*H*-1,2,3-triazol-4-il)metil cinamat (**47a**),
- (1-((9*H*-pirido[3,4-*b*]indol-1-il)metil)-1*H*-1,2,3-triazol-4-il)metil (*E*)-3-(3-fluorfenil)akrilat (**47b**),
- (1-((9*H*-pirido[3,4-*b*]indol-1-il)metil)-1*H*-1,2,3-triazol-4-il)metil (*E*)-3-(3-bromfenil)akrilat (**47c**),
- (1-((9*H*-pirido[3,4-*b*]indol-1-il)metil)-1*H*-1,2,3-triazol-4-il)metil (*E*)-3-(4-klorfenil)akrilat (**47d**),
- (1-((9*H*-pirido[3,4-*b*]indol-1-il)metil)-1*H*-1,2,3-triazol-4-il)metil (*E*)-3-(4-metoksifenil)akrilat (**47e**),
- (1-((1-metil-9*H*-pirido[3,4-*b*]indol-3-il)metil)-1*H*-1,2,3-triazol-4-il)metil cinamat (**48a**),
- (1-((1-metil-9*H*-pirido[3,4-*b*]indol-3-il)metil)-1*H*-1,2,3-triazol-4-il)metil (*E*)-3-(3-fluorfenil)akrilat (**48b**),
- (1-((1-metil-9*H*-pirido[3,4-*b*]indol-3-il)metil)-1*H*-1,2,3-triazol-4-il)metil (*E*)-3-(3-bromfenil)akrilat (**48c**),
- (1-((1-metil-9*H*-pirido[3,4-*b*]indol-3-il)metil)-1*H*-1,2,3-triazol-4-il)metil (*E*)-3-(4-klorfenil)akrilat (**48d**),
- (1-((1-metil-9*H*-pirido[3,4-*b*]indol-3-il)metil)-1*H*-1,2,3-triazol-4-il)metil (*E*)-3-(4-metoksifenil)akrilat (**48e**),
- 6-((1-cinamil-1*H*-1,2,3-triazol-4-il)metoksi)-1-metil-9*H*-pirido[3,4-*b*]indol (**49a**),
- (*E*)-6-((1-(3-(3-fluorfenil)alil)-1*H*-1,2,3-triazol-4-il)metoksi)-1-metil-9*H*-pirido[3,4-*b*]indol (**49b**),
- (*E*)-6-((1-(3-(3-bromfenil)alil)-1*H*-1,2,3-triazol-4-il)metoksi)-1-metil-9*H*-pirido[3,4-*b*]indol (**49c**),

- (*E*)-6-((1-(3-(4-klorfenil)alil)-1*H*-1,2,3-triazol-4-il)metoksi)-1-metil-9*H*-pirido[3,4-*b*]indol (**49d**),
- (*E*)-6-((1-(3-(4-metoksifenil)alil)-1*H*-1,2,3-triazol-4-il)metoksi)-1-metil-9*H*-pirido[3,4-*b*]indol (**49e**),
- (9-((1-cinamil-1*H*-1,2,3-triazol-4-il)metil)-1-metil-9*H*-pirido[3,4-*b*]indol-3-il)metanol (**50a**),
- (*E*)-(9-((1-(3-(3-bromfenil)alil)-1*H*-1,2,3-triazol-4-il)metil)-1-metil-9*H*-pirido[3,4-*b*]indol-3-il)metanol (**50c**),
- (*E*)-(9-((1-(3-(4-klorfenil)alil)-1*H*-1,2,3-triazol-4-il)metil)-1-metil-9*H*-pirido[3,4-*b*]indol-3-il)metanol (**50d**),
- (*E*)-(9-((1-(3-(4-metoksifenil)alil)-1*H*-1,2,3-triazol-4-il)metil)-1-metil-9*H*-pirido[3,4-*b*]indol-3-il)metanol (**50e**).

Harmicini **47-50** su novi, do sada neopisani spojevi. Sinteza harmicina i njihova čistoća praćene su tankoslojnom kromatografijom, a strukture su potvrđene uobičajenim metodama (IR, ^{1}H i ^{13}C NMR, MS). Analitički, spektrometrijski i spektroskopski podaci dani su u Tablicama 10-21. U IR spektrima harmicina **47** i **48** vidljiva je karakteristična vrpca C=O istezanja karbonila koja je, karakteristično za α,β-nezasićene estere, pomaknuta prema nižim valnim brojevima (1699-1715 cm^{-1}). Kemijski pomaci protona u ^{1}H, odnosno ugljika u ^{13}C NMR spektrima harmicina **47-50** u skladu su s predloženim strukturama. U ^{1}H NMR spektru svih spojeva vidljiv je CH signal (singlet, 1 proton) u aromatskom području (u rasponu 7,98–8,32 ppm) karakterističan za CH proton triazolskog prstena. U ^{13}C NMR spektru harmicina **47** i **48** vidljiv je signal za ugljikov atom karbonila na najvišem pomaku (≈ 165 ppm), dok se u ^{13}C NMR spketrima derivata **47b**, **48b** i **49b** (*m*-F-supstituirani derivati) jasno vide cijepanja signala ugljikovih atoma fenilnog prstena s fluorom. U MS spektrima svih harmicina vidi se pseudomolekulski ion. U MS spektrima spojeva **47c**, **48c**, **49c** i **50c** (*m*-Br-supstituirani derivati) vide se dva pseudomolekulska iona, zato što brom ima dva izotopa (^{79}Br i ^{81}Br), koja su prisutna u omjeru 1:1.

Tablica 10. Analitički i MS podaci za harmicine **47a-e**

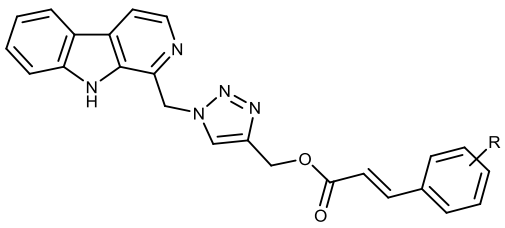

Spoj	R	Iskor. (%)	t_t (°C)	Molekulska formula	M_r	MS (*m/z*)
47a	H	49	181,5–183,5	$C_{24}H_{19}N_5O_2$	409,45	410,1 $(M+1)^+$
47b	*m*-F	56	185,5–187,5	$C_{24}H_{18}FN_5O_2$	427,44	428,1 $(M+1)^+$
47c	*m*-Br	37	184–186	$C_{24}H_{18}BrN_5O_2$	488,35	488,0 $(M+1)^+$ 489,9 $(M+1)^+$
47d	*p*-Cl	25	201–203,5	$C_{24}H_{18}ClN_5O_2$	443,89	444,0 $(M+1)^+$
47e	*p*-OCH_3	41	155–157,5	$C_{25}H_{21}N_5O_3$	439,48	440,1 $(M+1)^+$

Tablica 11. IR podaci za harmicine **47a-e**

Spoj	R	IR (ATR, ν_{max}/cm^{-1})
47a	H	3220, 3168, 3093, 3059, 3029, 2994, 2961, 2898, 2877, 2798, 2776, 1713, 1637, 1567, 1505, 1452, 1432, 1402, 1370, 1346, 1325, 1307, 1281, 1243, 1203, 1167, 1066, 1038, 1003, 972, 859, 820, 804, 764, 739, 707, 682, 641, 605, 593, 573, 547, 525, 483
47b	*m*-F	3311, 3230, 3198, 3147, 3105, 3063, 3019, 2998, 2973, 1715, 1639, 1585, 1569, 1502, 1485, 1472, 1449, 1429, 1403, 1390, 1349, 1323, 1272, 1234, 1190, 1168, 1147, 1122, 1075, 1060, 1035, 983, 954, 939, 874, 858, 837, 819, 780, 728, 671, 643, 605, 582, 562, 534, 521
47c	*m*-Br	3311, 3223, 3194, 3147, 3102, 3060, 2997, 2971, 1715, 1640, 1607, 1564, 1501, 1472, 1457, 1428, 1404, 1389, 1347, 1308, 1276, 1234, 1189, 1168, 1122, 1090, 1060, 1036, 984, 860, 830, 812, 777, 735, 670, 643, 605, 578, 542
47d	*p*-Cl	3227, 3192, 3096, 3061, 2993, 2965, 2926, 2894, 2872, 1713, 1642, 1594, 1568, 1503, 1490, 1468, 1453, 1431, 1404, 1370, 1346, 1308, 1271, 1242, 1201, 1171, 1148, 1087, 1068, 1038, 1012, 972, 868, 818, 775, 737, 695, 683, 669, 637, 593, 560, 547, 529, 491, 455
47e	*p*-OCH_3	3223, 3170, 3131, 3094, 3082, 2996, 2965, 2934, 2900, 2837, 1712, 1636, 1607, 1573, 1513, 1455, 1429, 1402, 1375, 1322, 1308, 1287, 1258, 1240, 1202, 1163, 1065, 1037, 1002, 971, 867, 852, 824, 774, 734, 592, 547, 527, 513

Tablica 12. ^{1}H i ^{13}C NMR spektroskopski podaci za harmicine **47a-e**

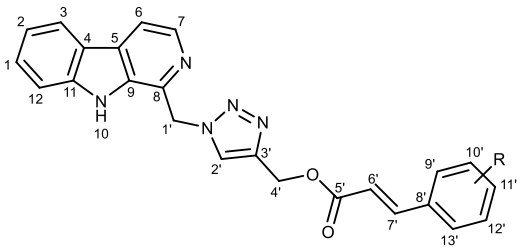

Spoj	R	^{1}H NMR (DMSO-d_6, δ ppm)	^{13}C NMR (DMSO-d_6, δ ppm)
47a	H	11,98 (s, 1H, 10), 8,32 (s, 1H, 2'), 8,30 (d, 1H, 7, *J* = 5,2 Hz), 8,27 (d, 1H, 3, *J* = 7,9 Hz), 8,13 (d, 1H, 6, *J* = 5,2 Hz), 7,73–7,66 (m, 4H, 12, 7', 9', 13'), 7,62–7,58 (m, 1H, 1), 7,44–7,38 (m, 3H, 10', 11', 12'), 7,31–7,26 (m, 1H, 2), 6,66 (d, 1H, 6', *J* = 16,0 Hz), 6,11 (s, 2H, 4'), 5,28 (s, 2H, 1')	165,93 (5'), 145,03 (7'), 141,79 (8), 140,70 (11), 137,98 (3'), 137,88 (7), 133,92 (9), 133,84 (8'), 130,57 (11'), 128,91 (9', 13'), 128,74 (5), 128,57 (1), 128,42 (10', 12'), 125,73 (2'), 121,92 (3), 120,74 (4), 119,66 (2), 117,65 (6'), 114,87 (6), 112,07 (12), 57,29 (4'), 51,21 (1')
47b	*m*-F	11,98 (s, 1H, 10), 8,32 (s, 1H, 2'), 8,30 (d, 1H, 7, *J* = 5,2 Hz), 8,27 (d, 1H, 3, *J* = 7,9 Hz), 8,13 (d, 1H, 6, *J* = 5,2 Hz), 7,69–7,63 (m, 3H, 12, 7', 9'), 7,61–7,59 (m, 1H, 1), 7,56 (dt, 1H, 13', *J* = 7,8, 1,2 Hz), 7,47–7,43 (m, 1H, 12'), 7,30–7,24 (m, 2H, 2, 11'), 6,75 (d, 1H, 6', *J* = 16,1 Hz), 6,11 (s, 2H, 4'), 5,28 (s, 2H, 1')	165,75 (5'), 162,40 (d, 10', *J* = 243,8 Hz), 143,66 (7'), 141,71 (8), 140,71 (11), 137,99 (3'), 137,89 (7), 136,49 (d, 8', *J* = 8,1 Hz), 133,85 (9), 130,87 (d, 12', *J* = 8,4 Hz), 128,75 (5), 128,59 (1), 125,78 (2'), 124,94 (d, 13', *J* = 2,5 Hz), 121,94 (3), 120,75 (4), 119,68 (2), 119,30 (6'), 117,26 (d, 11', *J* = 21,4 Hz), 114,89 (6), 114,58 (d, 9', *J* = 22,1 Hz), 112,08 (12), 57,40 (4'), 51,22 (1')
47c	*m*-Br	11,97 (s, 1H, 10), 8,32 (s, 1H, 2'), 8,30 (d, 1H, 7, *J* = 5,2 Hz), 8,26 (d, 1H, 3, *J* = 7,8 Hz), 8,13 (d, 1H, 6, *J* = 5,2 Hz), 7,98 (t, 1H, 9', *J* = 1,8 Hz), 7,73 (dt, 1H, 13', *J* = 7,8, 1,3 Hz), 7,69–7,57 (m, 4H, 1, 12, 7', 11'), 7,36 (t, 1H, 12', *J* = 7,9 Hz), 7,31–7,27 (m, 1H, 2), 6,75 (d, 1H, 6', *J* = 16,0 Hz), 6,11 (s, 2H, 4'), 5,28 (s, 2H, 1')	165,68 (5'), 143,33 (7'), 141,71 (8), 140,69 (11), 137,97 (3'), 137,87 (7), 136,45 (8'), 133,83 (9), 133,03 (9'), 130,93 (11', 12'), 128,74 (5), 128,57 (1), 127,32 (13'), 125,74 (2'), 122,28 (10'), 121,92 (3), 120,73 (4), 119,66 (2), 119,37 (6'), 114,87 (6), 112,07 (12), 57,40 (4'), 51,21 (1')
47d	*p*-Cl	11,97 (s, 1H, 10), 8,31 (s, 1H, 2'), 8,30 (d, 1H, 7, *J* = 5,3 Hz), 8,27 (d, 1H, 3, *J* = 7,9 Hz), 8,13 (d, 1H, 6, *J* = 5,2 Hz), 7,77–7,74 (m, 2H, 9', 13'), 7,70–7,64 (m, 2H, 12, 7'), 7,62–7,58 (m, 1H, 1), 7,50–7,45 (m, 2H, 10', 12'), 7,31–7,26 (m, 1H, 2), 6,69 (d, 1H, 6', *J* = 16,1 Hz), 6,11 (s, 2H, 4'), 5,28 (s, 2H, 1')	165,79 (5'), 143,60 (7'), 141,74 (8), 140,69 (11), 137,97 (3'), 137,87 (7), 135,08 (11'), 133,83 (9), 132,91 (8'), 130,15 (9', 13'), 128,94 (10', 12'), 128,74 (5), 128,57 (1), 125,73 (2'), 121,92 (3), 120,73 (4), 119,66 (2), 118,49 (6'), 114,87 (6), 112,07 (12), 57,35 (4'), 51,21 (1')
47e	*p*-$\overset{14'}{O}CH_3$	11,98 (s, 1H, 10), 8,32–8,29 (m, 2H, 2', 7), 8,27 (d, 1H, 3, *J* = 7,9 Hz), 8,12 (d, 1H, 6, *J* = 5,2 Hz), 7,69–7,59 (m, 5H, 1, 12, 7', 9', 13'), 7,28 (t, 1H, 2, *J* = 7,5 Hz), 6,96 (d, 2H, 10', 12', *J* = 8,4 Hz), 6,50 (d, 1H, 6', *J* = 16,0 Hz), 6,11 (s, 2H, 4'), 5,25 (s, 2H, 1'), 3,79 (s, 3H, 14')	166,22 (5'), 161,24 (11'), 144,85 (7'), 141,92 (8), 140,71 (11), 138,01 (3'), 137,88 (7), 133,85 (9), 130,26 (9', 13'), 128,74 (5), 128,58 (1), 126,56 (8'), 125,70 (2'), 121,94 (3), 120,75 (4), 119,67 (2), 114,88 (6, 6'), 114,38 (10', 12'), 112,09 (12), 57,11 (4'), 55,34 (14'), 51,21 (1')

Tablica 13. Analitički i MS podaci za harmicine **48a-e**

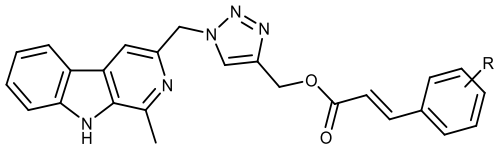

Spoj	R	Iskor. (%)	t_t (°C)	Molekulska formula	M_r	MS (*m/z*)
48a	H	36	194,5–195,5	$C_{25}H_{21}N_5O_2$	423,48	424,0 $(M+1)^+$
48b	*m*-F	60	197–198,5	$C_{25}H_{20}FN_5O_2$	441,47	442,1 $(M+1)^+$
48c	*m*-Br	53	204,5–205,5	$C_{25}H_{20}BrN_5O_2$	502,37	501,9 $(M+1)^+$ 503,9 $(M+1)^+$
48d	*p*-Cl	57	209–211	$C_{25}H_{20}ClN_5O_2$	457,92	458,0 $(M+1)^+$
48e	*p*-OCH_3	62	240,5–243	$C_{26}H_{23}N_5O_3$	453,50	454,1 $(M+1)^+$

Tablica 14. IR podaci za harmicine **48a-e**

Spoj	R	IR (ATR, ν_{max}/cm^{-1})
48a	H	3220, 3194, 3175, 3145, 3101, 3060, 3030, 2989, 2945, 1712, 1694, 1644, 1626, 1605, 1565, 1503, 1451, 1392, 1376, 1356, 1329, 1312, 1271, 1254, 1223, 1202, 1170, 1116, 1059, 1037, 1002, 972, 934, 898, 859, 843, 827, 804, 765, 752, 738, 708, 681, 642, 611, 587, 524, 480
48b	*m*-F	3223, 3198, 3166, 3104, 3067, 3043, 3012, 2970, 2895, 1707, 1627, 1608, 1583, 1568, 1506, 1483, 1449, 1387, 1355, 1320, 1271, 1252, 1213, 1151, 1115, 1084, 1057, 1036, 1008, 980, 942, 911, 898, 864, 832, 788, 766, 738, 693, 675, 649, 609, 586, 555, 537, 520, 480
48c	*m*-Br	3347, 3281, 3170, 3080, 3054, 3023, 2970, 2950, 1708, 1684, 1638, 1592, 1569, 1498, 1474, 1455, 1423, 1383, 1354, 1341, 1313, 1290, 1272, 1247, 1231, 1188, 1146, 1110, 1073, 1053, 1032, 1009, 980, 928, 899, 872, 829, 791, 766, 731, 697, 666, 649, 623, 586, 563, 549, 527
48d	*p*-Cl	3250, 3157, 3103, 3086, 3067, 3052, 1703, 1633, 1592, 1566, 1493, 1475, 1456, 1428, 1408, 1388, 1356, 1305, 1278, 1251, 1222, 1204, 1182, 1160, 1117, 1089, 1058, 1036, 1004, 964, 899, 865, 840, 823, 805, 753, 739, 719, 702, 646, 605, 586, 550, 524, 501, 456
48e	*p*-OCH_3	3236, 3201, 3165, 3103, 3068, 3036, 3007, 2965, 2940, 2911, 2839, 1699, 1626, 1601, 1574, 1514, 1456, 1426, 1389, 1357, 1307, 1290, 1252, 1223, 1207, 1179, 1155, 1115, 1056, 1023, 1009, 992, 971, 937, 898, 868, 830, 810, 776, 751, 735, 710, 693, 663, 652, 637, 608, 586, 555, 521

Tablica 15. ^{1}H i ^{13}C NMR spektroskopski podaci za harmicine **48a-e**

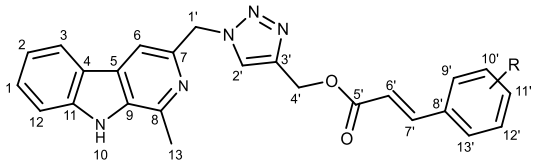

Spoj	R	^{1}H NMR (DMSO-d_6, δ ppm)	^{13}C NMR (DMSO-d_6, δ ppm)
48a	H	11,67 (s, 1H, 10), 8,26 (s, 1H, 2'), 8,17 (d, 1H, 3, *J* = 7,9 Hz), 7,99 (s, 1H, 6), 7,72–7,70 (m, 2H, 9', 13'), 7,67 (d, 1H, 7', *J* = 16,0 Hz), 7,60 (dt, 1H, 12, *J* = 8,2, 1,0 Hz), 7,55–7,53 (m, 1H, 1), 7,44–7,39 (m, 3H, 10', 11', 12'), 7,24–7,21 (m, 1H, 2), 6,65 (d, 1H, 6', *J* = 16,1 Hz), 5,77 (s, 2H, 4'), 5,27 (s, 2H, 1'), 2,75 (s, 3H, 13)	165,94 (5'), 145,02 (7'), 142,54 (7), 142,16 (11), 141,92 (3'), 140,78 (8), 134,00 (9), 133,93 (8'), 130,58 (11'), 128,91 (10', 12'), 128,42 (9', 13'), 128,10 (2'), 127,60 (5), 125,13 (1), 121,72 (3), 120,91 (4), 119,46 (2), 117,66 (6'), 112,10 (12), 112,05 (6), 57,34 (4'), 55,25 (1'), 20,40 (13)
48b	*m*-F	11,67 (s, 1H, 10), 8,26 (s, 1H, 2'), 8,18 (d, 1H, 3, *J* = 7,9 Hz, 3), 8,00 (s, 1H, 6), 7,67 (d, 1H, 7', *J* = 16,1 Hz), 7,65–7,62 (m, 1H, 9'), 7,61–7,59 (m, 1H, 13'), 7,56–7,53 (m, 2H, 1, 12), 7,46–7,43 (m, 1H, 12'), 7,27–7,22 (m, 2H, 2, 11'), 6,74 (d, 1H, 6', *J* = 16,0 Hz), 5,77 (s, 2H, 4'), 5,28 (s, 2H, 1'), 2,75 (s, 3H, 13)	165,73 (5'), 162,39 (d, 10', *J* = 243,8 Hz), 143,61 (7'), 142,52 (7), 142,16 (11), 141,83 (3'), 140,77 (8), 136,47 (d, 8', *J* = 8,1 Hz), 134,00 (9), 130,84 (d, 12', *J* = 8,4 Hz), 128,09 (2'), 127,60 (5), 125,14 (1), 124,91 (d, 13', *J* = 2,5 Hz), 121,71 (3), 120,90 (4), 119,44 (2), 119,29 (6'), 117,23 (d, 11', *J* = 21,3 Hz), 114,56 (d, 9', *J* = 22,1 Hz), 112,09 (12), 112,06 (6), 57,43 (4'), 55,25 (1'), 20,40 (13)
48c	*m*-Br	11,67 (s, 1H, 10), 8,26 (s, 1H, 2'), 8,17 (d, 1H, 3, *J* = 7,9 Hz), 7,99 (s, 1H, 6), 7,97 (t, 1H, 9', *J* = 1,8 Hz), 7,75–7,71 (m, 1H, 13'), 7,64 (d, 1H, 7', *J* = 16,0 Hz), 7,62–7,58 (m, 2H, 12, 11'), 7,56–7,52 (m, 1H, 1), 7,36 (t, 1H, 12', *J* = 7,9 Hz), 7,25–7,21 (m, 1H, 2), 6,74 (d, 1H, 6', *J* = 16,1 Hz), 5,77 (s, 2H, 4'), 5,28 (s, 2H, 1'), 2,75 (s, 3H, 13)	165,67 (5'), 143,31 (7'), 142,52 (7), 142,14 (11), 141,84 (3'), 140,77 (8), 136,44 (8'), 133,99 (9), 133,01 (9'), 130,91 (11', 12'), 128,08 (2'), 127,59 (5), 127,29 (13'), 125,11 (1), 122,27 (10'), 121,70 (3), 120,90 (4), 119,43 (2), 119,38 (6'), 112,08 (12), 112,03 (6), 57,44 (4'), 55,24 (1'), 20,39 (13)
48d	*p*-Cl	11,67 (s, 1H, 10), 8,26 (s, 1H, 2'), 8,18 (d, 1H, 3, *J* = 7,9 Hz), 8,00 (s, 1H, 6), 7,76–7,73 (m, 2H, 9', 13'), 7,66 (d, 1H, 7', *J* = 16,0 Hz), 7,60 (dt, 1H, 12, *J* = 8,3, 1,0 Hz), 7,56–7,53 (m, 1H, 1), 7,48–7,45 (m, 2H, 10', 12'), 7,24–7,22 (m, 1H, 2), 6,68 (d, 1H, 6', *J* = 16,1 Hz), 5,77 (s, 2H, 4'), 5,28 (s, 2H, 1'), 2,75 (s, 3H, 13)	165,80 (5'), 143,60 (7'), 142,53 (7), 142,17 (11), 141,88 (3'), 140,78 (8), 135,09 (8'), 134,01 (9), 132,92 (11'), 130,15 (9', 13'), 128,94 (10', 12'), 128,11 (2'), 127,61 (5), 125,13 (1), 121,72 (3), 120,91 (4), 119,46 (2), 118,51 (6'), 112,10 (12), 112,07 (6), 57,40 (4'), 55,26 (1'), 20,41 (13)
48e	*p*-$^{14'}OCH_3$	11,67 (s, 1H, 10), 8,25 (s, 1H, 2'), 8,18 (d, 1H, 3, *J* = 7,9 Hz), 7,99 (s, 1H, 6), 7,68–7,64 (m, 2H, 9', 13'), 7,64–7,59 (m, 2H, 12, 7'), 7,55–7,53 (m, 1H, 1), 7,24–7,22 (m, 1H, 2), 6,97–6,94 (m, 2H, 10', 12'), 6,49 (d, 1H, 6', *J* = 16,0 Hz), 5,77 (s, 2H, 4'), 5,25 (s, 2H, 1'), 3,79 (s, 3H, 14'), 2,75 (s, 3H, 13)	166,19 (5'), 161,20 (11'), 144,80 (7'), 142,53 (7), 142,14 (11), 142,03 (3'), 140,76 (8), 133,99 (9), 130,22 (9', 13'), 128,08 (2'), 127,59 (5), 126,54 (8'), 125,05 (1), 121,70 (3), 120,90 (4), 119,44 (2), 114,88 (6'), 114,35 (10', 12'), 112,08 (12), 112,04 (6), 57,14 (4'), 55,32 (14'), 55,23 (1'), 20,39 (13)

Tablica 16. Analitički i MS podaci za harmicine **49a-e**

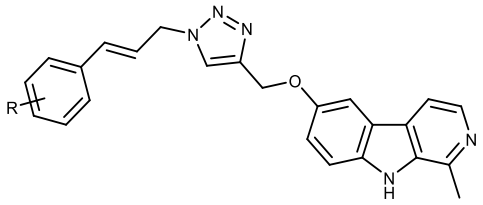

Spoj	R	Iskor. (%)	t_t (°C)	Molekulska formula	M_r	MS (*m/z*)
49a	H	70	205–206,5	$C_{24}H_{21}N_5O$	395,47	396,3 $(M+1)^+$
49b	*m*-F	44	145–147	$C_{24}H_{20}FN_5O$	413,46	414,2 $(M+1)^+$
49c	*m*-Br	50	181,5–183	$C_{24}H_{20}BrN_5O$	474,36	474,2 $(M+1)^+$ 476,2 $(M+1)^+$
49d	*p*-Cl	51	195–196,5	$C_{24}H_{20}ClN_5O$	429,91	430,4 $(M+1)^+$
49e	*p*-OCH_3	77	200–203	$C_{25}H_{23}N_5O_2$	425,49	426,3 $(M+1)^+$

Tablica 17. IR podaci za harmicine **49a-e**

Spoj	R	IR (ATR, ν_{max}/cm^{-1})
49a	H	3136, 3120, 3030, 2945, 2856, 2760, 2693, 2676, 1632, 1604, 1579, 1565, 1504, 1481, 1460, 1412, 1389, 1361, 1335, 1289, 1237, 1202, 1123, 1054, 1034, 1002, 967, 888, 858, 817, 780, 755, 725, 705, 694, 625, 584, 520, 502
49b	*m*-F	3357, 3293, 3166, 3071, 3052, 2975, 2937, 2900, 2866, 1601, 1583, 1568, 1493, 1473, 1459, 1404, 1379, 1365, 1330, 1286, 1262, 1207, 1149, 1120, 1067, 1054, 1039, 976, 938, 884, 847, 812, 792, 776, 752, 736, 715, 675, 641, 620, 593, 561, 528, 493, 456
49c	*m*-Br	3252, 3198, 3151, 3089, 3064, 3039, 3015, 2965, 2945, 2916, 2892, 1601, 1584, 1566, 1495, 1475, 1422, 1400, 1373, 1350, 1337, 1289, 1256, 1233, 1217, 1199, 1129, 1095, 1066, 1052, 1033, 1008, 977, 944, 882, 857, 807, 782, 738, 707, 674, 620, 589, 563, 542, 479
49d	*p*-Cl	3208, 3136, 3089, 3069, 2969, 2923, 2893, 2870, 2802, 1602, 1582, 1567, 1494, 1480, 1459, 1405, 1385, 1340, 1289, 1257, 1237, 1207, 1163, 1127, 1094, 1054, 1033, 1015, 987, 971, 950, 884, 857, 843, 818, 742, 702, 687, 662, 623, 583, 563, 533, 487
49e	*p*-OCH_3	3208, 3138, 3069, 2953, 2929, 2894, 2873, 2836, 2802, 1743, 1607, 1582, 1567, 1513, 1498, 1480, 1460, 1441, 1405, 1386, 1337, 1289, 1257, 1238, 1207, 1175, 1127, 1109, 1054, 1032, 1015, 987, 968, 884, 856, 819, 760, 741, 703, 666, 624, 582, 563, 529, 498, 477

Tablica 18. ^{1}H i ^{13}C NMR spektroskopski podaci za harmicine **49a-e**

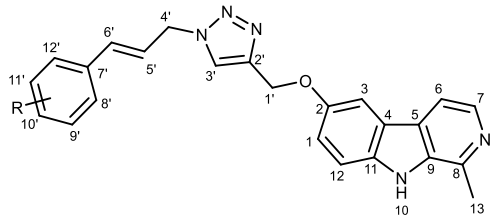

Spoj	R	^{1}H NMR (DMSO-d_6, δ ppm)	^{13}C NMR (DMSO-d_6, δ ppm)
49a	H	11,39 (s, 1H, 10), 8,30 (s, 1H, 3'), 8,16 (d, 1H, 7, *J* = 5,3 Hz), 7,91–7,89 (m, 2H, 3, 6), 7,51 (d, 1H, 12, *J* = 8,8 Hz), 7,45–7,22 (m, 6H, 1, 8', 9', 10', 11', 12'), 6,65–6,49 (m, 2H, 5', 6'), 5,26 (s, 2H, 1'), 5,21 (d, 2H, 4', *J* = 6,3 Hz), 2,74 (s, 3H, 13)	151,94 (2), 143,26 (2'), 142,22 (8), 136,98 (7), 135,70 (11), 135,42 (7'), 135,10 (9), 133,62 (5'), 128,68 (9', 11'), 128,14 (10'), 126,70 (4), 126,56 (8', 12'), 124,43 (3'), 123,72 (6'), 121,36 (5), 118,35 (1), 112,76 (6), 112,69 (12), 105,12 (3), 61,89 (1'), 51,34 (4'), 20,42 (13)
49b	*m*-F	11,41 (s, 1H, 10), 8,31 (s, 1H, 3'), 8,17 (d, 1H, 7, *J* = 5,4 Hz), 7,91–7,89 (m, 2H, 3, 6), 7,52 (d, 1H, 12, *J* = 8,8 Hz), 7,39–7,32 (m, 2H, 8', 11'), 7,27–7,23 (m, 2H, 1, 12'), 7,13–7,08 (m, 1H, 10'), 6,64–6,62 (m, 2H, 5', 6'), 5,26 (s, 2H, 1'), 5,23–5,21 (m, 2H, 4'), 2,75 (s, 3H, 13)	162,49 (d, 9', *J* = 243,3 Hz), 151,97 (2), 143,26 (2'), 142,16 (8), 138,36 (d, 7', *J* = 7,9 Hz), 136,80 (7), 135,48 (11), 135,07 (9), 132,34 (5'), 130,58 (d, 11', *J* = 8,5 Hz), 126,78 (4), 125,50 (6'), 124,47 (3'), 123,00 (d, 12', *J* = 1,7 Hz), 121,34 (5), 118,42 (1), 114,81 (d, 10', *J* = 21,3 Hz), 112,80 (d, 8', *J* = 17,4 Hz) 112,77 (6), 112,67 (12), 105,11 (3), 61,89 (1'), 51,16 (4'), 20,32 (13)
49c	*m*-Br	11,40 (s, 1H, 10), 8,31 (s, 1H, 3'), 8,16 (d, 1H, 7, *J* = 5,4 Hz), 7,92–7,89 (m, 2H, 3, 6), 7,71 (t, 1H, 8', *J* = 2,0 Hz), 7,51 (d, 1H, 12, *J* = 8,8 Hz), 7,48–7,43 (m, 2H, 10', 12'), 7,30 (t, 1H, 11', *J* = 7,8 Hz), 7,24 (dd, 1H, 1, *J* = 8,8, 2,5 Hz), 6,68–6,58 (m, 2H, 5', 6'), 5,26 (s, 2H, 1'), 5,21 (d, 2H, 4', *J* = 4,6 Hz), 2,74 (s, 3H, 13)	151,98 (2), 143,28 (2'), 142,20 (8), 138,30 (7'), 136,89 (7), 135,46 (11), 135,09 (9), 132,03 (5'), 130,77 (10', 11'), 129,05 (12'), 126,75 (4), 125,67 (6', 8'), 124,47 (3'), 122,17 (9'), 121,36 (5), 118,40 (1), 112,78 (6), 112,71 (12), 105,10 (3), 61,91 (1'), 51,20 (4'), 20,37 (13)
49d	*p*-Cl	11,39 (s, 1H, 10), 8,30 (s, 1H, 3'), 8,16 (d, 1H, 7, *J* = 5,4 Hz), 7,91–7,89 (m, 2H, 3, 6), 7,51 (d, 1H, 12, *J* = 8,8 Hz), 7,47–7,44 (m, 2H, 8', 12'), 7,39–7,36 (m, 2H, 9', 11'), 7,23 (dd, 1H, 1, *J* = 8,9, 2,5 Hz), 6,62–6,51 (m, 2H, 5', 6'), 5,26 (s, 2H, 1'), 5,21 (d, 2H, 4', *J* = 5,1 Hz), 2,74 (s, 3H, 13)	151,93 (2), 143,27 (2'), 142,22 (8), 136,98 (7), 135,44 (11), 135,10 (9), 134,68 (7'), 132,51 (10'), 132,23 (5'), 128,65 (8', 12'), 128,28 (9', 11'), 126,71 (4), 124,77 (6'), 124,48 (3'), 121,36 (5), 118,38 (1), 112,76 (6), 112,69 (12), 105,15 (3), 61,89 (1'), 51,23 (4'), 20,41 (13)
49e	*p*-OCH_3 (13')	11,39 (s, 1H, 10), 8,28 (s, 1H, 3'), 8,16 (d, 1H, 7, *J* = 5,4 Hz), 7,92–7,89 (m, 2H, 3, 6), 7,51 (d, 1H, 12, *J* = 8,8 Hz), 7,37 (d, 2H, 8', 12', *J* = 8,2 Hz), 7,23 (d, 1H, 1, *J* = 8,9 Hz), 6,88 (d, 2H, 9', 11', *J* = 8,2 Hz), 6,58 (d, 1H, 6', *J* = 15,8 Hz), 6,39–6,32 (m, 1H, 5'), 5,25 (s, 2H, 1'), 5,16 (d, 2H, 4', *J* = 6,5 Hz), 3,75 (s, 3H, 13'), 2,74 (s, 3H, 13)	159,22 (10'), 151,94 (2), 143,23 (2'), 142,21(8), 136,98 (7), 135,42 (11), 135,09 (9), 133,36 (5'), 128,30 (7'), 127,89 (8', 12'), 126,70 (4), 124,31 (3'), 121,36 (5), 121,11 (6'), 118,34 (1), 114,06 (9', 11'), 112,75 (6), 112,68 (12), 105,12 (3), 61,89 (1'), 55,11 (13'), 51,46 (4'), 20,41 (13)

Tablica 19. Analitički i MS podaci za harmicine **50a,c-e**

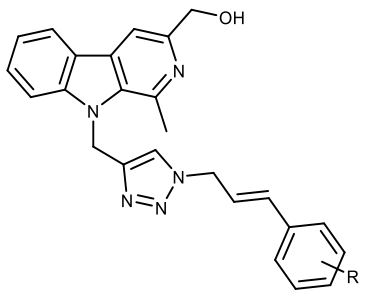

Spoj	R	Iskor. (%)	t_t (°C)	Molekulska formula	M_r	MS (*m/z*)
50a	H	49	197–200	$C_{25}H_{23}N_5O$	409,49	410,3 $(M+1)^+$
50c	*m*-Br	39	164,5–167,5	$C_{25}H_{22}BrN_5O$	488,39	488,1 $(M+1)^+$ 490,1 $(M+1)^+$
50d	*p*-Cl	41	183–186,5	$C_{25}H_{22}ClN_5O$	443,94	444,2 $(M+1)^+$
50e	*p*-OCH_3	43	202–205	$C_{26}H_{25}N_5O_2$	439,52	440,3 $(M+1)^+$

Tablica 20. IR podaci za harmicine **50a,c-e**

Spoj	R	IR (ATR, ν_{max}/cm^{-1})
50a	H	3113, 3060, 2966, 2917, 2859, 1657, 1619, 1560, 1512, 1445, 1402, 1362, 1337, 1290, 1252, 1220, 1190, 1156, 1136, 1122, 1062, 1043, 962, 934, 860, 842, 813, 780, 748, 691, 638, 620, 577, 530, 511, 477, 463
50c	*m*-Br	3117, 3060, 2959, 2922, 2861, 1619, 1592, 1560, 1471, 1460, 1445, 1380, 1358, 1336, 1290, 1252, 1222, 1199, 1154, 1120, 1095, 1062, 1044, 995, 965, 934, 875, 861, 829, 786, 747, 719, 685, 668, 636, 621, 577, 534, 492, 463
50d	*p*-Cl	3111, 3064, 2971, 2918, 28558, 2822, 1727, 1658, 1619, 1592, 1559, 1489, 1471, 1447, 1405, 1361, 1336, 1292, 1254, 1221, 1192, 1158, 1121, 1085, 1041, 1014, 964, 938, 861, 837, 819, 799, 779, 748, 719, 685, 637, 577, 537, 502, 462
50e	*p*-OCH_3	3180, 3119, 3067, 3024, 3002, 2945, 2923, 2869, 1622, 1563, 1488, 1462, 1441, 1379, 1364, 1333, 1298, 1254, 1222, 1203, 1160, 1135, 1122, 1067, 1037, 1003, 965, 915, 857, 771, 745, 696, 636, 582, 533, 509, 471, 454

Tablica 21. ^{1}H i ^{13}C NMR spektroskopski podaci za harmicine **50a,c-e**

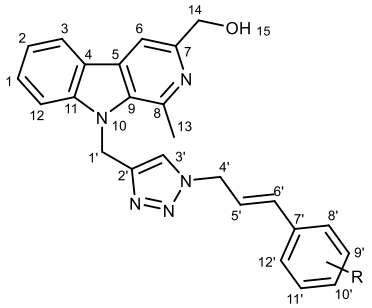

Spoj	R	^{1}H NMR (DMSO-d_6, δ ppm)	^{13}C NMR (DMSO-d_6, δ ppm)
50a	H	8,23 (d, 1H, 3, *J* = 7,7 Hz), 8,02 (s, 1H, 6), 7,98 (s, 1H, 3'), 7,82 (d, 1H, 12, *J* = 8,3 Hz), 7,59–7,55 (m, 1H, 1), 7,40–7,24 (m, 6H, 2, 8', 9', 10', 11', 12'), 6,51 (d, 1H, 6', *J* = 15,9 Hz), 6,47–6,35 (m, 1H, 5'), 5,90 (s, 2H, 1'), 5,33 (t, 1H, 15, *J* = 5,7 Hz), 5,07 (d, 2H, 4', *J* = 6,0 Hz), 4,67 (d, 2H, 14, *J* = 5,7 Hz), 3,05 (s, 3H, 13)	150,27 (8), 144,17 (7), 141,35 (11), 140,55 (9), 135,63 (7'), 133,45 (2'), 133,41 (5'), 129,10 (4), 128,66 (8', 12'), 128,10 (10'), 128,06 (3'), 126,51 (9', 11'), 123,66 (6'), 122,72 (1), 121,41 (3), 120,99 (5), 119,71 (2), 110,61 (12), 109,07 (6), 64,35 (14), 51,27 (1'), 39,73 (4'), 23,15 (13)
50c	*m*-Br	8,23 (d, 1H, 3, *J* = 7,7 Hz), 8,02 (s, 1H, 6), 7,97 (s, 1H, 3'), 7,82 (d, 1H, 12, *J* = 8,3 Hz), 7,70 (t, 1H, 8', *J* = 2,2 Hz), 7,57 (t, 1H, 1, *J* = 8,0 Hz), 7,47–7,42 (m, 2H, 10', 12'), 7,30–7,24 (m, 2H, 2, 11'), 6,67–6,60 (m, 2H, 5', 6'), 5,93 (s, 2H, 1'), 5,32 (t, 1H, 15, *J* = 5,7 Hz), 5,07 (d, 2H, 4', *J* = 5,1 Hz), 4,67 (d, 2H, 14, *J* = 5,6 Hz), 3,08 (s, 3H, 13)	150,26 (8), 144,16 (7), 141,34 (11), 140,54 (9), 138,20 (7'), 133,45 (2'), 131,73 (5'), 130,74 (10'), 130,69 (11'), 129,09 (4), 129,00 (8'), 128,04 (3'), 125,64 (12'), 125,56 (6'), 122,78 (1), 122,12 (9'), 121,40 (3), 120,99 (5), 119,71 (2), 110,60 (12), 109,06 (6), 64,34 (14), 51,11 (1'), 39,72 (4'), 23,13 (13)
50d	*p*-Cl	8,23 (d, 1H, 3, *J* = 7,8 Hz), 8,02 (s, 1H, 3'), 7,97 (s, 1H, 6), 7,82 (d, 1H, 12, *J* = 8,3 Hz), 7,57 (t, 1H, 1, *J* = 7,5 Hz), 7,43–7,35 (m, 4H, 8', 9', 11', 12'), 7,27 (t, 1H, 2, *J* = 7,4 Hz), 6,52–6,41 (m, 2H, 5', 6'), 5,90 (s, 2H, 1'), 5,32 (t, 1H, 15, *J* = 5,7 Hz), 5,07 (d, 2H, 4', *J* = 5,1 Hz), 4,67 (d, 2H, 14, *J* = 5,7 Hz), 3,05 (s, 3H, 13)	150,27 (8), 144,18 (7), 141,35 (11), 140,55 (9), 134,61 (7'), 133,44 (2'), 132,47 (10'), 132,05 (5'), 129,10 (4), 128,64 (8', 12'), 128,24 (9', 11'), 128,06 (3'), 124,71 (6'), 122,76 (1), 121,41 (3), 120,99 (5), 119,72 (2), 110,60 (12), 109,06 (6), 64,35 (14), 51,17 (1'), 39,73 (4'), 23,15 (13)
50e	*p*-$\overset{13'}{\text{O}}\text{CH}_3$	8,23 (d, 1H, 3, *J* = 7,8 Hz), 8,02 (s, 1H, 3'), 7,96 (s, 1H, 6), 7,82 (d, 1H, 12, *J* = 8,3 Hz), 7,57 (t, 1H, 1, *J* = 7,5 Hz), 7,34–7,30 (m, 2H, 8', 12'), 7,26 (t, 1H, 2, *J* = 7,5 Hz), 6,89–6,85 (m, 2H, 9', 11'), 6,47 (d, 1H, 6', *J* = 15,8 Hz), 6,25 (dt, 1H, 5', *J* = 15,8, 6,5 Hz), 5,90 (s, 2H, 1'), 5,33 (t, 1H, 15, *J* = 5,7 Hz), 5,03 (d, 2H, 4', *J* = 7,2 Hz), 4,67 (d, 2H, 14, *J* = 5,7 Hz), 3,74 (s, 3H, 13'), 3,05 (s, 3H, 13)	159,20 (10'), 150,26 (8), 144,14 (7), 141,35 (11), 140,56 (9), 133,45 (2'), 133,19 (5'), 129,09 (4), 128,24 (7'), 128,05 (3'), 127,86 (8', 12'), 122,61 (1), 121,40 (3), 121,05 (6'), 120,98 (5), 119,71 (2), 114,06 (9', 11'), 110,60 (12), 109,07 (6), 64,35 (14), 55,11 (13'), 51,41 (1'), 39,73 (4'), 23,15 (13)

4.1.9. Sinteza harmikina 51-65

Pripravljene su dvije serije spojeva, harmikini TT **51-58** i harmikini AT **59-65**, u 5 položaja β-karbolinskog prstena, C-1, C-3, O-6, O-7 i N-9. Harmikini TT **51-58** pripravljeni su klik-reakcijom u istim reakcijskim uvjetima koji su korišteni kod priprave harmicina **49** i **50** (Shema 23). C-1 i C-3 harmikini pripravljeni su reakcijom alkina 7-klorkinolina **42** i azida β-karbolina **6**, odnosno **11**. Nasuprot tome, O-6, O-7 i N-9 harmikini dobiveni su reakcijom azida 7-klorkinolina **38**, odnosno **40** te alkina β-karbolina **19**, **24** i **28**. Korištena su dva različita azida 7-klorkinolina radi variranja strukture poveznice, čime se povećava strukturna raznolikost hibrida. Reakcije su, kao kod priprave harmicina **49** i **50**, trajale 24 h. Obrada reakcijska smjese bila je jednostavna te je uključivala uparavanje otapala pod sniženim tlakom i pročišćavanje ostatka nakon uparavanja kromatografijom na koloni uz dodatak sloja Al_2O_3 kako bi se uklonili zaostali bakrovi ioni. Iskorištenja reakcija bila su zadovoljavajuća (38–66 %).

Harmikini AT **59**-**63** pripravljeni su reakcijama povezivanja 7-klorkinolinske kiseline **43** i β-karbolinskih amina **7**, **12**, **21**, **26** ili **30** uz *coupling* reagens T3P i bazu TEA (Metoda 1) (Shema 24). Budući da je harmikin **63** pokazao izuzetno antimalarijsko djelovanje, naknadno su sintetizirana njegova dva analoga, N-9-supstituirani harmikini **64** i **65** koji se razlikuju u duljini poveznice (Shema 24). Spojevi **64** i **65** pripravljeni su reakcijama povezivanja β-karbolinske kiseline **33** i 7-klorkinolinskih amina **44** i **45** uz *coupling reagens* HATU i bazu DIEA (Metoda 2). U obje metode karboksilne kiseline dodane su u suvišku (1,1 ekvivalent) kako bi se povećao prinos reakcije. Također, korištena je dvostruka količina baze (2,2 ekvivalenta) u odnosu na količinu karboksilne kiseline, jer baza ima dvije uloge: deprotoniranje kiseline i amina. Sve reakcije povezivanja provedene su na s.t. Neovisno o metodi, reakcije nisu napredovale do potpune konverzije reaktanata u produkte te su prekinute nakon 18 h. Reakcije povezivanja provedene Metodom 1 prekinute su dodatkom 5 %-tnog NaOH. Nusprodukt u reakciji, linearni trimerni propilfosfonat, u bazičnim uvjetima hidrolizira, a ionski razgradni produkti su, za razliku od amida, topljivi u vodi što omogućava kristalizaciju produkta u vodenoj otopini (214) te izolaciju odsisavanjem. Harmikini pripravljeni Metodom 2 taložili su se iz reakcijske smjese te su odsisani. Sirovi produkti pročišćeni su kromatografijom na koloni. Iskorištenja reakcija bila su umjereno dobra (26–43 %).

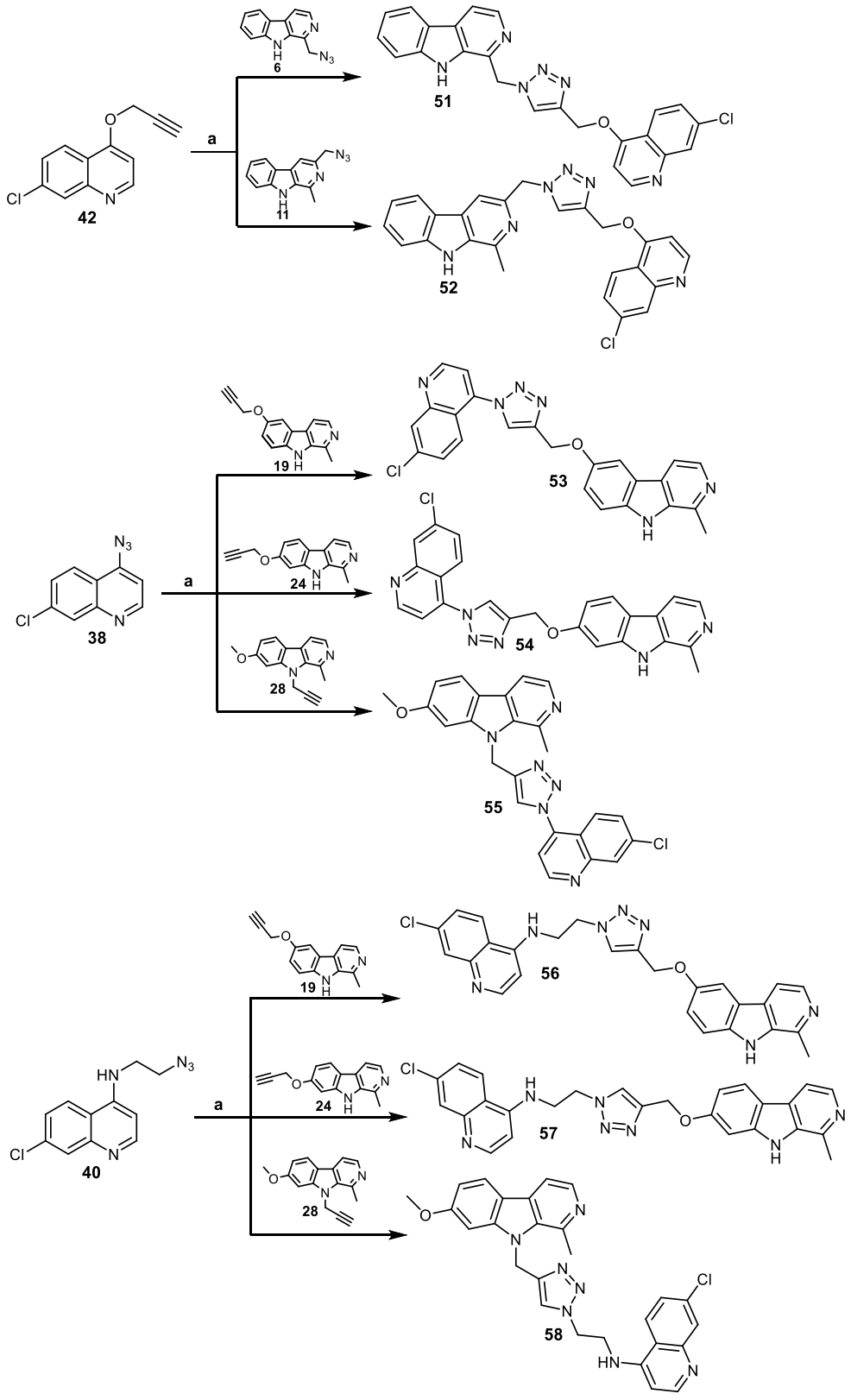

Shema 23. Sinteza harmikina TT **51**-**58**
Reagensi i uvjeti: (a) $Cu(CH_3COO)_2$, MeOH, s.t., 24 h.

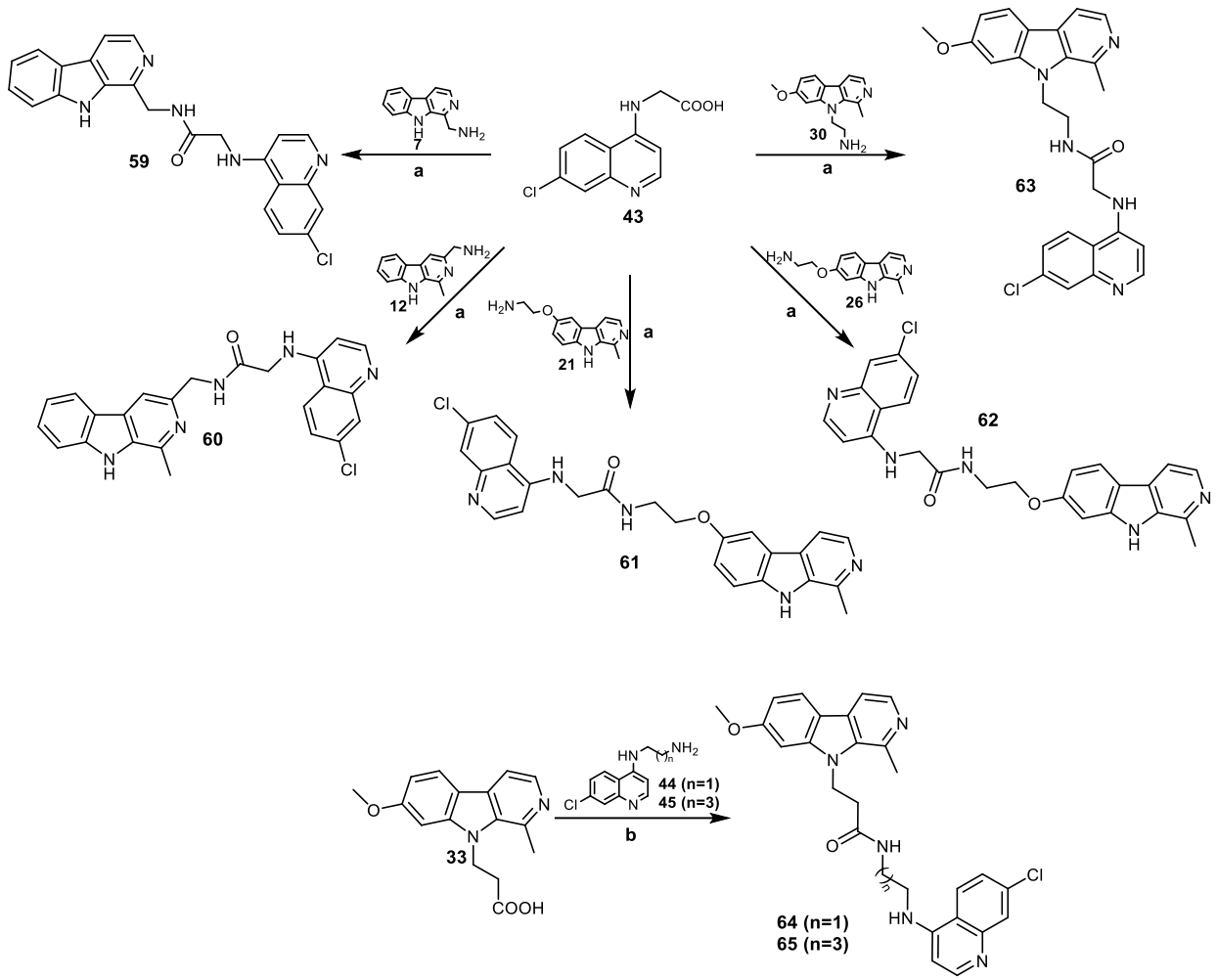

Shema 24. Sinteza harmikina AT **58**-**65**
Reagensi i uvjeti: (a) T3P, TEA, DMF, s.t., 18 h; (b) HATU, DIEA, CH_2Cl_2, s.t., 18 h.

Pripravljeni su spojevi:

- 1-((4-(((7-klorkinolin-4-il)oksi)metil)-1*H*-1,2,3-triazol-1-il)metil)-9*H*-pirido[3,4-*b*]indol (**51**),3
- 3-((4-(((7-klorkinolin-4-il)oksi)metil)-1*H*-1,2,3-triazol-1-il)metil)-1-metil-9*H*-pirido[3,4-*b*]indol (**52**),
- 6-((1-(7-klorkinolin-4-il)-1*H*-1,2,3-triazol-4-il)metoksi)-1-metil-9*H*-pirido[3,4-*b*]indol (**53**),
- 7-((1-(7-klorkinolin-4-il)-1*H*-1,2,3-triazol-4-il)metoksi)-1-metil-9*H*-pirido[3,4-*b*]indol (**54**),
- 9-((1-(7-klorkinolin-4-il)-1*H*-1,2,3-triazol-4-il)metil)-7-metoksi-1-metil-9*H*-pirido[3,4-*b*]indol (**55**),
- 7-klor-*N*-(2-(4-(((1-metil-9*H*-pirido[3,4-*b*]indol-6-il)oksi)metil)-1*H*-1,2,3-triazol-1-il)etil)kinolin-4-amin (**56**),

- 7-klor-*N*-(2-(4-(((1-metil-9*H*-pirido[3,4-*b*]indol-7-il)oksi)metil)-1*H*-1,2,3-triazol-1-il)etil)kinolin-4-amin (**57**),
- 7-klor-*N*-(2-(4-((7-metoksi-1-metil-9*H*-pirido[3,4-*b*]indol-9-il)metil)-1*H*-1,2,3-triazol-1-il)etil)kinolin-4-amin (**58**),
- *N*-((9*H*-pirido[3,4-*b*]indol-1-il)metil)-2-((7-klorkinolin-4-il)amino)acetamid (**59**),
- 2-((7-klorkinolin-4-il)amino)-*N*-((1-metil-9*H*-pirido[3,4-*b*]indol-3-il)metil)acetamid (**60**),
- 2-((7-klorkinolin-4-il)amino)-*N*-(2-((1-metil-9*H*-pirido[3,4-*b*]indol-6-il)oksi)etil)acetamid (**61**),
- 2-((7-klorkinolin-4-il)amino)-*N*-(2-((1-metil-9*H*-pirido[3,4-*b*]indol-7-il)oksi)etil)acetamid (**62**),
- 2-((7-klorkinolin-4-il)amino)-*N*-(2-(7-metoksi-1-metil-9*H*-pirido[3,4-*b*]indol-9-il)etil)acetamid (**63**),
- *N*-(2-((7-klorkinolin-4-il)amino)etil)-3-(7-metoksi-1-metil-9*H*-pirido[3,4-*b*]indol-9-il)propanamid (**64**),
- *N*-(4-((7-klorkinolin-4-il)amino)butil)-3-(7-metoksi-1-metil-9*H*-pirido[3,4-*b*]indol-9-il)propanamid (**65**).

Harmikini **51-65** su novi, do sada neopisani spojevi. Sinteza harmikina i njihova čistoća praćene su tankoslojnom kromatografijom, a strukture su potvrđene uobičajenim metodama (IR, ^{1}H i ^{13}C NMR, MS). Analitički, spektrometrijski i spektroskopski podaci dani su u Tablicama 22-27. U IR spektrima harmikina AT **59-65** vidljive su karakteristične vrpce za amidnu vezu: u rasponu 3220-3370 cm^{-1} vidljiva je vrpca N-H istezanja, dok su u rasponu 1620-1680 cm^{-1} vidljive dvije bliske vrpce koje odgovaraju C=O istezanju. Kemijski pomaci protona u ^{1}H, odnosno ugljika u ^{13}C NMR spektrima spojeva u skladu su s predloženim strukturama. U ^{1}H NMR spektrima harmikina TT **51-58** vidljiv je CH signal (singlet, 1 proton) u području 7,98–9,02 ppm karakterističan za triazolski prsten, dok je u ^{1}H NMR spektrima harmikina AT **59-65** vidljiv signal za proton NH skupine amida u području 8–8,80 ppm. ^{13}C NMR spektri sadrže signal za karbonilni ugljik amida na ≈ 170 ppm. U MS spektrima svih harmikina vidi se pseudomolekulski ion.

Tablica 22. Analitički i MS podaci za harmikine **51-58**

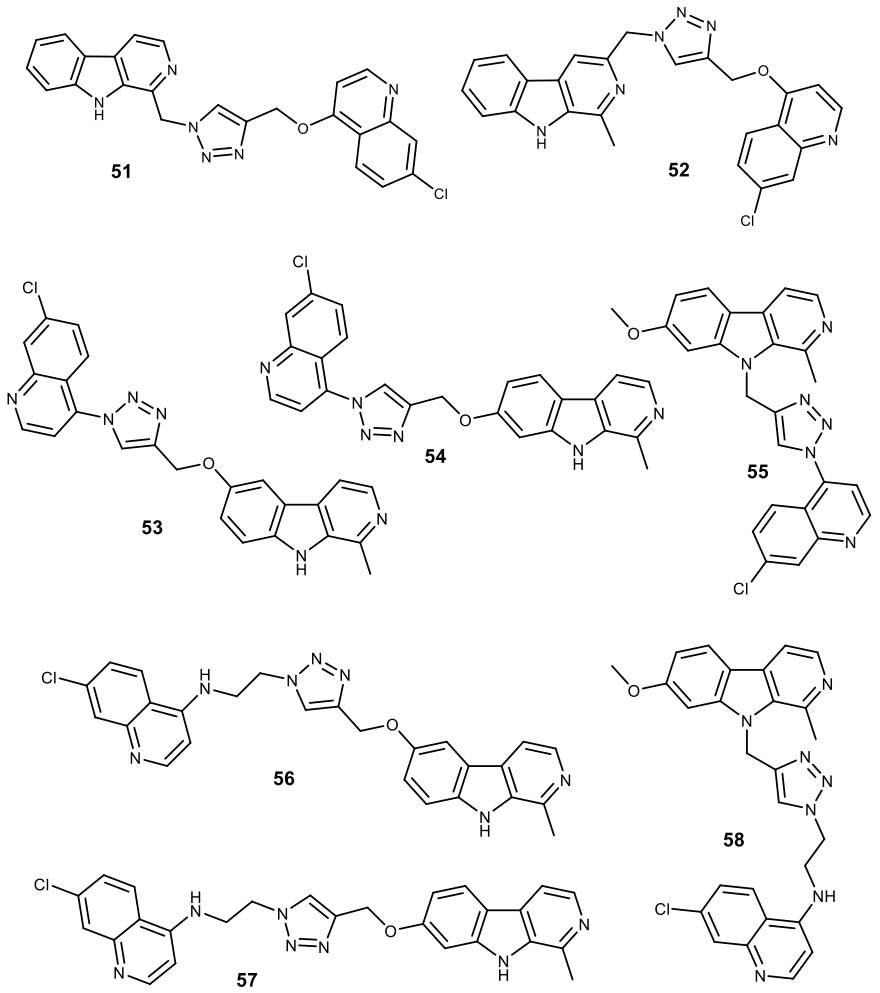

Spoj	Iskor. (%)	t_t (°C)	Molekulska formula	M_r	MS (*m/z*)
51	45	170-172	$C_{24}H_{17}ClN_6O$	440,89	441,0 $(M+1)^+$
52	40	172–174,5	$C_{25}H_{19}ClN_6O$	454,92	455,4 $(M+1)^+$
53	42	281,5–283	$C_{24}H_{17}ClN_6O$	440,89	441,4 $(M+1)^+$
54	50	236–239,5	$C_{24}H_{17}ClN_6O$	440,89	441,3 $(M+1)^+$
55	38	235–237	$C_{25}H_{19}ClN_6O$	454,92	455,3 $(M+1)^+$
56	43	272–273	$C_{26}H_{22}ClN_7O$	483,96	484,1 $(M+1)^+$
57	54	238–241	$C_{26}H_{22}ClN_7O$	483,96	482,1 $(M-1)^-$
58	66	244–245,5	$C_{27}H_{24}ClN_7O$	497,99	496,1 $(M-1)^-$

Tablica 23. IR podaci za harmicine **51-58**

Spoj	IR (ATR, ν_{max}/cm^{-1})
51	3235, 3058, 1619, 1604, 1566, 1541, 1488, 1454, 1432, 1374, 1322, 1299, 1228, 1136, 1100, 1054, 945, 856, 806, 755, 724, 656, 587, 541, 493, 478
52	3617, 3130, 3057, 2888, 2787, 1623, 1603, 1568, 1507, 1486, 1468, 1446, 1398, 1376, 1357, 1340, 1254, 1224, 1140, 1103, 1058, 1055, 1027, 971, 860, 812, 800, 749, 646, 589, 543, 479
53	3247, 3076, 3030, 2901, 1588, 1567, 1497, 1477, 1458, 1441, 1414, 1372, 1350, 1265, 1253, 1208, 1174, 1116, 1076, 1039, 1030, 1008, 987, 968, 878, 849, 829, 816, 803, 770, 736, 700, 672, 655, 621, 543, 500
54	3049, 1629, 1610, 1564, 1505, 1486, 1440, 1321, 1295, 1278, 1253, 1233, 1215, 1106, 1071, 1036, 996, 953, 920, 872, 822, 812, 801, 767, 629, 572
55	3143, 1621, 1561, 1499, 1442, 1406, 1372, 1345, 1255, 1223, 1194, 1171, 1138, 1115, 1036, 931, 925, 876, 813, 722, 623, 554
56	3201, 1608, 1583, 1544, 1498, 1456, 1429, 1383, 1365, 1352, 1330, 1248, 1207, 1170, 1061, 1139, 1050, 1026, 990, 909, 872, 845, 808, 765, 624, 492
57	3340, 3158, 3065, 2957, 1638, 1584, 1543, 1485, 1450, 1428, 1371, 1338, 1251, 1235, 1155, 1110, 1056, 874, 851, 813, 800, 761, 648, 858, 531
58	2957, 1619, 1578, 1495, 1441, 1428, 1403, 1369, 1355, 1324, 1252, 1224, 1193, 1171, 1082, 973, 926, 910, 875, 814, 764, 732, 641, 593, 462

Tablica 24. ^{1}H i ^{13}C NMR spektroskopski podaci za harmikine **51-58**

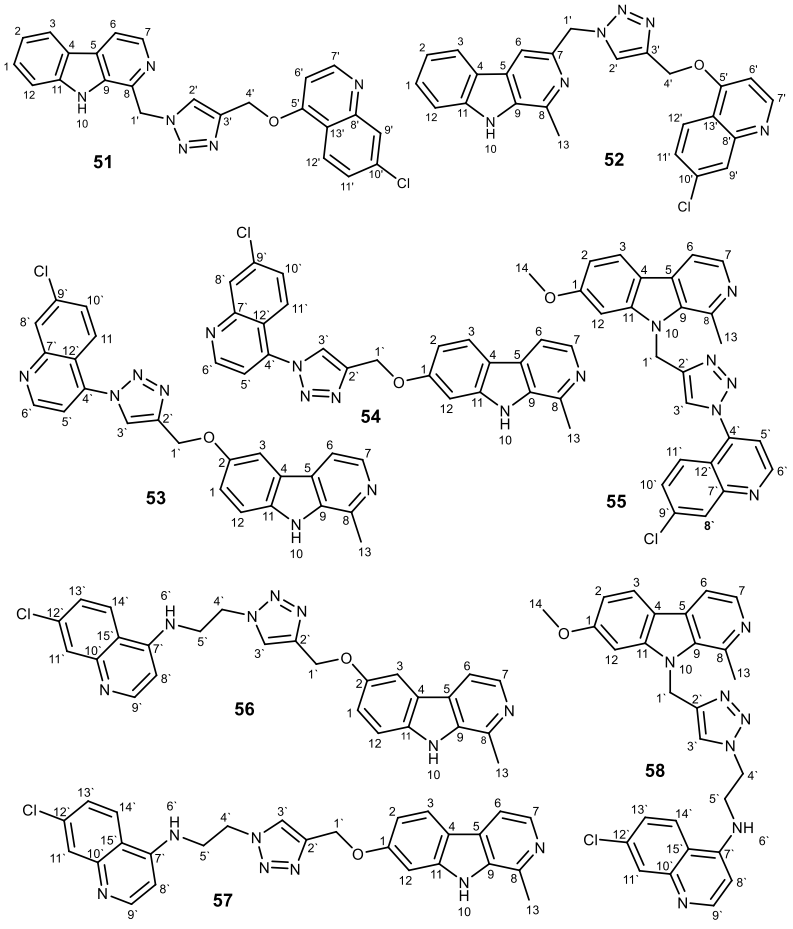

Spoj	^{1}H NMR (DMSO-d_6, δ ppm)	^{13}C NMR (DMSO-d_6, δ ppm)
51	11,93 (s, 1H, 10), 8,30 (s, 1H, 2'), 8,28–8,24 (m, 2H, 3, 7), 8,19 (d, 1H, 7', *J* = 7,8 Hz), 8,14 (d, 1H, 12', *J* = 8,6 Hz), 8,11 (d, 1H, 6, *J* = 5,1 Hz), 8,00 (d, 1H, 9', *J* = 1,9 Hz), 7,65 (dt, 1H, 12, *J* = 8,2, 0,9 Hz), 7,60–7,58 (m, 1H, 1), 7,38 (dd, 1H, 11', *J* = 8,6, 1,9 Hz), 7,29–7,27 (m, 1H, 2), 6,13 (d, 1H, 6', *J* = 7,8 Hz), 6,06 (s, 2H, 1'), 5,55 (s, 2H, 4')	175,78 (5'), 145,22 (7'), 141,86 (8), 140,68 (8'), 140,57 (11), 137,85 (7), 137,84 (3'), 136,92 (10'), 133,82 (9), 128,72 (5), 128,56 (9'), 127,86 (11'), 125,26 (4), 124,62 (12'), 123,75 (2'), 121,91 (1), 120,72 (13'), 119,65 (3), 116,69 (2), 114,85 (6), 112,05 (12), 109,78 (6'), 51,25 (4'), 46,88 (1')
52	11,66 (s, 1H, 10), 8,25 (s, 1H, 2'), 8,19 (d, 1H, 7', *J* = 7,8 Hz), 8,14 (d, 1H, 12', *J* = 8,6 Hz), 8,11 (d, 1H, 3, *J* = 7,9 Hz), 8,00 (d, 1H, 9', *J* = 1,8 Hz), 7,90 (s, 1H, 6), 7,59 (d, 1H, 12, *J* = 8,16 Hz), 7,56–7,52 (m, 1H, 1), 7,38 (dd, 1H, 11', *J* = 8,6, 1,8 Hz), 7,27–7,22 (m, 1H, 2), 6,13 (d, 1H, 6', *J* = 7,8 Hz), 5,73 (s, 2H, 1'), 5,55 (s, 2H, 4'), 2,71 (s, 3H, 13)	175,79 (5'), 145,24 (7'), 142,44 (7), 142,14 (8), 141,95 (11), 140,75 (3'), 140,55 (8'), 136,90 (10'), 133,95 (9), 128,09 (9'), 127,87 (11'), 127,55 (5), 125,28 (4), 124,08 (12'), 123,73 (2'), 121,62 (1), 120,87 (13'), 119,43 (3), 116,65 (2), 112,09 (12), 111,81 (6), 109,77 (6'), 55,19 (1'), 46,97 (4'), 20,34 (13)
53	11,42 (s, 1H, 10), 9,17 (d, 1H, 6', *J* = 4,6 Hz), 9,01 (s, 1H, 3'), 8,30 (d, 1H, 8', *J* = 2,2 Hz), 8,18 (d, 1H, 7, *J* = 5,3 Hz), 8,00–7,98 (m, 2H, 3, 11'), 7,93 (d, 1H, 6, *J* = 5,3 Hz), 7,89 (d, 1H, 5', *J* = 4,6 Hz), 7,75 (dd, 1H, 10', *J* = 9,1, 2,2 Hz), 7,55 (d, 1H, 12, *J* = 8,8 Hz), 7,31 (dd, 1H, 1, *J* = 8,8, 2,5 Hz), 5,42 (s, 2H, 1'), 2,75 (s, 3H, 13)	152,38 (6'), 151,88 (2), 149,38 (7'), 143,96 (2'), 142,25 (8), 140,38 (11), 137,00 (7), 135,56 (9), 135,36 (9'), 135,10 (4'), 128,98 (8'), 128,14 (10'), 126,85 (11'), 126,69 (5), 125,35 (3'), 121,39 (12'), 120,34 (4), 118,44 (1), 117,15 (5'), 112,82 (6), 112,69 (12), 105,40 (3), 61,80 (1'), 20,40 (13)
54	11,51 (s, 1H, 10), 9,17 (d, 1H, 6', *J* = 4,7 Hz), 9,02 (s, 1H, 3'), 8,30 (d, 1H, 8', *J* = 2,1 Hz), 8,17 (d, 1H, 7, *J* = 5,3 Hz), 8,11 (d, 1H, 3, *J* = 8,6 Hz), 8,01 (d, 1H, 11', *J* = 9,1 Hz), 7,90 (d, 1H, 5', *J* = 4,7 Hz), 7,83 (d, 1H, 6, *J* = 5,3 Hz), 7,79 (dd, 1H, 10', *J* = 9,1, 2,2 Hz), 7,27 (d, 1H, 12, *J* = 2,2 Hz), 6,99 (dd, 1H, 2, *J* = 8,6, 2,2 Hz), 5,47 (s, 2H, 1'), 2,74 (s, 3H, 13)	158,72 (1), 152,39 (6'), 149,39 (7'), 143,72 (2'), 141,79 (8), 141,37 (11), 140,36 (9), 137,74 (7), 135,39 (9'), 134,62 (4'), 129,03 (8'), 128,17 (10'), 127,14 (5), 127,00 (11'), 125,35 (3'), 122,73 (3), 120,34 (12'), 117,17 (5'), 115,31 (4), 111,99 (6), 109,45 (2), 96,03 (12), 61,29 (1'), 20,32 (13)
55	9,09 (d, 1H, 6', *J* = 4,7 Hz), 8,83 (s, 1H, 3'), 8,26 (d, 1H, 8', *J* = 2,2 Hz), 8,20 (d, 1H, 7, *J* = 5,2 Hz), 8,11 (d, 1H, 3, *J* = 8,6 Hz), 7,95–7,88 (m, 2H, 6, 11'), 7,78 (d, 1H, 5', *J* = 4,7 Hz), 7,74 (dd, 1H, 10', *J* = 9,1, 2,2 Hz), 7,42 (d, 1H, 12, *J* = 2,2 Hz), 6,90 (dd, 1H, 2, *J* = 8,6, 2,1 Hz), 6,05 (s, 2H, 1'), 3,92 (s, 3H, 14), 3,13 (s, 3H, 13)	160,62 (1), 152,29 (6'), 149,31 (7'), 144,79 (2'), 142,74 (8), 141,17 (11), 140,22 (9), 138,15 (7), 135,28 (4'), 134,75 (9'), 128,91 (8'), 128,62 (5), 128,10 (10'), 125,34 (3', 11'), 122,40 (3), 120,31 (12'), 117,20 (5'), 114,51 (4), 112,29 (6), 109,48 (2), 94,13 (12), 55,66 (14), 23,31 (13)
56	11,43 (s, 1H, 10), 8,41 (d, 1H, 9', *J* = 5,4 Hz), 8,32 (s, 1H, 3'), 8,20 (d, 1H, 14', *J* = 9,1 Hz), 8,16 (d, 1H, 7, *J* = 5,3 Hz), 7,92–7,85 (m, 2H, 3, 6), 7,81 (d, 1H, 11', *J* = 2,2 Hz), 7,54 (t, 1H, 6', *J* = 5,8 Hz), 7,50 (d, 1H, 12, *J* = 8,8 Hz), 7,44 (dd, 1H, 13', *J* = 9,0, 2,3 Hz), 7,20 (dd, 1H, 1, *J* = 8,8, 2,5 Hz), 6,57 (d, 1H, 8', *J* = 5,5 Hz), 5,21 (s, 2H, 1'), 4,70 (t, 2H, 4', *J* = 6,1 Hz), 3,82 (q, 2H, 5', *J* = 5,9 Hz), 2,75 (s, 3H, 13)	151,99 (2), 151,87 (9'), 149,76 (7'), 148,95 (10'), 142,97 (2'), 142,22 (8), 136,93 (7), 135,43 (11), 135,09 (9), 133,53 (12'), 127,47 (11'), 126,70 (5), 124,96 (3'), 124,35 (14'), 124,00 (13'), 121,35 (15'), 118,28 (1), 117,47 (4), 112,76 (6), 112,66 (12), 105,00 (3), 98,90 (8'), 61,91 (1'), 47,86 (4'), 42,46 (5'), 20,41 (13)
57	11,48 (s, 1H, 10), 8,41 (d, 1H, 9', *J* = 5,4 Hz), 8,32 (s, 1H, 3'), 8,19–8,15 (m, 2H, 7, 14'), 8,05 (d, 1H, 3, *J* = 8,6 Hz), 7,82–7,80 (m, 2H, 6, 11'), 7,54 (t, 1H, 6', *J* = 5,2 Hz), 7,45 (dd, 1H, 13', *J* = 9,0, 2,3 Hz), 7,17 (d, 1H, 12, *J* = 2,2 Hz), 6,88 (dd, 1H, 2, *J* = 8,7, 2,3 Hz), 6,57 (d, 1H, 8', *J* = 5,5 Hz), 5,25 (s, 2H, 1'), 4,70 (t, 2H, 4', *J* = 5,8 Hz), 3,82 (q, 2H, 5', *J* = 6,0 Hz), 2,73 (s, 3H, 13)	158,79 (1), 151,77 (9'), 149,82 (7'), 148,82 (10'), 142,70 (2'), 141,82 (8), 141,30 (11), 137,65 (7), 134,59 (9), 133,60 (12'), 127,38 (11'), 127,18 (5), 125,08 (3'), 124,40 (14'), 124,00 (13'), 122,64 (3), 117,44 (15'), 115,10 (4), 111,98 (6), 109,42 (2), 98,91 (8'), 95,82 (12), 61,45 (1'), 47,90 (4'), 42,43 (5'), 20,29 (13)

58	8,31 (d, 1H, 9', *J* = 5,4 Hz), 8,17 (d, 1H, 7, *J* = 5,2 Hz), 8,08 (d, 1H, 3, *J* = 8,6 Hz), 8,05 (d, 1H, 14', *J* = 9,1 Hz), 7,98 (s, 1H, 3'), 7,87 (d, 1H, 6, *J* = 5,2 Hz), 7,79 (d, 1H, 11', *J* = 2,2 Hz), 7,44–7,37 (m, 2H, 6', 13'), 7,26 (d, 1H, 12, *J* = 2,1 Hz), 6,87 (dd, 1H, 2, *J* = 8,6, 2,1 Hz), 6,45 (d, 1H, 8', *J* = 5,5 Hz), 5,83 (s, 2H, 1'), 4,57 (t, 2H, 4', *J* = 6,0 Hz), 3,83 (s, 3H, 14), 3,70 (q, 2H, 5', *J* = 5,9 Hz,), 2,98 (s, 3H, 13)	160,52 (1), 151,63 (9'), 149,73 (7'), 148,74 (10'), 143,88 (2'), 142,65 (8), 141,07 (11), 137,98 (7), 134,60 (9), 133,56 (12'), 128,49 (5), 127,34 (11'), 124,35 (3'), 123,78 (14'), 123,47 (13'), 122,34 (3), 117,33 (15'), 114,39 (4), 112,23 (6), 109,36 (2), 98,77 (8'), 93,95 (12), 55,53 (14), 47,86 (4'), 42,34 (5'), 23,11 (13)

Tablica 25. Analitički i MS podaci za harmikine **59-65**

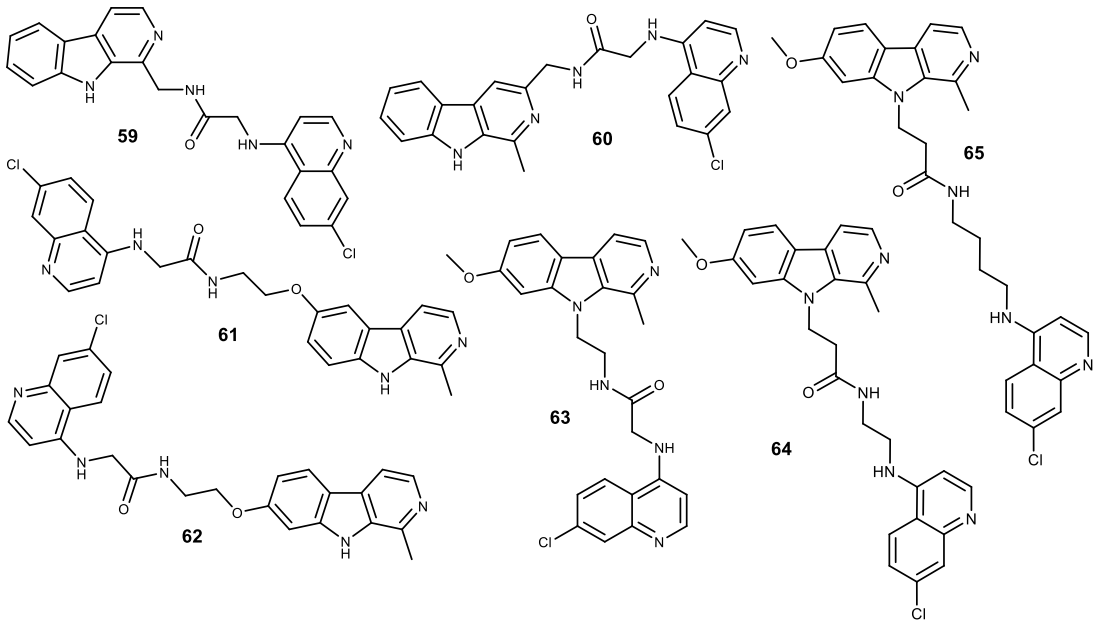

Spoj	Iskor. (%)	t_t (°C)	Molekulska formula	M_r	MS (*m/z*)
59	42	244–247	$C_{23}H_{18}ClN_5O$	415,88	416,1 $(M+1)^+$
60	28	274,5–277	$C_{24}H_{20}ClN_5O$	429,91	430,1 $(M+1)^+$
61	26	304–307	$C_{25}H_{22}ClN_5O_2$	459,93	460,0 $(M+1)^+$
62	30	275–277,5	$C_{25}H_{22}ClN_5O_2$	459,93	460,1 $(M+1)^+$
63	35	252,5–255	$C_{26}H_{24}ClN_5O_2$	473,96	474,1 $(M+1)^+$
64	35	224–227	$C_{27}H_{26}ClN_5O_2$	487,99	488,1 $(M+1)^+$
65	43	230–233	$C_{29}H_{30}ClN_5O_2$	516,04	516,4 $(M+1)^+$

Tablica 26. IR podaci za harmikine **59-65**

Spoj	IR (ATR, ν_{max}/cm^{-1})
59	3267, 1651, 1627, 1585, 1451, 1431, 1323, 1284, 1235, 1151, 1126, 1082, 1023, 986, 902, 871, 853, 742, 578, 563, 519
60	3616, 3285, 1662, 1629, 1587, 1502, 1453, 1431, 1375, 1328, 1234, 1150, 1083, 1014, 901, 851, 801, 737
61	3525, 3369, 3219, 3145, 3054, 2874, 1679, 1581, 1530, 1505, 1485, 1452, 1372, 1334, 1287, 1240, 1213, 1116, 1075, 990, 877, 854, 810, 793, 629, 614, 488, 467
62	3641, 3284, 3093, 1659, 1631, 1612, 1587, 1487, 1431, 1376, 1328, 1274, 1232, 1178, 1148, 1109, 1056, 974, 903, 878, 852, 801, 569
63	3268, 3063, 1656, 1625, 1582, 1445, 1408, 1375, 1343, 1280, 1251, 1198, 1174, 1140, 1081, 1047, 1025, 976, 809, 639, 597, 569
64	3226, 3060, 2967, 1645, 1624, 1582, 1547, 1503, 1449, 1409, 1342, 1300, 1284, 1267, 1231, 1167, 1140, 1120, 1083, 1042, 1017, 976, 946, 872, 853, 827, 814, 801, 764, 636, 595, 567, 546, 474
65	3306, 2936, 1642, 1624, 1577, 1499, 1448, 1408, 1366, 1330, 1305, 1227, 1205, 1166, 1187, 1119, 1046, 883, 849, 810, 546

Tablica 27. ^{1}H i ^{13}C NMR spektroskopski podaci za harmikine **59-65**

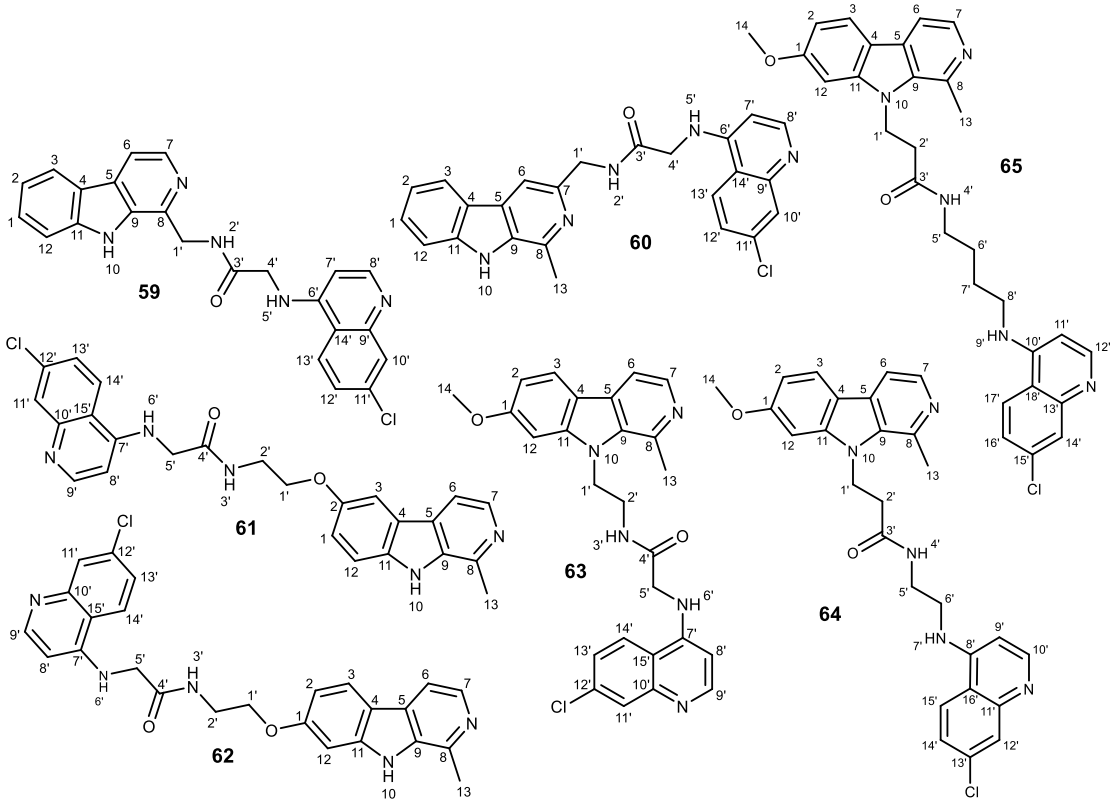

Spoj	^{1}H NMR (DMSO-d_6, δ ppm)	^{13}C NMR (DMSO-d_6, δ ppm)
59	11,54 (s, 1H, 10), 8,79 (t, 1H, 2', *J* = 5,5 Hz), 8,34 (d, 1H, 8', *J* = 5,4 Hz), 8,28–8,25 (m, 2H, 7, 13'), 8,22 (d, 1H, 3, *J* = 7,9 Hz), 8,03 (d, 1H, 6, *J* = 5,2 Hz), 7,83 (t, 1H, 5', *J* = 6,5 Hz), 7,81 (d, 1H, 10', *J* = 2,3 Hz), 7,59 (d, 1H, 12, *J* = 8,2 Hz), 7,56–7,53 (m, 1H, 1), 7,50 (dd, 1H, 12', *J* = 9,0, 2,3 Hz), 7,26–7,23 (m, 1H, 2), 6,40 (d, 1H, 7', *J* = 5,4 Hz), 4,81 (d, 2H, 1', *J* = 5,4 Hz), 4,07 (d, 2H, 4', *J* = 6,0 Hz)	169,38 (3'), 151,63 (8'), 150,35 (6'), 148,74 (9'), 141,33 (8), 140,40 (11), 137,30 (7), 133,56 (11'), 133,36 (9), 128,14 (1), 127,74 (5), 127,36 (10'), 124,41 (12'), 124,23 (13'), 121,76 (3), 120,83 (4), 119,42 (2), 117,56 (14'), 113,89 (6), 112,03 (12), 99,44 (7'), 45,81 (1'), 41,48 (4')
60	11,48 (s, 1H, 10), 8,71 (t, 1H, 2', *J* = 5,9 Hz), 8,44 (d, 1H, 8', *J* = 5,4 Hz), 8,29 (d, 1H, 13', *J* = 9,0 Hz), 8,05 (d, 1H, 3, *J* = 7,8 Hz), 7,90–7,79 (m, 2H, 5', 10'), 7,71 (s, 1H, 6), 7,60–7,46 (m, 3H, 1, 12, 12'), 7,26–7,19 (m, 1H, 2), 6,47 (d, 1H, 7', *J* = 5,4 Hz), 4,52 (d, 2H, 1', *J* = 5,8 Hz), 4,07 (d, 2H, 4', *J* = 6,0 Hz), 2,70 (s, 3H, 13)	168,98 (3'), 151,79 (8'), 150,26 (6'), 148,97 (9'), 146,08 (7), 141,11(8), 140,73 (11), 133,51 (11'), 133,45 (9), 127,82 (1), 127,65 (5), 127,46 (10'), 124,32 (12', 13'), 121,46 (3), 120,94 (4), 119,13 (2), 117,63 (14'), 111,95 (12), 109,34 (6), 99,28 (7'), 46,01 (1'), 44,21 (4'), 20,24 (13)
61	11,41 (s, 1H, 10), 8,41 (t, 1H, 3', *J* = 5,7 Hz), 8,29 (d, 1H, 9', *J* = 5,4 Hz), 8,27 (d, 1H, 14', *J* = 9,1 Hz), 8,15 (d, 1H, 7, *J* = 5,3 Hz), 7,88 (d, 1H, 6, *J* = 5,3 Hz), 7,82 (t, 1H, 6', *J* = 6,4 Hz), 7,81 (d, 1H, 11', *J* = 2,3 Hz), 7,73 (d, 1H, 3, *J* = 2,5 Hz), 7,52–7,48 (m, 2H, 12, 13'), 7,15 (dd, 1H, 1, *J* = 8,8, 2,5 Hz), 6,31 (d, 1H, 8', *J* = 5,4 Hz), 4,10 (t, 2H, 1', *J* = 5,6 Hz), 3,98 (d, 2H, 5', *J* = 5,9 Hz), 3,54 (q, 2H, 2', *J* = 5,6 Hz), 2,74 (s, 3H, 13)	169,14 (4'), 152,30 (2), 151,54 (9'), 150,39 (7'), 148,64 (10'), 142,18 (8), 136,88 (7), 135,36 (11), 135,08 (9), 133,57 (12'), 127,24 (11'), 126,70 (5), 124,36 (14'), 124,26 (13'), 121,37 (4), 118,23 (1), 117,52 (15'), 112,73 (6), 112,69 (12), 104,77 (3), 99,15 (8'), 66,99 (1'), 45,80 (5'), 38,50 (2'), 20,39 (13)
62	11,54 (s, 1H, 10), 8,46 (t, 1H, 3', *J* = 5,7 Hz), 8,30–8,28 (m, 2H, 9', 14'), 8,16 (d, 1H, 7, *J* = 5,3 Hz), 8,06 (d, 1H, 3, *J* = 8,6 Hz), 7,92 (t, 1H, 6', *J* = 6,1 Hz), 7,82 (d, 1H, 6, *J* = 5,3 Hz), 7,81 (d, 1H, 11', *J* = 2,3 Hz), 7,50 (dd, 1H, 13', *J* = 9,0, 2,3 Hz), 7,02 (d, 1H, 12, *J* = 2,2 Hz), 6,83 (dd, 1H, 2, *J* = 8,6, 2,2 Hz), 6,32 (d, 1H, 8', *J* = 5,5 Hz), 4,12 (t, 2H, 1', *J* = 5,6 Hz), 3,99 (d, 2H, 5', *J* = 5,9 Hz), 3,55 (q, 2H, 2', *J* = 5,6 Hz), 2,74 (s, 3H, 13)	169,16 (4'), 159,20 (1), 151,28 (9'), 150,57 (7'), 148,37 (10'), 141,96 (8), 141,23 (11), 137,51 (7), 134,57 (9), 133,69 (12'), 127,28 (5), 127,01 (11'), 124,42 (14'), 124,35 (13'), 122,68 (3), 117,48 (15'), 114,98 (4), 112,00 (6), 109,35 (2), 99,13 (8'), 95,41 (12), 66,42 (1'), 45,78 (5'), 38,38 (2'), 20,27 (13)
63	8,37 (t, 1H, 3', *J* = 6,0 Hz), 8,31 (d, 1H, 9', *J* = 5,3 Hz), 8,24 (d, 1H, 14', *J* = 9,0 Hz), 8,16 (d, 1H, 7, *J* = 5,2 Hz), 8,10 (d, 1H, 3, *J* = 8,6 Hz), 7,87 (d, 1H, 6, *J* = 5,1 Hz), 7,81 (d, 1H, 11', *J* = 2,3 Hz), 7,74 (t, 1H, 6', *J* = 6,1 Hz), 7,49 (dd, 1H, 13', *J* = 9,0, 2,3 Hz), 7,28 (d, 1H, 12, *J* = 2,2 Hz), 6,89 (dd, 1H, 2, *J* = 8,6, 2,2 Hz), 6,07 (d, 1H, 8', *J* = 5,4 Hz), 4,58 (t, 2H, 1', *J* = 7,1 Hz), 3,90 (s, 3H, 14), 3,85 (d, 2H, 5', *J* = 6,0 Hz), 3,52 (q, 2H, 2', *J* = 6,8 Hz), 2,96 (s, 3H, 13)	169,63 (4'), 160,57 (1), 151,91 (9'), 150,13 (7'), 148,95 (10'), 142,90 (8), 140,62 (11), 137,87 (7), 134,64 (9), 133,50 (12'), 128,43 (5), 127,53 (11'), 124,36 (14'), 124,22 (13'), 122,48 (3), 117,56 (15'), 114,31 (4), 112,30 (6), 109,25 (2), 98,97 (8'), 93,63 (12), 55,57 (14), 45,97 (1'), 43,29 (5'), 38,84 (2'), 23,14 (13)
64	8,40 (d, 1H, 10', *J* = 5,4 Hz), 8,23 (t, 1H, 4', *J* = 5,8 Hz), 8,20–8,12 (m, 2H, 7, 15'), 8,05 (d, 1H, 3, *J* = 8,6 Hz), 7,85 (d, 1H, 6, *J* = 5,1 Hz), 7,79 (d, 1H, 12', *J* = 2,2 Hz), 7,44 (dd, 1H, 14', *J* = 9,0, 2,3 Hz), 7,31 (t, 1H, 7', *J* = 5,5 Hz), 7,22 (d, 1H, 12, *J* = 2,2 Hz), 6,85 (dd, 1H, 2, *J* = 8,6, 2,2 Hz), 6,47 (d, 1H, 9', *J* = 5,5 Hz), 4,82 (t, 2H, 1', *J* = 7,2 Hz), 3,90 (s, 3H, 14), 3,27 (q, 2H, 6', *J* = 6,3 Hz), 3,17 (q, 2H, 5', *J* = 5,9 Hz), 2,97 (s, 3H, 13), 2,63 (t, 2H, 2', *J* = 7,2 Hz)	170,35 (3'), 160,43 (1), 151,89 (10'), 149,97 (8'), 149,07 (11'), 142,51 (8), 140,75 (11), 137,90 (7), 134,49 (9), 133,40 (13'), 128,56 (5), 127,52 (12'), 124,10 (15'), 123,94 (14'), 122,29 (3), 117,42 (16'), 114,32 (4), 112,21 (6), 109,20 (2), 98,57 (9'), 93,88 (12), 55,52 (14), 41,76 (1'), 40,87 (6'), 37,23 (5'), 36,34 (2'), 23,11 (13)

65	8,39 (d, 1H, 12', *J* = 5,6 Hz), 8,31 (d, 1H, 17', *J* = 9,0 Hz), 8,16 (d, 1H, 7, *J* = 5,2 Hz), 8,06 (d, 1H, 3, *J* = 8,6 Hz), 7,96 (t, 1H, 4', *J* = 5,6 Hz), 7,86 (d, 1H, 6, *J* = 5,2 Hz), 7,79 (d, 1H, 14', *J* = 2,3 Hz), 7,54–7,40 (m, 2H, 9', 16'), 7,20 (d, 1H, 12, *J* = 2,2 Hz), 6,85 (dd, 1H, 2, *J* = 8,6, 2,1 Hz), 6,43 (d, 1H, 11', *J* = 5,6 Hz), 4,79 (t, 2H, 1', *J* = 7,1 Hz), 3,90 (s, 3H, 14), 3,23–3,13 (m, 2H, 8'), 3,04 (q, 2H, 5', *J* = 6,5 Hz), 2,97 (s, 3H, 13), 2,60 (t, 2H, 2', *J* = 7,0 Hz), 1,53–1,43 (m, 2H, 6'), 1,36 (q, 2H, 7', *J* = 7,2 Hz)	169,59 (3'), 160,42 (1), 151,10 (12'), 150,48 (10'), 148,19 (13'), 142,54 (8), 140,71 (11), 137,75 (7), 134,48 (9), 133,71 (15'), 128,57 (5), 126,73 (14'), 124,28 (17'), 124,17 (16'), 122,26 (3), 117,27 (18'), 114,26 (4), 112,22 (6), 109,21 (2), 98,57 (11'), 93,91 (12), 55,50 (14), 42,01 (1'), 40,96 (8'), 38,17 (5'), 36,37 (2'), 26,49 (6'), 24,98 (7'), 23,04 (13)

4.1.10. Sinteza harmicena 66-83

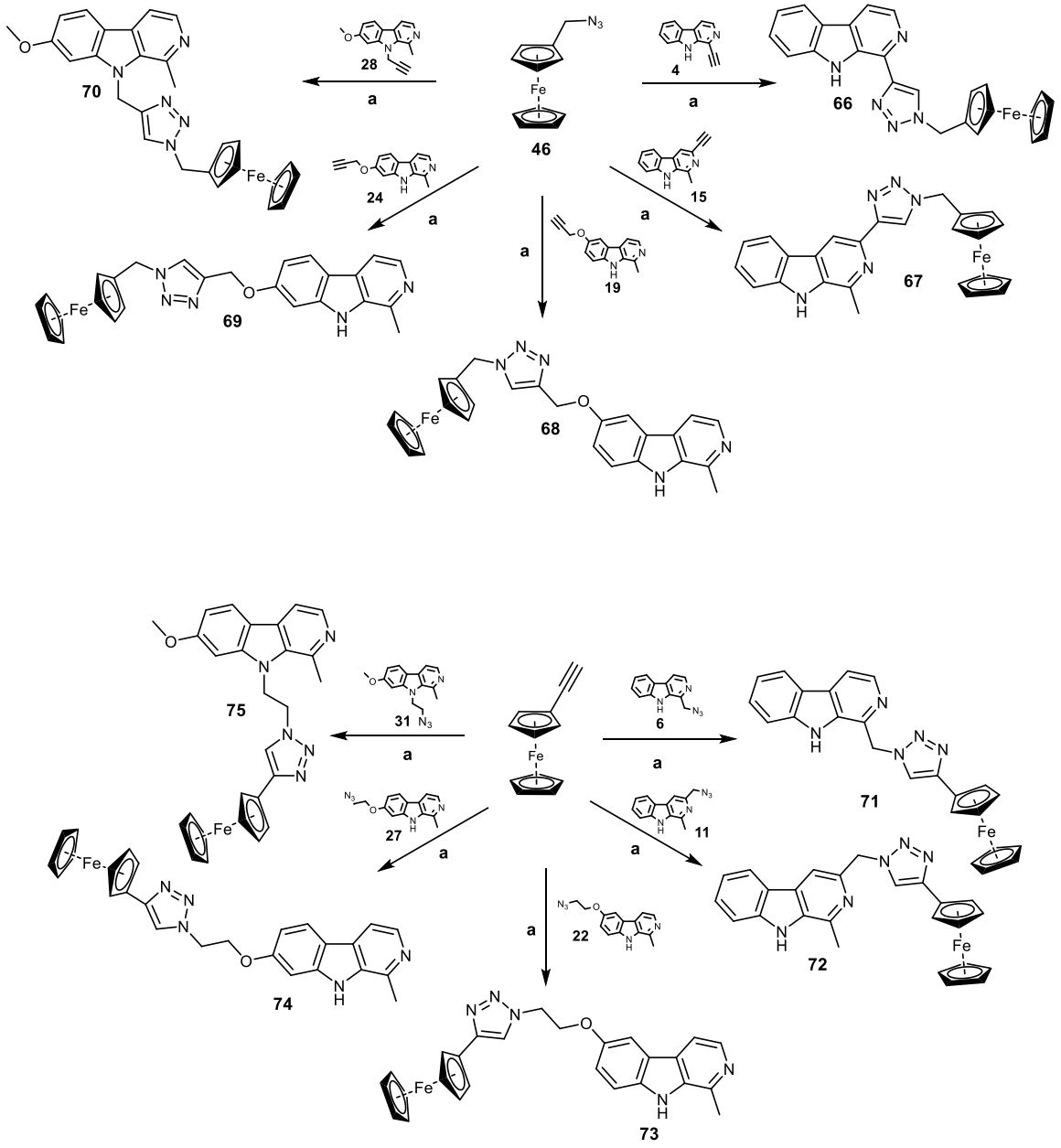

Shema 25. Sinteza harmicena TT
Reagensi i uvjeti: a) Na-askorbat, $CuSO_4 \times 5H_2O$, DMF/H_2O (2:1), s.t., 18 h.

Poput harmikina, harmiceni su pripravljeni u 5 položaja β-karbolinskog prstena, C-1, C-3, O-6, O-7 i N-9. Pripravljene su dvije serije spojeva, harmiceni TT **66**-**75** i harmiceni AT **76**-**83**. Unutar svake serije pripravljene su dvije podserije koje se razlikuju prema strukturi poveznice. Podserije harmicena TT **66**-**70** i harmicena AT **80**-**83** sadrže metilenski most između

triazola/amida i ferocena. S druge strane, podserije harmicena TT **71-75** i harmicena AT **76-79** sadrže triazol/amid izravno vezan za ferocenski prsten.

Harmiceni **66-70** pripravljeni su klik-reakcijom 1-azidometilferocena i β-karbolinskih alkina **4**, **15**, **19**, **24** i **28**, dok su harmiceni **71-75** pripravljeni klik-reakcijom etinilferocena i β-karbolinskih azida **6**, **11**, **22**, **27** i **31** (Shema 25). Istraženi su različiti načini provođenja klik-reakcija. Korištenje bakrovog(II) acetata u metanolu na s.t. rezultiralo je slabim napredovanjem reakcija uz veći broj nusprodukata. Grijanje reakcijske smjese u mikrovalnom reaktoru (50 °C, 1 h) nije imalo pozitivnog učinka na napredovanje reakcije i čistoću reakcijske smjese. Reakcije provedene pomoću natrijevog askorbata i $CuSO_4 \times 5H_2O$ u smjesi *tert*-butanola i vode (omjer 1:1) na s.t. napredovale su dobro, ali je reakcijska smjesa bila nečista. Korištenje istog prekatalizatora, uz promjenu otapala (smjesa DMF-a i vode, omjer 2:1) na s.t rezultiralo je uspješnom pripravom harmicena triazolskog tipa. Izolacija produkta uključivala je odsisavanje nastalog taloga/ekstrakciju te pročišćavanje kromatografijom na koloni uz dodatak sloja Al_2O_3 kako bi se uklonile zaostale bakrove soli. Iskorištenja reakcija bila su zadovoljavajuća (30–78 %).

Harmiceni AT **76-79** pripravljeni su reakcijom povezivanja ferocenkarboksilne kiseline i amina **7**, **12**, **26** i **30**, dok su harmicini **80-83** dobiveni reakcijom povezivanja ferocenoctene kiseline i istih amina (Shema 26). Reakcije su provedene korištenjem *coupling* reagensa HATU uz bazu DIEA u bezvodnom diklormetanu na s.t. tijekom 18 h. Analogno sintezi harmikina AT, ferocenkarboksilna, odnosno ferocenoctena kiselina dodane su u suvišku (1,1 ekvivalent) kako bi se povećao prinos reakcije te je korištena dvostruka količina DIEA (2,2 ekvivalenta) u odnosu na količinu karboksilne kiseline. Uspješno su pripravljeni derivati u položajima 1, 3, 7 i 9 β-karbolinskog prstena, dok priprava O-6 harmicena AT nije bila uspješna. Pokušaji optimiranja reakcijskih uvjeta, kao i provođenje sinteze preko drugih međuprodukata nije dalo željene rezultate. Harmiceni **76-79** izolirani su iz reakcijske smjese ekstrakcijom i pročišćeni kromatografijom na koloni uz pokretnu fazu diklormetan/aceton i rastrljavanjem u smjesi dietil-etera i petroletera. U pokretnoj fazi metanol je zamijenjen acetonom jer je primijećeno da tijekom kromatografije na koloni uz pokretnu fazu koja sadrži metanol dolazi do raspada spojeva. Harmicen **79** se istaložio iz reakcijske smjese te je odsisan, a ne ekstrahiran, i pročišćen kromatografijom na koloni uz pokretnu fazu diklormetan/aceton i rastrljavanjem u smjesi dietil-etera i petroletera. Zbog raspada tijekom pročišćavanja kromatografijom na koloni, harmiceni **80-83** pročišćeni su na drugačiji način. Spojevi **80** i **81** istaložili su se iz reakcijske smjese te su odsisani i prekristalizirani iz etanola, dok su spojevi **82** i **83** isprani zasićenom vodenom

otopinom NaCl i vodom, otapalo je upareno pod sniženim tlakom, a ostatak je rastrljan u smjesi dietil-etera i petroleter.

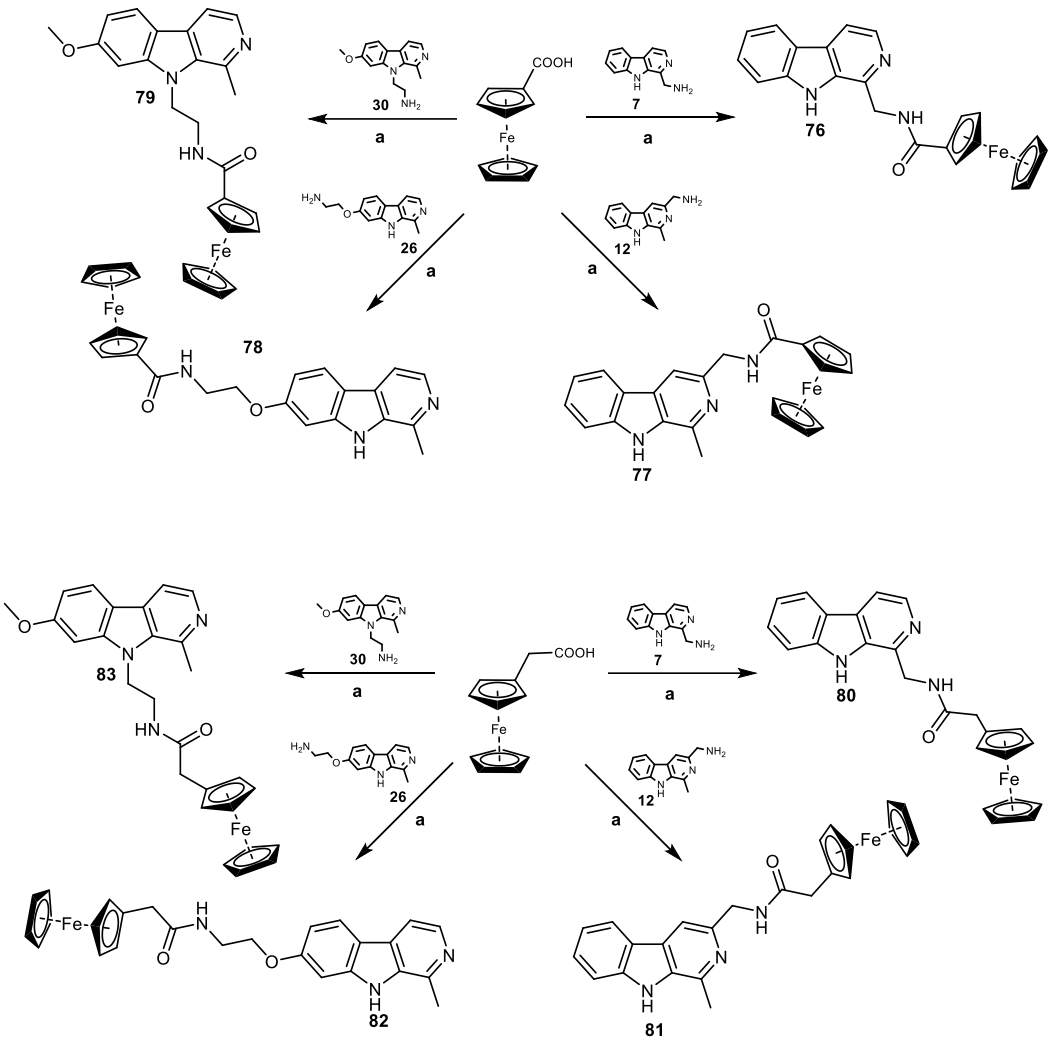

Shema 26. Sinteza harmicena AT
Reagensi i uvjeti: (a) HATU, DIEA, CH_2Cl_2, s.t., 18 h.

Pripravljeni su sljedeći spojevi:

- 1-(1-(ferocenilmetil)-1*H*-1,2,3-triazol-4-il)-9*H*-pirido[3,4-*b*]indol (**66**),
- 3-(1-(ferocenilmetil)-1*H*-1,2,3-triazol-4-il)-1-metil-9*H*-pirido[3,4-*b*]indol (**67**),
- 6-((1-(ferocenilmetil)-1*H*-1,2,3-triazol-4-il)metoksi)-1-metil-9*H*-pirido[3,4-*b*]indol (**68**),
- 7-((1-(ferocenilmetil)-1*H*-1,2,3-triazol-4-il)metoksi)-1-metil-9*H*-pirido[3,4-*b*]indol (**69**),
- 9-((1-(ferocenilmetil)-1*H*-1,2,3-triazol-4-il)metil)-7-metoksi-1-metil-9*H*-pirido[3,4-*b*]indol (**70**),
- 1-((4-ferocenil-1*H*-1,2,3-triazol-1-il)metil)-9*H*-pirido[3,4-*b*]indol (**71**),
- 3-((4-ferocenil-1*H*-1,2,3-triazol-1-il)metil)-1-metil-9*H*-pirido[3,4-*b*]indol (**72**),

- 6-(2-(4-ferocenil-1*H*-1,2,3-triazol-1-il)etoksi)-1-metil-9*H*-pirido[3,4-*b*]indol (**73**),
- 7-(2-(4-ferocenil-1*H*-1,2,3-triazol-1-il)etoksi)-1-metil-9*H*-pirido[3,4-*b*]indol (**74**),
- 9-(2-(4-ferocenil-1*H*-1,2,3-triazol-1-il)etil)-7-metoksi-1-metil-9*H*-pirido[3,4-*b*]indol (**75**),
- *N*-((9*H*-pirido[3,4-*b*]indol-1-il)metil)ferocenkarboksamid (**76**),
- *N*-((1-metil-9*H*-pirido[3,4-*b*]indol-3-il)metil)ferocenkarboksamid (**77**),
- *N*-(2-((1-metil-9*H*-pirido[3,4-*b*]indol-7-il)oksi)etil)ferocenkarboksamid (**78**),
- *N*-(2-(7-metoksi-1-metil-9*H*-pirido[3,4-*b*]indol-9-il)etil)ferocenkarboksamid (**79**),
- *N*-((9*H*-pirido[3,4-*b*]indol-1-il)metil)-2-ferocenilacetamid (**80**),
- 2-ferocenil-*N*-((1-metil-9*H*-pirido[3,4-b]indol-3-il)metil)acetamid (**81**),
- 2-ferocenil-*N*-(2-((1-metil-9*H*-pirido[3,4-b]indol-7-il)oksi)etil)acetamid (**82**),
- *N*-(2-(7-metoksi-1-metil-9*H*-pirido[3,4-*b*]indol-9-il)etil)-2-ferocenilacetamid (**83**).

Harmicini **66-83** su novi, do sada neopisani spojevi. Njihova sinteza i čistoća praćene su tankoslojnom kromatografijom, a strukture su potvrđene uobičajenim spektroskopskim metodama (IR, ^{1}H i ^{13}C NMR, MS). Analitički, spektrometrijski i spektroskopski podaci dani su u Tablicama 28-39.

U IR spektrima harmicena AT **76-83** vidljive su karakteristične vrpce za amidnu skupinu: u području 3470–3190 cm^{-1} vidljiva je vrpca N-H istezanja, dok su u rasponu 1620–1655 cm^{-1} vidljive dvije bliske vrpce koje odgovaraju C=O istezanju. U ^{1}H NMR spektru harmicena TT **66-75** vidljiv je CH signal triazola u području 8,2–8,8 ppm, dok ^{1}H NMR spektar harmicena AT **76-83** sadrži signal za proton NH skupine amida u području 8–8,60 ppm. U ^{13}C NMR spektrima spojeva **76-83** vidljiv je signal za karbonilni ugljik amida na ≈ 170 ppm. Dalje, NMR spektri svih harmicena sadrže signale karakteristične za protone/ugljike ferocenskog prstena: u ^{1}H NMR spektru u području 4-5 ppm vide se dva tripleta (supstituirani ciklopentadienilni prsten) i jedan singlet (nesupstituirani ciklopentadienilni prsten), dok ^{13}C NMR spekar otkriva tri signala (dva manja i jedan veći) u području 67–70 ppm. Kemijski pomaci drugih protona u ^{1}H, odnosno atoma ugljika u ^{13}C NMR spektrima spojeva u skladu su s predloženim strukturama. U MS spektrima svih harmicena vidi se pseudomolekulski ion.

Tablica 28. Analitički i MS podaci za harmicene **66-70**

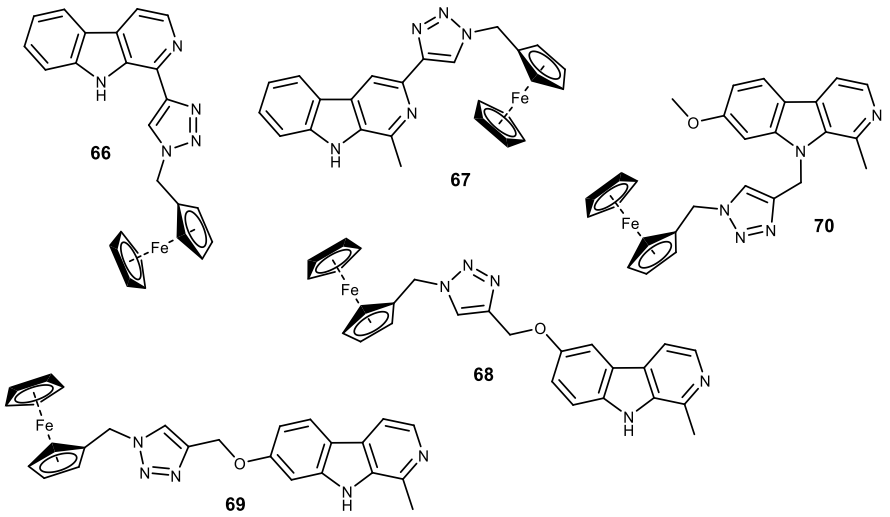

Spoj	Iskor. (%)	t_t (°C)	Molekulska Formula	M_r	MS (*m/z*)
66	51	229–230	$C_{24}H_{19}FeN_5$	433,30	434,1 $(M+1)^+$
67	45	183–186	$C_{25}H_{21}FeN_5$	447,32	447,9 $(M+1)^+$
68	68	244,5–248	$C_{26}H_{23}FeN_5O$	477,35	478,1 $(M+1)^+$
69	60	242–244	$C_{26}H_{23}FeN_5O$	477,35	478,1 $(M+1)^+$
70	30	187–190	$C_{27}H_{25}FeN_5O$	491,38	492,1 $(M+1)^+$

Tablica 29. IR podaci za harmicene **66-70**

Spoj	IR (ATR, ν_{max}/cm^{-1})
66	3385, 3172, 3105, 3065, 2991, 1625, 1576, 1489, 1452, 1437, 1419, 1351, 1314, 1282, 1254, 1239, 1152, 1103, 1000, 829, 807, 749, 629, 591, 548, 499, 479
67	3361, 2920, 2851, 1734, 1626, 1574, 1496, 1455, 1431, 1373, 1338, 1303, 1277, 1234, 1172, 1104, 1049, 1024, 1000, 924, 889, 818, 788, 775, 704, 631, 558, 584, 503, 478
68	3631, 3137, 3081, 2950, 1637, 1603, 1583, 1567, 1499, 1480, 1451, 1411, 1283, 1211, 1107, 1069, 1054, 1040, 1027, 849, 821, 765, 620, 504
69	3344, 3072, 2869, 2785, 1738, 1626, 1567, 1488, 1444, 1377, 1325, 1305, 1290, 1278, 1177, 1142, 1110, 1058, 1142, 1011, 965, 828, 813, 781, 661, 639, 598, 572, 505, 480
70	3135, 3090, 2929, 1709, 1623, 1564, 1499, 1449, 1408, 1325, 1252, 1227, 1193, 1174, 1106, 1042, 1000, 913, 815, 764, 732, 638, 596, 550, 481

Tablica 30. ^{1}H i ^{13}C NMR spketroskopski podaci za harmicene **66-70**

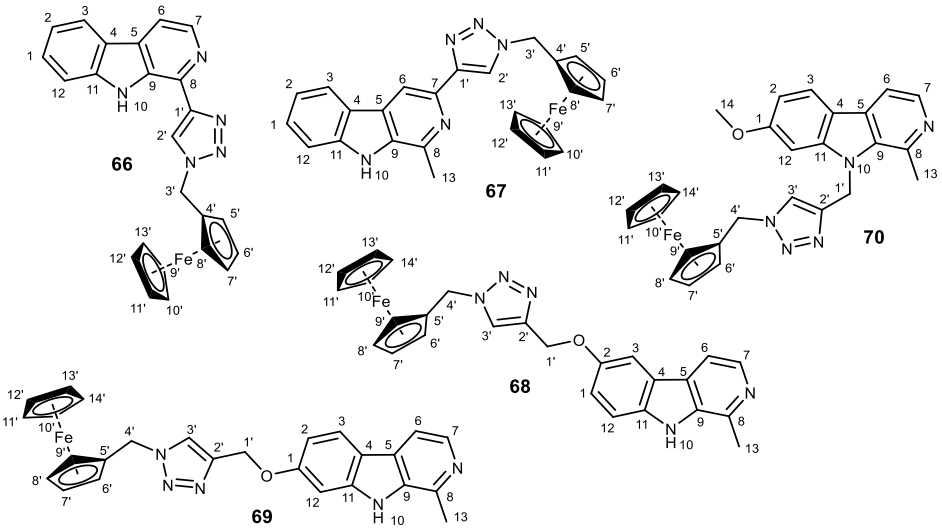

Spoj	^{1}H NMR (DMSO-d_6, δ ppm)	^{13}C NMR (DMSO-d_6, δ ppm)
66	11,53 (s, 1H, 10), 8,78 (s, 1H, 2'), 8,38 (d, 1H, 7, *J* = 5,2 Hz), 8,26–8,24 (m, 1H, 3), 8,11 (d, 1H, 6, *J* = 5,1 Hz), 7,91–7,90 (m, 1H, 12), 7,57–7,54 (m, 1H, 1), 7,27–7,25 (m, 1H, 2), 5,49 (s, 2H, 3'), 4,46 (t, 2H, 5', 8', *J* = 1,9 Hz), 4,24 (s, 5H, 9'–13'), 4,22 (t, 2H, 6', 7', *J* = 1,9 Hz)	147,60 (8), 141,15 (11), 137,83 (7), 133,68 (9), 131,74 (1'), 129,05 (4), 128,18 (2'), 122,94 (1), 121,47 (3), 120,40 (5), 119,51 (2), 114,11 (6), 113,23 (12), 82,36 (4'), 68,74 (5', 8'), 68,69 (9'-13'), 68,48 (6', 7'), 49,33 (3')
67	11,69 (s, 1H, 10), 8,58 (s, 1H, 2'), 8,41 (s, 1H, 6), 8,29 (d, 1H, 3, *J* = 7,9 Hz), 7,60 (d, 1H, 12, *J* = 8,1 Hz), 7,54 (t, 1H, 1, *J* = 7,6 Hz), 7,24 (t, 1H, 2, *J* = 7,4 Hz), 5,39 (s, 2H, 3'), 4,45 (t, 2H, 5', 8', *J* = 1,9 Hz), 4,23 (s, 5H, 9'–13'), 4,21 (t, 2H, 6', 7', *J* = 1,9 Hz), 2,80 (s, 3H, 13)	148,61 (7), 141,93 (11), 140,82 (8), 138,95 (9), 133,96 (1'), 128,02 (2'), 127,73 (4), 121,97 (1), 121,27 (5), 121,25 (3), 119,36 (2), 112,01 (6), 108,31 (12), 82,45 (4'), 68,86 (5, 8'), 68,68 (9'-13'), 68,44 (6',7'), 49,05 (3'), 20,48 (13)
68	11,37 (s, 1H, 10), 8,24 (s, 1H, 3'), 8,16 (d, 1H, 7, *J* = 5,3 Hz), 7,89–7,88 (m, 2H, 3, 6), 7,49 (d, 1H, 12, *J* = 8,8 Hz), 7,21 (dd, 1H, 1, *J* = 8,9, 2,5 Hz), 5,32 (s, 2H, 1'), 5,21 (s, 2H, 4'), 4,32 (t, 2H, 6', 9', *J* = 1,8 Hz), 4,16–4,14 (m, 7H, 7', 8', 10'–14'), 2,73 (s, 3H, 13)	151,88 (2), 142,95 (2'), 142,19 (8), 136,96 (7), 135,42 (11), 135,08 (9), 126,69 (4), 124,09 (3'), 121,34 (5), 118,39 (1), 112,73 (6), 112,67 (12), 105,20 (3), 82,49 (5'), 68,62 (10'-14'), 68,59 (6', 9'), 68,31 (7', 8'), 61,88 (1'), 48,92 (4'), 20,40 (13)
69	11,45 (s, 1H, 10), 8,23 (s, 1H, 3'), 8,15 (d, 1H, 7, *J* = 5,2 Hz), 8,05 (d, 1H, 3, *J* = 8,6 Hz), 7,80 (d, 1H, 6, *J* = 5,3 Hz), 7,16 (d, 1H, 12, *J* = 2,2 Hz), 6,89 (dd, 1H, 2, *J* = 8,7, 2,3 Hz), 5,33 (s, 2H, 1'), 5,25 (s, 2H, 4'), 4,34 (t, 2H, 6', 9', *J* = 1,9 Hz), 4,18–4,16 (m, 7H, 7', 8', 10'–14'), 2,72 (s, 3H, 13)	158,74 (1), 142,71 (8), 141,76 (2'), 141,33 (11), 137,74 (7), 134,58 (9), 127,13 (5), 124,15 (3'), 122,63 (3), 115,11 (4), 111,95 (6), 109,46 (2), 95,86 (12), 82,41 (5'), 68,66 (6', 9'), 68,64 (10'-14'), 68,36 (7', 8'), 61,45 (1'), 48,98 (4'), 20,32 (13)
70	8,16 (d, 1H, 7, *J* = 5,2 Hz), 8,07 (d, 1H, 3, *J* = 8,5 Hz), 7,98 (s, 1H, 3'), 7,86 (d, 1H, 6, *J* = 5,2 Hz), 7,32 (d, 1H, 12, *J* = 2,2 Hz), 6,87 (dd, 1H, 2, *J* = 8,5, 2,2 Hz), 5,86 (s, 2H, 1'), 5,21 (s, 2H, 4'), 4,23 (t, 2H, 6', 9', *J* = 1,8 Hz), 4,12 (t, 2H, 7', 8', *J* = 1,8 Hz), 4,06 (s, 5H, 10'–14'), 3,88 (s, 3H, 14), 3,03 (s, 3H, 13)	160,55 (1), 143,81 (2'), 142,67 (8), 141,13 (11), 138,05 (7), 134,66 (9), 128,54 (5), 122,55 (3'), 122,38 (3), 114,46 (4), 112,26 (6), 109,46 (2), 94,05 (12), 82,59 (5'), 68,54 (10'-14'), 68,44 (6', 9'), 68,21 (7', 8'), 55,62 (14), 48,77 (4'), 23,24 (13)

Tablica 31. Analitički i MS podaci za harmicene **71-75**

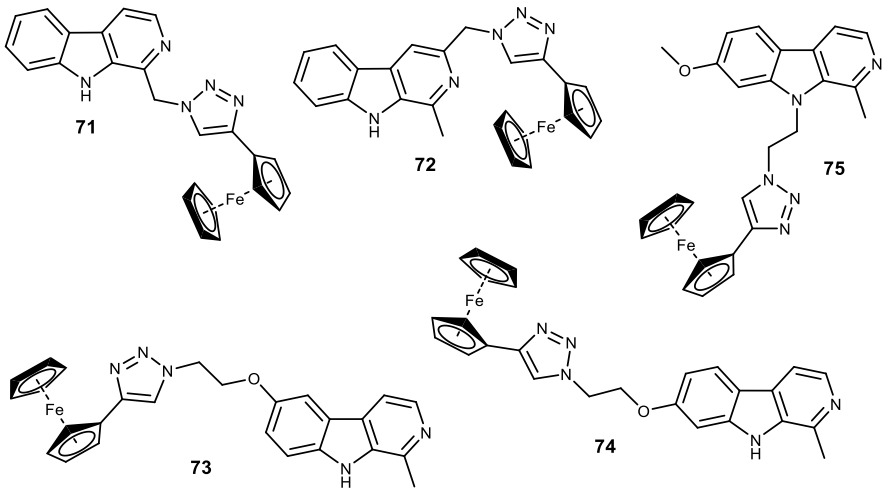

Spoj	Iskor. (%)	t_t (°C)	Molekulska Formula	M_r	MS (*m/z*)
71	78	252–255,5	$C_{24}H_{19}FeN_5$	433,30	434,9 $(M+1)^+$
72	62	242,5–244	$C_{25}H_{21}FeN_5$	447,32	448,9 $(M+1)^+$
73	37	201,5–204,0	$C_{26}H_{23}FeN_5O$	477,35	477,9 $(M+1)^+$
74	77	228,0–229,5	$C_{26}H_{23}FeN_5O$	477,35	477,9 $(M+1)^+$
75	63	218,0–220,0	$C_{27}H_{25}FeN_5O$	491,38	491,9 $(M+1)^+$

Tablica 32. IR podaci za harmicene **71-75**

Spoj	IR (ATR, ν_{max}/cm^{-1})
71	3249, 3138, 3094, 2987, 2953, 1625, 1585, 1567, 1497, 1455, 1430, 1389, 1321, 1236, 1212, 1189, 1094, 1058, 998, 875, 816, 794, 750, 730, 622, 592, 500
72	3148, 3101, 2993, 2891, 1737, 1627, 1566, 1506, 1456, 1443, 1351, 1328, 1251, 1219, 1086, 1057, 1019, 1000, 874, 815, 729, 680, 587, 506, 487
73	3133, 2949, 2872, 1583, 1568, 1497, 1458, 1286,1210, 1105, 1041, 988, 878, 818, 705, 621, 504
74	3125, 3077, 2959, 2850, 2772, 1623, 1566, 1443, 1426, 1301, 1278, 1240, 1185, 1108, 1053, 1042, 977, 874, 822, 810, 743, 720, 693, 638, 587, 570, 522, 513, 495, 483
75	2968, 1621, 1565, 1445, 1404, 1339, 1253, 1222, 1158, 1182, 1136, 1096, 1041, 1021, 970, 929, 877, 821, 807, 641, 590, 545, 501, 475

Tablica 33. ^{1}H i ^{13}C NMR spektroskopski podaci za harmicene **71-75**

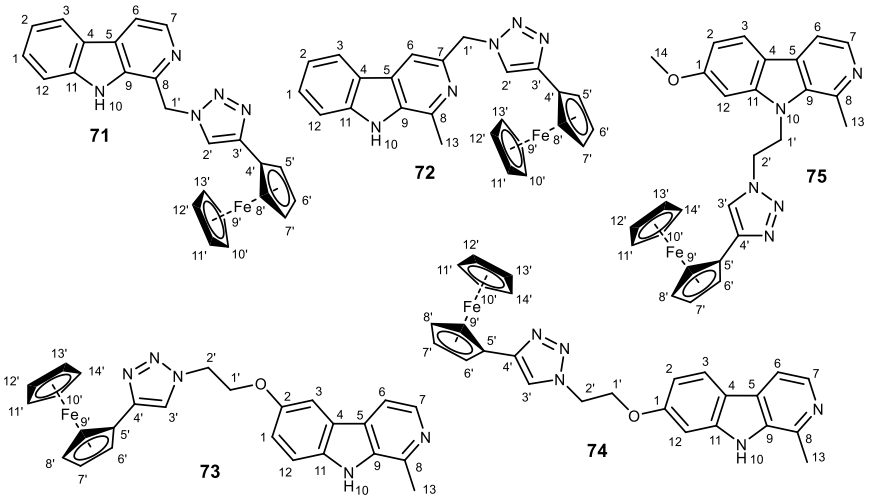

Spoj	^{1}H NMR (DMSO-d_6, δ ppm)	^{13}C NMR (DMSO-d_6, δ ppm)
71	11,95 (s, 1H, 10), 8,31 (d, 1H, 7, *J* = 5,2 Hz), 8,28–8,26 (m, 2H, 3, 2'), 8,13 (d, 1H, 6, *J* = 5,1 Hz), 7,70–7,68 (m, 1H, 12), 7,61–7,59 (m, 1H, 1), 7,30–7,27 (m, 1H, 2), 6,08 (s, 2H, 1'), 4,73 (t, 2H, 5', 8', *J* = 1,9 Hz), 4,28 (t, 2H, 6', 7', *J* = 1,8 Hz), 4,03 (s, 5H, 9'–13')	145,22 (8), 140,71 (11), 138,17 (3'), 137,86 (7), 133,85 (9), 128,71 (5), 128,54 (2'), 121,91 (3), 121,57 (1), 120,76 (4), 119,64 (2), 114,82 (6), 112,09 (12), 76,04 (4'), 69,23 (9'-13'), 68,21 (5', 8'), 66,34 (6', 7'), 51,24 (1')
72	11,66 (s, 1H, 10), 8,23 (s, 1H, 6), 8,16 (d, 1H, 3, *J* = 7,9 Hz), 7,90 (s, 1H, 2'), 7,60–7,59 (m, 1H, 12), 7,55–7,52 (m, 1H, 1), 7,24–7,21 (m, 1H, 2), 5,76 (s, 2H, 1'), 4,74 (t, 2H, 5', 8', *J* = 1,9 Hz), 4,29 (t, 2H, 6', 7', *J* = 1,9 Hz), 4,03 (s, 5H, 9'–13'), 2,76 (s, 3H, 13)	145,37 (8), 142,95 (7), 142,05 (11), 140,77 (3'), 133,94 (9), 128,08 (2'), 127,63 (5), 121,64 (3), 121,06 (1), 120,91 (4), 119,44 (2), 112,09 (6), 111,42 (12), 76,09 (4'), 69,26 (9'-13'), 68,21 (5', 8'), 66,32 (6', 7'), 55,10 (1'), 20,38 (13)
73	11,39 (s, 1H, 10), 8,29 (s, 1H, 3'), 8,15 (d, 1H, 7, *J* = 5,3 Hz), 7,87 (d, 1H, 6, *J* = 5,3 Hz), 7,78 (d, 1H, 3, *J* = 2,5 Hz), 7,48 (d, 1H, 12, *J* = 8,8 Hz), 7,16 (dd, 1H, 1, *J* = 8,8, 2,5 Hz), 4,82 (t, 2H, 1', *J* = 5,1 Hz), 4,73 (t, 2H, 6', 9', *J* = 1,9 Hz), 4,53 (t, 2H, 2', *J* = 5,2 Hz), 4,30 (t, 2H, 7', 8', *J* = 1,8 Hz), 4,01 (s, 5H, 10'–14'), 2,72 (s, 3H, 13)	151,85 (2), 145,24 (8), 142,24 (4'), 136,98 (7), 135,52 (11), 135,10 (9), 126,63 (4), 121,35 (5), 121,28 (3'), 118,14 (1), 112,77 (6), 112,64 (12), 105,13 (3), 76,05 (5'), 69,22 (10'-14'), 68,21 (6', 9'), 67,14 (1'), 66,34 (7', 8'), 49,24 (2'), 20,40 (13)
74	11,44 (s, 1H, 10), 8,30 (s, 1H, 3'), 8,14 (d, 1H, 7, *J* = 5,3 Hz), 8,05 (d, 1H, 3, *J* = 8,6 Hz), 7,79 (d, 1H, 6, *J* = 5,3 Hz), 7,03 (d, 1H, 12, *J* = 2,2 Hz), 6,85 (dd, 1H, 2, *J* = 8,6, 2,2 Hz), 4,83 (t, 2H, 1', *J* = 5,1 Hz), 4,73 (t, 2H, 6', 9', *J* = 1,9 Hz), 4,55 (t, 2H, 2', *J* = 5,1 Hz), 4,30 (t, 2H, 7', 8', *J* = 1,8 Hz), 4,01 (s, 5H, 10'–14'), 2,72 (s, 3H, 13)	158,62 (1), 145,25 (8), 141,72 (4'), 141,35 (11), 137,76 (7), 134,59 (9), 127,07 (5), 122,71 (3'), 121,34 (3), 115,33 (4), 111,98 (6), 109,17 (2), 95,73 (12), 76,01 (5'), 69,23 (10'-14'), 68,22 (6', 9'), 66,57 (1'), 66,35 (7', 8'), 49,09 (2'), 20,36 (13)
75	8,17 (d, 1H, 7, *J* = 5,2 Hz), 8,04 (d, 1H, 3, *J* = 8,5 Hz), 7,88 (d, 1H, 6, *J* = 5,2 Hz), 7,80 (s, 1H, 3'), 6,84–6,78 (m, 2H, 2, 12), 5,08 (t, 2H, 1', *J* = 5,6 Hz), 4,88 (t, 2H, 2', *J* = 5,6 Hz), 4,49 (t, 2H, 6', 9', *J* = 1,9 Hz), 4,22 (t, 2H, 7', 8', *J* = 1,9 Hz), 3,86–3,85 (m, 8H, 14, 10'–14'), 2,90 (s, 3H, 13)	160,51 (1), 145,15 (4'), 142,76 (8), 140,67 (11), 138,12 (7), 134,68 (9), 128,73 (4), 122,23 (3'), 121,79 (3), 114,10 (5), 112,26 (6), 109,81 (2), 92,93 (12), 75,78 (5'), 68,09 (10'-14'), 68,06 (6', 9'), 66,26 (7', 8'), 55,37 (14), 49,71 (1'), 44,47 (2'), 23,18 (13)

Tablica 34. Analitički i MS podaci za harmicene **76-79**

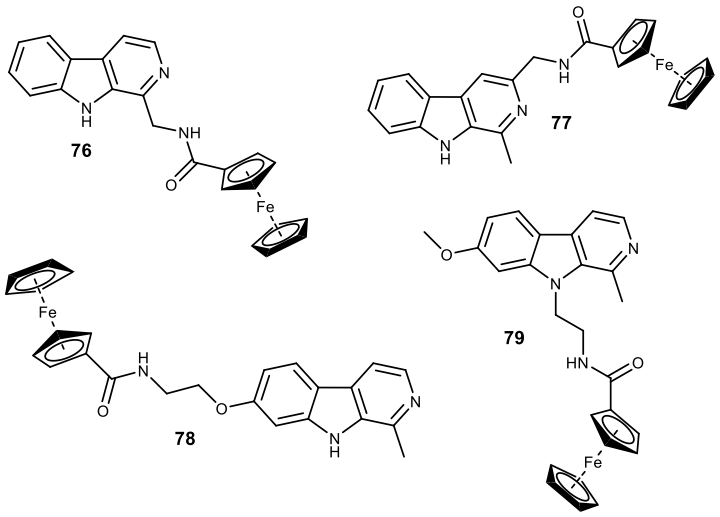

Spoj	Iskor. (%)	t_t (°C)	Molekulska formula	M_r	MS (*m/z*)
76	48	210–213	$C_{23}H_{19}FeN_3O$	409,27	410,0 (M+1)
77	39	240,5–243	$C_{24}H_{21}FeN_3O$	423,30	424,0 (M+1)
78	42	243–245,5	$C_{25}H_{23}FeN_3O_2$	453,32	454,0 (M+1)
79	50	225–227	$C_{26}H_{25}FeN_3O_2$	467,35	468,1 (M+1)

Tablica 35. IR podaci za harmicine **76-79**

Spoj	IR (ATR, ν_{max}/cm^{-1})
76	3623, 3467, 3085, 3050, 2962, 2928, 1711, 1649, 1622, 1531, 1503, 1444, 1408, 1375, 1340, 1300, 1249, 1229, 1195, 138, 1123, 1106, 1041, 1017, 914, 819, 801, 634, 598, 558
77	3324, 3226, 1634, 1574, 1532, 1498, 1447, 1380, 1348, 1297, 1248, 1104, 1026, 901, 814, 755, 738, 629, 528, 482
78	3216, 1716, 1622, 1551, 1451, 1422, 1376, 1312, 1278, 1236, 1217, 1105, 960, 842, 801, 741, 641, 605, 505,476
79	3623, 3467, 3085, 3050, 2962, 2928, 1711, 1649, 1622, 1531, 1503, 1444, 1408, 1375, 1340, 1300, 1249, 1229, 1195, 1177, 1138, 1123, 1107, 1041, 1016, 914, 819, 801, 634, 598, 558

Tablica 36. ^{1}H i ^{13}C NMR spketroskopski podaci za harmicene **76-79**

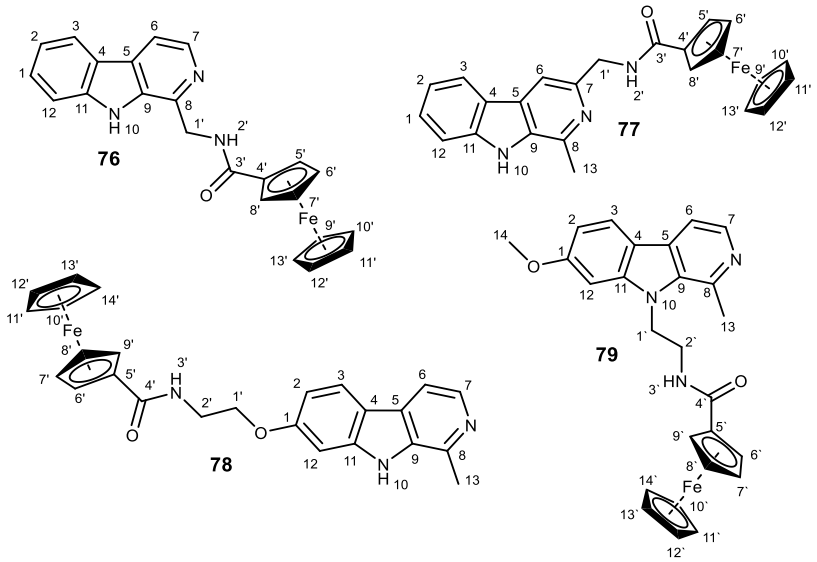

Spoj	^{1}H NMR (DMSO-d_6, δ ppm)	^{13}C NMR (DMSO-d_6, δ ppm)
76	11,49 (s, 1H, 10), 8,58 (t, 1H, 2', *J* = 6,0 Hz), 8,31 (d, 1H, 7, *J* = 5,2 Hz), 8,23 (d, 1H, 3, *J* = 7,8 Hz), 8,05 (d, 1H, 6, *J* = 5,2 Hz), 7,68 (d, 1H, 12, *J* = 8,2 Hz), 7,56 (t, 1H, 1, *J* = 7,6 Hz), 7,25 (t, 1H, 2, *J* = 7,5 Hz), 4,88–4,87 (m, 4H, 1', 5', 8'), 4,35 (t, 2H, 6', 7', *J* = 1,9 Hz), 4,07 (s, 5H, 9'–13')	169,83 (3'), 142,64 (8), 140,17 (11), 137,35 (7), 133,55 (9), 128,10 (3), 127,74 (5), 121,74 (1), 120,93 (4), 119,37 (2), 113,86 (6), 111,99 (12), 76,11 (4'), 70,10 (5', 8'), 69,31 (9'-13'), 68,30 (6', 7'), 41,73 (1')
77	11,51 (s, 1H, 10), 8,47 (t, 1H, 2', *J* = 6,1 Hz), 8,12 (d, 1H, 3, *J* = 7,9 Hz), 7,89 (s, 1H, 6), 7,57 (d, 1H, 12, *J* = 8,2 Hz), 7,52–7,48 (m, 1H, 1), 7,21–7,17 (m, 1H, 2), 4,90 (t, 2H, 5', 8', *J* = 1,9 Hz), 4,60 (d, 2H, 1', *J* = 6,0 Hz), 4,37 (t, 2H, 6', 7', *J* = 1,9 Hz), 4,20 (s, 5H, 9'–13'), 2,78 (s, 3H, 13)	168,94 (3'), 147,17 (7), 141,14 (8), 140,76 (11), 133,49 (9), 127,78 (3), 127,66 (5), 121,35 (1), 120,95 (4), 119,16 (2), 111,98 (12), 109,47 (6), 76,73 (4'), 69,96 (5', 8'), 69,25 (9'-13'), 68,28 (6', 7'), 44,31 (1'), 20,27 (13)
78	11,41 (s, 1H, 10), 8,14 (d, 1H, 7, *J* = 5,3 Hz,), 8,07–8,05 (m, 2H, 3', 3), 7,79 (d, 1H, 6, *J* = 5,3 Hz), 7,07 (d, 1H, 12, *J* = 2,4 Hz), 6,90 (dd, 1H, 2, *J* = 8,7, 2,2 Hz), 4,83 (t, 2H, 6', 9', *J* = 2,0 Hz), 4,35 (t, 2H, 7', 8', *J* = 1,9 Hz), 4,23 (t, 2H, 1', *J* = 5,7 Hz), 4,13 (s, 5H, 10'–14'), 3,63 (q, 2H, 2', *J* = 5,7 Hz), 2,71 (s, 3H, 13)	169,36 (4'), 159,31 (1), 141,89 (8), 141,28 (11), 137,74 (7), 134,55 (9), 127,17 (5), 122,69 (3), 114,98 (4), 111,93 (6), 109,22 (2), 95,38 (12), 76,31 (5'), 70,01 (6', 9'), 69,40 (10'-14'), 68,22 (7', 8'), 66,40 (1'), 38,49 (2'), 20,33 (13)
79	8,17 (d, 1H, 7, *J* = 5,1 Hz), 8,10–8,07 (m, 2H, 3, 3'), 7,88 (d, 1H, 6, *J* = 5,1 Hz), 7,32 (d, 1H, 12, *J* = 2,2 Hz), 6,88 (dd, 1H, 2, *J* = 8,5, 2,1 Hz), 4,69 (t, 2H, 6', 9', *J* = 1,9 Hz), 4,66 (t, 2H, 1', *J* = 7,1 Hz), 4,34 (t, 2H, 7', 8', *J* = 1,9 Hz), 4,07 (s, 5H, 10'–14'), 3,91 (s, 3H, 14), 3,60 (q, 2H, 2', *J* = 6,7 Hz), 3,04 (s, 3H, 13)	169,75 (4'), 160,52 (1), 143,00 (8), 140,66 (11), 137,82 (7), 134,67 (9), 128,43 (5), 122,39 (3), 114,28 (4), 112,26 (6), 109,20 (2), 93,78 (12), 76,40 (5'), 69,93 (6', 9'), 69,32 (10'-14'), 68,08 (7', 8'), 55,50 (14), 43,56 (1'), 39,10 (2'), 23,14 (13)

Tablica 37. Analitički i MS podaci za harmicene **80-83**

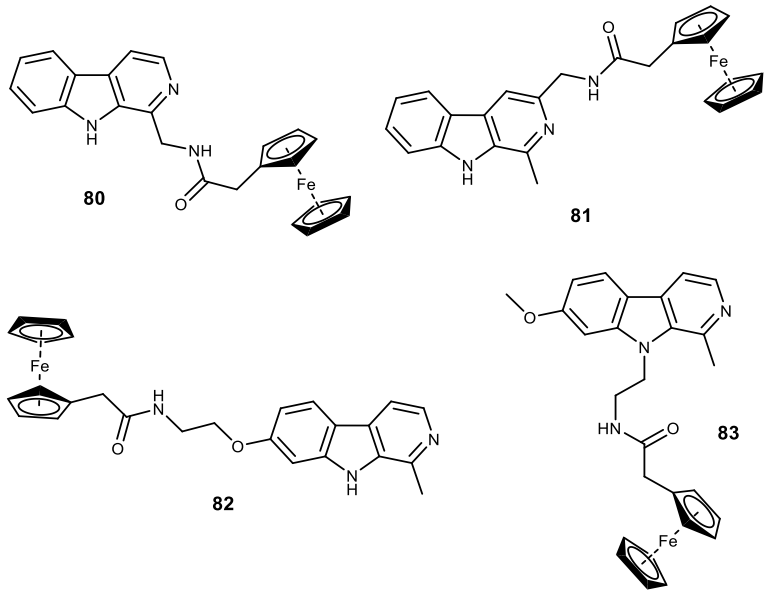

Spoj	Iskor. (%)	t_t (°C)	Molekulska formula	M_r	MS (*m/z*)
80	34	222,0–224,5	$C_{24}H_{21}FeN_3O$	423,30	424,1 $(M+1)^+$
81	39	247,5–250,0	$C_{25}H_{23}FeN_3O$	437,32	438,0 $(M+1)^+$
82	58	176,0–177,5	$C_{26}H_{25}FeN_3O_2$	467,35	468,1 $(M+1)^+$
83	69	170,5–172,0	$C_{27}H_{27}FeN_3O_2$	481,38	482,2 $(M+1)^+$

Tablica 38. IR podaci za harmicene **80-83**

Spoj	IR (ATR, ν_{max}/cm^{-1})
80	3333, 3219, 3168, 3099, 2995, 2898, 1651, 1568, 1521, 1502, 1445, 1436, 1413, 1361, 1321, 1285, 1248, 1151, 1106, 1045, 1026, 999, 878, 820, 740, 677, 595, 564, 504
81	3404, 3191, 3081, 2944, 1649, 1621, 1570, 1522, 1471, 1455, 1421, 1312, 1247, 1267, 1136, 1103, 1038, 1023, 997, 925, 826, 803, 753, 741, 693, 621, 584, 543, 500, 482
82	3222, 3055, 2875, 1656, 1630, 1539, 1484, 1434, 1378, 1324, 1299, 1273, 1238, 1174, 1134, 1106, 1073, 1037, 1023, 1002, 961, 924, 871, 814, 776, 738, 661, 634, 590, 567, 484
83	3341, 2931, 1655, 1624, 1566, 1503, 1451, 1439, 1410, 1347, 1330, 1300, 1251, 1195, 1172, 1141, 1104, 1048, 1024, 929, 835, 813, 794, 639, 567, 496, 482

Tablica 39. ^{1}H i^{13}C NMR spektroskopski podaci za harmicene **80-83**

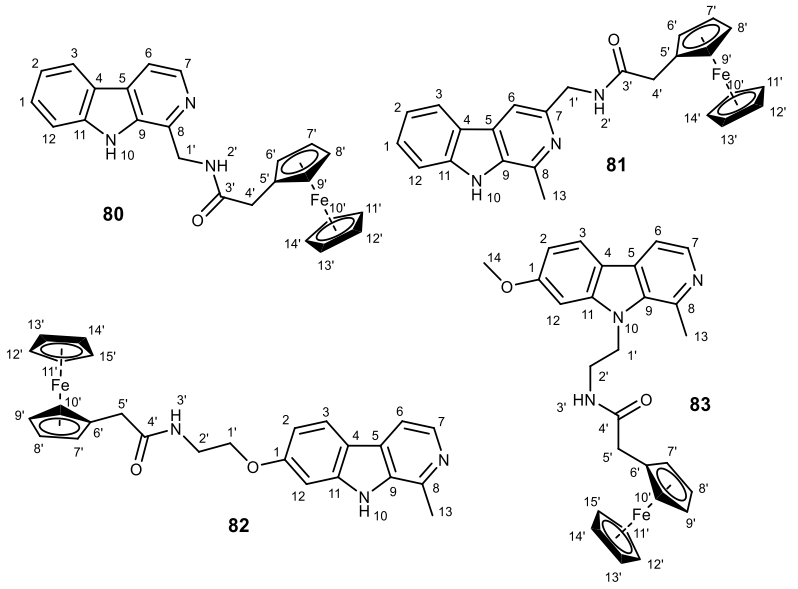

Spoj	^{1}H NMR (DMSO-d_6, δ ppm)	^{13}C NMR (DMSO-d_6, δ ppm)
80	11,50 (s, 1H, 10), 8,55 (t, 1H, 2', *J* = 5,4 Hz), 8,29 (d, 1H, 7, *J* = 5,2 Hz), 8,22 (d, 1H, 3, *J* = 7,8 Hz), 8,04 (d, 1H, 6, *J* = 5,2 Hz), 7,63 (d, 1H, 12, *J* = 8,2 Hz), 7,55 (t, 1H, 1, *J* = 7,6 Hz), 7,25 (t, 1H, 2, *J* = 7,4 Hz), 4,76 (d, 2H, 1', *J* = 5,4 Hz), 4,22 (t, 2H, 6', 9', *J* = 1,9 Hz), 4,05 (m, 7H, 7', 8', 10'–14'), 3,26 (s, 2H, 4')	170,47 (3'), 141,60 (8), 140,36 (11), 137,36 (7), 133,50 (9), 128,12 (3), 127,74 (5), 121,73 (1), 120,87 (4), 119,39 (2), 113,89 (6), 112,05 (12), 82,66 (5'), 68,58 (6', 9'), 68,41 (10'-14'), 67,11 (7', 8'), 41,52 (1'), 36,33 (4')
81	11,48 (s, 1H, 10), 8,42 (t, 1H, 2', *J* = 5,9 Hz), 8,10 (d, 1H, 3, *J* = 7,8 Hz), 7,73 (s, 1H, 6), 7,56 (d, 1H, 12, *J* = 8,2 Hz), 7,52–7,50 (m, 1H, 1), 7,21 (t, 1H, 2, *J* = 7,4 Hz), 4,46 (d, 2H, 1', *J* = 5,8 Hz), 4,27 (t, 2H, 6', 9', *J* = 1,9 Hz), 4,12 (s, 5H, 10'–14'), 4,10 (t, 2H, 7', 8', *J* = 1,9 Hz), 3,24 (s, 2H, 4'), 2,73 (s, 3H, 13)	169,93 (3'), 146,33 (7), 141,16 (8), 140,71 (11), 133,44 (9), 127,78 (3), 127,66 (5), 121,49 (1), 120,98 (4), 119,11 (2), 111,94 (12), 109,54 (6), 83,05 (5'), 68,63 (6', 9'), 68,45 (10'-14'), 67,15 (7', 8'), 44,28 (1'), 36,72 (4'), 20,28 (13)
82	11,40 (s, 1H, 10), 8,19 (t, 1H, 3', *J* = 5,5 Hz), 8,14 (d, 1H, 7, *J* = 5,3 Hz), 8,05 (d, 1H, 3, *J* = 8,6 Hz), 7,80 (d, 1H, 6, *J* = 5,3 Hz), 7,02 (d, 1H, 12, *J* = 2,2 Hz), 6,85 (dd, 1H, 2, *J* = 8,6, 2,2 Hz), 4,20 (t, 2H, 7', 10', *J* = 1,9 Hz), 4,13 (t, 2H, 1', *J* = 5,5 Hz), 4,11 (s, 5H, 11'–15'), 4,05 (t, 2H, 8', 9', *J* = 1,9 Hz), 3,51 (q, 2H, 2', *J* = 5,6 Hz), 3,16 (s, 2H, 5'), 2,72 (s, 3H, 13)	170,25 (4'), 159,17 (1), 141,84 (8), 141,29 (11), 137,75 (7), 134,56 (9), 127,16 (5), 122,63 (3), 115,00 (4), 111,93 (6), 109,30 (2), 95,40 (12), 82,72 (6'), 68,50 (7', 10'), 68,43 (11'-15'), 67,08 (8', 9'), 66,55 (1'), 38,40 (2'), 36,37 (5'), 20,35 (13)
83	8,17 (d, 1H, 7, *J* = 5,1 Hz), 8,09 (d, 1H, 3, *J* = 8,6 Hz), 8,01 (t, 1H, 3', *J* = 6,0 Hz), 7,88 (d, 1H, 6, *J* = 5,1 Hz), 7,27 (d, 1H, 12, *J* = 2,2 Hz), 6,89 (dd, 1H, 2, *J* = 8,6, 2,2 Hz), 4,57 (t, 2H, 1', *J* = 7,1 Hz), 4,13 (t, 2H, 7', 10', *J* = 1,9 Hz), 4,11 (s, 5H, 11'–15'), 4,05 (t, 2H, 8', 9', *J* = 1,8 Hz), 3,92 (s, 3H, 14), 3,45 (q, 2H, 2', *J* = 6,7 Hz), 3,07 (s, 2H, 5'), 2,95 (s, 3H, 13)	170,58 (4'), 160,52 (1), 142,86 (8), 140,61 (11), 137,80 (7), 134,64 (9), 128,43 (5), 122,40 (3), 114,31 (4), 112,25 (6), 109,24 (2), 93,64 (12), 82,12 (6'), 68,72 (7', 10'), 68,46 (11'-15'), 67,21 (8', 9'), 55,52 (14), 43,37 (1'), 38,73 (2'), 36,65 (5'), 23,08 (13)

4.2. FIZIKALNO-KEMIJSKA SVOJSTVA HIBRIDNIH DERIVATA HARMINA POŽELJNA ZA LJEKOVITE TVARI

Bitan korak u procesu dizajniranja i razvoja novih lijekova je određivanje fizikalno-kemijskih svojstava molekula kandidata na temelju kojih je moguće procijeniti svojstva poželjna za ljekovite tvari (engl. *drug-like properties* ili *drug-likeness*). Ovim pristupom može se u ranoj fazi razvoja lijeka izvršiti probir molekula, čime se skraćuje vrijeme i smanjuju troškovi istraživanja (215, 216).

Važno svojstvo poželjno za ljekovite tvari je oralna bioraspoloživost. Za procjenu oralne bioraspoloživosti predložena su različita pravila (2). Lipinski i suradnici su na temelju analize spojeva iz baze podataka Svjetskog indeksa lijekova (*World Drugs Index*) definirali 4 kriterija (temeljena na fizikalno-kemijskim svojstvima) koja molekula mora zadovoljiti da bi bila oralno aktivna. Kriteriji su poznatiji kao Lipinskijevo pravilo 5 jer su svi brojevi u tom pravilu višekratnici broja 5: relativna molekulska masa ljekovite tvari mora biti manja od 500, molekula ne smije sadržavati više od 5 donora vodikovih veza, molekula ne smije sadržavati više od 10 akceptora vodikovih veza, izračunata vrijednost log *P* mora biti manja od 5. Ukoliko molekula zadovoljava barem tri navedena kriterija izgledno je da će pokazati dobru oralnu bioraspoloživost (216–218).

Veber i suradnici su 2002. godine pokazali da fleksibilnost molekule (mjerena brojem veza u molekuli koje mogu slobodno rotirati) ima važnu ulogu u oralnoj bioraspoloživosti. Što je molekula fleksibilnija, vjerojatnije je da će oralna bioraspoloživost biti slabija. Također, zaključili su da se u procjeni oralne bioraspoloživosti zona polarne površine molekule (TPSA) može koristiti umjesto broja skupina koje mogu tvoriti vodikove veze. Predložili su sljedeće kriterije za procjenu: molekula ne smije sadržavati više od 10 veza koje mogu rotirati i TPSA ne smije biti veća od 140 Å ili molekula ne smije imati više od 10 veza koje mogu rotirati te ne smije imati više od 12 donora i akceptora vodikovih veza ukupno (219). Gelovanijeva pravila pak zahtijevaju da je molarna refraktivnost (MR) između 40 i 130 cm^3/mol, TPSA manja od 140 $Å^2$ te broj atoma u molekuli od 20 do 70 (220).

Harmicinima i harmikinima su korištenjem programa *Chemicalize.org* (221) određena sljedeća fizikalno-kemijska svojstva: broj atoma, relativna molekulska masa, log *P*, broj donora vodikove veze, broj akceptora vodikove veze, broj rotirajućih veza, molarna refraktivnost te zona polarne površine. Podaci su dani u Tablici 40.

Tablica 40. Fizikalno-kemijska svojstva harmicina i harmikina

Spoj	Broj atoma	M_r	log*P*[a]	DVV[b]	AVV[c]	Lipinskijeva pravila[d]	RV[e]	MR[f] (cm^3/mol)	TPSA[g] ($Å^2$)
47a	50	409,45	4,07	1	4	4	7	128,53	85,69
47b	50	427,44	4,22	1	4	4	7	128,74	85,69
47c	50	488,35	4,84	1	4	4	7	136,15	85,69
47d	50	443,89	4,68	1	4	4	7	133,33	85,69
47e	54	439,48	3,92	1	5	4	8	134,99	94,92
48a	53	423,48	4,21	1	4	4	7	133,12	85,69
48b	53	441,47	4,35	1	4	4	7	133,34	85,69
48c	53	502,37	4,97	1	4	3	7	140,74	85,69
48d	53	457,92	4,81	1	4	4	7	137,92	85,69
48e	57	453,50	4,05	1	5	4	8	139,58	94,92
49a	51	395,47	4,03	1	4	4	6	128,65	68,62
49b	51	413,46	4,18	1	4	4	6	128,87	68,62
49c	51	474,36	4,80	1	4	4	6	136,27	68,62
49d	51	429,91	4,64	1	4	4	6	133,46	68,62
49e	55	425,49	3,88	1	5	4	7	135,12	77,85
50a	54	409,49	3,73	1	4	4	6	133,38	68,76
50c	54	488,39	4,50	1	4	4	6	141	68,76
50d	54	443,94	4,33	1	4	4	6	138,18	68,76
50e	58	439,52	3,57	1	5	4	7	139,84	77,99
51	49	440,89	4,14	1	5	4	5	131,95	81,51
52	52	454,92	4,27	1	5	4	5	136,54	81,51
53	49	440,89	4,12	1	5	4	4	121,91	81,51
54	49	440,89	4,12	1	5	4	4	121,91	81,51
55	52	454,92	4,34	0	5	4	4	126,8	70,65
56	57	483,96	3,74	2	6	4	7	146,73	93,54
57	57	483,96	3,74	2	6	4	7	146,73	93,54
58	60	497,99	3,96	1	6	4	7	151,63	82,68
59	48	415,88	2,81	3	4	4	6	117,13	82,7
60	51	429,91	2,94	3	4	4	6	121,72	82,7
61	55	459,93	2,78	3	5	4	8	128,18	91,93
62	55	459,93	2,78	3	5	4	8	128,18	91,93
63	58	473,96	3,00	2	5	4	8	133,08	81,07
64	61	487,99	3,24	2	5	4	9	137,78	81,07
65	67	516,04	3,82	2	5	3	11	147,29	81,07

[a] log *P* – particijski koeficijent; [b] DVV – broj donora vodikove veze; [c] AVV – broj akceptora vodikove veze; [d] broj zadovoljenih Lipinskijevih kriterija (od četiri); [e] RV – broj rotirajućih veza; [f] MR – molarna refraktivnost; [g] TPSA – zona polarne površine.

Svojstva poželjna za ljekovite tvari procijenjena su s obzirom na Lipinskijeva, Veberova i Gelovanijeva pravila. Gotovo svi harmicini i harmikini zadovoljavaju 4/4 Lipinskijeva kriterija. Izuzetak su harmicin **48c** i harmikin **65** koji zadovoljavaju 3/4 Lipinskijeva kriterija jer je njihova M_r veća od 500. Svi hibridi, osim harmikina **65**, zadovoljavaju Veberova pravila.

Harmikin **65** blago odstupa od kriterija fleksibilnosti (ima 11 rotirajućih veza). Svi hibridi zadovoljavaju dva Gelovanijeva pravila vezana uz TPSA i broj atoma. Treće Gelovanijevo pravilo (MR u rasponu 40–130 cm^3/mol) zadovoljavaju harmicini **47a,b** i **49a,b** te harmikini **53-55** i **59-62**. Ostali hibridi blago odstupaju od tog pravila, osim harmikina **56-58** i **65** kod kojih su odstupanja značajnija. Temeljem prethodnih spoznaja, može se predvidjeti dobra oralna bioraspoloživost harmicina i harmikina.

Dalje, harmicinima **48c** i **49c** te harmikinu **51**, koji su pokazali dobro i selektivno antiproliferativno djelovanje te harmikinima **63** i **65**, koji su pokazali izuzetna antimalarijska djelovanja na eritrocitu fazu životnog ciklusa plazmodija, detaljnije su analizirana farmakokinetička svojstva (gastro-intestinalna apsorpcija, prolazak krvno-moždane barijere, supstrat P-glikoproteina, inhibicija CYP enzima, prolazak kroz *stratum corneum*) korištenjem programa *SwissADME* (222) (Tablica 41). P-glikoprotein je transmembranski protein koji izbacuje kesenobiotike iz stanice. U tumorskim stanicama izaziva rezistenciju na različite citostatike zbog čega je važno u ranoj fazi razvoj lijeka odrediti je li molekula od interesa supstrat ovog proteina. Na temelju podataka može se zaključiti da svi analizirani spojevi, osim derivata **48c**, imaju slična farmakokinetička svojstva: dobru apsorpciju iz GIT-a, ne prolaze KMB-u, supstrati su P-glikoproteina i potencijalni inhibitori CYP enzima. Derivat **48c** se razlikuje od ostalih analiziranih spojeva u tome što nije potencijalni suspstrat P-glikoproteina i inhibitor CYP1A2 i CYP2D6 enzima.

Tablica 41. Farmakokinetička svojstva odabranih spojeva

Spoj	**48c**	**49c**	**51**	**63**	**65**
GIT apsorpcija[a]	visoka	visoka	visoka	visoka	visoka
KMB prolazak[b]	–	–	–	–	–
Supstrat P-glikoproteina	–	+	+	+	+
CYP1A2 inhibitor[c]	–	+	+	+	+
CYP2C19 inhibitor	+	+	+	+	+
CYP2C9 inhibitor	+	+	+	+	+
CYP2D6 inhibitor	–	+	+	+	+
CYP3A4 inhibitor	+	+	+	+	+
log K_p (cm/s)[d]	–6,09	–5,71	–6,07	–6,00	–5,82

[a] GIT- gastrointestinalni trakt; [b] KMB – krvno-moždana barijera; [c] CYP – citokrom P450 enzim; [d] log K_p – koeficijent propusnost otopljene tvari kroz *stratum corneum*.

4.3. BIOLOŠKO DJELOVANJE HARMICINA, HARMIKINA I HARMICENA

4.3.1. ANTIPROLIFERATIVNO DJELOVANJE

Kako bi se dobio uvid u protutumorski potencijal hibridnih derivata harmina, ispitano je njihovo antiproliferativno djelovanje na 4 humane tumorske stanične linije: MCF-7, HepG2, HCT116 i SW620. Dodatno, djelovanje hibrida ispitano je na jednoj netumorskoj humanoj staničnoj liniji (Hek293T) kako bi se procijenila njihova selektivnost. Kao pozitivne kontrole u ispitivanjima korišteni su 5-FU i harmin. Vijabilnost stanica određena je MTT testom. IC_{50} vrijednost određena je za one spojeve koji su pri najvišoj ispitivanoj koncentraciji (50 μM) pokazali smanjenje vijabilnosti za najmanje 50 %. Dobiveni rezultati prikazani su u Tablici 42.

U seriji harmicina najsnažnije djelovanje ostvarili su O-6-supstituirani harmicini **49**, između kojih se posebno istaknuo derivat **49c**. Najjači učinak imali su protiv MCF-7 i HCT116 staničnih linija (IC_{50} vrijednosti < 10 μM), osim spoja **49e**, čiji je učinak na staničnu liniju HCT116 bio slabiji. Na MCF-7 staničnu liniju djelovali su jače od harmina i 5-FU. Djelovanje ovih spojeva na Hek293T staničnu liniju bilo je slabo, što ukazuje na selektivnost njihovog djelovanja (Tablica 42). Spoj **49c** ostvario je visoke indekse selektivnosti prema MCF-7 (SI = 8,8) i HCT 116 (SI = 10,6).

Nasuprot tome, C-1-, C-3- i N-9-supstituirani harmicini (**47**, **48** i **50**) nisu značajno inhibirali rast humanih tumorskih stanica, osim spoja **48c** koji je imao izraženo djelovanje na staničnu liniju MCF-7 (IC_{50} = 8,5 ± 0,6 μM, SI > 5,9) te spoja **50c** koji je umjereno, ali selektivno inhibirao rast MCF-7 i HepG2 staničnih linija (Tablica 42).

Zanimljivo je da su u svim podserijama harmicina, osim podserije **47** koja je općenito bila neaktivna, najsnažnije djelovanje pokazali *m*-Br-supstituirani derivati (**48c**, **49c**, **50c**) koji su ujedno bili i najlipofilniji. Ipak, vidljivo je da položaj supstituenta na β-karbolinskom prstenu ima veći utjecaj na antiproliferativno djelovanje od vrste i položaja supstituenta na fenilnom prstenu cimetnog dijela molekule.

Tablica 42. *In vitro* antiproliferativno djelovanje harmicina, harmikina i harmicena na humane tumorske stanične linije s izračunatim indeksima selektivnosti

Spoj	S/P[a]	IC_{50}[b] (μM)					SI[c]	
		MCF-7	HepG2	HCT116	SW620	Hek293T	MCF-7	HCT116
47a	C-1/T	33,1 ± 4,5	> 50	44,1 ± 4,1	> 50	30,1 ± 4,33	0,9	0,7
47b		> 50	> 50	> 50	17,6 ± 2,1	> 50	> 1	> 1
47c		> 50	> 50	> 50	> 50	> 50	> 1	> 1
47d		> 50	> 50	> 50	> 50	> 50	> 1	> 1
47e		21,8 ± 2,9	> 50	> 50	> 50	> 50	> 2,3	> 1
48a	C-3/T	> 50	> 50	> 50	> 50	> 50	> 1	> 1
48b		25,2 ± 4,2	> 50	22,9 ± 0,9	> 50	> 50	> 2	> 2,2
48c		8,5 ± 0,6	> 50	19,8 ± 1,4	20,8 ± 3,1	> 50	> 5,9	> 2,5
48d		18,2 ± 0,5	> 50	20,8 ± 1,7	22,9 ± 1,3	23,7 ± 2	1,3	1,1
48e		> 50	> 50	> 50	> 50	27,4 ± 2,2	< 0,5	< 0,5
49a	O-6/T	8,4 ± 0,4	12,1 ± 2,8	7,8 ± 1,4	18,9 ± 0,6	39 ± 1,5	4,6	5
49b		8,9 ± 0,4	14,6 ± 1,3	3,6 ± 0,9	> 50	31,4 ± 1,7	3,5	8,7
49c		4,3 ± 0,1	15,3 ± 2,2	3,6 ± 0,7	17,1 ± 1,5	38 ± 3,6	8,8	10,6
49d		8,2 ± 0,8	14,3 ± 1	3,7 ± 1	17,5 ± 2.3	17,9 ± 2,1	2,2	4,8
49e		5,6 ± 0,3	15 ± 1,2	36,5 ± 7,7	27,3 ± 0.9	23,8 ± 2,8	4,3	0,7
50a	N-9/T	> 50	> 50	> 50	> 50	> 50	> 1	> 1
50c		12,6 ± 2	15,8 ± 1,3	> 50	> 50	34,9 ± 2,5	2,8	< 0,7
50d		> 50	> 50	> 50	> 50	> 50	> 1	> 1
50e		35,9 ± 0,9	> 50	> 50	> 50	> 50	> 1,4	> 1
51	C-1/T	> 50	>50	12,7 ± 1	> 50	> 50	> 1	> 3,9
52	C-3/T	> 50	> 50	> 50	> 50	> 50	> 1	> 1
53	O-6/T	21,2 ± 0,4	27,6 ± 2,9	12,9 ± 0,7	> 50	> 50	> 2,4	> 3,9
54	O-7/T	1,6 ± 0,1	10 ± 1,6	2 ± 0,1	8,2 ± 0,3	5,7 ± 0,1	3,6	2,9
55	N-9/T	13,1 ± 0,1	38,2 ± 4,6	7,7 ± 0,4	> 50	10,6 ± 0,7	0,8	1,4
56	O-6/T	12,4 ± 0,5	22,8 ± 2,7	4,6 ± 0,2	7,1 ± 0,3	16,2 ± 0,6	1,3	3,5
57	O-7/T	1,9 ± 0,3	4,2 ± 1,5	2,8 ± 0,6	3,4 ± 0,2	4,6 ± 0,4	2,4	1,6
58	N-9/T	13 ± 1,3	19,3 ± 2,0	12,8 ± 0,9	18,1 ± 0,3	26,1 ± 0,4	2	2
59	C-1/A	7,1 ± 0,2	13,7 ± 1,6	7,4 ± 0,4	11,2 ± 1,4	22,7 ± 0,5	3,2	3,1
60	C-3/A	6,2 ± 0,6	16,2 ± 1,4	6 ± 0,5	10,5 ± 0,8	6,2 ± 0,5	1	1
61	O-6/A	> 50	> 50	> 50	> 50	> 50	> 1	> 1
62	O-7/A	10,8 ± 0,8	17,4 ± 1,7	7,3 ± 0,4	9,4 ± 0,6	12,3 ± 1,7	1,1	1,7

63	N-9/A	7,7 ± 0,2	21 ± 2,7	5,1 ± 0,2	3,3 ± 0,5	11,8 ± 1,1	1,5	2,3
64	N-9/A	6,8 ± 0,1	14,8 ± 2,1	6 ± 0,3	6,3 ± 0,2	7,4 ± 0,7	1,1	1,2
65	N-9/A	> 50	33,2 ± 2,5	7,2 ± 0,3	> 50	11,1 ± 1,2	< 0,2	1,5
66	C-1/T	> 50	> 50	7,6 ± 0,5	23,1 ± 6,4	> 50	> 1	> 6,6
67	C-3/T	3,7 ± 0,2	12,3 ± 5	35,2 ± 4,7	3,8 ± 0,4	46,5 ± 1	12,6	1,3
68	O-6/T	6,8 ± 0,2	17 ± 0,3	> 50	8,1 ± 0,2	43 ± 8,6	6,3	< 0,9
69	O-7/T	> 50	> 50	7,4 ± 0,4	> 50	> 50	> 1	> 6,8
70	N-9/T	> 50	> 50	14,6 ± 3,7	> 50	> 50	> 1	> 3,4
71	C-1/T	39,4 ± 7,9	43,9 ± 1,1	29,4 ± 4,6	> 50	> 50	> 1,3	> 1,7
72	C-3/T	17,7 ± 0,6	> 50	8,3 ± 1,4	19,7 ± 1,9	> 50	> 2,8	> 6
73	O-6/T	6,9 ± 0,5	8,4 ± 0,9	9 ± 0,7	6,5 ± 0,7	7,3 ± 2,8	1,1	0,8
74	O-7/T	8,0 ± 0,2	9,5 ± 0,5	38,6 ± 2,8	7,6 ± 0,1	17,1 ± 1,8	2,1	0,4
75	N-9/T	> 50	> 50	> 50	> 50	> 50	> 1	> 1
76	C-1/A	8,5 ± 1,5	> 50	16,8 ± 0,9	45,1 ± 3,7	> 50	> 5,9	> 3
77	C-3/A	19,9 ± 1,1	> 50	> 50	> 50	> 50	> 2,5	> 1
78	O-7/A	9,1 ± 1,4	15,6 ± 0,3	6,6 ± 0,8	9,9 ± 4	18,6 ± 0,2	2	2,8
79	N-9/A	30,5 ± 13,2	> 50	16,3 ± 3,2	> 50	> 50	> 1,6	> 3,1
80	C-1/A	> 50	> 50	> 50	> 50	> 50	> 1	> 1
81	C-3/A	36,9 ± 6,8	> 50	20,9 ± 1,5	25 ± 8,1	> 50	> 1,4	> 2,4
82	O-7/A	4,5 ± 0,3	7,4 ± 0,5	5,9 ± 1,3	4,2 ± 0,3	8,4 ± 0,3	1,9	1,4
83	N-9/A	13,2 ± 0,5	28 ± 2,5	7,5 ± 0,4	9,9 ± 1,1	30,8 ± 2,4	2,3	4,1
HAR[d]		13,5 ± 1,1	18,7 ± 0,8	4 ± 0,8	4,7 ± 0,6	12,6 ± 0,8	0,9	3,2
5-FU[e]		23,9 ± 5,9	5,5 ± 0,6	5,2 ± 2,8	9,4 ± 0,3	8,1 ± 0,8	0,3	1,6

[a] S/P – položaj supstitucije na β-karbolinskom prstenu/tip poveznice (T – triazol, A – amid); [b] IC_{50} – koncentracija spoja koja inhibira rast stanica za 50 %; [c] SI – indeks selektivnosti; [d] HAR – harmin; [e] 5-FU – 5-fluorouracil.

U usporedbi s harmicinima, harmikini su ispoljili značajno snažnije, ali uglavnom neselektivno antiproliferativno djelovanje na ispitane humane stanične linije (učinak harmikina na HepG2 i Hek293T bio je nešto slabiji) (Tablica 42). Uspoređeno je djelovanje harmikina unutar pojedine podserije, kao i djelovanje harmikina TT i AT u pojedinim položajima β-karbolinskog prstena.

Između harmikina TT antiproliferativno djelovanje je s obzirom na položaj supstitucije β-karbolinskog prstena opadalo prema obrascu: O-7 > N-9 > O-6 > C-1 > C-3. O-7-supstituirani derivati **54** i **57**, koji se razlikuju u duljini poveznice, ostvarili su najsnažnije antiproliferativno djelovanje u ovoj seriji spojeva (IC_{50} vrijednosti ≤ 10 μM). S druge strane, C-1- i C-3-supstituirani derivati **51** i **52** koji u položaju 4 kinolinskog prstena nisu imali amino, već etersku skupinu bili su neaktivni u najvećoj ispitivanoj koncentraciji, osim spoja **51** koji je umjereno, ali selektivno djelovao na HCT-116 (SI > 3,9). Zanimljiv je utjecaj duljine poveznice na antiproliferativno djelovanje. U slučaju O-7-supstituiranih derivata **54** i **57** vidljivo je da duljina poveznice ne utječe na djelovanje (oba derivata djelovala su podjednako snažno). Nasuprot tome, O-6-supstituirani derivat **56** koji je imao dužu poveznicu djelovao je snažnije od analoga, derivata **53** koji je imao triazol izravno vezan za kinolinski prsten. Potonji je umjereno, ali selektivno djelovao na MCF-7, HepG2 i HCT116.

Harmikini AT najsnažnije su djelovali na HCT116 (IC_{50} < 10 μM), osim spoja **61** (O-6 harmikin) koji nije bio učinkovit prema svim ispitivanim staničnim linijama u najvišoj koncentraciji. Moguće je da je zbog slabe topljivosti i taloženja u staničnom mediju njegovo antiproliferativno djelovanje izostalo. Amidi **60**, **63** i **64** pokazali su snažno antiproliferativno djelovanje na sve ispitivane stanične linije, osim na HepG2 na koju je učinak bio slabiji. Između amida u položaju N-9, derivat **65** s najduljom poveznicom ostvario je slabije djelovanje ili je bio neaktivan u odnosu na analoge s kraćom poveznicom što je posebno vidljivo u slučaju MCF-7, HepG2 i SW620 staničnih linija.

Usporedbom podserija vidljivo je da su C-1 i C-3 amidi (**59** i **60**) ostvarili snažnije djelovanje od triazolskih analoga supstituiranih u tim položajima (spojevi **51** i **53**). S druge strane, O-7-supstituirani triazoli **54** i **57** ostvarili su jače djelovanje od O-7-supstituiranog amida **62**. N-9-supstituirani amidi **63** i **64** pokazali su snažnije ili usporedljivo djelovanje u odnosu na N-9-supstituirane triazole **55** i **58**.

Harmiceni su pokazali dobro djelovanje humane tumorske stanične linije, između kojih su najosjetljivije bile MCF-7, HCT116 i SW620 (7 od 18 spojeva djelovalo je na ove stanične linije u niskim mikromolarnim vrijednostima). Najslabiji učinak imali su na HepG2 (samo su 3

od 18 spojeva djelovali na ovu staničnu liniju u niskim mikromolarnim vrijednostima). Harmiceni su na Hek293T djelovali slabo što upućuje na selektivnost njihovog djelovanja. Najsnažnije djelovanje pokazali su O-6-supstituirani triazol **73** i O-7-supstituirani amid **82**. O-7- i N-9-supstituirani amidi (**78**, **79**, **82**, **83**) djelovali su snažnije od triazolskih derivata supstituiranih u istim položajima. Nasuprot tome, C-1- i C-3-supstituirani triazoli (**66**, **67**, **71**, **72**) pokazali su blago snažnije antiproliferativno djelovanje od analognih amida. C-1-, O-7- i N-9-supstituirani triazoli (**66**, **69**, **70**) koji sadrže metilenski most između triazola i ferocena ostvarili su selektivno djelovanje na HCT116 (SI(**66**) > 6,6, SI(**69**) > 6,8, SI(**70**) > 3,4), dok njihovi analozi u čijoj strukturi su triazolski i ferocenski prsten izravno vezani nisu djelovali selektivno. Štoviše, spoj **74** slabo je djelovao na HCT116, dok je pokazao snažan citotoksični učinak prema ostalim ispitivanim staničnim linijama. S druge strane, C-3-supstituirani amid u čijoj strukturi su triazol i ferocen izravno vezani (**77**) djelovao je umjereno, ali selektivno na MCF-7 (SI > 2,5). Njegov analog, spoj **81** koji sadrži metilenski most, nije pokazao selektivnost. Može se zaključiti da prisutnost metilenskog mosta između triazola i ferocena, ovisno o vrsti poveznice, utječe na selektivnost harmicena. N-9-supstituirani triazol **75** i C-1-supstituirani amid **80** bili su neaktivni prema svim ispitivanim staničnim linijama u najvećoj ispitivanoj koncentraciji.

Kako bi se dobio uvid u mogući mehanizam djelovanja, harmicinima i harmicenima, hibridima harmina koje bi bilo poželjno razvijati kao potencijalne protutumorske lijekove, ispitana je lokalizacija u stanici. Na temelju rezultata antiproliferativnog djelovanja za ispitivanje su odabrani harmicin **49c**, koji je bio citotoksičan prema svim ispitivanim staničnim linijama, te harmiceni **69** (selektivan prema HCT116) i **82** (citotoksičan prema svim ispitivanim staničnim linijama), a u pokusu je korištena MCF-7 stanična linija. Sposobnost fluorescencije spojeva iskorištena je kako bi se pratila njihova lokalizacija u stanici korištenjem fluorescentnog mikroskopa. Analizom kontrole (netretirane stanice) nije uočena autofluorescencija. Utvrđeno da harmicin **49c** stvara točkasta obojenja u citoplazmi stanice (Slika 61a), ali ne i u staničnoj jezgri što isključuje interakciju s molekulom DNA kao potencijalni mehanizam djelovanja. Nasuprot tome, harmicen **69** izazvao je bojanje citoplazme te točkasta obojenja u jezgri što potvrđuje njegov ulazak jezgru (Slika 61b). U stanicama tretiranim harmicenom **82** uočeno je bojanje citoplazme, dok je fluorescencija jezgre bila slabije izražena. Zbog tehničkih ograničenja i spektralnih karakteristika ovog spoja nismo mogli optimirati uvjete pokusa te ne možemo sa sigurnošću donijeti zaključak o lokalizaciji spoja unutar stanice. Istraživanje detaljnog mehanizma protutumorskog djelovanja harmicina i harmicena prelazi okvire ovog doktorskog rada.

a)

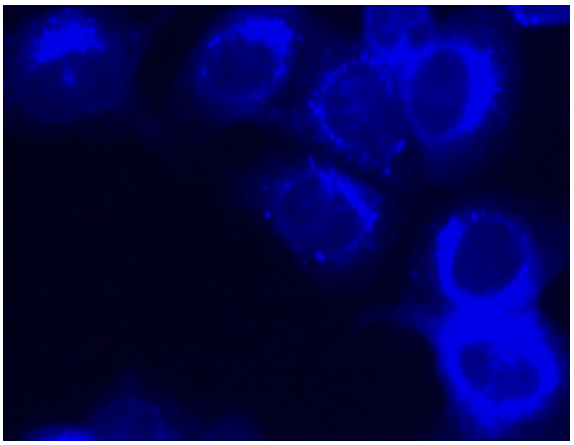

b)

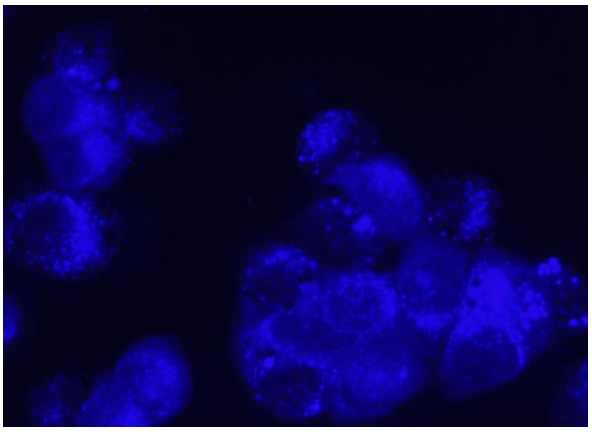

Slika 61. Unutarstanična lokalizacija: a) harmicina **49c**, b) harmicena **69** (povećanje 400 ×)

4.3.2. ANTIMALARIJSKO DJELOVANJE

Antimalarijsko djelovanje harmicina, harmikina i harmicena ispitano je na eritrocitnoj i hepatocitnoj fazi životnog ciklusa plazmodija.

4.3.2.1. Djelovanje na eritrocitnu fazu životnog ciklusa plazmodija

Djelovanje hibrida na eritrocitnu fazu ispitano je na dva soja *P. falciparum*: 3D7 i Dd2. Iznimno, antimalarijsko djelovanje odabranih harmikina ispitano je na dva multirezistentna soja: *Pf*K1 (soj otporan na CQ, pirimetamin i sulfadoksin, porijeklom iz Tajlanda) i *Pf*7G8 (soj otporan na CQ i pirimetamin, porijeklom iz Brazila). Rezultati antimalarijskog djelovanja harmicina, harmikina i harmicena na eritrocitu fazu životnog ciklusa plazmodija dani su Tablicama 43 i 46. Usporedbom djelovanja sve tri skupine spojeva, došli smo do zaključka da harmikini imaju najbolje antimalarijsko djelovanje, potom harmiceni te harmicini.

4.3.2.1.1. Harmikini

Djelovanje harmikina na eritrocitnu fazu životnog ciklusa plazmodija ispitano je u dva ciklusa (Tablica 43). Prvo je ispitan njihov učinak na *Pf*3D7 i *Pf*Dd2, dok je u drugom ciklusu ispitano djelovanje hibrida s IC_{50} (*Pf*3D7) < 100 nM na multirezistentne sojeve *Pf*K1 i *Pf*7G8, osim spoja **64**, koji nije bio dostupan, i derivata **59**, koji je dao nekonzistentne rezultate te je izostavljen iz analize. Strukturna raznolikost pripremljenih spojeva omogućila je donošenje nekoliko zaključaka vezanih uz SAR:

1) Harmikini AT i većina harmikina TT djelovala je snažnije od polaznog spoja, harmina. Primjerice, harmikin AT **63** imao je 3 reda veličine jači učinak na *Pf*3D7 od harmina.
2) Optimalni položaj za supstituciju β-karbolinskog prstena je N-9. Spojevi **58** i **63** (najučinkovitiji protiv *Pf*3D7) te **63** i **65** (najučinkovitiji protiv *Pf*Dd2) su N-9-supstituirani derivati.
3) Općenito, harmikini AT pokazali su snažnije djelovanje od harmikina TT protiv svih ispitanih sojeva *P. falciparum*.
4) U strukturi poveznice važna je amino skupina izravno vezana za klorkinolinski prsten. Harmikini koji ne sadrže amino skupinu (**53-55**) ostvarili su slabije djelovanje, dok su

derivati u čijoj strukturi je amino skupina zamijenjena eterskom (**51** i **52**) bili neaktivni.

Tablica 43. *In vitro* antiplazmodijsko djelovanje harmikina na eritrocitnu fazu životnog ciklusa plazmodija

Spoj	S/P[a]	IC_{50}[b] (nM)			
		***Pf*3D7**	***Pf*Dd2**	***Pf*K1**	***Pf*7G8**
51	C-1/T	> 28000	> 27777,8	n.o.[c]	n.o.
52	C-3/T	10841,4 ± 2569,4	5418,4 ± 552	n.o.	n.o.
53	O-6/T	3660,3 ± 370,4	7110,3 ± 2496,9	n.o.	n.o.
54	O-7/T	95,8 ± 1,7	202,7 ± 28,5	299,1 ± 102,7	195,0 ± 43,3
55	N-9/T	899,2 ± 106,9	1816,4 ± 350,3	n.o.	n.o.
56	O-6/T	65,7 ± 3,4	160,4 ± 44,0	140,6 ± 14,2	143,8 ± 105,5
57	O-7/T	57,3 ± 1,2	76,2 ± 14,4	33,5 ± 4,9	44,2 ± 6,0
58	N-9/T	11,6 ± 3,8	204,5 ± 9,9	163,2 ± 78,5	28,6 ± 5,3
59	C-1/A	54,0 ± 15,8	170,7 ± 2,5	n.o.	n.o.
60	C-3/A	13 ± 3,1	46,1 ± 3,9	48,8 ± 19,6	28,2 ± 2,7
61	O-6/A	303,4 ± 61,3	535,4 ± 131,9	n.o.	n.o.
62	O-7/A	234,4 ± 25,7	309,3 ± 61,9	n.o.	n.o.
63	N-9/A	2 ± 0,3	16,2 ± 2,83	24,8 ± 1,3	7,4 ± 1,3
64	N-9/A	19,0 ± 5,1	54,8 ± 9	n.o.	n.o.
65	N-9/A	34,6 ± 1,2	15,5 ± 0,9	20,2 ± 5,2	6,0 ± 0,3
CQ[c]		11 ± 3	364,2 ± 70,2	392,1 ± 39,5	220,3 ± 23,0
HAR		8250 ± 2830	>27777,8	n.o.	n. o.

[a] S/P – položaj supstitucije na β-karbolinskom/tip poveznice (T – triazol, A – amid);[b] IC_{50} – koncentracija spoja koja inhibira rast plazmodija za 50 %; [c] CQ – klorokin; [d] HAR - harmin

Uz nekoliko iznimaka, soj *Pf*3D7 bio je najosjetljiviji (IC_{50} vrijednosti 9 od 15 spojeva bile su niže od 100 nM). Spoj koji je djelovao najsnažnije, harmikin AT **63**, pokazao je 5,5 puta jače djelovanje od CQ (IC_{50} = 2 ± 0,3 nM). Harmikin TT **58** (IC_{50} = 11,6 ± 3,8 nM) i harmikin AT **60** (IC_{50} = 13 ± 3,1 nM) ostvarili su djelovanja usporediva s CQ (IC_{50} = 11 ± 3 nM). Važno je istaći da je većina harmikina snažno djelovala na rezistenente sojeve što potvrđuju izračunati indeksi rezistencije prikazani u Tablici 44. Učinak 10 od 15 harmikina na *Pf*Dd2 te 7 od 15 na *Pf*K1 i *Pf*7G8 bio je jači u odnosu na CQ. Najizraženije djelovanje imao je harmikin **65** koji se pokazao učinkovitijim protiv rezistentnih sojeva *P. falciparum* nego protiv soja *Pf*3D7 (36,7

puta jače djelovanje od CQ protiv *Pf*7G8, IC_{50} = 6,0 ± 0,3 nM). Harmikin **63** pokazao je 22,5 puta snažnije djelovanje na *Pf*Dd2, 15,9 puta jače na *Pf*K1 i 29,8 puta jače na *Pf*7G8 u odnosu na CQ. Zanimljiva je usporedba harmikina AT i TT koji su ostvarili najslabije djelovanje. Među harmikinima AT, O-6 i O-7 derivati (**61** i **62**) pokazali su dva reda veličine slabije djelovanje od harmikina **63**. S druge strane, u podseriji harmikina TT najslabije su djelovali C-1 (**51**) i C-3 (**52**) hibridi. Većina spojeva nije pokazala križnu rezistenciju sa sojevima otpornim na CQ pokazujući da zadržavaju istu aktivnost protiv sojeva osjetljivih i otpornih na CQ.

Tablica 44. Indeksi rezistencije harmikina

Spoj	**RI** [a]		
	IC_{50}(*Pf*Dd2)/ IC_{50}(*Pf*3D7)	**IC_{50}(*Pf*K1)/ IC_{50}(*Pf*3D7)**	**IC_{50}(*Pf*7G8)/ IC_{50}(*Pf*3D7)**
51	n.o. [b]	n.o.	n.o.
52	0,4	n.o.	n.o.
53	1,9	n.o.	n.o.
54	2,1	3,1	2,0
55	2	n.o.	n.o.
56	2,4	2,1	2,1
57	1,3	0,5	0,7
58	17,6	14	2,4
59	3,1	n.o.	n.o.
60	3,5	3,7	2,1
61	1,7	n.o.	n.o.
62	1,3	n.o.	n.o.
63	8,1	12,4	3,7
65	0,4	0,5	0,1
CQ	33,1	35,7	20,0

[a] RI – indeks rezistencije; [b] n.o. – nije određeno

Tablica 45. *In vitro* inhibicija polimerizacije hema u hemozoin

Spoj	IPH [a]	Spoj	IPH
51	–	**59**	–
52	+	**60**	–
53	++	**61**	–
54	++	**62**	+
55	–	**63**	+
56	++	**64**	–
57	++	**65**	–
58	+	**CQ**	++

IPH – inhibicija polimerizacije hemozoina *in vitro*, harmikini su grupirani s obziroma na % IPH u odnosu na referentni lijek (CQ): < 50 %, ne inhibiraju polimerizaciju hemozoina (–); između 50 i 75 %, umjereno inhibiraju polimerizaciju hemozoina (+); > 75 %, snažno inhibiraju polimerizaciju hemozoina (++).

Nadalje, harmikinima je ispitan mogući mehanizam djelovanja. Budući da su derivati CQ-a, postoji mogućnost da inhibiraju polimerizaciju hema u hemozoin. Kao model za proučavanje tvorbe hemozoina korišten je β-hematin, sintetski oblik hemozoina, koji se *in vitro* može prirediti iz hemina u kiseloj sredini. Rezultati ispitivanja inhibicije polimerizacije hema u hemozoina dani su u Tablici 45. Vidljivo je da sposobnost inhibicije polimerizacije hemozoina ne slijedi rezultate antimalarijskog djelovanja na eritrocitnu fazu životnog ciklusa plazmodija zbog čega se može zaključiti da se djelovanje spojeva temelji i na drugim mehanizmima, vjerojatno inhibiciji *Pf*Hsp90.

4.3.2.1.2. Harmiceni i harmicini

Harmiceni su pokazali umjereno djelovanje na eritrocitnu fazu životnog ciklusa plazmodija. Soj *Pf*3D7 uglavnom je bio osjetljiviji na djelovanje harmicena od soja *Pf*Dd2: 7 od 18 spojeva djelovalo je na *Pf*3D7 u submikromolarnim koncentracijama, dok su samo 2 od 18 spojeva djelovala na *Pf*Dd2 u tom rasponu koncentracija. Harmiceni su na *Pf*3D7 djelovali snažnije ili usporedljivo s harminom, osim derivata **69** i **76** koji su bili neaktivni pri najvišoj ispitivanoj koncentraciji, ali slabije od CQ. Na ovaj soj najsnažnije je djelovao O-7-supstituirani triazol **74** (IC_{50} = 0,15 ± 0,05 μM). Treba istaći da su harmiceni, osim derivata **69** i **76**, djelovali na *Pf*Dd2 snažnije od harmina koji je bio nedjelotvoran prema ovom soju. Najučinkovitiji je bio O-7-supstituirani amid **78** (IC_{50} = 0,66 ± 0,01 μM).

Nadalje, SAR analiza otkriva da položaj supstitucije na β-karbolinskom prstenu ima značajniji utjecaj na antimalarijsko djelovanje od vrste i strukture poveznice. Optimalan položaj za supstituciju na β-karbolinskom prstenu je O-7. Svi O-7-supstituirani harmiceni, osim derivata **69**, ostvarili su djelovanje u submikromolarnim koncentracijama, dok je O-7-supstituirani triazol **74** ostvario najjače djelovanje u ovoj seriji spojeva. Također, kod harmicena TT pogodno mjesto supstitucije je O-6, dok je kod harmicena AT to položaj N-9. Nažalost, priprava O-6-supstituiranih amida nije uspjela te nije ispitano kako taj položaj kod amida utječe na antimalarijsko djelovanje.

Tablica 46. *In vitro* antiplazmodijsko djelovanje harmicina i harmicena na eritrocitnu fazu životnog ciklusa plazmodija

Spoj	S/P[a]	IC_{50}[b] (μM)		Spoj	S/P[a]	IC_{50}[b] (μM)	
		*Pf*3D7	*Pf*Dd2			*Pf*3D7	*Pf*Dd2
47a	C-1/T	> 27,8	> 20,3	**66**	C-1/T	3,6 ± 1,1	4,4 ± 1,8
47b		> 17,3	> 20,1	**67**	C-3/T	2,6 ± 0,3	4 ± 0,6
47c		> 13,2	> 19,1	**68**	O-6/T	0,31 ± 0,01	1,1 ± 0,005
47d		> 55,6	> 55,6	**69**	O-7/T	> 55,56	> 55,56
47e		> 55,6	39,2 ± 0,3	**70**	N-9/T	2,1 ± 0,8	2,9 ± 0,1
48a	C-3/T	> 20	> 27,8	**71**	C-1/T	9,2 ± 2	11,2 ± 2,2
48b		> 27,8	> 27,8	**72**	C-3/T	7,1± 0,4	6,1 ± 1,4
48c		16,4 ± 3,4	11,1 ± 2,8	**73**	O-6/T	0,35 ± 0,2	0,89 ± 0,01
48d		21,4 ± 2,3	> 27,8	**74**	O-7/T	0,15 ± 0,05	1 ± 0,5
48e		> 27,8	> 27,8	**75**	N-9/T	1,4 ± 0,3	2,3 ± 0,3
49a	O-6/T	0,61 ± 0,09	2,12 ± 0,40	**76**	C-1/A	> 55,56	14 ± 1,95
49b		0,55 ± 0,08	2,28 ± 0,33	**77**	C-3/A	13,2 ± 8,5	8 ± 0,2
49c		0,26 ± 0,17	0,73 ± 0,40	**78**	O-7/A	0,3 ± 0,09	0,66 ± 0,01
49d		0,57 ± 0,06	0,95 ± 0,16	**79**	N-9/A	0,4 ± 0,18	2 ± 0,3
49e		0,60 ± 0,03	1,81 ± 0,04	**80**	C-1/A	1,3 ± 0,1	1,1 ± 0,01
50a	N-9/T	>27,8	>19,8	**81**	C-3/A	7,9 ± 2,2	13 ± 5,9
50c		6,3 ± 1	18,4 ± 2,4	**82**	O-7/A	0,42 ± 0,02	1,5 ± 0,1
50d		>19,9	>23,6	**83**	N-9/A	0,83 ± 0,22	1,8 ± 0,4
50e		18,2	>16,9	**CQ[c]**		0,003 ± 0,002	0,2 ± 0,1
				HAR[d]		8,3 ± 2,8	> 27,7

[a] S/P – položaj supstitucije na β-karbolinskom/tip poveznice (T – triazol, A – amid); [b] IC_{50} – koncentracija spoja koja inhibira rast plazmodija za 50 %; [c] CQ – klorokin; [d] HAR – harmin.

Strukturna raznolikost harmicina omogućila je analizu utjecaja položaja supstituenta na β-karbolinskom prstenu te vrste i položaja supstituenta na benzenskom prstenu DCK-a na antimalarijsko djelovanje. Uočeno je da je položaj O-6 β-karbolinskog prstena najpogodniji za supstituciju te da vrsta i položaj supstituenta na fenilnom prstenu DCK-i nema značajnijeg utjecaja na antimalarijsko djelovanje hibrida. O-6-supstituirani derivati **49** pokazali su umjereno antimalarijsko djelovanje (IC_{50} vrijednosti u submikromolarnom području), dok su C-1-, C-3- i N-9-supstituirani harmicini djelovali vrlo slabo ili su bili neaktivni pri najvišim ispitivanim koncentracijama. Derivati **49** snažnije su djelovali na *Pf*3D7 nego na *Pf*Dd2. Njihov

antimalarijski učinak bio je jedan red veličine snažniji od harmina, ali dva reda veličine slabiji od CQ-a. Najbolje djelovanje ostvario je *m*-Br-supstituirani hibrid **49c** (IC_{50} = 0,26 ± 0,17 μM).

C-1- i C-3-supstituirani harmicini (**47** i **48**) u poveznici, uz triazol, sadrže i estersku skupinu. Vjerovatno je u *in vitro* uvjetima došlo do hidrolize estera i razgradnje harmicina što je rezultiralo slabijim antimalarijskim djelovanjem. Međutim, trebalo bi sintetizirati analogne spojeve bez esterske poveznice i ispitati njihovo antimalarijsko djelovanje kako bi se potvrdila ova hipoteza.

Zanimljiva je usporedba djelovanja N-9-supstituiranih harmicina **50** sintetiziranih u okviru ovog doktorskog rada i onih koje su pripravili Rajić i suradnici (Slika 62). Novosintetizirani harmicini **50** sadrže hidroksimetilnu skupinu u položaju C-3, nemaju metoksi skupinu u položaju O-7 i općenito su neaktivni, dok prije objavljeni harmicini sadrže metoksi skupinu u položaju O-7, nesupstituirani su u položaju C-3 te ostvaruju antiplazmodijsko djelovanje u submikromolarnim koncentracijama. Može se zaključiti da je uvođenje alkoholne skupine u položaju C-3 i gubitak metoksi supstituenta u položaju O-7 rezultiralo gubitkom antimalarijskog djelovanja.

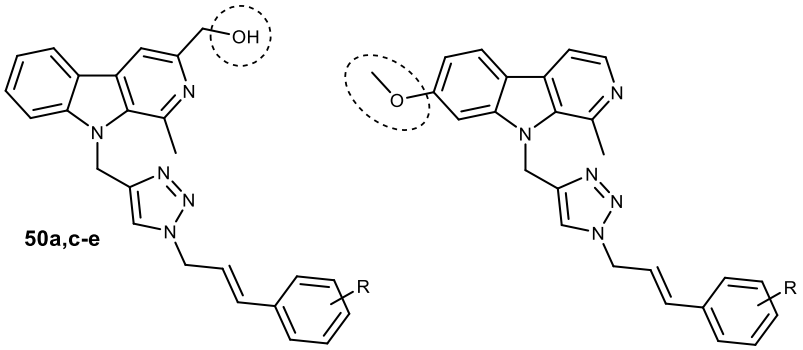

Slika 62. Usporedba strukturnih značajki dvije serije *N*-supstituiranih harmicina

4.3.2.1.3. Selektivnost antimalarijskog djelovanja hibridnih derivata β-karbolina

Kako bi se odredila selektivnost novosintetiziranih spojeva prema plazmodiju izračunati su indeksi selektivnosti (SI) izraženi kao omjer IC_{50} vrijednosti za HepG2 i IC_{50} vrijednosti za *Pf*3D7. Rezultati su prikazani u Tablici 47.

Tablica 47. Indeksi selektivnosti za harmicine, harmikine i harmicene

Spoj	SI[a]	Spoj	SI	Spoj	SI
47a	> 1,8	**50e**	> 2,7	**68**	> 54,8
47b	> 2,9	**51**	> 1,8	**69**	> 0,9
47c	> 3,8	**52**	> 4,6	**70**	23,8
47d	> 0,9	**53**	7,5	**71**	4,8
47e	> 0,9	**54**	104,4	**72**	> 7
48a	> 2,5	**55**	42,5	**73**	24
48b	> 1,8	**56**	346,4	**74**	63,3
48c	> 3	**57**	73,3	**75**	> 35,7
48d	> 2,3	**58**	1663,8	**76**	> 0,9
48e	> 1,8	**59**	254,1	**77**	> 3,8
49a	19,8	**60**	1246,2	**78**	52
49b	26,5	**61**	164,8	**79**	> 125
49c	58,8	**62**	74,2	**80**	> 38,5
49d	25	**63**	10500	**81**	> 6,3
49e	25,1	**64**	780	**82**	> 17,6
50a	> 1,8	**65**	959,5	**83**	33,7
50c	2,5	**66**	> 13,9		
50d	> 2,5	**67**	> 4,7		

[a] SI – indeks selektivnosti izražen kao omjer IC_{50} za HepG2 i IC_{50} za *Pf*3D7.

Između ostalih serija hibrida, harmikini su pokazali najveću selektivnost prema plazmodiju u odnosu na humane stanice. Citotoksični učinak ispoljili su u mikromolarnim koncentracijma, dok su antimalarijsko djelovanje ostvarili u niskim nanomolarnim koncentracijama što je rezultiralo visokim indeksima selektivnosti (Tablica 47). Derivati **54**, **56**, **59**, **61**, **64** i **65** djelovali su na plazmodij za tri reda veličine snažnije u odnosu na humane stanice, spojevi **58** i **60** za četiri reda veličine snažnije, dok spoj **63** djelovao čak pet redova

veličine snažnije. Visoki indeksi selektivnosti harmikina potvrđuju da njihovo antimalarijsko djelovanje nije isključivo posljedica citotoksičnosti već ciljanog antimalarijskog djelovanja. U seriji harmicina umjerenu selektivnost prema plazmodiju pokazali su derivati **49**, dok su u seriji harmicena dobru selektivnost ostvarili derivati **68**, **74**, **75**, **79**, **80** i **83**.

4.3.2.2. Djelovanje na hepatocitnu fazu životnog ciklusa plazmodija

Djelovanje novosintetiziranih hibrida na hepatocitnu fazu životnog ciklusa plazmodija ispitano je na Huh7 staničnoj liniji inficiranoj s *P. berghei*. Preliminarno, djelovanje hibrida ispitano je pri dvije koncentracije (1 i 10 μM) kako bi se dobio uvid u odnos antimalarijskog djelovanja i toksičnosti prema Huh7. Određena je količina parazita (izražena kao postotak infekcije) koja govori o učinku ispitivanih spojeva te vijabilnost stanica (izražena kao konfluentnost) koja daje uvid u citotoksičnost spojeva prema Huh7. Kao pozitivna kontrola korišteni su PQ (referentni lijek s djelovanjem na hepatocitnu fazu životnog ciklusa plazmodija) i harmin, a kao negativna kontrola DMSO. Preliminarnim ispitivanjem identificirani su spojevi koji pokazuju dobro djelovanje na hepatocitnu fazu, a nisu previše citotoksični na Huh7, zbog čega predstavljaju kandidate za određivanje IC_{50} vrijednosti.

Harmicini su na hepatocitnu fazu životnog ciklusa plazmodija djelovali umjereno, uglavnom slabije od PQ-a (Slike 63a i 63b).

a)

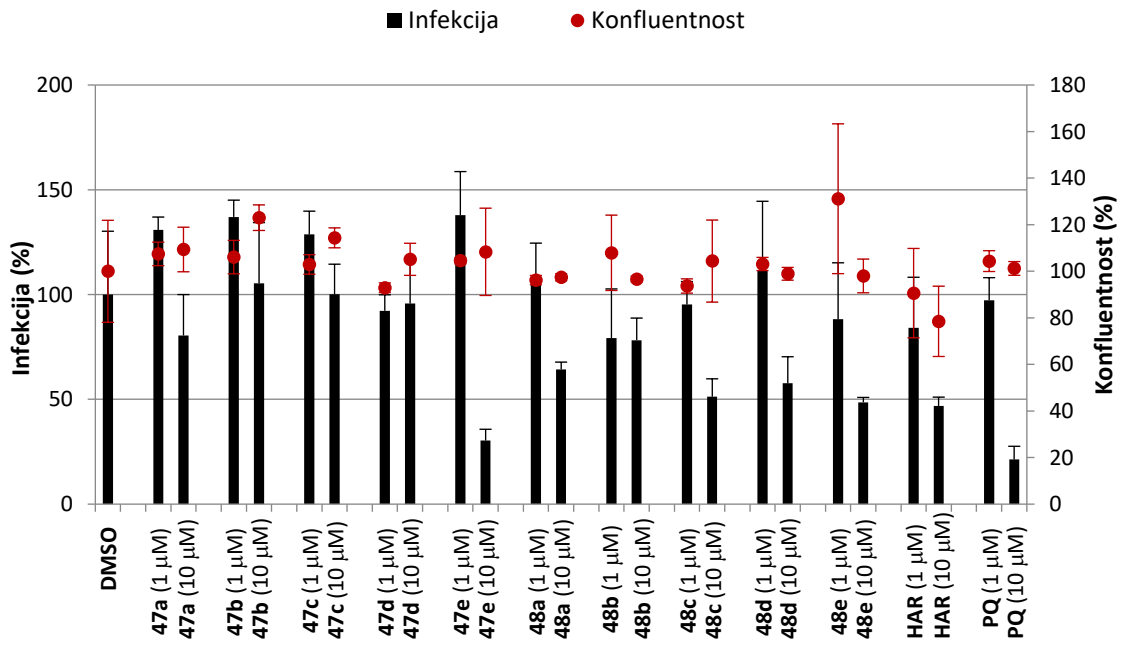

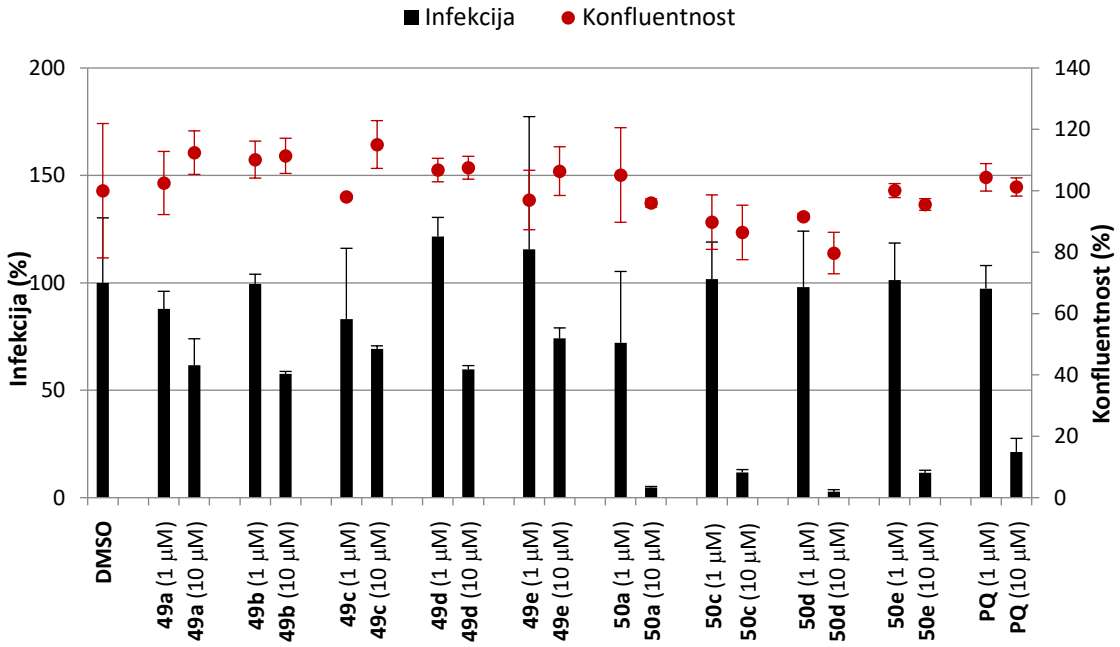

b)

Slika 63. *In vitro* djelovanje harmicina **47** i **48** (a) te **49** i **50** (b) na hepatocitnu fazu životnog ciklusa plazmodija. Ukupna količina parazita predstavljena je kao postotak infekcije (stupci), a vijabilnost stanica kao konfluentnost (točke).
HAR – harmin, PQ – primakin.

Svi harmikini su pri 10 μM značajno inhibirali infekciju Huh7 s *P. berghei* (Slika 64). Pri nižoj koncentraciji značajnije inhibitorno djelovanje na plazmodij pokazali su harmikini **53** i **54**. S obzirom da je pri višoj koncentraciji bio manje citotoksičan, za određivanje IC_{50} vrijednosti odabran je O-7 harmikin TT **53**. Njegovo djelovanje (IC_{50} = 0,548 ± 0,051 μM) bilo je 15,3 puta jače u odnosu na PQ (IC_{50} = 8,4 ± 3,4 μM).

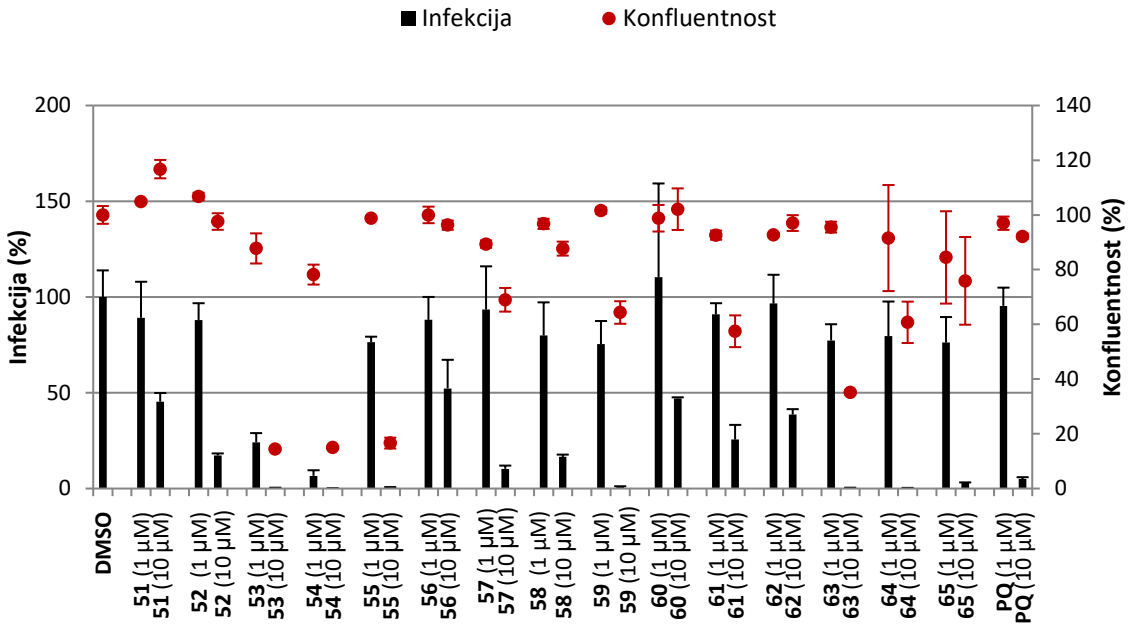

Slika 64. *In vitro* djelovanje harmikina **51-65** na hepatocitnu fazu životnog ciklusa plazmodija. Ukupna količina parazita predstavljena je kao postotak infekcije (stupci), a vijabilnost stanica kao konfluentnost (točke). PQ – primakin.

Harmiceni, osim spojeva **66** i **75**, su pri višoj ispitivanoj koncentraciji djelovali snažnije od PQ-a na hepatocitnu fazu životnog ciklusa plazmodija. Spoj **68** je pri toj koncentraciji ispoljio snažno citotoksično djelovanje na Huh7 što je moglo interferirati s rezultatima antimalarijskog djelovanja. Pri nižoj koncentraciji spojevi **68-71**, **76**, **80** i **81** djelovali su usporedivo ili snažnije od PQ-a, dok su spojevi **66**, **67**, **72** i **75** djelovali slabije od referentnog lijeka. Najsnažnije djelovanje na hepatocitnu fazu ostvario je spoj **80** (IC_{50} < 1 µM), uz izostanak citotoksičnog djelovanja na Huh7. Spojevi **66** i **75** pokazali su najslabije djelovanje na hepatocitnu fazu (pri obje koncentracije djelovali su slabije od PQ-a). Rezultati su prikazani na Slici 65.

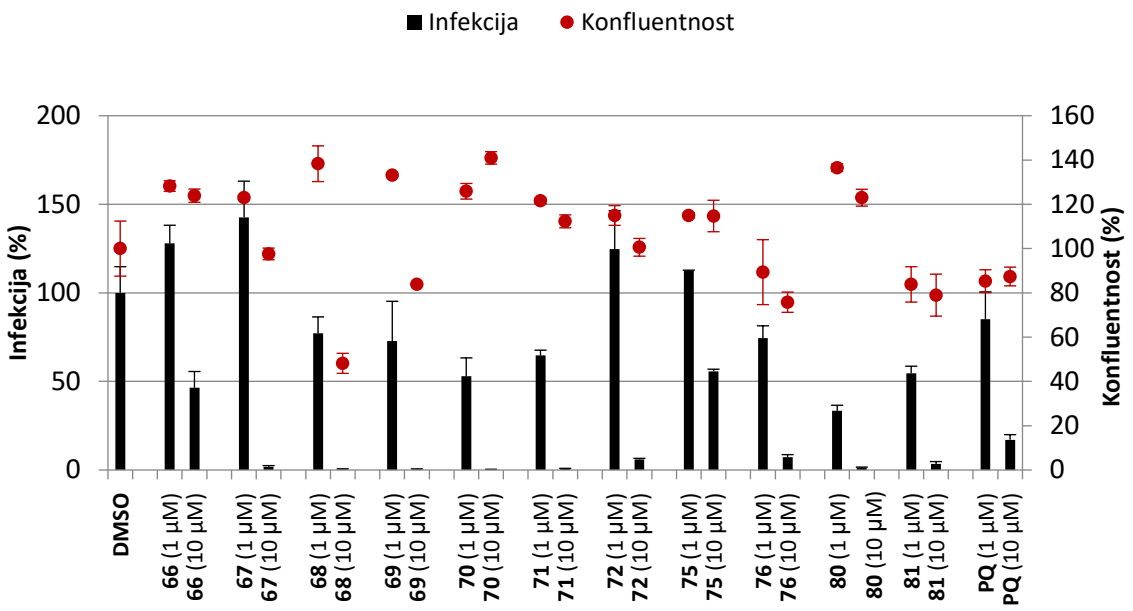

Slika 65. *In vitro* djelovanje harmicena na hepatocitnu fazu životnog ciklusa plazmodija. Ukupna količina parazita predstavljena je kao postotak infekcije (stupci), a vijabilnost stanica kao konfluentnost (točke). PQ – primakin.

5. ZAKLJUČCI

U ovom doktorskom radu sintetizirane su 3 nove serije hibridnih spojeva harmina: harmicini **47-50**, harmikini **51-65** i harmiceni **66-83**, te njihovi prekursori:

a) β-karbolinski alkini **4**, **13**, **15**, **19**, **24** i **28**, azidi **6**, **11**, **22**, **27** i **31**, amini **7**, **12**, **21**, **26** i **30** te karboksilna kiselina **33**,
b) propargilni esteri DCK-a **34**, azidi DCK-a **37**,
c) klorkinolinski azidi **38** i **40**, alkin **42**, karboksilna kiselina **43,** amini **44** i **45**,
d) azidometilferocen **46**.

Hibridni spojevi TT pripravljeni su klik-reakcijom. Harmicini **47** i **48** pripravljeni su klik-reakcijom propargilnih estera DCK-a **34** i β-karbolinskih azida **6**, odnosno **11**. S druge strane, harmicini **49** i **50** pripravljeni su klik-reakcijom azida DCK-a **37** i β-karbolinskih alkina **13**, odnosno **19**. Nadalje, harmikini TT pripravljeni su klik-reakcijom alkina **42** i β-karbolinskih azida **6** i **11** (spojevi **51** i **52**), odnosno klik-reakcijom azida **38** i **40** i alkina **19**, **24** i **28** (spojevi **53-58**). Konačno, harmiceni TT **66-70** pripravljeni su klik-reakcijom azidometilferocena i alkina **4**, **15**, **19**, **24** i **28**. S druge strane, triazoli **71-75** dobiveni su klik-reakcijom etinil-ferocena i azida **6**, **11**, **22**, **27** i **31**.

Hibridni spojevi AT pripravljeni su reakcijama povezivanja. Harmikini AT **59-63** dobiveni su reakcijom karboksilne kiseline **43** i amina **7**, **12**, **21**, **26** i **30**, dok su amidi **64** i **65** pripravljeni reakcijom karboksilne kiseline **33** i amina **44** i **45**. Harmiceni AT **76-83** pripravljeni su reakcijom povezivanja ferocenkarboksilne, odnosno ferocenoctene kiseline s aminima **7**, **12**, **21**, **26** i **30**.

Ispitano je biološko djelovanje sintetiziranih hibridnih spojeva: antiproliferativno djelovanje na humane stanične linije (četiri tumorske i jedna netumorska stanična linija) i antimalarijsko djelovanje na eritrocitnu i hepatocitnu fazu životnog ciklusa plazmodija.

Harmiceni su pokazali snažno i selektivno djelovanje na humane tumorske stanice. U ovoj seriji hibrida, najjače antiproliferativno djelovanje prema svim ispitivanim staničnim linijama ostvarili su spojevi **73** i **82**. Spojevi **66**, **69** i **70** pokazali su selektivno djelovanje prema HCT116, dok su spojevi **76** i **77** bili selektivni prema MCF-7. Harmikini su pokazali snažno, ali uglavnom neselektivno antiproliferativno djelovanje. O-7-supstituirani derivati **54** i **57** ostvarili su najjače djelovanje ($IC_{50} \leq 10$ μM), dok je spoj **51** bio selektivan prema HCT116. Između harmicina, najbolje antiproliferativno djelovanje pokazali su O-6-supstituirani derivati **49**, posebno prema MCF-7 i HCT116 staničnim linijama. Harmicin **49c** pokazao je selektivno djelovanje prema MCF-7. Pokus lokalizacije spojeva u stanici otkrio je da harmicen **69**, za razliku od harmicina **49c**, ulazi u staničnu jezgru

Najsnažnije antimalarijsko djelovanje na eritrocitnu fazu životnog ciklusa plazmodija pokazali su harmikini, koji su bili učinkoviti protiv *Pf*3D7 (IC_{50} vrijednosti 9 od 15 spojeva < 100 nM), ali i protiv rezistentnih sojeva *P. falciparum*. Najbolje djelovanje na *Pf*3D7 ostvarili su derivati **58** (IC_{50} = 11,6 ± 3,8 nM), **60** (IC_{50} = 13 ± 3,1 nM) i **63** (IC_{50} = 2 ± 0,3 nM), čije je djelovanje bilo 5,5 puta snažnije u odnosu na CQ. Spoj **65** snažnije je djelovao na rezistentne sojeve nego na *Pf*3D7 (IC_{50} (*Pf*Dd2) = 15,5 ± 0,9 nM, IC_{50} (*Pf*K1) = 20,2 ± 5,2 nM, IC_{50} (*Pf*7G8) = 6,0 ± 0,3 nM). Harmiceni i harmicini djelovali su na eritrocitnu fazu djelovali umjereno. Između harmicena, najbolje djelovanje pokazao je spoj **74** (IC_{50} = 0,15 ± 0,05 μM), dok su u seriji harmicina najbolje antimalarijsko djelovanje pokazali hibridi **49** (O-6-supstituirani spojevi) s IC_{50} vrijednostima u submikromolarnom području. Na hepatocitnu fazu životnog ciklusa plazmodija dobro djelovanje pokazali su harmikini (IC_{50}(**53**) = 0,548 ± 0,051 μM) i harmiceni (IC_{50}(**80**) < 1 μM).

Harmikini su pokazali najselektivnije antimalarijsko djelovanje u usporedbi s djelovanjem na humane stanice. Najselektivniji je bio derivat **63** (SI = 10500). Izrazito snažno i selektivno antimalarijsko djelovanje čini ih dobrim spojevima uzorima za razvoj novih potencijalnih antimalarika. S druge strane, harmicini i harmiceni, osim nekoliko iznimki, bili su manje selektivni prema plazmodiju. S obzirom da su pojedini spojevi iz ovih serija pokazali snažno i selektivno antiproliferativno djelovanje na tumorske stanice, mogli bi poslužiti kao spojevi uzori za razvoj novih citostatika.

6. LITERATURA

1. Cooper GM. The Cell: Molecular Approach. 8th ed. Oxford: Oxford University Press; 2019.

2. Graham LP. An introduction to medicinal chemistry. 6th ed. Oxford: Oxford University Press; 2017.

3. World Health Organization. Cancer. Preuzeto s: https://www.who.int/health-topics/cancer#tab=tab_1 (pristupljeno: 25. svibnja 2022.)

4. Vasan N, Baselga J, Hyman DM. A view on drug resistance in cancer. Nature 2019;575: 299–309.

5. Nurgali K, Jagoe RT, Abalo R. Adverse effects of cancer chemotherapy: anything new to improve tolerance and reduce sequelae? [Editorial] Front Pharmacol 2018;9:245.

6. Kumar K, Pradines B, Madamet M, Amalvict R, Benoit N, Kumar V. 1*H*-1,2,3-triazole tethered isatin-ferrocene conjugates: synthesis and *in vitro* antimalarial evaluation. Eur J Med Chem 2014;87:801–4.

7. Mishra M, Mishra VK, Kashaw V, Iyer AK, Kashaw SK. Comprehensive review on various strategies for antimalarial drug discovery. Eur J Med Chem 2017;125:1300–20.

8. Trampuz A, Jereb M, Muzlovic I, Prabhu RM. Clinical review: severe malaria. Crit Care 2003;7:315–23.

9. World Health Organization. World malaria report 2021. Preuzeto s: https://www.who.int/teams/global-malaria-programme/reports/world-malaria-report-2021 (pristupljeno: 25. svibnja 2022.)

10. Biamonte MA, Wanner J, le Roch KG. Recent advances in malaria drug discovery. Bioorg Med Chem Lett 2013;23:2829–43.

11. Schlitzer M. Antimalarial drugs – what is in use and what is in the pipeline. Arch Pharm 2008;341:149–63.

12. Varo R, Chaccour C, Bassat Q. Update on malaria. Med Clin 2020;155:395–402.

13. Singh Sidhu AB, Verdier-Pinard D, Fidock DA. Chloroquine resistance in *Plasmodium falciparum* malaria parasites conferred by *Pf*CRT mutations. Science 2002;298:210–3.

14. Kozlov M. Resistance to front-line malaria drugs confirmed in Africa. Nature 2021;597:604.

15. Caminade C, Kovats S, Rocklov J, Tompkins AM, Morse AP, Colón-González FJ, et al. Impact of climate change on global malaria distribution. Proc Natl Acad Sci USA 2014;111:3286–91.

16. World Health Organisation. WHO recommends groundbreaking malaria vaccine for children at risk. Preuzeto s: https://www.who.int/news/item/06-10-2021-who-recommends-groundbreaking-malaria-vaccine-for-children-at-risk (pristupljeno: 10. lipnja 2022.)

17. Centers for Disease Control and Prevention. Malaria - About Malaria - Biology. Preuzeto s: https://www.cdc.gov/malaria/about/biology/ (pristupljeno: 24. lipnja 2022.)

18. Agarwal D, Gupta RD, Awasthi SK. Are antimalarial hybrid molecules a close reality or a distant dream? Antimicrob Agents Chemother 2017;61:e00249-17.

19. Srivastava V, Lee H. Chloroquine-based hybrid molecules as promising novel chemotherapeutic agents. Eur J Pharmacol 2015;762:472–86.

20. Walsh JJ, Coughlan D, Heneghan N, Gaynor C, Bell A. A novel artemisinin-quinine hybrid with potent antimalarial activity. Bioorg Med Chem Lett 2007;17:3599–602.

21. Ecker A, Lehane AM, Clain J, Fidock DA. *Pf*CRT and its role in antimalarial drug resistance. Trends Parasitol 2012;28:504–14.

22. Andrews S, Burgess SJ, Skaalrud D, Kelly JX, Peyton DH. Reversal agent and linker variants of reversed chloroquines: activities against *Plasmodium falciparum*. J Med Chem 2010;53:916–9.

23. Laine AE, Lood C, Koskinen AMP. Pharmacological importance of optically active tetrahydro-β-carbolines and synthetic approaches to create the C1 stereocenter. Molecules 2014;19:1544–67.

24. Aaghaz S, Sharma K, Jain R, Kamal A. β-Carbolines as potential anticancer agents. Eur J Med Chem 2021;216:113321.

25. Cao R, Peng W, Wang Z, Xu A. β-Carboline alkaloids: biochemical and pharmacological functions. Curr Med Chem 2007;14:479–500.

26. Moura DJ, Richter MF, Boeira JM, Pêgas Henriques JA, Saffi J. Antioxidant properties of β-carboline alkaloids are related to their antimutagenic and antigenotoxic activities. Mutagenesis 2007;22:293–302.

27. Zhao F, Gao Z, Jiao W, Chen L, Chen L, Yao X. *In vitro* anti-inflammatory effects of β-carboline alkaloids, isolated from *Picrasma quassioides*, through inhibition of the iNOS pathway. Planta Med 2012;78:1906–11.

28. Zhang M, Sun D. Recent advances of natural and synthetic β-carbolines as anticancer agents. Anticancer Agents Med Chem 2015;15:537–47.

29. Shin HJ, Lee HSL, Lee DS. The synergistic antibacterial activity of 1-acetyl-β-carboline and β-lactams against methicillin-resistant *Staphylococcus aureus* (MRSA). J Microbiol Biotechnol 2010;20:501–5.

30. Nazari Formagio AS, Santos PR, Zanoli K, Ueda-Nakamura T, Düsman Tonin LT, Nakamura CV, et al. Synthesis and antiviral activity of β-carboline derivatives bearing a substituted carbohydrazide at C-3 against poliovirus and herpes simplex virus (HSV-1). Eur J Med Chem 2009;44:4695–701.

31. Gorki V, Walter NS, Singh R, Chauhan M, Dhingra N, Salunke DB, et al. β-Carboline derivatives tackling malaria: biological evaluation and docking analysis. ACS Omega 2020;5:17993–8006.

32. Smith KL, Ford GK, Jessop DS, Finn DP. Behavioural, neurochemical and neuroendocrine effects of the endogenous β-carboline harmane in fear-conditioned rats. J Psychopharmacol 2013;27:162–70.

33. Kaijima M, da Costa-Rochette L, Dodd RH, Rossier J, Naquet R. Hypnotic action of ethyl β-carboline-3-carboxylate, a benzodiazepine receptor antagonist, in cats. Electroencephalogr Clin Neurophysiol 1984;58:277–81.

34. Pogosyan SA, Grigoryan NP, Paronikyan RG. Synthesis and anticonvulsant activity of dihydrochlorides of indoline-3′spiro-1-(1,2,3,4-tetrahydro-β-carboline derivatives. Pharm Chem J 2007;41:527–8.

35. Lake RJ, Blunt JW, Munro MHG. Eudistomins from the New Zealand ascidian *Ritterella sigillinoides*. Aust J Chem 1989;42:1201–6.

36. Rao KV, Santarsiero BD, Mesecar AD, Schinazi RF, Tekwani BL, Hamann MT. New manzamine alkaloids with activity against infectious and tropical parasitic diseases from an Indonesian sponge. J Nat Prod 2003;66:823–8.

37. Pähkla R, Zilmer M, Kullisaar T, Rägo L. Comparison of the antioxidant activity of melatonin and pinoline *in vitro*. J Pineal Res 1998;24:96–101.

38. Cochrane. Reserpine for lowering blood pressure. Preuzeto s: https://www.cochrane.org/CD007655/HTN_reserpine-lowering-blood-pressure (pristupljeno: 1. lipnja 2022.)

39. DrugBank Online. Tadalafil: uses, interactions, mechanism of action. Preuzeto s: https://go.drugbank.com/drugs/DB00820 (pristupljeno: 1. lipnja 2022.)

40. Bouwman SA, Zoleko-Manego R, Renner KC, Schmitt EK, Mombo-Ngoma G, Grobusch MP. The early preclinical and clinical development of cipargamin (KAE609), a novel antimalarial compound. Travel Med Infect Dis 2020;36:101765.

41. Pictet A, Spengler T. Über die bildung von isochinolin-derivaten durch einwirkung von methylal auf phenyl-äthylamin, phenyl-alanin und tyrosin. Ber Dtsch Chem Ges 1911;44:2030–6.

42. Eagon S, Anderson MO. Microwave-assisted synthesis of tetrahydro-β-carbolines and β-carbolines. Eur J Org Chem 2014;2014:1653–65.

43. Kurti L, Czako B. Strategic applications of named reactions in organic synthesis. 1st ed. Amsterdam: Elsevier Academic Press; 2005.

44. Cao R, Fan W, Guo L, Ma Q, Zhang G, Li J, et al. Synthesis and structure-activity relationships of harmine derivatives as potential antitumor agents. Eur J Med Chem 2013;60:135–43.

45. Moloudizargari M, Mikaili P, Aghajanshakeri S, Asghari M, Shayegh J. Pharmacological and therapeutic effects of *Peganum harmala* and its main alkaloids. Pharmacogn Rev 2013;7:199–212.

46. Patel K, Gadewar M, Tripathi R, Prasad SK, Patel DK. A review on medicinal importance, pharmacological activity and bioanalytical aspects of β-carboline alkaloid ‘Harmine”. Asian Pac J Trop Biomed 2012;2:660–4.

47. Wikipedia. *Peganum harmala*. Preuzeto s: https://bs.m.wikipedia.org/wiki/Datoteka:Peganum_harmala_Baikonur_09.jpg (pristupljeno: 20. lipnja 2022.)

48. Ding Y, He J, Huang J, Yu T, Shi X, Zhang T, et al. Harmine induces anticancer activity in breast cancer cells via targeting TAZ. Int J Oncol 2019;54:1995–2004.

49. Li C, Wang Y, Wang C, Yi X, Li M, He X. Anticancer activities of harmine by inducing a pro-death autophagy and apoptosis in human gastric cancer cells. Phytomedicine 2017;28:10–8.

50. Wu LW, Zhang JK, Rao M, Zhang ZY, Zhu HJ, Zhang C. Harmine suppresses the proliferation of pancreatic cancer cells and sensitizes pancreatic cancer to gemcitabine treatment. OncoTargets Ther 2019;12:4585–93.

51. Ruan S, Jia F, Li J. Potential antitumor effect of harmine in the treatment of thyroid cancer. Evid Based Complement Alternat Med 2017;2017:9402615.

52. Hai-Rong C, Xiang H, Xiao-Rong Z. Harmine suppresses bladder tumor growth by suppressing vascular endothelial growth factor receptor 2-mediated angiogenesis. Biosci Rep 2019;39:20190155.

53. Kamani M, Ghanbari A, Taghadosi M, Mansouri K, Jalili C. Harmine augments the cytotoxic and anti-invasive potential of temozolomide against glioblastoma multiforme cells. Jundishapur J Nat Phar Prod 2022;17:115464.

54. Mota NSRS, Kviecinski MR, Felipe KB, Grinevicius VMAS, Siminski T, Almeida GM, et al. β-carboline alkaloid harmine induces DNA damage and triggers apoptosis by a mitochondrial pathway: study *in silico*, *in vitro* and *in vivo*. Int J Funct Nutr 2020;1:1.

55. Shahinas D, Liang M, Datti A, Pillai DR. A repurposing strategy identifies novel synergistic inhibitors of *Plasmodium falciparum* heat shock protein 90. J Med Chem 2010;53:3552–7.

56. Shahinas D, MacMullin G, Benedict C, Crandall I, Pillaid DR. Harmine is a potent antimalarial targeting Hsp90 and synergizes with chloroquine and artemisinin. Antimicrob Agents Chemother 2012;56:4207–13.

57. Shahinas D, Folefoc A, Pillai DR. Targeting *Plasmodium falciparum* Hsp90: towards reversing antimalarial resistance. Pathogens 2013;2:33–54.

58. Banumathy G, Singh V, Pavithra SR, Tatu U. Heat shock protein 90 function is essential for *Plasmodium falciparum* growth in human erythrocytes. J Biol Chem 2003;278:18336–45.

59. Pesce ER, Cockburn IL, Goble JL, Stephens LL, Blatch GL. Malaria heat shock proteins: drug targets that chaperone other drug targets. Infect Disord Drug Targets 2010;10:147–57.

60. Kamal A, Narasimha Rao MP, Swapna P, Srinivasulu V, Bagul C, Shaik AB, et al. Synthesis of β-carboline-benzimidazole conjugates using lanthanum nitrate as a catalyst and their biological evaluation. Org Biomol Chem 2014;12:2370–87.

61. Xiao S, Lin W, Wang C, Yang M. Synthesis and biological evaluation of DNA targeting flexible side-chain substituted β-carboline derivatives. Bioorg Med Chem Lett 2001;11:437–41.

62. Shankaraiah N, Siraj KP, Nekkanti S, Srinivasulu V, Sharma P, Senwar KR, et al. DNA-binding affinity and anticancer activity of β-carboline-chalcone conjugates as potential DNA intercalators: molecular modelling and synthesis. Bioorg Chem 2015;59:130–9.

63. Zhao M, Bi L, Wang W, Wang C, Baudy-Floc'h M, Ju J, et al. Synthesis and cytotoxic activities of β-carboline amino acid ester conjugates. Bioorg Med Chem 2006;14:6998–7010.

64. Shi B, Cao R, Fan W, Guo L, Ma Q, Chen X, et al. Design, synthesis and *in vitro* and *in vivo* antitumor activities of novel bivalent β-carbolines. Eur J Med Chem 2013;60:10–22.

65. Shankaraiah N, Jadala C, Nekkanti S, Senwar KR, Nagesh N, Shrivastava S, et al. Design and synthesis of C3-tethered 1,2,3-triazolo-β-carboline derivatives: anticancer

activity, DNA-binding ability, viscosity and molecular modeling studies. Bioorg Chem 2016;64:42–50.

66. Kamal A, Srinivasulu V, Nayak VL, Sathish M, Shankaraiah N, Bagul C, et al. Design and synthesis of C3-pyrazole/chalcone-linked beta-carboline hybrids: antitopoisomerase I, DNA-interactive, and apoptosis-inducing anticancer agents. ChemMedChem 2014;9:2084–98.

67. Sathish M, Chetan Dushantrao S, Nekkanti S, Tokala R, Thatikonda S, Tangella Y, et al. Synthesis of DNA interactive C3-trans-cinnamide linked β-carboline conjugates as potential cytotoxic and DNA topoisomerase I inhibitors. Bioorg Med Chem 2018;26:4916–29.

68. Kovvuri J, Nagaraju B, Nayak VL, Akunuri R, Rao MPN, Ajitha A, et al. Design, synthesis and biological evaluation of new β-carboline-bisindole compounds as DNA binding, photocleavage agents and topoisomerase I inhibitors. Eur J Med Chem 2018;143:1563–77.

69. Sathish M, Kavitha B, Nayak VL, Tangella Y, Ajitha A, Nekkanti S, et al. Synthesis of podophyllotoxin linked β-carboline congeners as potential anticancer agents and DNA topoisomerase II inhibitors. Eur J Med Chem 2018;144:557–71.

70. Kamal A, Sathish M, Nayak VL, Srinivasulu V, Kavitha B, Tangella Y, et al. Design and synthesis of dithiocarbamate linked β-carboline derivatives: DNA topoisomerase II inhibition with DNA binding and apoptosis inducing ability. Bioorg Med Chem 2015;23:5511–26.

71. Deveau AM, Labroli MA, Dieckhaus CM, Barthen MT, Smith KS, MacDonald TL. The synthesis of amino-acid functionalized β-carbolines as topoisomerase II inhibitors. Bioorg Med Chem Lett 2001;11:1251–5.

72. Al-Allaf TAK, Rashan LJ. Synthesis and cytotoxic evaluation of the first trans-palladium(II) complex with naturally occurring alkaloid harmine. Eur J Med Chem 1998;33:817–20.

73. Toshima K, Okuno Y, Nakajima Y, Matsumura S. β-Carboline–carbohydrate hybrids: molecular design, chemical synthesis and evaluation of novel DNA photocleavers. Bioorg Med Chem Lett 2002;12:671–3.

74. Huber K, Brault L, Fedorov O, Gasser C, Filippakopoulos P, Bullock AN, et al. 7,8-dichloro-1-oxo-β-carbolines as a versatile scaffold for the development of potent and selective kinase inhibitors with unusual binding modes. J Med Chem 2012;55:403–13.

75. Amoussou NG, Bigot A, Roussakis C, Robert JMH. Haspin: a promising target for the design of inhibitors as potent anticancer drugs. Drug Discov Today 2018;23:409–15.

76. Cuny GD, Ulyanova NP, Patnaik D, Liu JF, Lin X, Auerbach K, et al. Structure-activity relationship study of β-carboline derivatives as haspin kinase inhibitors. Bioorg Med Chem Lett 2012;22:2015–9.

77. Holderfield M, Deuker MM, McCormick F, McMahon M. Targeting RAF kinases for cancer therapy: BRAF mutated melanoma and beyond. Nat Rev Cancer 2014;14:455–67.

78. Xin B, Tang W, Wang Y, Lin G, Liu H, Jiao Y, et al. Design, synthesis and biological evaluation of β-carboline derivatives as novel inhibitors targeting B-Raf kinase. Bioorg Med Chem Lett 2012;22:4783–6.

79. Shen YC, Chen CY, Hsieh PW, Duh CY, Lin YM, Ko CL. The preparation and evaluation of 1-substituted 1,2,3,4-tetrahydro- and 3,4-dihydro-β-carboline derivatives as potential antitumor agents. Chem Pharm Bull 2005;53:32–6.

80. Samundeeswari S, Kulkarni MV, Joshi SD, Dixit SR, Jayakumar S, Ezhilarasi RM. Synthesis and human anticancer cell line studies on coumarin-β-carboline hybrids as possible antimitotic agents. ChemistrySelect 2016;1:5019–24.

81. Poje G, Rajić Z. lnhibitori histonskih deacetilaza kao protutumorski lijekovi. Farm Glas 2020;76:261–80.

82. Zhang Y, Ling Y, Xu C, Luo L, Cao J, Feng J, et al. Novel β-carboline/hydroxamic acid hybrids targeting both histone deacetylase and DNA display high anticancer activity via regulation of the p53 signaling pathway. J Med Chem 2015;58:9214–27.

83. Yang WS, Stockwell BR. Synthetic lethal screening identifies compounds activating iron-dependent, nonapoptotic cell death in oncogenic-RAS-harboring cancer cells. Chem Biol 2008;15:234–45.

84. Bialonska D, Zjawiony JK. Aplysinopsins - marine indole alkaloids: chemistry, bioactivity and ecological significance. Mar Drugs 2009;7:166–83.

85. Soni JP, Yeole Y, Shankaraiah N. β-Carboline-based molecular hybrids as anticancer agents: a brief sketch. RSC Med Chem 2021;12:730–50.

86. Ikeda R, Kimura T, Tsutsumi T, Tamura S, Sakai N, Konakahara T. Structure-activity relationship in the antitumor activity of 6-, 8- or 6,8-substituted 3-benzylamino-β-carboline derivatives. Bioorg Med Chem Lett 2012;22:3506–15.

87. Luo B, Song X. A comprehensive overview of β-carbolines and its derivatives as anticancer agents. Eur J Med Chem 2021;224:113688.

88. Boursereau Y, Coldham I. Synthesis and biological studies of 1-amino β-carbolines. Bioorg Med Chem Lett 2004;14:5841–4.

89. Thompson MJ, Louth JC, Little SM, Jackson MP, Boursereau Y, Chen B, et al. Synthesis and evaluation of 1-amino-6-halo-β-carbolines as antimalarial and antiprion agents. ChemMedChem 2012;7:578–86.

90. Kamboj A, Sihag B, Brar DS, Kaur A, Salunke DB. Structure activity relationship in β-carboline derived anti-malarial agents. Eur J Med Chem 2021;221:113536.

91. Barbaras D, Kaiser M, Brun R, Gademann K. Potent and selective antiplasmodial activity of the cyanobacterial alkaloid nostocarboline and its dimers. Bioorg Med Chem Lett 2008;18:4413–5.

92. Liew LPP, Fleming JM, Longeon A, Mouray E, Florent I, Bourguet-Kondracki ML, et al. Synthesis of 1-indolyl substituted β-carboline natural products and discovery of antimalarial and cytotoxic activities. Tetrahedron 2014;70:4910–20.

93. Yadav VD, Srivastava K, Tripathi R, Batra S. Synthesis of β-carboline-fused 1,4-oxazepines and their assessment as antiplasmodial agents. Tetrahedron 2017;73:5680–9.

94. Eagon S, Hammill JT, Bach J, Everson N, Sisley TA, Walls MJ, et al. Antimalarial activity of tetrahydro-β-carbolines targeting the ATP binding pocket of the *Plasmodium falciparum* heat shock 90 protein. Bioorg Med Chem Lett 2020;30:127502.

95. Kumar V, Sachdeva C, Waidha K, Sharma S, Ray D, Kumar Kaushik N, et al. *In Vitro* and *in silico* anti-plasmodial evaluation of newly synthesized β-carboline derivatives. ChemistrySelect 2021;6:5338–42.

96. Jaromin A, Gryzło B, Jamrozik M, Parapini S, Basilico N, Cegła M, et al. Synthesis, molecular docking and antiplasmodial activities of new tetrahydro-β-carbolines. Int J Mol Sci 2021;22:13569.

97. Perković I, Raić-Malić S, Fontinha D, Prudêncio M, Pessanha de Carvalho L, Held J, et al. Harmicines - harmine and cinnamic acid hybrids as novel antiplasmodial hits. Eur J Med Chem 2020;187:111927.

98. Marinović M, Perković I, Fontinha D, Prudêncio M, Held J, de Carvalho LP, et al. Novel harmicines with improved potency against *Plasmodium*. Molecules 2020;25:4376.

99. Guzman JD. Natural cinnamic acids, synthetic derivatives and hybrids with antimicrobial activity. Molecules 2014;19:19292–349.

100. Silva AT, Bento CM, Pena AC, Figueiredo LM, Prudêncio C, Aguiar L, et al. Cinnamic acid conjugates in the rescuing and repurposing of classical antimalarial drugs. Molecules 2019;25:66.

101. De P, Baltas M, Bedos-Belval F. Cinnamic acid derivatives as anticancer agents – a review. Curr Med Chem 2011;18:1672–703.

102. Sharma P. Cinnamic acid derivatives: a new chapter of various pharmacological activities. J Chem Pharm Res 2011;3:403–23.

103. Nimse SB, Pal D, Mazumder A, Mazumder R. Synthesis of cinnamanilide derivatives and their antioxidant and antimicrobial activity. J Chem 2015;2015:208910.

104. Amano R, Yamashita A, Kasai H, Hori T, Miyasato S, Saito S, et al. Cinnamic acid derivatives inhibit hepatitis C virus replication via the induction of oxidative stress. Antiviral Res 2017;145:123–30.

105. De P, De K, Veau D, Bedos-Belval F, Chassaing S, Baltas M. Recent advances in the development of cinnamic-like derivatives as antituberculosis agents. Expert Opin Ther Pat 2012;22:155–68.

106. Jabir NR, Khan FR, Tabrez S. Cholinesterase targeting by polyphenols: a therapeutic approach for the treatment of Alzheimer's disease. CNS Neurosci Ther 2018;24:753–62.

107. Pontiki E, Hadjipavlou-Litina D. Multi-target cinnamic acids for oxidative stress and inflammation: design, synthesis, biological evaluation and modeling studies. Molecules 2019;24:12.

108. Zhu R, Liu H, Liu C, Wang L, Ma R, Chen B, et al. Cinnamaldehyde in diabetes: a review of pharmacology, pharmacokinetics and safety. Pharmacol Res 2017;122:78–89.

109. Hapuarachchi SV, Cobbold SA, Shafik SH, Dennis ASM, McConville MJ, Martin RE, et al. The malaria parasite's lactate transporter *Pf*FNT is the target of antiplasmodial compounds identified in whole cell phenotypic screens. PLoS Pathog 2017 Feb 8;13:e1006180.

110. Kanaani J, Ginsburg H. Effects of cinnamic acid derivatives on in vitro growth of *Plasmodium falciparum* and on the permeability of the membrane of malaria-infected erythrocytes. Antimicrob Agents Chemother 1992;36:1102–8.

111. Pérez BC, Teixeira C, Figueiras M, Gut J, Rosenthal PJ, Gomes JRB, et al. Novel cinnamic acid/4-aminoquinoline conjugates bearing non-proteinogenic amino acids: towards the development of potential dual action antimalarials. Eur J Med Chem 2012;54:887–99.

112. Pérez BC, Teixeira C, Albuquerque IS, Gut J, Rosenthal PJ, Gomes JRB, et al. *N*-cinnamoylated chloroquine analogues as dual-stage antimalarial leads. J Med Chem 2013;56:556–67.

113. Gomes A, Prez B, Albuquerque I, Machado M, Prudpncio M, Nogueira F, et al. *N*-cinnamoylation of antimalarial classics: quinacrine analogues with decreased toxicity and dual-stage activity. ChemMedChem 2014;9:305–10.

114. Wiesner J, Mitsch A, Wissner P, Jomaa H, Schlitzer M. Structure-activity relationships of novel anti-malarial agents. Part 2: cinnamic acid derivatives. Bioorg Med Chem Lett 2001;11:423-4.

115. Seck R, Mansaly M, Gassama A, Cavé C, Cojean S. Synthesis and antimalarial activity of cinnamic acid derivatives. J Chem Pharm 2018;10:1-8.

116. Pérez BC, Fernandes I, Mateus N, Teixeira C, Gomes P. Recycling antimalarial leads for cancer: antiproliferative properties of *N*-cinnamoyl chloroquine analogues. Bioorg Med Chem Lett 2013;23:6769–72.

117. Gomes A, Fernandes I, Teixeira C, Mateus N, Sottomayor MJ, Gomes P. A quinacrine analogue selective against gastric cancer cells: insight from biochemical and biophysical studies. ChemMedChem 2016;11:2703–12.

118. Mabeta P, Pavić K, Zorc B. Insights into the mechanism of antiproliferative effects of primaquine-cinnamic acid conjugates on MCF-7 cells. Acta Pharm 2018;68:337–48.

119. Xu CC, Deng T, Fan ML, Lv WB, Liu JH, Yu BY. Synthesis and *in vitro* antitumor evaluation of dihydroartemisinin-cinnamic acid ester derivatives. Eur J Med Chem 2016;107:192–203.

120. Mushtaque M, Shahjahan. Reemergence of chloroquine (CQ) analogs as multi-targeting antimalarial agents: a review. Eur J Med Chem 2015;90:280–95.

121. World Health Organization. Model List of Essential Medicines. Preuzeto s: https://list.essentialmeds.org/ (pristupljeno 3. lipnja 2022.)

122. PubChem. Chloroquine. Preuzeto s: https://pubchem.ncbi.nlm.nih.gov/compound/Chloroquine (pristupljeno: 3. lipnja 2022.)

123. Kucharski DJ, Jaszczak MK, Boratyński PJ. A review of modifications of quinoline antimalarials: mefloquine and (hydroxy)chloroquine. Molecules 2022;27:1003.

124. Browning DJ. Pharmacology of chloroquine and hydroxychloroquine. In: Browning DJ, editor. Hydroxychloroquine and chloroquine retinopathy. New York: Springer, 2014:35-63.

125. Vardanyan RS, Hruby VJ. Synthesis of essential drugs. 1st ed. Amsterdam: Elsevier; 2006.

126. Surrey AR, Hammer HF. Some 7-substituted 4-aminoquinoline derivatives. J Am Chem Soc 1946;68:113–6.

127. Price CC, Roberts RM. The synthesis of 4-hydroxyquinolines; through ethoxymethylene malonic ester. J Am Chem Soc 1946;68:1204–8.

128. Northey EH, Dreisbach PF, inventors. Wyeth Holdings LLC, assignee. Preparation of 4-hydroxyquinolines. United States Patent US2478125A. 1949 Aug 2.

129. Lei ZN, Wu ZX, Dong S, Yang DH, Zhang L, Ke Z, et al. Chloroquine and hydroxychloroquine in the treatment of malaria and repurposing in treating COVID-19. Pharmacol Ther 2020;216:107672.

130. FDA. Aralen. Preuzeto s: https://www.accessdata.fda.gov/drugsatfda_docs/label/2017/006002s044lbl.pdf (pristupljeno: 25. svibnja 2022.)

131. Kapishnikov S, Grolimund D, Schneider G, Pereiro E, McNally JG, Als-Nielsen J, et al. Unraveling heme detoxification in the malaria parasite by in situ correlative X-ray fluorescence microscopy and soft X-ray tomography. Sci Rep 2017;7:1–12.

132. Graham LP, editor. Antimalarial agents : design and mechanism of action. 1st ed. Amsterdam: Elsevier; 2020.

133. Zorc B. Primjena klorokina i hidroksiklorokina u suvremenoj terapiji. Farm Glas 2021;77:465–78.

134. Drugs.com. Chloroquine Dosage. Preuzeto s: https://www.drugs.com/dosage/chloroquine.html (pristupljeno: 25. svibnja 2022.)

135. Zorc B. Klorokin i hidroksiklorokin u terapiji karcinoma. Farm Glas 2021;77:553–80.

136. Kamat S, Kumari M. Repurposing chloroquine against multiple diseases with special attention to SARS-CoV-2 and associated toxicity. Front Pharmacol 2021;12:576093.

137. Glick D, Barth S, Macleod KF. Autophagy: cellular and molecular mechanisms. J Pathol 2010;221:3–12.

138. Verbaanderd C, Maes H, Schaaf MB, Sukhatme VP, Pantziarka P, Sukhatme V, et al. Repurposing drugs in oncology (ReDO) - chloroquine and hydroxychloroquine as anti-cancer agents. Ecancermedicalscience 2017;11:781.

139. Zhou W, Wang H, Yang Y, Chen ZS, Zou C, Zhang J. Chloroquine against malaria, cancers and viral diseases. Drug Discov 2020;25:2012–22.

140. Zhang Y, Li Y, Li Y, Li R, Ma Y, Wang H, et al. Chloroquine inhibits MGC803 gastric cancer cell migration via the Toll-like receptor 9/nuclear factor kappa B signaling pathway. Mol Med Rep 2015;11:1366–71.

141. Kim J, Yip MLR, Shen X, Li H, Hsin LYC, Labarge S, et al. Identification of anti-malarial compounds as novel antagonists to chemokine receptor CXCR4 in pancreatic cancer cells. PLoS One 2012 Feb 3;7:e31004.

142. Loehberg CR, Strissel PL, Dittrich R, Strick R, Dittmer J, Dittmer A, et al. Akt and p53 are potential mediators of reduced mammary tumor growth by cloroquine and the mTOR inhibitor RAD001. Biochem Pharmacol 2012;83:480–8.

143. Carmeliet P, Jain RK. Principles and mechanisms of vessel normalization for cancer and other angiogenic diseases. Nat Rev Drug Discov 2011;10:417–27.

144. Martinez-Outschoorn UE, Pavlides S, Whitaker-Menezes D, Daumer KM, Milliman JN, Chiavarina B, et al. Tumor cells induce the cancer associated fibroblast phenotype via caveolin-1 degradation: implications for breast cancer and DCIS therapy with autophagy inhibitors. Cell Cycle 2010;9:2423–33.

145. Al-Bari AA. Chloroquine analogues in drug discovery: new directions of uses, mechanisms of actions and toxic manifestations from malaria to multifarious diseases. J Antimicrob Chemother 2015;70:1608–21.

146. Manivannan E, Karthikeyan C, Moorthy NSHN, Chaturvedi SC. The rise and fall of chloroquine/hydroxychloroquine as compassionate therapy of COVID-19. Front Pharmacol 2021;12:584940.

147. Cheruku SR, Maiti S, Dorn A, Scorneaux B, Bhattacharjee AK, Ellis WY, et al. Carbon isosteres of the 4-aminopyridine substructure of chloroquine: effects on pK(a), hematin

binding, inhibition of hemozoin formation, and parasite growth. J Med Chem 2003;46:3166–9.

148. Nsumiwa S, Kuter D, Wittlin S, Chibale K, Egan TJ. Structure-activity relationships for ferriprotoporphyrin IX association and β-hematin inhibition by 4-aminoquinolines using experimental and ab initio methods. Bioorg Med Chem 2013;21:3738–48.

149. Kaschula CH, Egan TJ, Hunter R, Basilico N, Parapini S, Taramelli D, et al. Structure-activity relationships in 4-aminoquinoline antiplasmodials. The role of the group at the 7-position. J Med Chem 2002;45:3531–9.

150. Ray S, Madrid PB, Catz P, Levalley SE, Furniss MJ, Rausch LL, et al. Development of a new generation of 4-aminoquinoline antimalarial compounds using predictive pharmacokinetic and toxicology models. J Med Chem 2010;53:3685–95.

151. Pou S, Winter RW, Nilsen A, Kelly JX, Li Y, Doggett JS, et al. Sontochin as a guide to the development of drugs against chloroquine-resistant malaria. Antimicrob Agents Chemother 2012;56:3475–80.

152. Singh A, Gut J, Rosenthal PJ, Kumar V. 4-Aminoquinoline-ferrocenyl-chalcone conjugates: synthesis and anti-plasmodial evaluation. Eur J Med Chem 2017;125:269–77.

153. Pereira GR, Brandão GC, Arantes LM, de Oliveira HA, de Paula RC, do Nascimento MFA, et al. 7-Chloroquinolinotriazoles: synthesis by the azide-alkyne cycloaddition click chemistry, antimalarial activity, cytotoxicity and SAR studies. Eur J Med Chem 2014;73:295–309.

154. Manohar S, Khan SI, Rawat DS. Synthesis of 4-aminoquinoline-1,2,3-triazole and 4-aminoquinoline-1,2,3-triazole-1,3,5-triazine hybrids as potential antimalarial agents. Chem Biol Drug Des 2011;78:124–36.

155. Guantai EM, Ncokazi K, Egan TJ, Gut J, Rosenthal PJ, Smith PJ, et al. Design, synthesis and *in vitro* antimalarial evaluation of triazole-linked chalcone and dienone hybrid compounds. Bioorg Med Chem 2010;18:8243–56.

156. Boechat N, Ferreira MDLG, Pinheiro LCS, Jesus AML, Leite MMM, Júnior CCS, et al. New compounds hybrids 1*H*-1,2,3-triazole-quinoline against *Plasmodium falciparum*. Chem Biol Drug Des 2014;84:325–32.

157. Singh A, Kalamuddin M, Mohmmed A, Malhotra P, Hoda N. Quinoline-triazole hybrids inhibit falcipain-2 and arrest the development of *Plasmodium falciparum* at the trophozoite stage. RSC Adv 2019;9:39410–21.

158. Kealy TJ, Pauson PL. A new type of organo-iron compound. Nature 1951;168:1039–40.

159. Wilkinson G, Rosenblum M, Whiting MC, Woodward RB. The structure of iron *bis*-cyclopentadienyl. J Am Chem Soc 1952;74:2125–6.

160. Neuse EW. Macromolecular ferrocene compounds as cancer drug models. J Inorg Organomet Polym Mater 2005;15:3–31.

161. Rapić V, Čakić Semenčić M. Organometalna i bioorganometalna kemija – ferocen i metalni karbonili. Kem Ind 2011;60:61–79.

162. Bhatt V. Essentials of coordination chemistry: a simplified approach with 3D visuals. 1st ed. Amsterdam: Elsevier Science; 2015.

163. Pavia DL, Kriz GS, Lampman GM, Engel RG. A small scale approach to organic laboratory techniques. 4th ed. Boston: Cengage Learning; 2015.

164. Woollins JD. Inorganic experiments. 3rd ed. Weinheim: Wiley-VCH; 2010.

165. Roux C, Biot C. Ferrocene-based antimalarials. Future Med Chem 2012;4:783–97.

166. Biot C, Glorian G, Maciejewski LA, Brocard JS, Domarle O, Blampain G, et al. Synthesis and antimalarial activity *in vitro* and *in vivo* of a new ferrocene-chloroquine analogue. J Med Chem 1997;40:3715–8.

167. Delhaes L, Biot C, Berry L, Delcourt P, Maciejewski LA, Camus D, et al. Synthesis of ferroquine enantiomers: first investigation of effects of metallocenic chirality upon antimalarial activity and cytotoxicity. Chembiochem 2002;3:418-23.

168. Wani WA, Jameel E, Baig U, Mumtazuddin S, Hun LT. Ferroquine and its derivatives: new generation of antimalarial agents. Eur J Med Chem 2015;101:534–51.

169. Wells TN, van Huijsduijnen RH. Ferroquine: welcome to the next generation of antimalarials. Lancet Infect Dis 2015;15:1365–6.

170. Biot C, Taramelli D, Forfar-Bares I, Maciejewski LA, Boyce M, Nowogrocki G, et al. Insights into the mechanism of action of ferroquine. Relationship between physicochemical properties and antiplasmodial activity. Mol Pharm 2005;2:185–93.

171. Patra M, Gasser G. The medicinal chemistry of ferrocene and its derivatives. Nat Rev Chem 2017;1:0066.

172. Biot C, Chavain N, Dubar F, Pradines B, Trivelli X, Brocard J, et al. Structure-activity relationships of 4-*N*-substituted ferroquine analogues: time to re-evaluate the mechanism of action of ferroquine. J Organomet Chem 2009;694:845–54.

173. Biot C, Daher W, Chavain N, Fandeur T, Khalife J, Dive D, et al. Design and synthesis of hydroxyferroquine derivatives with antimalarial and antiviral activities. J Med Chem 2006;49:2845–9.

174. Bellot F, Coslédan F, Vendier L, Brocard J, Meunier B, Robert A. Trioxaferroquines as new hybrid antimalarial drugs. J Med Chem 2010;53:4103–9.

175. Salas PF, Herrmann C, Cawthray JF, Nimphius C, Kenkel A, Chen J, et al. Structural characteristics of chloroquine-bridged ferrocenophane analogues of ferroquine may obviate malaria drug-resistance mechanisms. J Med Chem 2013;56:1596–613.

176. Top S, Tang J, Vessières A, Carrez D, Provot C, Jaouen G. Ferrocenyl hydroxytamoxifen: a prototype for a new range of oestradiol receptor site-directed cytotoxics. ChemComm 1996;8:955–6.

177. Vessières A, Corbet C, Heldt JM, Lories N, Jouy N, Laïos I, et al. A ferrocenyl derivative of hydroxytamoxifen elicits an estrogen receptor-independent mechanism of action in breast cancer cell lines. J Inorg Biochem 2010;104:503–11.

178. De Oliveira AC, Hillard EA, Pigeon P, Rocha DD, Rodrigues FAR, Montenegro RC, et al. Biological evaluation of twenty-eight ferrocenyl tetrasubstituted olefins: cancer cell growth inhibition, ROS production and hemolytic activity. Eur J Med Chem 2011;46:3778–87.

179. Hillard E, Vessières A, Thouin L, Jaouen G, Amatore C. Ferrocene-mediated proton-coupled electron transfer in a series of ferrocifen-type breast-cancer drug candidates. Angew Chem Int Ed Engl 2005;45:285–90.

180. Michard Q, Jaouen G, Vessieres A, Bernard BA. Evaluation of cytotoxic properties of organometallic ferrocifens on melanocytes, primary and metastatic melanoma cell lines. J Inorg Biochem 2008;102:1980–5.

181. Allard E, Passirani C, Garcion E, Pigeon P, Vessières A, Jaouen G, et al. Lipid nanocapsules loaded with an organometallic tamoxifen derivative as a novel drug-carrier system for experimental malignant gliomas. J Control Release 2008;130:146–53.

182. Citta A, Folda A, Bindoli A, Pigeon P, Top S, Vessières A, et al. Evidence for targeting thioredoxin reductases with ferrocenyl quinone methides. A possible molecular basis for the antiproliferative effect of hydroxyferrocifens on cancer cells. J Med Chem 2014;57:8849–59.

183. Bruyère C, Mathieu V, Vessières A, Pigeon P, Top S, Jaouen G, et al. Ferrocifen derivatives that induce senescence in cancer cells: selected examples. J Inorg Biochem 2014;141:144–51.

184. Cázares-Marinero JDJ, Buriez O, Labbé E, Top S, Amatore C, Jaouen G. Synthesis, characterization, and antiproliferative activities of novel ferrocenophanic suberamides against human triple-negative MDA-MB-231 and hormone-dependent MCF-7 breast cancer cells. Organometallics 2013;32:5926–34.

185. Sharma B, Kumar V. Has ferrocene really delivered its role in accentuating the bioactivity of organic scaffolds? J Med Chem 2021;64:16865–921.

186. Graciano IA, de Carvalho AS, de Carvalho da Silva F, Ferreira VF. 1,2,3-Triazole- and quinoline-based hybrids with potent antiplasmodial activity. Med Chem 2022;18:521–35.

187. Haldón E, Nicasio MC, Pérez PJ. Copper-catalysed azide-alkyne cycloadditions (CuAAC): an update. Org Biomol Chem 2015;13:9528–50.

188. Krzywik J, Nasulewicz-Goldeman A, Mozga W, Wietrzyk J, Huczyński A. Novel double-modified colchicine derivatives bearing 1,2,3-triazole: design, synthesis, and biological activity evaluation. ACS Omega 2021;6:26583–600.

189. Kolb HC, Finn MG, Sharpless KB. Click chemistry: diverse chemical function from a few good reactions. Angew Chem Int Ed Engl 2001;40:2004-21.

190. Saftić D, Krstulović L, Bajić Žinić MB. 1,3-Dipolarna cikloadicija (I. dio): dobivanje 1,2,3-triazolnih derivata u nukleozidnoj kemiji. Kem Ind 2015;64:481−98.

191. Sumanadasa SDM, Goodman CD, Lucke AJ, Skinner-Adams T, Saham I, Haque A, et al. Antimalarial activity of the anticancer histone deacetylase inhibitor SB939. Antimicrob Agents Chemother 2012;56:3849-56.

192. Singh V, Hutait S, Batra S. Baylis–Hillman reaction of 1-formyl-β-carboline: one-step synthesis of the canthin-6-one framework by an unprecedented cascade cyclization reaction. Eur J Org Chem 2009;2009:6211–6.

193. Singh D, Hazra CK, Malakar CC, Pandey SK, Kaith BS, Singh V. Indium-mediated domino allylation-lactonisation approach: diastereoselective synthesis of β-carboline C-3 tethered α-methylene γ-butyrolactones. ChemistrySelect 2018;3:4859–64.

194. Bálint B, Wéber C, Cruzalegui F, Burbridge M, Kotschy A. Structure-based design and synthesis of harmine derivatives with different selectivity profiles in kinase versus monoamine oxidase inhibition. ChemMedChem 2017;12:932–9.

195. Coghi P, Ng JPL, Nasim AA, Wong VKW. *N*-[7-chloro-4-[4-(phenoxymethyl)-1*H*-1,2,3-triazol-1-yl]quinoline]-acetamide. Molbank 2021;2021:M1213.

196. Terzić N, Konstantinović J, Tot M, Burojević J, Djurković-Djaković O, Srbljanović J, et al. Reinvestigating old pharmacophores: are 4-aminoquinolines and tetraoxanes potential two-stage antimalarials? J Med Chem 2016;59:264–81.

197. Starčević K, Pešić D, Toplak A, Landek G, Alihodžić S, Herreros E, et al. Novel hybrid molecules based on 15-membered azalide as potential antimalarial agents. Eur J Med Chem 2012;49:365–78.

198. Beus M, Fontinha D, Held J, Rajić Z, Uzelac L, Kralj M, et al. Primaquine and chloroquine fumardiamides as promising antiplasmodial agents. Molecules 2019; 24:2812.

199. Chiyanzu I, Clarkson C, Smith PJ, Lehman J, Gut J, Rosenthal PJ, et al. Design, synthesis and anti-plasmodial evaluation in vitro of new 4-aminoquinoline isatin derivatives. Bioorg Med Chem 2005;13:3249–61.

200. Tremmel T, Bracher F. New approaches to the synthesis of canthin-4-one alkaloids and synthetic analogues. Tetrahedron 2015;71:4640–6.

201. Lin G, Wang Y, Zhou Q, Tang W, Wang J, Lu T. A facile synthesis of 1-substituted βcarboline derivatives via minisci-reaction. Synth Commun 2011;41:3541–50.

202. Goddard-Borger ED, Stick RV. An efficient, inexpensive, and shelf-stable diazotransfer reagent: imidazole-1-sulfonyl azide hydrochloride. Org Lett 2007;9:3797–800.

203. Pavić K, Beus M, Poje G, Uzelac L, Kralj M, Rajić Z. Synthesis and biological evaluation of harmirins, novel harmine–coumarin hybrids as potential anticancer agents. Molecules 2021;26:6490.

204. Held J, Gebru T, Kalesse M, Jansen R, Gerth K, Müller R, et al. Antimalarial activity of the myxobacterial macrolide chlorotonil A. Antimicrob Agents Chemother 2014;58:6378–84.

205. Noedl H, Bronnert J, Yingyuen K, Attlmayr B, Kollaritsch H, Fukuda M. Simple histidine-rich protein 2 double-site sandwich enzyme-linked immunosorbent assay for use in malaria drug sensitivity testing. Antimicrob Agents Chemother 2005;49:3575–7.

206. Machado M, Sanches-Vaz M, Cruz JP, Mendes AM, Prudêncio M. Inhibition of *Plasmodium* hepatic infection by antiretroviral compounds. Front Cell Infect Microbiol 2017;7:329.

207. Ploemen IHJ, Prudêncio M, Douradinha BG, Ramesar J, Fonager J, van Gemert GJ, et al. Visualisation and quantitative analysis of the rodent malaria liver stage by real time imaging. PLoS One 2009 Nov 18;4:e7881.

208. Habrant D, Rauhala V, Koskinen AMP. Conversion of carbonyl compounds to alkynes: general overview and recent developments. Chem Soc Rev 2010;39:2007–17.

209. Michel P, Gennet D, Rassat A. A one-pot procedure for the synthesis of alkynes and bromoalkynes from aldehydes. Tetrahedron Lett 1999;40:8575–8.

210. Morri AK, Thummala Y, Doddi VR. The dual role of 1,8-diazabicyclo[5.4.0]undec-7-ene (DBU) in the synthesis of terminal aryl- and styryl-acetylenes via umpolung reactivity. Org Lett 2015;17:4640–3.

211. Ohira S. Methanolysis of dimethyl (1-diazo-2-oxopropyl) phosphonate: generation of dimethyl (diazomethyl) phosphonate and reaction with carbonyl compounds. Synth Commun 1989;19:561–4.

212. Kitamura M, Koga T, Yano M, Okauchi T. Direct synthesis of organic azides from alcohols using 2-azido-1,3- dimethylimidazolinium hexafluorophosphate. Synlett 2012;23:1335–8.

213. Kitamura M, Yano M, Tashiro N, Miyagawa S, Sando M, Okauchi T. Direct synthesis of organic azides from primary amines with 2-azido-1,3-dimethylimidazolinium hexafluorophosphate. Eur J Org Chem 2011;2011:458–62.

214. Davidson A, Foley DA, Frericks-Schmidt H, Ruggeri SG, Herman M, Lacasse S, et al. pH-dependent degradation of T3P-related byproducts. Org Process Res Dev 2021;25:621–6.

215. Di L, Kerns E, Carter G. Drug-like property concepts in pharmaceutical design. Curr Pharm Des 2009;15:2184–94.

216. Lipinski CA. Lead- and drug-like compounds: the rule-of-five revolution. Drug Discov Today Technol 2004;1:337–41.

217. Lipinski CA, Lombardo F, Dominy BW, Feeney PJ. Experimental and computational approaches to estimate solubility and permeability in drug discovery and development settings. Adv Drug Deliv Rev 1997;23:3–25.

218. Lipinski CA. Drug-like properties and the causes of poor solubility and poor permeability. J Pharmacol Toxicol Methods 2000;44:235–49.

219. Veber DF, Johnson SR, Cheng HY, Smith BR, Ward KW, Kopple KD. Molecular properties that influence the oral bioavailability of drug candidates. J Med Chem 2002;45:2615–23.

220. Luzina EL, Popov AV. Synthesis, evaluation of anticancer activity and COMPARE analysis of *N*-*bis*(trifluoromethyl)alkyl-*N*'-substituted ureas with pharmacophoric moieties. Eur J Med Chem 2012;53:364–73.

221. Chemicalize - Instant Cheminformatics Solutions. Preuzeto s: https://chemicalize.com/welcome (pristupljeno: 20. svibnja 2022.)

222. SwissADME. Preuzeto s: http://www.swissadme.ch/ (pristupljeno: 25. svibnja 2022.)

7. ŽIVOTOPIS

Goran Poje rođen je u Rijeci 3. travnja 1994. godine. Osnovnu školu i opću gimnaziju završio je u Čabru, a 2013. godine upisao je integrirani preddiplomski i diplomski studij farmacije na Farmaceutsko-biokemijskom fakultetu Sveučilišta u Zagrebu. Diplomski rad pod naslovom „Sinteza hidroksamske kiseline hibrida primakina i cimetne kiseline“ izradio je u Zavodu za farmaceutsku kemiju Farmaceutsko-biokemijskog fakulteta Sveučilišta u Zagrebu pod mentorstvom izv. prof. dr. sc. Zrinke Rajić. Studij je završio u rujnu 2018. godine polaganjem stručnog ispita za magistre farmacije čime je stekao naslov magistar farmacije i odobrenje za samostalni rad u ljekarničkoj djelatnosti. Od listopada 2018. godine zaposlen je kao asistent na projektu u Zavodu za farmaceutsku kemiju Farmaceutsko-biokemijskog fakulteta Sveučilišta u Zagrebu, u sklopu uspostavnog istraživačkog projekta „Derivati harmina kao potencijalni antimalarici“ financiranog sredstvima Hrvatske zaklade za znanost. Sudjeluje u izvođenju nastave iz kolegija Farmaceutska kemija 1 i Biokemija lijekova. Poslijediplomski doktorski studij Farmaceutsko-biokemijske znanosti (grana Farmacija) upisao je 2018. godine. Od akademske godine 2019./2020. predstavnik je studenata poslijediplomskog doktorskog studija u Studentskom zboru i Fakultetskom vijeću Farmaceutsko-biokemijskog fakulteta. Od 2014. do 2020. godine bio je voditelj priprema za državnu maturu iz kemije u Župi Marije Pomoćnice, Knežija. Član je Hrvatske ljekarničke komore i Hrvatskog kemijskog društva.

Objavio je 4 znanstvena i 2 stručna rada te aktivno sudjelovao na međunarodnim i domaćim znanstvenim skupovima s 2 usmena i 17 posterskih priopćenja. Bio je neposredni voditelj 6 diplomskih i 2 studentska rada. Održao je nekoliko radionica na Danima otvorenih vrata Farmaceutsko-biokemijskog fakulteta i Festivalu znanosti.

Znanstveni radovi (CC):

1) Marinović M, Poje G, Perković I, Fontinha D, Prudêncio M, Held J, et al. Further investigation of harmicines as novel antiplasmodial agents: Synthesis, structure-activity relationship and insight into the mechanism of action. Eur J Med Chem 2021;224:113687.

2) Pavić K, Beus M, Poje G, Uzelac L, Kralj M, Rajić Z. Synthesis and Biological Evaluation of Harmirins, Novel Harmine-Coumarin Hybrids as Potential Anticancer Agents. Molecules 2021;26:6490.

3) Poje G, Pessanha de Carvalho L, Held J, Moita D, Prudêncio M, Perković I, et. al. Design and synthesis of harmiquins, harmine and chloroquine hybrids as potent antiplasmodial agents. Eur J Med Chem 2022;238:114408.

4) Poje G, Marinović M, Pavić K, Mioč M, Kralj M, Pessanha de Carvalho L, Held J, Perković I, Rajić Z. Harmicens, novel harmine and ferrocene hybrids: design, synthesis and biological activity. Int J Mol Sci 2022;23:9315.

PRILOG A

Prilog sadrži IR, NMR i MS spektre harmicina, harmikina i harmicena opisanih u ovom doktorskom radu.

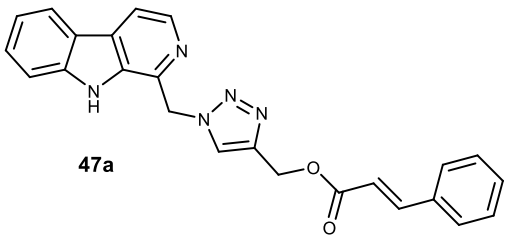

47a

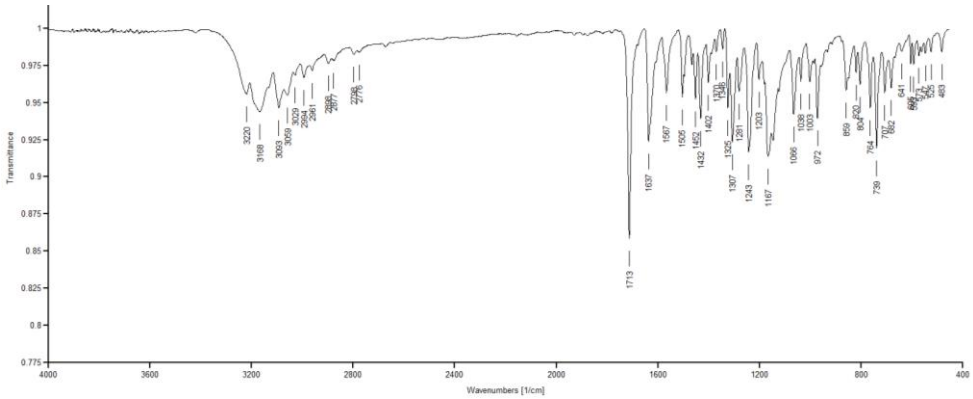
Transmittance
Wavenumbers [1/cm]
3220
3168
3053
3009
2941
2886
2877
2776
1713
1637
1567
1505
1452
1432
1402
1361
1325
1307
1281
1243
1203
1167
1086
1038
1033
972
859
802
764
739
702
641
493

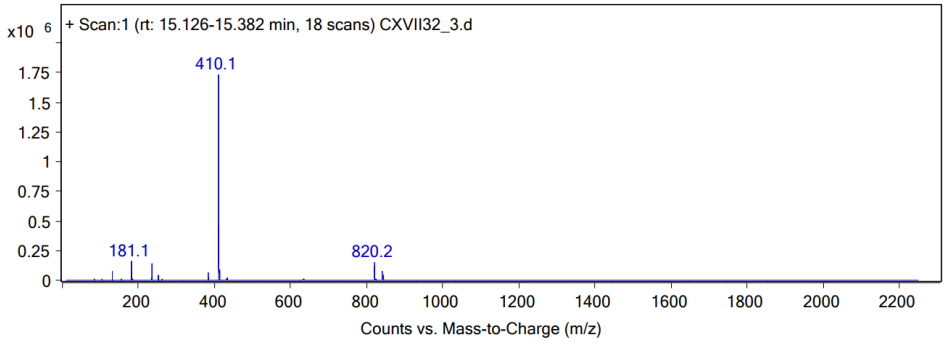
x10 6
+ Scan:1 (rt: 15.126-15.382 min, 18 scans) CXVII32_3.d
410.1
181.1
820.2
Counts vs. Mass-to-Charge (m/z)

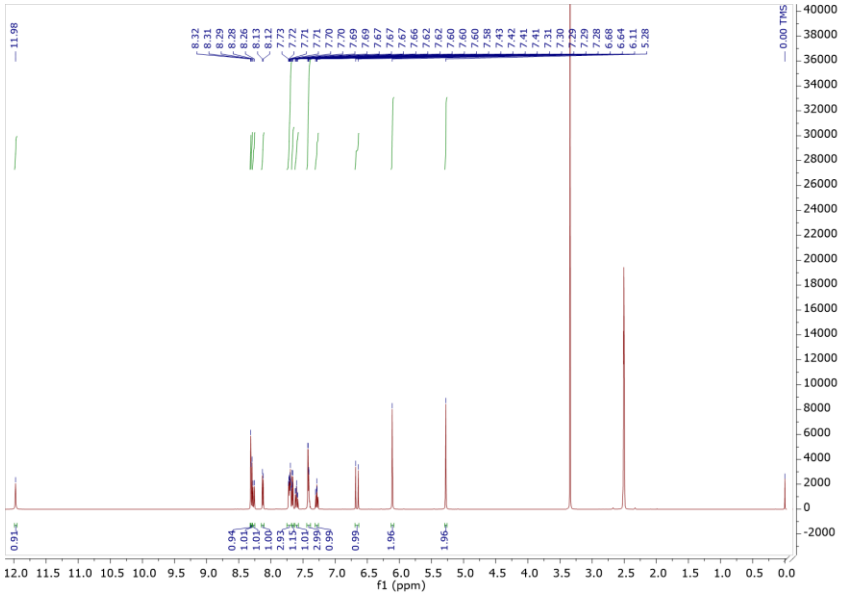
11.98
0.00 TMS
f1 (ppm)

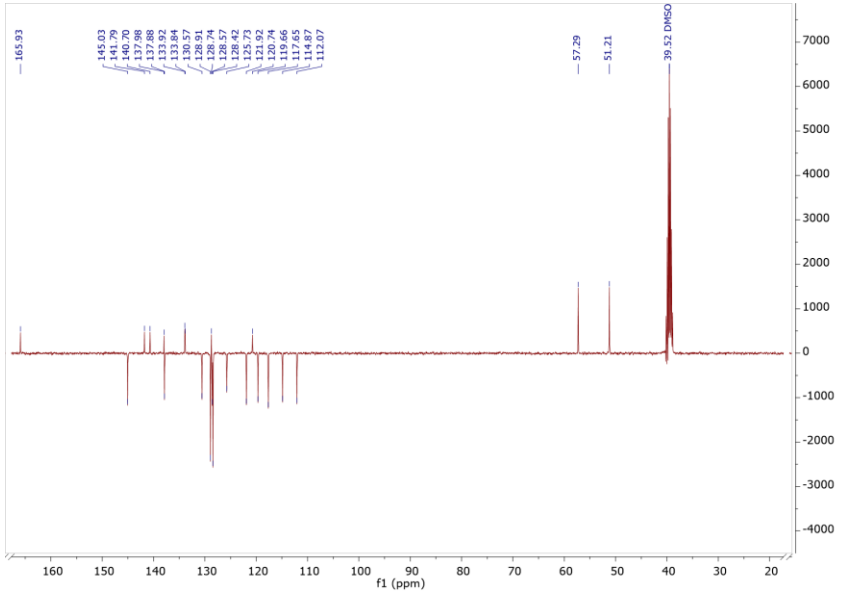
165.93
145.03
141.79
140.70
137.98
137.88
133.92
133.84
130.57
129.81
128.74
128.57
128.42
125.73
121.92
120.74
117.66
117.65
114.87
112.07
57.29
51.21
39.52 DMSO
f1 (ppm)

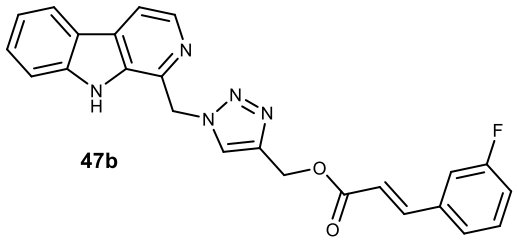
N
H
N
N
N
O
O
F

47b

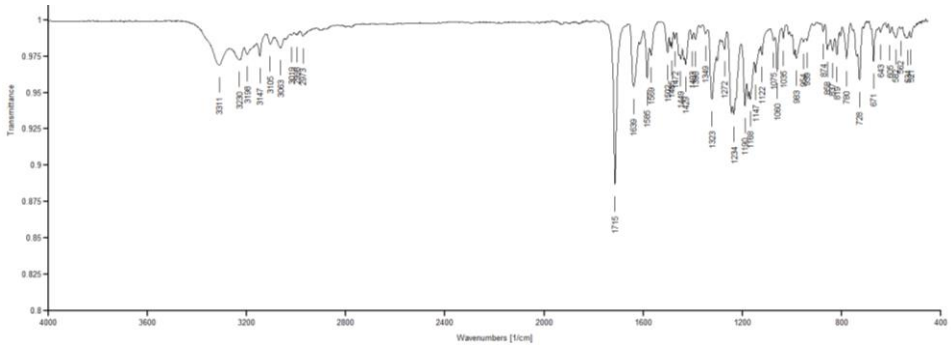
Transmittance
Wavenumbers [1/cm]
4000
3600
3200
2800
2400
2000
1600
1200
800
400

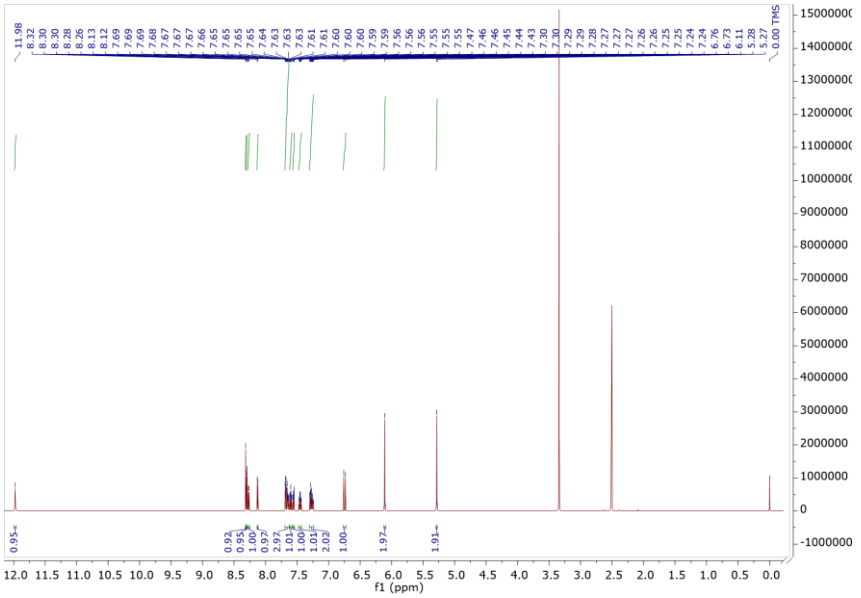
f1 (ppm)

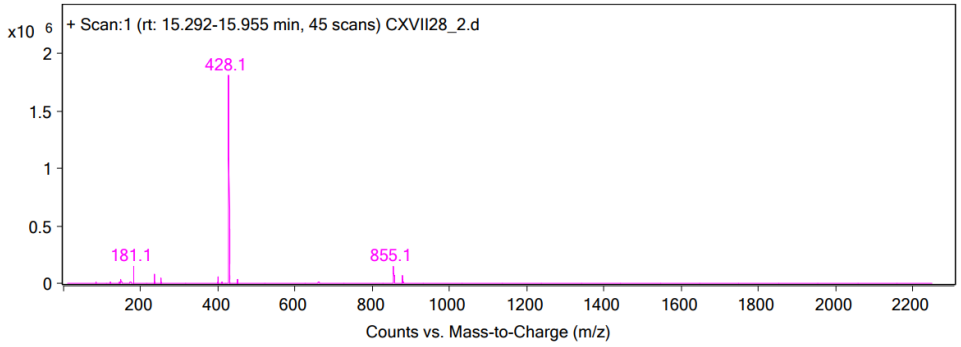
x10 6
+ Scan:1 (rt: 15.292-15.955 min, 45 scans) CXVII28_2.d
428.1
181.1
855.1
Counts vs. Mass-to-Charge (m/z)

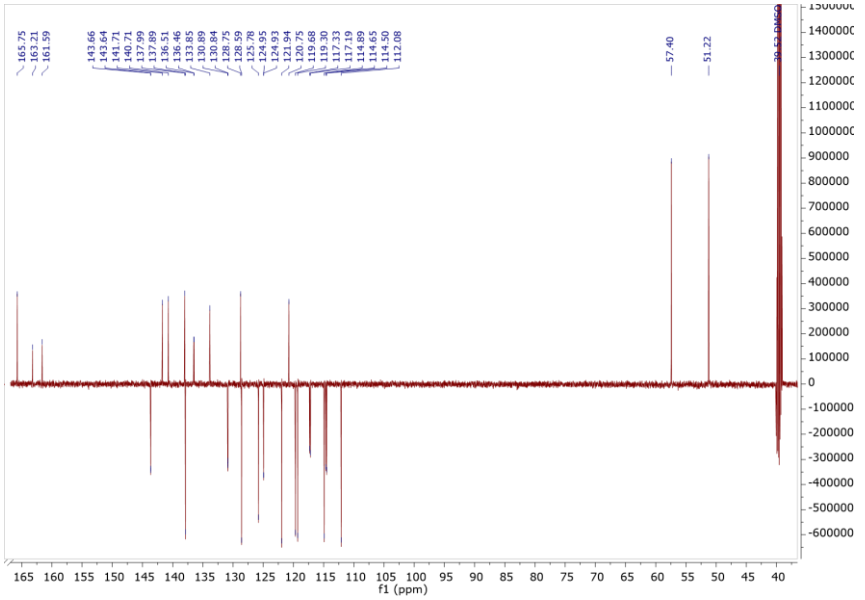
57.40
51.22
f1 (ppm)

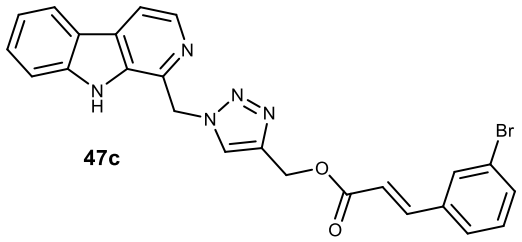
47c
Br
N
H
N
N
N
O
O

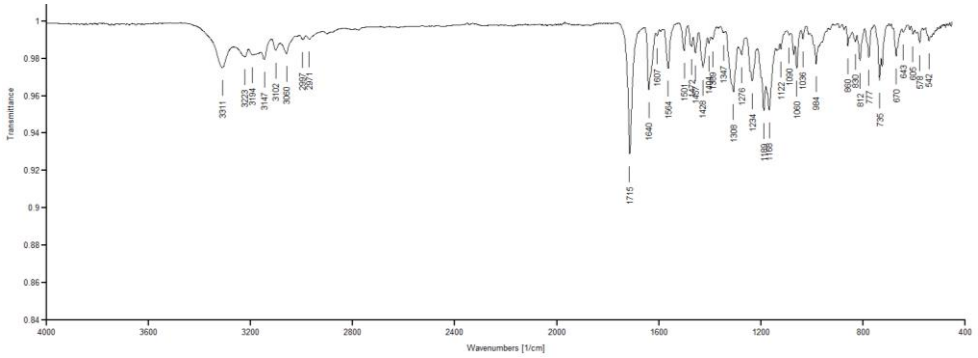
Transmittance
Wavenumbers [1/cm]
3311
3223
3154
3147
3102
3060
2951
2851
1715
1640
1607
1564
1501
1487
1428
1347
1308
1276
1234
1188
1122
1060
1036
984
890
850
812
777
735
670
643
605
578
542

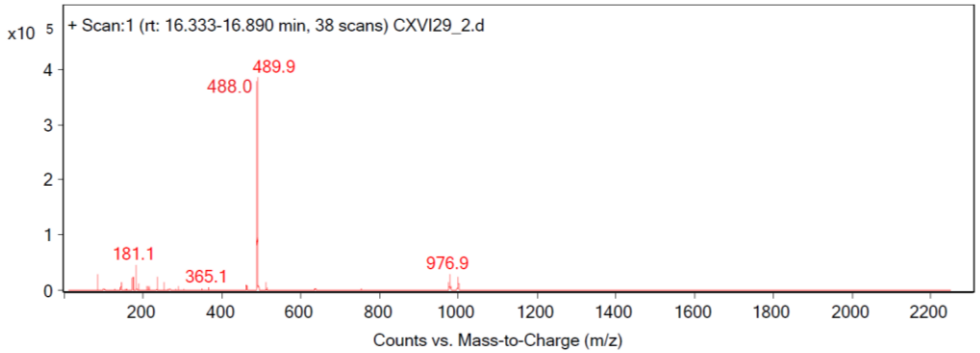
x10 5
+ Scan:1 (rt: 16.333-16.890 min, 38 scans) CXVI29_2.d
489.9
488.0
181.1
365.1
976.9
Counts vs. Mass-to-Charge (m/z)

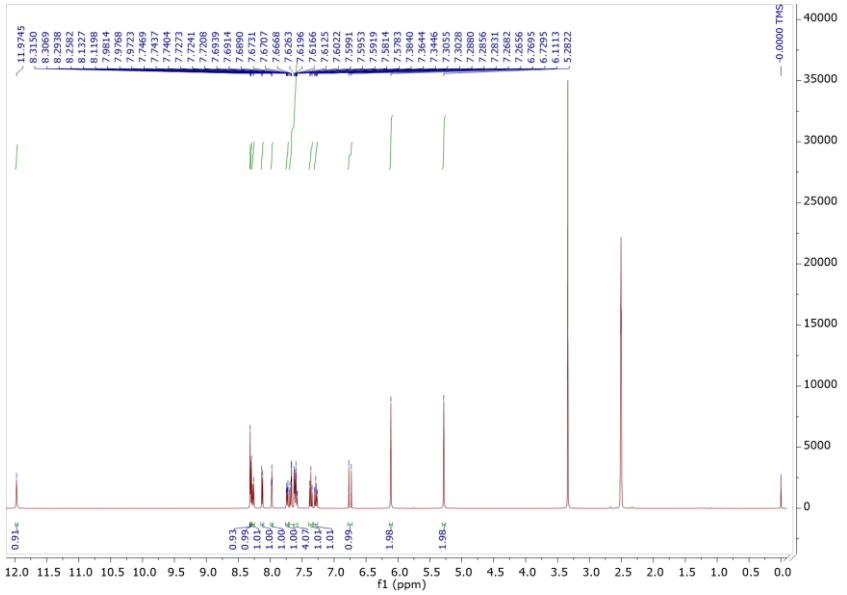
11.9745
8.3150
8.3069
8.2938
8.2382
8.2327
8.1198
7.9814
7.9768
7.9723
7.7469
7.7437
7.7404
7.7273
7.7241
7.7208
7.6939
7.6914
7.6890
7.6731
7.6700
7.6669
7.6263
7.6196
7.6166
7.6125
7.6022
7.5991
7.5955
7.5919
7.5814
7.5783
7.3840
7.3644
7.3446
7.3255
7.3028
7.2880
7.2856
7.2831
7.2682
7.2656
6.7695
6.2935
6.1113
5.2822
-0.0000 TMS
f1 (ppm)

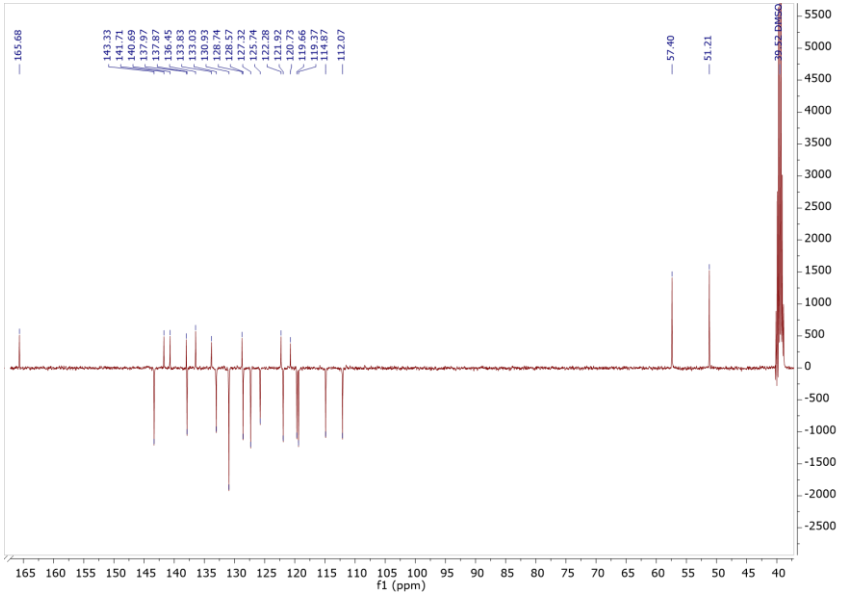
165.68
143.33
141.71
140.69
137.97
137.87
136.45
133.83
133.03
130.93
128.74
128.57
127.32
125.74
122.28
121.32
120.73
119.66
119.37
114.87
112.07
57.40
51.21
39.53 DMSO
f1 (ppm)

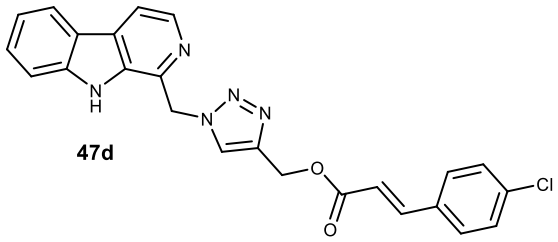
47d
N
H
N
N
N
O
O
Cl

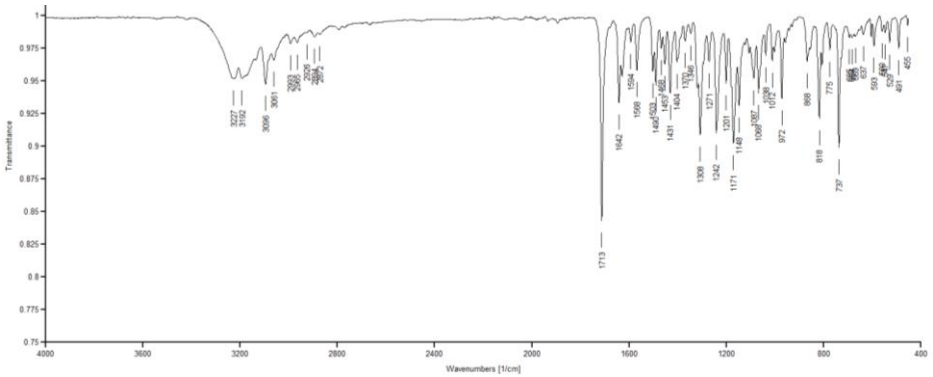
Transmittance
Wavenumbers [1/cm]

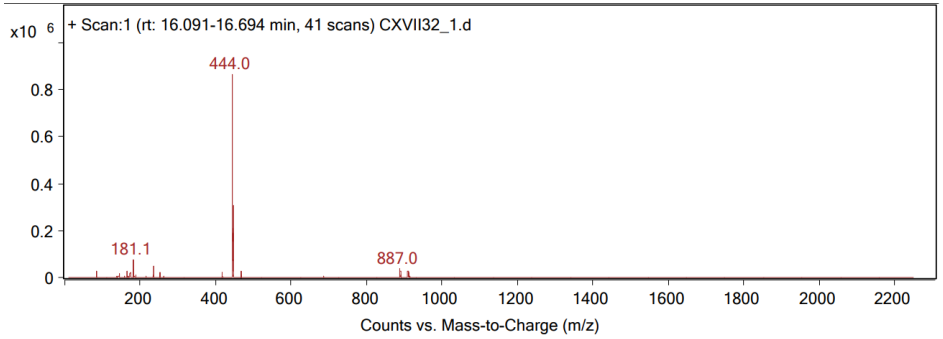
x10 6
+ Scan:1 (rt: 16.091-16.694 min, 41 scans) CXVII32_1.d
444.0
181.1
887.0
Counts vs. Mass-to-Charge (m/z)

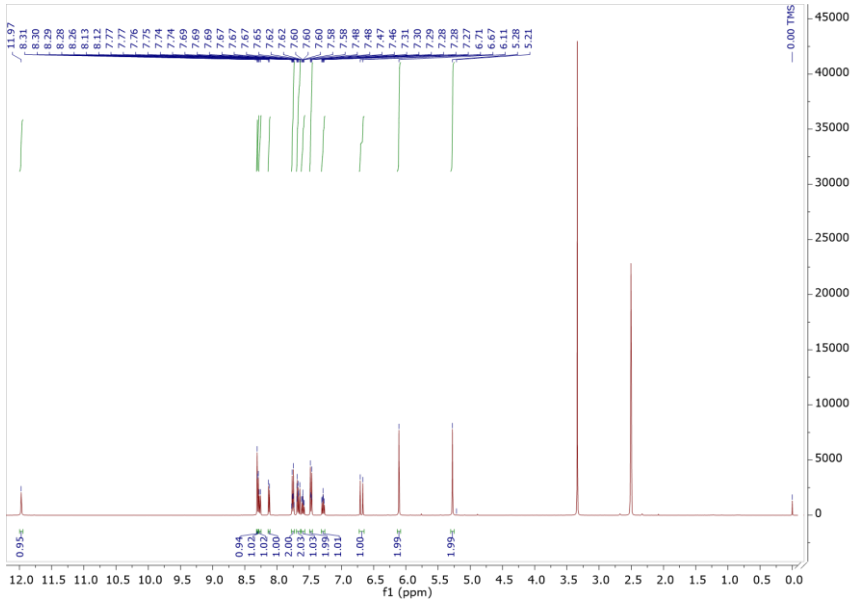
0.00 TMS
f1 (ppm)

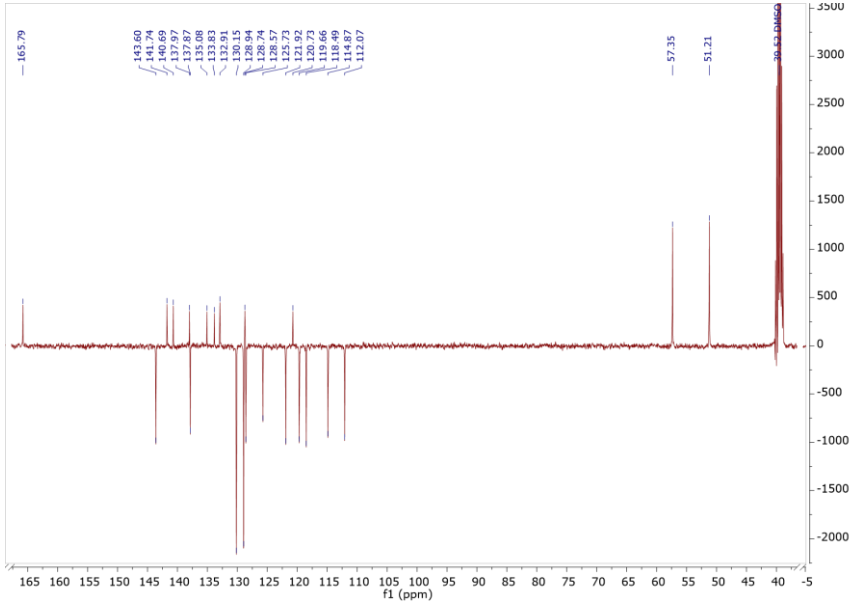
165.79
143.60
141.74
140.69
137.97
137.87
135.08
133.83
132.91
130.15
129.94
128.74
128.57
125.73
121.92
120.73
119.66
118.49
114.87
112.07
57.35
51.21
f1 (ppm)

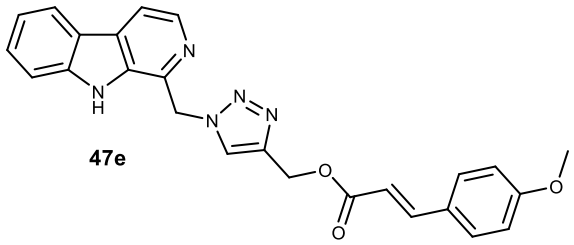

47e

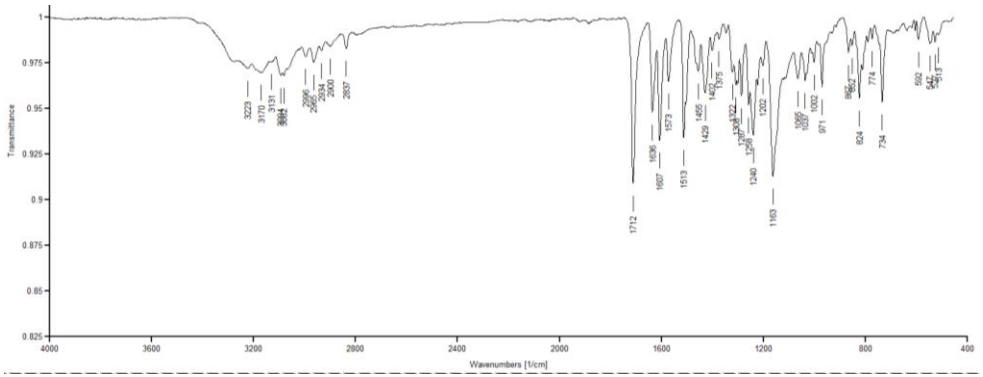
Transmittance
Wavenumbers [1/cm]

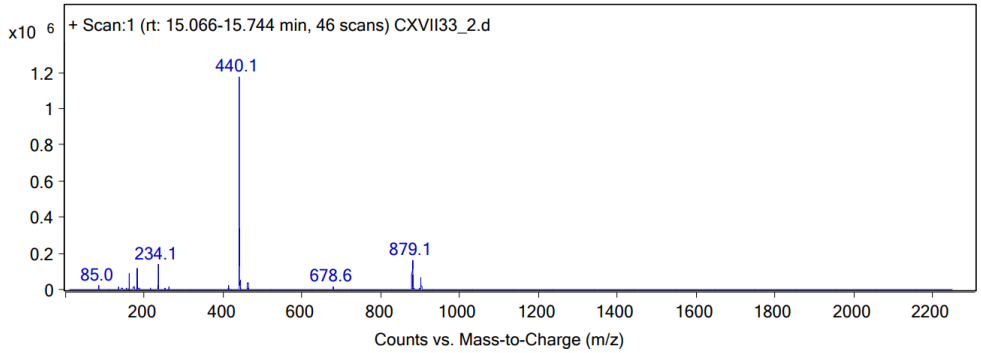
x10 6
+ Scan:1 (rt: 15.066-15.744 min, 46 scans) CXVII33_2.d
440.1
234.1
85.0
678.6
879.1
Counts vs. Mass-to-Charge (m/z)

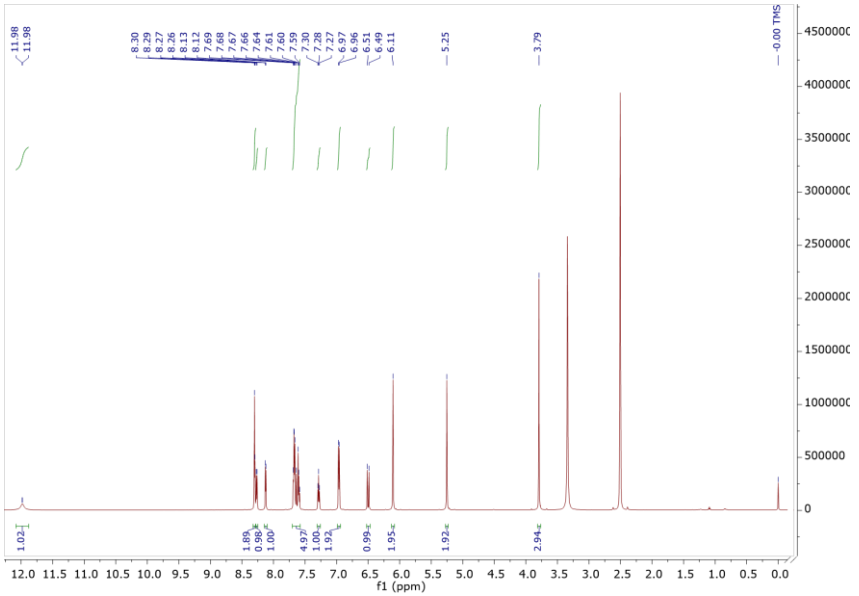
f1 (ppm)

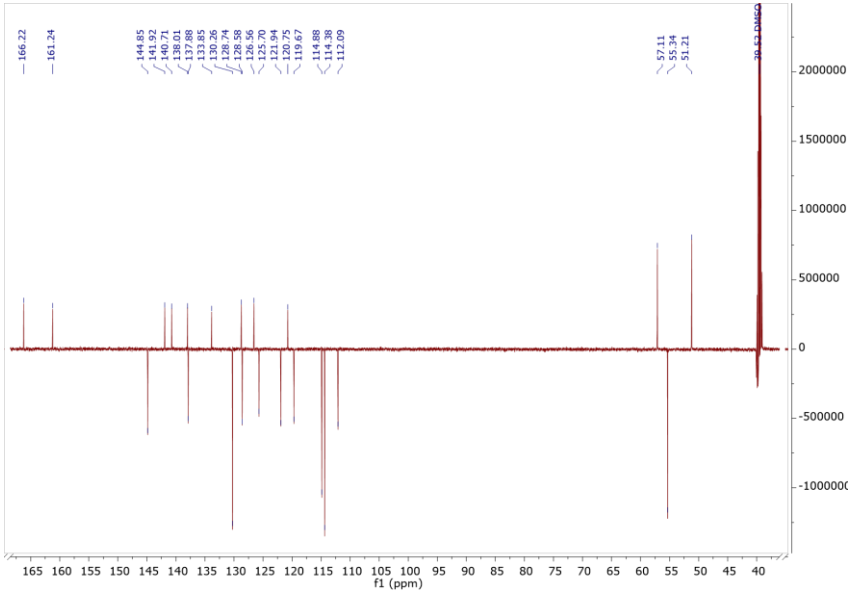
f1 (ppm)

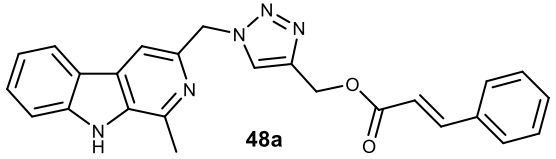

48a

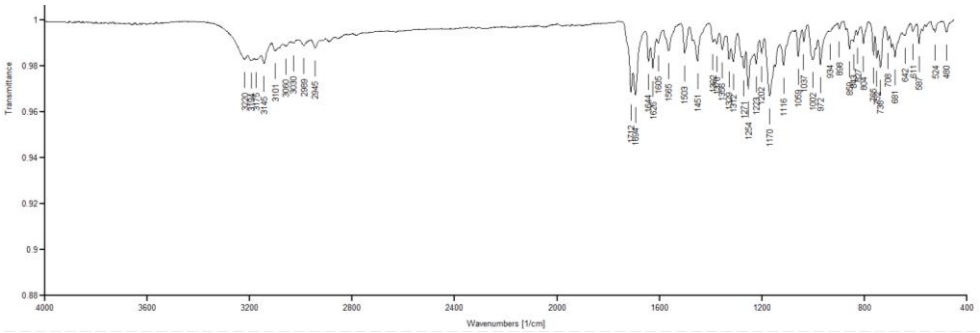

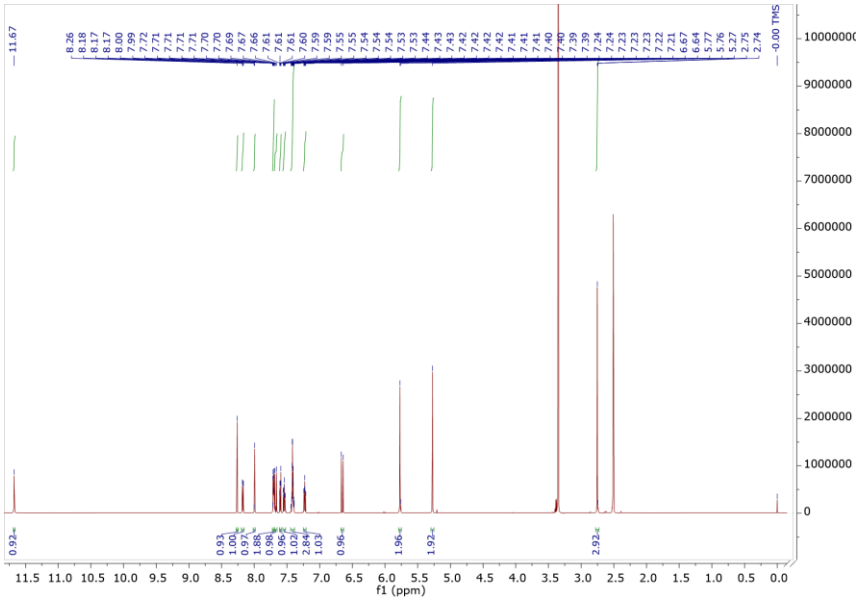

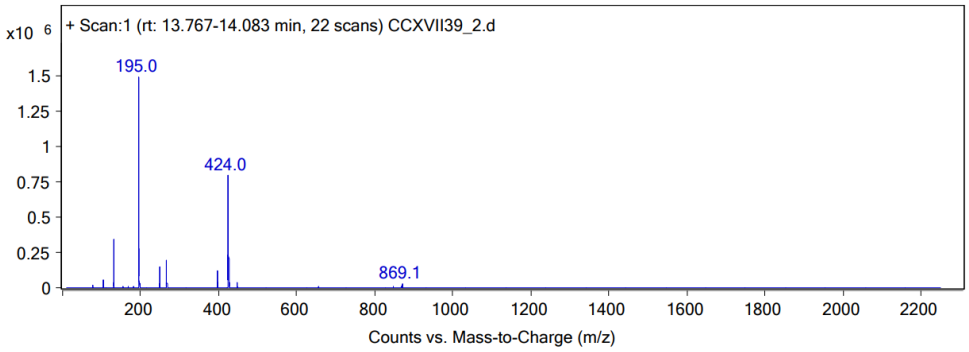
+ Scan:1 (rt: 13.767-14.083 min, 22 scans) CCXVII39_2.d
x10 6
195.0
424.0
869.1
Counts vs. Mass-to-Charge (m/z)

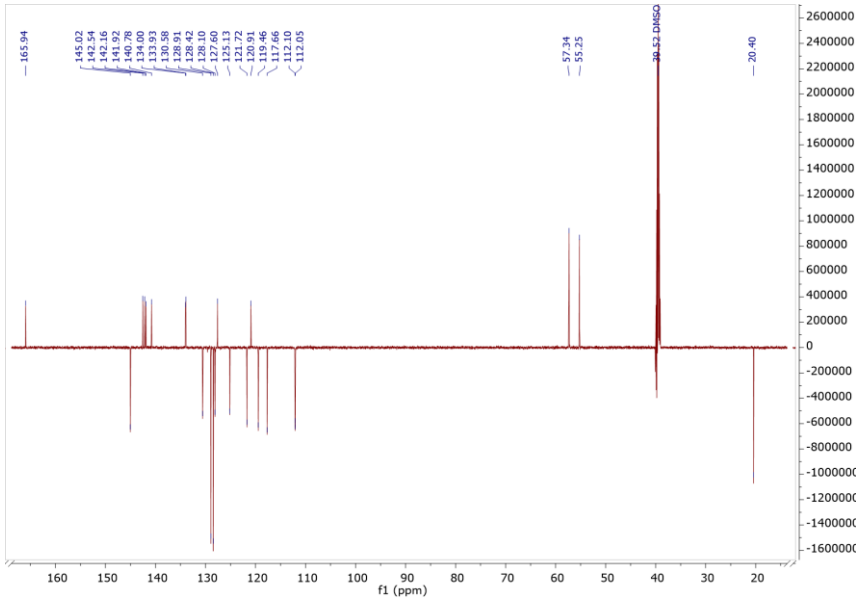

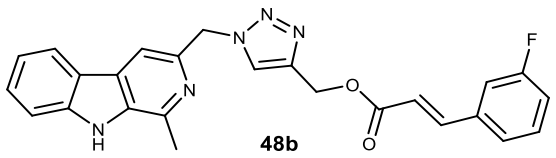
F
N
N
N
O
O
N
H

48b

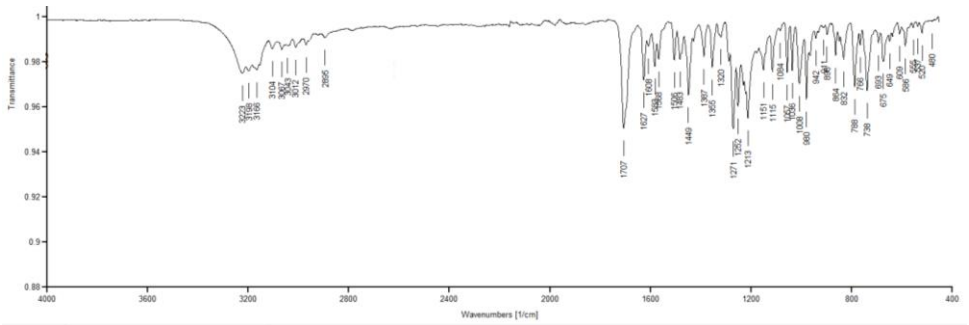
Transmittance
Wavenumbers [1/cm]

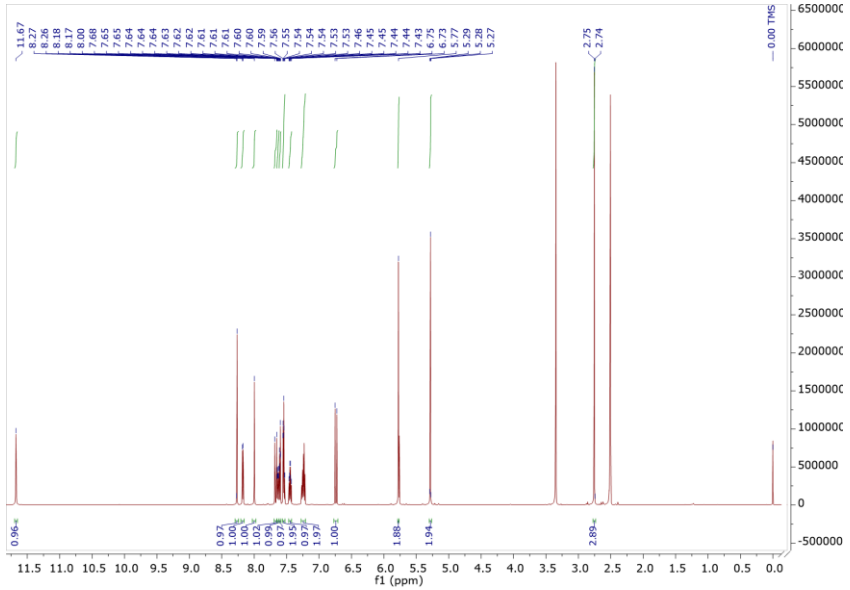
f1 (ppm)

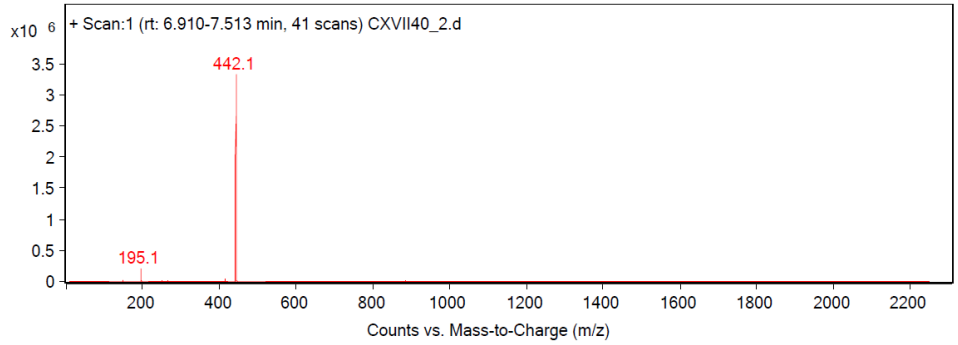
x10 6
+ Scan:1 (rt: 6.910-7.513 min, 41 scans) CXVII40_2.d
442.1
195.1
Counts vs. Mass-to-Charge (m/z)

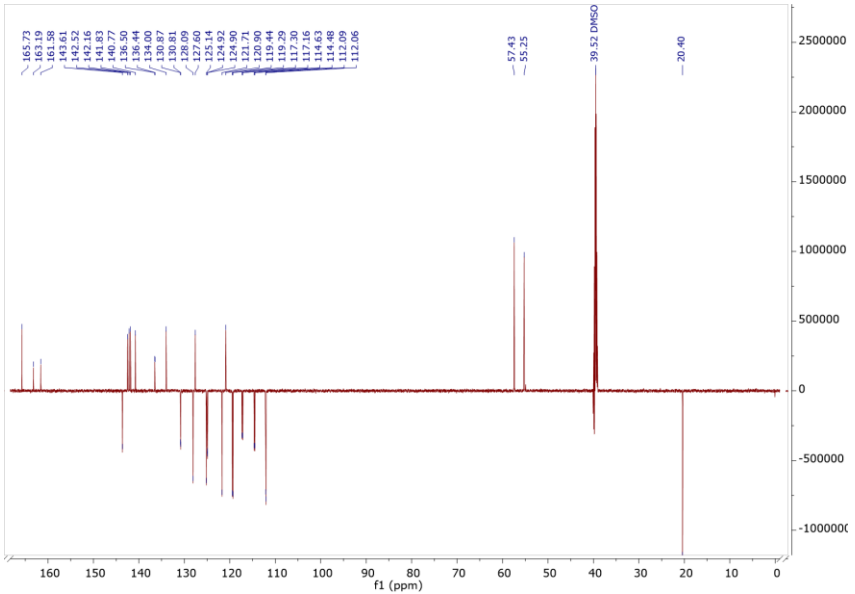
39.52 DMSO
f1 (ppm)

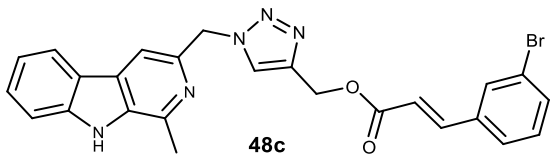
Br
N
N
N
O
O
N
H

48c

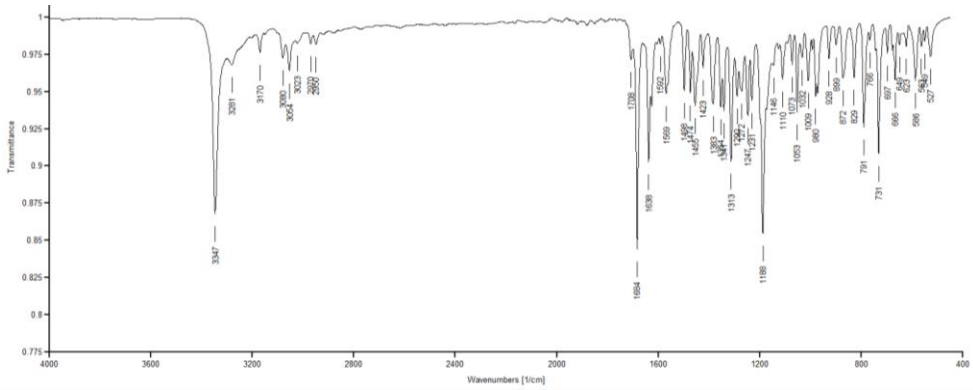
Transmittance
Wavenumbers [1/cm]

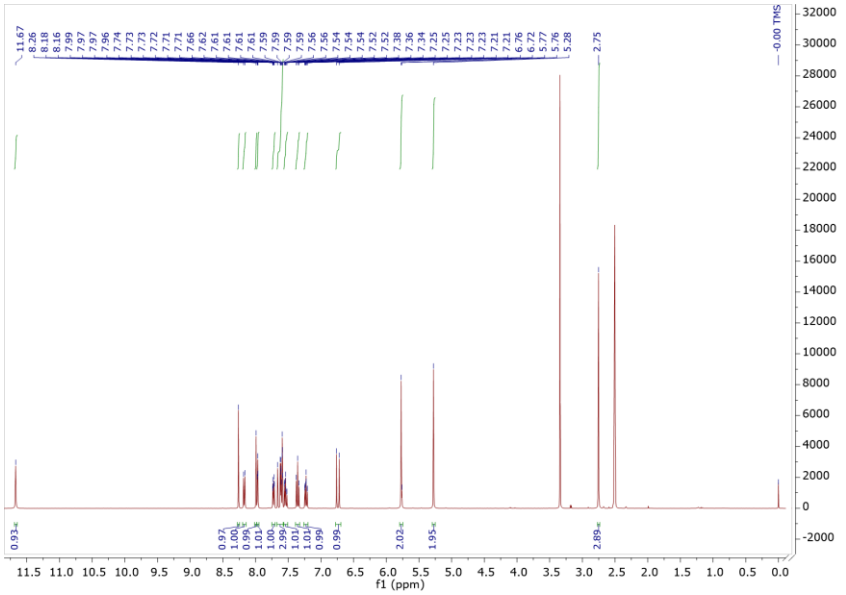
f1 (ppm)

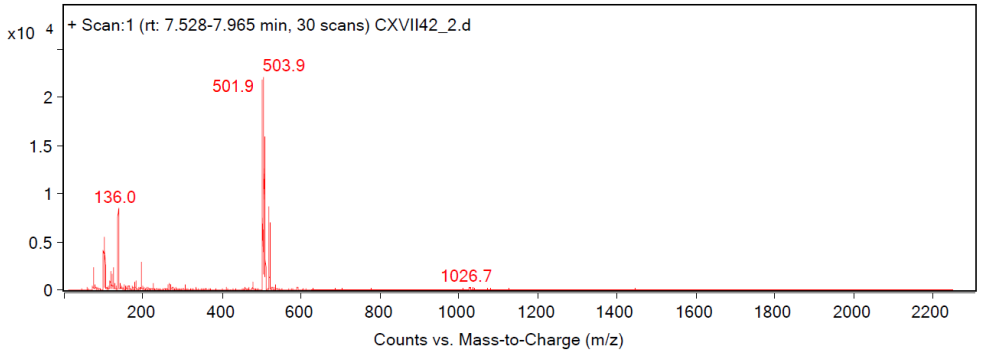
x10 4
+ Scan:1 (rt: 7.528-7.965 min, 30 scans) CXVII42_2.d
503.9
501.9
136.0
1026.7
Counts vs. Mass-to-Charge (m/z)

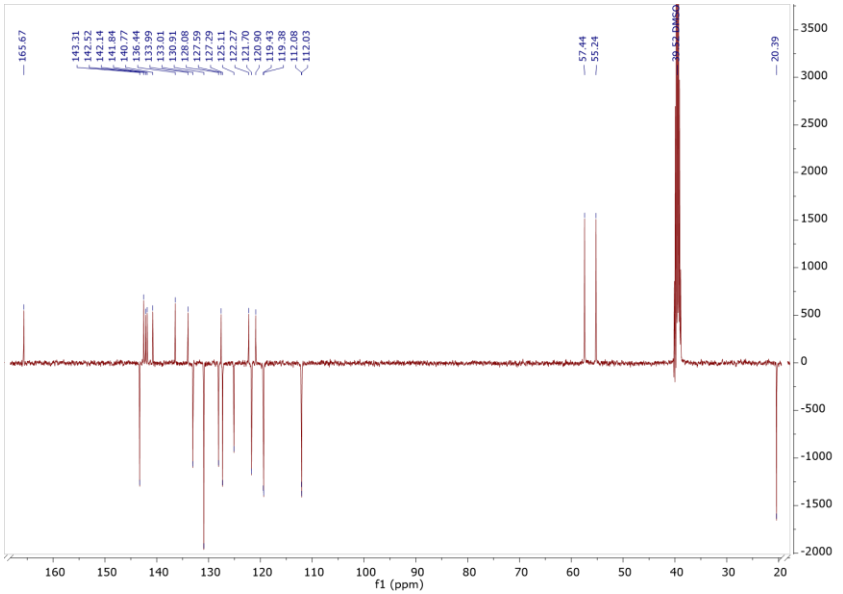
f1 (ppm)

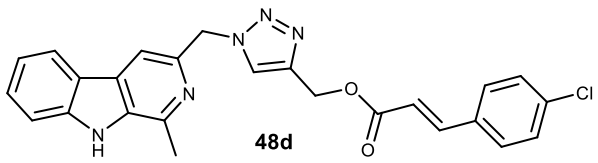
N
N
N
H
O
O
Cl

48d

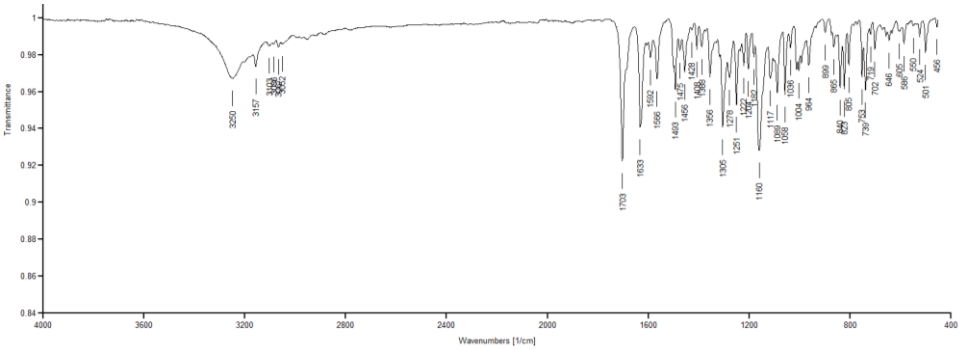
Transmittance
Wavenumbers [1/cm]
4000
3600
3200
2800
2400
2000
1600
1200
800
400

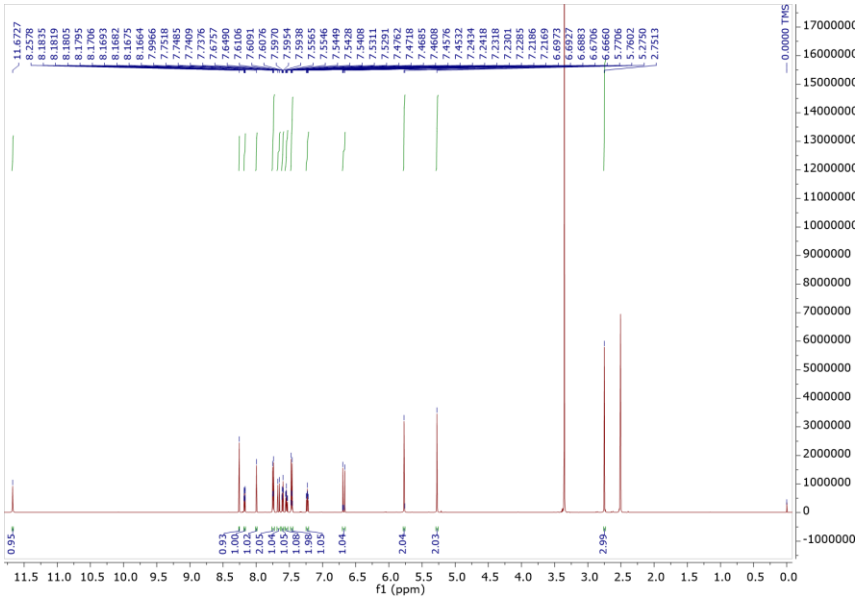
f1 (ppm)

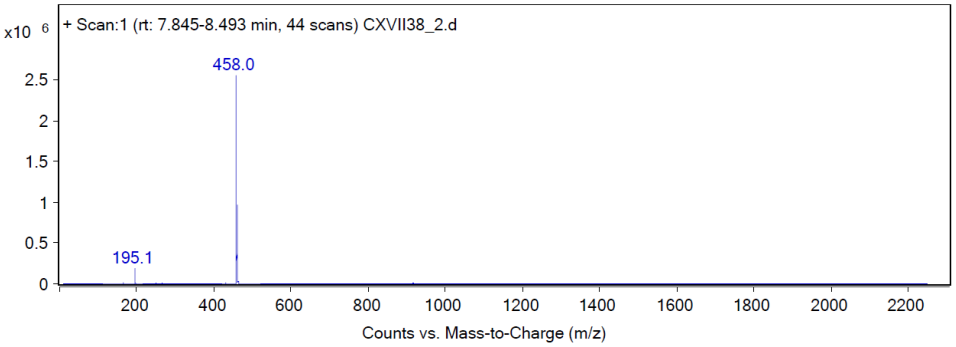
x10 6
+ Scan:1 (rt: 7.845-8.493 min, 44 scans) CXVII38_2.d
458.0
195.1
Counts vs. Mass-to-Charge (m/z)

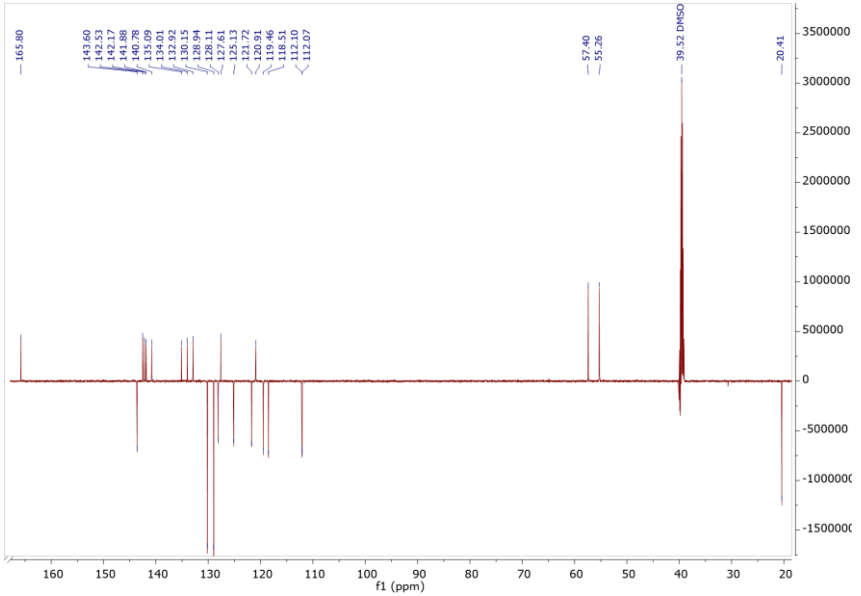
39.52 DMSO
f1 (ppm)

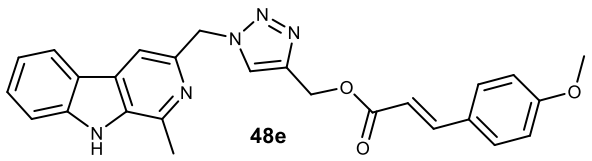

48e

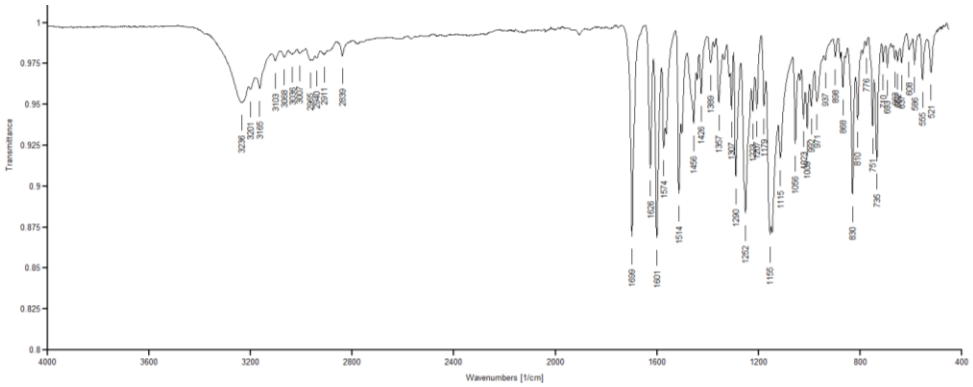
Transmittance
Wavenumbers [1/cm]

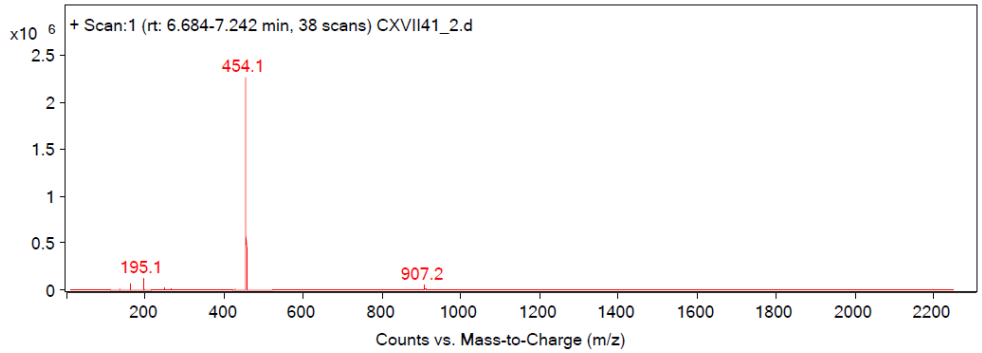
x10 6
+ Scan:1 (rt: 6.684-7.242 min, 38 scans) CXVII41_2.d
454.1
195.1
907.2
Counts vs. Mass-to-Charge (m/z)

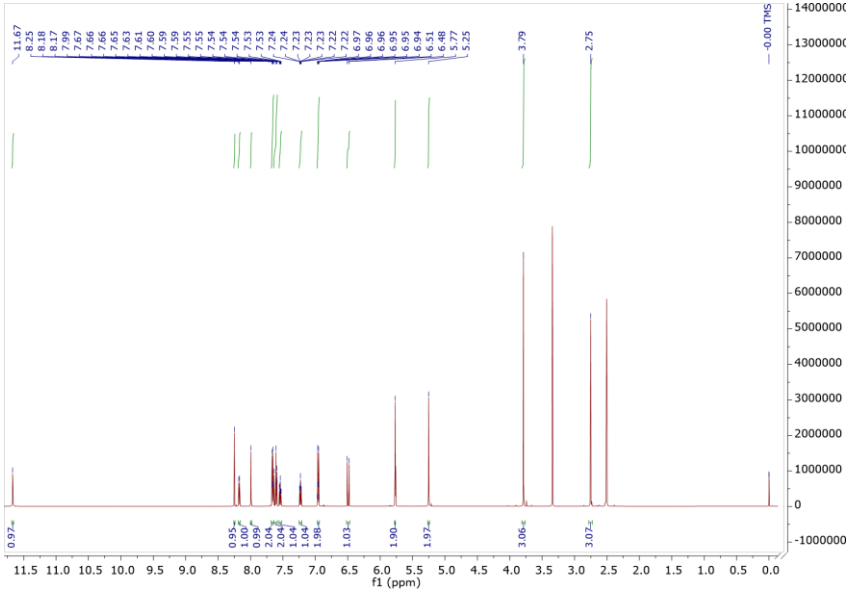
f1 (ppm)

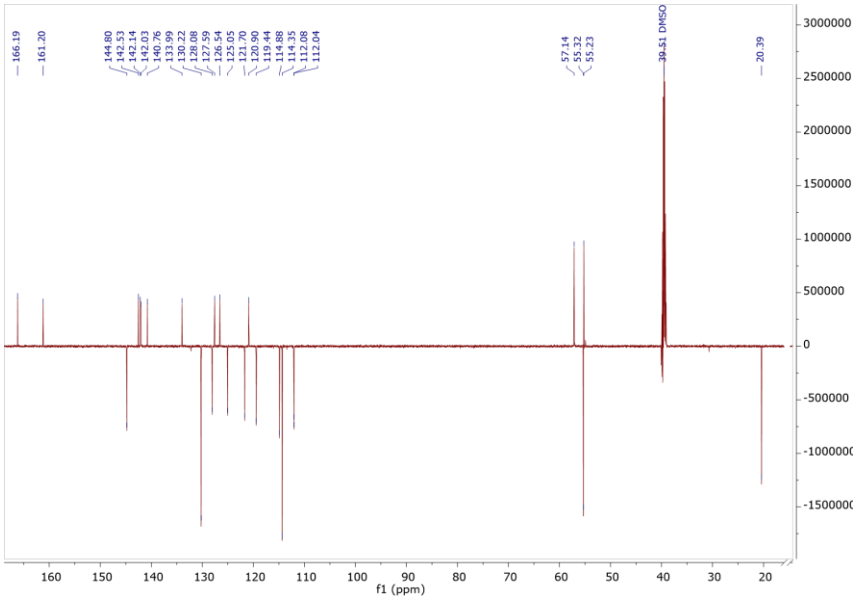
f1 (ppm)

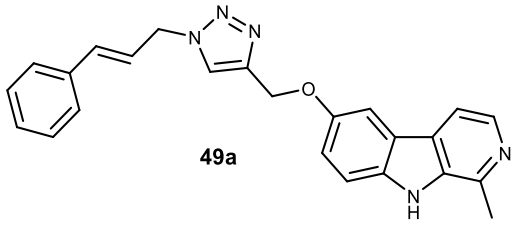
N
N
N
O
N
H

49a

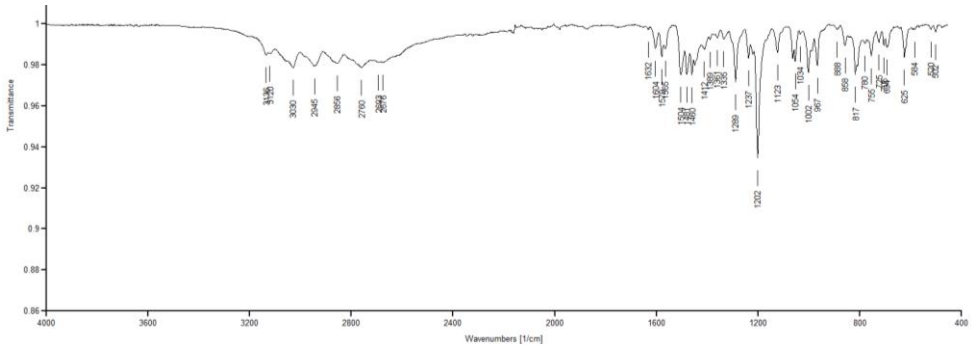
Transmittance
Wavenumbers [1/cm]

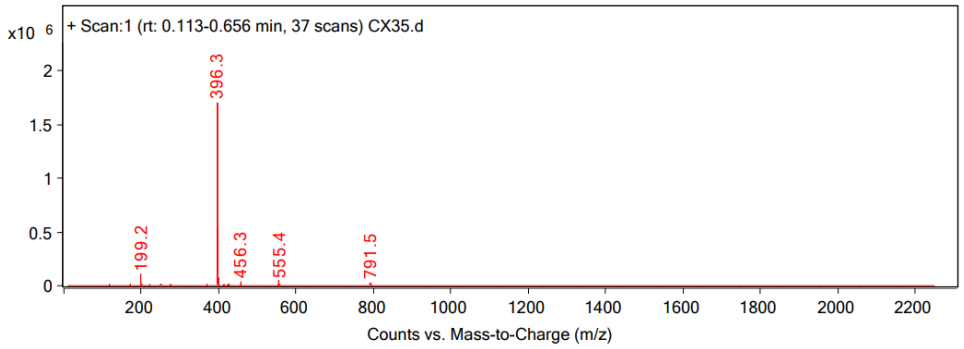
x10 6
+ Scan:1 (rt: 0.113-0.656 min, 37 scans) CX35.d
396.3
199.2
456.3
555.4
791.5
Counts vs. Mass-to-Charge (m/z)

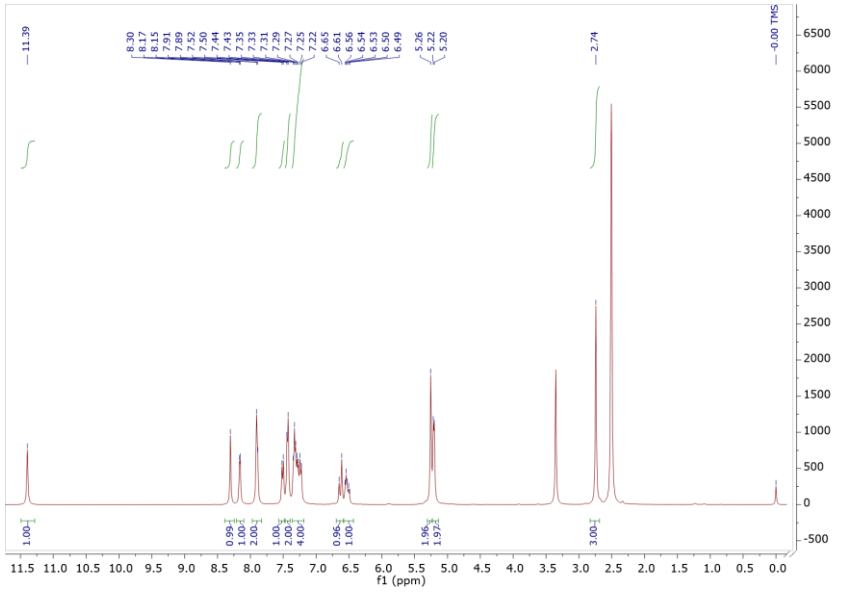
11.39
2.74
0.00 TMS
f1 (ppm)

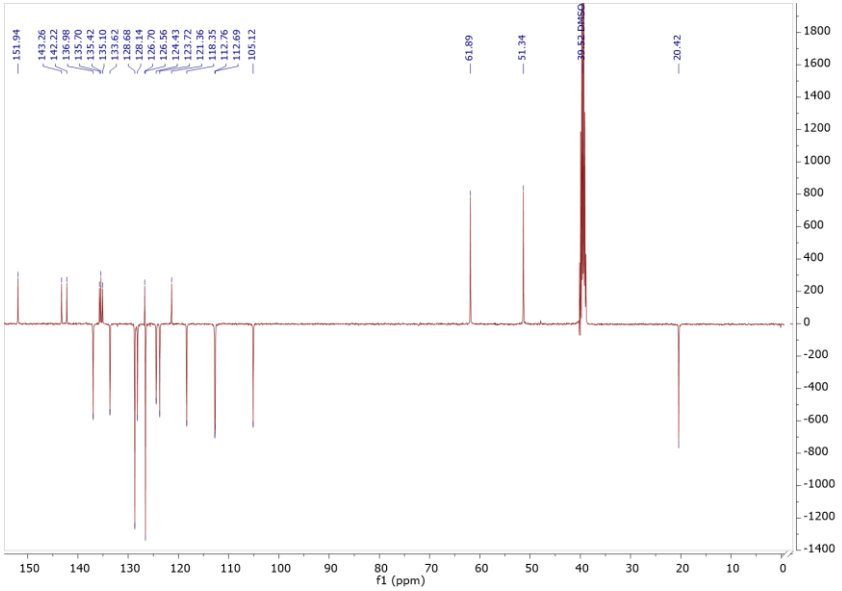
151.94
143.26
143.22
136.98
135.70
135.42
135.10
133.62
128.68
128.14
126.70
126.56
124.43
123.72
121.36
118.35
112.76
112.69
105.12
61.89
51.34
39.52 DMSO
20.42
f1 (ppm)

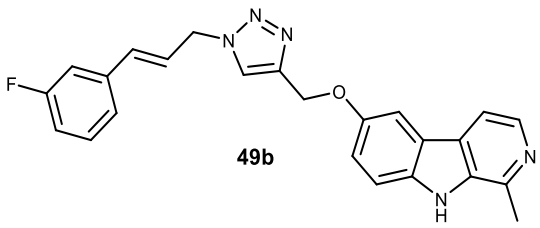
F
N
N
N
O
N
H

49b

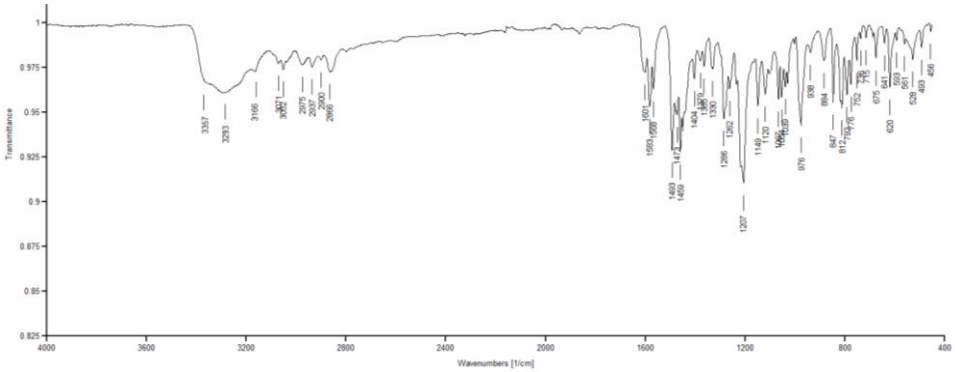
Transmittance
Wavenumbers [1/cm]

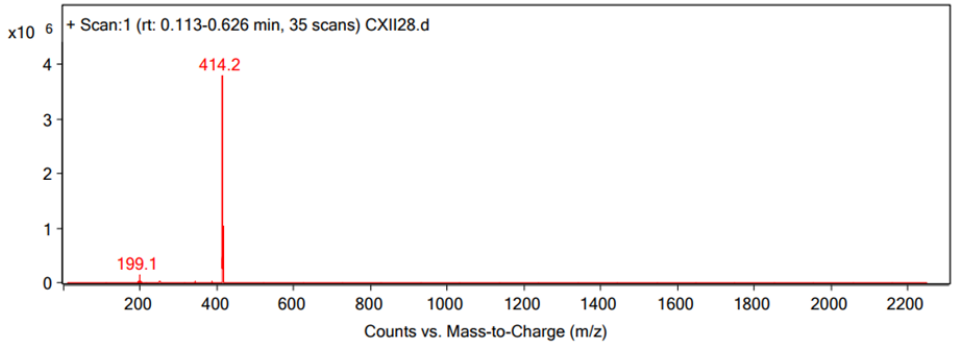
x10 6
+ Scan:1 (rt: 0.113-0.626 min, 35 scans) CXII28.d
414.2
199.1
Counts vs. Mass-to-Charge (m/z)

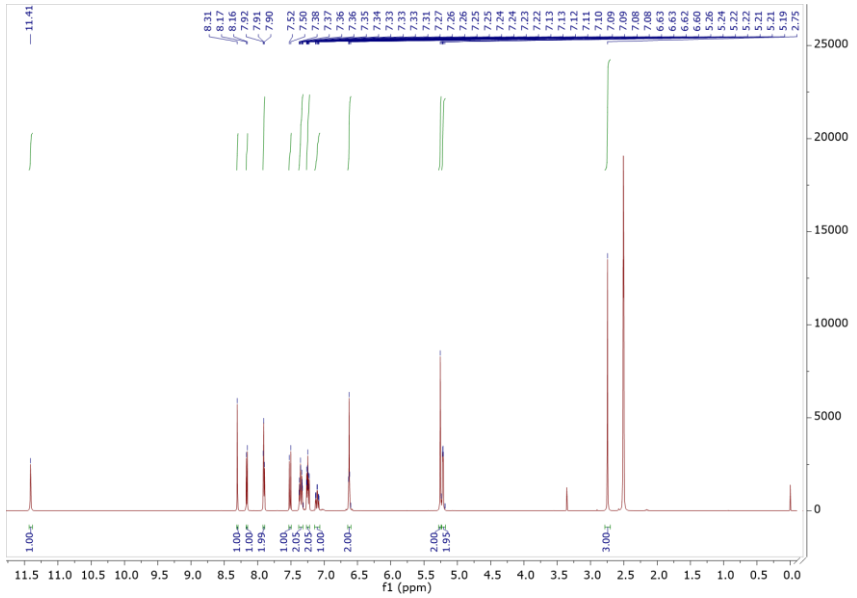
f1 (ppm)

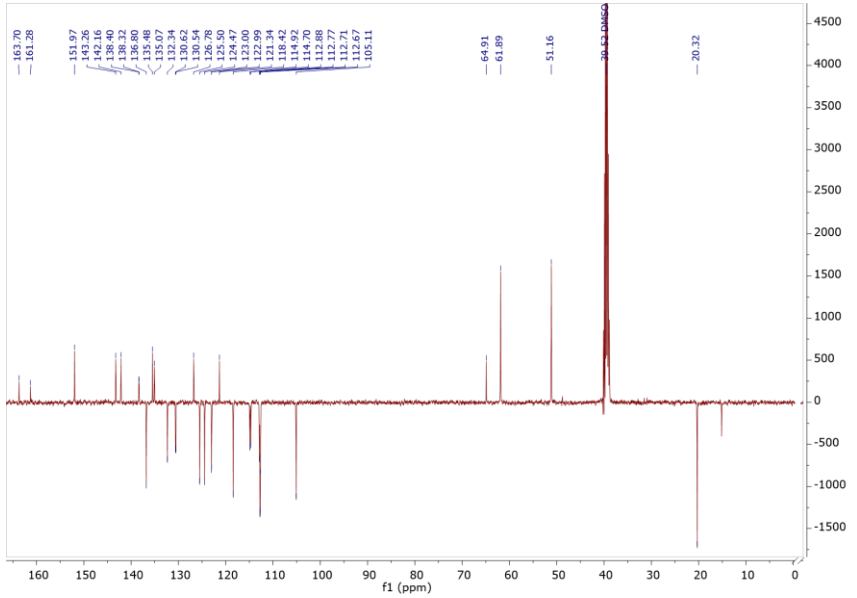
f1 (ppm)

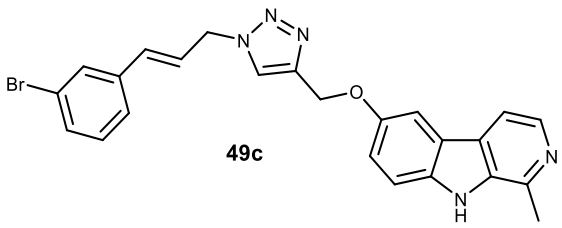
Br
N
N
N
O
N
H

49c

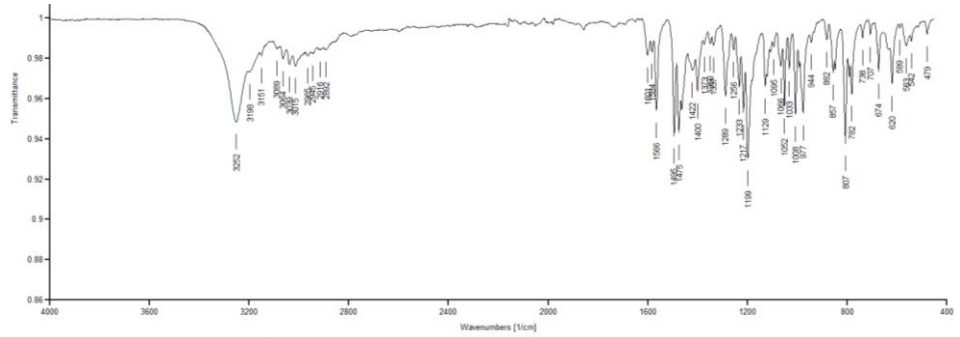
Transmittance
Wavenumbers [1/cm]

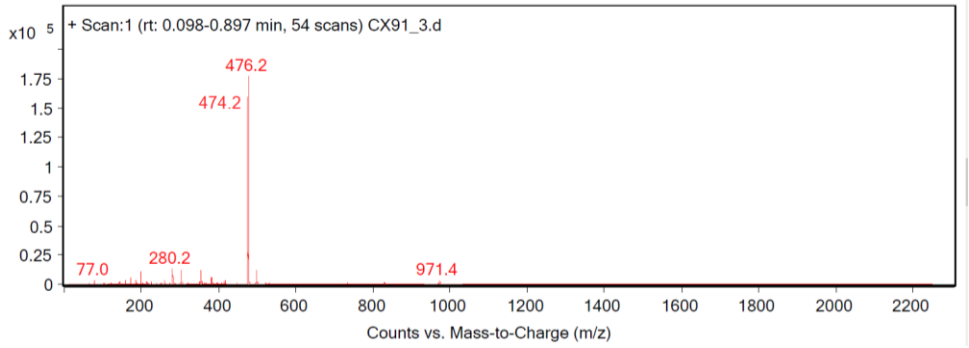
x10 5
+ Scan:1 (rt: 0.098-0.897 min, 54 scans) CX91_3.d
476.2
474.2
77.0
280.2
971.4
Counts vs. Mass-to-Charge (m/z)

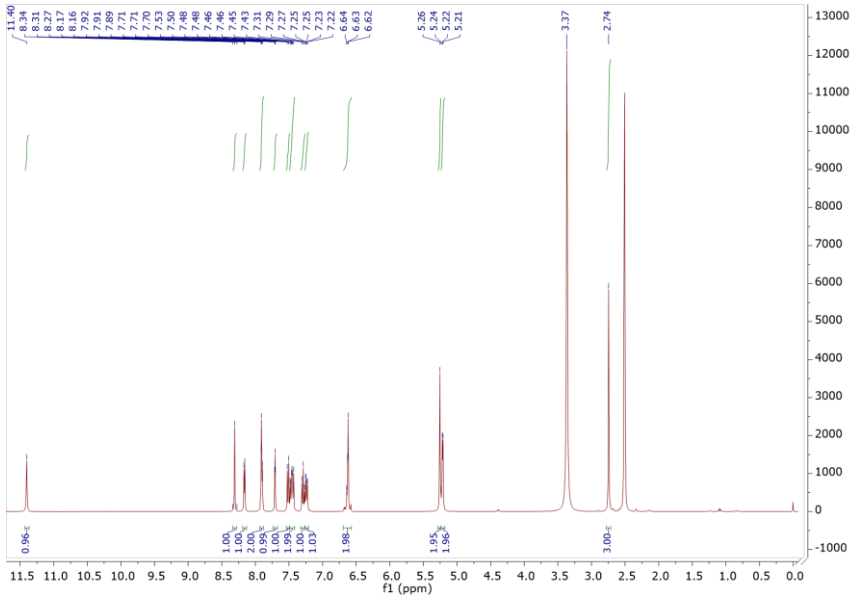
f1 (ppm)

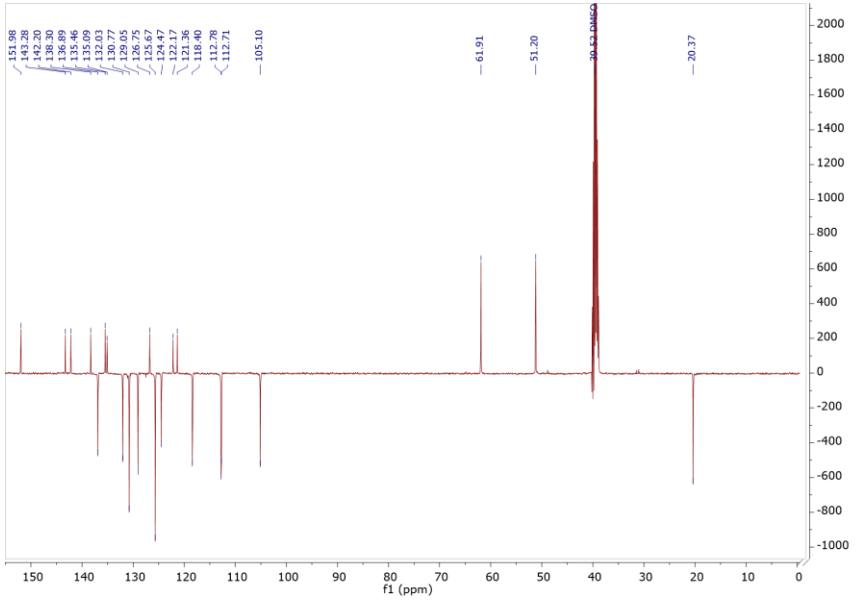
f1 (ppm)

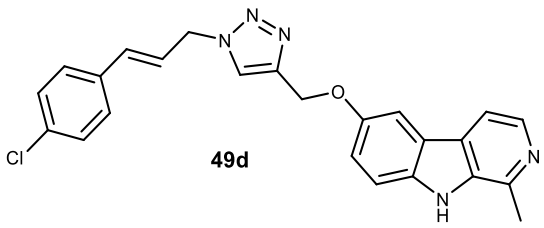
Cl
N
N
N
O
N
H

49d

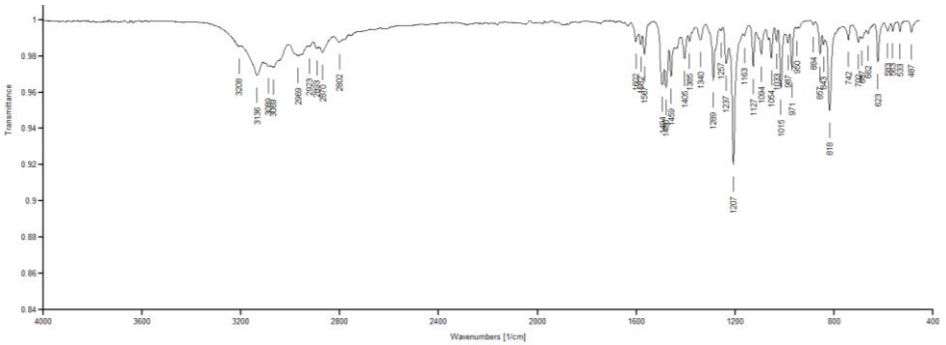
Transmittance
Wavenumbers [1/cm]

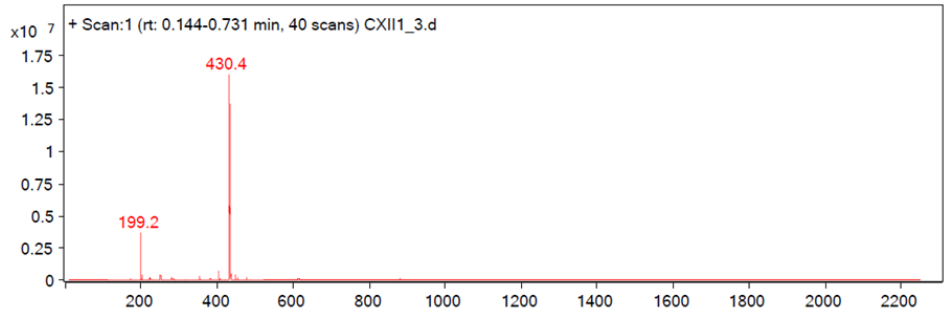
x10 7
+ Scan:1 (rt: 0.144-0.731 min, 40 scans) CXII1_3.d
430.4
199.2

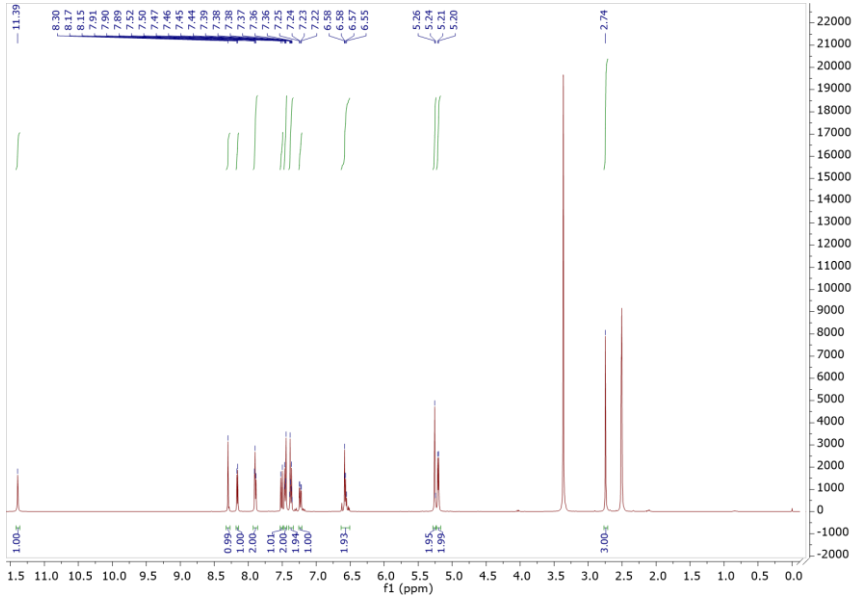
f1 (ppm)

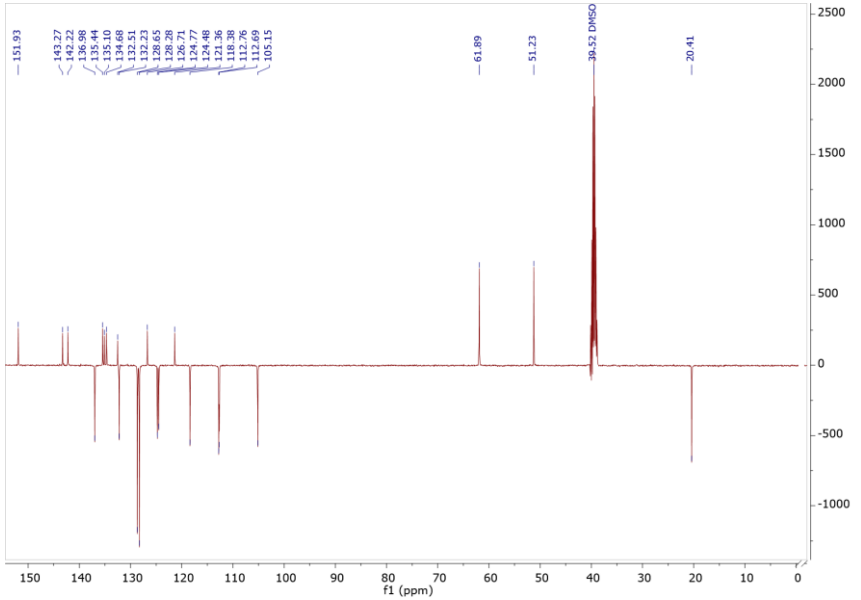
DMSO
f1 (ppm)

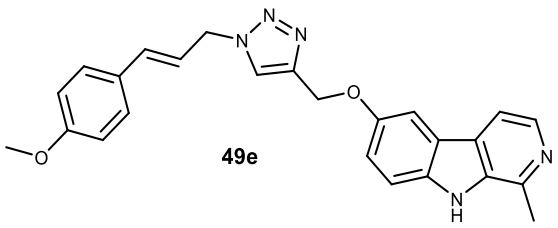
N
N
N
O
O
N
H
49e

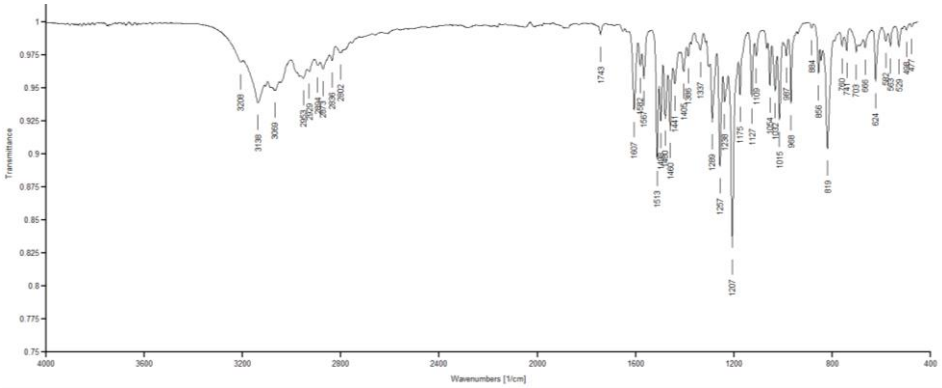
Transmittance
Wavenumbers [1/cm]

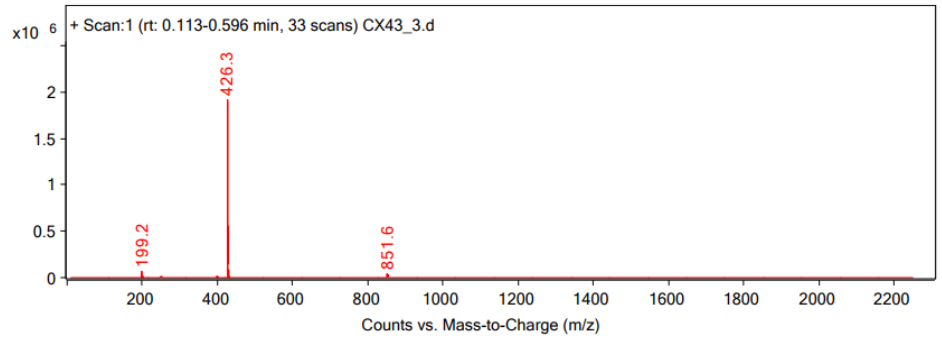
x10 6
+ Scan:1 (rt: 0.113-0.596 min, 33 scans) CX43_3.d
426.3
199.2
851.6
Counts vs. Mass-to-Charge (m/z)

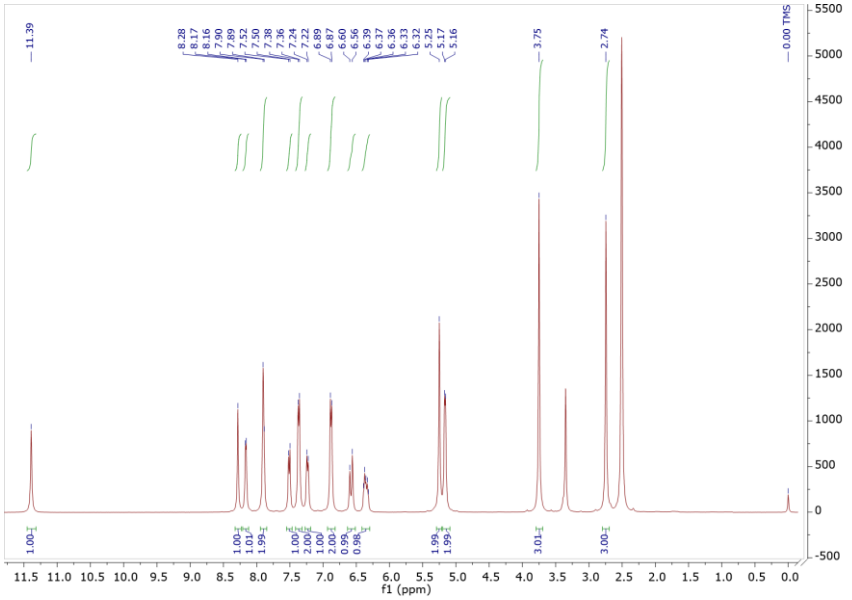
f1 (ppm)

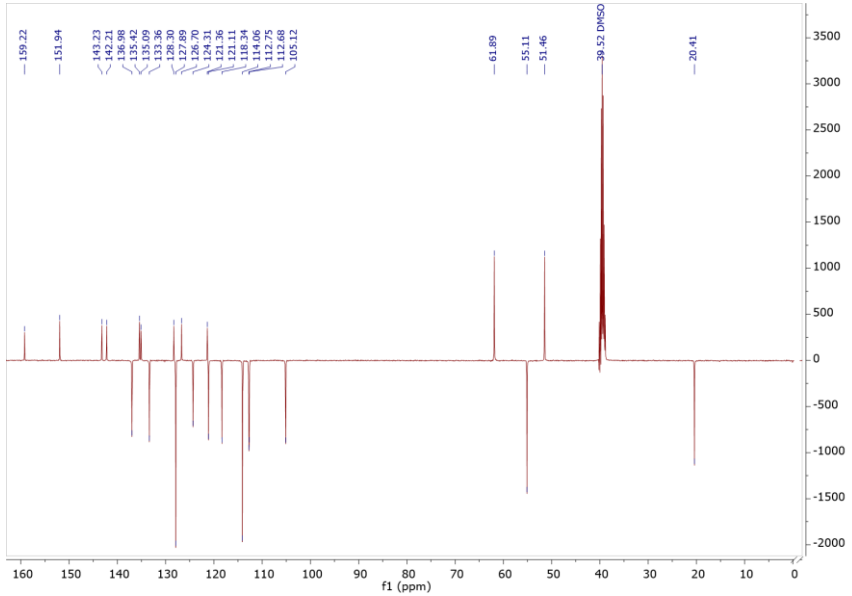
f1 (ppm)

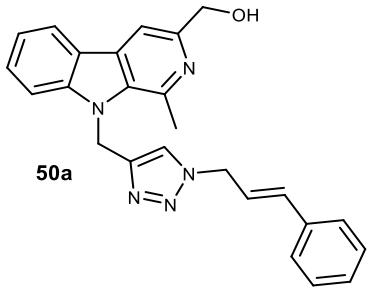
OH
N
N
N
N
N

50a

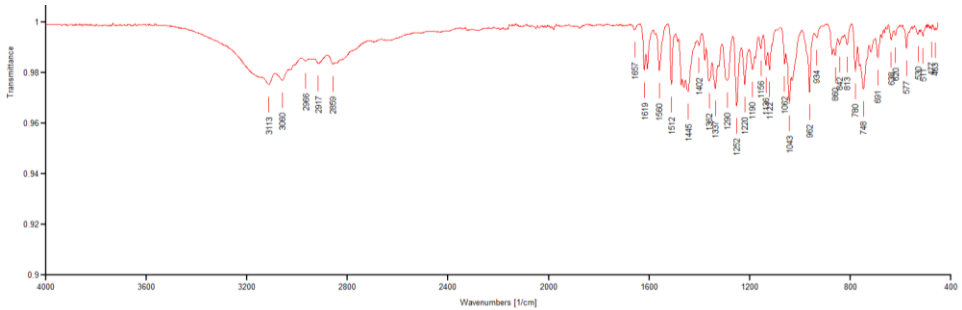
Transmittance
Wavenumbers [1/cm]
3113
3060
2966
2917
2859
1667
1619
1590
1512
1445
1402
1382
1338
1290
1252
1220
1190
1156
1128
1092
1043
984
962
895
845
819
780
748
691
577

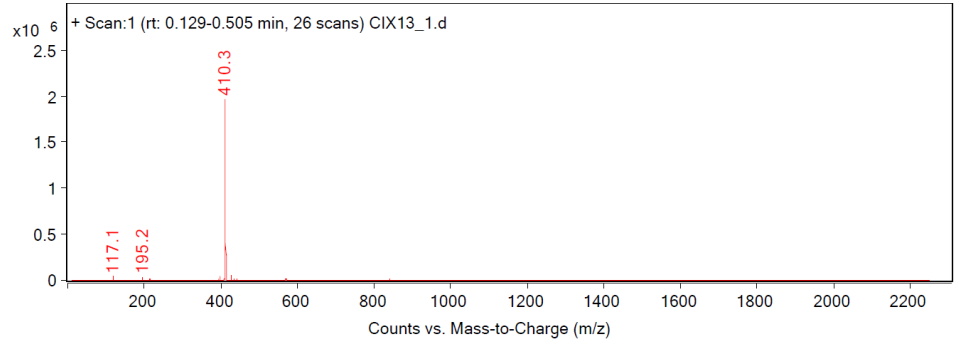
x10 6
+ Scan:1 (rt: 0.129-0.505 min, 26 scans) CIX13_1.d
410.3
117.1
195.2
Counts vs. Mass-to-Charge (m/z)

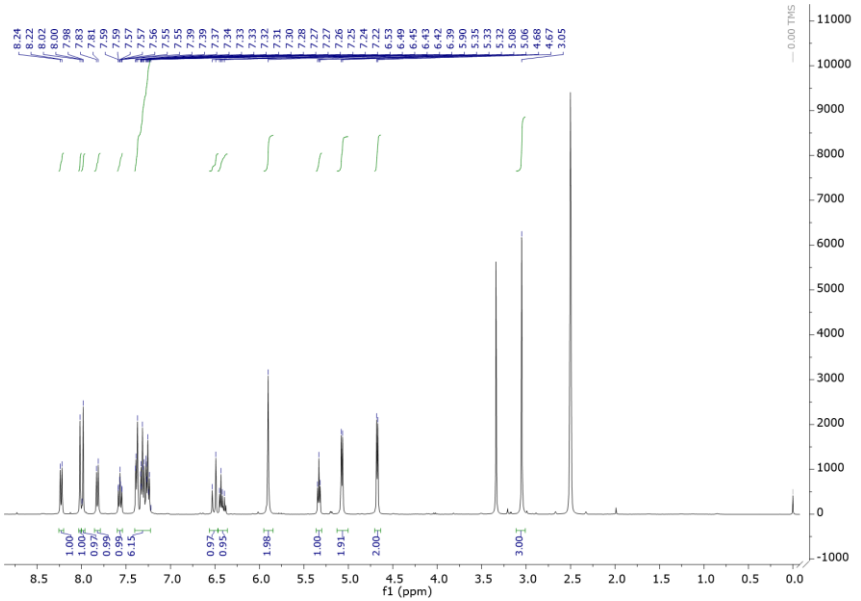
f1 (ppm)

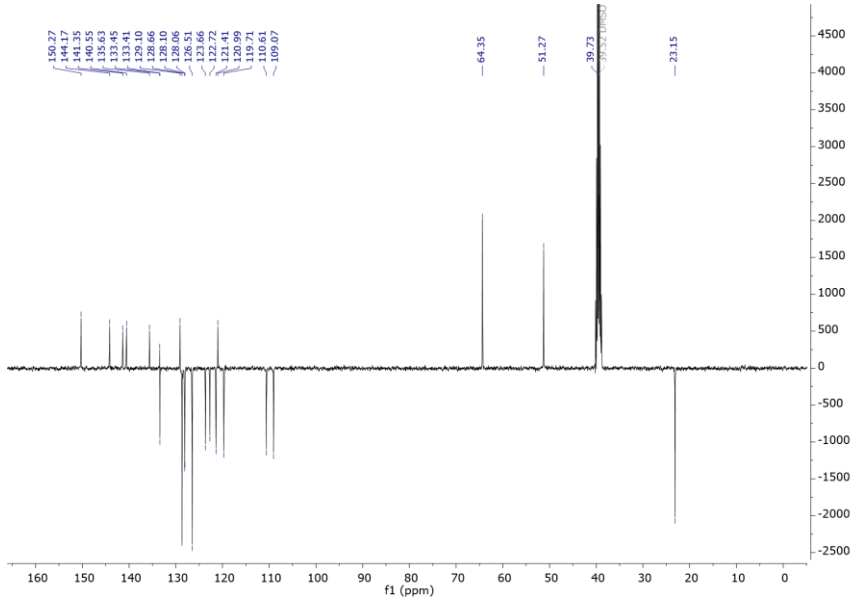
64.35
51.27
39.73
23.15
f1 (ppm)

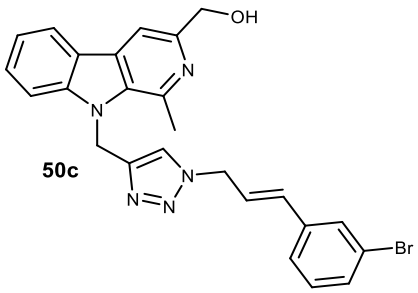
OH
N
N
N
N
Br

50c

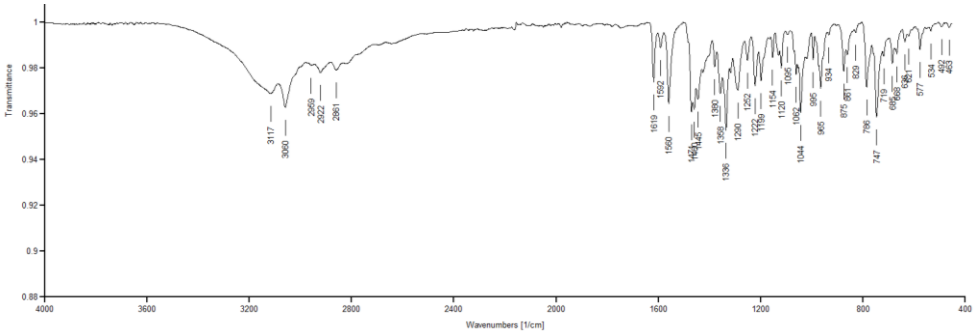
Transmittance
Wavenumbers [1/cm]

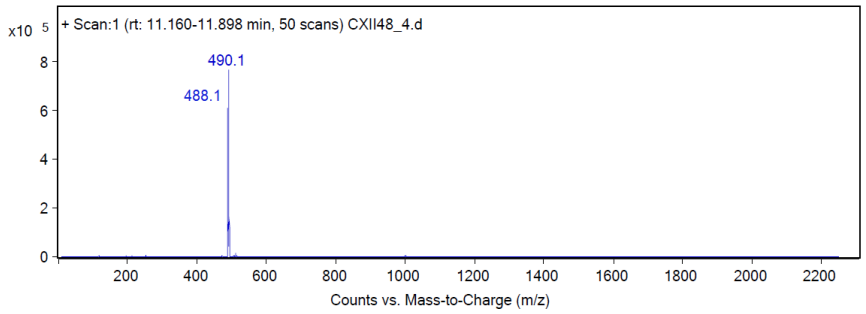
x10 5
+ Scan:1 (rt: 11.160-11.898 min, 50 scans) CXII48_4.d
490.1
488.1
Counts vs. Mass-to-Charge (m/z)

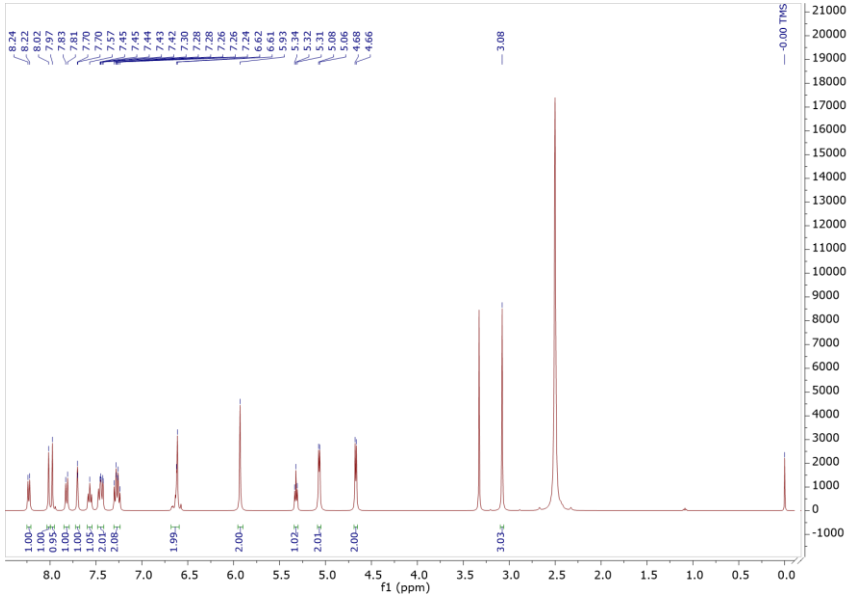
f1 (ppm)

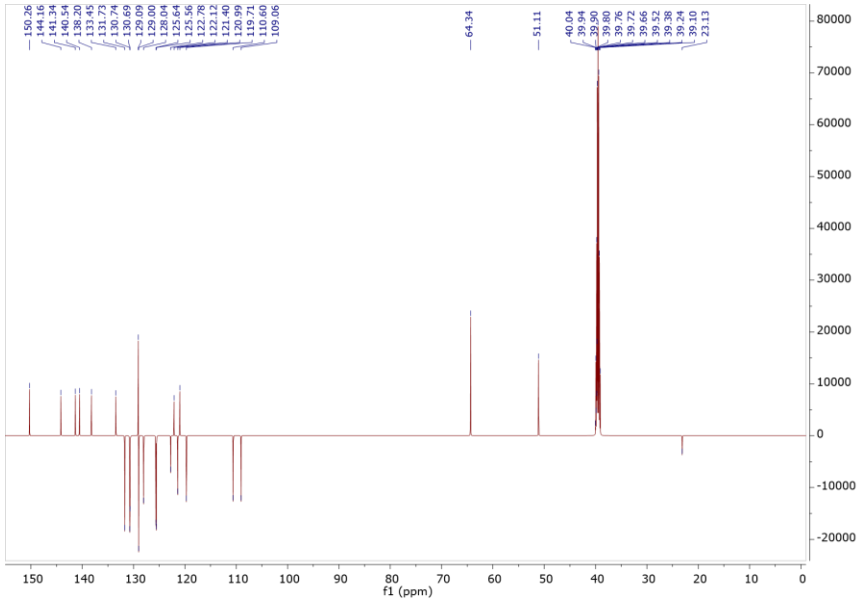
f1 (ppm)

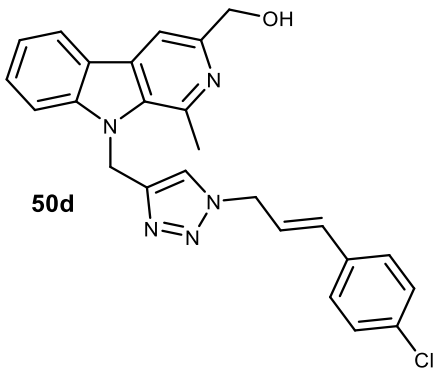
OH
N
N
N
N
N
Cl

50d

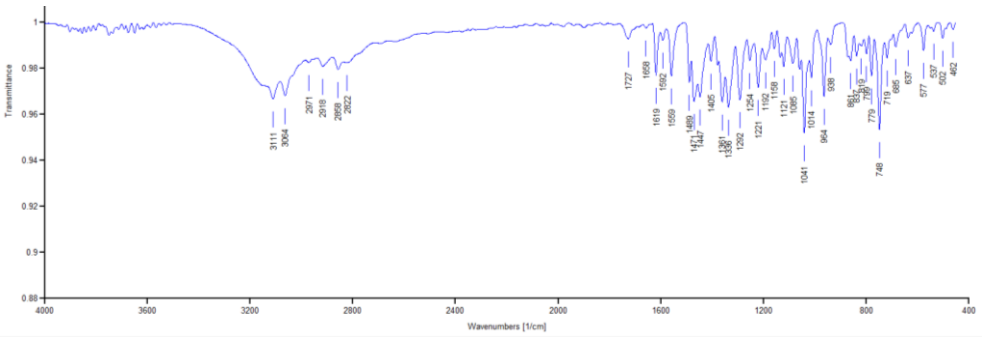
Transmittance
Wavenumbers [1/cm]

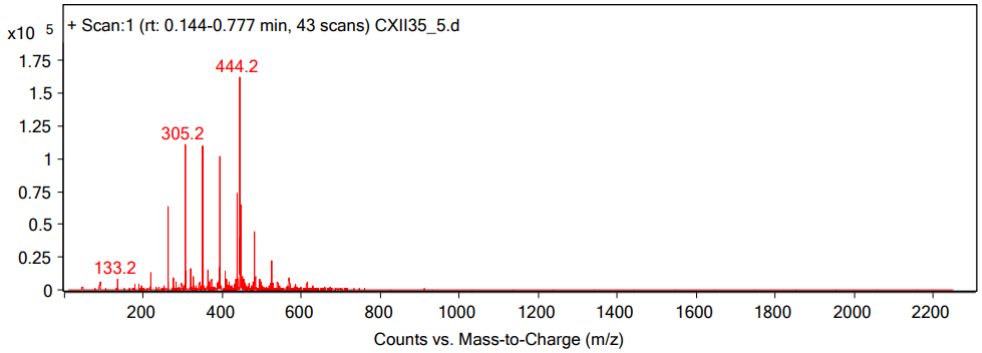
x10 5
+ Scan:1 (rt: 0.144-0.777 min, 43 scans) CXII35_5.d
444.2
305.2
133.2
Counts vs. Mass-to-Charge (m/z)

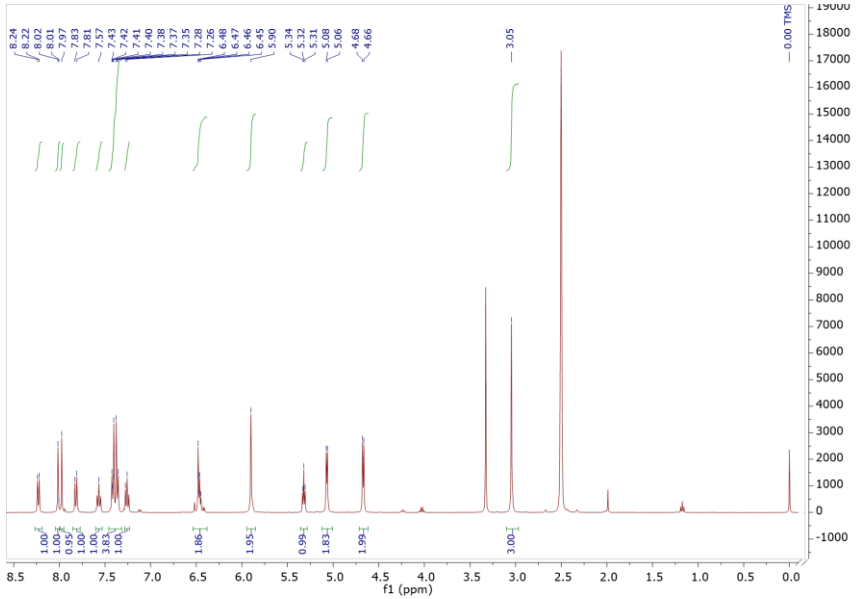
f1 (ppm)

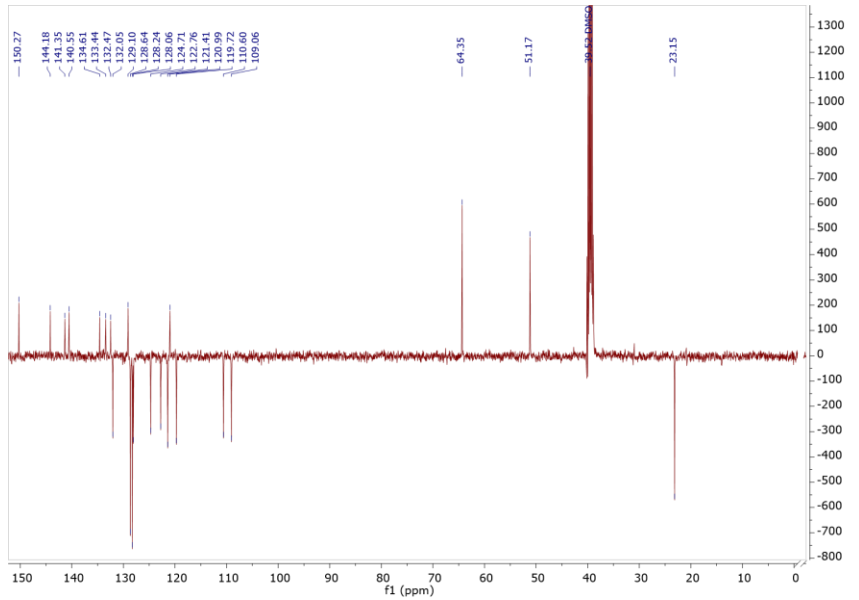
f1 (ppm)

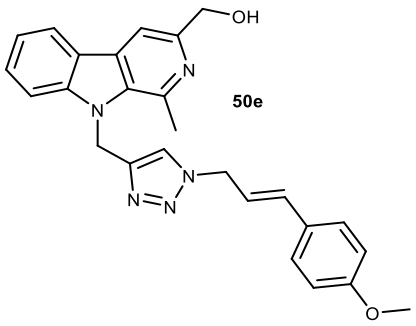
OH
N
N
N
N
O

50e

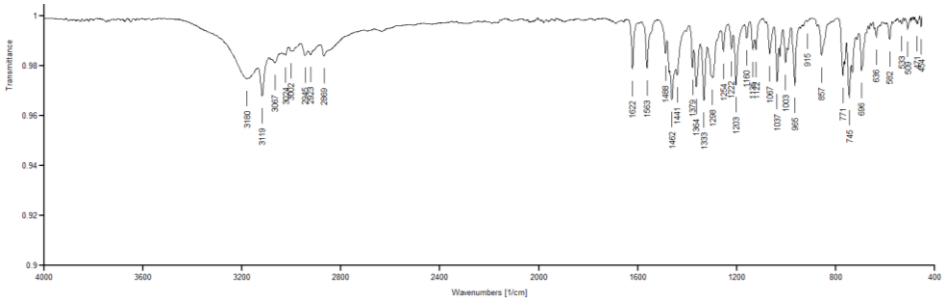
Transmittance
Wavenumbers [1/cm]

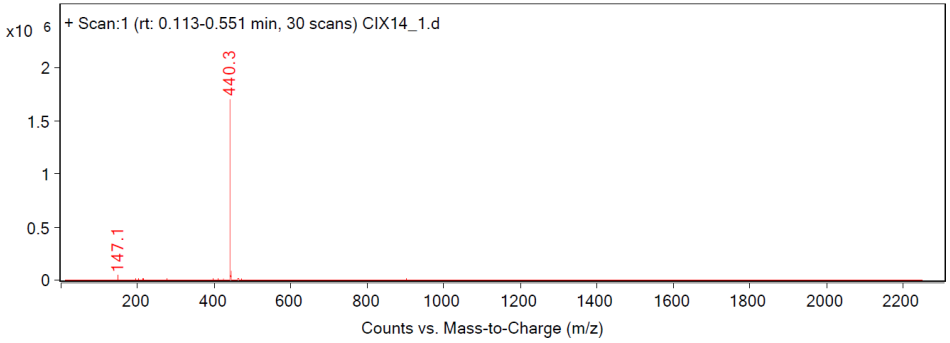
x10 6
+ Scan:1 (rt: 0.113-0.551 min, 30 scans) CIX14_1.d
440.3
147.1
Counts vs. Mass-to-Charge (m/z)

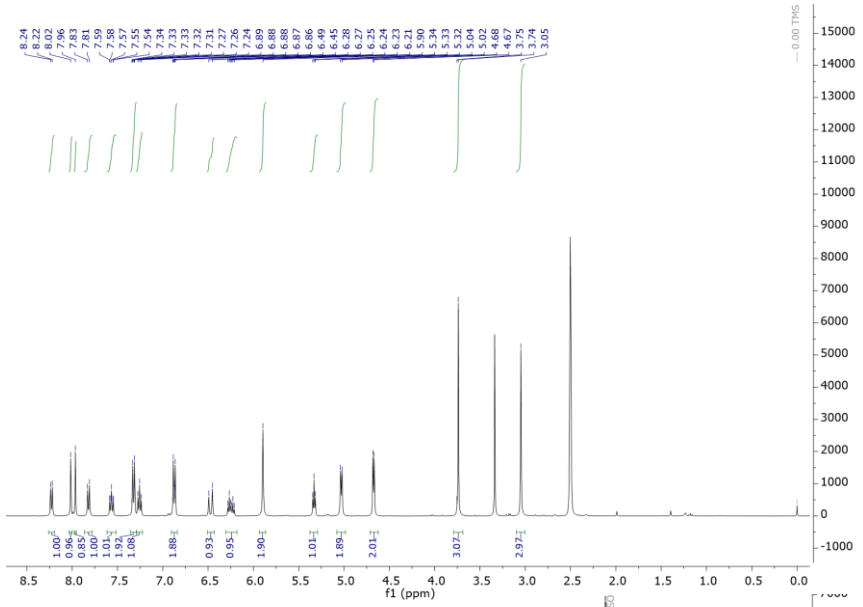
f1 (ppm)

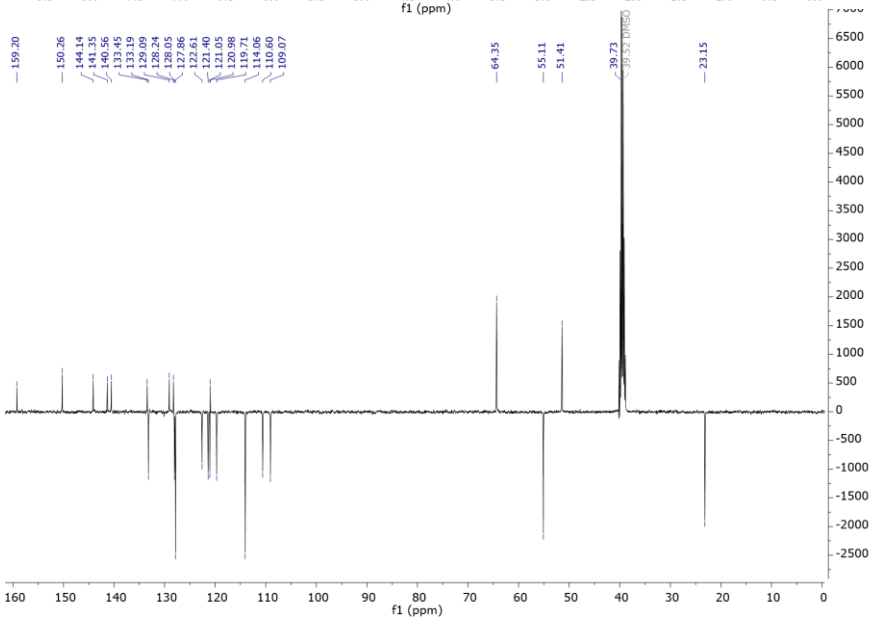
f1 (ppm)

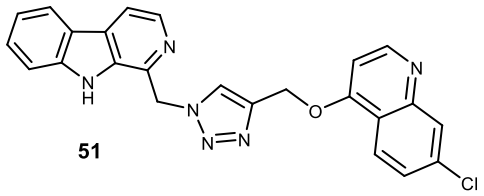

51

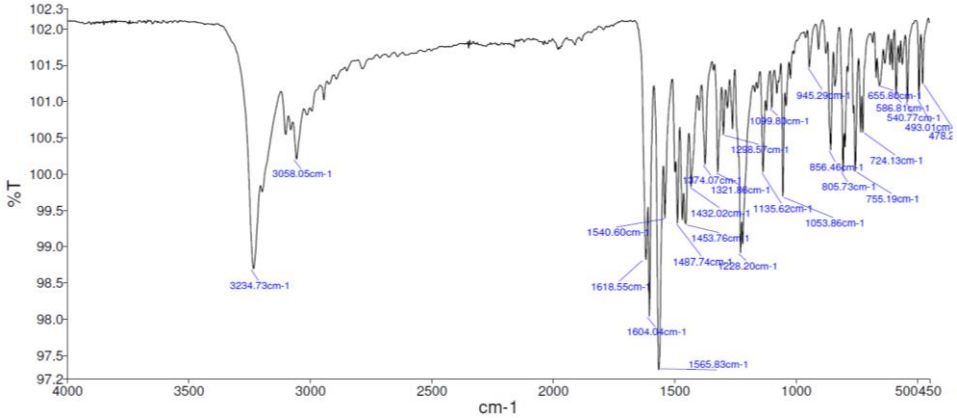
% T
cm-1
3234.73cm-1
3058.05cm-1
1618.55cm-1
1604.04cm-1
1565.83cm-1
1540.60cm-1
1487.74cm-1
1453.76cm-1
1432.02cm-1
1374.07cm-1
1321.86cm-1
1298.57cm-1
1228.20cm-1
1135.62cm-1
1099.80cm-1
1053.86cm-1
945.29cm-1
856.46cm-1
805.73cm-1
755.19cm-1
724.13cm-1
655.86cm-1
586.81cm-1
540.77cm-1
493.01cm-1

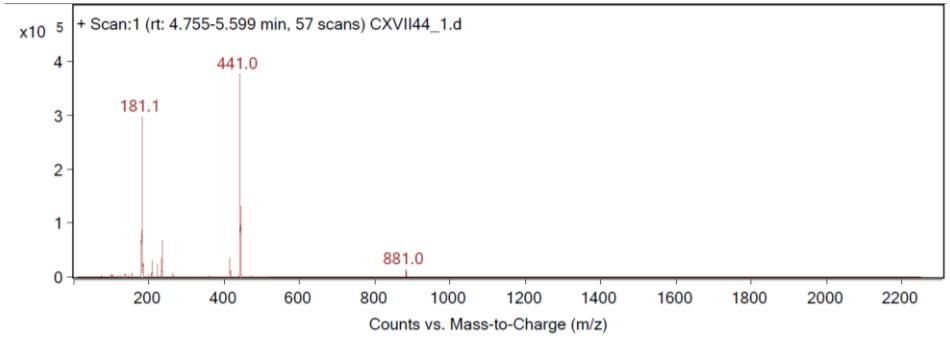
+ Scan:1 (rt: 4.755-5.599 min, 57 scans) CXVII44_1.d
x10 5
441.0
181.1
881.0
Counts vs. Mass-to-Charge (m/z)

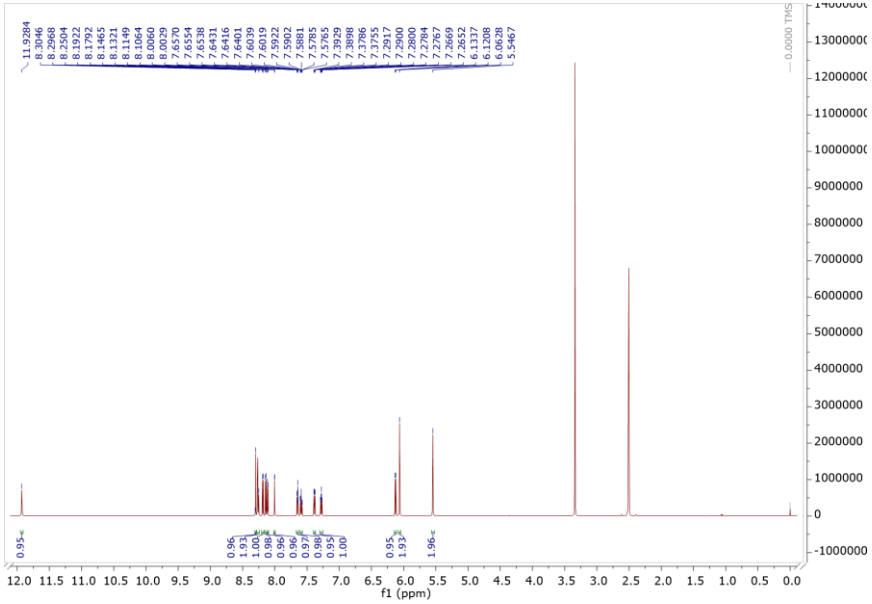
f1 (ppm)

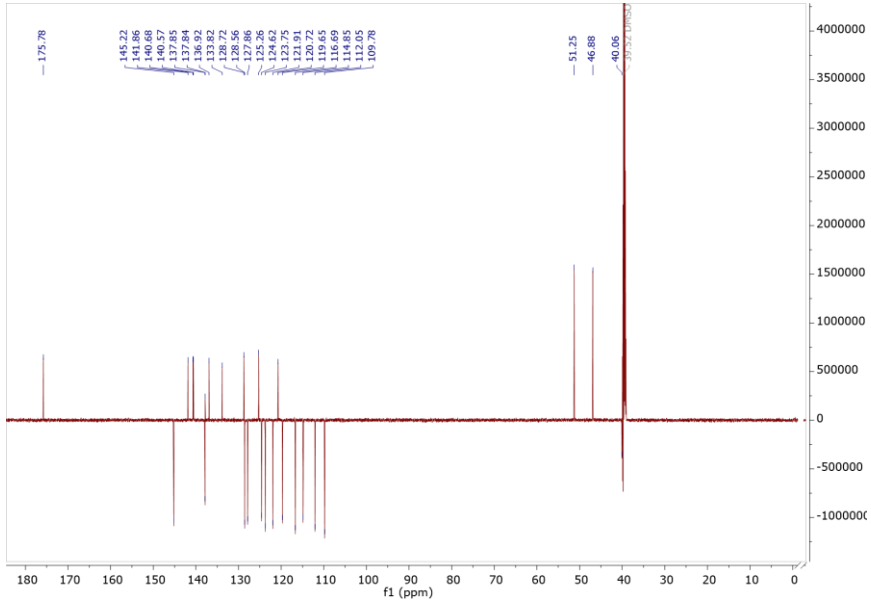
f1 (ppm)

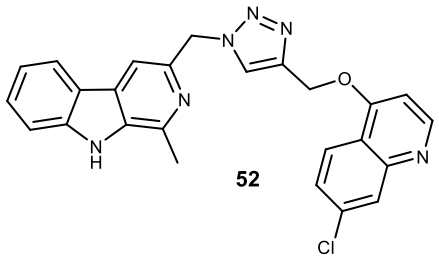
N
N
N
O
N
H
Cl

52

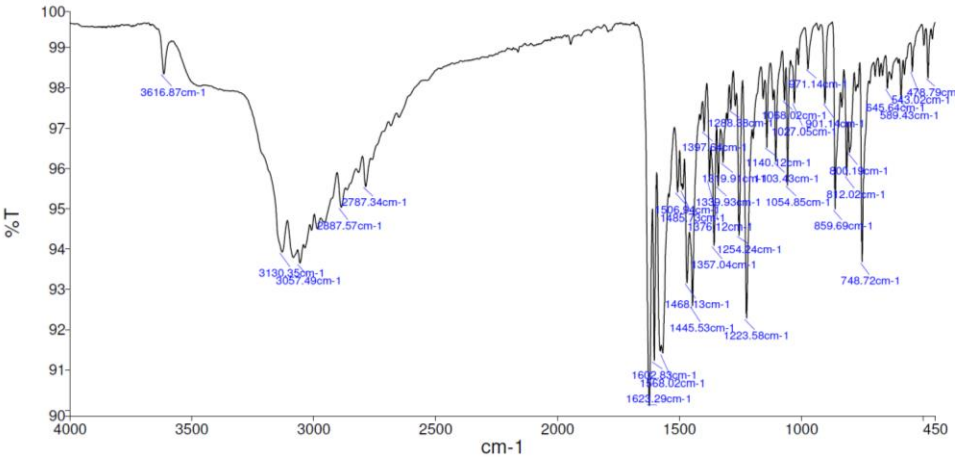
%T
cm-1
3616.87cm-1
3130.95cm-1
3057.49cm-1
2887.57cm-1
2787.34cm-1
1602.83cm-1
1568.02cm-1
1623.29cm-1
1468.13cm-1
1445.53cm-1
1223.58cm-1
1357.04cm-1
1254.24cm-1
1054.85cm-1
859.69cm-1
748.72cm-1

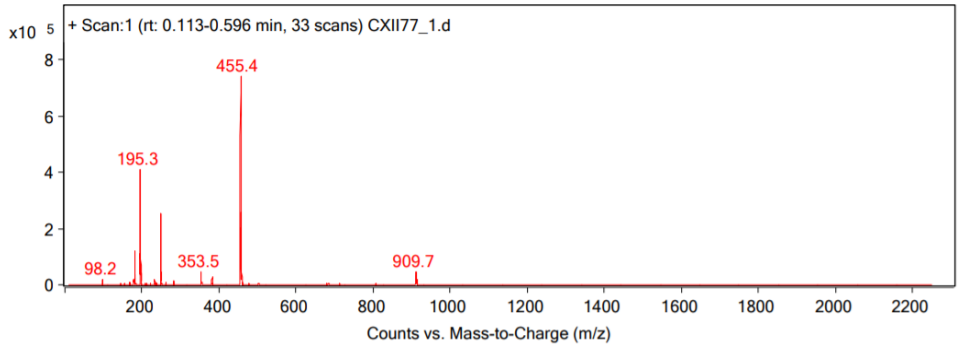
x10
+ Scan:1 (rt: 0.113-0.596 min, 33 scans) CXII77_1.d
455.4
195.3
98.2
353.5
909.7
Counts vs. Mass-to-Charge (m/z)

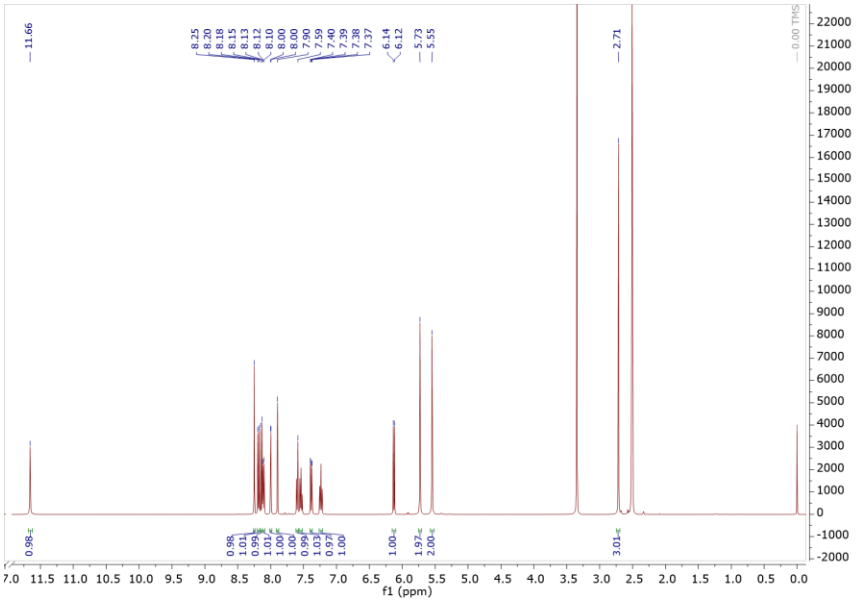
11.66
8.25
8.20
8.18
8.15
8.13
8.12
8.10
8.00
7.99
7.90
7.59
7.40
7.39
7.38
7.37
6.14
6.12
5.73
5.55
2.71
0.00 TMS
f1 (ppm)

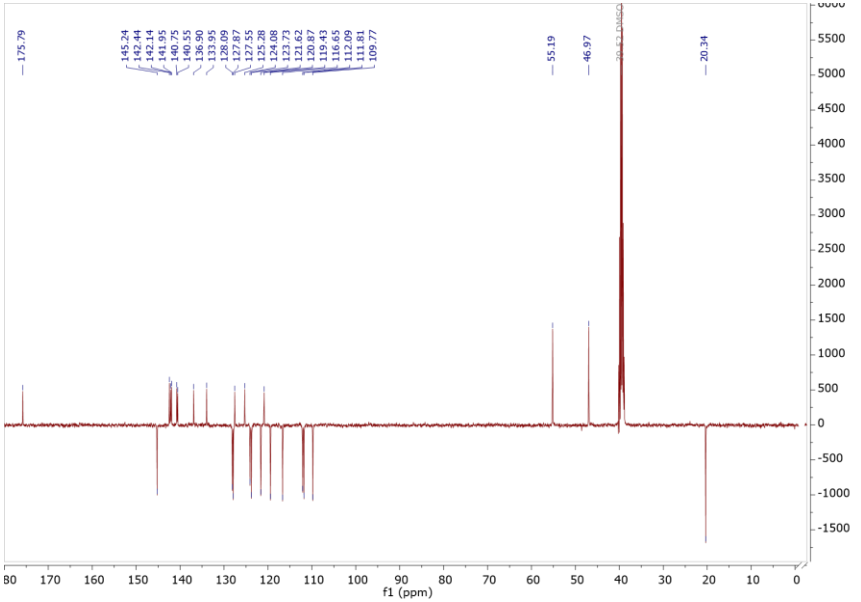
175.79
145.24
142.44
142.14
141.95
140.75
140.55
136.90
133.95
130.89
127.87
127.55
125.28
124.08
123.73
121.62
120.87
119.43
116.65
112.09
111.81
109.77
55.19
46.97
20.34
f1 (ppm)

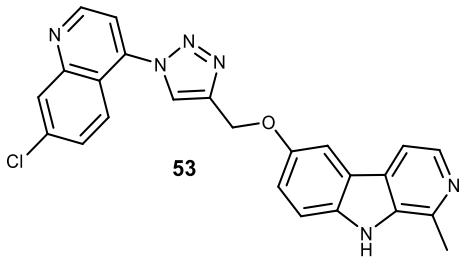
Cl
N
N
N
N
O
N
H

53

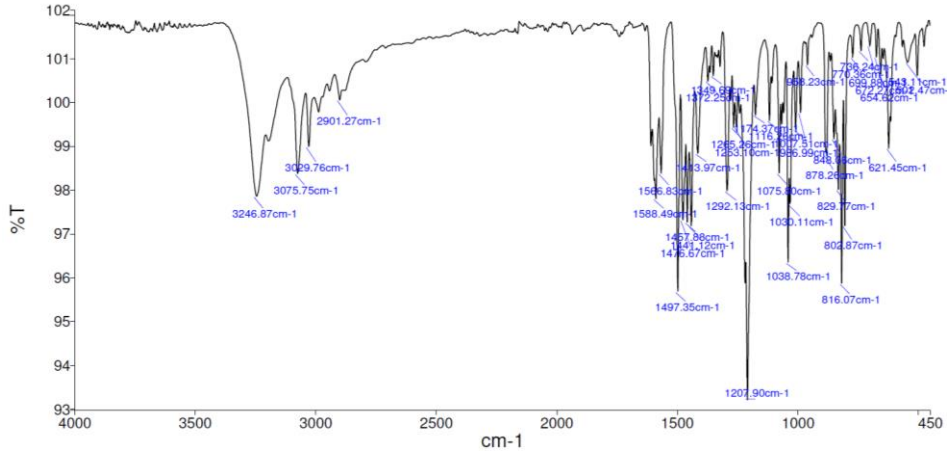
%T
cm-1
3246.87cm-1
3075.75cm-1
3029.76cm-1
2901.27cm-1
1588.49cm-1
1497.35cm-1
1457.86cm-1
1441.12cm-1
1378.67cm-1
1292.13cm-1
1207.90cm-1
1075.80cm-1
1038.78cm-1
1030.11cm-1
878.26cm-1
829.77cm-1
816.07cm-1
802.87cm-1
621.45cm-1

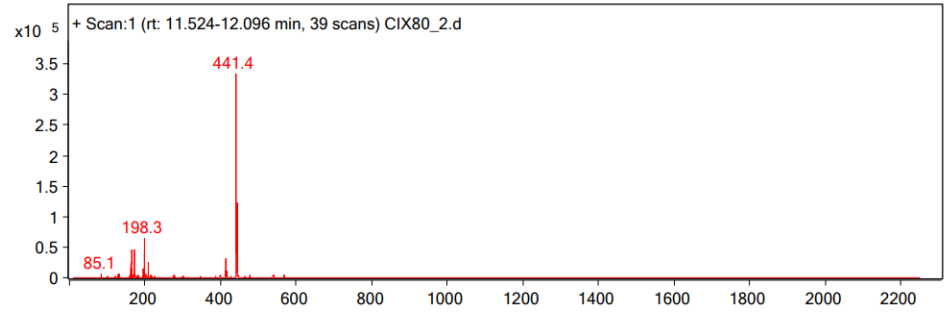
x10 5
+ Scan:1 (rt: 11.524-12.096 min, 39 scans) CIX80_2.d
441.4
198.3
85.1

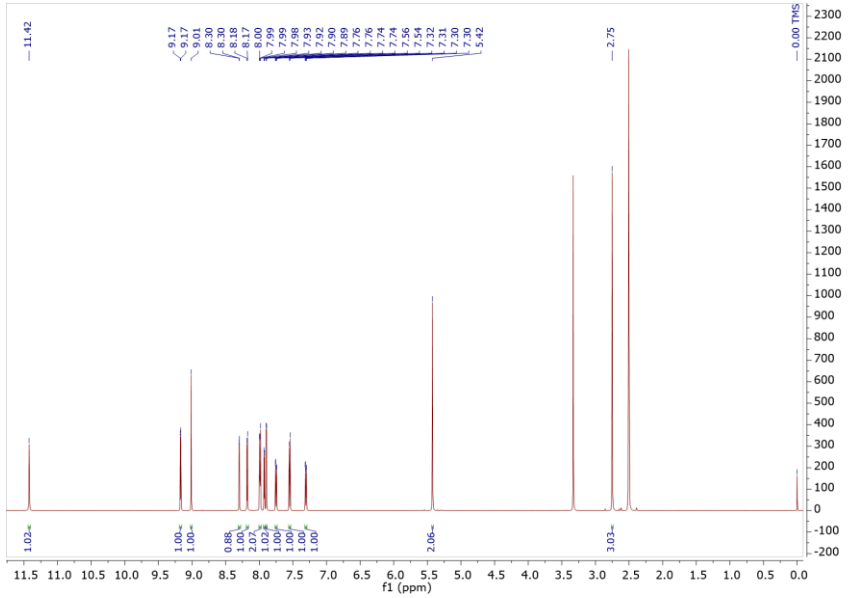
11.42
9.17
9.17
9.01
8.30
8.30
8.18
8.17
8.00
7.99
7.99
7.98
7.93
7.92
7.90
7.89
7.76
7.76
7.74
7.74
7.56
7.54
7.32
7.31
7.30
7.30
5.42
2.75
0.00 TMS
1.02
1.00
1.00
0.88
1.00
2.07
1.02
1.00
1.00
1.00
2.06
3.03
f1 (ppm)

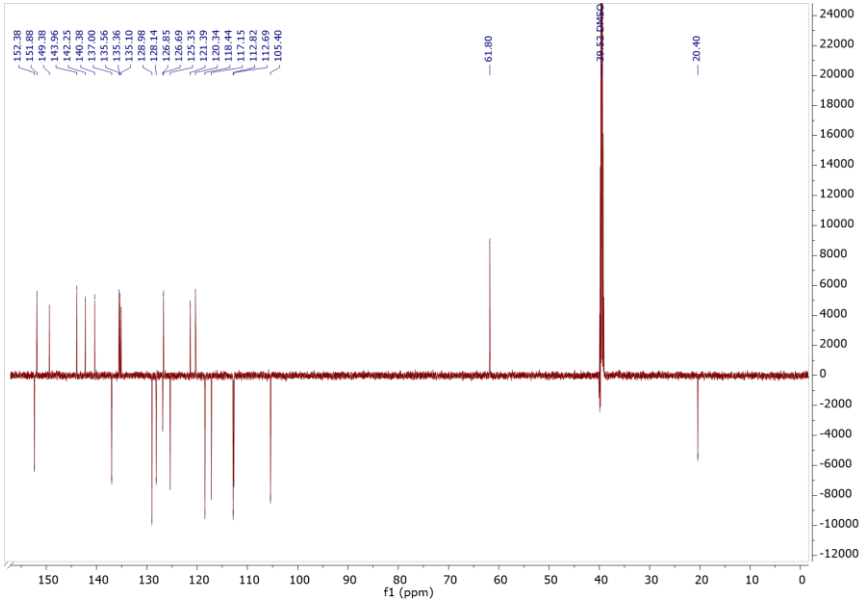
152.38
151.88
149.38
143.96
142.25
140.38
137.00
135.56
135.36
135.10
130.86
128.14
126.85
126.69
125.35
121.39
120.34
118.44
117.15
112.22
112.69
105.40
61.80
39.43 DMSO
20.40
f1 (ppm)

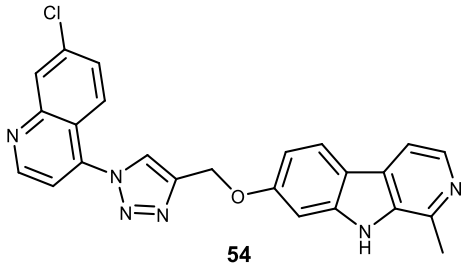
Cl
N
N
N=N
O
N
H

54

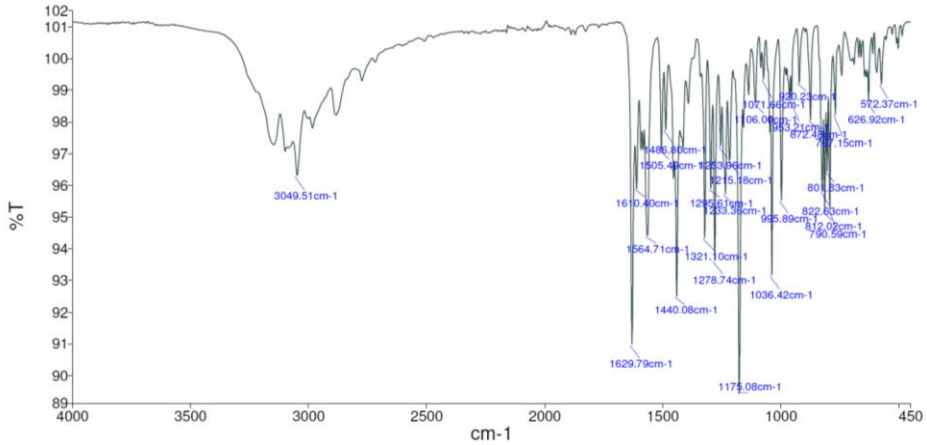
%T
cm-1
3049.51cm-1
1629.79cm-1
1564.71cm-1
1440.08cm-1
1321.10cm-1
1278.74cm-1
1175.08cm-1
1036.42cm-1
572.37cm-1
626.92cm-1

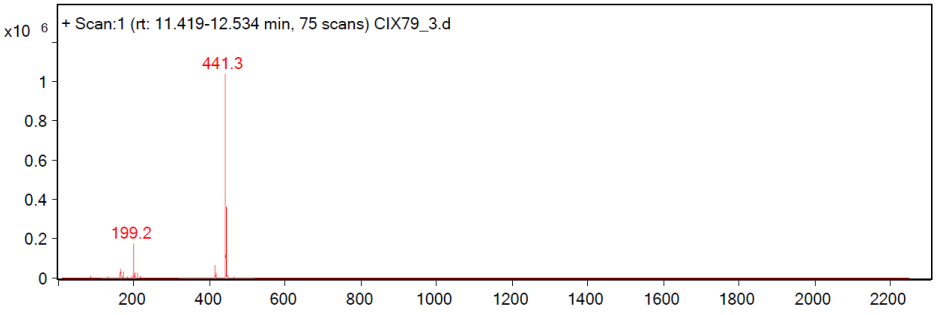
x10 6
+ Scan:1 (rt: 11.419-12.534 min, 75 scans) CIX79_3.d
441.3
199.2

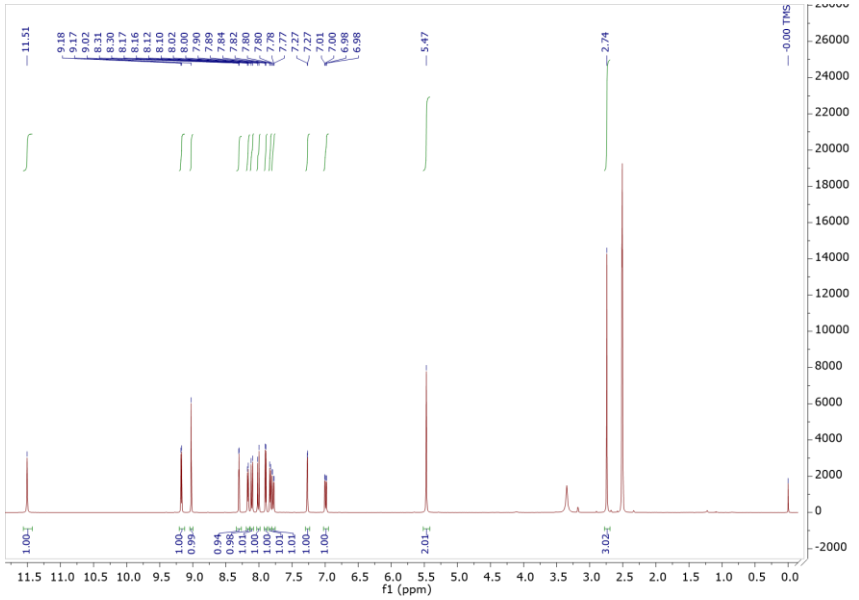
11.51
9.18
9.17
9.02
8.31
8.30
8.17
8.16
8.12
8.10
8.02
8.00
7.90
7.89
7.84
7.82
7.80
7.78
7.77
7.27
7.01
7.00
6.98
5.47
2.74
0.00 TMS
f1 (ppm)

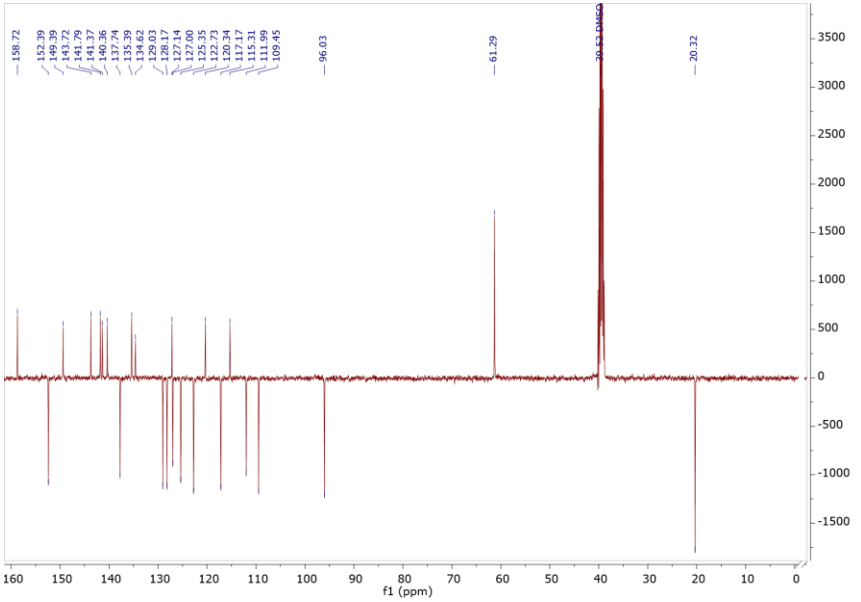
158.72
152.39
149.39
143.72
141.79
141.37
140.36
137.74
135.39
134.62
129.03
128.17
127.14
127.00
125.35
122.73
120.34
117.17
115.31
111.99
109.45
96.03
61.29
39.52 DMSO
20.32
f1 (ppm)

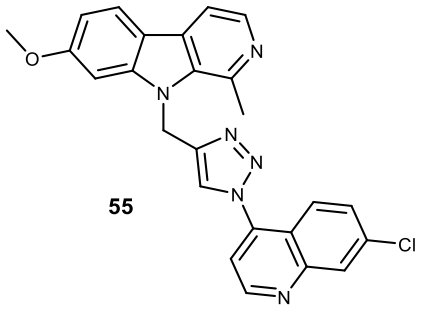
O
N
N
N
N
Cl
N

55

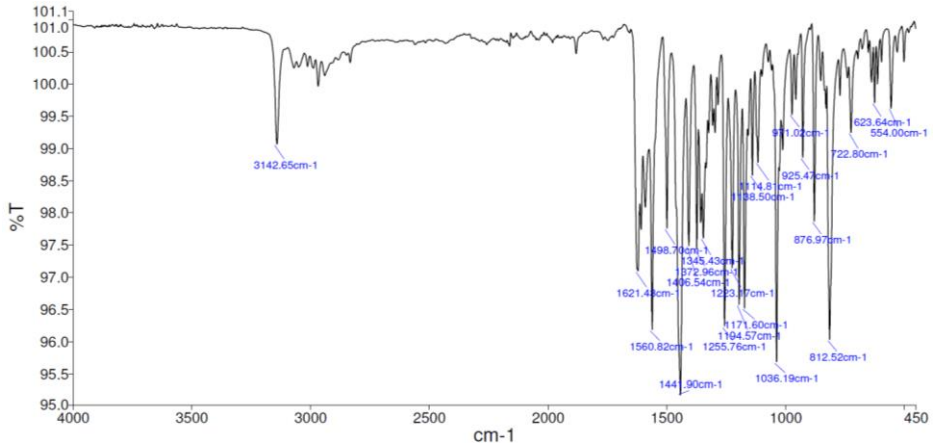
%T
cm-1
3142.65cm-1
1621.48cm-1
1560.82cm-1
1441.90cm-1
1036.19cm-1
812.52cm-1
876.97cm-1
722.80cm-1
623.64cm-1
554.00cm-1

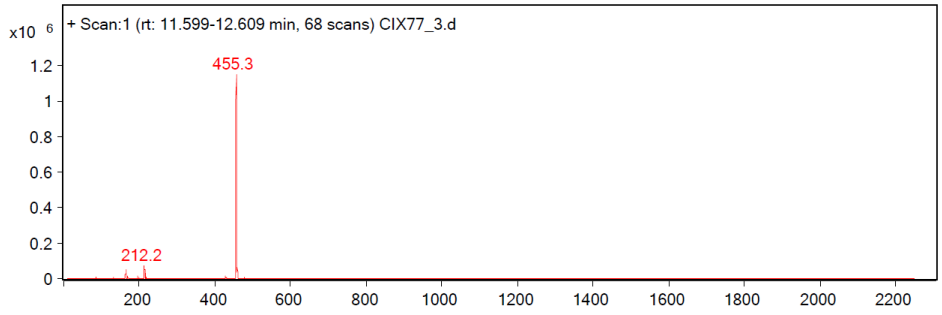
+ Scan:1 (rt: 11.599-12.609 min, 68 scans) CIX77_3.d
x10 6
455.3
212.2

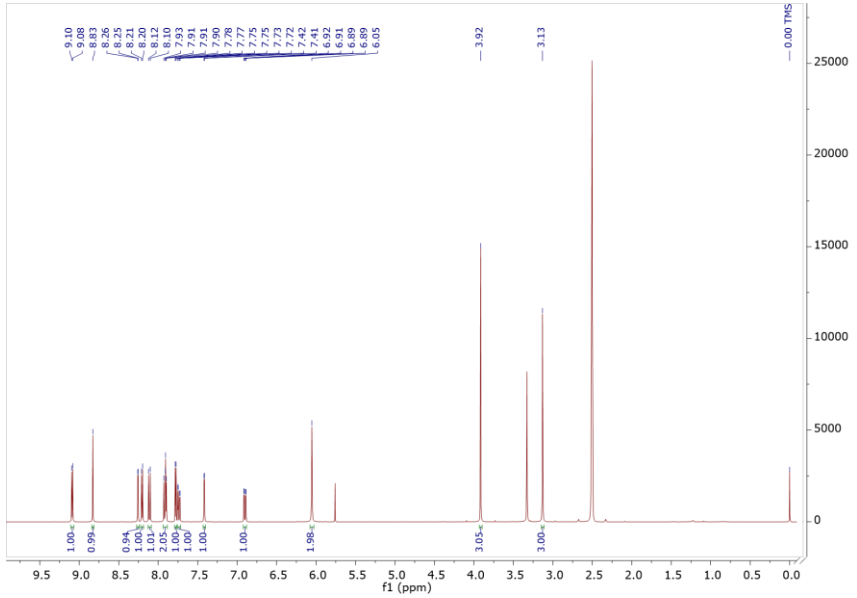
3.92
3.13
0.00 TMS
f1 (ppm)

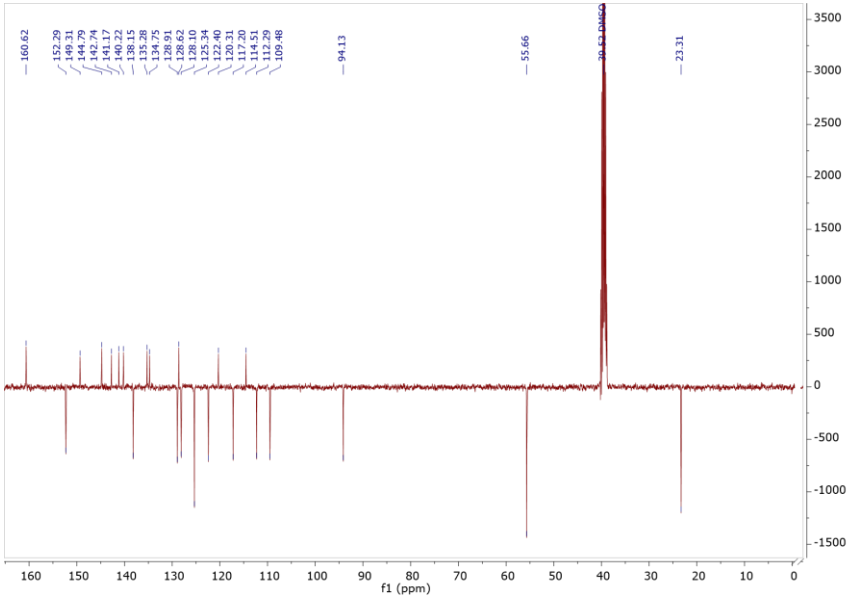
160.62
152.29
149.31
144.79
141.74
141.17
140.22
138.15
135.28
134.75
128.91
128.62
128.10
125.34
122.40
120.31
117.20
114.51
112.29
109.48
94.13
55.66
39.52 DMSO
23.31
f1 (ppm)

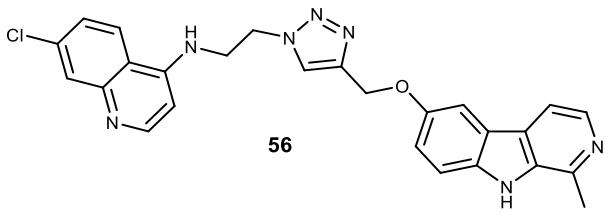
Cl
H
N
N
N
N
O
N
N
H

56

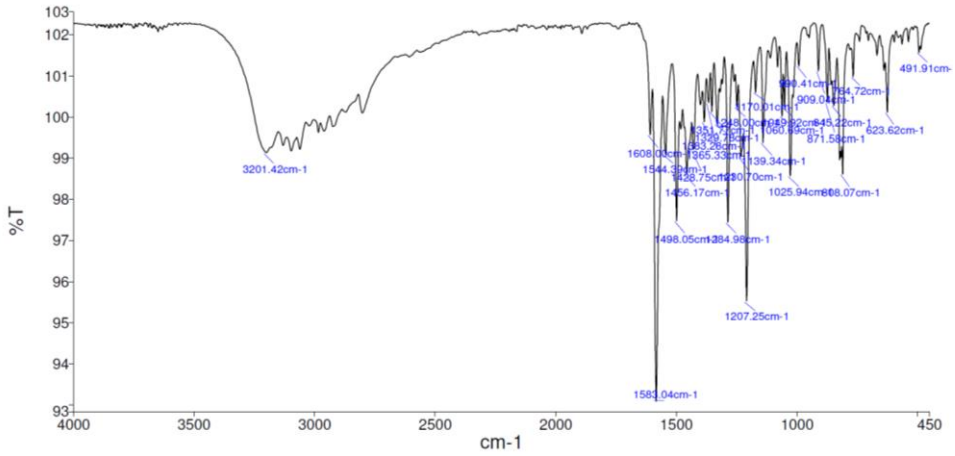
%T
cm-1
3201.42cm-1
1608.03cm-1
1544.32cm-1
1498.05cm-1
1207.25cm-1
1025.94cm-1
808.07cm-1
491.91cm-1

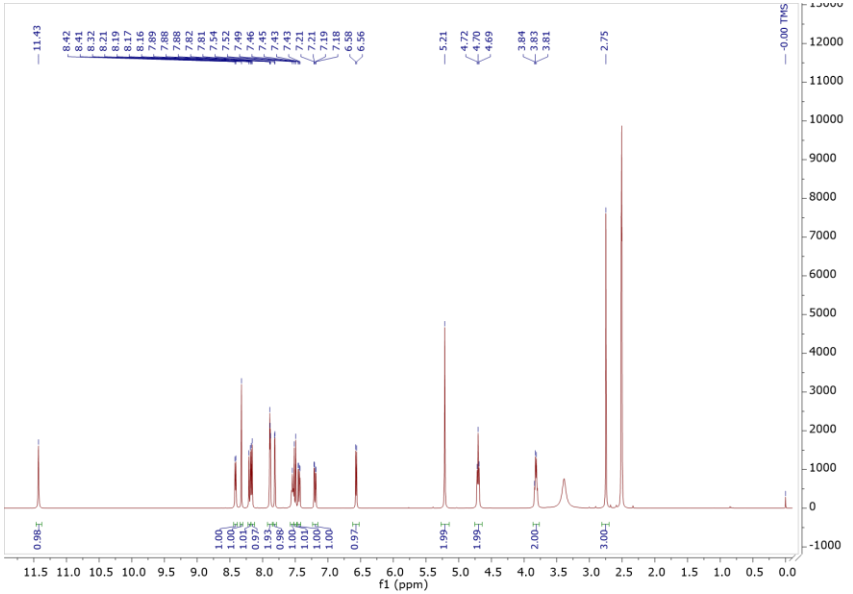
11.43
8.42
8.41
8.32
8.21
8.19
8.17
8.16
7.89
7.88
7.82
7.81
7.54
7.52
7.49
7.46
7.45
7.43
7.21
7.19
7.18
6.58
6.56
5.21
4.72
4.70
4.69
3.84
3.83
3.81
2.75
-0.00 TMS
f1 (ppm)

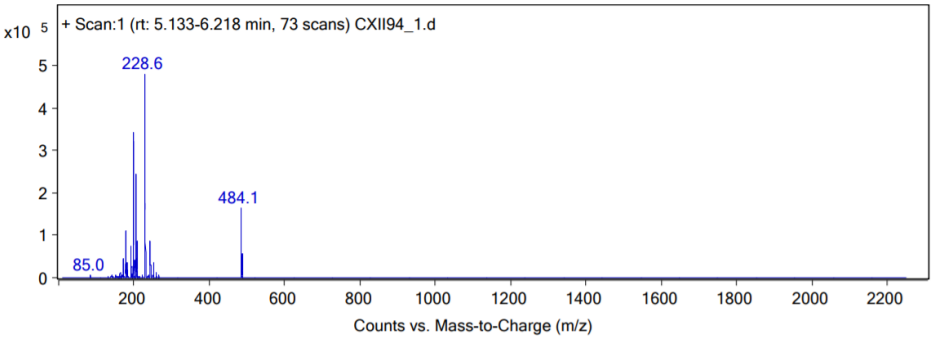
x10
+ Scan:1 (rt: 5.133-6.218 min, 73 scans) CXII94_1.d
228.6
484.1
85.0
Counts vs. Mass-to-Charge (m/z)

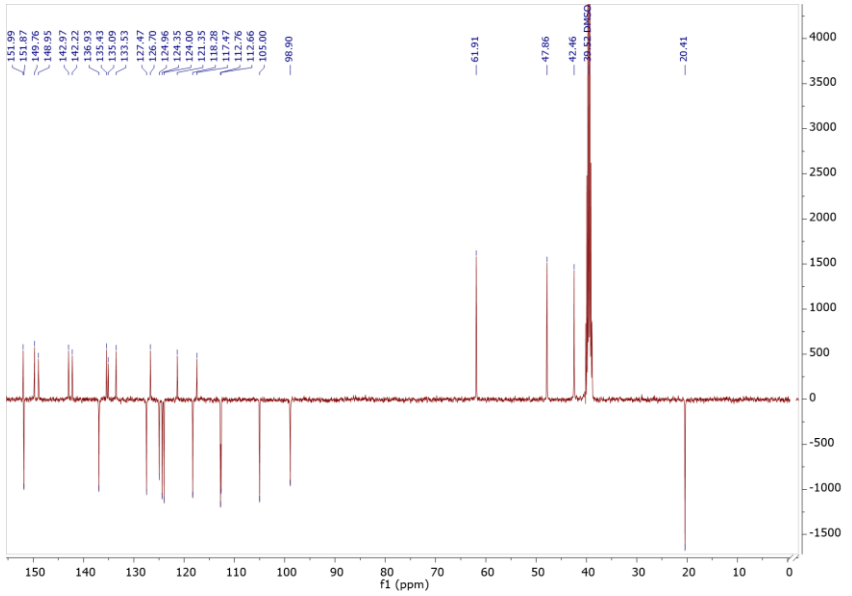
151.99
151.87
149.76
148.95
142.97
142.23
136.93
135.43
135.09
133.53
127.47
126.70
124.96
124.35
124.00
121.35
118.38
117.47
112.76
112.66
105.00
98.90
61.91
47.86
42.46
39.53 DMSO
20.41
f1 (ppm)

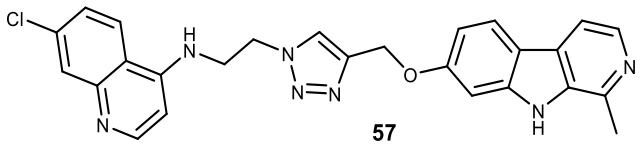
Cl
H
N
N
N
N
O
N
H
N

57

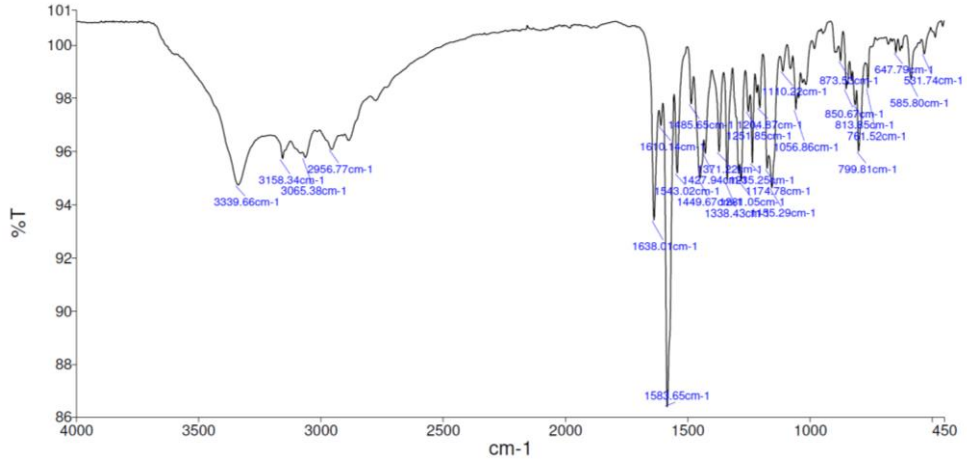
%T
cm-1
3339.66cm-1
3158.34cm-1
3065.38cm-1
2956.77cm-1
1638.01cm-1
1583.65cm-1
1543.02cm-1
1449.67cm-1
1338.43cm-1
1174.78cm-1
1056.86cm-1
799.81cm-1
761.52cm-1
585.80cm-1
551.74cm-1

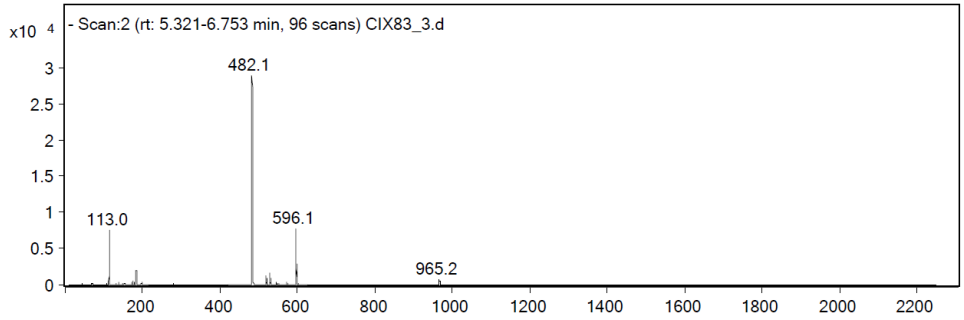
x10
- Scan:2 (rt: 5.321-6.753 min, 96 scans) CIX83_3.d
482.1
113.0
596.1
965.2

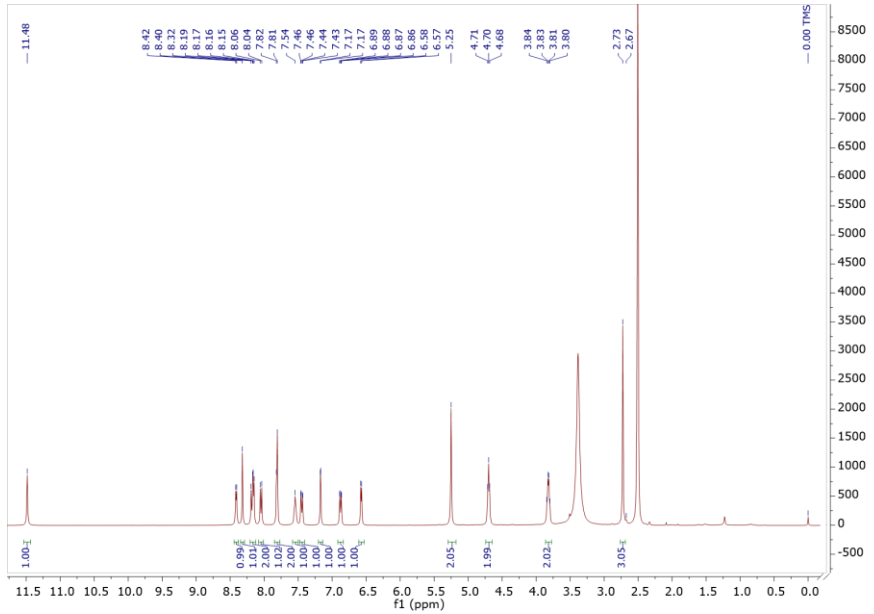
f1 (ppm)

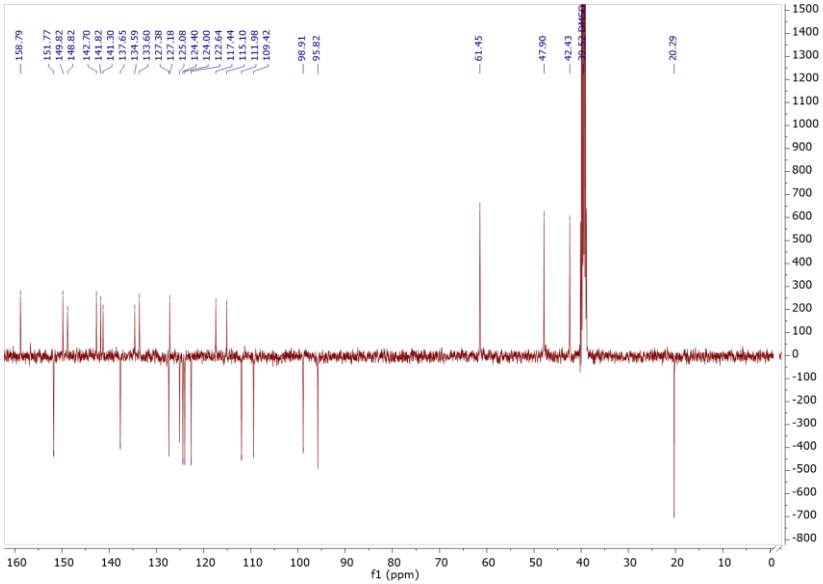
f1 (ppm)

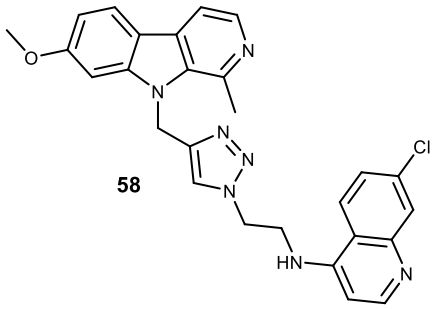
O
N
N
N
N
HN
N
Cl

58

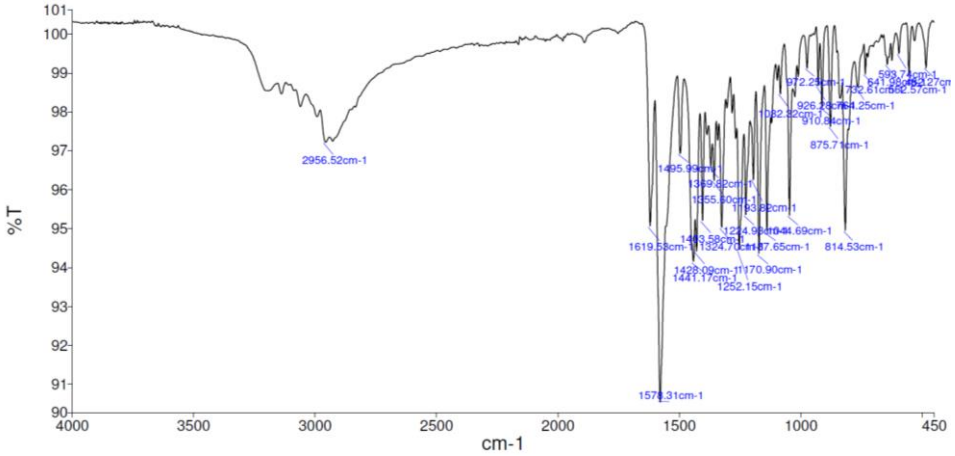
%T
cm-1
2956.52cm-1
1619.53cm-1
1578.31cm-1
1441.17cm-1
1428.09cm-1
1252.15cm-1
1170.90cm-1
814.53cm-1
875.71cm-1

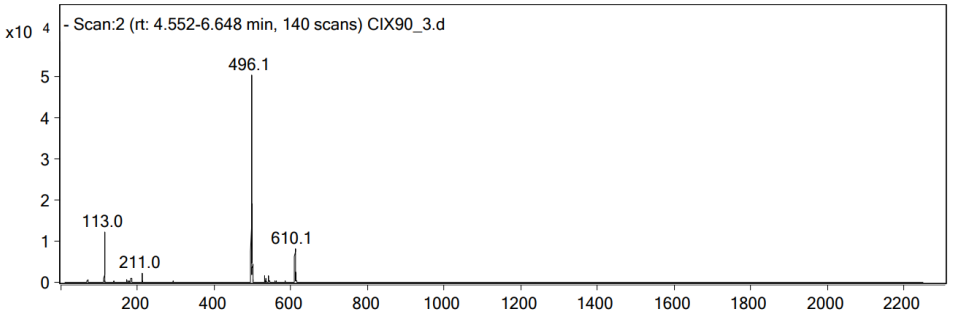
x10
- Scan:2 (rt: 4.552-6.648 min, 140 scans) CIX90_3.d
496.1
610.1
211.0
113.0

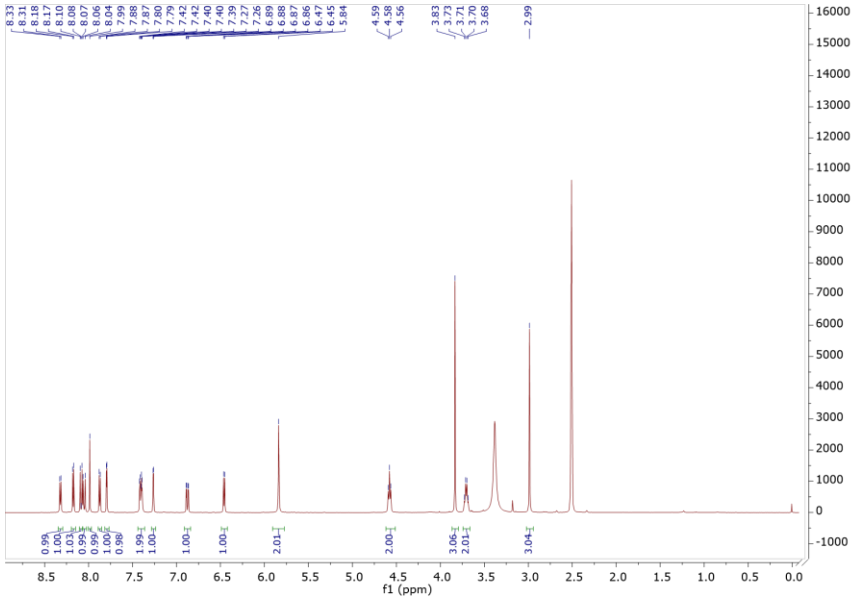
f1 (ppm)

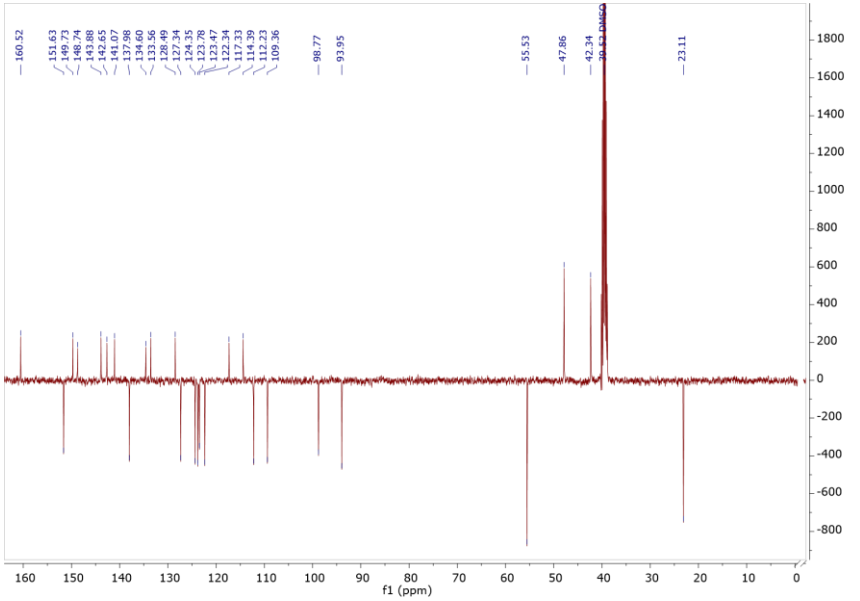
f1 (ppm)

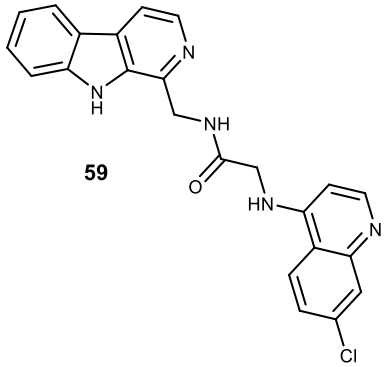
N
H
NH
O
HN
N
Cl

59

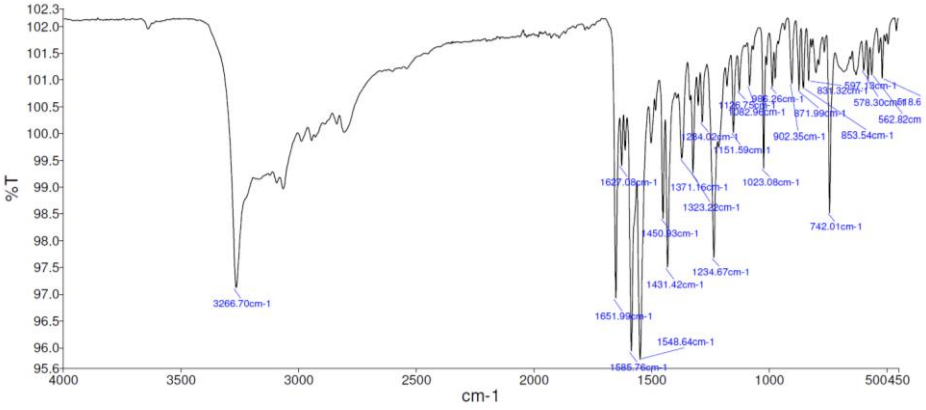
%T
cm-1
3266.70cm-1
1651.99cm-1
1548.64cm-1
1585.76cm-1
1431.42cm-1
1450.93cm-1
1627.08cm-1
1371.16cm-1
1323.22cm-1
1234.67cm-1
1284.02cm-1
1151.59cm-1
1023.08cm-1
902.35cm-1
871.99cm-1
853.54cm-1
742.01cm-1
562.82cm

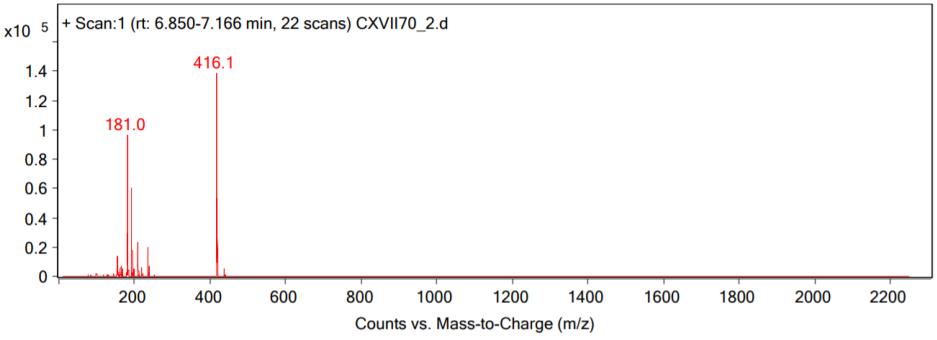
x10
+ Scan:1 (rt: 6.850-7.166 min, 22 scans) CXVII70_2.d
416.1
181.0
Counts vs. Mass-to-Charge (m/z)

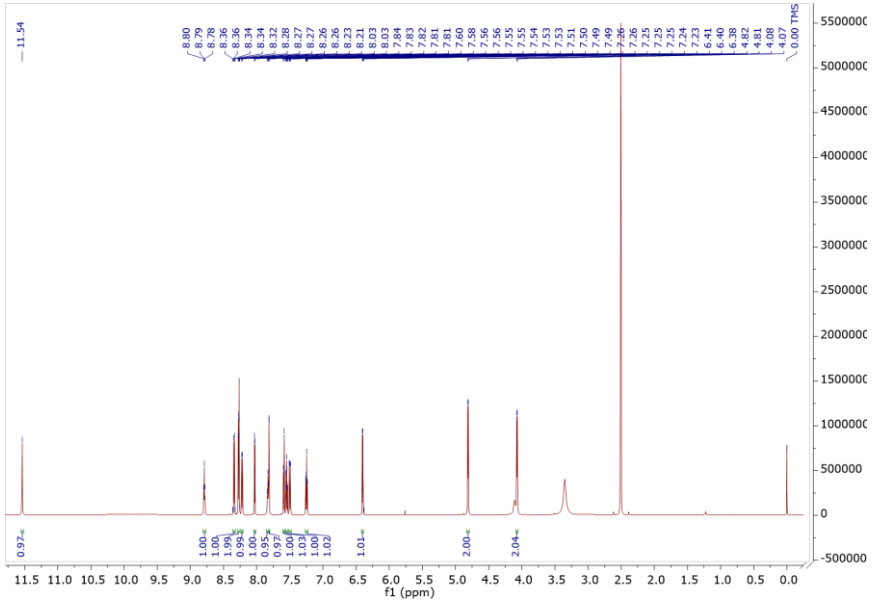
11.54
0.00 TMS
f1 (ppm)

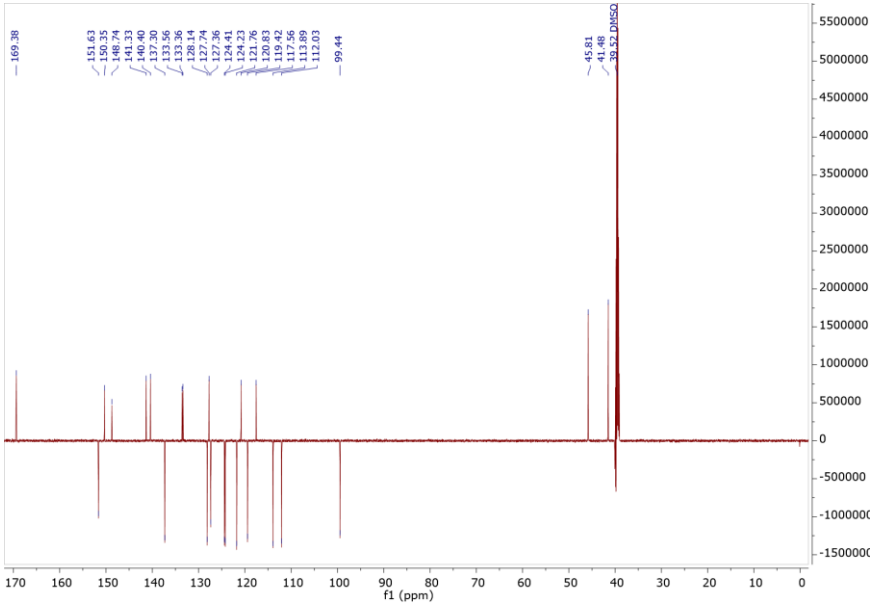
169.38
151.63
150.35
148.74
141.33
140.40
137.30
133.56
133.36
128.14
127.74
127.36
124.41
124.23
121.76
120.83
119.42
117.56
113.89
112.03
99.44
45.81
41.48
39.52 DMSO
f1 (ppm)

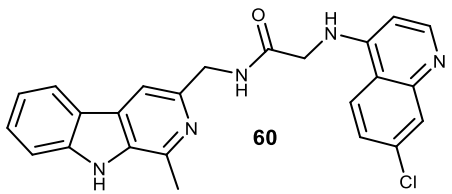
O
H
N
N
H
N
N
H
Cl

60

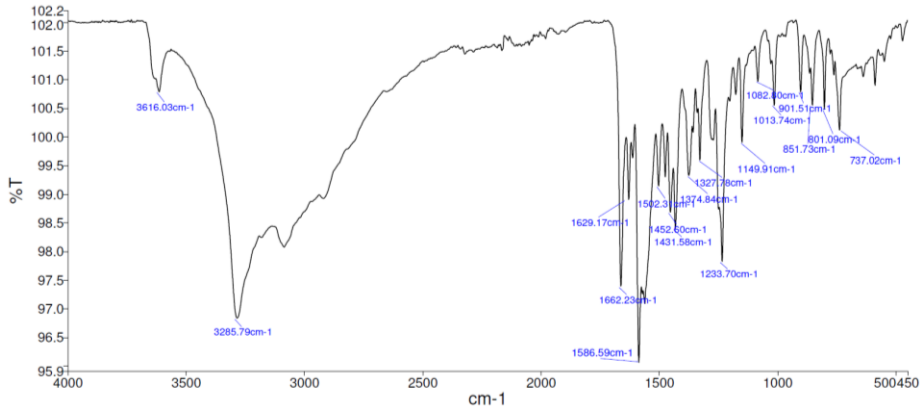
%T
cm-1
3616.03cm-1
3285.79cm-1
1629.17cm-1
1662.23cm-1
1586.59cm-1
1502.31cm-1
1452.60cm-1
1431.58cm-1
1374.84cm-1
1327.78cm-1
1233.70cm-1
1149.91cm-1
1082.40cm-1
1013.74cm-1
901.51cm-1
851.73cm-1
801.09cm-1
737.02cm-1

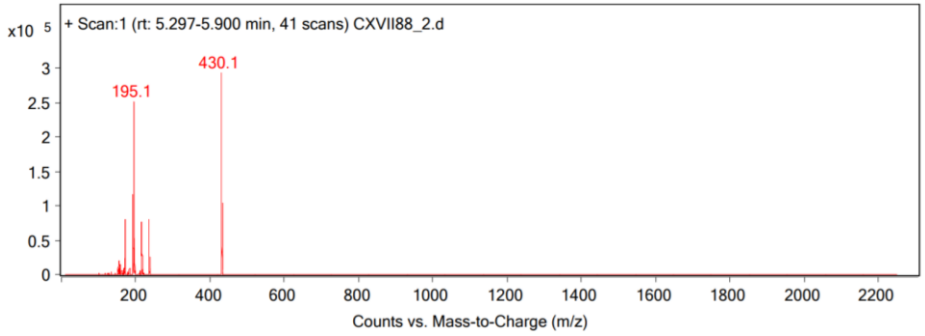
x10 5
+ Scan:1 (rt: 5.297-5.900 min, 41 scans) CXVII88_2.d
195.1
430.1
Counts vs. Mass-to-Charge (m/z)

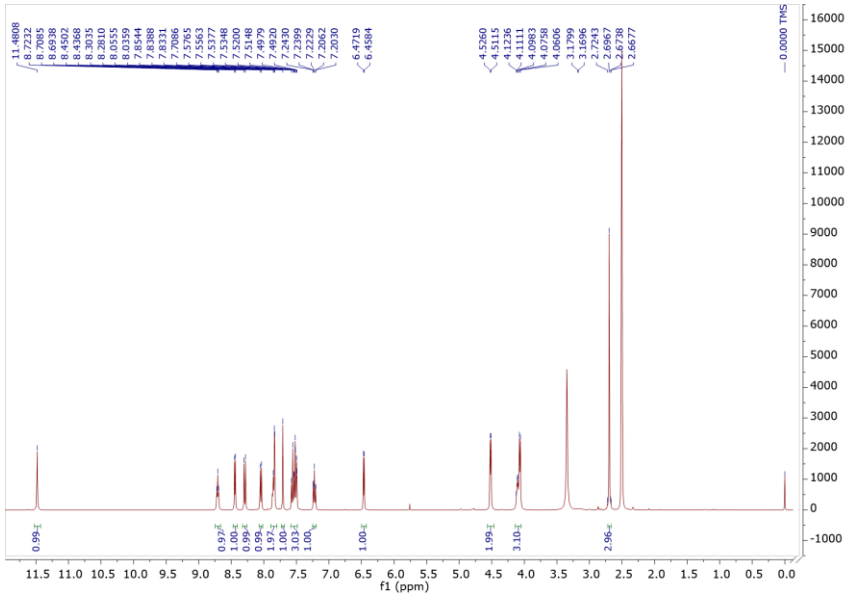
f1 (ppm)
0.0000 TMS

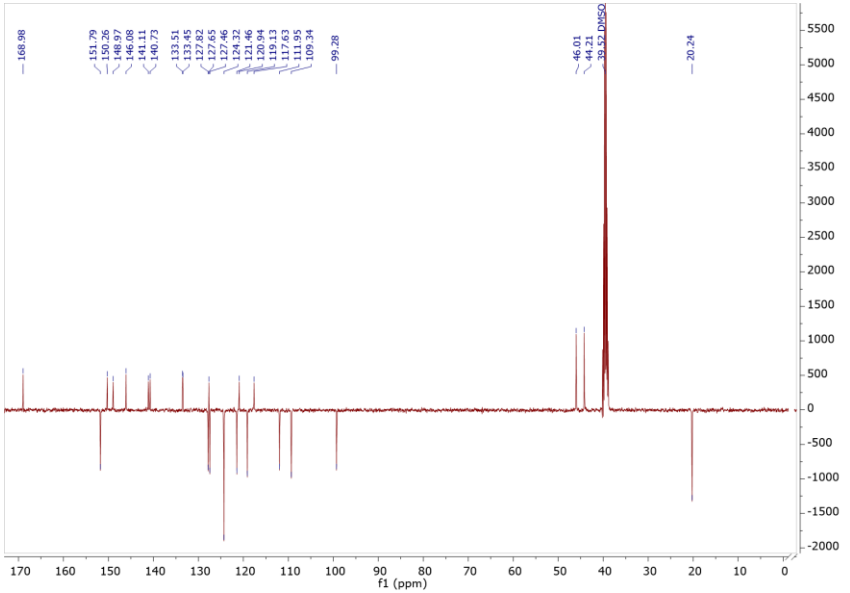
f1 (ppm)
39.52 DMSO

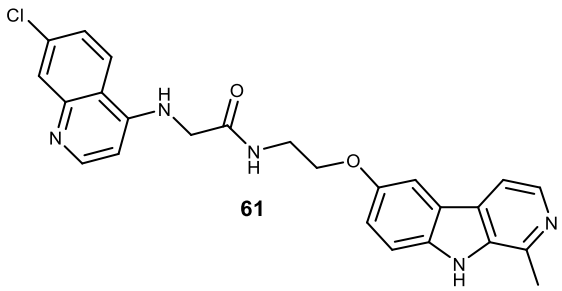
Cl
N
H
N
O
H
N
O
N
H
N

61

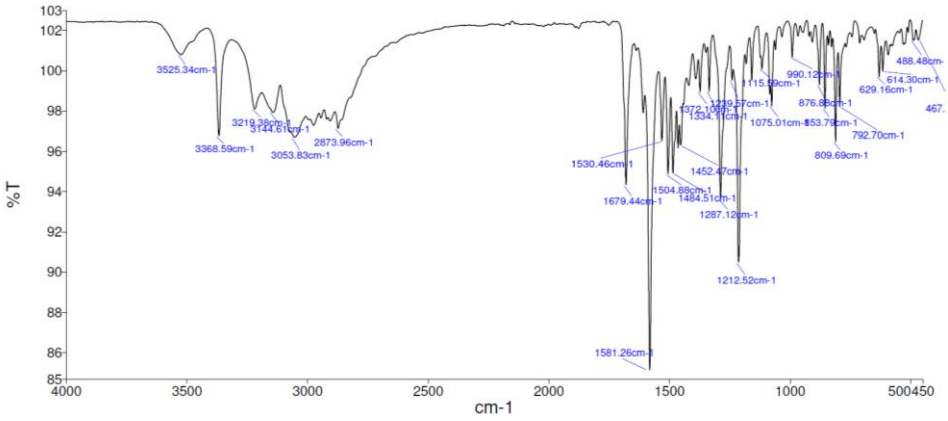
%T
cm-1
3525.34cm-1
3368.59cm-1
3219.38cm-1
3144.61cm-1
3053.83cm-1
2873.96cm-1
1679.44cm-1
1581.26cm-1
1530.46cm-1
1504.88cm-1
1484.51cm-1
1452.47cm-1
1287.12cm-1
1212.52cm-1
1075.01cm-1
990.12cm-1
876.88cm-1
853.79cm-1
809.69cm-1
792.70cm-1
629.16cm-1
614.30cm-1
488.48cm-1

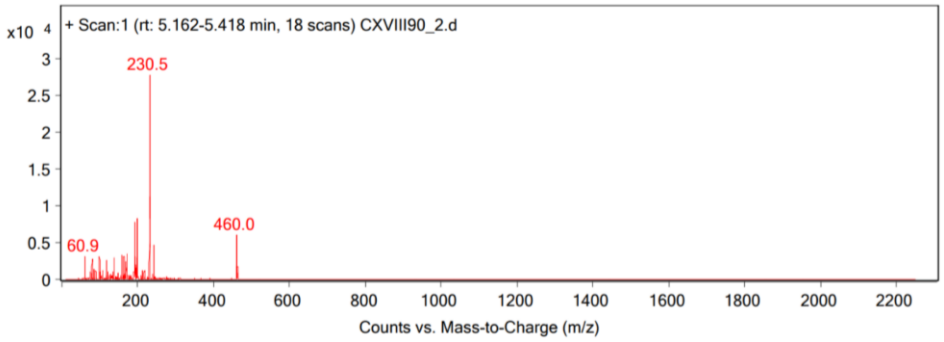
x10 4
+ Scan:1 (rt: 5.162-5.418 min, 18 scans) CXVIII90_2.d
230.5
460.0
60.9
Counts vs. Mass-to-Charge (m/z)

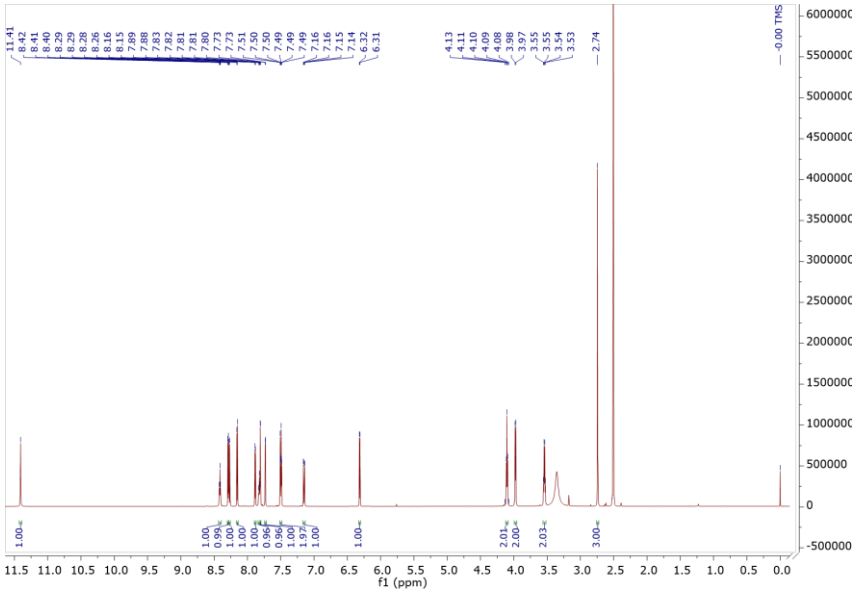
f1 (ppm)
-0.00 TMS
2.74

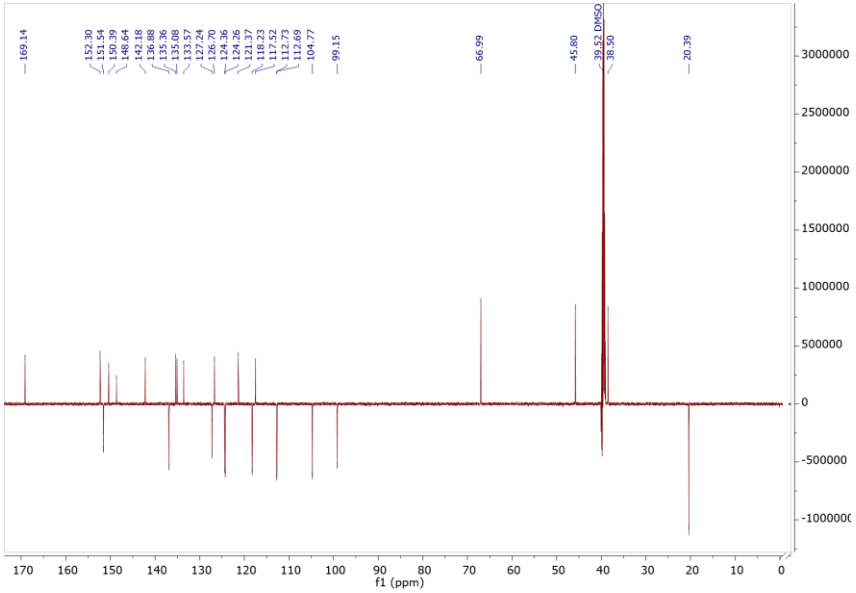
f1 (ppm)
169.14
152.30
151.54
150.39
148.64
142.88
139.36
135.08
133.57
127.24
126.70
124.36
124.26
121.37
118.23
117.52
112.73
112.69
104.77
99.15
66.99
45.80
39.52 DMSO
38.50
20.39

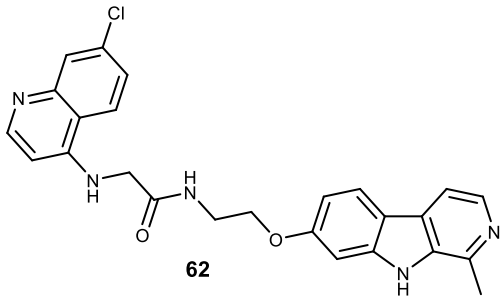
Cl
N
H
N
O
H
N
O
N
H
N

62

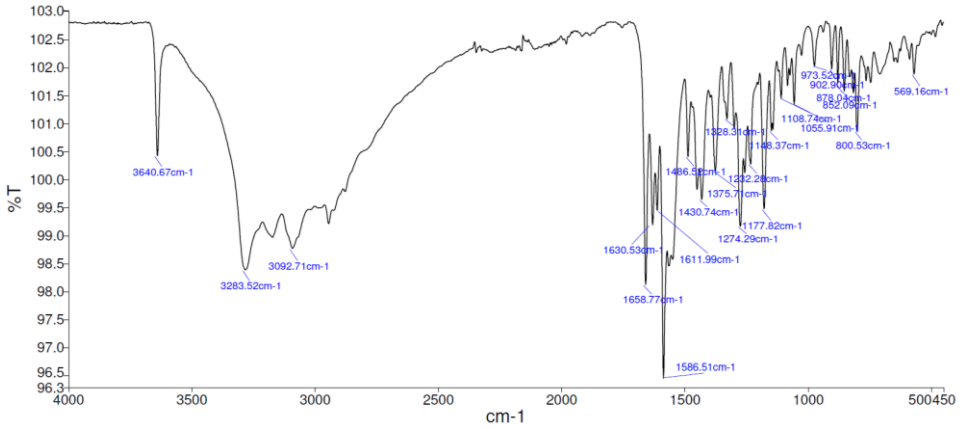
%T
cm-1
3640.67cm-1
3283.52cm-1
3092.71cm-1
1658.77cm-1
1630.53cm-1
1611.99cm-1
1586.51cm-1
1486.58cm-1
1430.74cm-1
1375.77cm-1
1328.31cm-1
1274.29cm-1
1232.28cm-1
1177.82cm-1
1148.37cm-1
1108.74cm-1
1055.91cm-1
973.52cm-1
902.90cm-1
878.04cm-1
852.09cm-1
800.53cm-1
569.16cm-1

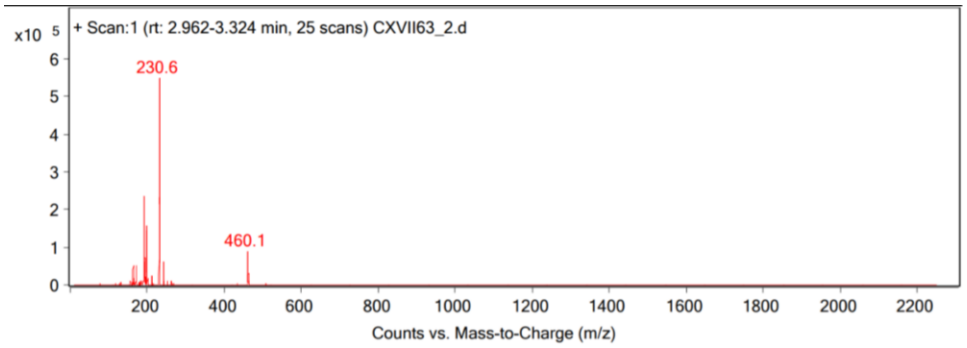
x10
+ Scan:1 (rt: 2.962-3.324 min, 25 scans) CXVII63_2.d
230.6
460.1
Counts vs. Mass-to-Charge (m/z)

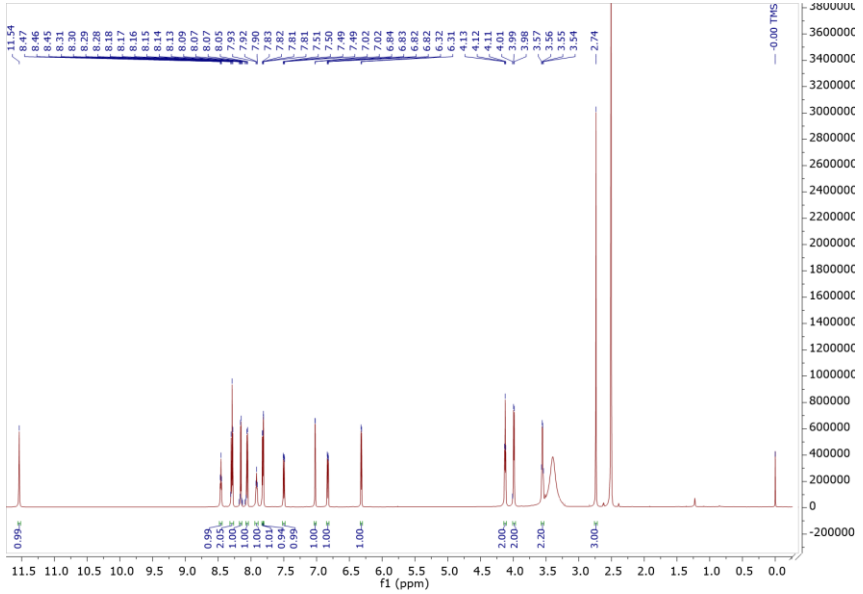
f1 (ppm)

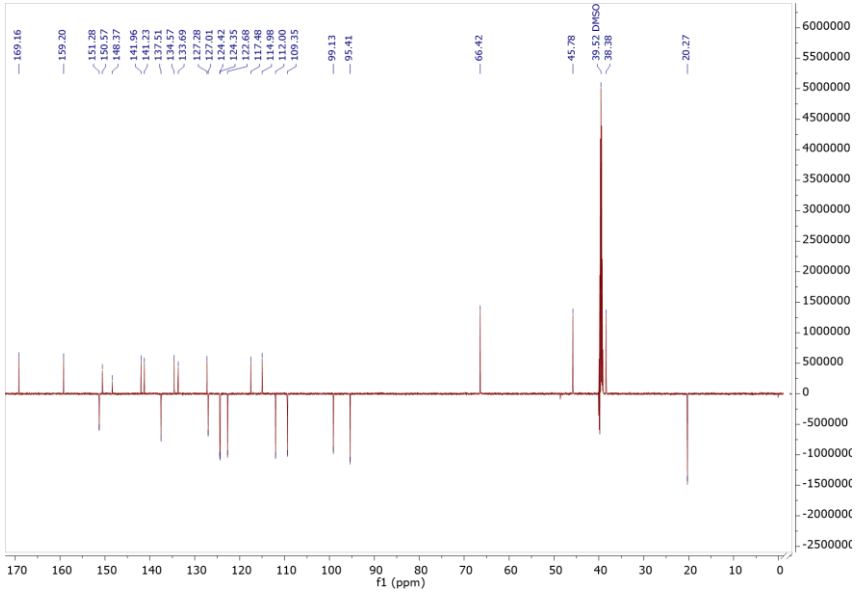
f1 (ppm)

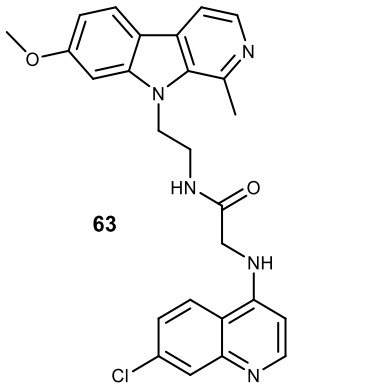
O
N
HN
O
NH
Cl
N

63

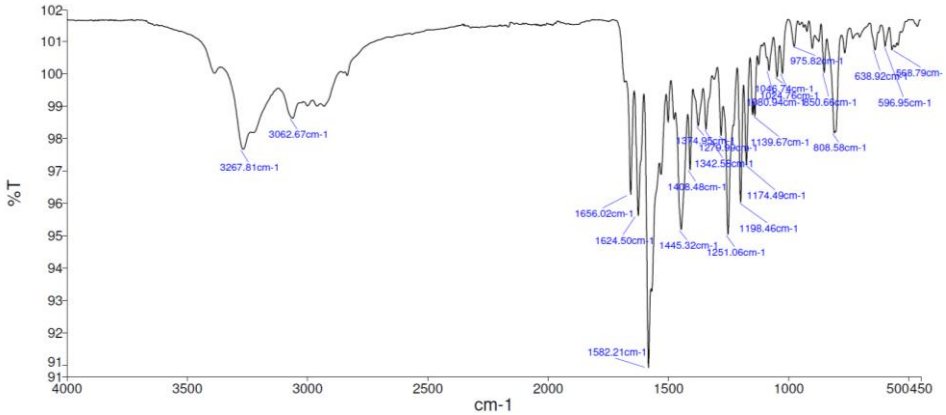
%T
cm-1
3267.81cm-1
3062.67cm-1
1656.02cm-1
1624.50cm-1
1582.21cm-1
1445.32cm-1
1408.48cm-1
1342.58cm-1
1251.06cm-1
1198.46cm-1
1174.49cm-1
1139.67cm-1
1046.74cm-1
1024.76cm-1
980.94cm-1
975.82cm-1
850.66cm-1
808.58cm-1
638.92cm-1
596.95cm-1

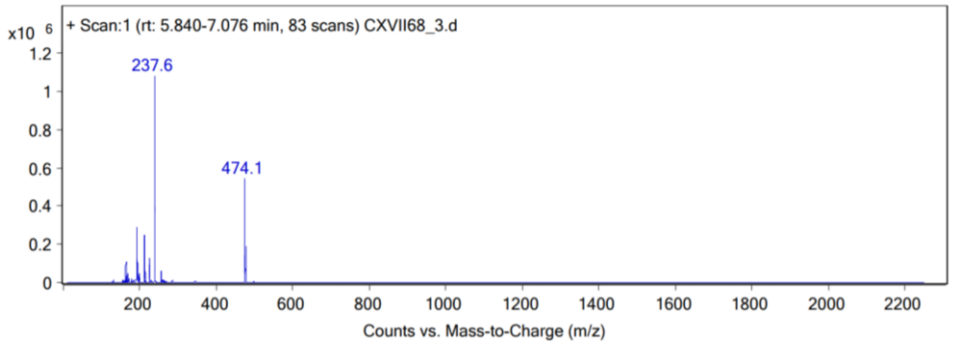
x10 6
+ Scan:1 (rt: 5.840-7.076 min, 83 scans) CXVII68_3.d
237.6
474.1
Counts vs. Mass-to-Charge (m/z)

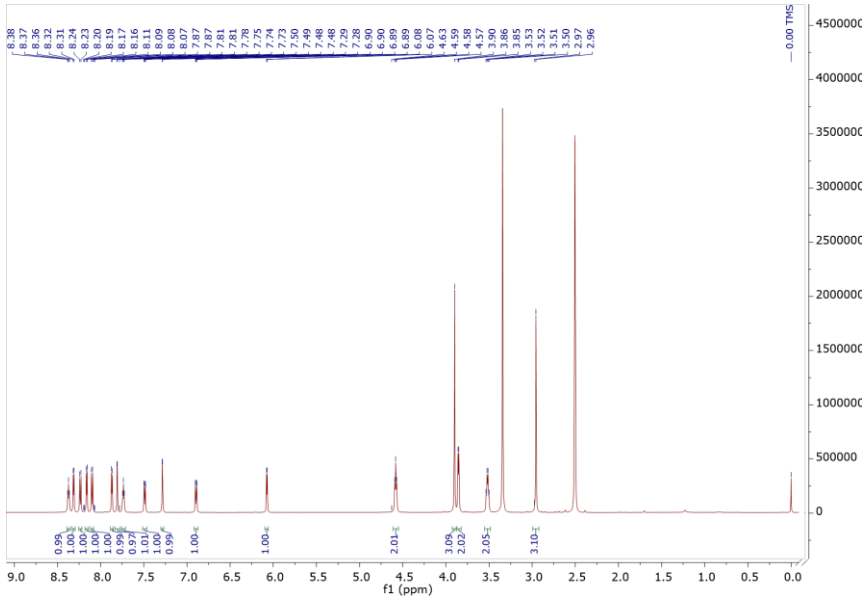
0.00 TMS
f1 (ppm)

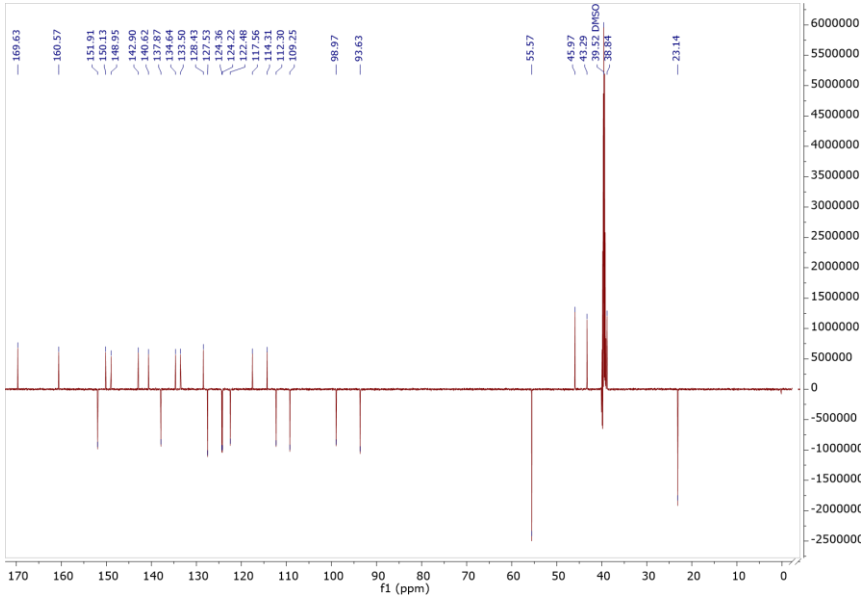
169.63
160.57
151.91
150.13
148.95
142.90
140.62
137.87
134.64
133.50
128.43
127.53
124.36
124.22
122.48
117.56
114.31
112.30
109.25
98.97
93.63
55.57
45.97
43.29
39.52 DMSO
38.84
23.14
f1 (ppm)

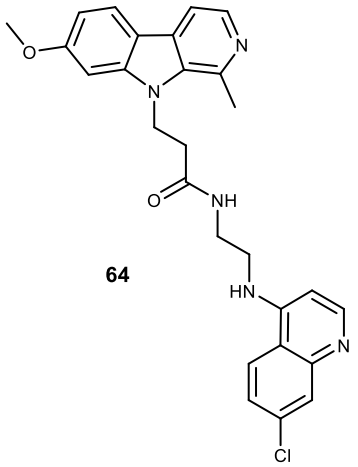
O
N
N
O
NH
HN
N
Cl

64

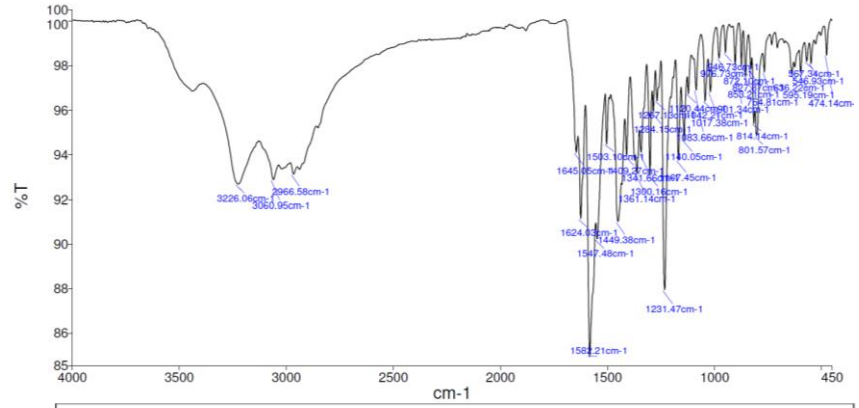
%T
cm-1
3226.06cm-1
2966.58cm-1
3050.95cm-1
1624.03cm-1
1449.38cm-1
1547.48cm-1
1231.47cm-1
1582.21cm-1
1543.10cm-1
1140.05cm-1
1361.14cm-1
814.14cm-1
801.57cm-1

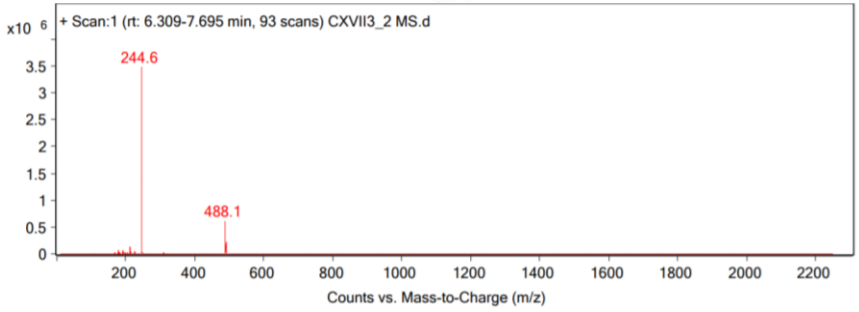
x10 6
+ Scan:1 (rt: 6.309-7.695 min, 93 scans) CXVII3_2 MS.d
244.6
488.1
Counts vs. Mass-to-Charge (m/z)

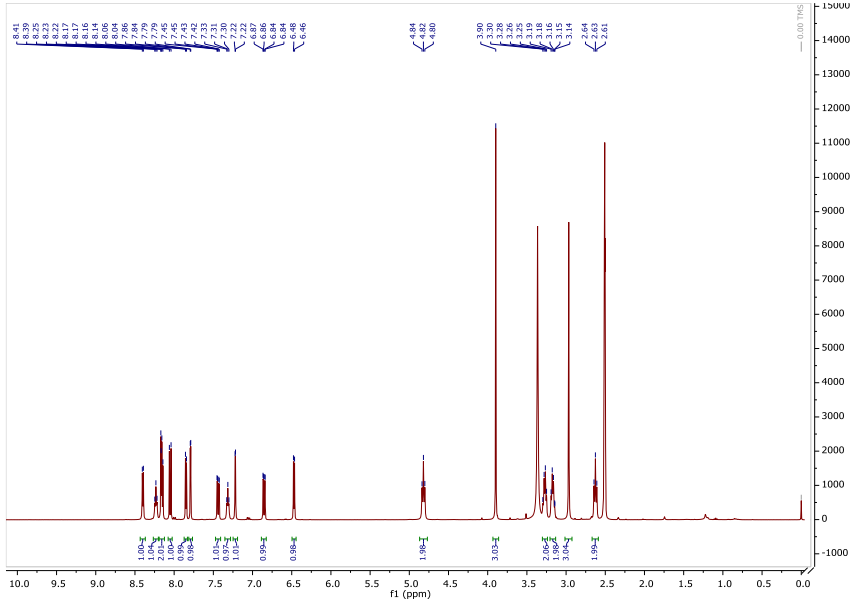
f1 (ppm)

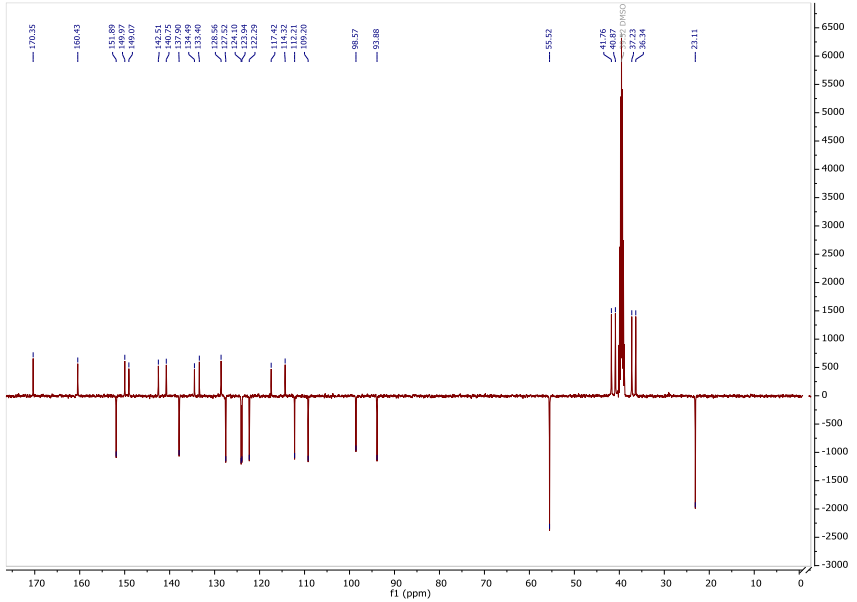
f1 (ppm)

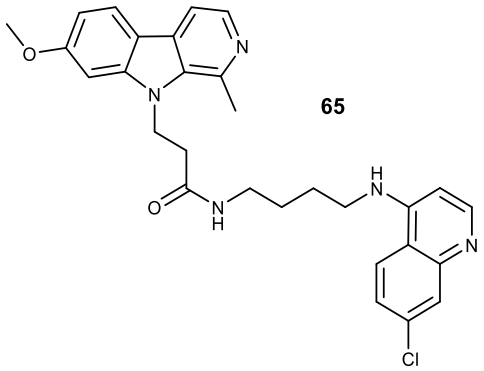
O
N
N
H
O
N
H
N
Cl

65

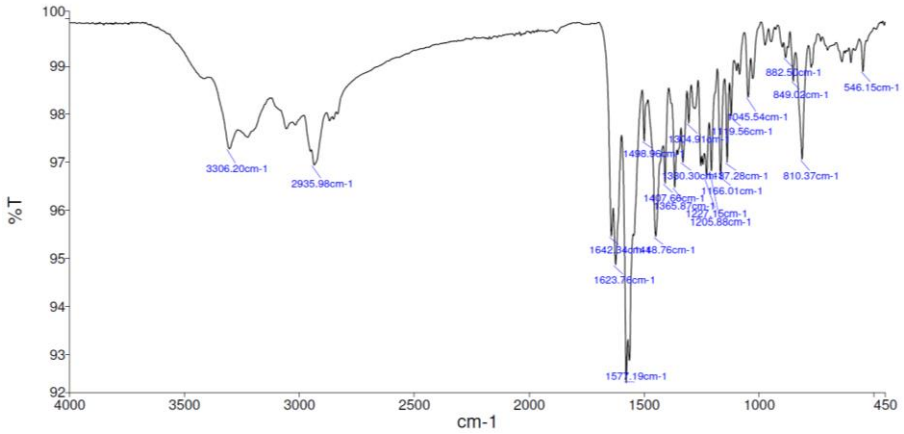
%T
cm-1
3306.20cm-1
2935.98cm-1
1642.84cm-1
1623.76cm-1
1577.19cm-1
1498.96cm-1
1497.68cm-1
1205.88cm-1
1166.01cm-1
1045.54cm-1
882.53cm-1
849.02cm-1
810.37cm-1
546.15cm-1

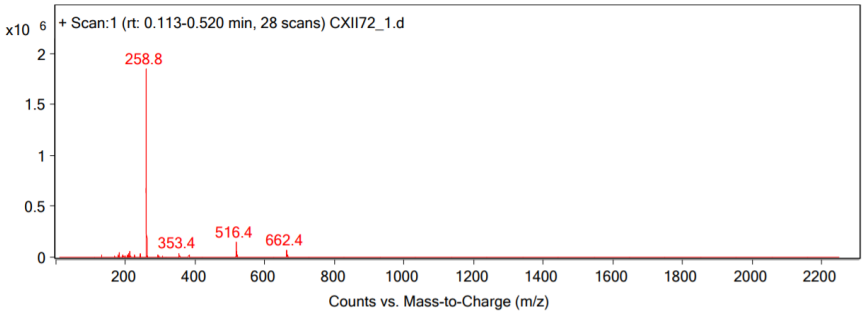
x10 6
+ Scan:1 (rt: 0.113-0.520 min, 28 scans) CXII72_1.d
258.8
353.4
516.4
662.4
Counts vs. Mass-to-Charge (m/z)

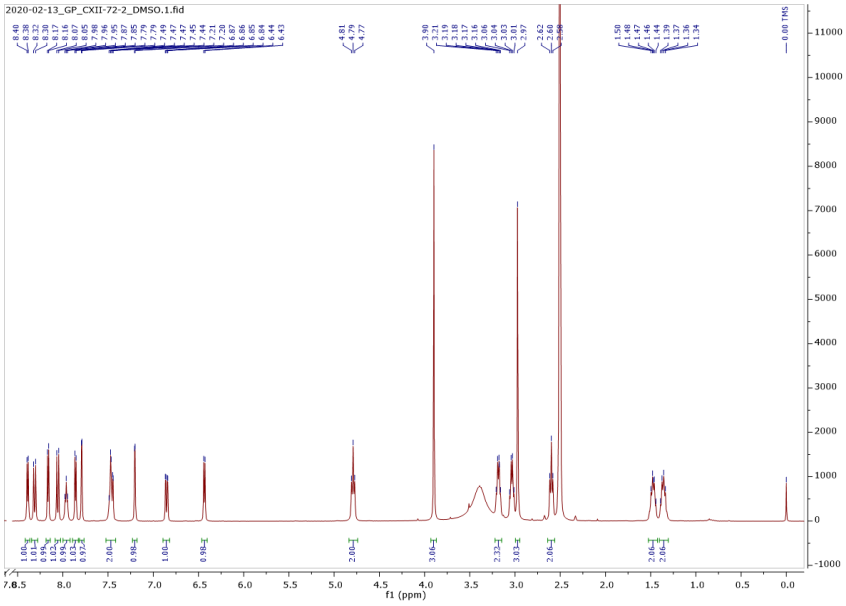
2020-02-13_GP_CXII-72-2_DMSO.1.fid
f1 (ppm)

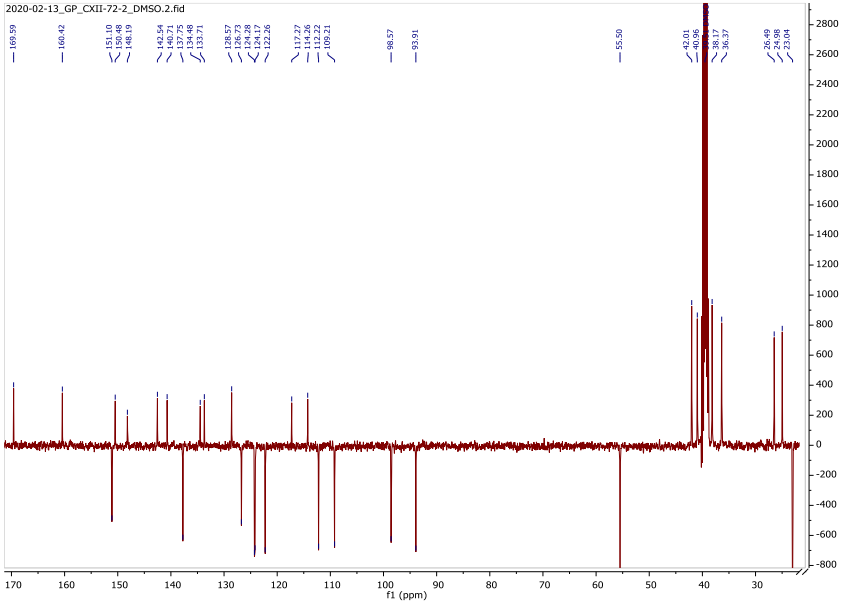
2020-02-13_GP_CXII-72-2_DMSO.2.fid
f1 (ppm)

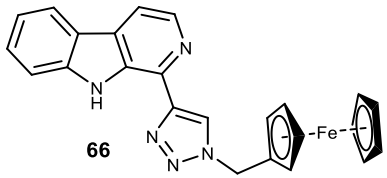
N
H
N
N
N
Fe

66

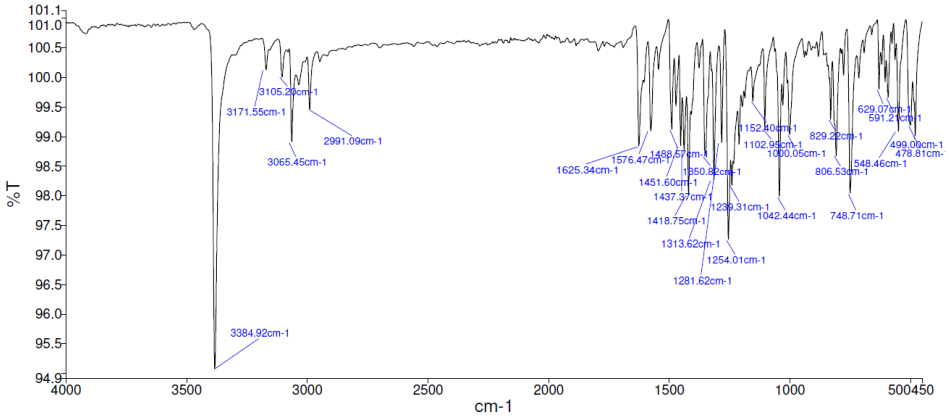
%T
cm-1
3384.92cm-1
3171.55cm-1
3105.22cm-1
3065.45cm-1
2991.09cm-1
1625.34cm-1
1576.47cm-1
1488.57cm-1
1451.60cm-1
1437.37cm-1
1418.75cm-1
1350.82cm-1
1313.62cm-1
1281.62cm-1
1254.01cm-1
1239.31cm-1
1152.40cm-1
1102.96cm-1
1042.44cm-1
1000.05cm-1
829.22cm-1
806.53cm-1
748.71cm-1
629.07cm-1
591.21cm-1
548.46cm-1
499.09cm-1
478.81cm-1

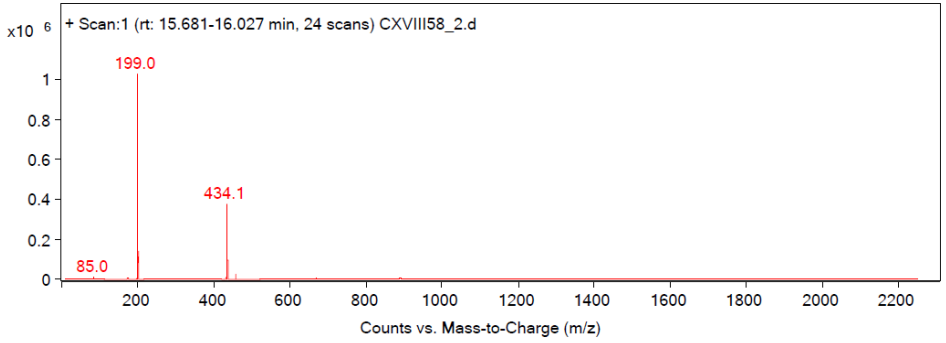
+ Scan:1 (rt: 15.681-16.027 min, 24 scans) CXVIII58_2.d
x10 6
199.0
434.1
85.0
Counts vs. Mass-to-Charge (m/z)

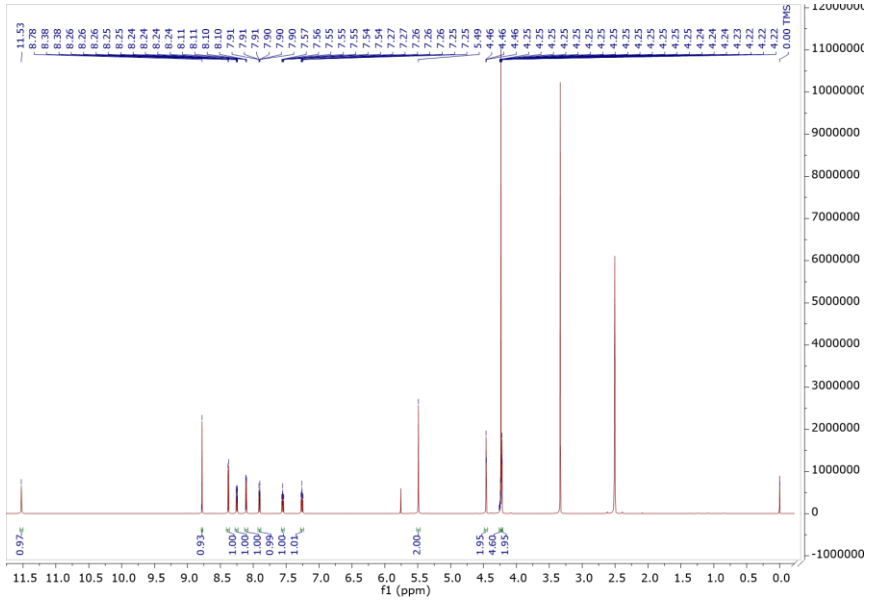
f1 (ppm)

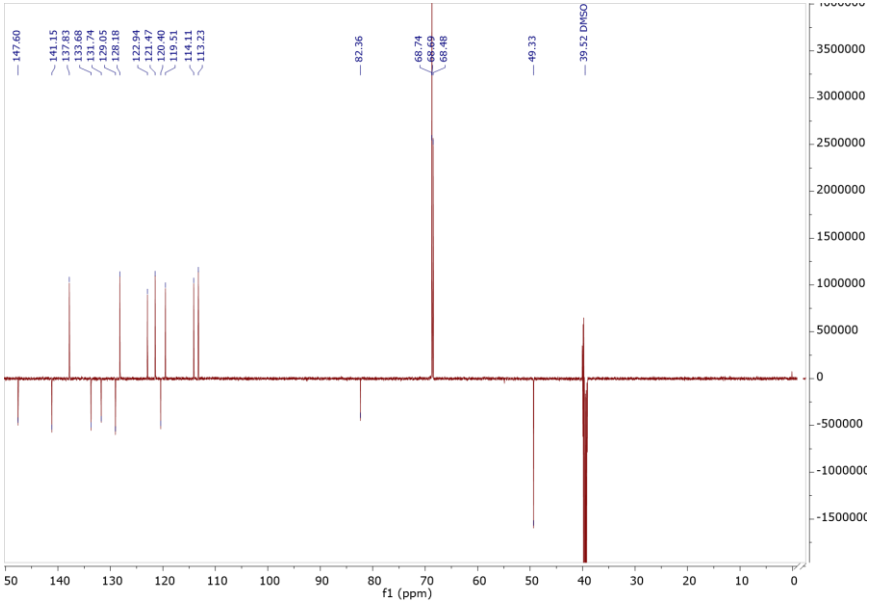
147.60
141.15
137.83
133.68
131.74
129.65
128.18
122.94
121.47
120.40
119.51
114.11
113.23
82.36
68.74
68.69
68.48
49.33
39.52 DMSO
f1 (ppm)

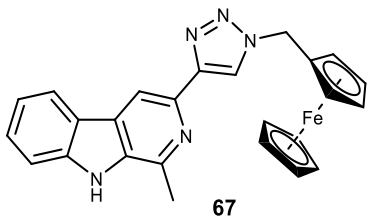
N
N
N
Fe
N
H

67

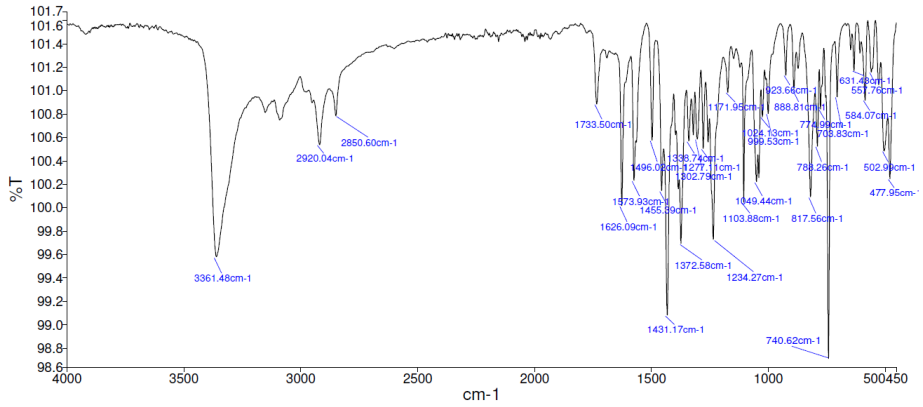
%T
cm-1
3361.48cm-1
2920.04cm-1
2850.60cm-1
1733.50cm-1
1626.09cm-1
1573.93cm-1
1455.59cm-1
1372.58cm-1
1431.17cm-1
1234.27cm-1
1103.88cm-1
1049.44cm-1
817.56cm-1
740.62cm-1

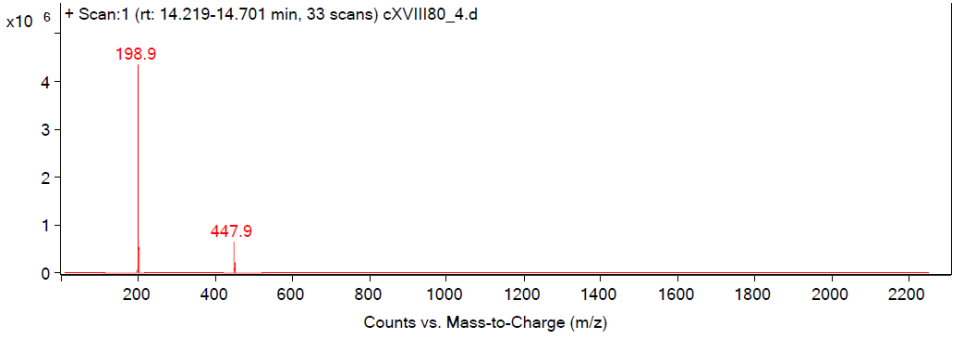
x10 6
+ Scan:1 (rt: 14.219-14.701 min, 33 scans) cXVIII80_4.d
198.9
447.9
Counts vs. Mass-to-Charge (m/z)

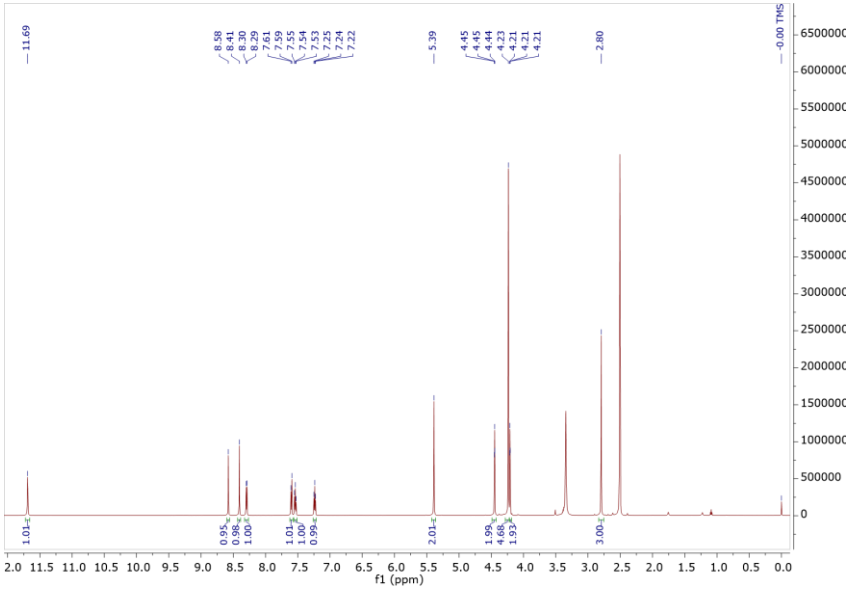
11.69
8.58
8.41
8.30
8.29
7.61
7.59
7.55
7.54
7.53
7.25
7.24
7.22
5.39
4.45
4.44
4.23
4.21
4.21
2.80
0.00 TMS
f1 (ppm)

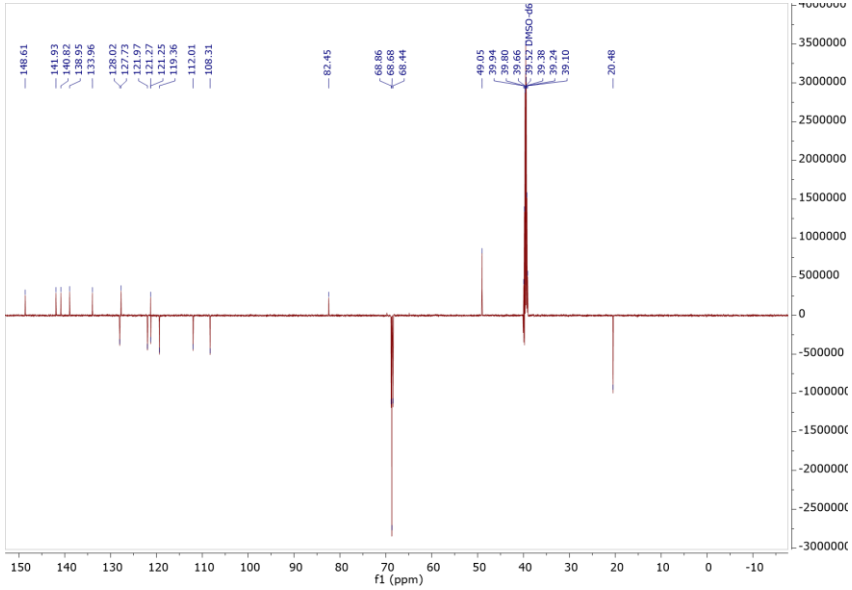
148.61
141.93
140.82
138.95
133.96
128.02
127.73
121.97
121.27
121.25
119.36
112.01
108.31
82.45
68.86
68.68
68.44
49.05
39.94
39.80
39.66
DMSO-d6
39.38
39.24
39.10
20.48
f1 (ppm)

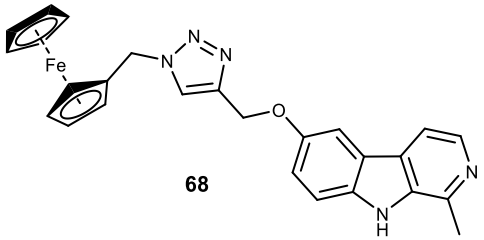
Fe
N
N
N
O
N
H

68

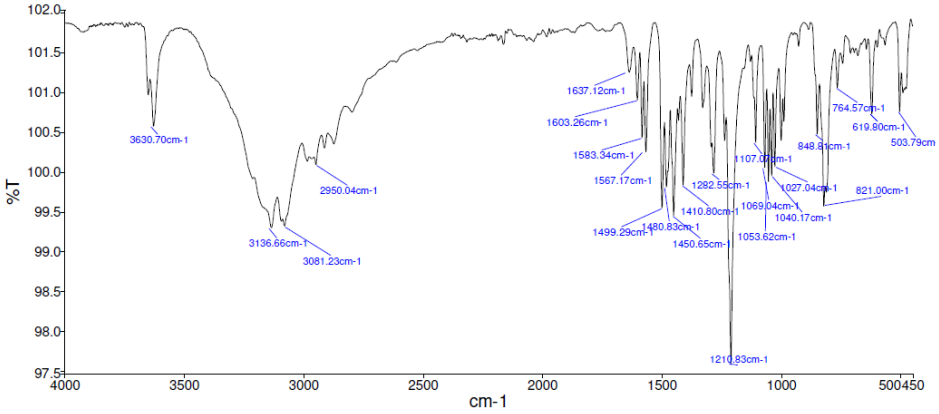
%T
cm-1
3630.70cm-1
3136.66cm-1
3081.23cm-1
2950.04cm-1
1637.12cm-1
1603.26cm-1
1583.34cm-1
1567.17cm-1
1499.29cm-1
1480.83cm-1
1450.65cm-1
1410.80cm-1
1282.55cm-1
1210.83cm-1
1107.05cm-1
1069.04cm-1
1053.62cm-1
1040.17cm-1
1027.04cm-1
848.81cm-1
821.00cm-1
764.57cm-1
619.80cm-1
503.79cm

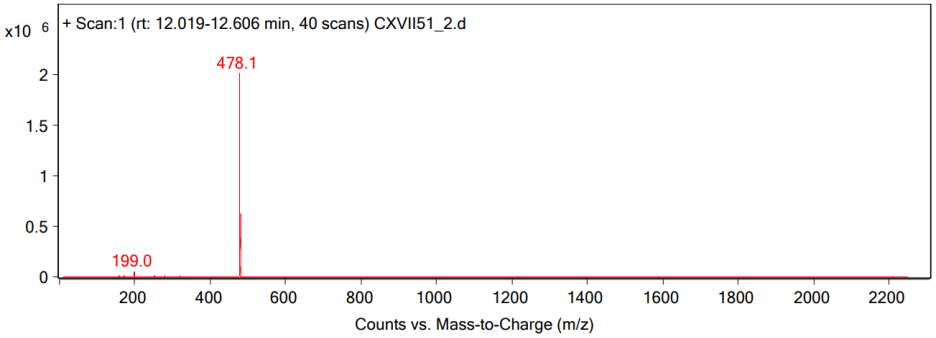
x10 6
+ Scan:1 (rt: 12.019-12.606 min, 40 scans) CXVII51_2.d
478.1
199.0
Counts vs. Mass-to-Charge (m/z)

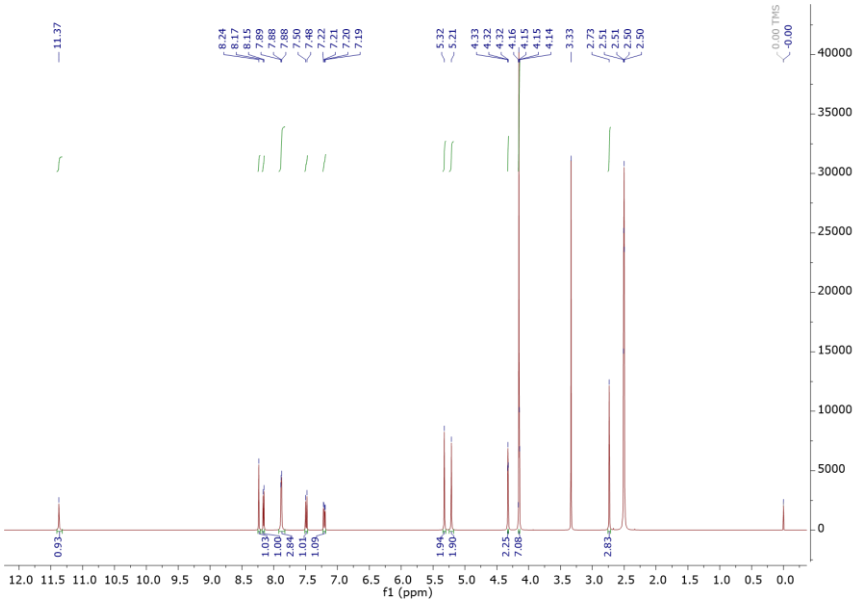
f1 (ppm)

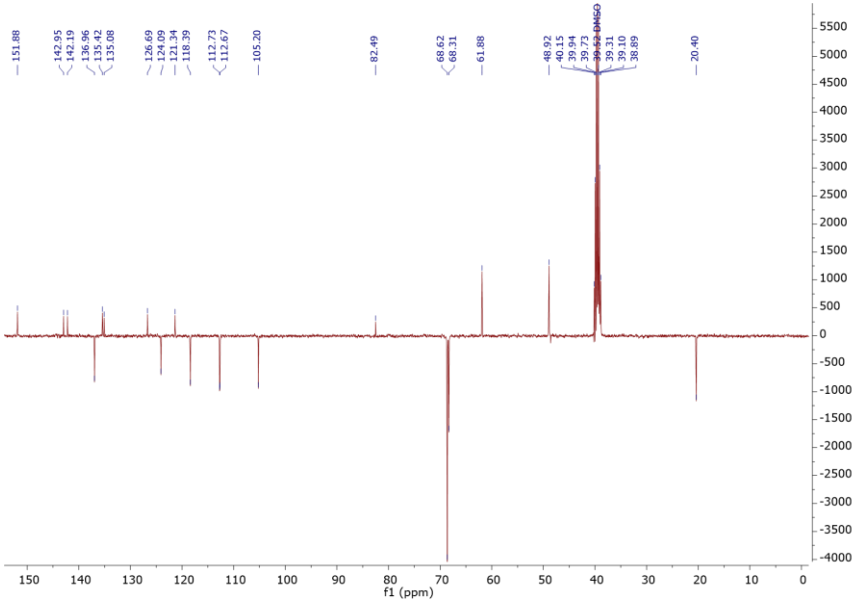
f1 (ppm)

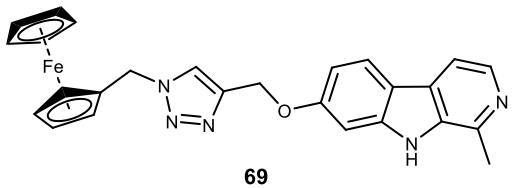
Fe
N
N
N
O
N
H

69

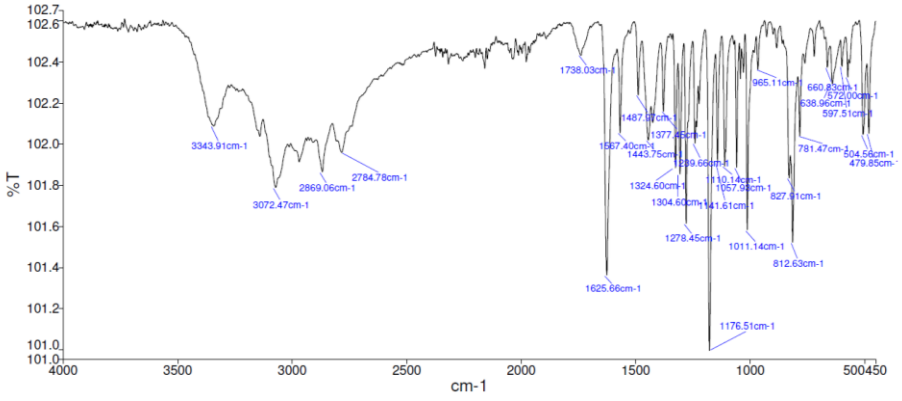
%T
cm-1
3343.91cm-1
3072.47cm-1
2869.06cm-1
2784.78cm-1
1738.03cm-1
1625.66cm-1
1587.40cm-1
1487.17cm-1
1443.75cm-1
1377.65cm-1
1324.60cm-1
1304.60cm-1
1278.45cm-1
1239.66cm-1
1176.51cm-1
1141.61cm-1
1057.93cm-1
1011.14cm-1
965.11cm-1
827.61cm-1
812.63cm-1
781.47cm-1
660.83cm-1
597.51cm-1
572.00cm-1
538.96cm-1
504.56cm-1
479.85cm-1

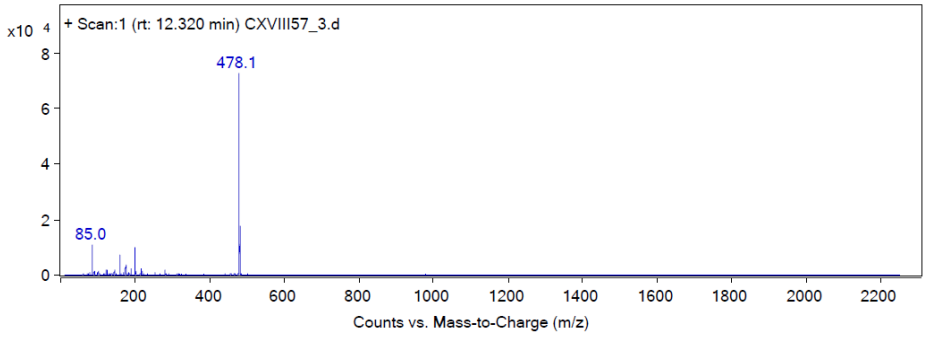
x10
+ Scan:1 (rt: 12.320 min) CXVIII57_3.d
478.1
85.0
Counts vs. Mass-to-Charge (m/z)

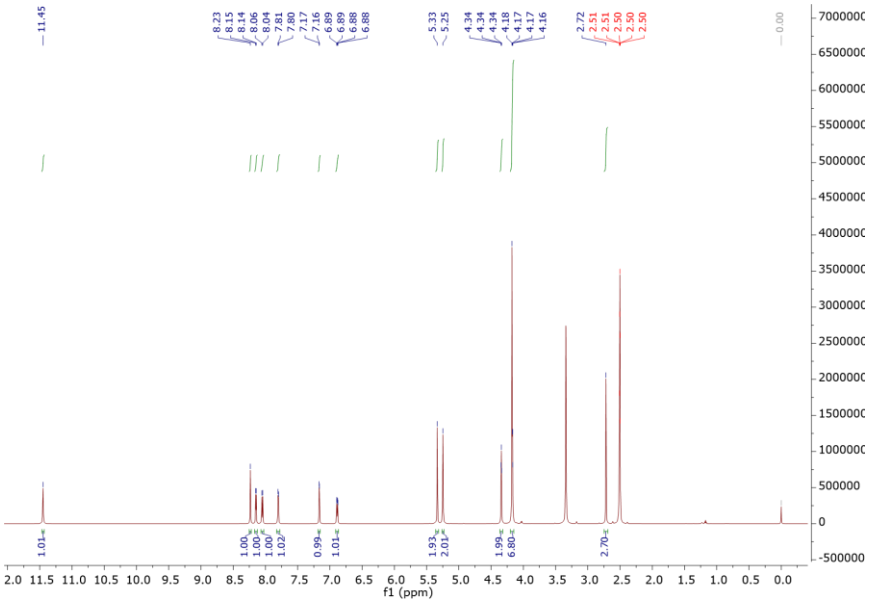
f1 (ppm)

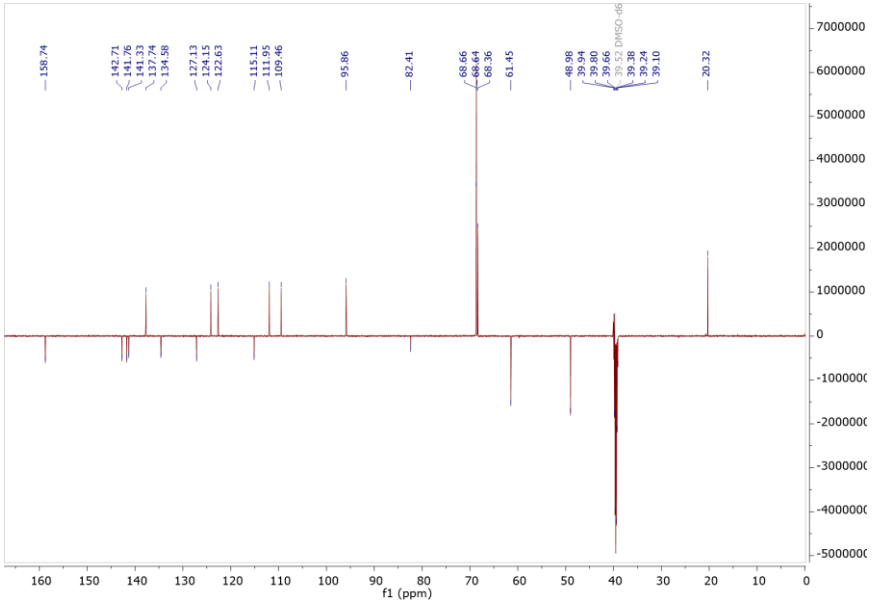
f1 (ppm)

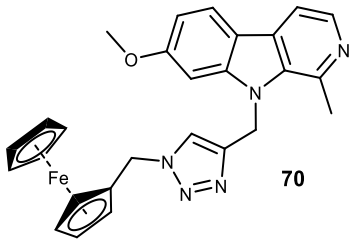
O
N
Fe
N
N
N

70

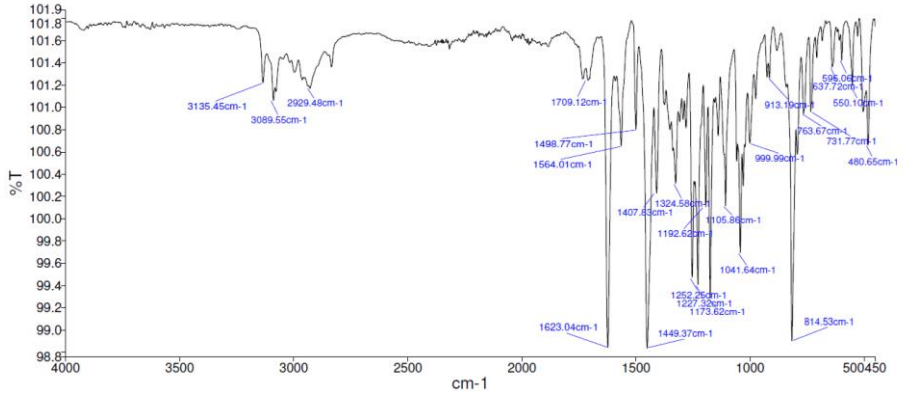
%T
cm-1
3135.45cm-1
3089.55cm-1
2929.48cm-1
1709.12cm-1
1498.77cm-1
1564.01cm-1
1407.83cm-1
1324.58cm-1
1192.62cm-1
1105.86cm-1
1041.64cm-1
1252.25cm-1
1227.32cm-1
1173.62cm-1
1623.04cm-1
1449.37cm-1
913.19cm-1
999.99cm-1
763.67cm-1
731.77cm-1
814.53cm-1
596.06cm-1
637.72cm-1
550.10cm-1
480.65cm-1

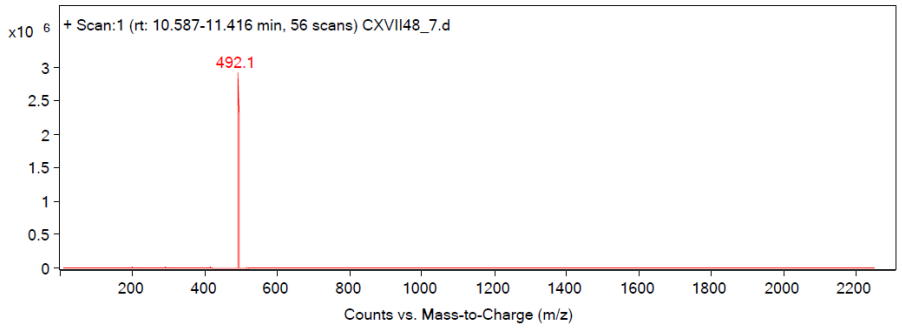
x10 6
+ Scan:1 (rt: 10.587-11.416 min, 56 scans) CXVII48_7.d
492.1
Counts vs. Mass-to-Charge (m/z)

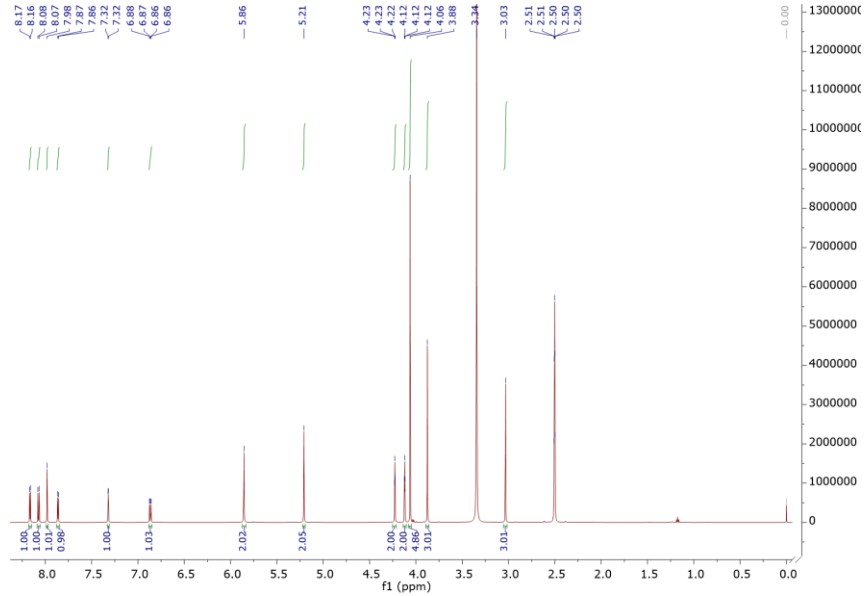
8.17
8.16
8.08
8.07
7.89
7.87
7.86
7.32
6.88
6.87
6.86
6.86
5.86
5.21
4.23
4.23
4.22
4.12
4.12
4.12
4.06
3.88
3.34
3.03
2.51
2.51
2.50
2.50
2.50
f1 (ppm)

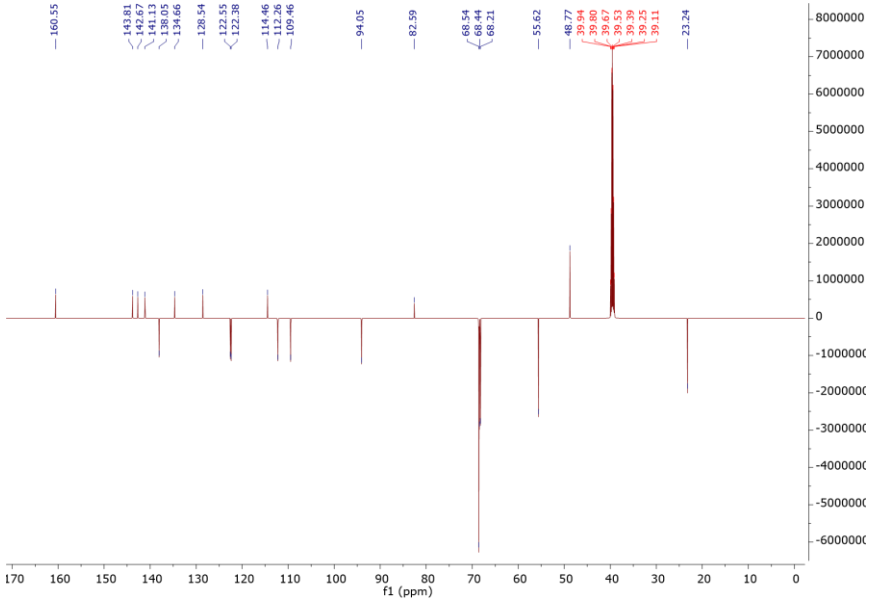
160.55
143.81
142.67
141.13
138.05
134.66
128.54
122.55
122.38
114.46
112.26
109.46
94.05
82.59
68.54
68.44
68.21
55.62
48.77
39.94
39.80
39.67
39.53
39.39
39.25
39.11
23.24
f1 (ppm)

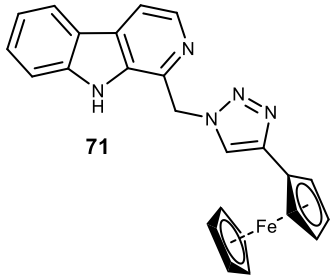
N
H
N
N
N
N
Fe

71

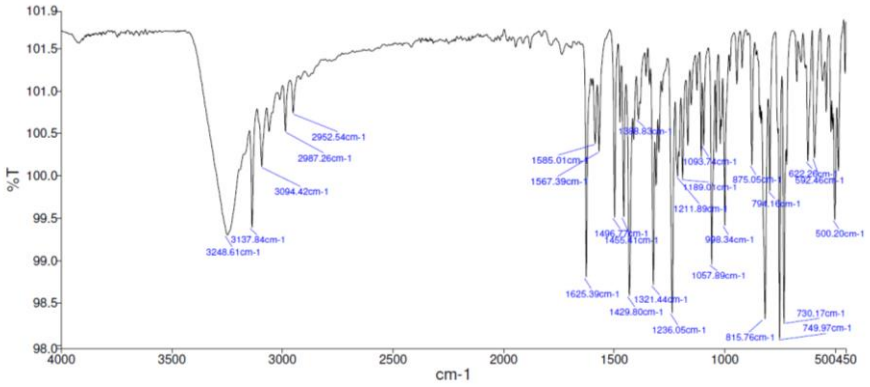
%T
cm-1
3248.61cm-1
3137.84cm-1
3094.42cm-1
2987.26cm-1
2952.54cm-1
1625.39cm-1
1585.01cm-1
1567.39cm-1
1429.80cm-1
1321.44cm-1
1236.05cm-1
1057.89cm-1
998.34cm-1
815.76cm-1
749.97cm-1
730.17cm-1
500.20cm-1

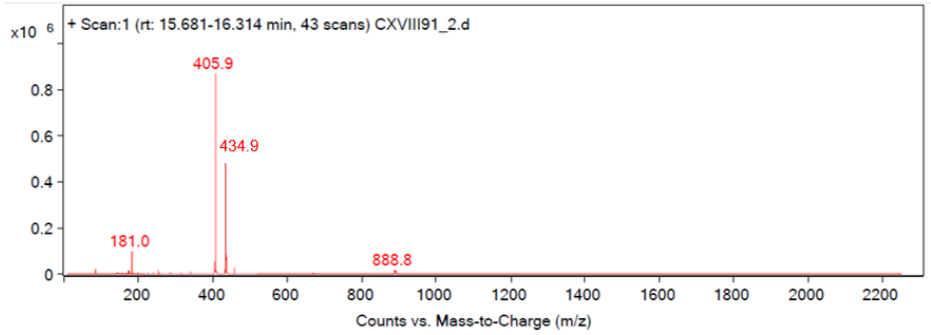
+ Scan:1 (rt: 15.681-16.314 min, 43 scans) CXVIII91_2.d
x10 6
405.9
434.9
181.0
888.8
Counts vs. Mass-to-Charge (m/z)

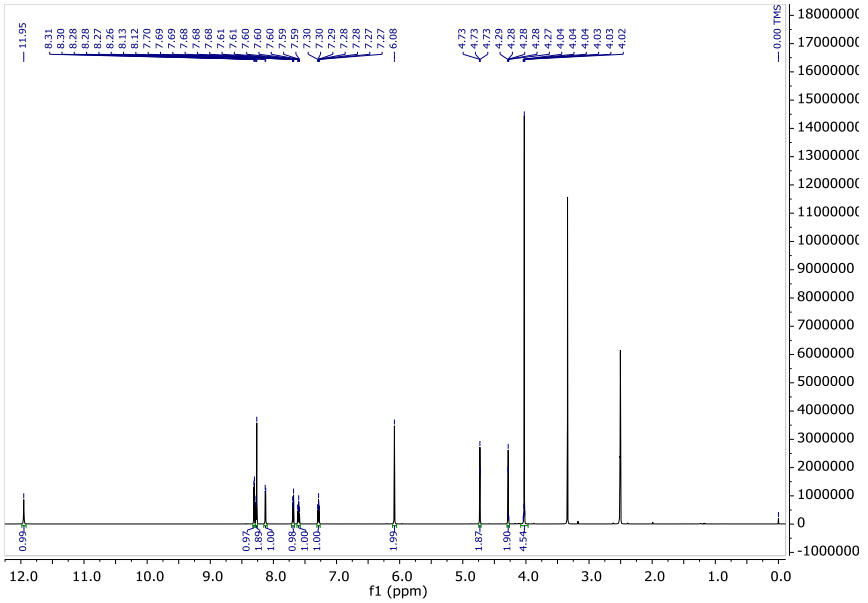
f1 (ppm)

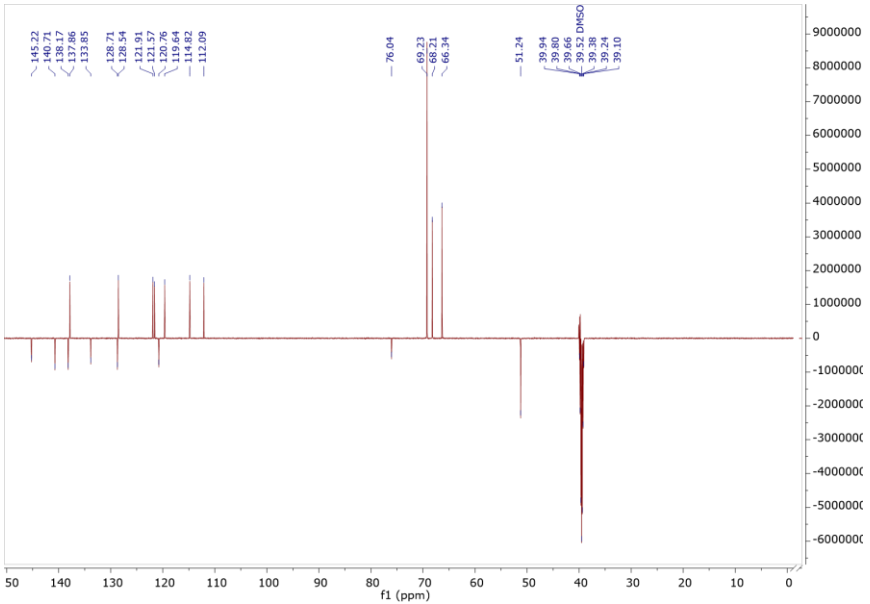
f1 (ppm)

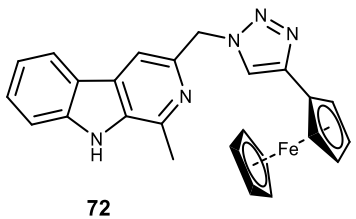
N
N
N
N
H
Fe

72

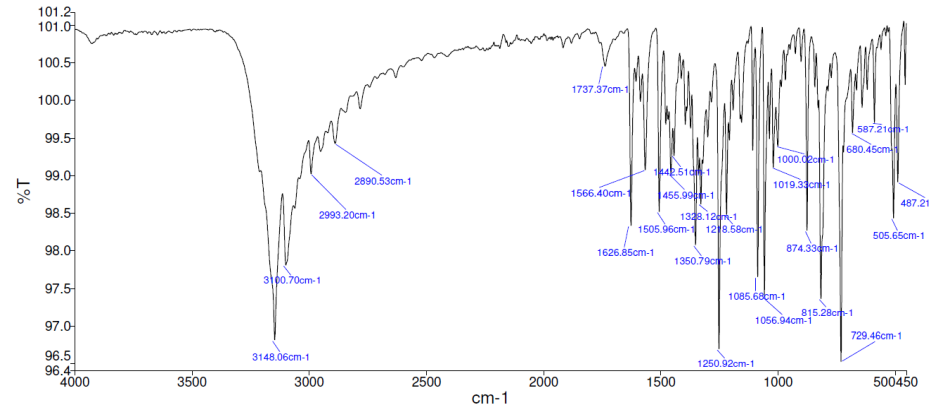
%T
cm-1
3148.06cm-1
3100.70cm-1
2993.20cm-1
2890.53cm-1
1737.37cm-1
1626.85cm-1
1566.40cm-1
1505.96cm-1
1442.51cm-1
1455.99cm-1
1328.12cm-1
1218.58cm-1
1350.79cm-1
1250.92cm-1
1085.68cm-1
1056.94cm-1
1000.02cm-1
1019.33cm-1
874.33cm-1
815.28cm-1
729.46cm-1
680.45cm-1
587.21cm-1
505.65cm-1
487.21

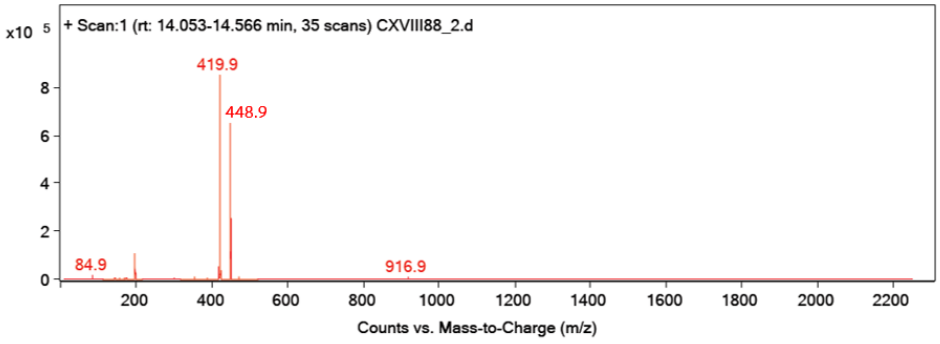
x10
+ Scan:1 (rt: 14.053-14.566 min, 35 scans) CXVIII88_2.d
419.9
448.9
84.9
916.9
Counts vs. Mass-to-Charge (m/z)

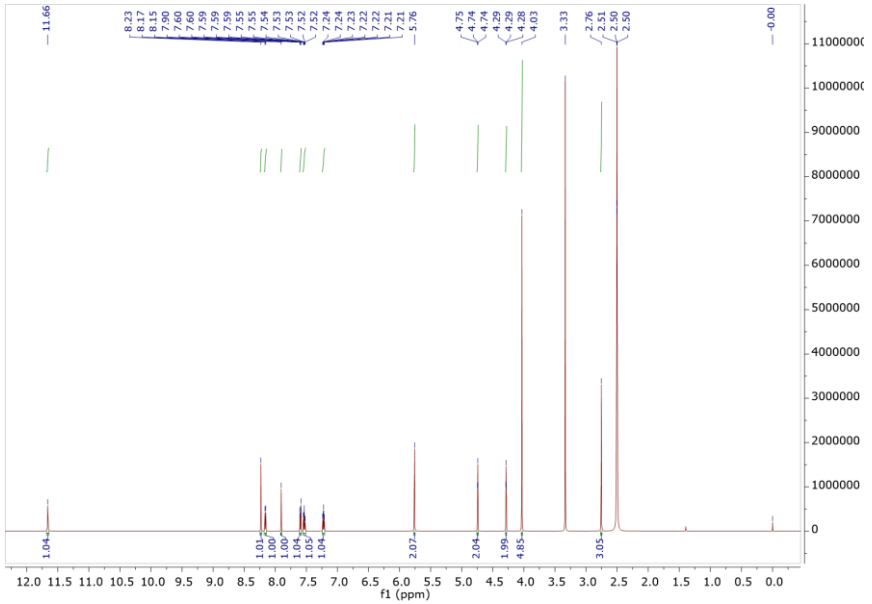
f1 (ppm)

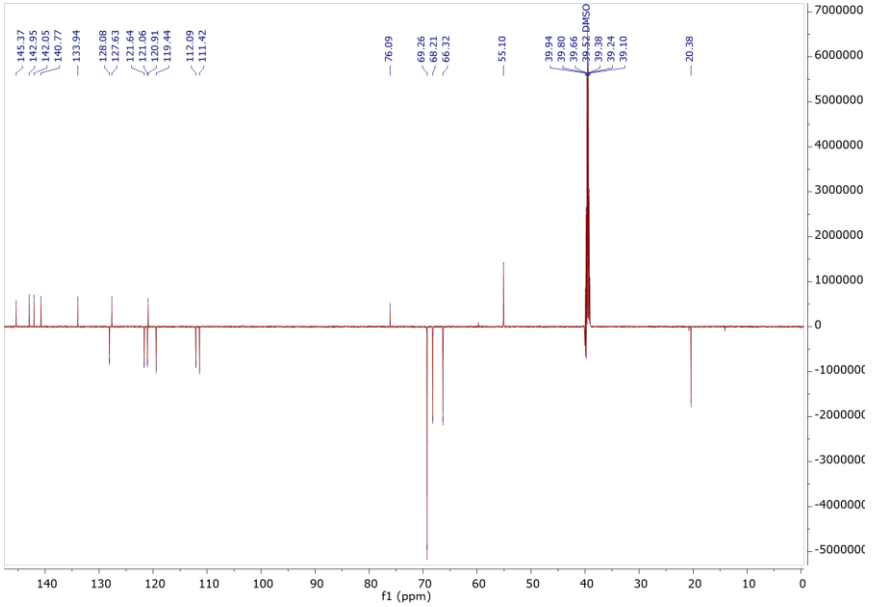
DMSO
f1 (ppm)

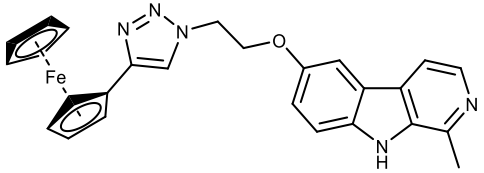
Fe
N
N
N
O
N
H

73

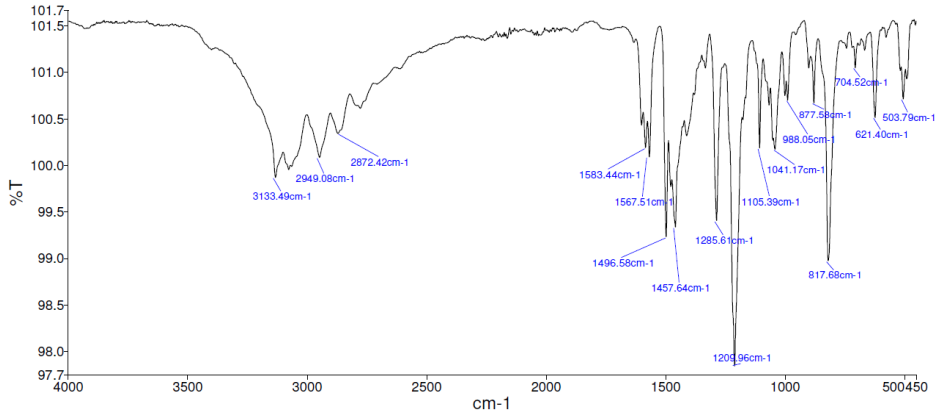
%T
cm-1
3133.49cm-1
2949.08cm-1
2872.42cm-1
1583.44cm-1
1567.51cm-1
1496.58cm-1
1457.64cm-1
1285.61cm-1
1209.96cm-1
1105.39cm-1
1041.17cm-1
988.05cm-1
877.58cm-1
817.68cm-1
704.52cm-1
621.40cm-1
503.79cm-1

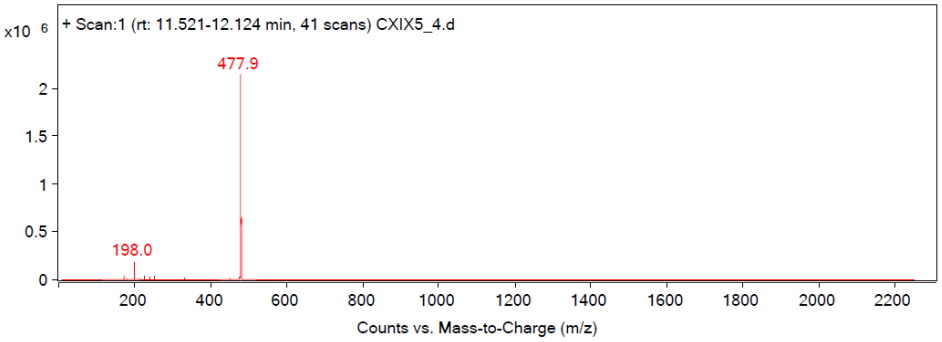
+ Scan:1 (rt: 11.521-12.124 min, 41 scans) CXIX5_4.d
x10 6
477.9
198.0
Counts vs. Mass-to-Charge (m/z)

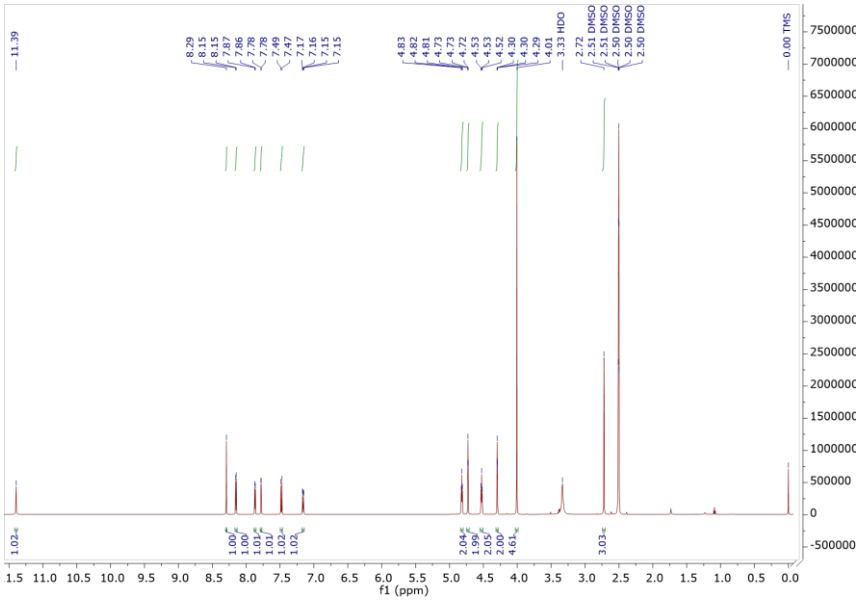
f1 (ppm)

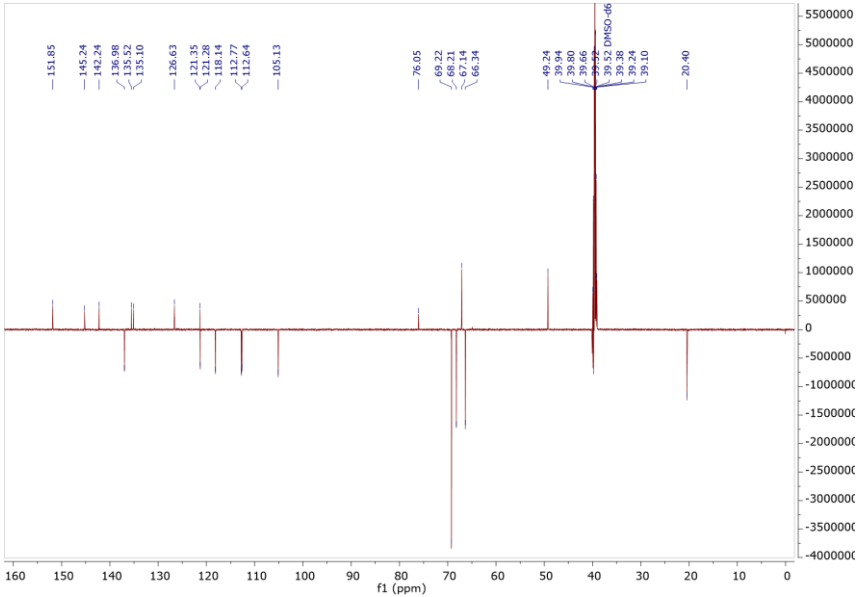
f1 (ppm)

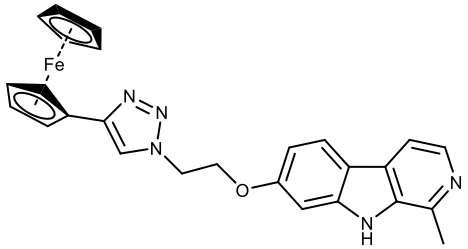
Fe
N
N
N
O
N
H

74

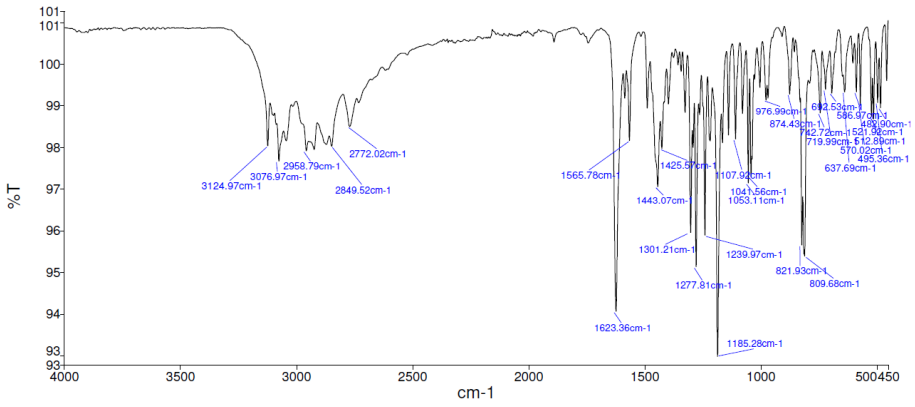
%T
cm-1
3124.97cm-1
3076.97cm-1
2958.79cm-1
2849.52cm-1
2772.02cm-1
1623.36cm-1
1565.78cm-1
1443.07cm-1
1425.57cm-1
1301.21cm-1
1277.81cm-1
1239.97cm-1
1185.28cm-1
1107.92cm-1
1041.56cm-1
1053.11cm-1
976.99cm-1
874.43cm-1
821.93cm-1
809.68cm-1
762.72cm-1
719.99cm-1
637.69cm-1
570.02cm-1
521.96cm-1
495.36cm-1

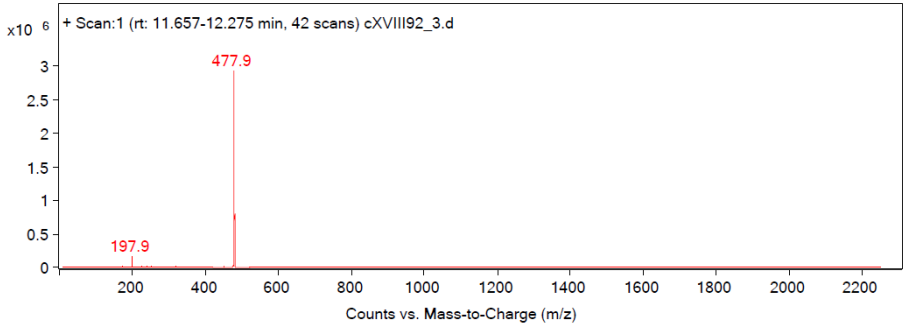
+ Scan:1 (rt: 11.657-12.275 min, 42 scans) cXVIII92_3.d
x10 6
477.9
197.9
Counts vs. Mass-to-Charge (m/z)

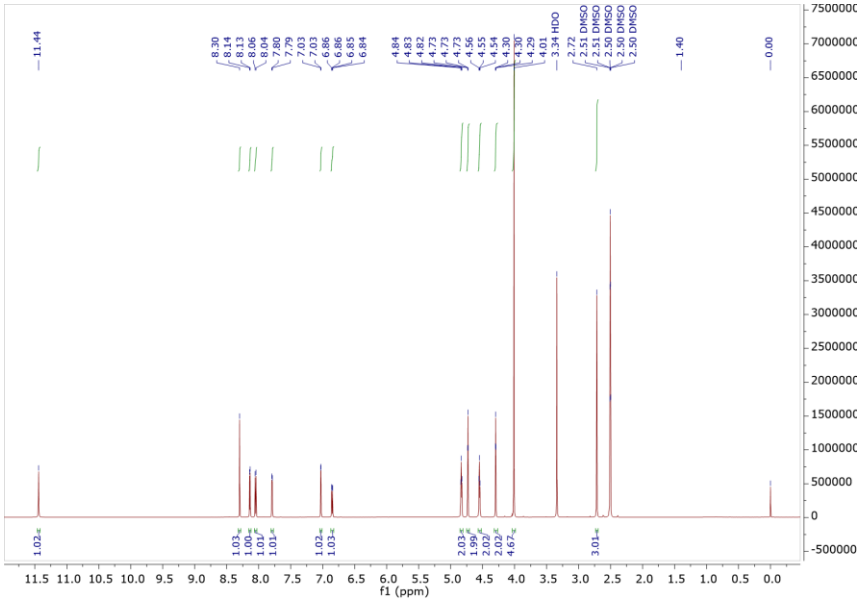
11.44
8.30
8.14
8.13
8.06
8.04
7.80
7.79
7.73
7.03
6.86
6.85
6.84
4.84
4.83
4.82
4.73
4.73
4.73
4.56
4.55
4.54
4.30
4.30
4.29
4.01
3.34 HDO
2.72
2.51 DMSO
2.51 DMSO
2.50 DMSO
2.50 DMSO
2.50 DMSO
1.40
0.00
f1 (ppm)

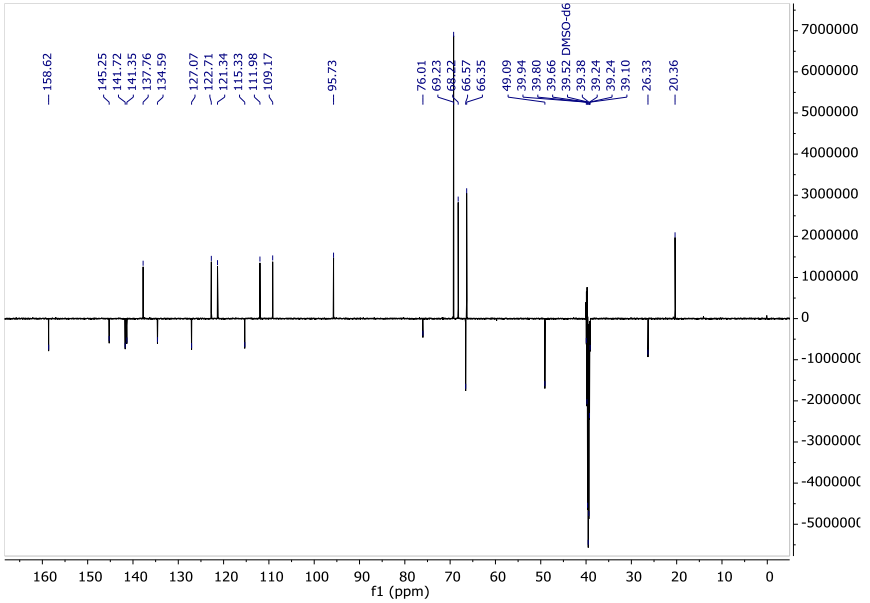
158.62
145.25
141.72
141.35
137.76
134.59
127.07
122.71
121.34
115.33
111.98
109.17
95.73
76.01
69.23
68.22
66.57
66.35
49.09
39.94
39.80
39.66
39.52 DMSO-d6
39.38
39.24
39.24
39.10
26.33
20.36
f1 (ppm)

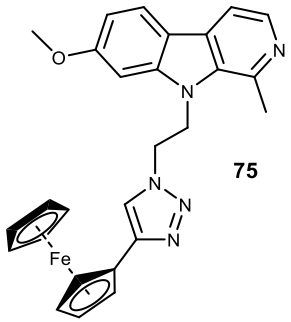
O
N
N
N
N
Fe

75

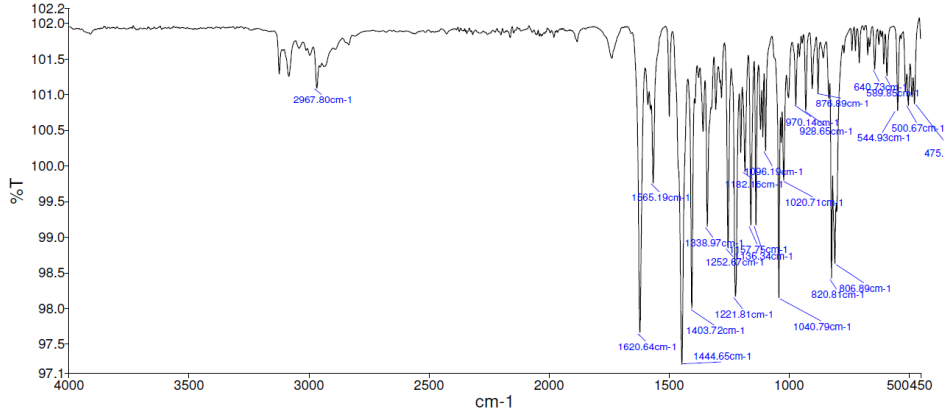
%T
cm-1
2967.80cm-1
1620.64cm-1
1565.19cm-1
1444.65cm-1
1403.72cm-1
1338.97cm-1
1252.67cm-1
1221.81cm-1
1040.79cm-1
1020.71cm-1
820.81cm-1
544.93cm-1
500.67cm-1

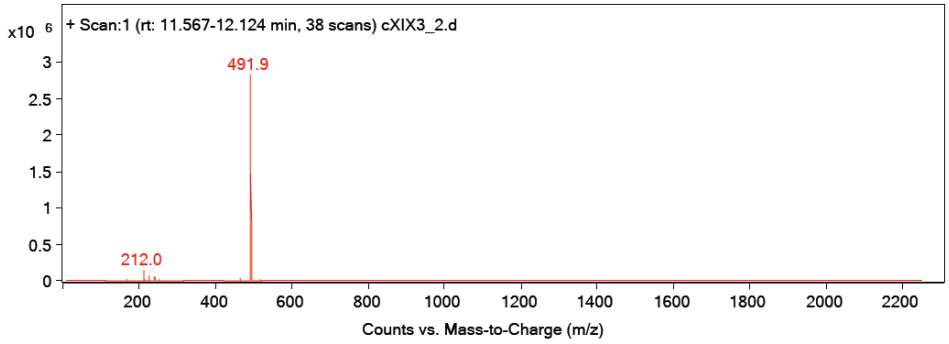
+ Scan:1 (rt: 11.567-12.124 min, 38 scans) cXIX3_2.d
x10 6
491.9
212.0
Counts vs. Mass-to-Charge (m/z)

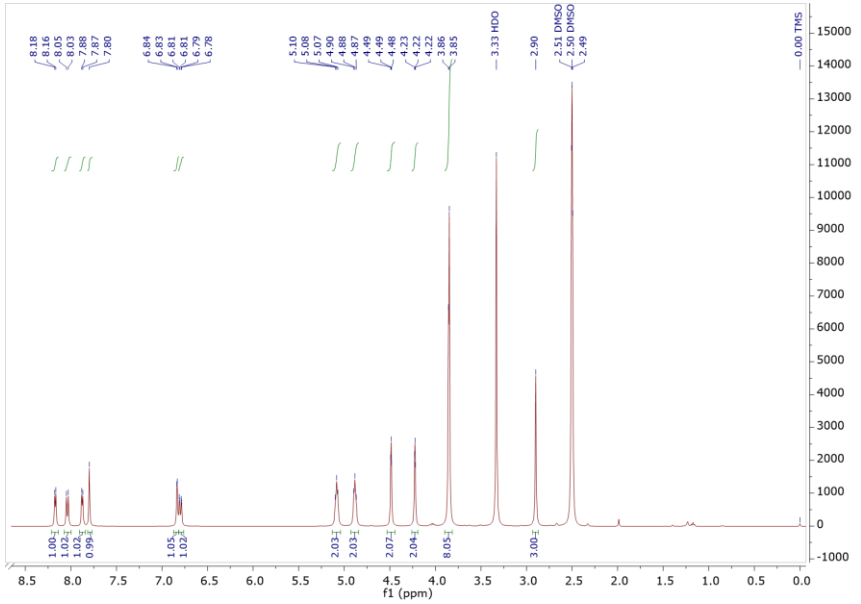
f1 (ppm)

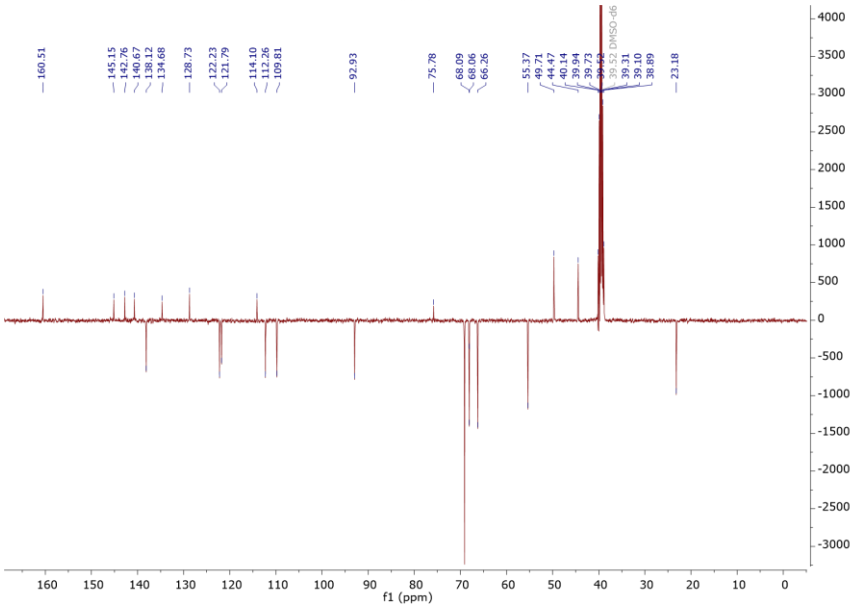
f1 (ppm)

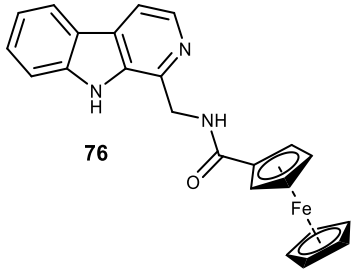
N
H
NH
O
Fe

76

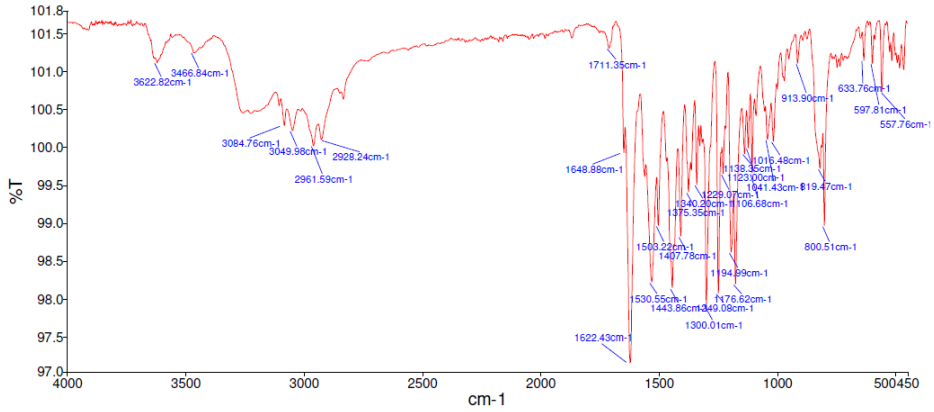
%T
cm-1
3622.82cm-1
3466.84cm-1
3084.76cm-1
3049.98cm-1
2928.24cm-1
2961.59cm-1
1711.35cm-1
1648.88cm-1
913.90cm-1
633.76cm-1
597.81cm-1
557.76cm-1
1503.22cm-1
1407.78cm-1
1194.99cm-1
800.51cm-1
1530.55cm-1
1443.86cm-1
1349.08cm-1
1300.01cm-1
1622.43cm-1

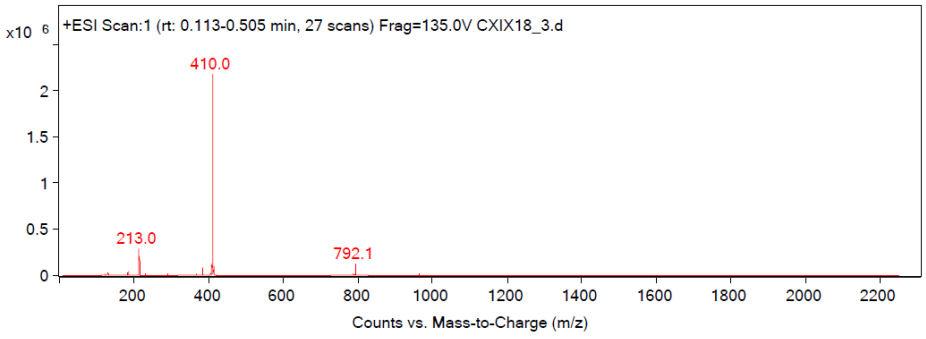
x10 6
+ESI Scan:1 (rt: 0.113-0.505 min, 27 scans) Frag=135.0V CXIX18_3.d
410.0
213.0
792.1
Counts vs. Mass-to-Charge (m/z)

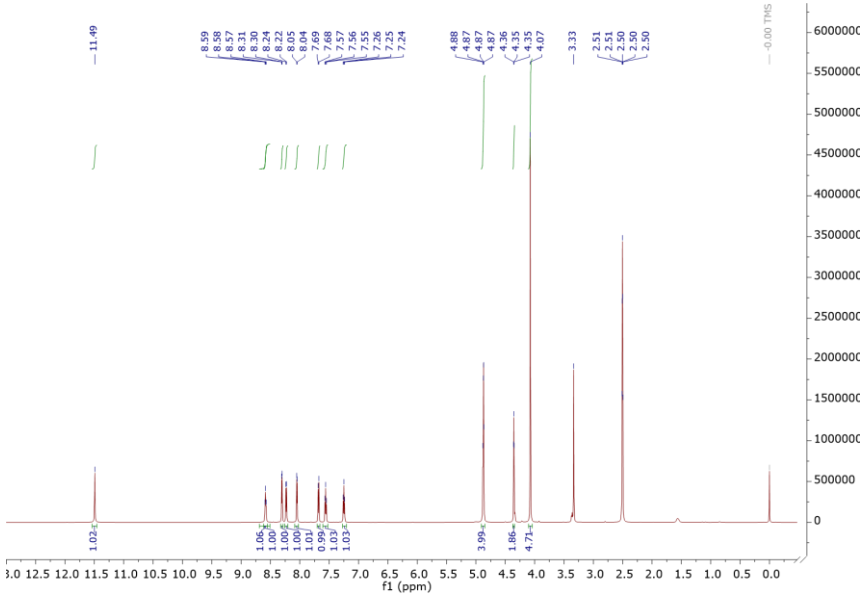
11.49
8.59
8.58
8.57
8.31
8.30
8.24
8.22
8.05
8.04
7.69
7.68
7.57
7.56
7.55
7.26
7.25
7.24
4.88
4.87
4.87
4.87
4.36
4.35
4.35
4.07
3.33
2.51
2.51
2.50
2.50
2.50
0.00 TMS
f1 (ppm)

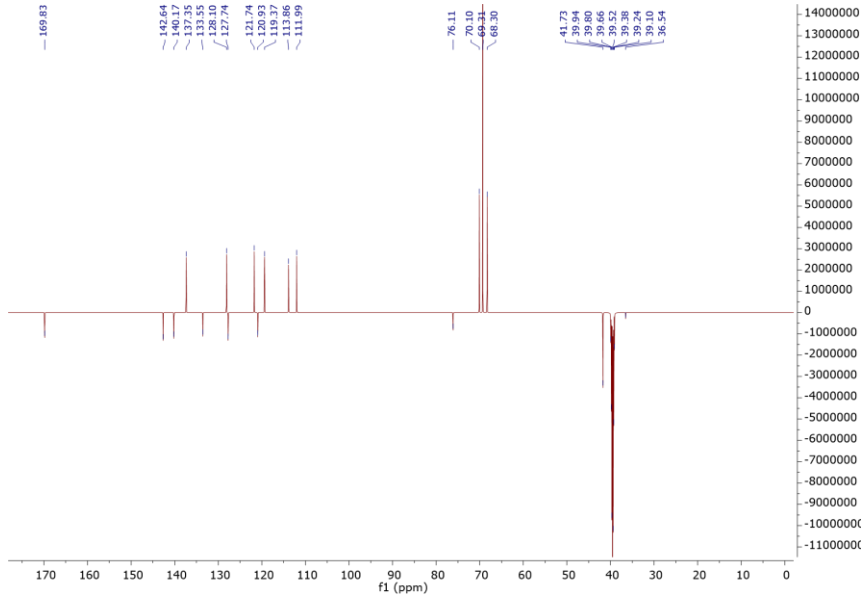
169.83
142.64
140.17
137.35
133.55
128.10
127.74
121.74
120.93
119.37
113.86
111.99
76.11
70.10
69.31
68.30
41.73
39.94
39.80
39.66
39.52
39.38
39.24
39.10
36.54
f1 (ppm)

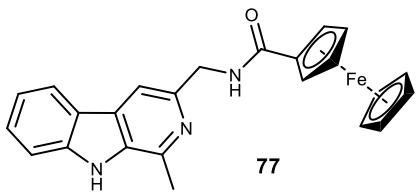
O
N
H
Fe
N
H

77

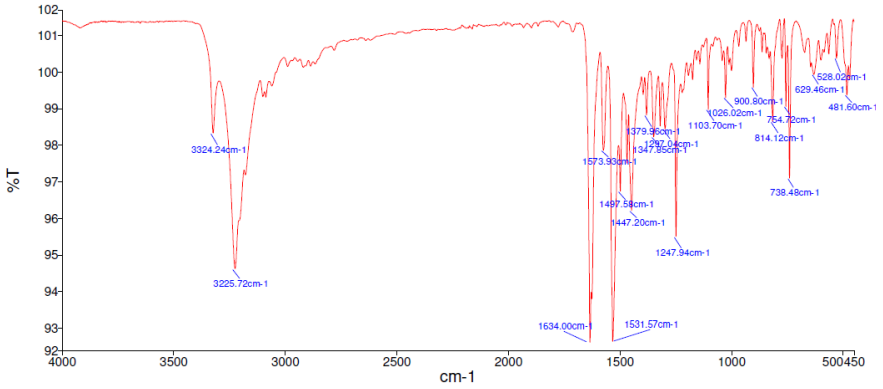
%T
cm-1
3324.24cm-1
3225.72cm-1
1634.00cm-1
1573.93cm-1
1531.57cm-1
1497.58cm-1
1447.20cm-1
1379.96cm-1
1347.85cm-1
1297.04cm-1
1247.94cm-1
1103.70cm-1
1026.02cm-1
900.80cm-1
814.12cm-1
754.72cm-1
738.48cm-1
629.46cm-1
528.02cm-1
481.60cm-1

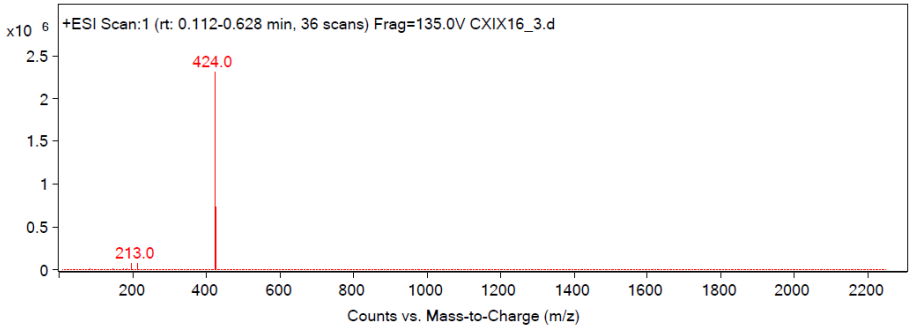
x10 6
+ESI Scan:1 (rt: 0.112-0.628 min, 36 scans) Frag=135.0V CXIX16_3.d
424.0
213.0
Counts vs. Mass-to-Charge (m/z)

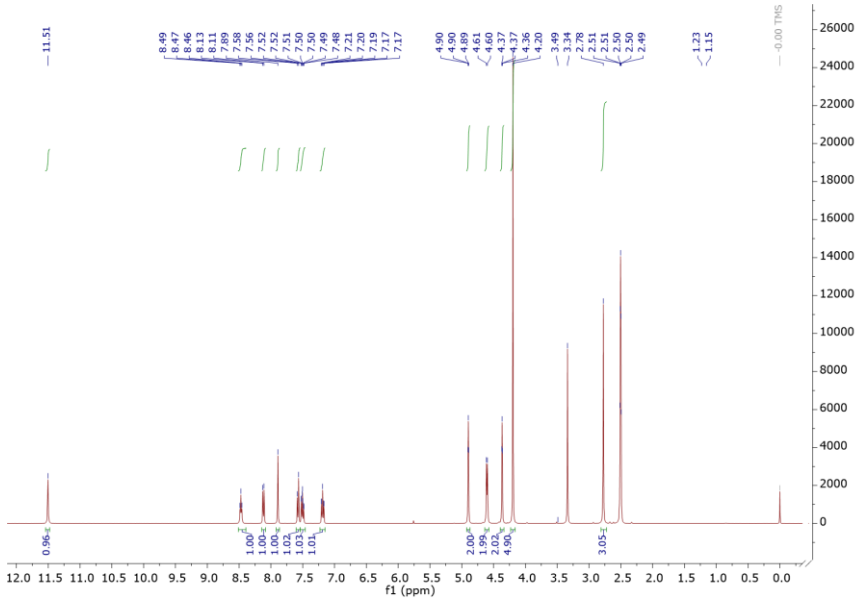
f1 (ppm)

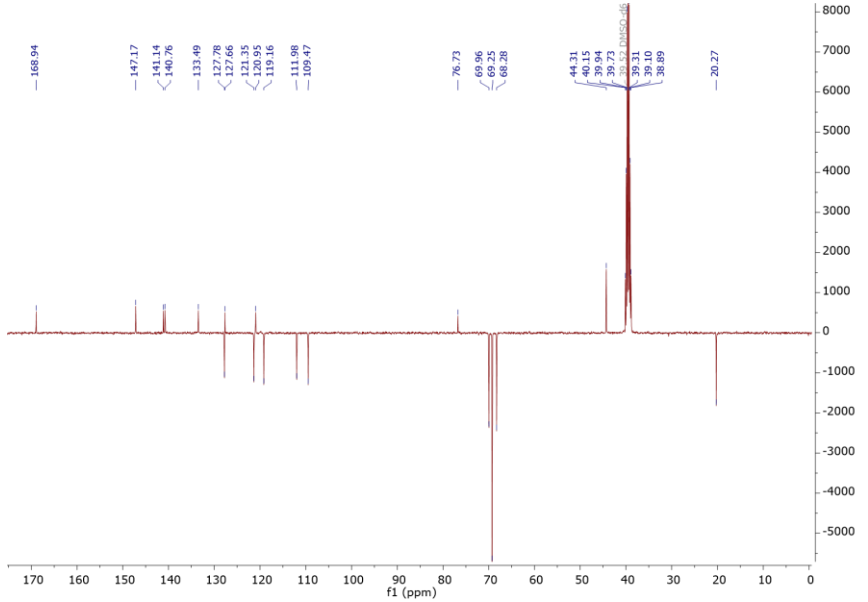
f1 (ppm)

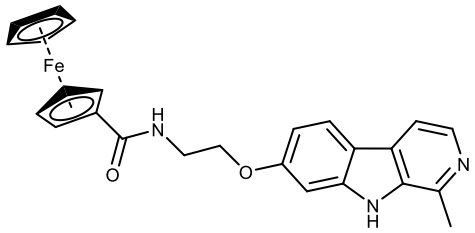
Fe
H
N
O
O
N
H
N

78

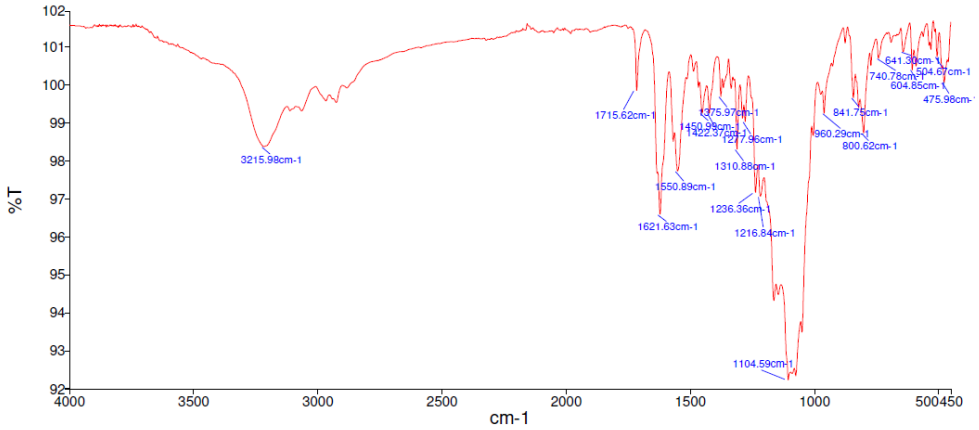
%T
cm-1
3215.98cm-1
1715.62cm-1
1621.63cm-1
1550.89cm-1
1450.98cm-1
1422.37cm-1
1375.97cm-1
1327.96cm-1
1310.88cm-1
1236.36cm-1
1216.84cm-1
1104.59cm-1
960.29cm-1
841.75cm-1
800.62cm-1
740.78cm-1
641.30cm-1
604.85cm-1
504.67cm-1
475.98cm-1

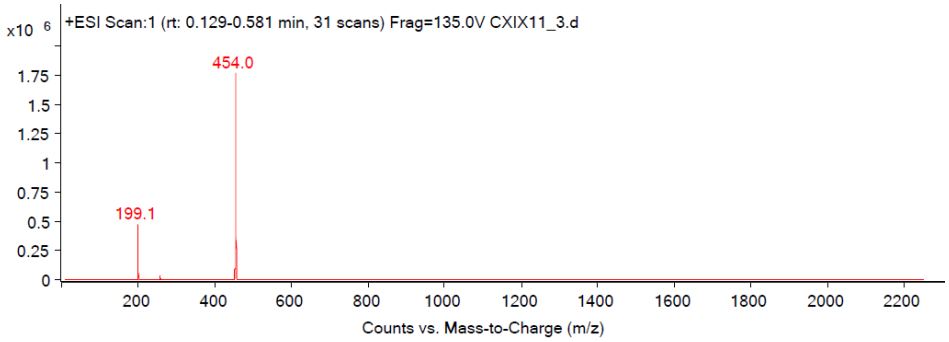
+ESI Scan:1 (rt: 0.129-0.581 min, 31 scans) Frag=135.0V CXIX11_3.d
x10 6
454.0
199.1
Counts vs. Mass-to-Charge (m/z)

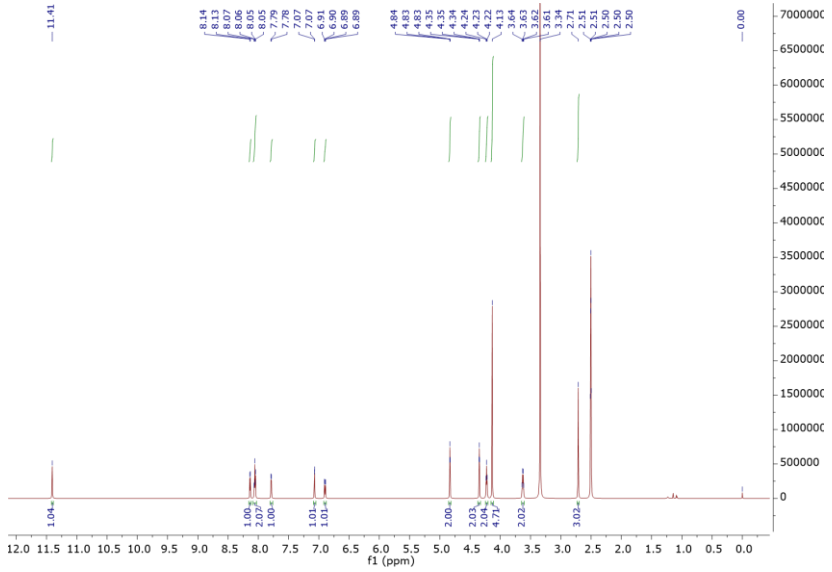
f1 (ppm)

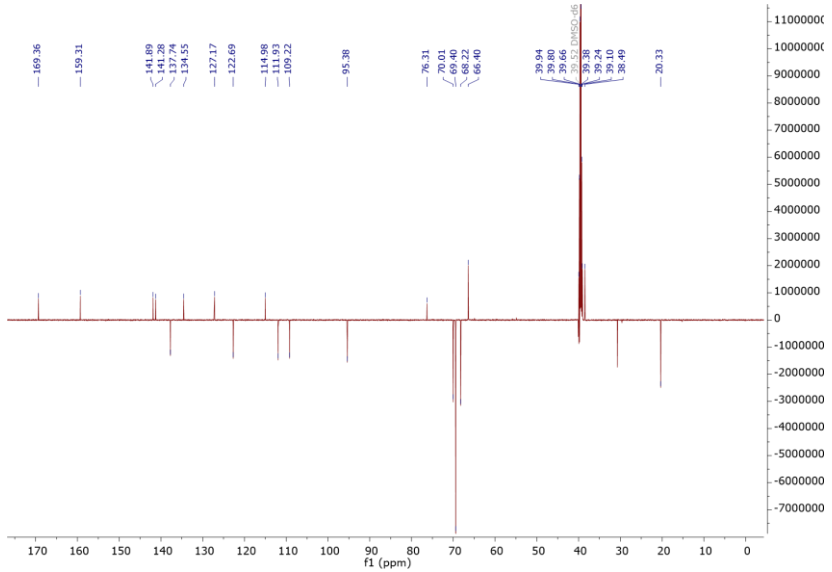
f1 (ppm)

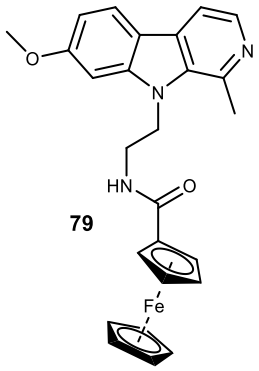
O
N
HN
O
Fe

79

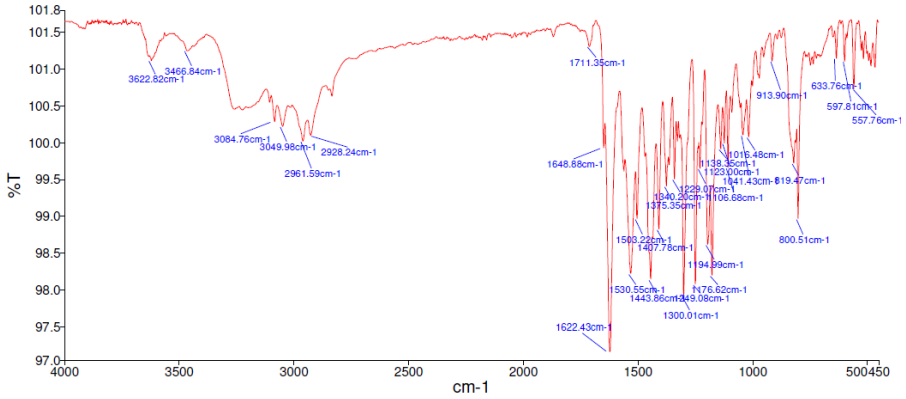
%T
cm-1
3622.82cm-1
3466.84cm-1
3084.76cm-1
3049.98cm-1
2961.59cm-1
2928.24cm-1
1711.35cm-1
1648.68cm-1
1622.43cm-1
1530.55cm-1
1503.22cm-1
1443.86cm-1
1407.76cm-1
1375.35cm-1
1349.08cm-1
1300.01cm-1
1194.99cm-1
1176.62cm-1
1138.35cm-1
1123.00cm-1
1106.68cm-1
1016.48cm-1
913.90cm-1
800.51cm-1
633.76cm-1
597.81cm-1
557.76cm-1

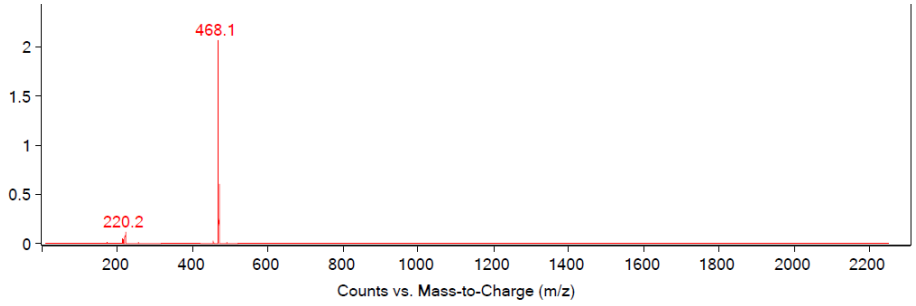
468.1
220.2
Counts vs. Mass-to-Charge (m/z)

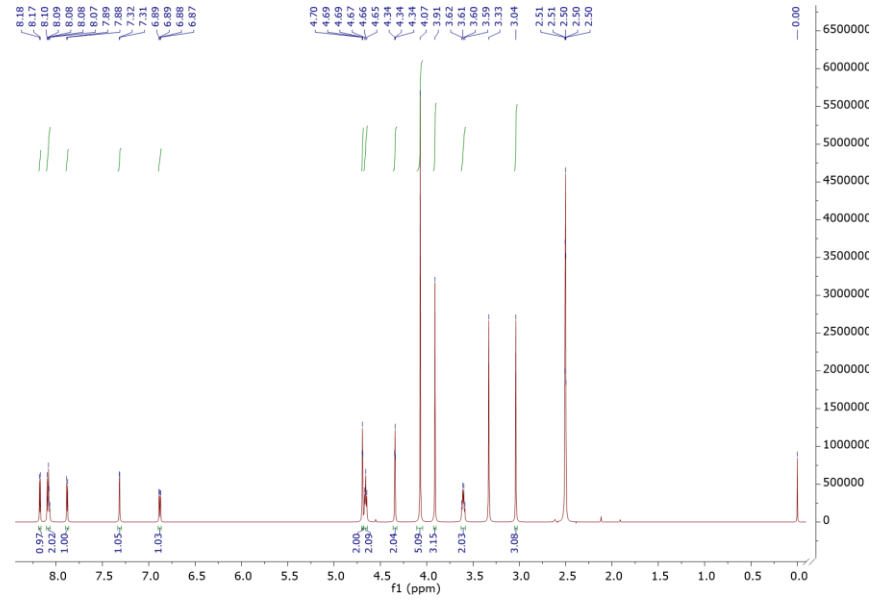
f1 (ppm)

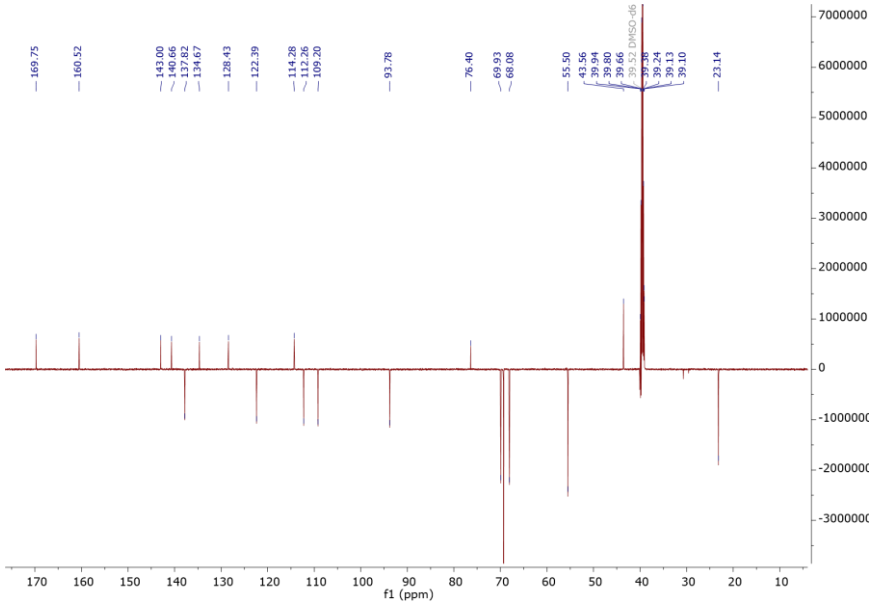
f1 (ppm)

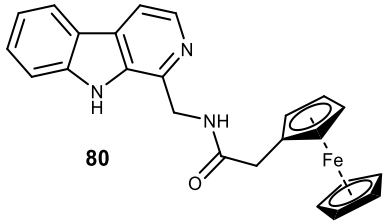
N
H
NH
O
Fe

80

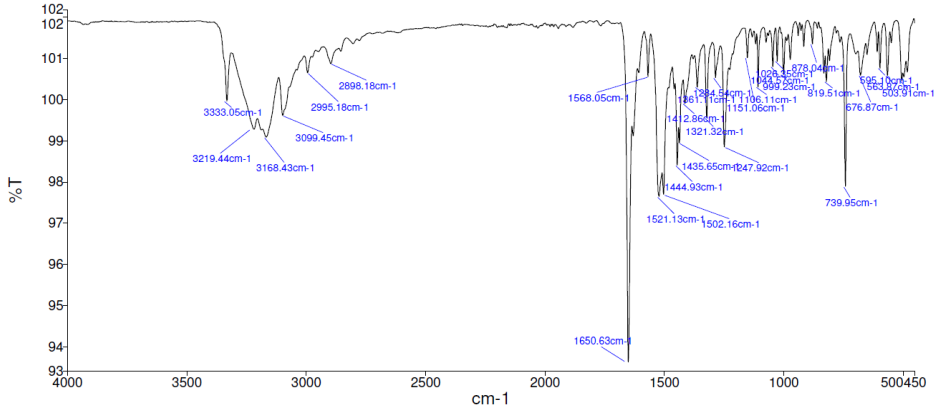
%T
cm-1
3333.05cm-1
3219.44cm-1
3168.43cm-1
3099.45cm-1
2995.18cm-1
2898.18cm-1
1650.63cm-1
1568.05cm-1
1521.13cm-1
1502.16cm-1
1444.93cm-1
1435.65cm-1
1412.86cm-1
1321.32cm-1
1247.92cm-1
1151.06cm-1
1106.11cm-1
819.51cm-1
739.95cm-1
676.87cm-1
503.91cm-1

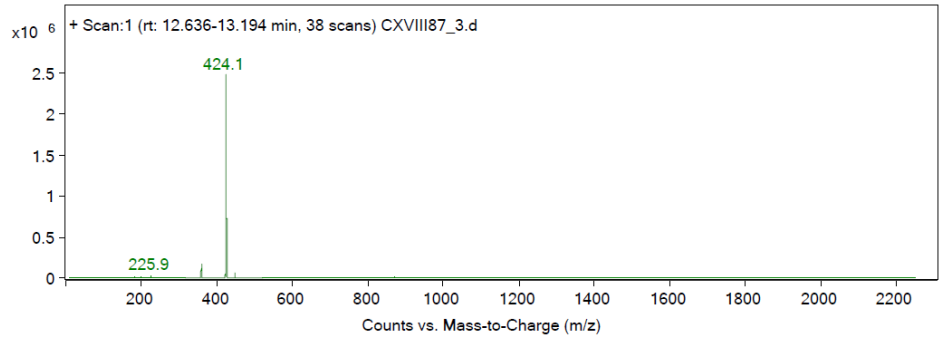
x10 6
+ Scan:1 (rt: 12.636-13.194 min, 38 scans) CXVIII87_3.d
424.1
225.9
Counts vs. Mass-to-Charge (m/z)

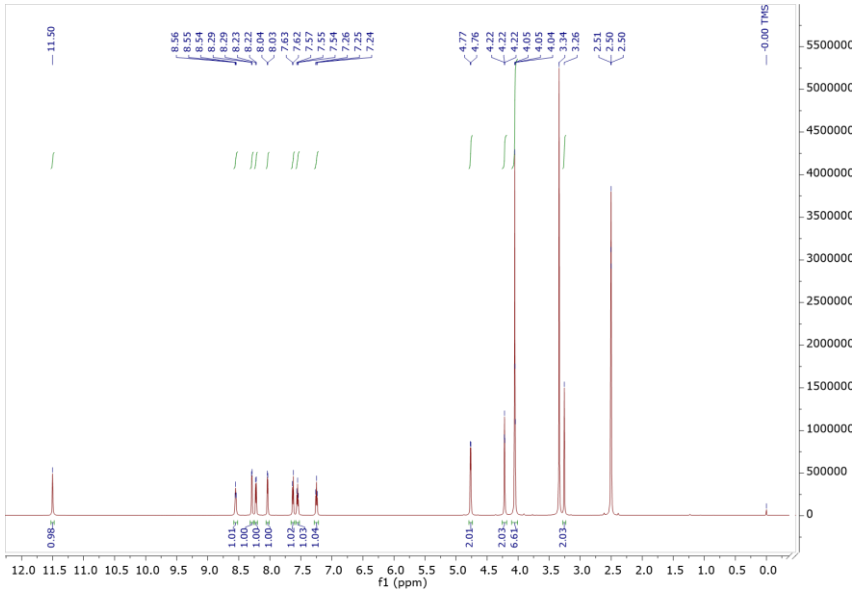
11.50
8.56
8.55
8.54
8.29
8.28
8.23
8.22
8.04
8.03
7.63
7.62
7.57
7.55
7.54
7.26
7.25
7.24
4.77
4.76
4.22
4.22
4.05
4.05
4.04
3.34
3.26
2.51
2.50
2.50
-0.00 TMS
0.98
1.01
1.00
1.00
1.00
1.02
1.03
1.04
2.01
2.03
6.61
2.03
f1 (ppm)

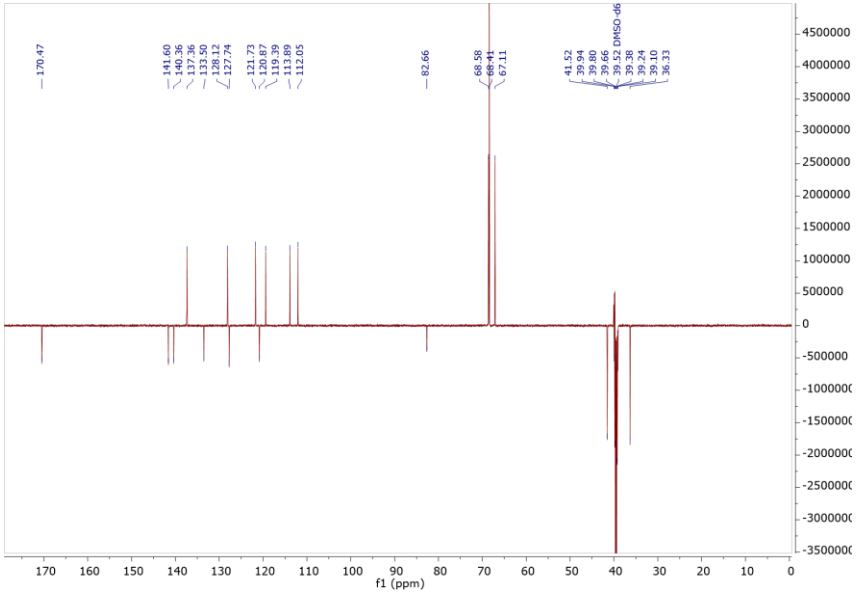
170.47
141.60
140.36
137.36
133.50
128.12
127.74
121.73
120.87
119.39
113.89
112.05
82.66
68.58
68.41
67.11
41.52
39.94
39.80
39.66
39.52 DMSO-d6
39.38
39.24
39.10
36.33
f1 (ppm)

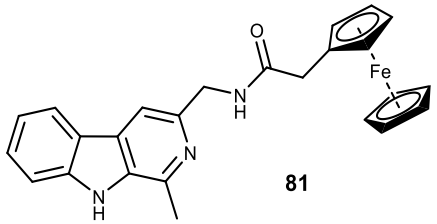
O
N
H
Fe
N
N
H

81

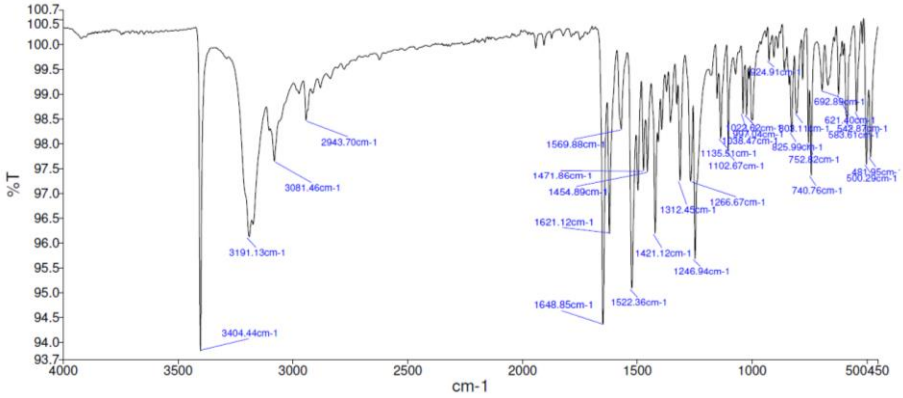
%T
cm-1
3404.44cm-1
3191.13cm-1
3081.46cm-1
2943.70cm-1
1648.85cm-1
1621.12cm-1
1569.88cm-1
1522.36cm-1
1471.86cm-1
1454.89cm-1
1421.12cm-1
1312.45cm-1
1266.67cm-1
1246.94cm-1
1135.51cm-1
1102.67cm-1
752.82cm-1
740.76cm-1

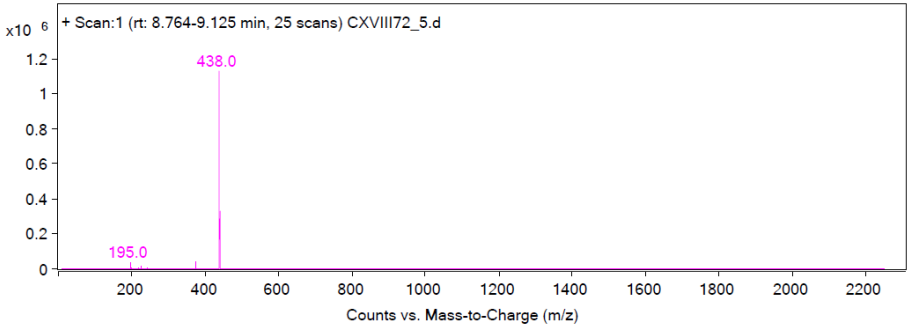
+ Scan:1 (rt: 8.764-9.125 min, 25 scans) CXVIII72_5.d
x10 6
438.0
195.0
Counts vs. Mass-to-Charge (m/z)

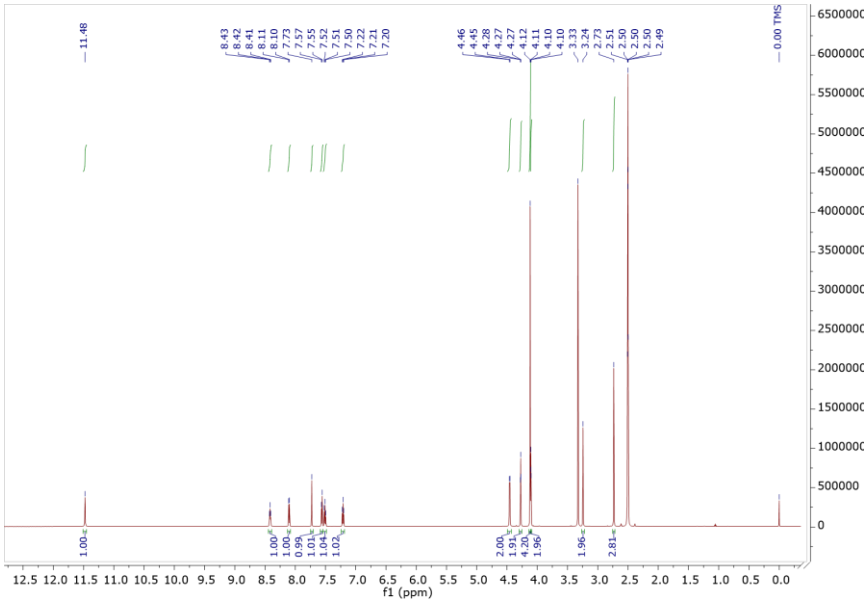
11.48
0.00 TMS
f1 (ppm)

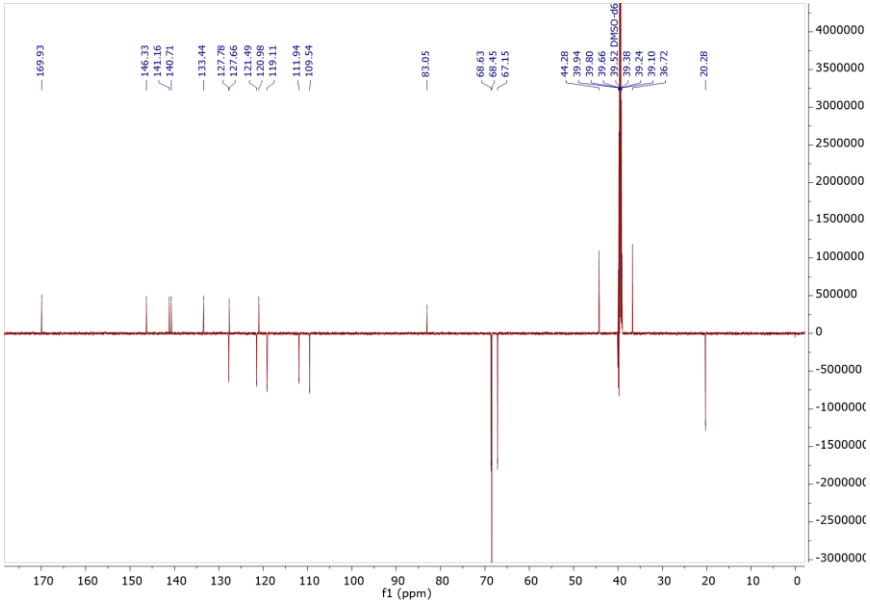
169.93
146.33
141.16
140.71
133.44
127.78
127.66
121.49
120.98
119.11
111.94
109.54
83.05
68.63
68.45
67.15
44.28
39.94
39.80
39.66
39.52 DMSO-d6
39.38
39.24
39.10
36.72
20.28
f1 (ppm)

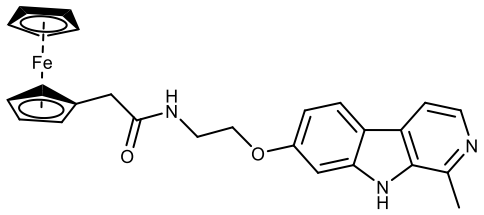
Fe
H
N
O
O
N
H

82

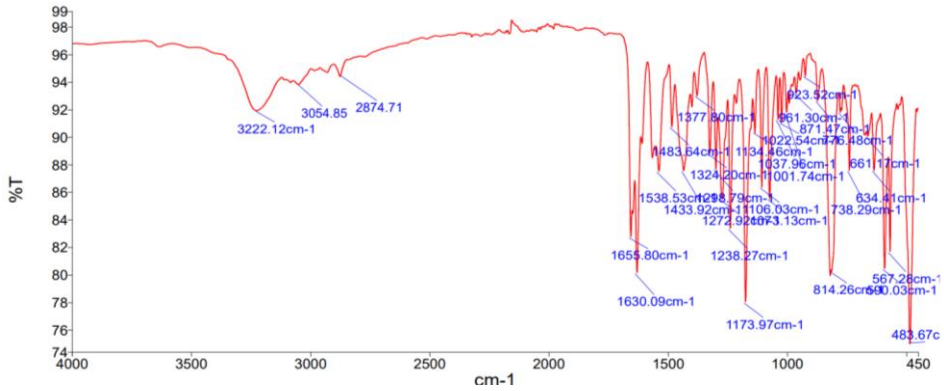
%T
cm-1
3222.12cm-1
3054.85
2874.71
1655.80cm-1
1630.09cm-1
1238.27cm-1
1173.97cm-1
1538.53cm-1
1433.92cm-1
1324.20cm-1
1483.64cm-1
1377.80cm-1
1272.92cm-1
1134.46cm-1
1106.03cm-1
1073.13cm-1
1037.96cm-1
1001.74cm-1
923.52cm-1
871.47cm-1
814.26cm-1
738.29cm-1
661.17cm-1
634.41cm-1
567.28cm-1
483.67c

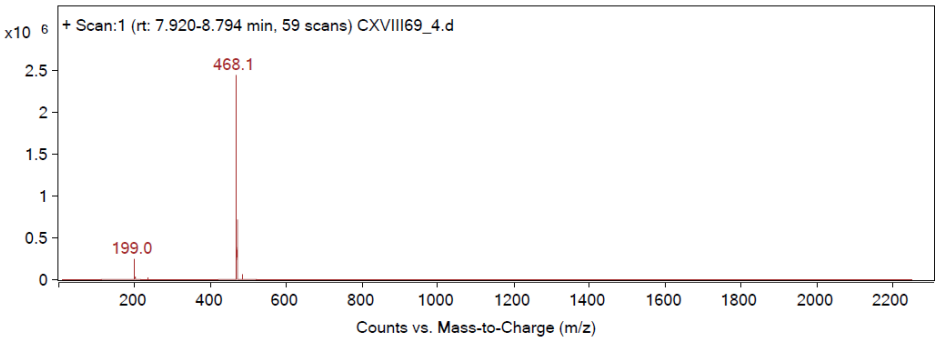
x10 6
+ Scan:1 (rt: 7.920-8.794 min, 59 scans) CXVIII69_4.d
468.1
199.0
Counts vs. Mass-to-Charge (m/z)

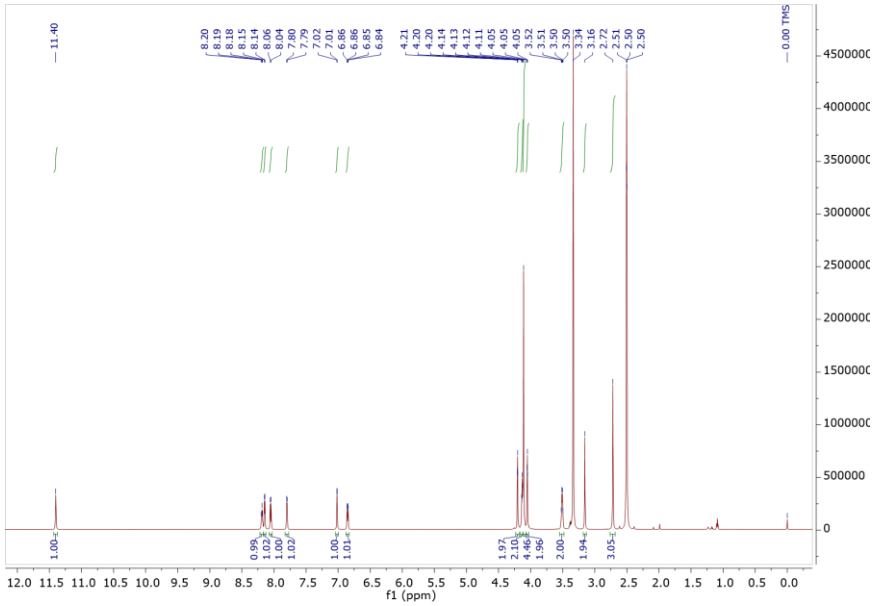
11.40
0.00 TMS
f1 (ppm)

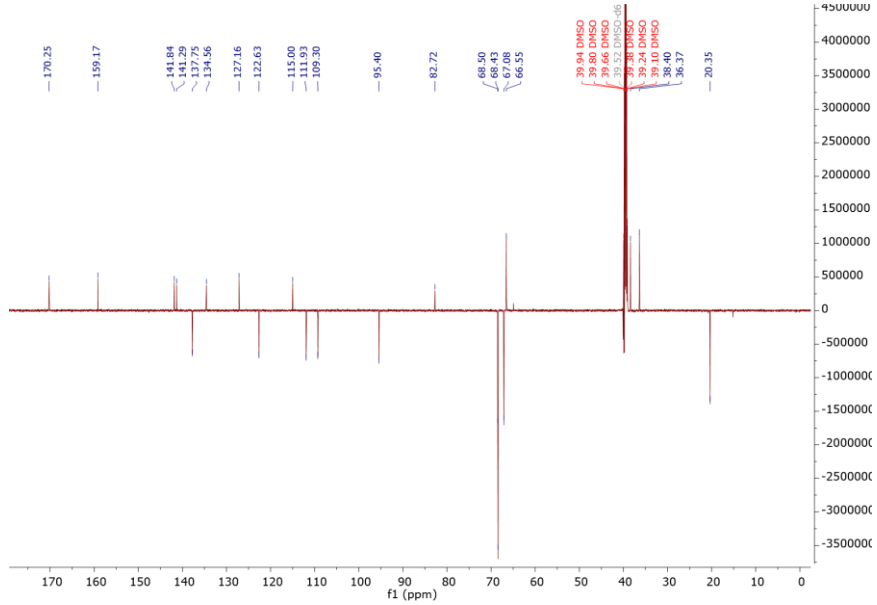
170.25
159.17
141.84
141.29
137.75
134.56
127.16
122.63
115.00
111.93
109.30
95.40
82.72
68.50
68.43
67.08
66.55
39.94 DMSO
39.80 DMSO
39.66 DMSO
39.52 DMSO
39.38 DMSO
39.24 DMSO
39.10 DMSO
38.40
36.37
20.35
f1 (ppm)

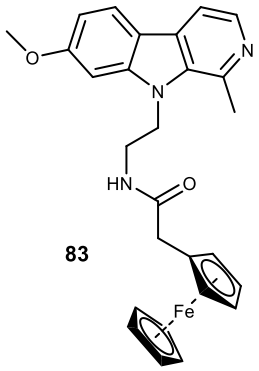
O
N
N
HN
O
Fe

83

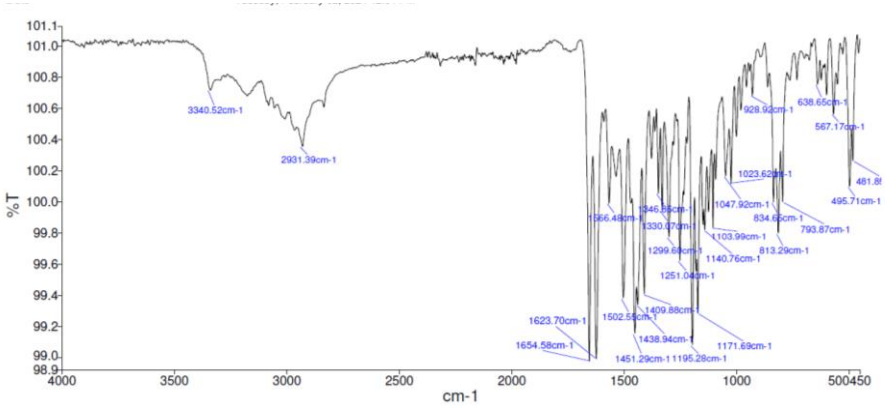
%T
cm-1
3340.52cm-1
2931.39cm-1
1623.70cm-1
1654.58cm-1
1438.94cm-1
1451.29cm-1
1195.28cm-1
1171.69cm-1
1409.88cm-1
1502.55cm-1
1299.69cm-1
1251.04cm-1
1140.76cm-1
1103.99cm-1
1047.92cm-1
1023.62cm-1
928.92cm-1
834.65cm-1
813.29cm-1
793.87cm-1
638.65cm-1
567.17cm-1
495.71cm-1

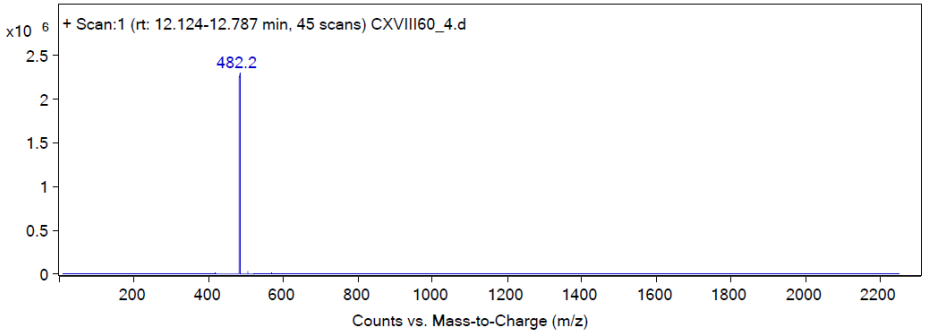
x10 6
+ Scan:1 (rt: 12.124-12.787 min, 45 scans) CXVIII60_4.d
482.2
Counts vs. Mass-to-Charge (m/z)

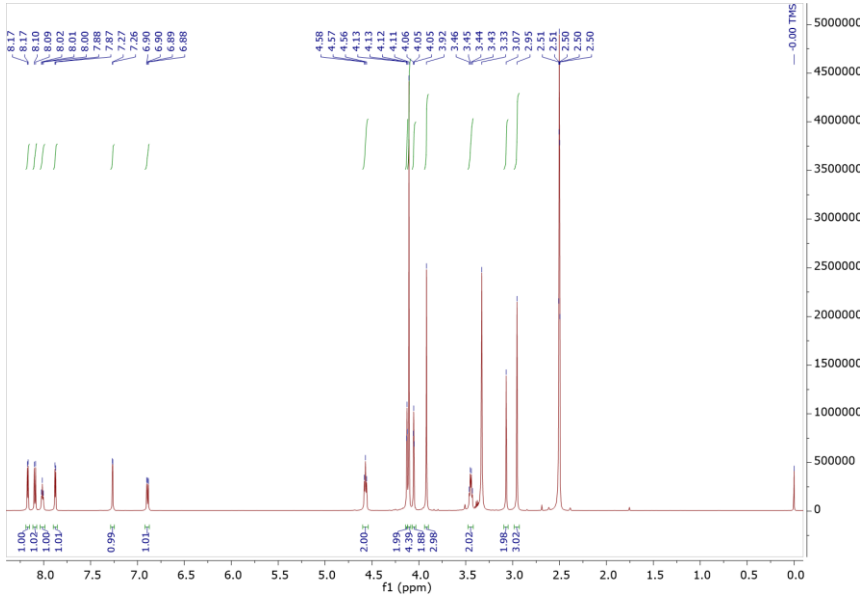
f1 (ppm)
0.00 TMS

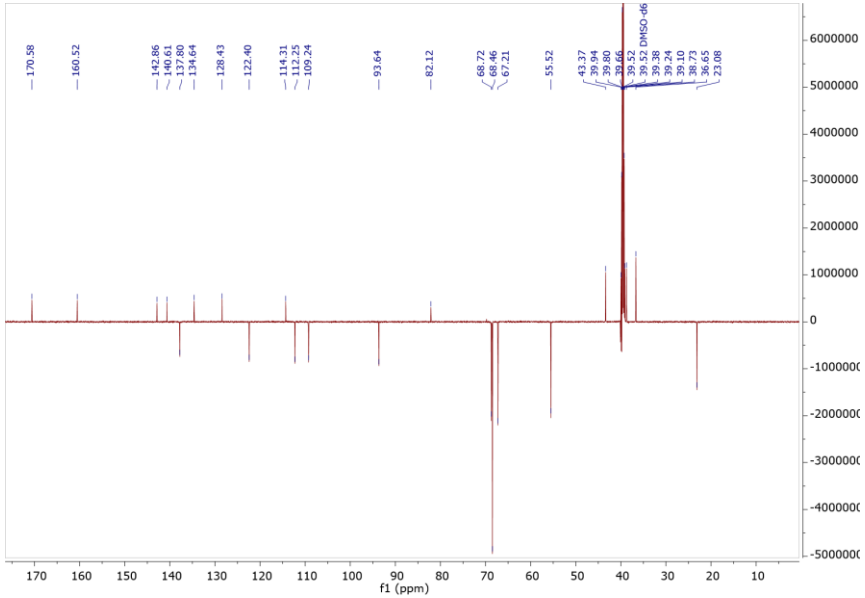
f1 (ppm)
DMSO-d6

PRILOG B

Prilog sadrži tri znanstvena rada objavljena u časopisima zastupljenim u bazi Current Contents koji obrađuju problematiku iznesenu u ovom doktorskom radu:

1) Marinović M, Poje G, Perković I, Fontinha D, Prudêncio M, Held J, et al. Further investigation of harmicines as novel antiplasmodial agents: Synthesis, structure-activity relationship and insight into the mechanism of action. Eur J Med Chem 2021;224:113687.

2) Poje G, Pessanha de Carvalho L, Held J, Moita D, Prudêncio M, Perković I, et. al. Design and synthesis of harmiquins, harmine and chloroquine hybrids as potent antiplasmodial agents. Eur J Med Chem 2022;238:114408.

3) Poje G, Marinović M, Pavić K, Mioč M, Kralj M, Pessanha de Carvalho L, Held J, Perković I, Rajić Z. Harmicens, novel harmine and ferrocene hybrids: design, synthesis and biological activity. Int J Mol Sci 2022;23:9315.

European Journal of Medicinal Chemistry 224 (2021) 113687

Contents lists available at ScienceDirect

European Journal of Medicinal Chemistry

journal homepage: http://www.elsevier.com/locate/ejmech

Further investigation of harmicines as novel antiplasmodial agents: Synthesis, structure-activity relationship and insight into the mechanism of action

Marina Marinović [a, 1], Goran Poje [a, 1], Ivana Perković [a], Diana Fontinha [b], Miguel Prudêncio [b], Jana Held [c], Lais Pessanha de Carvalho [c], Tana Tandarić [d], Robert Vianello [d], Zrinka Rajić [a, *]

[a] University of Zagreb Faculty of Pharmacy and Biochemistry, A. Kovačića 1, 10000, Zagreb, Croatia
[b] Instituto de Medicina Molecular João Lobo Antunes, Faculdade de Medicina, Universidade de Lisboa, Av. Prof. Egas Moniz, 1649-028, Lisboa, Portugal
[c] University of Tübingen, Institute of Tropical Medicine, Wilhelmstraße 27, 72074, Tübingen, Germany
[d] Rudjer Bošković Institute, Division of Organic Chemistry and Biochemistry, Bijenička Cesta 54, 10 000, Zagreb, Croatia

ARTICLE INFO

Article history:
Received 26 April 2021
Received in revised form
2 July 2021
Accepted 3 July 2021
Available online 5 July 2021

Keywords:
Harmine
β-Carboline
Cinnamic acid
Hybrid compounds
Antiplasmodial activity
*Pf*Hsp90
P. berghei
P. falciparum

ABSTRACT

The rise of the resistance of the malaria parasite to the currently approved therapy urges the discovery and development of new efficient agents. Previously we have demonstrated that harmicines, hybrid compounds composed from β-carboline alkaloid harmine and cinnamic acid derivatives, linked *via* either triazole or amide bond, exert significant antiplasmodial activity. In this paper, we report synthesis, antiplasmodial activity and cytotoxicity of expanded series of novel triazole- and amide-type harmicines. Structure-activity relationship analysis revealed that amide-type harmicines **27**, prepared at N-9 of the β-carboline core, exhibit superior potency against both erythrocytic stage of *P. falciparum* and hepatic stages of *P. berghei*. Notably, harmicine **27a**, *m*-(trifluoromethyl)cinnamic acid derivative, exhibited the most favourable selectivity index (SI = 1105). Molecular dynamics simulations revealed the ATP binding site of *P. falciparum* heat shock protein 90 as a druggable binding location, confirmed the usefulness of the harmine's N-9 substitution and identified favourable N–H … π interactions involving Lys45 and the aromatic phenyl unit in the attached cinnamic acid fragment as crucial for the enhanced biological activity. Thus, those compounds were identified as promising and valuable leads for further derivatization in the search of novel, more efficient antiplasmodial agents.

1. Introduction

Malaria is the deadliest human protozoan infectious disease widely spread in the tropical and subtropical areas of the world. Five identified species of the parasite responsible for causing human malaria are *Plasmodium falciparum*, *P. vivax*, *P. ovale*, *P. malariae* and *P. knowlesi*. Of these, *P. falciparum* and *P. vivax* are responsible for more than 95% of malaria cases in the world [1–3]. Despite years of continuous efforts, it is still a major cause of morbidity and mortality (229 million cases and 409 000 deaths in 2019), especially among young children and pregnant women [3]. As existing antimalarial drugs are becoming less effective due to the emergence of resistant strains of *P. falciparum*, there is an urgent need for novel and effective agents to combat malaria [2].

One of the widely employed approaches to find novel antimalarial chemotherapeutic agents is the design of hybrid molecules [4–8]. Hybrids represent chemical entities in which at least two pharmacological agents, acting on the same disease, are covalently linked in a single molecule. Ideally, the novel molecule should have greater activity than the sum of its parts and reduce the risk of drug resistance, drug-drug interactions and adverse effects. In the antimalarial field, hybrids comprised of agents belonging to the most of the known antimalarial drug classes have shown enhanced activity *in vitro* and *in vivo* [5]. Among those compounds, conjugates with cinnamic acid and its derivatives (CADs) have been extensively explored by us and others [9–13] and recently reviewed by Gomes and co-workers [14].

* Corresponding author.
E-mail address: zrajic@pharma.hr (Z. Rajić).
[1] Both authors contributed equally to this work.

https://doi.org/10.1016/j.ejmech.2021.113687
0223-5234/

In our previous work, we presented harmicines, hybrid compounds derived from harmine, a β-carboline alkaloid with antiplasmodial properties, and CADs [10,15]. The reported harmicines differ in 1) the type of the linker between two moieties, which is either a triazole ring or an amide bond, 2) the position of the substitution on the harmine's β-carboline core, which is either O-7 or N-9, and 3) type of CAD. Harmicines exerted remarkable antiplasmodial activity against erythrocytic and hepatic stages of the *Plasmodium* infection, while molecular dynamics (MD) simulations confirmed binding of the most active compounds within the ATP binding site of *P. falciparum* heat shock protein 90 (*Pf*Hsp90), crucial for the intraerythrocytic development of *Plasmodium* [16,17].

To further extend our knowledge of the harmicines structure-activity relationship, we decided to derivatize the harmine scaffold at C-1, C-3, O-6 and N-9 of the β-carboline core and combine it with different CADs (Fig. 1). Both triazole-type (TT) and amide-type (AT) harmicines were prepared. As a continuation of our research, we investigated their antiplasmodial activity against both erythrocytic and hepatic stages of the *Plasmodium* parasite, as well as cytotoxicity against human liver hepatocellular carcinoma cell line (HepG2). We also report computational analysis of their binding to *Pf*Hsp90 using MD simulations.

2. Results and discussion

2.1. Chemistry

The synthetic part of this work could be divided into two parts: 1) synthesis of TT harmicines and 2) synthesis of AT harmicines, with a general synthetic scheme shown in Fig. 2, while the detailed reactions and conditions are given in Schemes 1–4.

TT harmicines (**5a-e**, **14a-e**, **15a-e**, **20a-e**) were prepared by Cu(I) catalysed azide-alkyne cycloaddition (CuAAC). Different reagents and reaction conditions were used depending on the position of the β-carboline ring functionalization. Harmine-based azides **3** or **10** and CAD-based alkynes **4a-e** served as building blocks for the synthesis of TT harmicines at C-1 (**5a-e**) or C-3 (**15a-e**), respectively. CuAAC was performed with $CuSO_4 \times 5H_2O$ in the presence of sodium ascorbate, as a source of Cu(I) ions, in *t*-BuOH/H_2O 1:1 mixture. On the contrary, the starting compounds for the synthesis of TT harmicines at O-6 (**20a-e**) and N-9 (**14a-e**) were harmine-based alkynes **12** or **19** and cinnamyl azides **13a-e**. In this case, the reaction was carried out in MeOH, with Cu(II) acetate (MeOH acts as a reducing agent to generate Cu(I)).

To obtain the required starting compounds for CuAAC, synthetic routes to alkynes and azides were developed. Harmine-based azides **3** and **10** were generated in several steps: 1) synthesis of substituted β-carbolines **1** and **8** at positions 1 and 3 [18,19], 2) synthesis of the corresponding alcohols **2** and **9** [20], and 3) conversion of alcohols to azides **3** and **10** *via* 2-azido-1,3-dimethylimidazolinium hexafluorophosphate (ADMP) and 1,8-diazabicyclo(5.4.0)undec-7-ene (DBU) [21]. Alcohol **9** was also alkylated at N-9 with propargyl bromide in the presence of Cs_2CO_3, to obtain alkyne **12**. Next, we have prepared β-carboline **17**, substituted with a methoxy group at C-6, a starting compound for harmicines **20a-e** and **23a-h**. Subsequent demethylation yielded phenol **18**, which was further propargylated to yield alkyne **19**. CADs were efficiently transformed to CAD-based alkynes **4a-e** and cinnamyl azides **13a-e**. Alkynes **4a-e** were successfully prepared by the reaction of CAD with propargyl bromide, in the presence of K_2CO_3, while the synthesis of cinnamyl azides **13a-e** involved several steps: esterification of CADs, reduction to the corresponding alcohols, and conversion to azides *via* ADMP/DBU, as described previously [10].

On the other hand, synthesis of AT harmicines (**7a-h**, **16a-h**, **23a-h**, **27a**,**b**) was straightforward and involved two steps: 1) synthesis of harmine-based primary amines **6**, **11**, **22** and **26** and 2) coupling reactions with different CADs. The above listed primary amines were obtained by either the reduction of azides **3** and **10** by catalytic hydrogenation or the O-6 alkylation of phenol **18**/N-9 alkylation of harmine with 2-(Boc-amino)ethyl bromide, followed by the removal of the Boc-protecting group under acidic conditions [15]. Coupling reactions were efficiently performed by activating CADs with 1-[bis(dimethylamino)methylene]-1*H*-1,2,3-triazolo

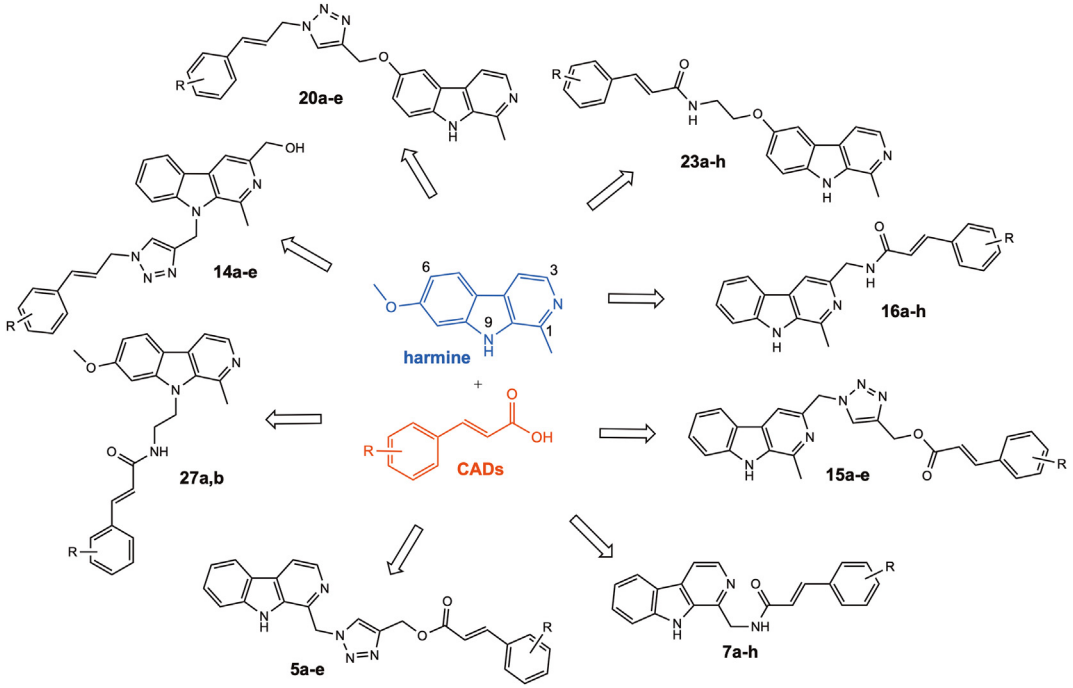

Fig. 1. Novel harmicines.

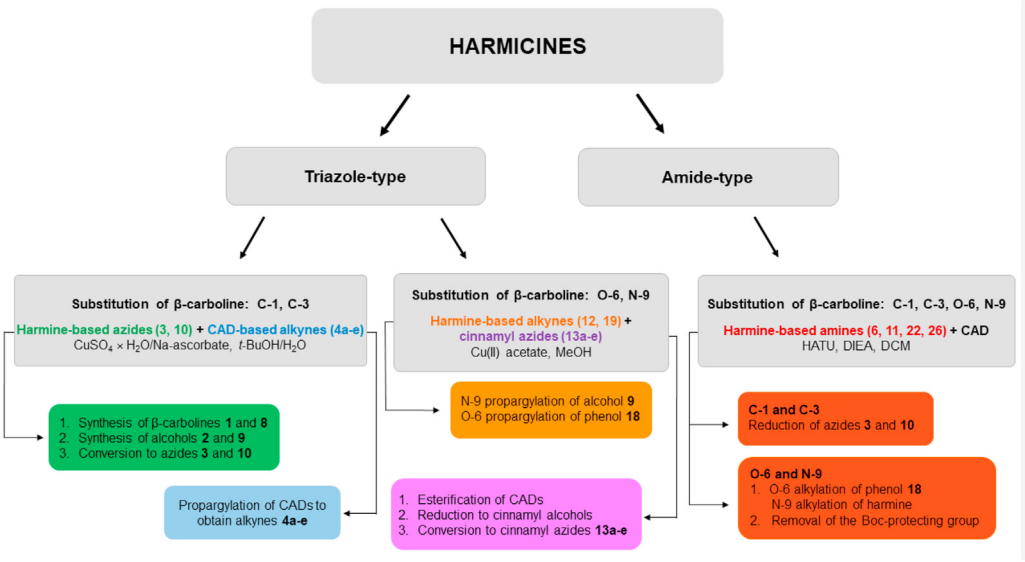

Fig. 2. Synthesis of triazole-type (TT) and amide-type (AT) harmicines.

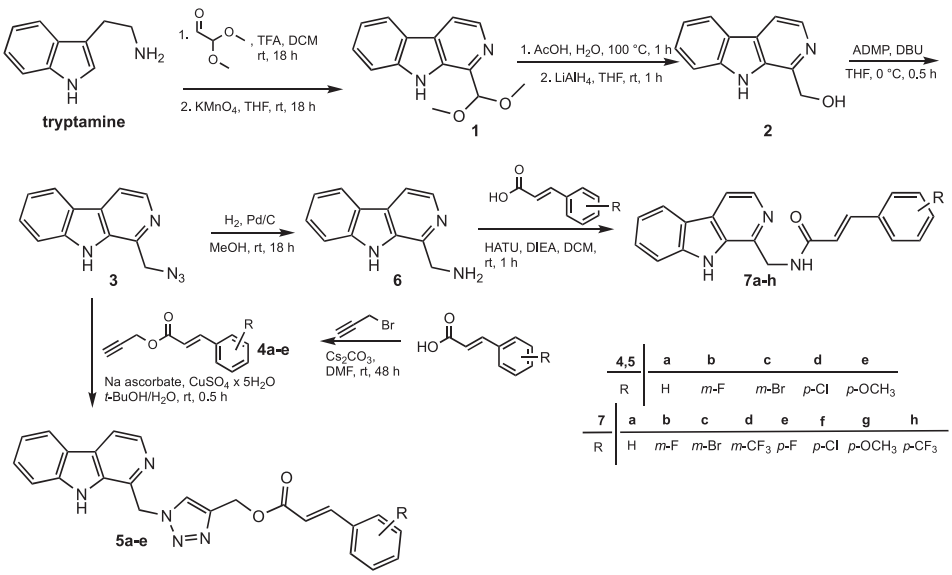

Scheme 1. Synthesis of TT harmicines **5a**-**e** and AT harmicines **7a**-**h**.

[4,5-*b*]pyridinium-3-oxide hexafluorophosphate (HATU), in the presence of *N,N*-diisopropylethylamine (DIEA), followed by the addition of an appropriate harmine-based amine. The reactions proceeded smoothly, in dichloromethane at room temperature for 1 h.

Altogether, we have obtained 45 new compounds in high purity, as determined by HPLC-ESI/MS analysis (>95%) or CHN analysis (values for C, H, and N within 0.4% of the calculated values for the proposed formula). Spectroscopic and spectrometric methods (^{1}H and ^{13}C NMR, IR, MS) were used to confirm the proposed structures. The data obtained are provided in short in the Materials and Methods section, and in detail in the Supplementary Material. The evaluation of the drug-like properties, *i.e.* relevant physicochemical parameters included in the Lipinski's rule and Gelovani's rules, using Chemicalize.org software [22] disclosed that both TT and AT harmicines are in complete agreement with both sets of rules, respectively (Table S15).

2.2. Biological evaluations

2.2.1. In vitro antiplasmodial activity and SAR analysis

The ability of novel harmicines to inhibit the erythrocytic stage of *P. falciparum* infection (chloroquine-sensitive (*Pf*3D7) and chloroquine-resistant (*Pf*Dd2) strains), as well as infection of the human hepatoma cell line (Huh7) by *P. berghei* parasites, was evaluated as described previously [23–27]. The diversity of the harmicines allowed us to explore the significance of certain structural features for the activity: 1) position of the substitution at the β-carboline ring, 2) linker between β-carboline and CAD, and 3) position and the type of substituent on the phenyl ring in CAD.

The results of the *in vitro* screening of blood schizonticidal activity indicated significant differences in antiplasmodial activities between harmicines prepared at the different positions of the β-carboline ring (Table 1). In general, the activity decreased according to the pattern: N-9 > O-6 > C-3 > C-1, except for TT harmicines **14**

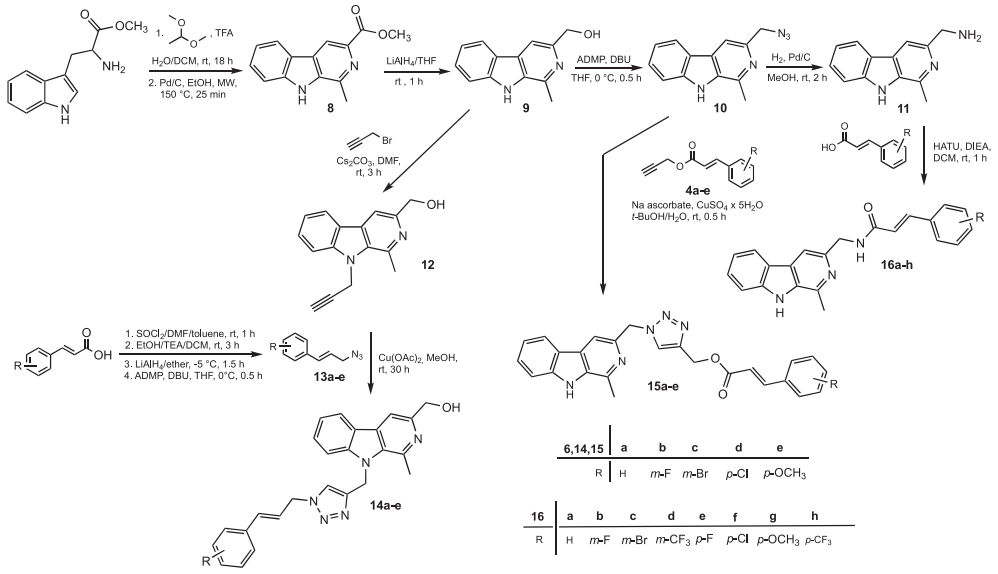

Scheme 2. Synthesis of TT harmicines **14a**-**e**, **15a**-**e** and AT harmicines **16a**-**h**.

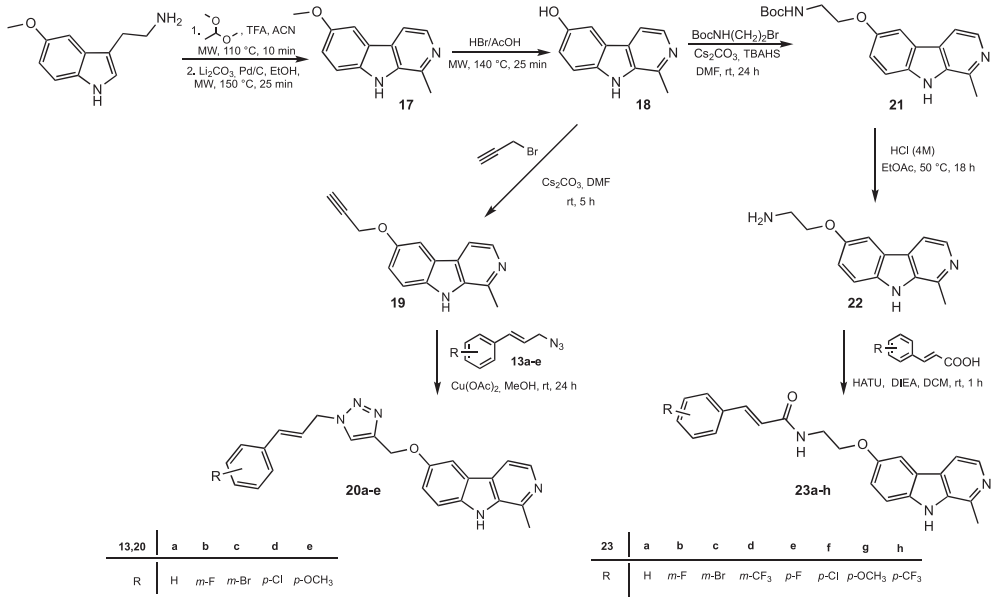

Scheme 3. Synthesis of TT harmicines **20a**-**e** and AT harmicines **23a**-**h**.

(substitution at N-9), which were among the least active compounds.

The most active compounds, AT harmicines **27a**,**b**, hybrids comprised of harmine-based amine at N-9 (compound **26**) and *m*- or *p*-(trifluoromethyl)cinnamic acid, displayed at least two orders of magnitude stronger activities than the parent compound, harmine, in nanomolar (*Pf*3D7) and submicromolar concentrations (*Pf*Dd2). These results are in agreement with IC_{50} values obtained previously for the series of AT harmicines, in which the derivative with *p*-chloro substituent (trifluoromethyl isostere) in the cinnamic scaffold exerted the highest activity [15]. Interestingly, harmicines **14**, also hybrids at N-9, with triazole linker and an additional hydroxymethyl substituent at C-3, exerted lower activity than harmine, with the exception of compound **14c**, *m*-bromocinnamic acid derivative. It is noteworthy that the analogues TT harmicines reported by Perković et al., without C-3 hydroxymethyl substituent, exhibited activities in submicromolar concentrations, suggesting that such substitution results in the loss of activity [10].

Harmicines **20** and **23**, both bearing substituents at O-6, showed similar activities in submicromolar and micromolar concentrations, regardless of the type of the linker. Comparison of the antiplasmodial activities within the series of TT harmicines **20** showed that the substituent R^1 on cinnamic moiety had a minor effect on the activity. Compound **20c**, a *m*-bromocinnamic acid derivative, exerted on average 2.2-fold higher activity than the other compounds. Among the AT harmicines, compounds **23d** and **23h**, *m*- and *p*-(trifluoromethyl)cinnamic acid derivatives, exhibited the highest antiplasmodial activities, which were still 2 to 3-fold lower than the activities of analogous compounds **27a** and **27b**.

On the other hand, considering the antiplasmodial activities of the AT and TT harmicines **16** and **15**, hybrids at C-3, two conclusions could be drawn. First, the IC_{50} values were in the micromolar range.

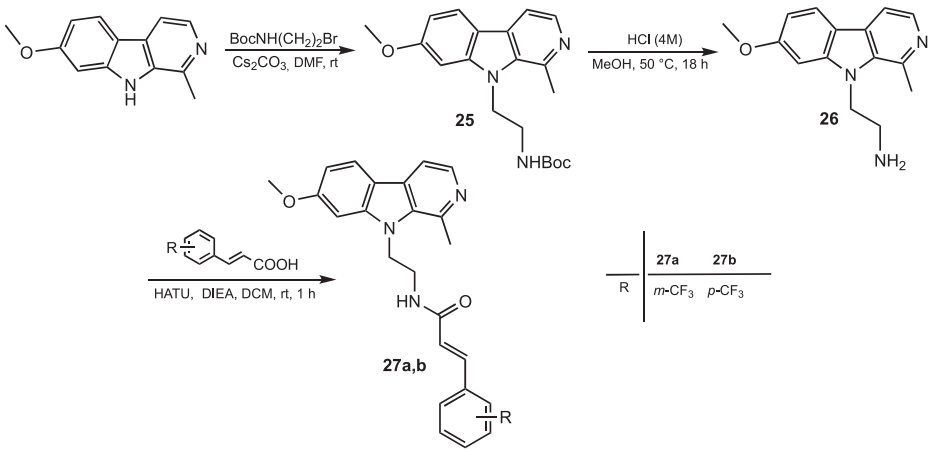

Scheme 4. Synthesis of harmicines **27**.

Table 1
In vitro antiplasmodial activity of harmicines **5**, **7**, **14**–**16**, **20**, **23** and **27** against the erythrocytic stage of *P. falciparum* (*Pf*3D7 and *Pf*Dd2 strains).

TT harmicines	β-carboline substitution	IC_{50}[a] (μM)		AT harmicines	IC_{50} (μM)	
		*Pf*3D7	*Pf*Dd2		*Pf*3D7	*Pf*Dd2
5a	C-1	>27.78[b]	>20.25	**7a**	>27.99	>55.56
5b		>17.32	>20.07	**7b**	>27.78	>27.78
5c		>13.24	>19.07	**7c**	>27.78	>27.78
				7d	>27.78	>27.78
				7e	>13.89	>13.89
5d		>55.56	>55.56	**7f**	>27.78	>27.78
5e		>55.56	39.20 ± 0.25	**7g**	>27.78	>27.78
				7h	>55.56	>55.56
15a	C-3	>20.04	>27.78	**16a**	5.78 ± 1.05	10.18 ± 1.68
15b		>27.78	>27.78	**16b**	5.74 ± 0.33	12.71 ± 1.76
15c		16.41 ± 3.35	11.14 ± 2.76	**16c**	3.23 ± 0.32	1.48 ± 035
				16d	2.01 ± 0.09	7.40 ± 0.74
				16e	4.13 ± 0.61	13.30 ± 7.41
15d		21.44 ± 2.27	>27.78	**16f**	2.92 ± 0.03	8.38 ± 3.16
15e		>27.78	>27.78	**16g**	6.50 ± 0.29	10.72 ± 3.18
				16h	2.30 ± 0.41	5.97 ± 1.33
20a	O-6	0.61 ± 0.09	2.12 ± 0.40	**23a**	1.55 ± 0.45	2.47 ± 0.25
20b		0.55 ± 0.08	2.28 ± 0.33	**23b**	1.11 ± 0.14	1.30 ± 0.09
20c		0.26 ± 0.17	0.73 ± 0.40	**23c**	0.19 ± 0.02	0.63 ± 0.22
				23d	0.12 ± 0.02	0.32 ± 0.08
				23e	0.95 ± 0.06	1.67 ± 0.06
20d		0.57 ± 0.06	0.95 ± 0.16	**23f**	0.36 ± 0.02	0.92 ± 0.06
20e		0.60 ± 0.03	1.81 ± 0.04	**23g**	1.17 ± 0.03	2.86 ± 0.52
				23h	0.12 ± 0.02	0.35 ± 0.06
14a	N-9	>27.78	>19.78			
14c		6.28 ± 1.04	18.41 ± 2.42			
14d		>19.92	>23.60			
14e		18.19	>16.93			
				27a	0.06 ± 0.02	0.33 ± 0.06
				27b	0.04 ± 0.003	0.17 ± 0.01
CQ[d]		0.003 ± 0.002	0.20 ± 0.10	HAR[e]	8.25 ± 2.83	>27.7

[c] Results represent mean ± SD, $n \geq 2$.
[a] IC_{50}, the concentration of the tested compound necessary for 50% growth inhibition.
[b] The exact IC_{50} could not be obtained, as activity could only be detected at the highest tested concentration.
[d] CQ, chloroquine;[e] HAR, harmine.

This result, together with those obtained for harmicines **14**, indicate that the position 3 of the β-carboline ring is not optimal for substitution. Secondly, there is a marked difference in the antiplasmodial activities of harmicines **15** and **16**. AT harmicines **16** were significantly more potent than their triazole-linker counterparts, compounds **15**. Comparison of the activities of the homologous compounds from the series **16** and **15** revealed at least a 3.5-fold (**16a** *vs* **15a**) increase in the activity. The most pronounced effect was observed for harmicines **16g** and **15d** (a 7.3-fold increase in the activity). Remarkably, the comparison of IC_{50} values of AT and TT harmicines, hybrids at N-9 of the β-carboline, reported earlier, revealed the same tendency [10,15].

Harmicines **5** and **7**, prepared at C-1of the β-carboline core, were inactive against the erythrocytic stage of *P. falciparum*, at the highest concentration tested, regardless of the type of the linker and CAD used for conjugation.

As a continuation of our research, screening of *in vitro* activities of harmicines **5**, **7**, **14**, **15**, **16**, **20**, **23** and **27** against the hepatic stages

of *Plasmodium* parasite was performed. Both AT and TT harmicines were initially tested at two concentrations, 1 and 10 μM. The results obtained have shown that the potency of harmicines against the hepatic stages followed a similar pattern as against the erythrocytic stage of *Plasmodium* infection (Fig. 3). The most pronounced activity was observed for harmicines **27** and **14**, prepared at N-9 of the β-carboline ring, followed by **20** and **23** (O-6), **15** and **16** (C-3) and finally harmicines **5** and **7** (C-1), which were mostly inactive. In general, AT harmicines exhibited better activity, *i.e.* **27** > **14**, **23** > **20**, **16** > **15**. In view of those results, compound **27a**, *m*-(trifluoromethyl)cinnamic acid derivative, was selected as the most promising for IC_{50} determination (Fig. S1). The obtained IC_{50} value was 4.3-fold lower than IC_{50} of the reference drug primaquine (1.94 ± 0.68 μM *vs* 8.4 ± 3.4 μM) [28].

2.2.2. *In vitro cytotoxicity screening and selectivity*

Cytotoxicity of the harmicines active against the erythrocytic stage of *P. falciparum* was evaluated against HepG2, as described previously [29] (Table 2). In addition, the selectivity index (SI) for each harmicine was calculated as the fractional ratio between the IC_{50}s for HepG2 and *P. falciparum Pf*3D7 strain (Table 2).

To our delight, the most active compounds against *Pf*3D7, **27a**,**b**, exhibited favourable SIs. Remarkably, the most selective compound of all prepared harmicines was **27a** (SI = 1105). A comparison of the IC_{50} values obtained for harmicines prepared at O-6 revealed that, in general, TT harmicines **20** were more cytotoxic to HepG2 cells than AT harmicines **23** ($IC_{50} \leq 10$ μM, with the exception of the compound **20e**). It is worth mentioning that harmicines **23e**-**g** were not cytotoxic at all at the highest concentration tested.

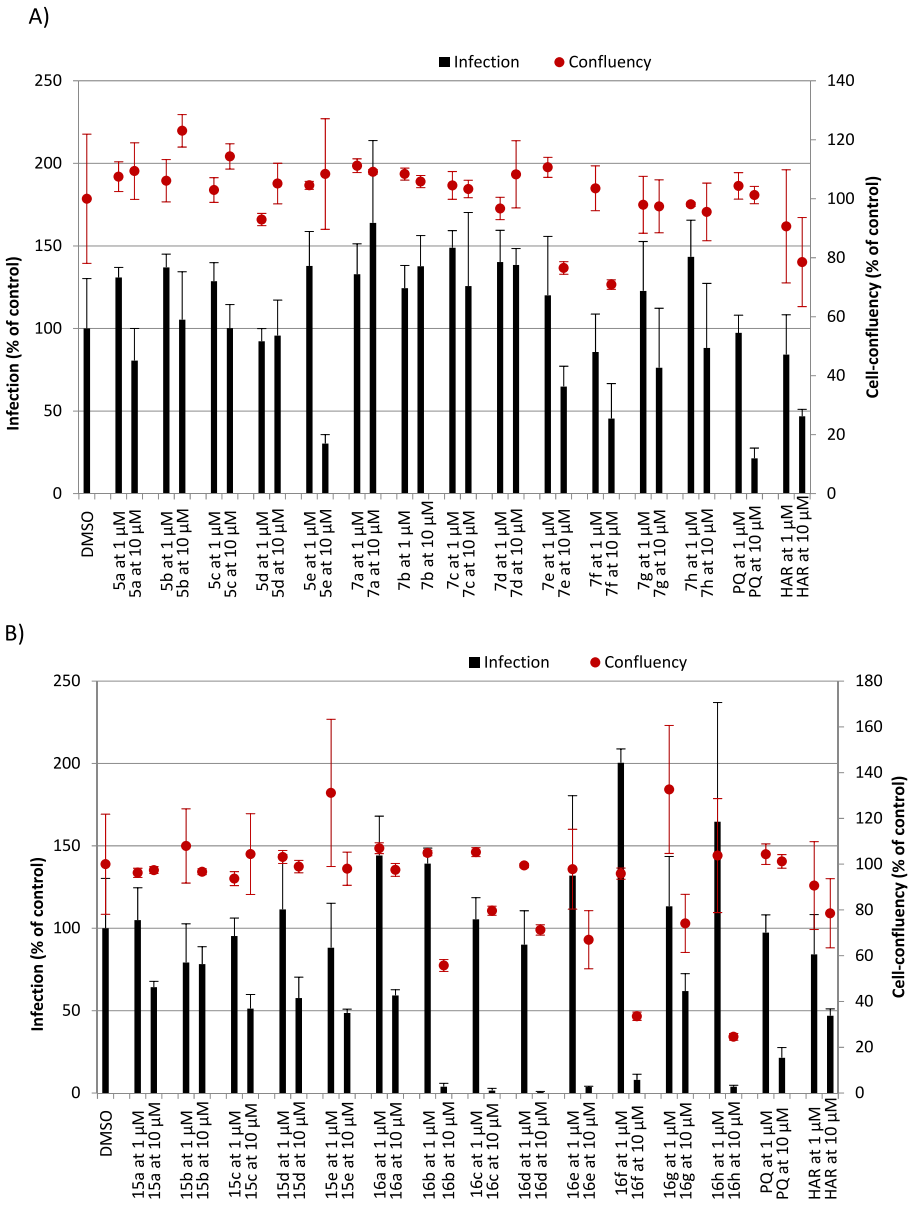

Fig. 3. *In vitro* activity of harmicines against *P. berghei* liver stages: a) **5a**-**e** and **7a**-**h**, b) **15a**-**e** and **16a**-**h**, c) **20a**-**e** and **23a**-**h** and d) **14a**,**c**-**d** and **27a**,**b** at 1 and 10 μM concentrations. Total parasite load (infection scale, bars) and cell viability (cell confluency scale, dots) are shown. Results were normalized to the negative control, DMSO, and are represented as mean ± SD, n = 1 (PQ, primaquine; HAR, harmine).

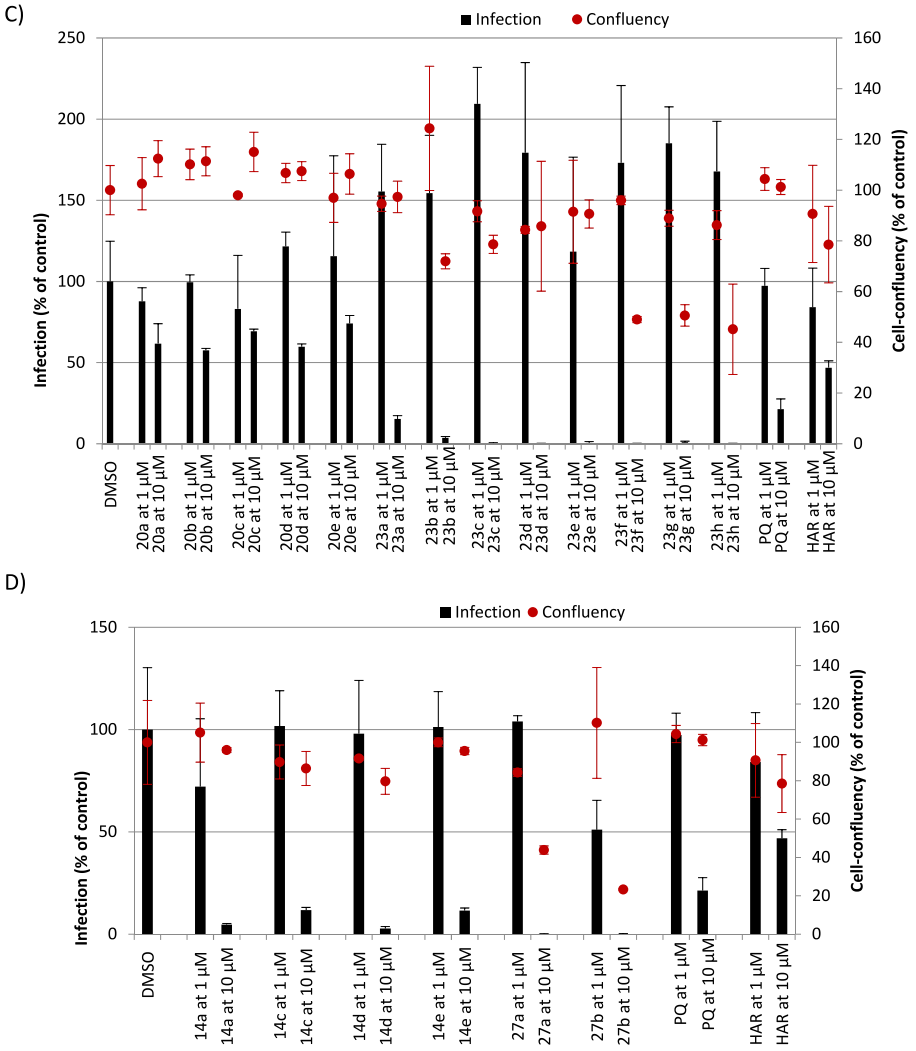

Fig. 3. (*continued*).

Cytotoxicity of other tested harmicines did not differ much from their antiplasmodial activities against erythrocytic stages (in most cases their SI was below 7). Therefore, those compounds can't be considered for future development as antimalarial agents. However, those results open the window for their repurposing as anticancer agents, which will be explored in our future investigations.

2.3. Molecular dynamics simulations

Given a very large number of compounds evaluated in this work, we utilized MD simulations on a representative set of systems, selected to feature the most potent derivative **27b**, together with **7b**, **16a** and **23h**, which should provide enough structural and electronic information to discriminate among various substitution patterns and their biological activities, while offering guidelines how to focus subsequent synthetic efforts towards even more effective analogues based on the employed organic framework.

The calculated binding free energies (ΔG_{BIND}) for the studied systems are given in Table 3, together with their decomposition into contributions from individual residues. The residues considered for the analysis include those identified as responsible for the

Table 2
In vitro cytotoxicity screening of harmicines against HepG2 and calculated selectivity indices.

Compd.	IC_{50}[a] (μM)	SI[b]	Compd.	IC_{50}[a] (μM)	SI[b]
14c	>125[c]	19.90	**20d**	3.95 ± 0.83	6.93
15c	110.19 ± 56.92	6.71	**20e**	88.01 ± 50.81	146.68
15d	70.50 ± 25.64	3.29	**23a**	12.02 ± 4.95	7.75
16a	7.05 ± 0.11	1.29	**23b**	37.57 ± 3.10	33.85
16b	15.83 ± 3.23	2.76	**23c**	7.57 ± 2.56	39.84
16c	9.64 ± 4.71	2.98	**23d**	6.14 ± 0.11	51.17
16d	9.37 ± 4.90	4.66	**23e**	>250	263.16
16e	12.46 ± 5.26	2.99	**23f**	>250	694.44
16f	11.33 ± 0.65	3.88	**23g**	>250	213.68
16g	10.38 ± 4.15	1.60	**23h**	3.59 ± 1.26	29.92
16h	33.26 ± 1.66	14.46	**27a**	66.32 ± 3.79	1105.33
20a	10.13 ± 3.50	16.61	**27b**	5.84 ± 1.67	146
20b	10.51 ± 5.39	19.11	HAR[d]	>250	30
20c	6.13 ± 2.71	23.58			

[a] IC_{50}, the concentration of the tested compound necessary for 50% growth inhibition.
[b] SI, selectivity index, the ratio between IC_{50} (HepG2) and IC_{50} (*Pf*3D7).
[c] The exact IC_{50} could not be obtained, as activity could only be detected at the highest tested concentration.
[d] HAR, harmine.

Table 3
Total binding free energies (ΔG_{BIND}) and their decomposition on a per-residue basis following the MM-GBSA analysis of the obtained molecular dynamics trajectories.[a].

System	7b	16a	23h	27b	HAR[b]
Total ΔG_{BIND}	−21.3	−25.8	−22.9	−30.0	−7.5
Lys44	−0.13	−1.41	−0.51	−1.89	0.00
Arg98	−1.63	0.04	−1.71	−1.67	0.00
Asn37	−2.25	−2.17	−1.80	−1.40	0.00
Met84	−0.89	−1.63	−2.06	−1.26	0.00
Ala41	−0.58	−1.51	−1.59	−1.02	0.00
Tyr47	0.01	−0.02	0.01	−0.68	0.00
Phe124	−0.78	−0.73	−0.74	−0.68	0.00
Ile82	−0.10	−0.98	−1.30	−0.64	0.00
Asp40	0.14	−0.79	−0.48	−0.63	0.00
Leu93	−0.61	−0.61	−0.58	−0.47	0.00
Ile173	−0.21	−0.66	−0.56	−0.43	−0.01
Thr171	−0.37	−1.03	−0.75	−0.37	0.00
Leu34	−0.13	−0.48	−0.19	−0.31	0.00
Ala38	−0.15	−0.82	−0.69	−0.23	0.00
Lys102	0.01	0.01	0.01	0.03	−0.34
Asp52	0.01	0.01	0.01	0.04	0.00
Thr95	0.02	0.03	0.03	0.04	0.00
Arg167	0.03	0.04	0.02	0.05	0.00
Glu48	0.03	0.06	0.08	0.13	0.00
Asp43	0.05	0.04	0.04	0.20	0.00
Asp79	0.23	1.51	1.62	0.31	0.00

[a] Residues are selected to list those belonging to the ATP binding pocket (Asn37, Asp79, Arg98, Phe124, in bold) and all of those with contributions higher than −0.20 and lower than 0.03 kcal mol^{-1} for the most potent **27b**. All values are in kcal mol^{-1}.
[b] HAR, harmine.

binding of ATP within the ATP binding pocket of *Pf*Hsp90 (Asn37, Asp79, Arg98, Phe124) [30,31] and all those with contributions higher than −0.20 and lower than 0.03 kcal mol^{-1} for the most potent **27b**.

It turns out that all compounds are associated with negative ΔG_{BIND} values, implying that their binding is exergonic and favourable. All four systems are clearly positioned within the ATP binding site of *Pf*Hsp90 (Fig. 4), as they form significant interactions with residues that define that site, which underlines the importance of this structural element as a druggable target. Still, their orientations and specific ligand-protein interactions are largely different, thus resulting in diverse affinities.

The binding of **27b** is the most exergonic, ΔG_{BIND}(**27b**) = −30.0 kcal mol^{-1}, thus confirming its highest biological activity measured here. Its harmine fragment enters deeper within the binding site, where it uses its aromatic framework to interact with Asn37 (N−H … π interactions) and Met84 (C−H … π interactions), evidenced in their significant individual contributions

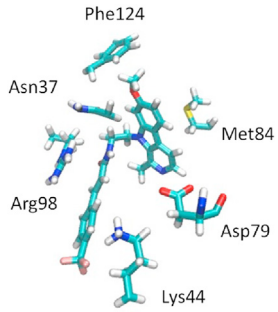

Fig. 5. Specific interactions governing the binding of the most potent **27b** within the ATP binding site of the *Pf*Hsp90 protein.

of −1.40 and −1.26 kcal mol^{-1}, respectively (Fig. 5), or its attached −OMe group to form C−H … π interactions with Phe124 (−0.68 kcal mol^{-1}). The mentioned three residues already contribute around 11% of the total binding energy, which is significant. In addition, the introduced N-9 amide functionality further promotes the binding, first by allowing Arg98 to stack above the amide linker (−1.67 kcal mol^{-1}), and second, even more significantly, to facilitate positive N−H … π contacts between the cationic Lys44 residue and the terminal *p*-CF_3-phenyl unit, being persistent during simulations (Fig. S2). The latter promotes Lys44 as the most dominant *Pf*Hsp90 residue in binding **27b**, related with the individual contribution of −1.89 kcal mol^{-1}. Taken together, indicated five residues already account for 23% of the total binding energy, suggesting that **27b** is rather well positioned within the binding site. All of this clearly confirms the suitability of the N-9 substitution as a useful strategy in designing effective compounds and justifies placing an aromatic unit at an appropriate distance from the harmine N-9 site to benefit the binding, where the amide linker seems to be optimal and well-tuned for the purpose. In addition, knowing that the *p*-CF_3 group exerts an electron-withdrawing effect on the attached phenyl ring, which likely diminishes the mentioned N−H … π interactions with Lys44, it would be useful to consider replacing *p*-CF_3 with different electron-donating groups, which will be tackled in the subsequent synthetic work. Having said that, among others, *p*-OMe does not appear suitable as such a derivative possesses reduced activity [15], albeit lower toxicity, so other substituents would have to be evaluated.

The effect of the anionic Asp79 is also interesting and worth discussing. This is a significant residue, since it is also identified as part of the ATP binding motif, yet its interactions with **27b** are strongly

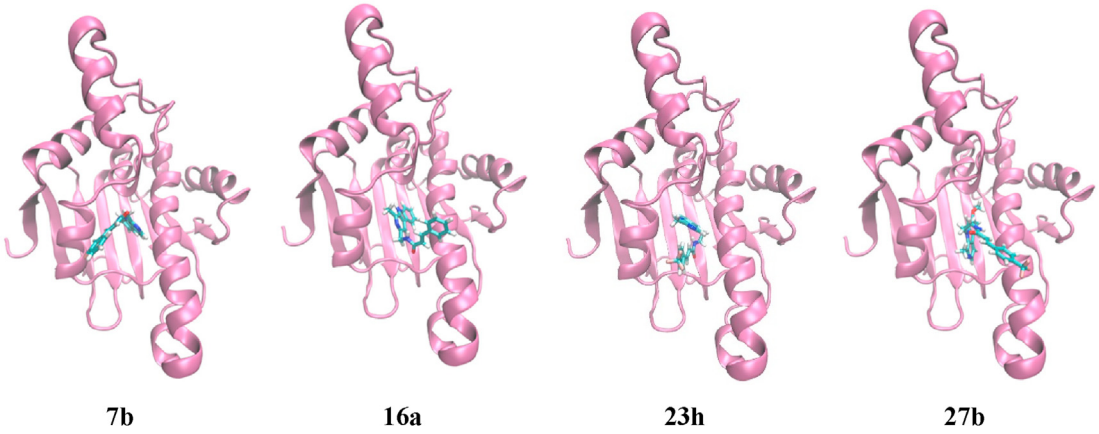

Fig. 4. Position of the investigated ligands within the ATP binding site of the *Pf*Hsp90 protein.

disfavouring the binding, as Asp79 is associated with a positive contribution of +0.31 kcal mol^{-1}, being the highest endergonic among all residues. The underlying reason is that Asp79 is located in the vicinity of the harmine's pyridine unit without any notable favourable contacts that could counterbalance a negative steric and electronic interference from the anionic carboxylate. This suggests that despite its mostly optimal design, **27b** could further benefit from modifying its pyridine unit with something that could revert this fragment into a favourable pairing with Asp79. Yet, this is not achieved in **16a**, as the binding affinity of this C-3 derivative is reduced by 4.2 kcal mol^{-1} to ΔG_{BIND}(**16a**) = −25.8 kcal mol^{-1}, suggesting that the introduced amide-linked cinnamic acid moiety is likely too large for this purpose. There, the unfavourable interaction with Asp79 is even enhanced (Fig. S3), as its individual contribution rises from +0.31 in **27b** to +1.51 kcal mol^{-1}. Such structural modification even changes the binding orientation so that, for example, the entire positive contribution from Arg98, observed in **27b**, is lost here, which leads to a reduced affinity, being in line with experiments. An even less favourable outcome is seen in **7b**, where an analogous structural modification occurs on the other part of the pyridine ring, the C-1 atom, where the resulting binding affinity is further reduced to ΔG_{BIND}(**7b**) = −21.3 kcal mol^{-1}, being the lowest among considered systems, thus confirming its low activity observed experimentally. Even though **7b** seems to be able to compensate the unfavourable contribution from Asp79 down to +0.23 kcal mol^{-1}, its position within the ATP binding site disfavours favourable contributions from several significant residues, including Lys44, which is diminished to only −0.13 kcal mol^{-1}, despite, for example, improving the contribution of Asn37 up to −2.25 kcal mol^{-1} due to positive N−H … π interactions.

In general, all considered systems, selected to correspond to different substitution patterns, show much more exergonic binding affinities than the parent harmine, which justifies the utilized synthetic strategy. The calculated value of ΔG_{BIND}(harmine) = −7.5 kcal mol^{-1}, demonstrates its poor binding features, being consistent with its elevated IC_{50} value of 8.25 μM (Table 1). In addition, although the relationship between IC_{50} and ΔG_{BIND} values is not so straightforward in absolute terms, their relative ratio is connected through the Cheng-Prusoff equation [32]. In this context, harmine's IC_{50} value roughly translates to the binding energy of −6.9 kcal mol^{-1}, thus placing our calculations in close agreement with experiments, and confirming the validity of the employed computational setup. Harmine seems like a good reference, since it was identified as a selective inhibitor of *Pf*Hsp90, which is essential for the erythrocytic development of *Plasmodium* [16,33] and our calculations show it predominantly binds outside the ATP binding site (Table 3). Hence, the approach to structurally modify harmine is likely to lead to more efficient compounds, although, in some cases evaluated here, the introduced amide/triazole-linked cinnamic acid unit, despite being placed at right positions on the harmine's scaffold, appears as too bulky or electronically less optimized to maximize the effect. Nevertheless, computations confirm the substitution at the N-9 position as the most promising route in this respect, which likely opens the door towards further improvements in the desired biological activities.

3. Conclusions

In conclusion, we have successfully prepared and characterized 45 novel harmicines of the triazole- and amide-type in the positions 1, 3, 6 and 9 of the β-carboline ring. Further, we evaluated their antiplasmodial activities against erythrocytic and hepatic stages of the *Plasmodium* infection and cytotoxicity against HepG2. The results clearly showed remarkable blood shizontocidal activity in nanomolar concentrations, as well as selectivity of amide-type harmicines **27**, in comparison to other compounds. Harmicines **27** were also the most active against hepatic stages of *P. berghei* (4.3-fold more active than the reference drug primaquine). Molecular dynamics simulations revealed that all investigated compounds bind within the ATP binding site and confirmed **27b** as the most potent derivative. In addition, Lys44 was identified as crucial for the enhanced activity, evident in favourable N−H … π contacts with the phenyl ring within the attached cinnamic acid unit, particularly when the latter is introduced at the harmine's N-9 position, being in line with the experiments. Lastly, computations underlined the unfavourable contribution from the ATP binding site residue Asp79, seen in the steric and electronic interference with the bound ligands, which defines a promising route to advance the developed synthetic methodology towards even more efficient compounds based on the employed organic framework. Taken together with previously obtained results, this study revealed amide-type harmicines at N-9 of the β-carboline ring as the best performers against *Plasmodium*. Our ongoing work focuses on establishing a reliable quantitative structure-activity relationship model, with the final goal of identifying lead compounds for further development.

4. Materials and Methods

4.1. Chemistry

4.1.1. General information

Melting points were determined on a Stuart Melting Point Apparatus (Barloworld Scientific, UK) in open capillaries and were uncorrected. FTIR-ATR spectra were recorded using a Fourier-Transform Infrared Attenuated Total Reflection UATR Two spectrometer (PerkinElmer, Waltham, MA, USA) in the range from 450 to 4000 cm^{-1}. ^{1}H and ^{13}C NMR spectra were recorded on a Bruker Avance III HD operating at 300, 400 or 600 MHz for the ^{1}H and 75, 101 or 151 MHz for the ^{13}C nuclei (Bruker, Billerica, MA, USA). Samples were measured in DMSO-d_6 solutions at 20 °C in 5 mm NMR tubes. Chemical shifts (δ) are reported in parts per million (ppm) using tetramethylsilane (TMS) as a reference in the ^{1}H and DMSO residual peak as a reference in the ^{13}C spectra (39.52 ppm). Coupling constants (J) are reported in hertz (Hz). Mass spectra were recorded on Agilent 1200 Series HPLC coupled with Agilent 6410 Triple Quad (Agilent Technologies, St. Clara, CA, USA). The mobile phase consisted of Milli Q water as component A and MeOH (HPLC grade, J. T. Baker) as component B, and as the stationary phase, Zorbax XDC C18 column (4.6 × 75 mm, 3.5 μm) was used. Gradient elution was used at a flow rate of 0.5 mL/min, and 5 μL of analyte solution was injected per analysis. The starting conditions and gradient steepness were adjusted according to the analyte polarity. Diode array detector was utilized, while the data were presented as a total wavelength chromatogram (TWC). Mass spectrometry conditions were as follows: electrospray ionization (ESI) in positive and negative mode was used. Capillary voltage and current were set to 4.0 kV and 20 nA, respectively. Nebulizer pressure was set to 15 psi, while the drying gas (nitrogen) temperature and flow were 300 °C and 11 L/min. For the MS data analysis, Agilent MassHunter software (Agilent Technologies, St. Clara, CA, USA) was used. Elemental analyses were performed on a CHNS LECO analyser (LECO Corporation, St. Joseph, MI, USA). Analyses indicated by the symbols of the elements were within ±0.4% of their theoretical values. Microwave-assisted reactions were performed in a microwave reactor CEM Discover (CEM, USA) in a glass reaction vessel. All compounds were routinely checked by TLC with silica gel 60F-254 glass plates (Merck, Germany) using DCM/MeOH 8:1, 85:15, 95:5, 97:3, cyclohexane/EtOAc/MeOH 1:1:0.5 and cyclohexane/EtOAc 2:1, 9:1 as the solvent systems. Spots were visualized by UV light (λ = 254 nm; 365 nm) and iodine vapour. Column chromatography was performed on silica gel 0.063−0.200 mm (Sigma-Aldrich, USA)

with the same eluents used for TLC, with an additional Al_2O_3 layer to remove Cu-salts (compounds **5a**-**e**, **14a**,**c**-**d**, **15a**-**e**, **20a**-**e**). All chemicals and solvents were of analytical grade and purchased from commercial sources. CADs were purchased as predominantly *trans* stereoisomers (≥99%).

Harmine, acetic acid, hydrochloric acid, cinnamic acid, *m*-fluorocinnamic acid, *p*-fluorocinnamic acid, *p*-methoxycinnamic acid, *p*-chlorocinnamic acid, *m*-(trifluoromethyl)cinnamic acid, *p*-(trifluoromethyl)cinnamic acid, *t*-BuOH, acetaldehyde dimethyl acetal, 2,2-dimethoxyacetaldehyde, DBU, lithium aluminium hydride, toluene, lithium carbonate, 10% palladium on activated charcoal were purchased from Sigma-Aldrich (USA). Caesium carbonate, 2-(*tert*-butoxycarbonylamino)ethyl bromide, tryptamine, 5-methoxytryptamine, L-tryptophan methyl ester hydrochloride, tetrabutylammonium hydrogensulfate, ADMP, HATU, *m*-bromocinnamic acid, propargyl bromide and DMF were purchased from TCI Chemicals (Japan). Hydrobromic acid (47%), dry tetrahydrofuran and aluminium oxide were purchased from Merck (Germany), DIEA, copper(II) acetate and TEA from Alfa Aesar (USA), 1 M hydrochloric acid in EtOAc, trifluoroacetic acid, DCM and dry diethyl ether from Thermo Fischer Scientific (USA), diethyl ether from ITW Reagents (Germany), cyclohexane, EtOAc, MeOH, absolute EtOH and petroleum ether from Honeywell (USA), acetonitrile from CARLO ERBA Reagents (France), DMF, sodium hydroxide, sodium bicarbonate and potassium carbonate from Kemika (Croatia), anhydrous sodium sulphate, potassium permanganate, ammonium chloride and sodium chloride from Gram-Mol (Croatia), thionyl chloride from Fluka (Switzerland), sodium ascorbate from Acros Organics (Belgium), copper(II) sulphate pentahydrate from Zorka Šabac (Serbia).

β-carbolines **1**, **8**, **17** and alcohol **9** were prepared according to the literature procedures [18–20,34]. Alcohol **2** is a known compound, but prepared by alternative methods [35,36]. Phenol **18** was prepared according to the modified literature procedure from β-carboline **17** using HBr/glacial acetic acid mixture, under the MW irradiation [37]. Among alkynes **4**, only **4c** is a new compound. Nevertheless, the established synthetic method for their preparation differs from the one described in the literature [38]. Although amine **6** is commercially available, we have included its synthesis and characterization, since those data are not available. Cinnamyl azides **13a**-**e**, as well as compounds **25** and **26** were prepared according to our published methods [10,15].

*4.1.2. Synthesis of (9H-pyrido [3,4]-b]indol-1-yl)methanol (**2**)*

A solution of β-carboline **1** (0.700 g, 2.889 mmol), AcOH (3.63 mL) and H_2O (5.45 mL) was refluxed for 1 h at 100 °C. After cooling to rt, pH was adjusted to 9 with 5% NaOH and the reaction mixture extracted with EtOAc (3 × 50 mL). The collected organic layers were filtered through phase separator and solvent evaporated under the reduced pressure. Obtained yellow crude (0.453 g, 2.309 mmol) was suspended in dry THF (6 mL). Afterwards $LiAlH_4$ (0.175 g, 4.618 mmol) was added in small portions, and the reaction mixture was stirred under argon atmosphere for 1 h at rt. The reaction was quenched with H_2O (20 mL), pH adjusted to 8 with 1% HCl, and the resulting solution extracted with EtOAc (4 × 50 mL). The collected organic layers were filtered through phase separator and solvent evaporated under the reduced pressure. The crude product was triturated with diethyl ether, to obtain alcohol **2**. Yield: 0.417 g (91%).

*4.1.3. General procedure for the synthesis of azides **3** and **10***

To a solution of **2** or **9** (1.447 mmol) in dry THF (5 mL), ADMP (1.032 g, 3.618 mmol) and DBU (0.584 mL, 3.907 mmol) were added at 0 °C. The reaction was stirred at 0 °C for 0.5 h, diluted with saturated NH_4Cl solution (40 mL) and extracted with DCM (2 × 30 mL). Organic layers were collected and extracted with brine (2 × 30 mL) and H_2O (1 × 20 mL), filtered through phase separator and solvent evaporated under the reduced pressure. The crude product (brownish oil) was purified by column chromatography (cyclohexane/EtOAc/MeOH 1:1:0.5).

*4.1.3.1. 1-(azidomethyl)-9H-pyrido[3,4-b]indole (**3**).* Alcohol **2**: 0.287 g. Yield: 0.236 g (73%); oil; IR (ATR, ν/cm^{-1}) 3663, 3451, 3288, 3059, 2937, 2855, 2105, 1730, 1631, 1566, 1493, 1428, 1371, 1321, 1248, 1118, 1052, 971, 938, 873, 824, 751, 718, 620, 579, 432; ^{1}H NMR (DMSO-d_6) δ 11.78 (s, 1H), 8.36 (d, 1H, J = 5.2 Hz), 8.29-8.23 (m, 1H), 8.13 (d, 1H, J = 5.2 Hz), 7.64 (dt, 1H, J = 8.3, 0.9 Hz), 7.60-7.57 (m, 1H), 7.29-7.26 (m, 1H), 4.89 (s, 2H); ^{13}C NMR (DMSO-d_6) δ 140.58, 139.19, 137.75, 133.86, 128.50, 128.44, 121.87, 120.74, 119.57, 114.77, 112.02, 51.59.

*4.1.3.2. 3-(azidomethyl)-1-methyl-9H-pyrido[3,4-b]indole (**10**).* Alcohol **9**: 0.307 g. Yield: 0.261 g (76%); oil; IR (ATR, ν/cm^{-1}) 3671, 3451, 3239, 3051, 2937, 2863, 2447, 2325, 2104, 1689, 1631, 1566, 1509, 1452, 1403, 1354, 1264, 1085, 1036, 971, 848, 759, 718, 644, 579, 431; ^{1}H NMR (DMSO-d_6) δ 11.66 (s, 1H), 8.20 (d, 1H, J = 7.9 Hz), 8.00 (s, 1H), 7.62-7.60 (m, 1H), 7.57-7.53 (m, 1H), 7.26-7.23 (m, 1H), 4.57 (s, 2H), 2.78 (s, 3H); ^{13}C NMR (DMSO-d_6) δ 143.23, 142.12, 140.74, 133.94, 128.02, 127.56, 121.74, 121.01, 119.39, 112.07, 111.72, 55.30, 20.41.

*4.1.4. General procedure for the synthesis of alkynes **4a**-**e***

An appropriate CAD (3.375 mmol) and K_2CO_3 (0.653 g, 4.725 mmol) were suspended in dry DMF (5 mL). Under the argon atmosphere, propargyl bromide (0.601 mL, 5.4 mmol, 80% solution in toluene) was added dropwise, and the reaction was stirred at rt for 48 h. Upon completion, the reaction mixture was diluted with H_2O (50 mL) and extracted with EtOAc (3 × 40 mL). The collected organic layers were washed with H_2O (2 × 100 mL), dried over anhydrous sodium sulphate and solvent evaporated under the reduced pressure. The crude product (oil) was purified by column chromatography (cyclohexane/EtOAc/MeOH 1:1:0.5).

*4.1.4.1. Prop-2-yn-1-yl cinnamate (**4a**).* CAD: 0.500 g of *trans*-cinnamic acid; yield: 0.584 g (93%).

*4.1.4.2. Prop-2-yn-1-yl (E)-3-(3-fluorophenyl)acrylate (**4b**).* CAD: 0.561 g of *m*-fluorocinnamic acid; yield: 0.648 g (94%).

*4.1.4.3. Prop-2-yn-1-yl (E)-3-(3-bromophenyl)acrylate (**4c**).* CAD: 0.766 g of *m*-bromocinnamic acid; yield: 0.779 g (87%); mp 79.0–81.0 °C; IR (ATR, ν/cm^{-1}) 3416, 3279, 3060, 3042, 2940, 2132, 1716, 1637, 1561, 1479, 1419, 1360, 1295, 1201, 1169, 1073, 991, 965, 851, 780, 754, 696, 665, 632, 554; ^{1}H NMR (DMSO-d_6) δ 8.02 (t, 1H, J = 1.8 Hz), 7.78 (dt, 1H, J = 7.7, 1.4 Hz), 7.69 (d, 1H, J = 16.1 Hz), 7.64-7.62 (m, 1H), 7.39 (t, 1H, J = 7.9 Hz), 6.79 (d, 1H, J = 16.1 Hz), 4.84 (d, 2H, J = 2.4 Hz), 3.59 (t, 1H, J = 2.5 Hz); ^{13}C NMR (DMSO-d_6) δ 165.21, 143.81, 136.38, 133.17, 130.99, 130.97, 127.45, 122.32, 118.90, 77.80, 51.93; ESI-MS: decomposition.

*4.1.4.4. Prop-2-yn-1-yl (E)-3-(4-chlorophenyl)acrylate (**4d**).* CAD: 0.616 g of *p*-chlorocinnamic acid; yield: 0.7 g, (94%).

*4.1.4.5. Prop-2-yn-1-yl (E)-3-(4-methoxyphenyl)acrylate (**4e**).* CAD: 0.601 g of *p*-methoxycinnamic acid; yield: 0.540 g, (74%).

*4.1.5. General procedure for the synthesis of harmicines **5a**-**e***

Azide **3** (0.04 g, 0.179 mmol) and a corresponding alkyne **4a-e** (0.197 mmol) were suspended in 5 mL of a 1:1 H_2O/*t*-BuOH mixture. Sodium ascorbate (0.2 mmol, 200 μL of freshly prepared 1 M

solution in H_2O) was added, followed by $CuSO_4 \times 5H_2O$ (0.02 mmol, 20 μL of 1 M solution in H_2O). The mixture was stirred at rt for 0.5 h, diluted with 5 mL of ice-cold H_2O and filtered. A yellow precipitate was washed with H_2O (3 × 2 mL), dried under vacuum, purified by column chromatography (mobile phase DCM/MeOH 95:5). The crude product was triturated with diethyl ether/petroleum ether mixture/recrystallized from EtOH.

*4.1.5.1. (1-((9H-pyrido[3,4-b]indol-1-yl)methyl)-1H-1,2,3-triazol-4-yl)methyl cinnamate (**5a**).* Alkyne **4a**: 0.037 g; purification: trituration with diethyl ether/petroleum ether mixture; yield: 0.036 g (49%); mp 181.5–183.5 °C; IR (ATR, ν/cm^{-1}) 3220, 3168, 3093, 3059, 3029, 2994, 2961, 2898, 2877, 2798, 2776, 1713, 1637, 1567, 1505, 1452, 1432, 1402, 1370, 1346, 1325, 1307, 1281, 1243, 1203, 1167, 1066, 1038, 1003, 972, 859, 820, 804, 764, 739, 707, 682, 641, 605, 593, 573, 547, 525, 483; ^{1}H NMR (DMSO-d_6) δ 11.98 (s, 1H), 8.32 (s, 1H), 8.30 (d, 1H, J = 5.2 Hz), 8.27 (d, 1H, J = 7.9 Hz), 8.13 (d, 1H, J = 5.2 Hz), 7.73-7.66 (m, 4H), 7.62-7.58 (m, 1H), 7.44-7.38 (m, 3H), 7.31-7.26 (m, 1H), 6.66 (d, 1H, J = 16.0 Hz), 6.11 (s, 2H), 5.28 (s, 2H); ^{13}C NMR (DMSO-d_6) δ 165.93, 145.03, 141.79, 140.70, 137.98, 137.88, 133.92, 133.84, 130.57, 128.91, 128.74, 128.57, 128.42, 125.73, 121.92, 120.74, 119.66, 117.65, 114.87, 112.07, 57.29, 51.21; ESI-MS: *m/z* 410.1 (M+1)$^+$; Anal. Calcd. for $C_{24}H_{19}N_5O_2$: C, 70.40; H, 4.68; N, 17.10; found: C, 70.27; H, 4.47; N, 17.35.

*4.1.5.2. (1-((9H-pyrido[3,4-b]indol-1-yl)methyl)-1H-1,2,3-triazol-4-yl)methyl (E)-3-(3-fluorophenyl)acrylate (**5b**).* Alkyne **4b**: 0.040 g; purification: trituration with diethyl ether/petroleum ether mixture; yield: 0.043 g (56%); mp 185.5–187.5 °C; IR (ATR, ν/cm^{-1}) 3311, 3230, 3198, 3147, 3105, 3063, 3019, 2998, 2973, 1715, 1639, 1585, 1569, 1502, 1485, 1472, 1449, 1429, 1403, 1390, 1349, 1323, 1272, 1234, 1190, 1168, 1147, 1122, 1075, 1060, 1035, 983, 954, 939, 874, 858, 837, 819, 780, 728, 671, 643, 605, 582, 562, 534, 521; ^{1}H NMR (DMSO-d_6) δ 11.98 (s, 1H), 8.32 (s, 1H), 8.30 (d, 1H, J = 5.2 Hz), 8.27 (d, 1H, J = 7.9 Hz), 8.13 (d, 1H, J = 5.2 Hz), 7.69-7.63 (m, 3H), 7.61-7.59 (m, 1H), 7.56 (dt, 1H, J = 7.8, 1.2 Hz), 7.47-7.43 (m, 1H), 7.30-7.24 (m, 2H), 6.75 (d, 1H, J = 16.1 Hz), 6.11 (s, 2H), 5.28 (s, 2H); ^{13}C NMR (DMSO-d_6) δ 165.75, 162.40 (d, J = 243.8 Hz), 143.66, 141.71, 140.71, 137.99, 137.89, 136.49 (d, J = 8.1 Hz), 133.85, 130.87 (d, J = 8.4 Hz), 128.75, 128.59, 125.78, 124.94 (d, J = 2.5 Hz), 121.94, 120.75, 119.68, 119.30, 117.26 (d, J = 21.4 Hz), 114.89, 114.58 (d, J = 22.1 Hz), 112.08, 57.40, 51.22; ESI-MS: *m/z* 428.1 (M+1)$^+$; Anal. Calcd. for $C_{24}H_{18}FN_5O_2$: C, 67.44; H, 4.24; N, 16.38; found: C, 67.40; H, 4.49; N, 16.21.

*4.1.5.3. (1-((9H-pyrido[3,4-b]indol-1-yl)methyl)-1H-1,2,3-triazol-4-yl)methyl (E)-3-(3-bromophenyl)acrylate (**5c**).* Alkyne **4c**: 0.052 g; purification: recrystallisation from EtOH; yield: 0.032 g (37%); mp 184.0–186.0 °C; IR (ATR, ν/cm^{-1}) 3311, 3223, 3194, 3147, 3102, 3060, 2997, 2971, 1715, 1640, 1607, 1564, 1501, 1472, 1457, 1428, 1404, 1389, 1347, 1308, 1276, 1234, 1189, 1168, 1122, 1090, 1060, 1036, 984, 860, 830, 812, 777, 735, 670, 643, 605, 578, 542; ^{1}H NMR (DMSO-d_6) δ 11.97 (s, 1H), 8.32 (s, 1H), 8.30 (d, 1H, J = 5.2 Hz), 8.26 (d, 1H, J = 7.8 Hz), 8.13 (d, 1H, J = 5.2 Hz), 7.98 (t, 1H, J = 1.8 Hz), 7.73 (dt, 1H, J = 7.8, 1.3 Hz), 7.69-7.57 (m, 4H), 7.36 (t, 1H, J = 7.9 Hz), 7.31-7.27 (m, 1H), 6.75 (d, 1H, J = 16.0 Hz), 6.11 (s, 2H), 5.28 (s, 2H); ^{13}C NMR (DMSO-d_6) δ 165.68, 143.33, 141.71, 140.69, 137.97, 137.87, 136.45, 133.83, 133.03, 130.93, 128.74, 128.57, 127.32, 125.74, 122.28, 121.92, 120.73, 119.66, 119.37, 114.87, 112.07, 57.40, 51.21; ESI-MS: *m/z* 488.0 (M+1)$^+$, 489.9 (M+1)$^+$; Anal. Calcd. for $C_{24}H_{18}BrN_5O_2$: C, 59.03; H, 3.72; N, 14.34; found: C, 59.19; H, 3.94; N, 14.52.

*4.1.5.4. (1-((9H-pyrido[3,4-b]indol-1-yl)methyl)-1H-1,2,3-triazol-4-yl)methyl (E)-3-(4-chlorophenyl)acrylate (**5d**).* Alkyne **4d**: 0.043 g; purification: trituration with diethyl ether/petroleum ether mixture; yield: 0.02 g (25%); mp 201.0–203.5 °C; IR (ATR, ν/cm^{-1}) 3227, 3192, 3096, 3061, 2993, 2965, 2926, 2894, 2872, 1713, 1642, 1594, 1568, 1503, 1490, 1468, 1453, 1431, 1404, 1370, 1346, 1308, 1271, 1242, 1201, 1171, 1148, 1087, 1068, 1038, 1012, 972, 868, 818, 775, 737, 695, 683, 669, 637, 593, 560, 547, 529, 491, 455; ^{1}H NMR (DMSO-d_6) δ 11.97 (s, 1H), 8.31 (s, 1H), 8.30 (d, 1H, J = 5.3 Hz), 8.27 (d, 1H, J = 7.9 Hz), 8.13 (d, 1H, J = 5.2 Hz), 7.77-7.74 (m, 2H), 7.70-7.64 (m, 2H), 7.62-7.58 (m, 1H), 7.50-7.45 (m, 2H), 7.31-7.26 (m, 1H), 6.69 (d, 1H, J = 16.1 Hz), 6.11 (s, 2H), 5.28 (s, 2H); ^{13}C NMR (DMSO-d_6) δ 165.79, 143.60, 141.74, 140.69, 137.97, 137.87, 135.08, 133.83, 132.91, 130.15, 128.94, 128.74, 128.57, 125.73, 121.92, 120.73, 119.66, 118.49, 114.87, 112.07, 57.35, 51.21; ESI-MS: *m/z* 444.0 (M+1)$^+$; Anal. Calcd. for $C_{24}H_{18}ClN_5O_2$: C, 64.94; H, 4.09; N, 15.78; found: C, 64.75; H, 4.27; N, 15.93.

*4.1.5.5. (1-((9H-pyrido[3,4-b]indol-1-yl)methyl)-1H-1,2,3-triazol-4-yl)methyl (E)-3-(4-methoxyphenyl)acrylate (**5e**).* Alkyne **4e**: 0.043 g; purification: trituration with diethyl ether/petroleum ether mixture; yield: 0.032 g (41%); mp 155.0–157.5 °C; IR (ATR, ν/cm^{-1}) 3223, 3170, 3131, 3094, 3082, 2996, 2965, 2934, 2900, 2837, 1712, 1636, 1607, 1573, 1513, 1455, 1429, 1402, 1375, 1322, 1308, 1287, 1258, 1240, 1202, 1163, 1065, 1037, 1002, 971, 867, 852, 824, 774, 734, 592, 547, 527, 513; ^{1}H NMR (DMSO-d_6) δ 11.98 (s, 1H), 8.32-8.29 (m, 2H), 8.27 (d, 1H, J = 7.9 Hz), 8.12 (d, 1H, J = 5.2 Hz), 7.69-7.59 (m, 5H), 7.28 (t, 1H, J = 7.5 Hz), 6.96 (d, 2H, J = 8.4 Hz), 6.50 (d, 1H, J = 16.0 Hz), 6.11 (s, 2H), 5.25 (s, 2H), 3.79 (s, 3H); ^{13}C NMR (DMSO-d_6) δ 166.22, 161.24, 144.85, 141.92, 140.71, 138.01, 137.88, 133.85, 130.26, 128.74, 128.58, 126.56, 125.70, 121.94, 120.75, 119.67, 114.88, 114.38, 112.09, 57.11, 55.34, 51.21; ESI-MS: *m/z* 440.1 (M+1)$^+$; Anal. Calcd. for $C_{25}H_{21}N_5O_3$: C, 68.33; H, 4.82; N, 15.94; found: C, 68.27; H, 4.99; N, 15.68.

*4.1.6. General procedure for the synthesis of amines **6** and **11***

A suspension of **3** or **10** (0.856 mmol) and 10% Pd/C (0.041 g) in MeOH (5 mL) was stirred at rt under hydrogen atmosphere for 18 h (compound **6**) or 2 h (compound **11**). Upon completion, the reaction mixture was filtered through celite, and the solvent was removed under the reduced pressure. The crude product was triturated with diethyl ether/petroleum ether mixture.

*4.1.6.1. (9H-pyrido[3,4-b]indol-1-yl)methanamine (**6**).* Azide **3**: 0.191 g; yield: 0.120 g (71%); IR (ATR, ν/cm^{-1}) 3347, 3282, 3120, 3051, 2955, 2856, 2776, 1625, 1600, 1562, 1501, 1477, 1460, 1430, 1355, 1327, 1316, 1240, 1212, 1163, 1127, 1108, 1071, 960, 896, 848, 829, 772, 747, 671, 595, 564, 516; ^{1}H NMR (DMSO-d_6) δ 8.26 (d, 1H, J = 5.2 Hz), 8.21 (dt, 1H, J = 7.8, 1.0 Hz), 7.97 (d, 1H, J = 5.2 Hz), 7.63-7.62 (m, 1H), 7.55-7.52 (m, 1H), 7.24-7.22 (m, 1H), 4.19 (s, 2H); ^{13}C NMR (DMSO-d_6) δ 146.51, 140.35, 137.18, 133.23, 127.82, 127.42, 121.60, 120.88, 119.15, 113.19, 112.01, 44.59; ESI-MS: *m/z* 196.0 (M − 1)$^-$.

*4.1.6.2. (1-methyl-9H-pyrido[3,4-b]indol-3-yl)methanamine (**11**).* Azide **10**: 0.203 g; yield: 0.110 g (61%); IR (ATR, ν/cm^{-1}) 3338, 3239, 3130, 3057, 2978, 2940, 2914, 2882, 2850, 2783, 2737, 2690, 2637, 1626, 1606, 1566, 1503, 1453, 1401, 1374, 1344, 1317, 1284, 1250, 1176, 1147, 1103, 1083, 1009, 970, 945, 891, 838, 813, 775, 734, 643, 588, 545; ^{1}H NMR (DMSO-d_6) δ 11.42 (s, 1H), 8.14 (d, 1H, J = 7.6 Hz), 7.91 (s, 1H), 7.57-7.47 (m, 2H), 7.20 (t, 1H, J = 6.9 Hz), 3.89 (s, 2H), 2.73 (s, 3H); ^{13}C NMR (DMSO-d_6) δ 151.13, 140.89, 140.74, 133.29, 127.76, 127.62, 121.53, 121.19, 118.98, 111.89, 109.01, 47.59, 20.38; ESI-MS: *m/z* 210.0 (M − 1)$^-$.

*4.1.7. General procedure for the synthesis of harmicines **7a-h***

A solution of a corresponding CAD (0.212 mmol), DIEA (0.073 mL, 0.424 mmol) and HATU (0.081 g, 0.212 mmol) in DCM

(4 mL) was stirred at rt for 20 min, followed by the addition of amine **6** (0.038 g, 0.193 mmol). The reaction mixture was stirred at rt for 1 h. The formed precipitate was filtered off. After purification by column chromatography (DCM/MeOH 8:1) and trituration with diethyl ether, compounds **7a-h** were obtained.

*4.1.7.1. N-((9H-pyrido[3,4-b]indol-1-yl)methyl)cinnamamide (**7a**).* CAD: 0.031 g of *trans*-cinnamic acid; yield: 0.033 g (52%); mp 225.0–227.0 °C; IR (ATR, ν/cm^{-1}) 3375, 3328, 3226, 3195, 3101, 3060, 2901, 1661, 1623, 1576, 1514, 1435, 1404, 1325, 1243, 1205, 994, 914, 811, 767, 731, 718, 706, 620, 565, 490, 478; ^{1}H NMR (DMSO-d_6) δ 11.64 (s, 1H), 8.79 (t, 1H, J = 5.4 Hz), 8.33 (d, 1H, J = 5.2 Hz), 8.25 (d, 1H, J = 7.9 Hz), 8.08 (d, 1H, J = 5.3 Hz), 7.67-7.64 (m, 1H), 7.61-7.50 (m, 4H), 7.46-7.35 (m, 3H), 7.29-7.24 (m, 1H), 6.88 (d, 1H, J = 15.8 Hz), 4.92 (d, 2H, J = 5.3 Hz); ^{13}C NMR (DMSO-d_6) δ 165.43, 141.41, 140.45, 139.04, 137.34, 134.92, 133.52, 129.49, 128.94, 128.17, 127.82, 127.58, 122.10, 121.76, 120.87, 119.45, 113.96, 112.08, 41.65; ESI-MS: m/z 328.1 (M+1)$^+$; HPLC purity > 99.5%.

*4.1.7.2. (E)-N-((9H-pyrido[3,4-b]indol-1-yl)methyl)-3-(3-fluorophenyl)acrylamide (**7b**).* CAD: 0.035 g of *m*-fluorocinnamic acid; yield: 0.034 g (51%); mp 224.5–225.5 °C; IR (ATR, ν/cm^{-1}) 3350, 3217, 3149, 3080, 2995, 2905, 2814, 1672, 1627, 1586, 1516, 1448, 1409, 1325, 1273, 1239, 1225, 1146, 1011, 968, 878, 851, 807, 784, 728, 611, 564, 521; ^{1}H NMR (DMSO-d_6) δ 11.63 (s, 1H), 8.78 (t, 1H, J = 5.4 Hz), 8.32 (d, 1H, J = 5.2 Hz), 8.24 (d, 1H, J = 7.8 Hz), 8.07 (d, 1H, J = 5.2 Hz), 7.64 (d, 1H, J = 8.2 Hz), 7.57 (t, 1H, J = 7.6 Hz), 7.52 (d, 1H, J = 15.8 Hz), 7.49-7.43 (m, 3H), 7.26 (t, 1H, J = 7.4 Hz), 7.23-7.20 (m, 1H), 6.94 (d, 1H, J = 15.8 Hz), 4.92 (d, 2H, J = 5.3 Hz); ^{13}C NMR (DMSO-d_6) δ 165.08, 162.46 (d, J = 244.0 Hz), 141.26, 140.45, 137.71 (d, J = 2.4 Hz), 137.58 (d, J = 7.8 Hz), 137.37, 133.48, 130.90 (d, J = 8.4 Hz), 128.16, 127.80, 123.75 (d, J = 2.5 Hz), 123.70, 121.76, 120.87, 119.44, 116.14 (d, J = 21.2 Hz), 113.96 (d, J = 21.8 Hz), 112.07, 41.65; ESI-MS: m/z 346.1 (M+1)$^+$; HPLC purity 98.2%.

*4.1.7.3. (E)-N-((9H-pyrido[3,4-b]indol-1-yl)methyl)-3-(3-bromophenyl)acrylamide (**7c**).* CAD: 0.048 g of *m*-bromocinnamic acid; yield: 0.056 g (72%); mp 236.5–239.0 °C; IR (ATR, ν/cm^{-1}) 3191, 3016, 1671, 1626, 1564, 1497, 1471, 1437, 1392, 1328, 1222, 1128, 1078, 971, 929, 820, 778, 722, 667, 584; ^{1}H NMR (DMSO-d_6) δ 11.62 (s, 1H), 8.74 (t, 1H, J = 5.4 Hz), 8.31 (d, 1H, J = 5.2 Hz), 8.23 (d, 1H, J = 7.8 Hz), 8.06 (d, 1H, J = 5.2 Hz), 7.80 (t, 1H, J = 1.9 Hz), 7.63 (d, 1H, J = 8.2 Hz), 7.59 (d, 1H, J = 7.8 Hz), 7.57-7.54 (m, 2H), 7.47 (d, 1H, J = 15.8 Hz), 7.37 (t, 1H, J = 7.9 Hz), 7.25 (t, 1H, J = 7.4 Hz), 6.94 (d, 1H, J = 15.8 Hz), 4.91 (d, 2H, J = 5.3 Hz); ^{13}C NMR (DMSO-d_6) δ 165.01, 141.20, 140.46, 137.53, 137.34, 137.30, 133.46, 131.98, 131.02, 130.06, 128.17, 127.82, 126.49, 123.82, 122.26, 121.76, 120.85, 119.44, 113.96, 112.06, 41.62; ESI-MS: m/z 405.9 (M+1)$^+$, 407.9 (M+1)$^+$; HPLC purity 99.4%.

*4.1.7.4. (E)-N-((9H-pyrido[3,4-b]indol-1-yl)methyl)-3-(3-(trifluoromethyl)phenyl)acrylamide (**7d**).* CAD: 0.046 g of *m*-(trifluoromethyl)cinnamic acid; yield: 0.040 g (52%); mp 225.5–226.5 °C; IR (ATR, ν/cm^{-1}) 3197, 3014, 1669, 1628, 1560, 1498, 1438, 1329, 1226, 1177, 1167, 1109, 1077, 972, 885, 804, 742, 721, 691, 581; ^{1}H NMR (DMSO-d_6) δ 11.65 (s, 1H), 8.78 (t, 1H, J = 5.3 Hz), 8.33 (d, 1H, J = 5.2 Hz), 8.24 (dt, 1H, J = 7.9, 1.0 Hz), 8.07 (d, 1H, J = 5.2 Hz), 7.96 (t, 1H, J = 2.0 Hz), 7.90 (d, 1H, J = 7.8 Hz), 7.73 (d, 1H, J = 7.8 Hz), 7.67-7.63 (m, 2H), 7.60 (d, 1H, J = 15.8 Hz), 7.58-7.55 (m, 1H), 7.28-7.25 (m, 1H), 7.06 (d, 1H, J = 15.9 Hz), 4.93 (d, 2H, J = 5.3 Hz); ^{13}C NMR (DMSO-d_6) δ 164.96, 141.19, 140.47, 137.35, 137.26, 136.19, 133.47, 131.37, 130.05, 129.74 (q, J = 31.7 Hz), 128.15, 127.80, 125.72 (q, J = 2.7 Hz), 124.33, 124.06 (q, J = 273.3 Hz), 123.92 (q, J = 3.6 Hz), 121.75, 120.87, 119.44, 113.96, 112.07, 41.67; ESI-MS: m/z 396.1 (M+1)$^+$; HPLC purity 97.3%.

*4.1.7.5. (E)-N-((9H-pyrido[3,4-b]indol-1-yl)methyl)-3-(4-fluorophenyl)acrylamide (**7e**).* CAD: 0.035 g of *p*-fluorocinnamic acid; yield: 0.045 g (67%); mp 231.5–233.0 °C; IR (ATR, ν/cm^{-1}) 3380, 3244, 3147, 3075, 2989, 2900, 1655, 1616, 1599, 1556, 1505, 1430, 1426, 1413, 1354, 1325, 1239, 1220, 1161, 1128, 1098, 1010, 977, 828, 755, 734, 628, 508; ^{1}H NMR (DMSO-d_6) δ 11.62 (s, 1H), 8.75 (t, 1H, J = 5.4 Hz), 8.32 (d, 1H, J = 5.2 Hz), 8.24 (d, 1H, J = 7.8 Hz), 8.06 (d, 1H, J = 5.2 Hz), 7.66-7.63 (m, 3H), 7.56 (t, 1H, J = 7.6 Hz), 7.51 (d, 1H, J = 15.8 Hz), 7.27-7.24 (m, 3H), 6.83 (d, 1H, J = 15.8 Hz), 4.91 (d, 2H, J = 5.3 Hz); ^{13}C NMR (DMSO-d_6) δ 165.31, 162.69 (d, J = 247.0 Hz), 141.39, 140.42, 137.80, 137.35, 133.49, 131.56 (d, J = 3.0 Hz), 129.71 (d, J = 8.4 Hz), 128.12, 127.77, 122.00 (d, J = 1.7 Hz), 121.73, 120.86, 119.41, 115.89 (d, J = 21.8 Hz), 113.92, 112.05, 41.64; ESI-MS: m/z 346.1 (M+1)$^+$; Anal. Calcd. for $C_{21}H_{16}FN_3O$: C, 73.03; H, 4.67; N, 12.17; found: C, 73.15; H, 4.81; N, 12.29.

*4.1.7.6. (E)-N-((9H-pyrido[3,4-b]indol-1-yl)methyl)-3-(4-chlorophenyl)acrylamide (**7f**).* CAD: 0.039 g of *p*-chlorocinnamic acid; yield: 0.036 g (52%); mp 241.0–243.5 °C (decomp.); IR (ATR, ν/cm^{-1}) 3384, 3275, 3053, 1671, 1627, 1532, 1505, 1494, 1457, 1435, 1405, 1323, 1237, 1219, 1094, 1028, 1013, 972, 819, 732, 609, 589, 573, 495; ^{1}H NMR (DMSO-d_6) δ 11.62 (s, 1H), 8.79 (t, 1H, J = 5.4 Hz), 8.32 (d, 1H, J = 5.2 Hz), 8.24 (d, 1H, J = 7.8 Hz), 8.06 (d, 1H, J = 5.2 Hz), 7.65-7.61 (m, 3H), 7.58-7.55 (m, 1H), 7.52-7.48 (m, 3H), 7.26 (t, 1H, J = 7.4 Hz), 6.89 (d, 1H, J = 15.8 Hz), 4.91 (d, 2H, J = 5.4 Hz); ^{13}C NMR (DMSO-d_6) δ 165.20, 141.35, 140.45, 137.67, 137.38, 133.92, 133.51, 129.29, 128.99, 128.16, 127.80, 122.93, 121.77, 120.88, 119.45, 113.96, 112.08, 41.66; ESI-MS: m/z 362.1 (M+1)$^+$; Anal. Calcd. for $C_{21}H_{16}ClN_3O$: C, 69.71; H, 4.46; N, 11.61; found: C, 69.95; H, 4.31; N, 11.99.

*4.1.7.7. (E)-N-((9H-pyrido[3,4-b]indol-1-yl)methyl)-3-(4-methoxyphenyl)acrylamide (**7g**).* CAD: 0.038 g of *p*-methoxycinnamic acid; yield: 0.034 g (49%); mp 230.5–232.0 °C; IR (ATR, ν/cm^{-1}) 3350, 3173, 3097, 3006, 1662, 1624, 1603, 1511, 1432, 1366, 1325, 1254, 1240, 1174, 1029, 981, 914, 818, 791, 733, 596, 528, 506; ^{1}H NMR (DMSO-d_6) δ 11.58 (s, 1H), 8.66 (t, 1H, J = 5.5 Hz), 8.29 (d, 1H, J = 5.3 Hz), 8.22 (d, 1H, J = 7.8 Hz), 8.04 (d, 1H, J = 4.7 Hz), 7.62 (d, 1H, J = 8.2 Hz), 7.56-7.51 (m, 3H), 7.44 (d, 1H, J = 15.7 Hz), 7.24 (t, 1H, J = 7.5 Hz), 6.96 (d, 2H, J = 8.2 Hz), 6.69 (d, 1H, J = 15.7 Hz), 4.88 (d, 2H, J = 5.5 Hz), 3.77 (s, 3H); ^{13}C NMR (DMSO-d_6) δ 165.82, 160.39, 141.57, 140.46, 138.83, 137.34, 133.54, 129.20, 128.20, 127.85, 127.49, 121.78, 120.90, 119.57, 119.48, 114.42, 113.98, 112.10, 55.28, 41.67; ESI-MS: m/z 358.1 (M+1)$^+$; HPLC purity 99.0%.

*4.1.7.8. (E)-N-((9H-pyrido[3,4-b]indol-1-yl)methyl)-3-(4-(trifluoromethyl)phenyl)acrylamide (**7h**).* CAD: 0.046 g of *p*-(trifluoromethyl)cinnamic acid; yield: 0.050 g (65%); mp 262.5–265.0 °C; IR (ATR, ν/cm^{-1}) 3341, 3236, 1664, 1622, 1504, 1436, 1416, 1323, 1239, 1217, 1155, 1116, 1068, 1013, 988, 826, 755, 740, 572, 532, 494; ^{1}H NMR (DMSO-d_6) δ 11.65 (s, 1H), 8.87 (t, 1H, J = 5.4 Hz), 8.33 (d, 1H, J = 5.3 Hz), 8.25 (d, 1H, J = 7.9 Hz), 8.08 (d, 1H, J = 5.3 Hz), 7.83-7.76 (m, 4H), 7.66-7.54 (m, 3H), 7.29-7.24 (m, 1H), 7.03 (d, 1H, J = 15.8 Hz), 4.94 (d, 2H, J = 5.3 Hz); ^{13}C NMR (DMSO-d_6) δ 164.89, 141.23, 140.46, 139.04, 137.38, 137.32, 133.49, 129.21 (q, J = 32.3 Hz), 128.20, 128.16, 127.81, 125.81 (q, J = 3.0 Hz), 124.95, 124.12 (q, J = 272.7 Hz), 121.76, 120.87, 119.44, 113.96, 112.07, 41.66; ESI-MS: m/z 396.1 (M+1)$^+$; HPLC purity 99.4%.

*4.1.8. Synthesis of (1-methyl-9-(prop-2-yn-1-yl)-9H-pyrido[3,4-b]indol-3-yl)methanol (**12**)*

Alcohol **9** (0.200 g, 0.942 mmol) was dissolved in dry DMF (5 mL). Under argon atmosphere caesium carbonate (0.430 g, 1.319 mmol) was added, followed by dropwise addition of

propargyl bromide (0.126 mL, 1.130 mmol, 80% solution in toluene). The reaction mixture was stirred at rt for 5 h. Upon completion, the reaction mixture was diluted with H_2O (50 mL) and extracted with EtOAc (3 × 40 mL). The collected organic layers were washed with H_2O (2 × 100 mL), dried over anhydrous sodium sulphate and the solvent evaporated under the reduced pressure. After purification by column chromatography (DCM/MeOH 95:5) and trituration with diethyl ether, alkyne **12** was obtained as a white solid.

Yield: 0.170 g (72%); mp 225.0–230.0 °C (decomp.); IR (ATR, ν/cm^{-1}) 3154, 2929, 2823, 2109, 1621, 1561, 1475, 1453, 1360, 1333, 1283, 1206, 1139, 1063, 1040, 965, 933, 877, 744, 724, 641, 578; ^{1}H NMR (DMSO-d_6) δ 8.25 (d, 1H, J = 7.8 Hz), 8.03 (s, 1H), 7.78 (d, 1H, J = 8.3 Hz), 7.63-7.58 (m, 1H), 7.29 (t, 1H, J = 7.4 Hz), 5.45 (d, 2H, J = 2.4 Hz), 5.35 (t, 1H, J = 5.8 Hz), 4.68 (d, 2H, J = 5.8 Hz), 3.35 (t, 1H, J = 2.4 Hz), 3.04 (s, 3H); ^{13}C NMR (DMSO-d_6) δ 150.83, 141.27, 140.52, 133.22, 129.53, 128.23, 121.52, 121.05, 120.04, 110.37, 109.11, 75.50, 64.34, 34.19, 22.45; ESI-MS: m/z 251.1 (M+1)$^+$.

*4.1.9. General procedure for the synthesis of harmicines **14a-e***

To a solution of alkyne **12** (0.040 g, 0.160 mmol) and the corresponding cinnamyl azide **13a-e** (0.176 mmol) in MeOH (5 mL), a catalytic amount of $Cu(OAc)_2$ was added. The reaction mixture was stirred at rt for 24 h. Upon completion of the reaction, the solvent was removed under the reduced pressure. The residue was purified by column chromatography with DCM/MeOH, cyclohexane/EtOAc/MeOH or EtOAc/MeOH as a mobile phase. The crude product was triturated with diethyl ether/petroleum ether to obtain harmicines **14a-e**. Compound **14b** was obtained, but decomposed quickly at −20 °C.

*4.1.9.1. (9-((1-cinnamyl-1H-1,2,3-triazol-4-yl)methyl)-1-methyl-9H-pyrido[3,4-b]indol-3-yl)methanol (**14a**).* **13a**: 0.028 g; mobile phase: cyclohexane/EtOAc/MeOH 3:1:0.5; yield: 0.032 g (49%); mp 197.0–200.0 °C; IR (ATR, ν/cm^{-1}) 3113, 3060, 2966, 2917, 2859, 1657, 1619, 1560, 1512, 1445, 1402, 1362, 1337, 1290, 1252, 1220, 1190, 1156, 1136, 1122, 1062, 1043, 962, 934, 860, 842, 813, 780, 748, 691, 638, 620, 577, 530, 511, 477, 463; ^{1}H NMR (DMSO-d_6) δ 8.23 (d, 1H, J = 7.7 Hz), 8.02 (s, 1H), 7.98 (s, 1H), 7.82 (d, 1H, J = 8.3 Hz), 7.59-7.55 (m, 1H), 7.40-7.24 (m, 6H), 6.51 (d, 1H, J = 15.9 Hz), 6.47-6.35 (m, 1H), 5.90 (s, 2H), 5.33 (t, 1H, J = 5.7 Hz), 5.07 (d, 2H, J = 6.0 Hz), 4.67 (d, 2H, J = 5.7 Hz), 3.05 (s, 3H); ^{13}C NMR (DMSO-d_6) δ 150.27, 144.17, 141.35, 140.55, 135.63, 133.45, 133.41, 129.10, 128.66, 128.10, 128.06, 126.51, 123.66, 122.72, 121.41, 120.99, 119.71, 110.61, 109.07, 64.35, 51.27, 39.73, 23.15; ESI-MS: m/z 410.3 (M+1)$^+$; Anal. Calcd. for $C_{25}H_{23}N_5O$: C, 73.33; H, 5.66; N, 17.10; found: C, 73.19; H, 5.39; N, 17.34.

*4.1.9.2. (E)-(9-((1-(3-(3-bromophenyl)allyl)-1H-1,2,3-triazol-4-yl)methyl)-1-methyl-9H-pyrido[3,4-b]indol-3-yl)methanol (**14c**).* **13c**: 0.042 g; mobile phase: DCM/MeOH 95:5; yield: 0.031 g, (39%); mp 164.5–167.5 °C; IR (ATR, ν/cm^{-1}) 3117, 3060, 2959, 2922, 2861, 1619, 1592, 1560, 1471, 1460, 1445, 1380, 1358, 1336, 1290, 1252, 1222, 1199, 1154, 1120, 1095, 1062, 1044, 995, 965, 934, 875, 861, 829, 786, 747, 719, 685, 668, 636, 621, 577, 534, 492, 463; ^{1}H NMR (DMSO-d_6) δ 8.23 (d, 1H, J = 7.7 Hz), 8.02 (s, 1H), 7.97 (s, 1H), 7.82 (d, 1H, J = 8.3 Hz), 7.70 (t, 1H, J = 2.2 Hz), 7.57 (t, 1H, J = 8.0 Hz), 7.47-7.42 (m, 2H), 7.30-7.24 (m, 2H), 6.67-6.60 (m, 2H), 5.93 (s, 2H), 5.32 (t, 1H, J = 5.7 Hz), 5.07 (d, 2H, J = 5.1 Hz), 4.67 (d, 2H, J = 5.6 Hz), 3.08 (s, 3H); ^{13}C NMR (DMSO-d_6) δ 150.26, 144.16, 141.34, 140.54, 138.20, 133.45, 131.73, 130.74, 130.69, 129.09, 129.00, 128.04, 125.64, 125.56, 122.78, 122.12, 121.40, 120.99, 119.71, 110.60, 109.06, 64.34, 51.11, 39.72, 23.13; ESI-MS: m/z 488.1 (M+1)$^+$, 490.1 (M+1)$^+$; Anal. Calcd. for $C_{25}H_{22}BrN_5O$: C, 61.48; H, 4.54; N, 14.34; found: C, 61.78; H, 4.59; N, 14.62.

*4.1.9.3. (E)-(9-((1-(3-(4-chlorophenyl)allyl)-1H-1,2,3-triazol-4-yl)methyl)-1-methyl-9H-pyrido[3,4-b]indol-3-yl)methanol (**14d**).* **13d**: 0.034 g; mobile phase: EtOAc/MeOH 10:0.5; yield: 0.029 g, (41%); mp 183.0–186.5 °C; IR (ATR, ν/cm^{-1}) 3111, 3064, 2971, 2918, 2858, 2822, 1727, 1658, 1619, 1592, 1559, 1489, 1471, 1447, 1405, 1361, 1336, 1292, 1254, 1221, 1192, 1158, 1121, 1085, 1041, 1014, 964, 938, 861, 837, 819, 799, 779, 748, 719, 685, 637, 577, 537, 502, 462; ^{1}H NMR (DMSO-d_6) δ 8.23 (d, 1H, J = 7.8 Hz), 8.02 (s, 1H), 7.97 (s, 1H), 7.82 (d, 1H, J = 8.3 Hz), 7.57 (t, 1H, J = 7.5 Hz), 7.43-7.35 (m, 4H), 7.27 (t, 1H, J = 7.4 Hz), 6.52-6.41 (m, 2H), 5.90 (s, 2H), 5.32 (t, 1H, J = 5.7 Hz), 5.07 (d, 2H, J = 5.1 Hz), 4.67 (d, 2H, J = 5.7 Hz), 3.05 (s, 3H); ^{13}C NMR (DMSO-d_6) δ 150.27, 144.18, 141.35, 140.55, 134.61, 133.44, 132.47, 132.05, 129.10, 128.64, 128.24, 128.06, 124.71, 122.76, 121.41, 120.99, 119.72, 110.60, 109.06, 64.35, 51.17, 39.73, 23.15; ESI-MS: m/z 444.2 (M+1)$^+$; Anal. Calcd. for $C_{25}H_{22}ClN_5O$: C, 67.64; H, 5.00; N, 15.78; found: C, 67.34; H, 5.16; N, 15.63.

*4.1.9.4. (E)-(9-((1-(3-(4-methoxyphenyl)allyl)-1H-1,2,3-triazol-4-yl)methyl)-1-methyl-9H-pyrido[3,4-b]indol-3-yl)methanol (**14e**).* **13e**: 0.033 g; mobile phase: DCM/MeOH 95:5; yield: 0.030 g, (43%); mp 202.0–205.0 °C; IR (ATR, ν/cm^{-1}) 3180, 3119, 3067, 3024, 3002, 2945, 2923, 2869, 1622, 1563, 1488, 1462, 1441, 1379, 1364, 1333, 1298, 1254, 1222, 1203, 1160, 1135, 1122, 1067, 1037, 1003, 965, 915, 857, 771, 745, 696, 636, 582, 533, 509, 471, 454; ^{1}H NMR (DMSO-d_6) δ 8.23 (d, 1H, J = 7.8 Hz), 8.02 (s, 1H), 7.96 (s, 1H), 7.82 (d, 1H, J = 8.3 Hz), 7.57 (t, 1H, J = 7.5 Hz), 7.34-7.30 (m, 2H), 7.26 (t, 1H, J = 7.5 Hz), 6.89-6.85 (m, 2H), 6.47 (d, 1H, J = 15.8 Hz), 6.25 (dt, 1H, J = 15.8, 6.5 Hz), 5.90 (s, 2H), 5.33 (t, 1H, J = 5.7 Hz), 5.03 (d, 2H, J = 7.2 Hz), 4.67 (d, 2H, J = 5.7 Hz), 3.74 (s, 3H), 3.05 (s, 3H); ^{13}C NMR (DMSO-d_6) δ 159.20, 150.26, 144.14, 141.35, 140.56, 133.45, 133.19, 129.09, 128.24, 128.05, 127.86, 122.61, 121.40, 121.05, 120.98, 119.71, 114.06, 110.60, 109.07, 64.35, 55.11, 51.41, 39.73, 23.15; ESI-MS: m/z 440.3 (M+1)$^+$; Anal. Calcd. for $C_{26}H_{25}N_5O_2$: C, 71.05; H, 5.73; N, 15.93; found: C, 71.27; H, 5.79; N, 15.72.

*4.1.10. General procedure for the synthesis of harmicines **15a-e***

To a suspension of azide **10** (0.04 g, 0.169 mmol) and a corresponding alkyne **4a-e** (0.186 mmol) in 5 mL of a 1:1H_2O/*t*-BuOH mixture, sodium ascorbate (0.2 mmol, 200 μL of freshly prepared 1 M solution in H_2O) and $CuSO_4 \times 5H_2O$ (0.02 mmol, 20 μL of 1 M solution in H_2O) were added. The mixture was stirred at rt for 0.5 h, diluted with 5 mL of ice-cold H_2O and filtered. A yellow precipitate was washed with H_2O (3 × 2 mL) and dried under vacuum. After purification by column chromatography (mobile phase DCM/MeOH 95:5) and trituration with diethyl ether/petroleum ether mixture, compounds **15a-e** were obtained as white solids.

*4.1.10.1. (1-((1-methyl-9H-pyrido[3,4-b]indol-3-yl)methyl)-1H-1,2,3-triazol-4-yl)methyl cinnamate (**15a**).* Alkyne **4a**: 0.035 g; yield: 0.026 g (36%); mp 194.5–195.5 °C; IR (ATR, ν/cm^{-1}) 3220, 3194, 3175, 3145, 3101, 3060, 3030, 2989, 2945, 1712, 1694, 1644, 1626, 1605, 1565, 1503, 1451, 1392, 1376, 1356, 1329, 1312, 1271, 1254, 1223, 1202, 1170, 1116, 1059, 1037, 1002, 972, 934, 898, 859, 843, 827, 804, 765, 752, 738, 708, 681, 642, 611, 587, 524, 480; ^{1}H NMR (DMSO-d_6) δ 11.67 (s, 1H), 8.26 (s, 1H), 8.17 (d, 1H, J = 7.9 Hz), 7.99 (s, 1H), 7.72-7.70 (m, 2H), 7.67 (d, 1H, J = 16.0 Hz), 7.60 (dt, 1H, J = 8.2, 1.0 Hz), 7.55-7.53 (m, 1H), 7.44-7.39 (m, 3H), 7.24-7.21 (m, 1H), 6.65 (d, 1H, J = 16.1 Hz), 5.77 (s, 2H), 5.27 (s, 2H), 2.75 (s, 3H); ^{13}C NMR (DMSO-d_6) δ 165.94, 145.02, 142.54, 142.16, 141.92, 140.78, 134.00, 133.93, 130.58, 128.91, 128.42, 128.10, 127.60, 125.13, 121.72, 120.91, 119.46, 117.66, 112.10, 112.05, 57.34, 55.25, 20.40; ESI-MS: m/z 424.0 (M+1)$^+$; Anal. Calcd. for $C_{25}H_{21}N_5O_2$: C, 70.91; H, 5.00; N, 16.54; found: C, 70.83; H, 5.17; N, 16.69.

*4.1.10.2. (1-((1-methyl-9H-pyrido[3,4-b]indol-3-yl)methyl)-1H-1,2,3-triazol-4-yl)methyl (E)-3-(3-fluorophenyl)acrylate (**15b**).* Alkyne **4b**: 0.038 g, yield: 0.045 g (60%); mp 197.0–198.5 °C; IR (ATR, ν/cm^{-1}) 3223, 3198, 3166, 3104, 3067, 3043, 3012, 2970, 2895, 1707, 1627, 1608, 1583, 1568, 1506, 1483, 1449, 1387, 1355, 1320, 1271, 1252, 1213, 1151, 1115, 1084, 1057, 1036, 1008, 980, 942, 911, 898, 864, 832, 788, 766, 738, 693, 675, 649, 609, 586, 555, 537, 520, 480; ^{1}H NMR (DMSO-d_6) δ 11.67 (s, 1H), 8.26 (s, 1H), 8.18 (d, 1H, J = 7.9 Hz), 8.00 (s, 1H), 7.67 (d, 1H, J = 16.1 Hz), 7.65-7.62 (m, 1H), 7.61-7.59 (m, 1H), 7.56-7.53 (m, 2H), 7.46-7.43 (m, 1H), 7.27-7.22 (m, 2H), 6.74 (d, 1H, J = 16.0 Hz), 5.77 (s, 2H), 5.28 (s, 2H), 2.75 (s, 3H); ^{13}C NMR (DMSO-d_6) δ 165.73, 162.39 (d, J = 243.8 Hz), 143.61, 142.52, 142.16, 141.83, 140.77, 136.47 (d, J = 8.1 Hz), 134.00, 130.84 (d, J = 8.4 Hz), 128.09, 127.60, 125.14, 124.91 (d, J = 2.5 Hz), 121.71, 120.90, 119.44, 119.29, 117.23 (d, J = 21.3 Hz), 114.56 (d, J = 22.1 Hz), 112.09, 112.06, 57.43, 55.25, 20.40; ESI-MS: m/z 442.1 (M+1)$^+$; HPLC purity 97.6%.

*4.1.10.3. (1-((1-methyl-9H-pyrido[3,4-b]indol-3-yl)methyl)-1H-1,2,3-triazol-4-yl)methyl (E)-3-(3-bromophenyl)acrylate (**15c**).* Alkyne **4c**: 0.049 g; yield: 0.045 g (53%); mp 204.5–205.5 °C; IR (ATR, ν/cm^{-1}) 3347, 3281, 3170, 3080, 3054, 3023, 2970, 2950, 1708, 1684, 1638, 1592, 1569, 1498, 1474, 1455, 1423, 1383, 1354, 1341, 1313, 1290, 1272, 1247, 1231, 1188, 1146, 1110, 1073, 1053, 1032, 1009, 980, 928, 899, 872, 829, 791, 766, 731, 697, 666, 649, 623, 586, 563, 549, 527; ^{1}H NMR (DMSO-d_6) δ 11.67 (s, 1H), 8.26 (s, 1H), 8.17 (d, 1H, J = 7.9 Hz), 7.99 (s, 1H), 7.97 (t, 1H, J = 1.8 Hz), 7.75-7.71 (m, 1H), 7.64 (d, 1H, J = 16.0 Hz), 7.62-7.58 (m, 2H), 7.56-7.52 (m, 1H), 7.36 (t, 1H, J = 7.9 Hz), 7.25-7.21 (m, 1H), 6.74 (d, 1H, J = 16.1 Hz), 5.77 (s, 2H), 5.28 (s, 2H), 2.75 (s, 3H); ^{13}C NMR (DMSO-d_6) δ 165.67, 143.31, 142.52, 142.14, 141.84, 140.77, 136.44, 133.99, 133.01, 130.91, 128.08, 127.59, 127.29, 125.11, 122.27, 121.70, 120.90, 119.43, 119.38, 112.08, 112.03, 57.44, 55.24, 20.39; ESI-MS: m/z 501.9 (M+1)$^+$, 503.9 (M+1)$^+$; HPLC purity 97.4%.

*4.1.10.4. (1-((1-methyl-9H-pyrido[3,4-b]indol-3-yl)methyl)-1H-1,2,3-triazol-4-yl)methyl (E)-3-(4-chlorophenyl)acrylate (**15d**).* Alkyne **4d**: 0.041 g; yield: 0.044 g (57%); mp 209.0–211.0 °C; IR (ATR, ν/cm^{-1}) 3250, 3157, 3103, 3086, 3067, 3052, 1703, 1633, 1592, 1566, 1493, 1475, 1456, 1428, 1408, 1388, 1356, 1305, 1278, 1251, 1222, 1204, 1182, 1160, 1117, 1089, 1058, 1036, 1004, 964, 899, 865, 840, 823, 805, 753, 739, 719, 702, 646, 605, 586, 550, 524, 501, 456; ^{1}H NMR (DMSO-d_6) δ 11.67 (s, 1H), 8.26 (s, 1H), 8.18 (d, 1H, J = 7.9 Hz), 8.00 (s, 1H), 7.76-7.73 (m, 2H), 7.66 (d, 1H, J = 16.0 Hz), 7.60 (dt, 1H, J = 8.3, 1.0 Hz), 7.56-7.53 (m, 1H), 7.48-7.45 (m, 2H), 7.24-7.22 (m, 1H), 6.68 (d, 1H, J = 16.1 Hz), 5.77 (s, 2H), 5.28 (s, 2H), 2.75 (s, 3H); ^{13}C NMR (DMSO-d_6) δ 165.80, 143.60, 142.53, 142.17, 141.88, 140.78, 135.09, 134.01, 132.92, 130.15, 128.94, 128.11, 127.61, 125.13, 121.72, 120.91, 119.46, 118.51, 112.10, 112.07, 57.40, 55.26, 20.41; ESI-MS: m/z 458.0 (M+1)$^+$; HPLC purity 98.3%.

*4.1.10.5. (1-((1-methyl-9H-pyrido[3,4-b]indol-3-yl)methyl)-1H-1,2,3-triazol-4-yl)methyl (E)-3-(4-methoxyphenyl)acrylate (**15e**).* Alkyne **4e**: 0.040 g; yield: 0.048 g (62%); mp 240.5–243.0 °C; IR (ATR, ν/cm^{-1}) 3236, 3201, 3165, 3103, 3068, 3036, 3007, 2965, 2940, 2911, 2839, 1699, 1626, 1601, 1574, 1514, 1456, 1426, 1389, 1357, 1307, 1290, 1252, 1223, 1207, 1179, 1155, 1115, 1056, 1023, 1009, 992, 971, 937, 898, 868, 830, 810, 776, 751, 735, 710, 693, 663, 652, 637, 608, 586, 555, 521; ^{1}H NMR (DMSO-d_6) δ 11.67 (s, 1H), 8.25 (s, 1H), 8.18 (d, 1H, J = 7.9 Hz), 7.99 (s, 1H), 7.68-7.64 (m, 2H), 7.64-7.59 (m, 2H), 7.55-7.53 (m, 1H), 7.24-7.22 (m, 1H), 6.97-6.94 (m, 2H), 6.49 (d, 1H, J = 16.0 Hz), 5.77 (s, 2H), 5.25 (s, 2H), 3.79 (s, 3H), 2.75 (s, 3H); ^{13}C NMR (DMSO-d_6) δ 166.19, 161.20, 144.80, 142.53, 142.14, 142.03, 140.76, 133.99, 130.22, 128.08, 127.59, 126.54, 125.05, 121.70, 120.90, 119.44, 114.88, 114.35, 112.08, 112.04, 57.14, 55.32, 55.23, 20.39; ESI-MS: m/z 454.1 (M+1)$^+$; HPLC purity 98.6%.

*4.1.11. General procedure for the synthesis of harmicines **16a-h***

A solution of a corresponding CAD (0.162 mmol), DIEA (0.056 mL, 0.324 mmol) and HATU (0.062 g, 0.162 mmol) in DCM (4 mL) was stirred at rt for 20 min, followed by the addition of amine **11** (0.031 g, 0.147 mmol). The resulting solution was stirred at rt for 1 h. Purification was performed by either Method A or Method B.

Method A: The resulting precipitate was filtered off, purified by column chromatography (DCM/MeOH 8:1) and triturated with diethyl ether/petroleum ether mixture.

Method B: After completion of the reaction, the solvent was evaporated and EtOAc (10 mL) was added. The formed precipitate was filtered off, purified by column chromatography (DCM/MeOH 8:1) and triturated with diethyl ether/petroleum ether mixture.

*4.1.11.1. N-((1-methyl-9H-pyrido[3,4-b]indol-3-yl)methyl)cinnamamide (**16a**).* CAD: 0.024 g of *trans*-cinnamic acid; purification: Method A; yield: 0.032 g (64%); mp 207.0–208.0; IR (ATR, ν/cm^{-1}) 3352, 3284, 3089, 3048, 2896, 2851, 1659, 1621, 1568, 1510, 1451, 1388, 1354, 1319, 1284, 1246, 1206, 1176, 1075, 1015, 973, 899, 871, 741, 714, 643, 612, 587, 557, 487; ^{1}H NMR (DMSO-d_6) δ 11.54 (s, 1H), 8.69 (t, 1H, J = 5.7 Hz), 8.19 (d, 1H, J = 7.8 Hz), 7.88 (s, 1H), 7.60-7.58 (m, 3H), 7.53-7.49 (m, 2H), 7.44-7.41 (m, 2H), 7.39-7.37 (m, 1H), 7.21 (t, 1H, J = 7.4 Hz), 6.81 (d, 1H, J = 15.8 Hz), 4.62 (d, 2H, J = 5.8 Hz), 2.78 (s, 3H); ^{13}C NMR (DMSO-d_6) δ 164.89, 146.07, 141.27, 140.79, 138.77, 134.98, 133.55, 129.41, 128.92, 127.86, 127.79, 127.52, 122.38, 121.70, 120.99, 119.17, 111.93, 110.08, 44.64, 20.26; ESI-MS: m/z 342.4 (M+1)$^+$; HPLC purity 97.1%.

*4.1.11.2. (E)-3-(3-fluorophenyl)-N-((1-methyl-9H-pyrido[3,4-b]indol-3-yl)methyl)acrylamide (**16b**).* CAD: 0.027 g of *m*-fluorocinnamic acid; purification: Method A; yield: 0.022 g (41%); mp 118.0–119.0 °C; IR (ATR, ν/cm^{-1}) 3242, 3080, 2972, 2907, 2783, 1658, 1620, 1571, 1501, 1451, 1420, 1341, 1247, 1144, 1032, 983, 899, 859, 779, 740, 632, 561, 517; ^{1}H NMR (DMSO-d_6) δ 11.52 (s, 1H), 8.69 (t, 1H, J = 5.5 Hz), 8.18 (d, 1H, J = 7.4 Hz), 7.87 (s, 1H), 7.59-7.42 (m, 6H), 7.24-7.19 (m, 2H), 6.85 (d, 1H, J = 15.7 Hz), 4.61 (d, 2H, J = 4.3 Hz), 2.77 (s, 3H); ^{13}C NMR (DMSO-d_6) δ 164.59, 162.46 (d, J = 243.9 Hz), 146.03, 141.35, 140.75, 137.63 (d, J = 7.9 Hz), 137.47, 133.57, 130.89 (d, J = 8.3 Hz), 127.83, 127.73, 123.97, 123.67, 121.68, 121.00, 119.15, 116.07 (d, J = 21.4 Hz), 113.92 (d, J = 21.8 Hz), 111.94, 110.07, 44.73, 20.34; ESI-MS: m/z 360.3 (M+1)$^+$; Anal. Calcd. for $C_{22}H_{18}FN_3O$: C, 73.52; H, 5.05; N, 11.69; found: C, 73.35; H, 5.27; N, 11.83.

*4.1.11.3. (E)-3-(3-bromophenyl)-N-((1-methyl-9H-pyrido[3,4-b]indol-3-yl)methyl)acrylamide (**16c**).* CAD: 0.037 g of *m*-bromocinnamic acid; purification: Method A; yield: 0.018 g (28%); mp 121.5–123.5 °C; IR (ATR, ν/cm^{-1}) 3243, 3082, 1743, 1725, 1655, 1617, 1562, 1501, 1452, 1419, 1470, 1396, 1340, 1248, 1234, 1150, 1069, 1029, 984, 899, 863, 779, 741, 697, 666, 638, 609, 561; ^{1}H NMR (DMSO-d_6) δ 11.54 (s, 1H), 8.68 (t, 1H, J = 5.8 Hz), 8.18 (d, 1H, J = 7.9 Hz), 7.87 (s, 1H), 7.80 (t, 1H, J = 1.8 Hz), 7.61-7.56 (m, 3H), 7.52 (t, 1H, J = 7.4 Hz), 7.47 (d, 1H, J = 15.8 Hz), 7.39 (t, 1H, J = 7.9 Hz), 7.21 (t, 1H, J = 7.4 Hz), 6.87 (d, 1H, J = 15.8 Hz), 4.62 (d, 2H, J = 5.8 Hz), 2.78 (s, 3H); ^{13}C NMR (DMSO-d_6) δ 164.53, 146.00, 141.36, 140.76, 137.60, 137.12, 133.58, 131.93, 131.03, 130.03, 127.83, 127.73, 126.42, 124.09, 122.26, 121.68, 121.00, 119.15, 111.94, 110.06, 44.73, 20.34; ESI-MS: m/z 420.0 (M+1)$^+$, 422.0 (M+1)$^+$; HPLC purity 98.3%.

*4.1.11.4. (E)-N-((1-methyl-9H-pyrido[3,4-b]indol-3-yl)methyl)-3-(3-(trifluoromethyl)phenyl)acrylamide (**16d**).* CAD: 0.035 g of *m*-(trifluoromethyl)cinnamic acid; purification: Method B; yield: 0.023 g

(39%); mp 235.5–237.0 °C (decomp.); IR (ATR, ν/cm^{-1}) 3339, 3251, 3084, 2992, 2950, 2893, 2855, 2786, 1664, 1622, 1570, 1517, 1470, 1451, 1396, 1331, 1284, 1249, 1229, 1165, 1122, 1095, 1072, 1020, 969, 937, 899, 864, 803, 777, 738, 695, 657, 596, 559, 524, 507; ^{1}H NMR (DMSO-d_6) δ 11.53 (s, 1H), 8.70 (t, 1H, J = 5.8 Hz), 8.18 (d, 1H, J = 7.9 Hz), 7.95 (t, 1H, J = 2.0 Hz), 7.90 (d, 1H, J = 7.8 Hz), 7.88 (s, 1H), 7.74 (d, 1H, J = 7.8 Hz), 7.67 (t, 1H, J = 7.8 Hz), 7.61-7.58 (m, 2H), 7.54-7.51 (m, 1H), 7.22-7.20 (m, 1H), 6.96 (d, 1H, J = 15.9 Hz), 4.63 (d, 2H, J = 5.8 Hz), 2.78 (s, 3H); ^{13}C NMR (DMSO-d_6) δ 164.49, 145.97, 141.37, 140.77, 137.06, 136.23, 133.58, 131.31, 130.07, 129.73 (q, J = 31.7 Hz), 127.85, 127.75, 125.69 (q, J = 3.5 Hz), 124.06 (q, J = 272.8 Hz), 124.56, 123.88 (q, J = 3.5 Hz), 121.69, 121.01, 119.16, 111.95, 110.07, 44.74, 20.34; ESI-MS: m/z 410.1 (M+1)$^+$; HPLC purity 98.4%.

*4.1.11.5. E)-3-(4-fluorophenyl)-N-((1-methyl-9H-pyrido[3,4-b]indol-3-yl)methyl)acrylamide (**16e**).* CAD: 0.027 g of *p*-fluorocinnamic acid; purification: Method A; yield: 0.018 g (34%); mp 217.5–219.5 °C (decomp.); IR (ATR, ν/cm^{-1}) 3243, 3077, 2993, 2950, 2913, 2890, 2851, 2785, 1655, 1620, 1597, 1571, 1553, 1507, 1451, 1416, 1394, 1341, 1318, 1282, 1249, 1226, 1156, 1124, 1094, 1033, 1011, 984, 933, 899, 859, 830, 788, 739, 693, 643, 608, 591, 565, 506, 462; ^{1}H NMR (DMSO-d_6) δ 11.52 (s, 1H), 8.67 (t, 1H, J = 5.1 Hz), 8.18 (d, 1H, J = 7.8 Hz), 7.87 (s, 1H), 7.67-7.63 (m, 2H), 7.59-7.48 (m, 3H), 7.26 (t, 2H, J = 8.7 Hz), 7.20 (t, 1H, J = 7.4 Hz), 6.75 (d, 1H, J = 15.8 Hz), 4.61 (d, 2H, J = 5.5 Hz), 2.77 (s, 3H); ^{13}C NMR (DMSO-d_6) δ 164.81, 162.66 (d, J = 246.9 Hz), 146.14, 141.32, 140.75, 137.57, 133.56, 131.62 (d, J = 3.2 Hz), 129.66 (d, J = 8.4 Hz), 127.82, 127.72, 122.28, 121.68, 121.00, 119.14, 115.90 (d, J = 21.7 Hz), 111.93, 110.04, 44.70, 20.33; ESI-MS: m/z 360.1 (M+1)$^+$; HPLC purity 98.8%.

*4.1.11.6. (E)-3-(4-chlorophenyl)-N-((1-methyl-9H-pyrido[3,4-b]indol-3-yl)methyl)acrylamide (**16f**).* CAD: 0.030 g of *p*-chlorocinnamic acid; purification: Method A; yield: 0.012 g (21%); mp 255.0–257.5 °C (decomp.); IR (ATR, ν/cm^{-1}) 3649, 3239, 3055, 2918, 2874, 2798, 1982, 1925, 1897, 1662, 1624, 1551, 1502, 1454, 1404, 1318, 1283, 1251, 1220, 1176, 1088, 1044, 1011, 976, 902, 867, 815, 735, 646, 590, 550, 497; ^{1}H NMR (DMSO-d_6) δ 11.53 (s, 1H), 8.70 (t, 1H, J = 5.8 Hz), 8.18 (d, 1H, J = 7.9 Hz), 7.87 (s, 1H), 7.63-7.56 (m, 3H), 7.54-7.46 (m, 4H), 7.23-7.18 (m, 1H), 6.81 (d, 1H, J = 15.8 Hz), 4.61 (d, 2H, J = 5.7 Hz), 2.77 (s, 3H); ^{13}C NMR (DMSO-d_6) δ 164.67, 146.08, 141.33, 140.75, 137.41, 133.96, 133.82, 133.56, 129.22, 128.97, 127.82, 127.72, 123.19, 121.68, 121.00, 119.14, 111.93, 110.06, 44.72, 20.33; ESI-MS: m/z 374.0 (M − 1)$^-$; Anal. Calcd. for $C_{22}H_{18}ClN_3O$: C, 70.30; H, 4.83; N, 11.18; found: C, 70.39; H, 4.65; N, 11.37.

*4.1.11.7. (E)-3-(4-methoxyphenyl)-N-((1-methyl-9H-pyrido[3,4-b]indol-3-yl)methyl)acrylamide (**16g**).* CAD: 0.029 g of *p*-methoxycinnamic acid; purification: Method A; yield: 0.028 g (51%); mp 263.0–264.0 °C (decomp.); IR (ATR, ν/cm^{-1}) 3249, 3162, 3079, 2964, 2910, 2835, 2787, 2684, 1652, 1603, 1555, 1512, 1454, 1419, 1345, 1287, 1251, 1175, 1109, 1026, 987, 932, 900, 873, 827, 778, 744, 592, 549, 520; ^{1}H NMR (DMSO-d_6) δ 11.54 (s, 1H), 8.59 (t, 1H, J = 5.6 Hz), 8.18 (d, 1H, J = 7.9 Hz), 7.87 (s, 1H), 7.59-7.50 (m, 4H), 7.45 (d, 1H, J = 15.8 Hz), 7.20 (t, 1H, J = 7.5 Hz), 6.98 (d, 2H, J = 8.2 Hz), 6.66 (d, 1H, J = 15.8 Hz), 4.61 (d, 2H, J = 5.9 Hz), 3.79 (s, 3H), 2.78 (s, 3H); ^{13}C NMR (DMSO-d_6) δ 165.20, 160.29, 146.31, 141.29, 140.75, 138.47, 133.54, 129.09, 127.81, 127.73, 127.55, 121.68, 121.01, 119.89, 119.14, 114.38, 111.93, 109.98, 55.25, 44.66, 20.33; ESI-MS: m/z 372.3 (M+1)$^+$; Anal. Calcd. for $C_{23}H_{21}N_3O_2$: C, 74.37; H, 5.70; N, 11.31; found: C, 74.19; H, 5.93; N, 11.54.

*4.1.11.8. (E)-N-((1-methyl-9H-pyrido[3,4-b]indol-3-yl)methyl)-3-(4-(trifluoromethyl)phenyl)acrylamide (**16h**).* CAD: 0.035 g of *p*-(trifluoromethyl)cinnamic acid; purification: Method A; yield: 0.026 g (43%); mp 264.5–266.5 °C; IR (ATR, ν/cm^{-1}) 3339, 3263, 3058, 2920, 1666, 1626, 1575, 1496, 1452, 1413, 1324, 1248, 1164, 1120, 1065, 1012, 972, 900, 858, 822, 778, 737, 702, 586, 522, 491; ^{1}H NMR (DMSO-d_6) δ 11.54 (s, 1H), 8.79 (t, 1H, J = 5.8 Hz), 8.18 (d, 1H, J = 7.9 Hz), 7.88 (s, 1H), 7.82-7.76 (m, 4H), 7.59-7.49 (m, 3H), 7.23-7.18 (m, 1H), 6.94 (d, 1H, J = 15.8 Hz), 4.63 (d, 2H, J = 5.7 Hz), 2.77 (s, 3H); ^{13}C NMR (DMSO-d_6) δ 164.43, 145.97, 141.38, 140.77, 139.09, 137.12, 133.59, 129.17 (q, J = 31.8 Hz), 128.16, 127.84, 127.74, 125.81 (q, J = 3.9 Hz), 125.20, 124.13 (q, J = 272.0 Hz), 121.70, 121.01, 119.16, 111.95, 110.14, 44.78, 20.34; ESI-MS: m/z 410.1 (M+1)$^+$; HPLC purity 97.3%.

*4.1.12. Synthesis of 1-methyl-6-(prop-2-yn-1-yloxy)-9H-pyrido[3,4-b]indole (**19**)*

To a solution of compound **18** (0.200 g, 1.009 mmol) in dry DMF (5 mL), under argon atmosphere caesium carbonate (0.460 g, 1.413 mmol) was added, followed by the dropwise addition of propargyl bromide (0.135 mL, 1.211 mmol, 80% solution in toluene). The reaction mixture was stirred at rt for 6 h. Upon completion, reaction mixture was diluted with H_2O (50 mL) and extracted with EtOAc (3 × 40 mL). The collected organic layers were washed with H_2O (2 × 100 mL), dried over anhydrous sodium sulphate and the solvent was evaporated under the reduced pressure. After purification by column chromatography (DCM/MeOH = 97:3 → 95:5) and trituration with diethyl ether, **19** was obtained as a white solid. Yield: 0.122 g (51%); mp 175.5–177.5 °C; IR (ATR, ν/cm^{-1}) 3292, 3122, 3054, 2950, 2860, 2766, 2716, 2366, 2330, 2128, 2058, 1866, 1764, 1736, 1606, 1570, 1506, 1476, 1448, 1412, 1380, 1334, 1292, 1260, 1200, 1120, 1068, 1030, 986, 944, 914, 886, 818, 758, 646, 524; ^{1}H NMR (DMSO-d_6) δ 11.42 (s, 1H), 8.17 (d, 1H, J = 5.4 Hz), 7.88 (d, 1H, J = 5.3 Hz), 7.81 (d, 1H, J = 2.5 Hz), 7.53 (d, 1H, J = 8.9 Hz), 7.23 (dd, 1H, J = 8.8, 2.5 Hz), 4.88 (d, 2H, J = 2.4 Hz), 3.56 (t, 1H, J = 2.4 Hz), 2.75 (s, 3H); ^{13}C NMR (DMSO-d_6) δ 151.09, 142.26, 137.03, 135.67, 135.12, 126.63, 121.27, 118.34, 112.72, 112.62, 105.62, 78.04, 56.26, 20.40; ESI-MS: m/z 237.1 (M+1)$^+$.

*4.1.13. General procedure for the synthesis of harmicines **20a-e***

To a solution of alkyne **19** (0.050 g, 0.212 mmol) and the corresponding cinnamyl azide **13a-e** (0.254 mmol) in MeOH (5 mL), catalytic amount of $Cu(OAc)_2$ was added. The reaction mixture was stirred at rt for 24 h. Upon completion of the reaction, the solvent was removed under the reduced pressure. The residue was purified by column chromatography with DCM/MeOH or cyclohexane/EtOAc/MeOH as a mobile phase. The crude product was triturated with diethyl ether/petroleum ether mixture to obtain harmicines **20a-e**.

*4.1.13.1. 6-((1-Cinnamyl-1H-1,2,3-triazol-4-yl)methoxy)-1-methyl-9H-pyrido[3,4-b]indole (**20a**).* **13a**:0.040 g; mobile phase: DCM/MeOH 8:1; yield: 0.059 g (70%); mp 205.0–206.5 °C; IR (ATR, ν/cm^{-1}) 3136, 3120, 3030, 2945, 2856, 2760, 2693, 2676, 1632, 1604, 1579, 1565, 1504, 1481, 1460, 1412, 1389, 1361, 1335, 1289, 1237, 1202, 1123, 1054, 1034, 1002, 967, 888, 858, 817, 780, 755, 725, 705, 694, 625, 584, 520, 502; ^{1}H NMR (DMSO-d_6) δ 11.39 (s, 1H), 8.30 (s, 1H), 8.16 (d, 1H, J = 5.3 Hz), 7.91-7.89 (m, 2H), 7.51 (d, 1H, J = 8.8 Hz), 7.45-7.22 (m, 6H), 6.65-6.49 (m, 2H), 5.26 (s, 2H), 5.21 (d, 2H, J = 6.3 Hz), 2.74 (s, 3H); ^{13}C NMR (DMSO-d_6) δ 151.94, 143.26, 142.22, 136.98, 135.70, 135.42, 135.10, 133.62, 128.68, 128.14, 126.70, 126.56, 124.43, 123.72, 121.36, 118.35, 112.76, 112.69, 105.12, 61.89, 51.34, 20.42; ESI-MS: m/z 396.3 (M+1)$^+$; Anal. Calcd. for $C_{24}H_{21}N_5O$: C, 72.89; H, 5.35; N, 17.71; found: C, 72.74; H, 5.52; N, 17.56.

*4.1.13.2. (E)-6-((1-(3-(3-fluorophenyl)allyl)-1H-1,2,3-triazol-4-yl)methoxy)-1-methyl-9H-pyrido[3,4-b]indole (**20b**).* **13b**: 0.045 g; mobile phase: cyclohexane/EtOAc/MeOH 1:1:0.5 and DCM/MeOH 9:1; yield: 0.039 g (44%); mp 145.0–147.0 °C; IR (ATR, ν/cm^{-1}) 3357,

3293, 3166, 3071, 3052, 2975, 2937, 2900, 2866, 1601, 1583, 1568, 1493, 1473, 1459, 1404, 1379, 1365, 1330, 1286, 1262, 1207, 1149, 1120, 1067, 1054, 1039, 976, 938, 884, 847, 812, 792, 776, 752, 736, 715, 675, 641, 620, 593, 561, 528, 493, 456; ^{1}H NMR (DMSO-d_6) δ 11.41 (s, 1H), 8.31 (s, 1H), 8.17 (d, 1H, J = 5.4 Hz), 7.91-7.89 (m, 2H), 7.52 (d, 1H, J = 8.8 Hz), 7.39-7.32 (m, 2H), 7.27-7.23 (m, 2H), 7.13-7.08 (m, 1H), 6.64-6.62 (m, 2H), 5.26 (s, 2H), 5.23-5.21 (m, 2H), 2.75 (s, 3H); ^{13}C NMR (DMSO-d_6) δ 162.49 (d, J = 243.3 Hz), 151.97, 143.26, 142.16, 138.36 (d, J = 7.9 Hz), 136.80, 135.48, 135.07, 132.34, 130.58 (d, J = 8.5 Hz), 126.78, 125.50, 124.47, 130.00 (d, J = 1.7 Hz), 121.34, 118.42, 114.81 (d, J = 21.3 Hz), 112.80 (d, J = 17.4 Hz), 112.77, 112.67, 105.11, 61.89, 51.16, 20.32; ESI-MS: m/z 414.2 $(M+1)^+$; Anal. Calcd. for $C_{24}H_{20}FN_5O$: C, 69.72; H, 4.88; N, 16.94; found: C, 69.47; H, 4.61; N, 17.15.

*4.1.13.3. (E)-6-((1-(3-(3-bromophenyl)allyl)-1H-1,2,3-triazol-4-yl) methoxy)-1-methyl-9H-pyrido[3,4-b]indole (**20c**).* **13c**: 0.060 g; mobile phase: cyclohexane/EtOAc/MeOH 3:1:0.75; yield: 0.051 g (50%); mp 181.5–183.0 °C; IR (ATR, ν/cm^{-1}) 3252, 3198, 3151, 3089, 3064, 3039, 3015, 2965, 2945, 2916, 2892, 1601, 1584, 1566, 1495, 1475, 1422, 1400, 1373, 1350, 1337, 1289, 1256, 1233, 1217, 1199, 1129, 1095, 1066, 1052, 1033, 1008, 977, 944, 882, 857, 807, 782, 738, 707, 674, 620, 589, 563, 542, 479; ^{1}H NMR (DMSO-d_6) δ 11.40 (s, 1H), 8.31 (s, 1H), 8.16 (d, 1H, J = 5.4 Hz), 7.92-7.89 (m, 2H), 7.71 (t, 1H, J = 2.0 Hz), 7.51 (d, 1H, J = 8.8 Hz), 7.48-7.43 (m, 2H), 7.30 (t, 1H, J = 7.8 Hz), 7.24 (dd, 1H, J = 8.8, 2.5 Hz), 6.68-6.58 (m, 2H), 5.26 (s, 2H), 5.21 (d, 2H, J = 4.6 Hz), 2.74 (s, 3H); ^{13}C NMR (DMSO-d_6) δ 151.98, 143.28, 142.20, 138.30, 136.89, 135.46, 135.09, 132.03, 130.77, 129.05, 126.75, 125.67, 124.47, 122.17, 121.36, 118.40, 112.78, 112.71, 105.10, 61.91, 51.20, 20.37; ESI-MS: m/z 474.2 $(M+1)^+$, 476.2 $(M+1)^+$. Anal. Calcd. for $C_{24}H_{20}BrN_5O$: C, 60.77; H, 4.25; N, 14.76; C, 60.92; H, 4.43; N, 14.56.

*4.1.13.4. (E)-6-((1-(3-(4-chlorophenyl)allyl)-1H-1,2,3-triazol-4-yl) methoxy)-1-methyl-9H-pyrido[3,4-b]indole (**20d**).* **13d**: 0.049 g; mobile phase: cyclohexane/EtOAc/MeOH 1:1:0.5; yield: 0.046 g (51%); mp 195.0–196.5 °C; IR (ATR, ν/cm^{-1}) 3208, 3136, 3089, 3069, 2969, 2923, 2893, 2870, 2802, 1602, 1582, 1567, 1494, 1480, 1459, 1405, 1385, 1340, 1289, 1257, 1237, 1207, 1163, 1127, 1094, 1054, 1033, 1015, 987, 971, 950, 884, 857, 843, 818, 742, 702, 687, 662, 623, 583, 563, 533, 487; ^{1}H NMR (DMSO-d_6) δ 11.39 (s, 1H), 8.30 (s, 1H), 8.16 (d, 1H, J = 5.4 Hz), 7.91-7.89 (m, 2H), 7.51 (d, 1H, J = 8.8 Hz), 7.47-7.44 (m, 2H), 7.39-7.36 (m, 2H), 7.23 (dd, 1H, J = 8.9, 2.5 Hz), 6.62-6.51 (m, 2H), 5.26 (s, 2H), 5.21 (d, 2H, J = 5.1 Hz), 2.74 (s, 3H); ^{13}C NMR (DMSO-d_6) δ 151.93, 143.27, 142.22, 136.98, 135.44, 135.10, 134.68, 132.51, 132.23, 128.65, 128.28, 126.71, 124.77, 124.48, 121.36, 118.38, 112.76, 112.69, 105.15, 61.89, 51.23, 20.41; ESI-MS: m/z 430.4 $(M+1)^+$; Anal. Calcd. for $C_{24}H_{20}ClN_5O$: C, 67.05; H, 4.69; N, 16.29; found: C, 67.22; H, 4.78; N, 16.31.

*4.1.13.5. (E)-6-((1-(3-(4-methoxyphenyl)allyl)-1H-1,2,3-triazol-4-yl) methoxy)-1-methyl-9H-pyrido[3,4-b]indole (**20e**).* **13e**: 0.048 g; mobile phase: cyclohexane/EtOAc/MeOH 1:1:0.5; yield: 0.069 g (77%); mp 200.0–203.0 °C; IR (ATR, ν/cm^{-1}) 3208, 3138, 3069, 2953, 2929, 2894, 2873, 2836, 2802, 1743, 1607, 1582, 1567, 1513, 1498, 1480, 1460, 1441, 1405, 1386, 1337, 1289, 1257, 1238, 1207, 1175, 1127, 1109, 1054, 1032, 1015, 987, 968, 884, 856, 819, 760, 741, 703, 666, 624, 582, 563, 529, 498, 477; ^{1}H NMR (DMSO- d_6) δ 11.39 (s, 1H), 8.28 (s, 1H), 8.16 (d, 1H, J = 5.4 Hz), 7.92-7.89 (m, 2H), 7.51 (d, 1H, J = 8.8 Hz), 7.37 (d, 2H, J = 8.2 Hz), 7.23 (d, 1H, J = 8.9 Hz), 6.88 (d, 2H, J = 8.2 Hz), 6.58 (d, 1H, J = 15.8 Hz), 6.39-6.32 (m, 1H), 5.25 (s, 2H), 5.16 (d, 2H, J = 6.5 Hz), 3.75 (s, 3H), 2.74 (s, 3H); ^{13}C NMR (DMSO-d_6) δ 159.22, 151.94, 143.23, 142.21, 136.98, 135.42, 135.09, 133.36, 128.30, 127.89, 126.70, 124.31, 121.36, 121.11, 118.34, 114.06, 112.75, 112.68, 105.12, 61.89, 55.11, 51.46, 20.41; ESI-MS: m/z 426.3 $(M+1)^+$; Anal. Calcd. for $C_{25}H_{23}N_5O_2$: C, 70.57; H, 5.45; N, 16.46; found: C, 70.72; H, 5.63; N, 16.65.

*4.1.14. Tert-butyl (2-((1-methyl-9H-pyrido[3,4-b]indol-6-yl)oxy) ethyl)carbamate (**21**)*

To a stirred solution of **18** (0.647 g, 3.264 mmol) in dry DMF (6 mL), under argon atmosphere, caesium carbonate (2.978 g, 9.139 mmol) and tetrabutylammonium hydrogensulphate (0.887 g, 2.611 mmol) was added. The resulting suspension was stirred at rt for 20 min, followed by the addition of 2-(*tert*-butoxycarbonylamino)ethyl bromide (2.926 g, 13.056 mmol). The reaction mixture was stirred at rt for 24 h, poured into H_2O (50 mL) and extracted with EtOAc (3 × 50 mL). The collected organic layers were washed with H_2O, filtered through phase separator and evaporated under the reduced pressure. After purification by column chromatography (DCM/MeOH 8:1) and trituration with diethyl ether/petroleum ether mixture, compound **21** was obtained. Yield: 0.624 g (56%); ^{1}H NMR (DMSO-d_6) δ 11.42 (s, 1H), 8.16 (d, 1H, J = 5.3 Hz), 7.92 (d, 1H, J = 5.3 Hz), 7.77 (d, 1H, J = 1.7 Hz), 7.51 (d, 1H, J = 8.8 Hz), 7.18 (dd, 1H, J = 8.8, 2.3 Hz), 7.06 (t, 1H, J = 5.0 Hz), 4.05 (t, 2H, J = 5.8 Hz), 3.39-3.34 (m, 2H), 2.75 (s, 3H), 1.40 (s, 9H); ^{13}C NMR (DMSO-d_6) δ 155.73, 152.39, 142.04, 136.57, 135.41, 135.03, 126.88, 121.35, 118.42, 112.78, 112.75, 104.68, 77.76, 67.19, 39.61, 28.24, 20.23; ESI-MS: m/z 342.4 $(M+1)^+$.

*4.1.15. 2-((1-Methyl-9H-pyrido[3,4-b]indol-6-yl)oxy)ethan-1-amine (**22**)*

A solution of the **21** (0.642 g, 1.880 mmol) and 4.7 mL 4 M HCl (18.80 mmol) in EtOAc (6 mL) was stirred at 50 °C for 18 h. Upon completion, solvent was removed under the reduced pressure. The residue was dissolved in H_2O (20 mL), basified to pH 11 with 5% NaOH. The resulting precipitate was filtered off. After trituration with diethyl ether, 0.313 g, (69%) of **22** was obtained; mp 170.5–172.0 °C; IR (ATR, ν/cm^{-1}) 3645, 3359, 3241, 3065, 2925, 2869, 1605, 1581, 1566, 1500, 1478, 1458, 1401, 1288, 1234, 1211, 1126, 1071, 1059, 992, 905, 884, 847, 825, 816, 741, 703, 632; ^{1}H NMR (DMSO-d_6) δ 11.36 (s, 1H), 8.15 (d, 1H, J = 5.3 Hz), 7.90 (d, 1H, J = 5.3 Hz), 7.74 (d, 1H, J = 2.3 Hz), 7.50 (d, 1H, J = 8.8 Hz), 7.19 (dd, 1H, J = 8.8, 2.5 Hz), 4.02 (t, 2H, J = 5.8 Hz), 2.94 (t, 2H, J = 5.7 Hz), 2.74 (s, 3H); ^{13}C NMR (DMSO-d_6) δ 152.47, 141.87, 136.70, 135.19, 134.93, 126.54, 121.29, 117.98, 112.34, 112.18, 104.86, 71.06, 40.87, 19.97; ESI-MS: m/z 242.2 $(M+1)^+$.

*4.1.16. General procedure for the synthesis of harmicines **23a-h***

A solution of a corresponding CAD (0.249 mmol), DIEA (0.086 mL, 0.498 mmol) and HATU (0.095 g, 0.249 mmol) in DCM (4 mL) was stirred at rt for 20 min, followed by the addition of amine **22** (0.050 g, 0.208 mmol). The resulting solution was stirred at rt for 1 h. The formed precipitate was filtered off. After purification by column chromatography (DCM/MeOH 8:1) and trituration with diethyl ether/petroleum ether mixture compounds **23a-h** were obtained.

*4.1.16.1. N-(2-((1-methyl-9H-pyrido[3,4-b]indol-6-yl)oxy)ethyl)cinnamamide (**23a**).* CAD: 0.037 g of *trans*-cinnamic acid; yield: 0.045 g (58%); mp 128.0–129.5 °C; IR (ATR, ν/cm^{-1}) 3640, 3220, 3062, 2986, 2938, 2811, 2609, 1871, 1665, 1622, 1545, 1502, 1458, 1422, 1343, 1286, 1209, 1121, 1074, 970, 897, 808, 766, 714, 659, 630, 574, 512, 483; ^{1}H NMR (DMSO-d_6) δ 11.39 (s, 1H), 8.45 (t, 1H, J = 5.6 Hz), 8.16 (d, 1H, J = 5.3 Hz), 7.91 (d, 1H, J = 5.3 Hz), 7.81 (d, 1H, J = 2.5 Hz), 7.57 (d, 2H, J = 7.3 Hz), 7.53-7.46 (m, 2H), 7.44-7.36 (m, 3H), 7.22 (dd, 1H, J = 8.9, 2.6 Hz), 6.73 (d, 1H, J = 15.9 Hz), 4.17 (t, 2H, J = 5.6 Hz), 3.64 (q, 2H, J = 5.6 Hz), 2.74 (s, 3H); ^{13}C NMR (DMSO-d_6) δ 165.27, 152.37, 142.04, 138.83, 136.54, 135.46, 135.03, 134.89, 129.45, 128.93, 127.52, 126.90, 122.07, 121.37, 118.43, 112.79, 112.77,

104.73, 67.12, 38.67, 20.20; ESI-MS: *m/z* 372.0 $(M+1)^+$; HPLC purity > 99.5%.

*4.1.16.2. (E)-3-(3-fluorophenyl)-N-(2-((1-methyl-9H-pyrido[3,4-b]indol-6-yl)oxy)ethyl)acrylamide (**23b**).* CAD: 0.041 g of *m*-fluorocinnamic acid; yield: 0.062 g (76%); mp 225.0–226.0 °C; IR (ATR, ν/cm^{-1}) 3658, 3236, 3068, 2974, 2936, 2882, 2822, 2608, 1871, 1666, 1625, 1585, 1551, 1501, 1448, 1344, 1286, 1248, 1207, 1146, 1075, 1037, 974, 902, 856, 807, 738, 666, 630, 573, 519, 467; ^{1}H NMR (DMSO-d_6) δ 11.38 (s, 1H), 8.46 (t, 1H, J = 5.5 Hz), 8.16 (d, 1H J = 5.4 Hz), 7.91 (d, 1H, J = 5.3 Hz), 7.80 (d, 1H, J = 2.4 Hz), 7.51 (d, 1H, J = 8.9 Hz), 7.50-7.40 (m, 4H), 7.24-7.19 (m, 2H), 6.77 (d, 1H, J = 15.8 Hz), 4.17 (t, 2H, J = 5.5 Hz), 3.64 (q, 2H, J = 5.5 Hz), 2.74 (s, 3H); ^{13}C NMR (DMSO-d_6) δ 164.99, 162.45 (d, J = 243.8 Hz), 152.32, 142.15, 137.54, 137.49, 136.83, 135.37, 135.07, 130.89 (d, J = 8.4 Hz), 126.76, 123.65, 121.40, 118.29, 116.11 (d, J = 21.2 Hz), 113.93 (d, J = 21.8 Hz), 112.74, 112.72, 104.73, 67.07, 38.71, 20.34; ESI-MS: *m/z* 390.4 $(M+1)^+$; HPLC purity > 99.5%.

*4.1.16.3. (E)-3-(3-bromophenyl)-N-(2-((1-methyl-9H-pyrido[3,4-b]indol-6-yl)oxy)ethyl)acrylamide (**23c**).* CAD: 0.057 g of *m*-bromocinnamic acid; yield: 0.062 g (77%); mp 230.5–232.5 °C; IR (ATR, ν/cm^{-1}) 3646, 3171, 3062, 2975, 2939, 2879, 2792, 2613, 1664, 1620, 1566, 1501, 1460, 1384, 1345, 1287, 1199, 1110, 1072, 970, 856, 811, 781, 736, 667, 631, 561; ^{1}H NMR (DMSO-d_6) δ 11.40 (s, 1H), 8.43 (t, 1H, J = 5.5 Hz), 8.16 (d, 1H, J = 5.4 Hz), 7.92 (d, 1H, J = 5.4 Hz), 7.81 (d, 1H, J = 2.3 Hz), 7.79 (t, 1H, J = 1.8 Hz), 7.59-7.56 (m, 2H), 7.52 (d, 1H, J = 8.8 Hz), 7.45 (d, 1H, J = 15.8 Hz), 7.38 (t, 1H, J = 7.9 Hz), 7.22 (dd, 1H, J = 8.8, 2.4 Hz), 6.78 (d, 1H, J = 15.8 Hz), 4.17 (t, 2H, J = 5.5 Hz), 3.64 (q, 2H, J = 5.4 Hz), 2.75 (s, 3H); ^{13}C NMR (DMSO-d_6) δ 164.92, 152.33, 142.09, 137.50, 137.19, 136.68, 135.42, 135.05, 131.97, 131.02, 130.04, 126.83, 126.40, 123.76, 122.25, 121.38, 118.37, 112.76, 104.74, 67.08, 38.71, 20.27; ESI-MS: *m/z* 450.3 $(M+1)^+$, 452.3 $(M+1)^+$; HPLC purity > 99.5%.

*4.1.16.4. (E)-N-(2-((1-methyl-9H-pyrido[3,4-b]indol-6-yl)oxy)ethyl)-3-(3-(trifluoromethyl)phenyl)acrylamide (**23d**).* CAD: 0.054 g of *p*-(trifluoromethyl)cinnamic acid; yield: 0.058 g (64%); mp 216.5–218.0 °C; IR (ATR, ν/cm^{-1}) 3676, 3222, 3100, 3067, 2988, 2937, 2881, 2820, 2611, 1665, 1624, 1545, 1501, 1440, 1331, 1286, 1200, 1167, 1117, 1073, 1031, 971, 863, 805, 738, 691, 658, 630, 574, 465; ^{1}H NMR (DMSO-d_6) δ 11.41 (s, 1H), 8.46 (t, 1H, J = 5.6 Hz), 8.16 (d, 1H, J = 5.4 Hz), 7.93-7.88 (m, 3H), 7.81 (d, 1H, J = 2.6 Hz), 7.73 (d, 1H, J = 7.8 Hz), 7.66 (t, 1H, J = 7.8 Hz), 7.57 (d, 1H, J = 15.8 Hz), 7.52 (d, 1H, J = 8.8 Hz), 7.22 (dd, 1H, J = 8.8, 2.5 Hz), 6.88 (d, 1H, J = 15.9 Hz), 4.18 (t, 2H, J = 5.5 Hz), 3.65 (q, 2H, J = 5.6 Hz), 2.75 (s, 3H); ^{13}C NMR (DMSO-d_6) δ 164.88, 152.34, 142.10, 137.14, 136.69, 136.13, 135.43, 135.06, 131.30, 130.06, 129.73 (q, J = 32.3 Hz), 126.83, 125.73 (q, J = 3.0 Hz), 124.23, 124.04 (q, J = 273.7 Hz), 123.88 (q, J = 3.0 Hz), 121.38, 118.37, 112.76, 104.74, 67.09, 38.74, 20.27; ESI-MS: *m/z* 440.1 $(M+1)^+$; Anal. Calcd. for $C_{24}H_{20}F_3N_3O_2$: C, 65.60; H, 4.59; N, 9.56; found C, 65.80; H, 4.37; N, 9.71.

*4.1.16.5. (E)-3-(4-fluorophenyl)-N-(2-((1-methyl-9H-pyrido[3,4-b]indol-6-yl)oxy)ethyl)acrylamide (**23e**).* CAD: 0.041 g of *p*-fluorocinnamic acid; yield: 0.065 g (80%); mp 226.5–227.5 °C; IR (ATR, ν/cm^{-1}) 3659, 3311, 3225, 3099, 3045, 2990, 2938, 2165, 1870, 1667, 1625, 1542, 1502, 1422, 1347, 1286, 1208, 1160, 1122, 1074, 976, 897, 824, 740, 630, 576, 501, 459; ^{1}H NMR (DMSO-d_6) δ 11.40 (s, 1H), 8.43 (t, 1H, J = 5.4 Hz), 8.16 (d, 1H, J = 5.4 Hz), 7.92 (d, 1H, J = 5.3 Hz), 7.81 (d, 1H, J = 2.2 Hz), 7.66-7.62 (m, 2H), 7.53-7.46 (m, 2H), 7.28-7.21 (m, 3H), 6.68 (d, 1H, J = 15.8 Hz), 4.17 (t, 2H, J = 5.5 Hz), 3.64 (q, 2H, J = 5.4 Hz), 2.75 (s, 3H); ^{13}C NMR (DMSO-d_6) δ 165.21, 162.68 (d, J = 247.0 Hz), 152.35, 142.10, 137.65, 136.71, 135.41, 135.05, 131.53 (d, J = 2.6 Hz), 129.68 (d, J = 8.4 Hz), 126.82, 121.97, 121.39, 118.36, 115.90 (d, J = 21.7 Hz), 112.76, 104.72, 67.11, 38.68, 20.28; ESI-MS: *m/z* 390.4 $(M+1)^+$; HPLC purity > 99.5%.

*4.1.16.6. (E)-3-(4-chlorophenyl)-N-(2-((1-methyl-9H-pyrido[3,4-b]indol-6-yl)oxy)ethyl)acrylamide (**23f**).* CAD: 0.045 g of *p*-chlorocinnamic acid; yield: 0.071 g (84%); mp 228.5–229.5 °C; IR (ATR, ν/cm^{-1}) 3642, 3231, 3066, 2989, 2939, 2164, 2113, 1872, 1665, 1621, 1548, 1502, 1406, 1342, 1288, 1208, 1075, 976, 938, 897, 809, 742, 630, 575, 490; ^{1}H NMR (DMSO-d_6) δ 11.40 (s, 1H), 8.46 (t, 1H, J = 5.3 Hz), 8.16 (d, 1H, J = 5.3 Hz), 7.91 (d, 1H, J = 5.3 Hz), 7.80 (d, 1H, J = 2.0 Hz), 7.60 (d, 2H, J = 8.4 Hz), 7.51 (d, 1H, J = 8.9 Hz), 7.49-7.45 (m, 3H), 7.22 (dd, 1H, J = 8.8, 2.3 Hz), 6.73 (d, 1H, J = 15.8 Hz), 4.17 (t, 2H, J = 5.4 Hz), 3.64 (q, 2H, J = 5.3 Hz), 2.74 (s, 3H); ^{13}C NMR (DMSO-d_6) δ 165.08, 152.33, 142.11, 137.49, 136.72, 135.41, 135.05, 133.87, 129.22, 128.97, 126.81, 122.88, 121.39, 118.35, 112.76, 104.73, 67.09, 38.70, 20.29; ESI-MS: *m/z* 406.3 $(M+1)^+$; Anal. Calcd. for $C_{23}H_{20}ClN_3O_2$: C, 68.06; H, 4.97; N, 10.35; found C, 68.16; H, 4.78; N, 10.25.

*4.1.16.7. (E)-3-(4-methoxyphenyl)-N-(2-((1-methyl-9H-pyrido[3,4-b]indol-6-yl)oxy)ethyl)acrylamide (**23g**).* CAD: 0.044 g of *p*-methoxycinnamic acid; yield: 0.063g (75%); mp 241.5–242.5 °C; IR (ATR, ν/cm^{-1}) 3210, 3133, 3058, 2971, 2941, 2873, 2775, 2601, 2164, 1983, 1886, 1651, 1602, 1554, 1514, 1461, 1425, 1353, 1284, 1230, 1205, 1175, 1125, 1064, 1033, 983, 862, 827, 761, 699, 624, 555, 521; ^{1}H NMR (DMSO-d_6) δ 11.39 (s, 1H), 8.34 (t, 1H, J = 5.5 Hz), 8.16 (d, 1H, J = 5.4 Hz), 7.91 (d, 1H, J = 5.3 Hz), 7.80 (d, 1H, J = 2.4 Hz), 7.53-7.50 (m, 3H), 7.43 (d, 1H, J = 15.8 Hz), 7.22 (dd, 1H, J = 8.8, 2.5 Hz), 6.98 (d, 2H, J = 8.8 Hz), 6.58 (d, 1H, J = 15.8 Hz), 4.16 (t, 2H, J = 5.6 Hz), 3.79 (s, 3H), 3.63 (q, 2H, J = 5.5 Hz), 2.74 (s, 3H); ^{13}C NMR (DMSO-d_6) δ 165.59, 160.32, 152.35, 142.13, 138.54, 136.80, 135.37, 135.06, 129.09, 127.45, 126.77, 121.40, 119.58, 118.30, 114.38, 112.74, 104.71, 67.16, 55.24, 38.63, 20.33; ESI-MS: *m/z* 402.4 $(M+1)^+$; HPLC purity > 99.5%.

*4.1.16.8. (E)-N-(2-((1-methyl-9H-pyrido[3,4-b]indol-6-yl)oxy)ethyl)-3-(4-(trifluoromethyl)phenyl)acrylamide (**23h**).* CAD: 0.054 g of *p*-(trifluoromethyl)cinnamic acid; yield: 0.057 g (62%); mp 231.5–233.5 °C; IR (ATR, ν/cm^{-1}) 3645, 3269, 3061, 2932, 2875, 1667, 1628, 1559, 1501, 1461, 1417, 1384, 1328, 1286, 1234, 1202, 1166, 1119, 1067, 1016, 976, 953, 882, 829, 814, 728, 708, 614, 591, 562, 522, 495; ^{1}H NMR (DMSO-d_6) δ 11.41 (s, 1H), 8.54 (t, 1H, J = 5.5 Hz), 8.16 (d, 1H, J = 5.3 Hz), 7.92 (d, 1H, J = 5.3 Hz), 7.81-7.76 (m, 5H), 7.57-7.51 (m, 2H), 7.22 (dd, 1H, J = 8.9, 2.5 Hz), 6.86 (d, 1H, J = 15.8 Hz), 4.18 (t, 2H, J = 5.5 Hz), 3.65 (q, 2H, J = 5.4 Hz), 2.75 (s, 3H); ^{13}C NMR (DMSO-d_6) δ 164.82, 152.34, 142.09, 139.00, 137.19, 136.65, 135.44, 135.05, 129.20 (q, J = 32.3 Hz), 128.16, 126.85, 125.80 (q, J = 3.0 Hz), 124.87, 124.11 (q, J = 272.7 Hz), 121.38, 118.39, 112.78, 104.74, 67.06, 38.75, 20.25; MS: *m/z* 440.1 $(M+1)^+$; Anal. Calcd. for $C_{24}H_{20}F_3N_3O_2$: C, 65.60; H, 4.59; N, 9.56; found: C, 65.72; H, 4.37; N, 9.21.

*4.1.17. General procedure for the synthesis of harmicines **27a,b***

Harmicines **27a**,**b** were prepared according to the published procedure [26,27]. In short, a solution of a corresponding CAD (0.182 mmol), DIEA (0.063 mL, 0.364 mmol) and HATU (0.069 g, 0.182 mmol) in DCM (4 mL) was stirred at rt for 20 min, followed by the addition of amine **26** (0.042 g, 0.165 mmol). The resulting solution was stirred at rt for 1 h. The formed precipitate was filtered off. After purification by column chromatography (DCM/MeOH 8:1) and trituration with diethyl ether/petroleum ether mixture compounds **27a**,**b** were obtained.

*4.1.17.1. (E)-N-(2-(7-methoxy-1-methyl-9H-pyrido[3,4-b]indol-9-yl)ethyl)-3-(3-(trifluoromethyl)phenyl)acrylamide (**27a**).* CAD: 0.039 g

of *m*-(trifluoromethyl)cinnamic acid; yield: 0.033 g (44%); mp 220.5–222.5 °C; IR (ATR, ν/cm^{-1}) 3177, 2978, 2930, 1679, 1623, 1570, 1500, 1450, 1409, 1377, 1343, 1328, 1281, 1270, 1253, 1221, 1199, 1185, 1169, 1139, 1114, 1096, 1079, 1043, 1018, 991, 981, 803, 694, 659, 556, 530; ^{1}H NMR (DMSO-d_6) δ 8.42 (t, 1H, J = 6.0 Hz), 8.18 (d, 1H, J = 5.2 Hz), 8.09 (d, 1H, J = 8.5 Hz), 7.91-7.87 (m, 3H), 7.74 (dd, 1H, J = 7.7, 1.6 Hz), 7.66 (t, 1H, J = 7.8 Hz), 7.54 (d, 1H, J = 15.8 Hz), 7.27 (d, 1H, J = 2.2 Hz), 6.87 (dd, 1H, J = 8.6, 2.2 Hz), 6.68 (d, 1H, J = 15.8 Hz), 4.68 (t, 2H, J = 7.0 Hz), 3.90 (s, 3H), 3.61 (q, 2H, J = 6.6 Hz), 2.99 (s, 3H); ^{13}C NMR (DMSO-d_6) δ 165.35, 160.52, 142.92, 140.66, 137.87, 137.51, 135.98, 134.68, 131.26, 130.09, 129.76 (q, J = 31.7 Hz), 128.51, 125.86 (q, J = 3.6 Hz), 124.06 (q, J = 3.6 Hz), 124.04 (q, J = 272.5 Hz), 123.81, 122.41, 114.33, 112.29, 109.37, 93.57, 55.41, 43.37, 39.13, 23.10; ESI-MS: *m/z* 454.2 (M+1)$^+$; HPLC purity 98.2%.

*4.1.17.2. (E)-N-(2-(7-methoxy-1-methyl-9H-pyrido[3,4-b]indol-9-yl) ethyl)-3-(4-(trifluoromethyl)phenyl)acrylamide (**27b**).* CAD: 0.039 g of *p*-(trifluoromethyl)cinnamic acid; yield: 0.034 g (45%); mp 252.0–254.5 °C; IR (ATR, ν/cm^{-1}) 3188, 3005, 2962, 2844, 1680, 1633, 1569, 1445, 1412, 1321, 1253, 1199, 1165, 1108, 1066, 974, 831, 801, 597, 573; ^{1}H NMR (DMSO-d_6) δ 8.50 (t, 1H, J = 6.0 Hz), 8.18 (d, 1H, J = 5.1 Hz), 8.09 (d, 1H, J = 8.6 Hz), 7.89 (d, 1H, J = 5.2 Hz), 7.78 (s, 4H), 7.53 (d, 1H, J = 15.8 Hz), 7.27 (d, 1H, J = 2.2 Hz), 6.87 (dd, 1H, J = 8.6, 2.2 Hz), 6.68 (d, 1H, J = 15.8 Hz), 4.68 (t, 2H, J = 6.9 Hz), 3.90 (s, 3H), 3.61 (q, 2H, J = 6.7 Hz), 3.00 (s, 3H); ^{13}C NMR (DMSO-d_6) δ 165.27, 160.52, 142.92, 140.62, 138.83, 137.83, 137.51, 134.64, 129.29 (q, J = 31.8 Hz), 128.52, 128.21, 125.81 (q, J = 3.5 Hz), 124.44, 124.09 (q, J = 272.0 Hz), 122.40, 114.30, 112.28, 109.40, 93.51, 55.40, 43.32, 39.13, 23.06; ESI-MS: *m/z* 454.1 (M+1)$^+$; HPLC purity 99.1%.

4.2. In vitro drug sensitivity assay against P. falciparum erythrocytic stages

Antiplasmodial activity of harmicines **5**, **7**, **14**–**16**, **20** and **23** was evaluated against two laboratory *P. falciparum* strains (3D7, CQ-sensitive strain, and Dd2, CQ-resistant strain), as previously described, using the histidine-rich protein 2 (HRP2) assay [23,24]. Briefly, 96-well plates were pre-coated with the tested compounds in a three-fold dilution before ring-stage parasites were added in complete culture medium at a haematocrit of 1.5% and a parasitaemia of 0.05%. After three days of incubation at 37 °C, 5% CO_2 and 5% oxygen, plates were frozen until analysed by HRP2-ELISA. All compounds were evaluated in duplicate in at least two independent experiments. The IC_{50} was determined by nonlinear regression analysis of log concentration-response curves using the drc-package v0.9.0 of R v2.6.1 [25].

4.3. In vitro activity against P. berghei hepatic stages

In vitro activity of harmicines **5**, **7**, **14**–**16**, **20** and **23** against the liver stage of *P. berghei* infection was assessed as previously described [26,27]. Briefly, Huh7 cells were routinely cultured in 1640 Roswell Park Memorial Institute (RPMI) medium supplemented with 10% (*v*/*v*) fetal bovine serum, 1% (*v*/*v*) glutamine, 1% (*v*/*v*) penicillin/streptomycin, 1% non-essential amino acids, and 10 mM 2-[4-(2-hydroxyethyl)piperazin-1-yl]ethane-1-sulphonic acid (HEPES). For drug screening experiments, Huh7 cells were seeded at 1 × 10^4 cell/well of a 96-well plate and incubated overnight at 37 °C with 5% CO_2. 10 mM stock solutions of test compounds were prepared in DMSO and were serially diluted in infection medium, *i.e.* culture medium supplemented with gentamicin (50 μg/ml) and amphotericin B (0.8 μg/ml), to obtain the test concentrations. On the day of the infection, the culture medium was replaced by the serial dilutions of test compounds and incubated for 1 h at 37 °C with 5% CO_2. Next, 1 × 10^4 firefly luciferase-expressing *P. berghei* sporozoites, freshly isolated from the salivary glands of female infected *Anopheles stephensi* mosquitoes, were added to the cultures, plates were centrifuged at 1800×*g* for 5 min at room temperature and incubated at 37 °C with 5% CO_2. To assess the effect of each compound concentration on cell viability, cultures were incubated with Alamar Blue (Invitrogen, UK) at 46 h post infection (hpi), according to the manufacturer's recommendations. Parasite load was then assessed by a bioluminescence assay (Biotium, Fremont, CA, USA), using a multi-plate reader Infinite M200 (Tecan, Switzerland). Nonlinear regression analysis was employed to fit the normalized results of the dose-response curves, and IC_{50} values were determined using GraphPad Prism 6.0 (GraphPad software, La Jolla, CA, USA).

4.4. In vitro cytotoxicity assay

Cytotoxicity against a human cell line (HepG2) was evaluated using the neutral red assay [29]. In brief, human cells were seeded to a 96 well plate in a complete culture medium, before on the following day a serial dilution of the respective compound was added. After one day incubation, cytotoxicity was evaluated by the addition of Neutral Red, subsequent lysis of cells and measurement of absorbance in a plate reader. The IC_{50} was determined as for the *in vitro* drug assay against *P. falciparum*. To assess the safety of a compound, SI was calculated as the fractional ratio between the IC_{50}s for HepG2 and *P. falciparum* 3D7 strain.

4.5. Molecular dynamics simulations

MD simulations were performed on a *Pf*Hsp90 *N*-terminal domain X-ray structure collected from the Protein Data Bank (accession code 3K60). Ligands (ADP and SO_4^{2-}) were removed from the model and selected compounds were placed in the ATP binding pocket, including harmine as a reference. Original crystal waters were removed so that the water molecules from the bulk solvent could diffuse into the protein during equilibration and production MD runs. The investigated ligands were parameterized by performing the geometry optimization and RESP charge calculations in the Gaussian 16 program [39] at the HF/6–31G(d) level to be consistent with the employed GAFF force field, while the *Pf*Hsp90 protein was modelled with the AMBER ff14SB force field. Such protein complexes were solvated in a truncated octahedral box of TIP3P water molecules (10 Å-thick buffer), neutralized by Na^+ ions and submitted to geometry optimization in the AMBER 16 program [39] by employing periodic boundary conditions in all directions. Optimized systems were gradually heated from 0 to 300 K and equilibrated during 30 ps using NVT conditions, followed by productive and unconstrained MD simulations of 300 ns by employing a time step of 2 fs at a constant pressure (1 atm) and temperature (300 K), with the latter held constant using a Langevin thermostat with a collision frequency of 1 ps^{-1}. Bonds involving hydrogen atoms were constrained using the SHAKE algorithm [40] while the long-range electrostatic interactions were calculated employing the Particle Mesh Ewald method [41] The nonbonded interactions were truncated at 10.0 Å.

The binding free energies, ΔG_{BIND}, of each ligand within the *Pf*Hsp90 ATP binding site were calculated using the established MM-GBSA protocol [42,43] available in AmberTools16 [39], and in line with our earlier reports [10,15,44,45]. For that purpose, 1000 snapshots collected from the last 30 ns of the corresponding MD trajectories were utilized. The calculated MM-GBSA binding free energies were decomposed into specific residue contributions on a per-residue basis according to the established procedure [46,47]. This protocol calculates contributions to ΔG_{BIND} arising from each amino

acid residue and identifies the nature of the energy change in terms of interaction and solvation energies or entropic contributions.

Declaration of competing interest

The authors declare that they have no known competing financial interests or personal relationships that could have appeared to influence the work reported in this paper.

Acknowledgement

The authors acknowledge the financial support by the Croatian Science Foundation (research project UIP-2017-05-5160), University of Zagreb (support for 2019), and Fundação para a Ciência e Tecnologia, Portugal (FCT) (grant 02/SAICT/2017/29550). The work of doctoral student M. Marinović has been fully supported by the Young researcher's career development project - training of doctoral students of the Croatian Science Foundation founded by the European Union from the European Social Fund. T.T. and R.V. would like to thank the Zagreb University Computing Centre (SRCE) for granting computational resources on the ISABELLA cluster.

Abbreviations

ADMP	2-azido-1,3-dimethylimidazolinium hexafluorophosphate
AT	amide-type
ATR	attenuated total reflection
Boc	*tert*-butyloxycarbonyl
CAD	cinnamic acid derivative;
CQ	chloroquine;
DBU	1,8-diazabicyclo(5.4.0)undec-7-ene
DCM	dichloromethane
DIEA	*N,N*-diisopropylethylamine;
DMF	*N,N*-dimethylformamide;
ESI	electrospray ionization
EtOAc	ethyl acetate
EtOH	ethanol
ΔG_{BIND}	binding free energies
HAR	harmine
HATU	1-[bis(dimethylamino)methylene]-1*H*-1,2,3-triazolo [4,5-*b*]pyridinium-3-oxidhexafluorophosphate
HEPES	2-[4-(2-hydroxyethyl)piperazin-1-yl]ethane-1-sulphonic acid; hpi, hours post infection
HRP2	histidine-rich protein 2
HepG2	human liver hepatocellular carcinoma cell line;
IC_{50}	the concentration of the tested compound necessary for 50% growth inhibition
MD	molecular dynamics
MeOH	methanol
*Pf*3D7	chloroquine-sensitive strain of *P. falciparum*
*Pf*Dd2	chloroquine-resistant strain of *P. falciparum*
*Pf*Hsp90	*P. falciparum* heat shock protein 90
PQ	primaquine
SI	selectivity index
t-BuOH	*t*-buthanol
TEA	triethylamine
TMS	tetramethylsilane
TT	triazole-type
TWC	total wavelength chromatogram

Appendix A. Supplementary data

Supplementary data to this article can be found online at https://doi.org/10.1016/j.ejmech.2021.113687.

References

[1] M. Mishra, V.K. Mishra, V. Kashaw, A.K. Iyer, S.K. Kashaw, Comprehensive review on various strategies for antimalarial drug discovery, Eur. J. Med. Chem. 125 (2017) 1300–1320, https://doi.org/10.1016/j.ejmech.2016.11.025.
[2] P. Jourdan, J.P. Schneider, J. Dassonville-Klimpt, A. Sonnet, Recent Advances in Antimalarial Drugs: Structures, Mechanisms of Action and Clinical Trials, in: A. Méndez-Vilas (Ed.), Antimicrob. Res. Nov. Bioknowledge Educ. Programs, Formatex Research Center, Badajoz, 2017, pp. 599–609.
[3] WHO, World Malaria Report 2019, 2019. Colombia.
[4] A. Müller-Schiffmann, H. Sticht, C. Korth, Hybrid compounds: from simple combinations to nanomachines, BioDrugs 26 (2012) 21–31, https://doi.org/10.2165/11597630-000000000-00000.
[5] R. Oliveira, D. Miranda, J. Magalhães, R. Capela, M.J. Perry, P.M.O. Neill, R. Moreira, F. Lopes, From hybrid compounds to targeted drug delivery in antimalarial therapy, Bioorg. Med. Chem. 23 (2015) 5120–5130, https://doi.org/10.1016/j.bmc.2015.04.017.
[6] S. Shaveta, P. Mishra, Singh, Hybrid molecules: the privileged scaffolds for various pharmaceuticals, Eur. J. Med. Chem. 124 (2016) 500–536, https://doi.org/10.1016/j.ejmech.2016.08.039.
[7] J.J. Walsh, A. Bell, Hybrid drugs for malaria, Curr. Pharmaceut. Des. 15 (2009) 2970–2985.
[8] M. Fonte, N. Tassi, P. Gomes, C. Teixeira, Acridine-based antimalarials-from the very first synthetic antimalarial to recent developments, Molecules 26 (2021) 600, https://doi.org/10.3390/molecules26030600.
[9] B. Pérez, C. Teixeira, J. Gut, P.J. Rosenthal, J.R.B. Gomes, P. Gomes, Cinnamic acid/chloroquinoline conjugates as potent agents against chloroquine-resistant plasmodium falciparum, ChemMedChem 7 (2012) 1537–1540, https://doi.org/10.1002/cmdc.201200257.
[10] I. Perković, S. Raić-Malić, D. Fontinha, M. Prudêncio, L. Pessanha de Carvalho, J. Held, T. Tandarić, R. Vianello, B. Zorc, Z. Rajić, Harmicines - harmine and cinnamic acid hybrids as novel antiplasmodial hits, Eur. J. Med. Chem. 187 (2020), 111927, https://doi.org/10.1016/j.ejmech.2019.111927.
[11] B.C. Pérez, C. Teixeira, M. Figueiras, J. Gut, P.J. Rosenthal, J.R.B. Gomes, P. Gomes, Novel cinnamic acid/4-aminoquinoline conjugates bearing non-proteinogenic amino acids: towards the development of potential dual action antimalarials, Eur. J. Med. Chem. 54 (2012) 887–899, https://doi.org/10.1016/j.ejmech.2012.05.022.
[12] B.C. Pérez, C. Teixeira, I.S. Albuquerque, J. Gut, P.J. Rosenthal, J.R.B. Gomes, M. Prudeîncio, P. Gomes, N-Cinnamoylated chloroquine analogues as dual-stage antimalarial leads, J. Med. Chem. 56 (2013) 556–567, https://doi.org/10.1021/jm301654b.
[13] B. Pérez, C. Teixeira, I.S. Albuquerque, J. Gut, P.J. Rosenthal, M. Prudêncio, P. Gomes, PRIMACINS, N-cinnamoyl-primaquine conjugates, with improved liver-stage antimalarial activity, Medchemcomm 3 (2012) 1170–1172, https://doi.org/10.1039/c2md20113e.
[14] A. Teresa Silva, C.M. Bento, A.C. Pena, L.M. Figueiredo, C. Prudêncio, L. Aguiar, T. Silva, R. Ferraz, M. Salomé Gomes, C. Teixeira, P. Gomes, F. Borges, J. Garrido, T. Barros Silva, Cinnamic acid conjugates in the rescuing and repurposing of classical antimalarial drugs, Molecules 25 (2020) 66, https://doi.org/10.3390/molecules25010066.
[15] M. Marinović, I. Perković, D. Fontinha, M. Prudêncio, J. Held, L.P. de Carvalho, T. Tandarić, R. Vianello, B. Zorc, Z. Rajić, Novel harmicines with improved potency against Plasmodium, Molecules 25 (2020) 4376, https://doi.org/10.3390/molecules25194376.
[16] D. Shahinas, G. MacMullin, C. Benedict, I. Crandall, D.R. Pillaid, Harmine is a potent antimalarial targeting Hsp90 and synergizes with chloroquine and artemisinin, Antimicrob. Agents Chemother. 56 (2012) 4207–4213, https://doi.org/10.1128/AAC.00328-12.
[17] T. Wang, P. Mäser, D. Picard, Inhibition of plasmodium falciparum Hsp90 contributes to the antimalarial activities of aminoalcohol-carbazoles, J. Med. Chem. 59 (2016) 6344–6352, https://doi.org/10.1021/acs.jmedchem.6b00591.
[18] S. Eagon, M.O. Anderson, Microwave-assisted synthesis of tetrahydro-β-carbolines and β-carbolines, Eur. J. Org Chem. 2014 (2014) 1653–1665, https://doi.org/10.1002/ejoc.201301580.
[19] N. Devi, D. Singh, Honey, S. Mor, S. Chaudhary, R.K. Rawal, V. Kumar, A.K. Chowdhury, V. Singh, In(OTf)3 catalysed an expeditious synthesis of β-carboline-imidazo[1,2-: A] pyridine and imidazo[1,2- a] pyrazine conjugates, RSC Adv. 6 (2016) 43881–43891, https://doi.org/10.1039/c6ra04841b.
[20] D. Singh, C.K. Hazra, C.C. Malakar, S.K. Pandey, B.S. Kaith, V. Singh, Indium-mediated domino allylation-lactonisation approach: diastereoselective synthesis of β-carboline C-3 tethered α-methylene γ-butyrolactones, Chemistry 3 (2018) 4859–4864, https://doi.org/10.1002/slct.201800006.
[21] M. Kitamura, T. Koga, M. Yano, T. Okauchi, Direct synthesis of organic azides from alcohols using 2-azido-1,3- dimethylimidazolinium hexafluorophosphate, Synlett 23 (2012) 1335–1338, https://doi.org/10.1055/s-0031-1290958.
[22] Chemicalize ChemAxon. https://chemicalize.com/, 2018. (Accessed 20 July 2020).
[23] J. Held, T. Gebru, M. Kalesse, R. Jansen, K. Gerth, R. Müller, B. Mordmüller, Antimalarial activity of the myxobacterial macrolide chlorotonil A, Antimicrob. Agents Chemother. 58 (2014) 6378–6384, https://doi.org/10.1128/AAC.03326-14.
[24] H. Noedl, J. Bronnert, K. Yingyuen, B. Attlmayr, H. Kollaritsch, M. Fukuda,

Simple histidine-rich protein 2 double-site sandwich enzyme-linked immunosorbent assay for use in malaria drug sensitivity testing, Antimicrob. Agents Chemother. 49 (2005) 3575–3577, https://doi.org/10.1128/AAC.49.8.3575-3577.2005.
[25] R Core Team, A Language and Environment for Statistical Computing, R Foundation for Statistical Computing, Vienna, Austria, 2018. https://www.r-project.org/. (Accessed 20 July 2020).
[26] M. Machado, M. Sanches-Vaz, J.P. Cruz, A.M. Mendes, M. Prudêncio, Inhibition of Plasmodium hepatic infection by antiretroviral compounds, Front. Cell. Infect. Microbiol. 7 (2017) 329, https://doi.org/10.3389/fcimb.2017.00329.
[27] I.H.J. Ploemen, M. Prudêncio, B.G. Douradinha, J. Ramesar, J. Fonager, G.-J. van Gemert, A.J.F. Luty, C.C. Hermsen, R.W. Sauerwein, F.G. Baptista, M.M. Mota, A.P. Waters, I. Que, C.W.G.M. Lowik, S.M. Khan, C.J. Janse, B.M.D. Franke-Fayard, Visualisation and quantitative analysis of the rodent malaria liver stage by real time imaging, PloS One 4 (2009), e7881, https://doi.org/10.1371/journal.pone.0007881.
[28] M. Beus, D. Fontinha, J. Held, Z. Rajić, L. Uzelac, M. Kralj, M. Prudêncio, B. Zorc, Primaquine and chloroquine fumardiamides as promising antiplasmodial agents, Molecules 24 (2019) 2812, https://doi.org/10.3390/molecules24152812.
[29] E. Borenfreund, J.A. Puerner, A simple quantitative procedure using monolayer cultures for cytotoxicity assays (HTD/NR-90), J. Tissue Cult. Methods 9 (1985) 7–9, https://doi.org/10.1007/BF01666038.
[30] K.D. Corbett, J.M. Berger, Structure of the ATP-binding domain of plasmodium falciparum Hsp90, Proteins Struct. Funct. Bioinforma. 78 (2010) 2738–2744, https://doi.org/10.1002/prot.22799.
[31] S.M. Roe, C. Prodromou, R. O'Brien, J.E. Ladbury, P.W. Piper, L.H. Pearl, Structural basis for inhibition of the Hsp90 molecular chaperone by the antitumor antibiotics radicicol and geldanamycin, J. Med. Chem. 42 (1999) 260–266, https://doi.org/10.1021/jm980403y.
[32] H.C. Cheng, The power issue: determination of KB or Ki from IC50 - a closer look at the Cheng-Prusoff equation, the Schild plot and related power equations, J. Pharmacol. Toxicol. Methods 46 (2001) 61–71, https://doi.org/10.1016/S1056-8719(02)00166-1.
[33] D. Shahinas, M. Liang, A. Datti, D.R. Pillai, A repurposing strategy identifies novel synergistic inhibitors of plasmodium falciparum heat shock protein 90, J. Med. Chem. 53 (2010) 3552–3557, https://doi.org/10.1021/jm901796s.
[34] M. Cain, R.W. Weber, F. Guzman, J.M. Cook, S.A. Barker, K.C. Rice, J.N. Crawley, S.M. Paul, P. Skolnick, β-Carbolines: synthesis and neurochemical and pharmacological actions on brain benzodiazepine receptors, J. Med. Chem. 25 (1982) 1081–1091, https://doi.org/10.1021/jm00351a015.
[35] T. Szabó, V. Hazai, B. Volk, G. Simig, M. Milen, First total synthesis of the β-carboline alkaloids trigonostemine A, trigonostemine B and a new synthesis of pityriacitrin and hyrtiosulawesine, Tetrahedron Lett. 60 (2019) 1471–1475, https://doi.org/10.1016/j.tetlet.2019.04.044.
[36] G. Lin, Y. Wang, Q. Zhou, W. Tang, J. Wang, T. Lu, A facile synthesis of 1-substituted βcarboline derivatives via minisci-reaction, Synth. Commun. 41 (2011) 3541–3550, https://doi.org/10.1080/00397911.2010.519092.
[37] Y. Schott, M. Decker, H. Rommelspacher, J. Lehmann, 6-Hydroxy- and 6-methoxy-β-carbolines as acetyl- and butyrylcholinesterase inhibitors, Bioorg, Med. Chem. Lett. 16 (2006) 5840–5843, https://doi.org/10.1016/j.bmcl.2006.08.067.
[38] W. Seppelt, H.-J. Neubauer, H. Adolphi, P. Hofmeister, Propargyl Cinnamates, Process for Their Production and Their Application in Pest Control, EP0235722B1, 1989. https://patents.google.com/patent/EP0235722B1/en. (Accessed 15 March 2021).
[39] D.A. Case, R.M. Betz, D.S. Cerutti, T.E. Cheatham, T.A. Darden, R.E. Duke, T.J. Giese, H. Gohlke, A.W. Goetz, N. Homeyer, S. Izadi, P. Janowski, J. Kaus, A. Kovalenko, T.S. Lee, S. LeGrand, P. Li, C. Lin, T. Luchko, R. Luo, B. Madej, D. Mermelstein, K.M. Merz, G. Monard, H. Nguyen, H.T. Nguyen, I. Omelyan, A. Onufriev, D.R. Roe, A. Roitberg, C. Sagui, C.L. Simmerling, W.M. Botello-Smith, J. Swails, R.C. Walker, J. Wang, R.M. Wolf, X. Wu, L. Xiao, P.A. Kollman, Amber 16 (2016).
[40] J.P. Ryckaert, G. Ciccotti, H.J.C. Berendsen, Numerical integration of the cartesian equations of motion of a system with constraints: molecular dynamics of n-alkanes, J. Comput. Phys. 23 (1977) 327–341, https://doi.org/10.1016/0021-9991(77)90098-5.
[41] T. Darden, D. York, L. Pedersen, Particle mesh Ewald: an N·log(N) method for Ewald sums in large systems, J. Chem. Phys. 98 (1993) 10089–10092, https://doi.org/10.1063/1.464397.
[42] T. Hou, J. Wang, Y. Li, W. Wang, Assessing the performance of the MM/PBSA and MM/GBSA methods. 1. The accuracy of binding free energy calculations based on molecular dynamics simulations, J. Chem. Inf. Model. 51 (2011) 69–82, https://doi.org/10.1021/ci100275a.
[43] S. Genheden, U. Ryde, The MM/PBSA and MM/GBSA methods to estimate ligand-binding affinities, Expet Opin. Drug Discov. 10 (2015) 449–461, https://doi.org/10.1517/17460441.2015.1032936.
[44] T. Tandarić, R. Vianello, Computational insight into the mechanism of the irreversible inhibition of monoamine oxidase enzymes by the anti-parkinsonian propargylamine inhibitors rasagiline and selegiline, ACS Chem. Neurosci. 10 (2019) 3532–3542, https://doi.org/10.1021/acschemneuro.9b00147.
[45] L. Hok, J. Mavri, R. Vianello, The effect of deuteration on the H2 receptor histamine binding profile: a computational insight into modified hydrogen bonding interactions, Molecules 25 (2020) 1–17, https://doi.org/10.3390/molecules25246017.
[46] G. Rastelli, A. Del Rio, G. Degliesposti, M. Sgobba, Fast and accurate predictions of binding free energies using MM-PBSA and MM-GBSA, J. Comput. Chem. 31 (2010) 797–810, https://doi.org/10.1002/jcc.21372.
[47] H. Gohlke, C. Kiel, D.A. Case, Insights into protein-protein binding by binding free energy calculation and free energy decomposition for the Ras-Raf and Ras-RalGDS complexes, J. Mol. Biol. 330 (2003) 891–913, https://doi.org/10.1016/S0022-2836(03)00610-7.

European Journal of Medicinal Chemistry 238 (2022) 114408

Contents lists available at ScienceDirect

European Journal of Medicinal Chemistry

journal homepage: www.elsevier.com/locate/ejmech

Design and synthesis of harmiquins, harmine and chloroquine hybrids as potent antiplasmodial agents

Goran Poje [a], Lais Pessanha de Carvalho [b], Jana Held [b,c], Diana Moita [d], Miguel Prudêncio [d], Ivana Perković [a], Tana Tandarić [e], Robert Vianello [e], Zrinka Rajić [a,*]

[a] University of Zagreb Faculty of Pharmacy and Biochemistry, A. Kovačića 1, 10000, Zagreb, Croatia
[b] University of Tübingen, Institute of Tropical Medicine, Wilhelmstraße 27, 72074, Tübingen, Germany
[c] German Center for Infection Research (DZIF), Partner Site Tübingen, 72074, Tübingen, Germany
[d] Instituto de Medicina Molecular João Lobo Antunes, Faculdade de Medicina, Universidade de Lisboa, Av. Prof. Egas Moniz, 1649-028, Lisboa, Portugal
[e] Rudjer Bošković Institute, Division of Organic Chemistry and Biochemistry, Bijenička cesta 54, 10 000, Zagreb, Croatia

ARTICLE INFO

Keywords:
Harmine
β-Carboline
Chloroquine
Hybrid compounds
Antiplasmodial activity
*Pf*Hsp90
P. falciparum

ABSTRACT

Malaria remains one of the major health problems worldwide. The lack of an effective vaccine and the increasing resistance of *Plasmodium* to the approved antimalarial drugs demands the development of novel antiplasmodial agents that can effectively prevent and/or treat this disease.

Harmiquins represent hybrids that combine two moieties with different mechanisms of antiplasmodial activity in one molecule, *i.e.*, a chloroquine (CQ) scaffold, known to inhibit heme polymerization and a β-carboline ring capable of binding to *P. falciparum* heat shock protein 90 (*Pf*Hsp90). Here we present their synthesis, evaluation of biological activity and potential mechanism of action. The synthesized hybrids differed in the type of linker employed (triazole ring or amide bond) and in the position of the substitution on the β-carboline core of harmine. The antiplasmodial activity of harmiquins was evaluated against the erythrocytic stage of the *Plasmodium* life cycle, and their cytotoxic effect was tested on HepG2 cells. The results showed that harmiquins exerted remarkable activity against both CQ-sensitive (*Pf*3D7) and CQ-resistant (*Pf*Dd2, *Pf*K1, and *Pf*7G8). *P. falciparum* strains. The most active compound, harmiquine **32**, displayed single-digit nanomolar IC_{50} value against *Pf*3D7 ($IC_{50} = 2.0 \pm 0.3$ nM). Importantly, it also showed significantly higher activity than CQ against the resistant *Plasmodium* strains and had a very high selectivity index (4450). Harmiquins may act through the inhibition of heme polymerization and binding to the ATP binding site of the *Pf*Hsp90, which would explain their increased activity against the CQ-resistant *Plasmodium* strains. These results establish harmiquins as valuable antiplasmodial hits for future optimization.

1. Introduction

Malaria, an infectious disease caused by five species of *Plasmodium* parasites, affected 241 million people and claimed 627 000 lives in 2020, which is an increase of 6% in malaria cases and 12% in malaria deaths, in comparison to 2019, with the majority of patients being pregnant women and children [1,2]. The complex life cycle of *Plasmodium* includes an asymptomatic hepatic and a symptomatic erythrocytic stage in humans and a sporogenic stage in the *Anopheles* mosquito [3,4]. Known antimalarial drugs, such as chloroquine (CQ) and artemisinin, act solely against the erythrocytic stage of infection. CQ, a 4-amino-7--chloroquinoline derivative, is a potent inhibitor of intraparasitic hemozoin formation, resulting in the accumulation of highly toxic free heme [5,6]. It was introduced as malaria therapy in the 1940s and quickly became the drug of choice due to its rapid action, low cost, lack of serious side effects and wide availability [7,8]. However, the use of large amounts of CQ led to the emergence of resistant *Plasmodium* species and a decline in its clinical utility [4,9,10]. The introduction of artemisinin-based combination therapies (ACT) in 2001 and aggressive vector control led to a successful reduction of malaria incidence and deaths [1]. Unfortunately, such decline has stagnated in recent years. The main reason for the increase in 2020 was the disruption of services during the COVID-19 pandemic, along with the rise of the resistant *Plasmodium* strains (for example *Pf*Kelch13 mutations) that also

* Corresponding author.
E-mail address: zrajic@pharma.hr (Z. Rajić).

https://doi.org/10.1016/j.ejmech.2022.114408
Received 13 March 2022; Received in revised form 7 April 2022; Accepted 20 April 2022
Available online 30 April 2022

contributed to the treatment failure rates [1,11]. There has been considerable progress in the development of an effective vaccine against malaria. RTS,S malaria vaccine (Mosquirix®) has been recommended by WHO in October 2021 after an interim analysis of an ongoing phase IV study for use in children from 5 months of age in endemic regions and new, possibly more effective vaccines are in development [1,12]. Still, the vaccine efficacy is only moderate and waning over time. Therefore, effective antimalarial treatments remain the main pillar for acute infections.

Over the years, medicinal chemists have made intensive efforts to design and synthesise a large number of CQ analogues/derivatives, with the aim of overcoming the problems of drug resistance [13,14]. A more recent approach attracting much attention is molecular hybridization, *i.e.*, the fusion of at least two pharmacophores with individual antimalarial activity, either directly or *via* a spacer, to form a single, dual-acting antimalarial agent [15–19]. The advantages of hybrid compounds include higher efficacy, the ability to act on different stages of the parasite's life cycle, a reduction in side effects and a lower risk of adverse drug-drug interactions [20].

We have successfully employed molecular hybridization for the preparation of harmicines, comprising harmine, β-carboline type alkaloid, and cinnamic acid derivatives [21–23]. Harmine, as well as other natural and synthetic β-carbolines have been extensively investigated due to their antimalarial activities [24,25]. In addition, it has been shown that harmine is a selective inhibitor of *P. falciparum* heat shock protein 90 (*Pf*Hsp90), a molecular chaperone essential for the intra-erythrocytic development of the parasite [26–28]. Importantly, inhibition of *Pf*Hsp90 in combination with other antimalarial drugs can prevent the development of drug resistance by affecting resistance mechanisms [27,29,30]. Harmicines have shown remarkable and selective activity *in vitro* against erythrocytic and hepatic stages of the *Plasmodium* life cycle, possibly due to their effective binding to the ATP binding site of *Pf*Hsp90, as revealed by molecular dynamics (MD) simulations [21–23].

Therefore, as the next step in our search for novel antiplasmodial agents, we decided to combine the harmine and CQ scaffolds to produce dual-acting hybrid agents, harmiquins (Fig. 1). In addition to antiplasmodial activity based on inhibition of both heme polymerization and *Pf*Hsp90, harmiquins have the potential to protect against or overcome drug resistance. Here we present the synthesis of the harmiquin library, evaluation of its *in vitro* antiplasmodial activity against the erythrocytic stage of the *Plasmodium* life cycle, and cytotoxicity against the human hepatocellular carcinoma cell line (HepG2). Their possible mechanism of action, *i.e.* inhibition of heme polymerization and binding to *Pf*Hsp90 is also discussed.

2. Results and discussion

2.1. Chemistry

In this work, we report the synthesis of a harmiquine library consisting of two series of hybrid compounds differing in the type of linker employed, which is either triazole ring or an amide bond. We have chosen to refer to the hybrids bearing a triazole ring as triazole-type harmiquins (TT, **18**–**25**), and the harmiquins bearing an amide bond as amide-type (AT, **26**–**32**). 1,2,3-Triazoles have been widely used in drug discovery due to their advantageous properties such as stability to acid/base hydrolysis, reductive/oxidative conditions, and metabolic degradation, as well as their ability to actively bind to biomolecular targets through the formation of hydrogen bonds, dipole-dipole and π-stacking interactions [31–33]. In addition, triazole hybrids have been recognised as potential antimalarial agents [34]. Amide bond, a widely employed bioisoster of triazoles, was chosen as an alternative linker [35]. Additional structural diversity was achieved by derivatizing harmine's β-carboline core at five different positions, namely C-1, C-3, O-6, O-7 and N-9, with the aim of establishing a reliable SAR.

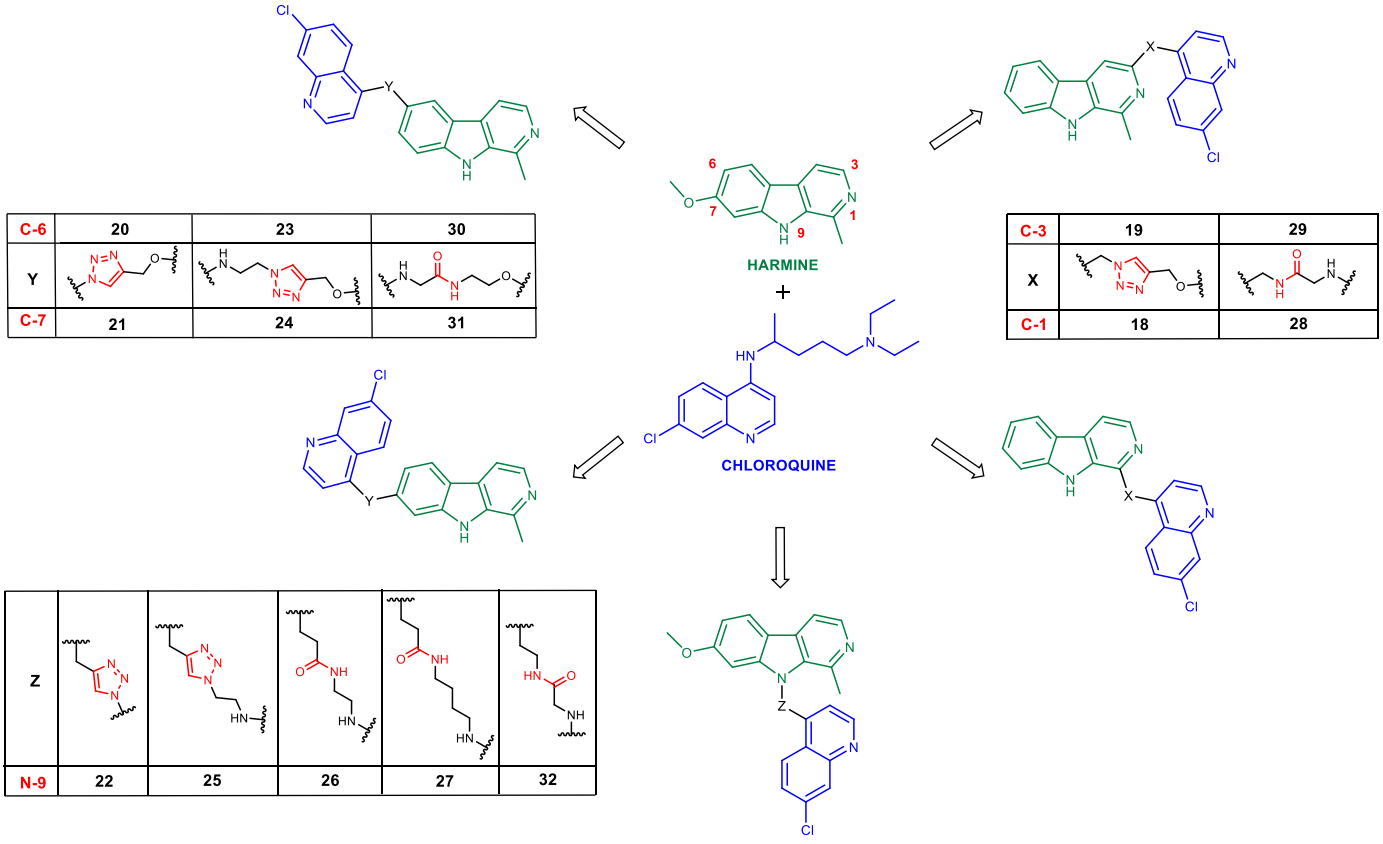

Fig. 1. Harmiquins.

TT harmiquins were prepared by Cu(I)-catalysed azide-alkyne cycloaddition (CuAAC), which is referred to as the "click chemistry reaction" and is known for its robustness, high reliability, and regiospecificity [31,36]. On the other hand, AT harmiquins were synthesized by a simple and straightforward coupling reaction. Therefore, the first step towards achieving our goal was the synthesis of intermediates, namely alkynes, azides, carboxylic acids, and amines. To this end, we prepared 7-chloroquinoline-based alkyne **1**, azides **2**, **3**, amines **4**, **5**, and carboxylic acid **6** (Scheme 1), as well as harmine-based azides **7**, **9**, amines **8**, **10**, **12**, **14**, **16**, alkynes **11**, **13**, **15**, and carboxylic acid **17** (Schemes 2 and 3), according to the procedures published by us or others [18,21–23,37–44].

Briefly, alkyne **1** was prepared by treating 4,7-dichloroquinoline with glacial acetic acid followed by alkylation of the obtained phenol with propargyl bromide/Cs_2CO_3. The synthesis of azide **3** involved a two-step procedure, substitution with 2-aminoethanol and conversion of the alcohol to azide using 2-azido-1,3-dimethyl-imidazolinium hexafluorophosphate (ADMP) and base 1,8-diazabicyclo(5.4.0)undec-7-ene (DBU) [37,38]. Finally, 7-chloroquinoline-based intermediates **2**, **4**, **5** and **6** were obtained by nucleophilic substitution of 4,7-dichloroquinoline with: 1) sodium azide, 2) ethylenediamine, 3) 1,4-diaminobutane and 4) glycine, respectively [38–40].

The preparation of β-carboline-based intermediates was more complex, as it involved the synthesis of C-1, C-3 and C-6 substituted β-carbolines by Pictet-Spengler condensation of tryptamine or its analogues with the corresponding aldehyde to give tetrahydro-β-carbolines, followed by oxidation [41–43]. The acetal group at C-1 was hydrolyzed in a mixture of AcOH/H_2O and the aldehyde obtained was reduced to alcohol with $LiAlH_4$. The reduction under similar conditions was applied for the conversion of the ester group at C-3 to alcohol. Finally, the alcohols were converted to azides **7** and **9** using ADMP/DBU and further reduced to amines **8** and **10** [23]. The ether group at position C-6 was hydrolyzed in a mixture of CH_3COOH/HBr affording phenol, which was alkylated with either propargyl bromide/Cs_2CO_3 to give alkyne **11** or 2-(Boc-amino)ethyl bromide/Cs_2CO_3, followed by the removal of the Boc protecting group under acidic conditions to obtain amine **12** [23].

On the other hand, the synthesis of alkynes/amines at C-7 (**13**/**14**) and N-9 (**15**/**16**) was carried out by alkylation of harmole or harmine with propargyl bromide/Cs_2CO_3 or 2-(Boc-amino)ethyl bromide/Cs_2CO_3 and subsequent deprotection [21,22]. Harmine-based carboxylic acid **17** was prepared in two steps. Michael addition between harmine and methyl acrylate gave the corresponding ester, which was further hydrolyzed to acid **17** [44].

7-Chloroquinoline-based alkyne **1** and harmine-based azides **7** or **9** served as building blocks for the synthesis of TT harmiquins at C-1 (**18**) and C-3 (**19**). In contrast, the starting compounds for the synthesis of TT harmiquins at O-6 (**20**, **23**), O-7 (**21**, **24**) and N-9 (**22**, **25**) were 7-chloroquinoline-based azides **2** or **3** and harmine-based alkynes **11**, **13**, **15** (Scheme 4). In both cases, the CuAAC reactions using the Cu(II) acetate precatalyst in methanol proceeded smoothly and led to TT harmiquins **18**–**25** in good yields.

AT harmiquins were prepared by reacting either 7-chloroquinoline-based amines **4**, **5** and harmine-based carboxylic acid **17** (compounds **26** and **27**) or 7-chloroquinoline-based carboxylic acid **6** and harmine-based amines **8**, **10**, **12**, **14**, **16** (compounds **28**–**32**) (Scheme 5). Different coupling reagents were employed depending on the reactants. Harmiquins **26** and **27** were prepared using 1-[bis(dimethylamino)methylene]-1*H*-1,2,3-triazolo[4,5-*b*]pyridinium-3-oxide hexafluorophosphate (HATU) and *N,N*-diisopropylethylamine (DIEA) in DCM. On the other hand, due to the better reaction yields and shorter reaction times, propylphosphonic anhydride/triethylamine (T3P/TEA) in DMF were used for the synthesis of harmiquins **28**–**32**.

Harmiquins were fully characterized by standard spectrometric and spectroscopic methods, namely MS, IR, ^1H and ^{13}C NMR. The data obtained are briefly given in the Materials and Methods section and in detail in the Supplementary Material. Their purity was checked by elemental analysis (the values found for C, H, N were within 0.4% of those calculated for the proposed formula). Their drug-like properties, *i.*

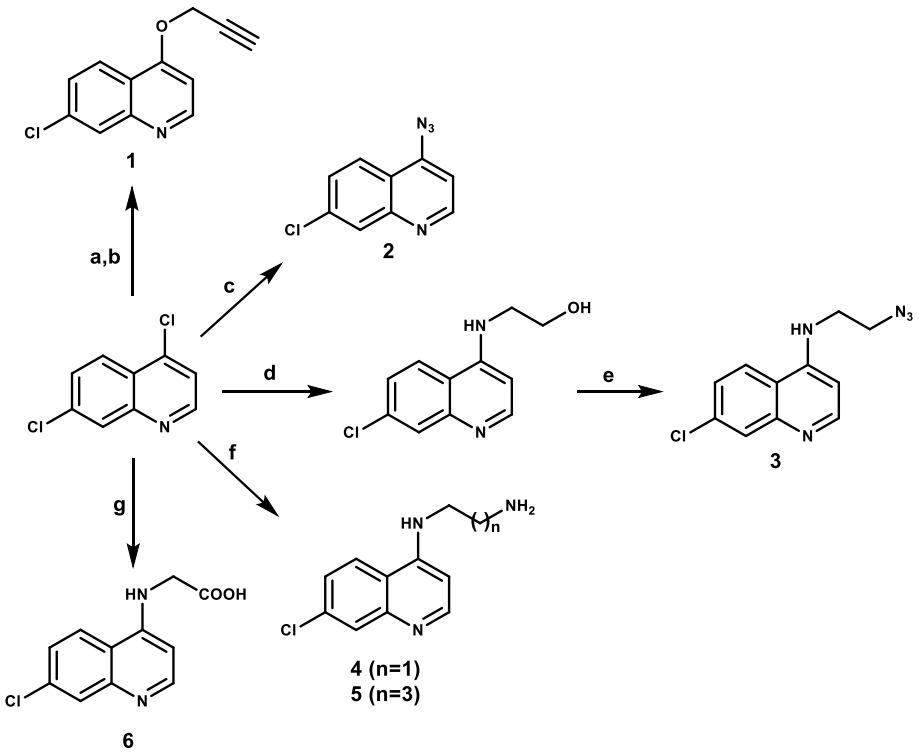

Scheme 1. Synthesis of 7-chloroquinoline-based intermediates **1**–**6**. Reagents and reaction conditions: (a) AcOH, 125 °C, 1 h; (b) $HC{\equiv}CCH_2Br$, Cs_2CO_3, DMF, rt, 1 h; (c) NaN_3, DMF, 65 °C, 18 h; (d) $H_2N(CH_2)_2OH$, TEA, 120 °C, 2 h; (e) ADMP, DBU, THF, 0 °C, 1.5 h; (f) $H_2NCH_2(CH_2)_nNH_2$, 95 °C, 1 h; (g) H_2NCH_2COOH, C_6H_5OH, 125 °C, 18 h.

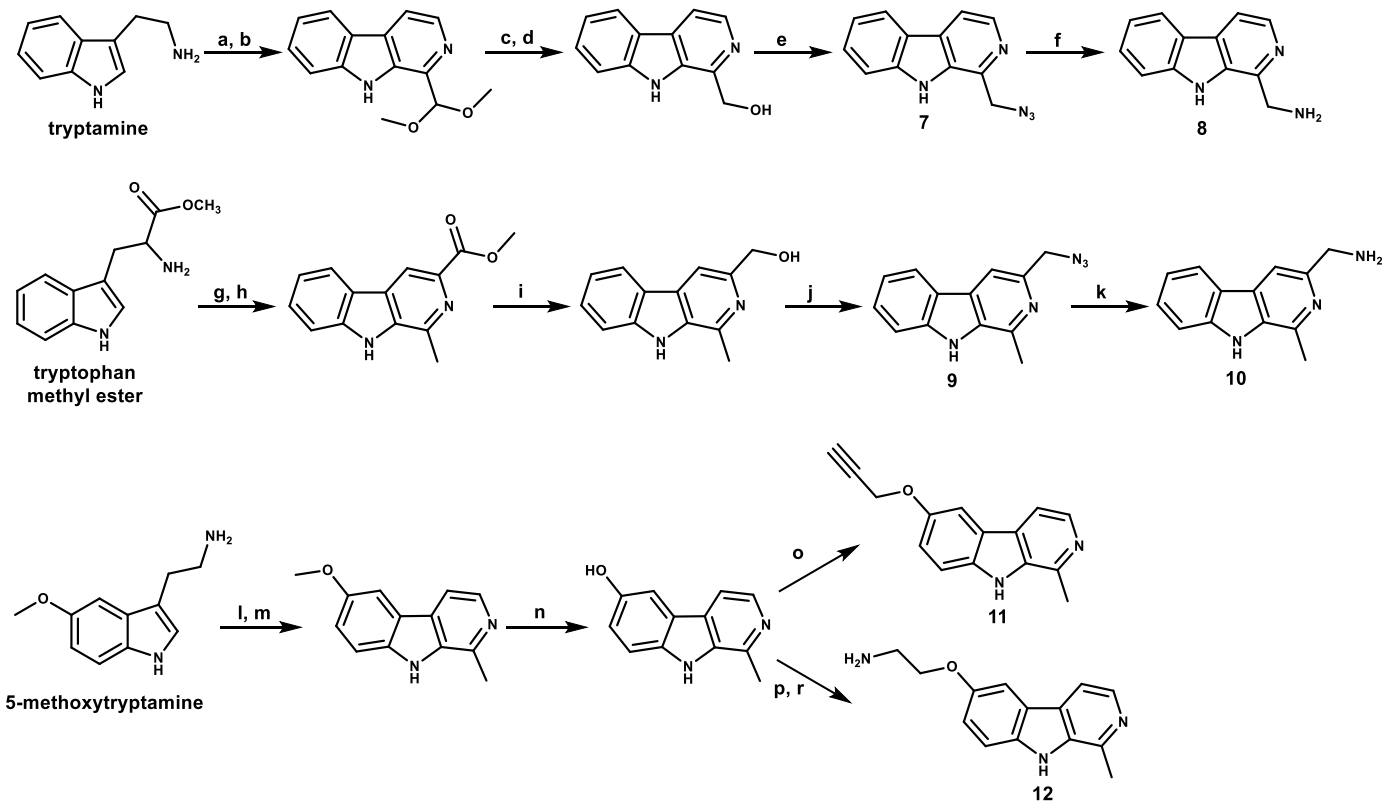

Scheme 2. Synthesis of β-carboline-based intermediates **7**–**12**. Reagents and reaction conditions: (a) $(CH_3O)_2CHCHO$, TFA, DCM, rt, 18 h; (b) $KMnO_4$, THF, rt, 48 h; (c) AcOH, H_2O, 100 °C, 1 h; (d) $LiAlH_4$, THF, rt, 1 h; (e) ADMP, DBU, THF, 0 °C, 0.5 h; (f) H_2/Pd/C, MeOH, rt, 18 h; (g) $(CH_3O)_2CHCH_3$, TFA, DCM, rt, 18 h; (h) Pd/C, EtOH, MW, 150 °C, 25 min; (i) $LiAlH_4$, THF, rt, 1 h; (j) ADMP, DBU, THF, 0 °C, 0.5 h; (k) H_2/Pd/C, MeOH, rt, 2 h; (l) $(CH_3O)_2CHCH_3$, TFA, ACN, MW, 110 °C, 10 min; (m) Pd/C, Li_2CO_3, EtOH, MW, 150 °C, 25 min; (n) HBr/AcOH, MW, 140 °C, 25 min; (o) $HC{\equiv}CCH_2Br$, Cs_2CO_3, DMF, rt, 3 h; (p) $BocNH(CH_2)_2Br$, Cs_2CO_3, TBAHS, DMF, rt, 24 h; (r) HCl/EtOAc, 50 °C, 18 h.

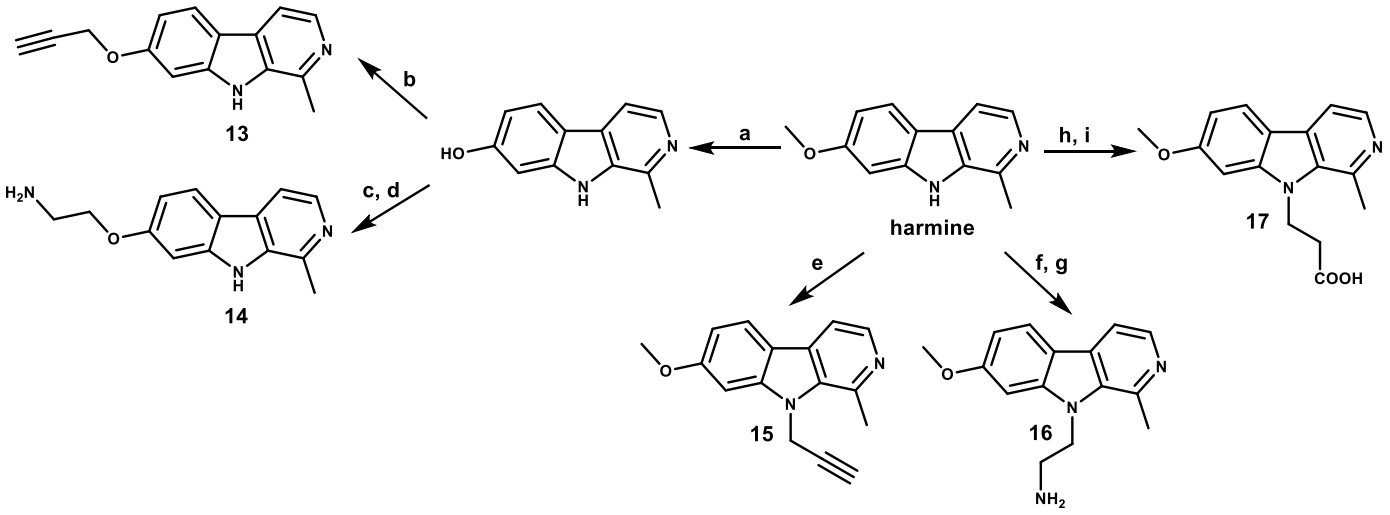

Scheme 3. Synthesis of harmine-based intermediates **13**–**17**. Reagents and reaction conditions: (a) HBr/AcOH, MW, 140 °C, 25 min; (b) $HC{\equiv}CCH_2Br$, Cs_2CO_3, DMF, rt, 3 h; (c) $BocNH(CH_2)_2Br$, Cs_2CO_3, DMF, 90 °C, 18 h; (d) HCl/MeOH, 50 °C, 18 h; (e) $HC{\equiv}CCH_2Br$, Cs_2CO_3, DMF, rt, 3 h; (f) $BocNH(CH_2)_2Br$, Cs_2CO_3, DMF, 90 °C, 18 h; (g) HCl/MeOH, 50 °C, 18 h; h) $CH_2{=}CHCOOCH_3$, DBU, ACN, 60 °C, 48 h; (i) LiOH × H_2O, MeOH/H_2O, rt, 1 h.

e. the relevant physicochemical parameters included in Lipinski's and Gelovani's rules, were also evaluated by Chemicalize.org software [45]. The results have shown that all harmiquins, apart from compound **27**, are in full compliance with both sets of rules (Table S1).

2.2. Biological evaluations

2.2.1. In vitro antiplasmodial activity and structure-activity relationship analysis

The activity of harmiquins against the erythrocytic stage of the *Plasmodium* life cycle was investigated *in vitro* in two rounds using a previously described method (Table 1a) [46–48]. First, all synthesized

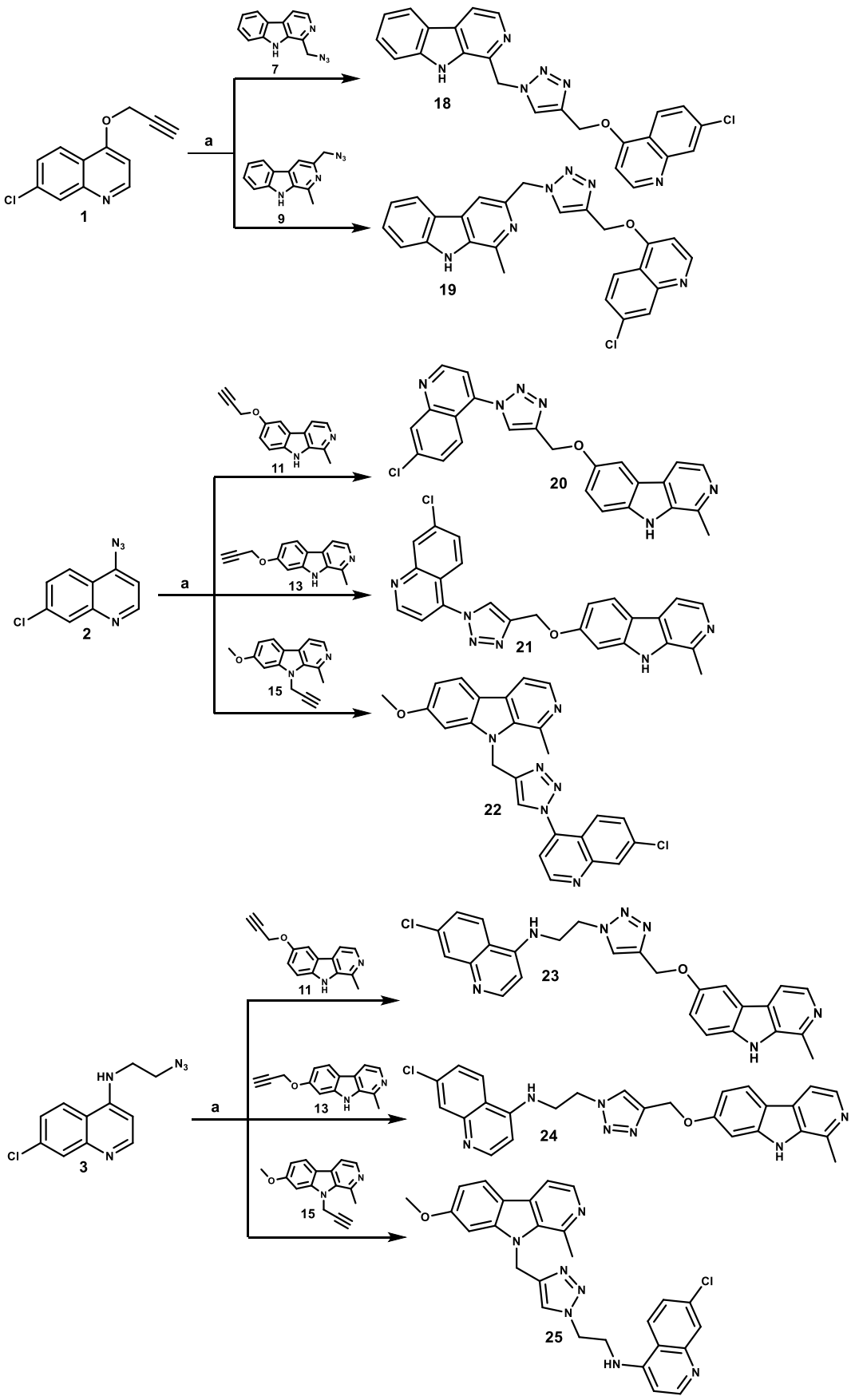

Scheme 4. Synthesis of TT harmiquins **18**–**25**. Reagents and reaction conditions: (a) $Cu(CH_3COO)_2$, MeOH, rt, 24 h.

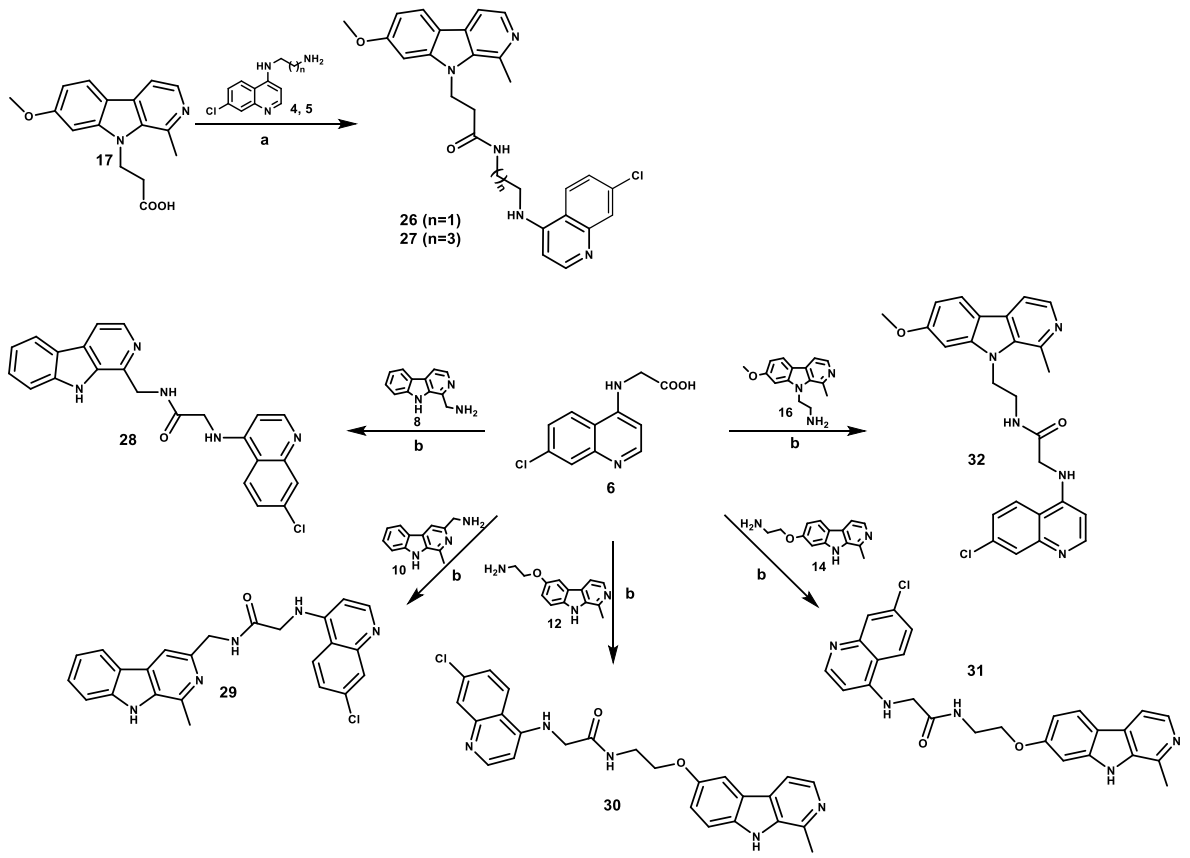

Scheme 5. Synthesis of AT harmiquins **26**–**32**. Reagents and reaction conditions: (a) HATU, DIEA, DCM, rt, 18 h; (b) T3P, TEA, DMF, rt, 18 h.

Table 1a
In vitro antiplasmodial activity of harmiquins against the erythrocytic stage of *P. falciparum* (*Pf*3D7, *Pf*Dd2, *Pf*K1 and *Pf*7G8 strains).

Compd.	IC_{50}[a] (nM)			
	*Pf*3D7	*Pf*Dd2	*Pf*K1	*Pf*7G8
18	>28 000[b]	>27777.8	n.d.[f]	n.d.
19	10841.4 ± 2569.4[c]	5418.4 ± 552	n.d.	n.d.
20	3660.3 ± 370.4	7110.3 ± 2496.9	n.d.	n.d.
21	95.8 ± 1.7	202.7 ± 28.5	299.1 ± 102.7	195.0 ± 43.3
22	899.2 ± 106.9	1816.4 ± 350.3	n.d.	n.d.
23	65.7 ± 3.4	160.4 ± 44.0	140.6 ± 14.2	143.8 ± 105.5
24	57.3 ± 1.2	76.2 ± 14.4	33.5 ± 4.9	44.2 ± 6.0
25	11.6 ± 3.8	204.5 ± 9.89	163.2 ± 78.5	28.6 ± 5.3
26	19.0 ± 5.1	54.8 ± 9	n.d.	n.d.
27	34.6 ± 1.2	15.5 ± 0.9	20.2 ± 5.2	6.0 ± 0.3
28	54.0 ± 15.8	170.7 ± 2.51	n.d.	n.d.
29	13 ± 3.1	46.1 ± 3.87	48.8 ± 19.6	28.2 ± 2.7
30	303.4 ± 61.3	535.4 ± 131.9	n.d.	n.d.
31	234.4 ± 25.7	309.3 ± 61.9	n.d.	n.d.
32	2 ± 0.3	16.2 ± 2.83	24.8 ± 1.3	7.4 ± 1.3
CQ[d]	11 ± 3	364.2 ± 70.2	392.1 ± 39.5	220.3 ± 23.0
HAR[e]	8250 ± 2830	>27777.8	n.d.	n.d.

[a] IC_{50}, the concentration of the tested compound necessary for 50% growth inhibition.
[b] The exact IC_{50} could not be obtained, as activity could only be detected at the highest tested concentration.
[c] Results represent mean ± SD, $n \geq 2$.
[d] CQ, chloroquine.
[e] HAR, harmine.
[f] n.d., not determined.

compounds were tested against a CQ-sensitive (*Pf*3D7) and a multi-resistant (*Pf*Dd2) *P. falciparum* strain with high level CQ resistance. The second round of evaluation included compounds with an IC_{50}(*Pf*3D7) < 100 nM (with the exception of compound **20**, which was not available; compound **28** gave different results and was therefore not included), against multi-resistant strains, with high level CQ resistance *Pf*K1 (CQ-pyrimethamine-sulfadoxine-resistant strain, originally from Thailand) and low level CQ resistance *Pf*7G8 (CQ-pyrimethamine-r-esistant strain, originally from Brazil). Resistance index, which represents fold difference, *i.e.* fractional ratio between the IC_{50} values obtained for sensitive and resistant strains, was calculated for each compound and is presented in Table 1b.

Table 1b
Resistance indices based on IC_{50} fold changes between CQ-sensitive (3D7) and CQ-resistant (Dd2, K1 and 7G8) *P. falciparum* strains.

Compd.	Resistance indices		
	IC_{50}(*Pf*Dd2)/IC_{50} (*Pf*3D7)	IC_{50}(*Pf*K1)/IC_{50} *Pf*3D7	IC_{50}(*Pf*7G8)/ IC_{50}(*Pf*3D7)
18	n.d.[a]	n.d.	n.d.
19	0.4	n.d.	n.d.
20	1.9	n.d.	n.d.
21	2.1	3.1	2.0
22	2	n.d.	n.d.
23	2.4	2.1	2.1
24	1.3	0.5	0.7
25	17.6	14	2.4
2	0.4	0.5	0.1
28	3.1	n.d.	n.d.
29	3.5	3.7	2.1
30	1.7	n.d.	n.d.
31	1.3	n.d.	n.d.
32	8.1	12.4	3.7
CQ	33.1	35.7	20.0

[a] n.d., not determined.

Harmiquins showed remarkable activity against the erythrocytic stage of *P. falciparum* life cycle. The structural diversity of the prepared compounds allowed us to draw some important conclusions about their structure-activity relationship (SAR).

1) AT harmiquins and most TT harmiquins were significantly more active than the parent compound harmine. For example, AT harmiquine **32** exerted over 3 orders of magnitude more pronounced antimalarial activity against *Pf*3D7 than harmine.
2) The optimal position for the substitution of the β-carboline ring is N-9. Compounds **32** (AT) and **25** (TT) were the most active against *Pf*3D7, whereas compounds **32** and **27** (both AT harmiquins) were the most active against the resistant *P. falciparum* strains.
3) In general, AT harmiquins were more active than TT harmiquins against all strains of *P. falciparum* tested.
4) It is evident that the -NH- group attached to the quinoline is an important structural feature contributing to the antimalarial activity, since the -NH- group containing compounds (all AT harmiquins and TT harmiquins **23**–**25**) show more pronounced activity than TT harmiquins with the triazole ring directly attached to the quinoline (compounds **20**–**22**) and TT harmiquins with an ether group in the same position (compounds **18** and **19**), which show a sharp decrease in the activity.
5) Six out of seven AT harmiquins and four out of eight TT harmiquins displayed stronger activities than CQ against the resistant *P. falciparum* strains. AT harmiquine **27** exerted the most pronounced activity (36.7-fold higher than CQ against *Pf*7G8, $IC_{50} = 6.0 \pm 0.3$ nM).

With few exceptions, the *Pf*3D7 strain was the most sensitive (9/15 compounds showed activity less than 100 nM). The most active compound, AT harmiquine **32**, displayed a single-digit nanomolar IC_{50} value ($IC_{50} = 2 \pm 0.3$ nM), which was also 5.5-fold higher than the activity of CQ itself. TT harmiquine **25** and AT harmiquine **29** (substituted at C-3) exerted IC_{50} values similar to CQ, 11.6 ± 3.8 and 13 ± 3.1 nM, respectively. However, harmiquine **32** displayed 22.5-fold higher activity than CQ against *Pf*Dd2, 15.9-fold higher against *Pf*K1, and 29.8-fold higher against *Pf*7G8. Moreover, 10/15 harmiquins exhibited higher activity than CQ against *Pf*Dd2 and 7/15 against *Pf*K1 and *Pf*7G8. In addition, AT harmiquine **27** (substituted at N-9) showed stronger activity against the resistant *P. falciparum* strains than against *Pf*3D7.

Remarkably, two TT harmiquins differing only by the position of the substitution at the β-carboline ring, compounds **25** (N-9) and **24** (O-7), showed significantly different activities against *P. falciparum* strains. While the most active TT harmiquine against *Pf*3D7 was compound **25**, harmiquine **24** exhibited the most pronounced activity against the resistant strains (*Pf*K1 and *Pf*7G8).

It is interesting to note that the least active AT harmiquins and TT harmiquins differ by the position of the substitution at the β-carboline ring. Among AT harmiquins, compounds **30** and **31**, substituted at O-6 and O-7, had two orders of magnitude less activity than harmiquine **32**. On the other hand, by far the least active TT harmiquins were those in which harmine was substituted at C-1 (**18**) and C-3 (**19**). Since these harmiquins contain an ether group attached to the quinoline instead of -NH-, it would be interesting to see if analogous compounds with -NH- group would have higher activity.

Most of the compounds did not show cross-resistance with the CQ-resistant strains, showing that they retain the same activity against CQ resistant and sensitive strains (Table 1b). The very active compounds **16** and **32** displayed a relevant IC_{50} fold change against *Pf*Dd2 and *Pf*K1 indicating cross-resistance, but the loss of activity was much less pronounced than with CQ.

2.2.2. *In vitro cytotoxicity screening and selectivity*

Screening of the cytotoxic activity of harmiquins against HepG2 was performed to evaluate their selectivity against *Plasmodium* over mammalian cells. For this purpose, the selectivity index was calculated for each compound as a fractional ratio between the IC_{50} values obtained for HepG2, and the *P. falciparum* 3D7 strain. The cytotoxicity of all compounds tested was similar, and the majority of harmiquins exhibited IC_{50} values in the 5–20 μM range (Table 2). Since most harmiquins showed antimalarial activity in the nanomolar range, we concluded that harmiquins have significant selectivity against *Plasmodium*. Most AT harmiquins showed more than 2 orders of magnitude higher activity against the parasite than against mammalian cells (SI > 100). Remarkably, compounds **32** and **29**, the most active harmiquins, exhibited more than 3 orders of magnitude less activity toward mammalian cells (SI = 4450 and 1431, respectively). Among TT harmiquins, only compound **25** showed significant selectivity (SI = 828).

2.2.3. *Inhibition of heme polymerization*

During erythrocytic stage of infection, *Plasmodium* degrades hemoglobin in its digestive vacuole under acidic conditions to globin and Fe (II) heme, which is rapidly oxidized to toxic Fe(III) hematin and further polymerized to hemozoin. Antimalarials, such as CQ, inhibit this unique detoxification process leading to the death of the parasite [49]. Thus, we decided to investigate whether harmiquins exert their activity at least in part through that mechanism. A synthetic form of hemozoin, β-hematin, can be generated *in vitro* from hemin under acidic conditions and it is routinely used as the model of hematin crystallisation. The amount of

Table 2
In vitro cytotoxicity screening of harmiquins against HepG2 and calculated selectivity indices.

Compd.	IC_{50}[a] (μM)	SI[b]	Compd.	IC_{50}[a] (μM)	SI[b]
18	>25[c]	>0.90[d]	**26**	12.8 ± 2.4	795.03
19	>100	>9.22	**27**	>25	>722.54
20	5.5 ± 3.3	1.50	**28**	7.8 ± 1.5	144.44
21	6.4 ± 4.2	66.81	**29**	18.6 ± 7.3	1430.76
22	19.7 ± 8.3	21.91	**30**	>20	>66.01
23	15.0 ± 1.5	228.31	**31**	15.93 ± 0.8	68.08
24	6.3 ± 1.9	109.95	**32**	8.9 ± 1.0	4450
25	14.0 ± 1.4	828.57	HAR[e]	>250	>30

[a] IC_{50}, the concentration of the tested compound necessary for 50% growth inhibition.
[b] SI, selectivity index, the ratio between IC_{50} (HepG2) and IC_{50} (*Pf*3D7).
[c] The exact IC_{50} could not be obtained, as activity could only be detected at the highest tested concentration.
[d] The exact SI could not be obtained, as exact IC_{50} could not be obtained.
[e] HAR, harmine.

β-hematin formed is inversely proportional to the activity of antimalarial compound, *i.e.* less amount of β-hematin equals higher inhibitory activity of the compound.

In vitro ability of the test compounds to inhibit β-hematin formation was examined by the methods previously reported [50]. Harmiquins, along with the reference drug CQ, were assayed at 1 mM and data are given in Table 3. Compounds were divided into 3 groups: inactive (<50% inhibitory activity of CQ), active (between 50 and 75% of the activity of CQ), and highly active (>75% of the activity of CQ). Interestingly, TT harmiquins significantly inhibited heme polymerization (4 out of 8 compounds were highly active), whereas AT harmiquins were not as effective (only two compounds were active). The ability of the test compounds to inhibit heme polymerization did not correlate completely with the antiplasmodial activities obtained against the erythrocytic stage *in vitro* (Table 1a), suggesting that other mechanisms are involved.

2.3. Molecular dynamics simulations

Computational analysis was utilized to provide an insight into the binding of a representative set of derivatives towards P*f*Hsp90 and to rationalize their measured affinities. We mostly focused on AT harmiquins, given their higher activity over analogous TT harmiquins, and considered most potent **29** and **32**, together with their structural analogues **28**, **30** and **31**. In addition, we also included compound **27**, given its structural similarity with **32**, differing in the type of the amide linkage and a longer alkyl spacer, therefore possessing larger flexibility. Lastly, all obtained values are discussed relative to two parent compounds, harmine and CQ, that will serve as reference systems.

The calculated binding free energies (ΔG_{BIND}) are given in Table 4, together with their decomposition into contributions from individual residues. The specific residues included in the analysis are those belonging to the ATP binding pocket (Asn37, Asp79, Arg98, Phe124) [51,52], and all of those with contributions higher than −0.20 and lower than 0.06 kcal mol^{-1} for the most active **32**. In other words, data in Table 4 identify residues mostly favouring and mostly disfavouring the binding of **32** to P*f*Hsp90.

Calculated ΔG_{BIND} values are all exergonic, thereby indicating a favourable binding of all derivatives towards P*f*Hsp90, which agrees with their demonstrated biological activities. A reference ligand harmine reveals the poorest binding features, as its affinity is significantly lower than in other systems, being ΔG_{BIND} = −7.5 kcal mol^{-1}. Furthermore, data in Table 4 clearly advise that harmine is not binding within the ATP binding site, as none of the residues defining this structural element on P*f*Hsp90, nor those in their vicinity, reveal any contribution to its binding energy. Still, such a low affinity is consistent with its high IC_{50} value of 8.25 μM (Table 1), and, although a relationship between IC_{50} and ΔG_{BIND} values is not so straightforward, the IC_{50} value measured for harmine roughly translates to a binding affinity of −6.9 kcal mol^{-1}, which places both sets of data in excellent agreement and validates our computational strategy.

Table 3
In vitro ability of harmiquins to inhibit heme polymerization.

Compd.	Activity[a]	Compd.	Activity[a]
18	–	**26**	–
19	+	**27**	–
20	++	**28**	–
21	++	**29**	–
22	–	**30**	–
23	++	**31**	+
24	++	**32**	+
25	+	CQ	++

[a] Ability of the test compounds to inhibit heme polymerization *in vitro* was calculated as a % of the inhibitory effect displayed by reference drug CQ in the same experiment; test compounds were ranked as follows: <50%, not active (–); between 50 and 75%, moderately active (+); >75%, highly active (++).

Interestingly, the other constituting fragment of our designed derivatives, CQ is, on its own, a better binder than harmine, and, although its P*f*Hsp90 inhibition is not demonstrated in the literature, it reveals a higher affinity of ΔG_{BIND} = −21.2 kcal mol^{-1}. Moreover, it most favourably attaches within the ATP binding site (Fig. 2), as crucial residues Asn37, Arg98 and Phe124 are promoting its binding with individual contributions of −0.75, −0.34 and −0.58 kcal mol^{-1}, respectively, solely being responsible for around 8% of its total ΔG_{BIND} value. On the other hand, all new derivatives further exceed the binding affinity of both harmine and CQ, which firmly justifies the employed synthetic strategy that led to more potent conjugates. Specifically, our analysis confirmed the highest activity of compounds **29** and **32**, with the calculated affinities of −37.2 and −38.2 kcal mol^{-1}, respectively, thereby demonstrating their better positioning within the P*f*Hsp90 interior. Both ligands are placed firmly within the ATP binding site (Fig. 2), and, in both cases, the binding to P*f*Hsp90 is dominated by Ile82. The latter surpasses all other residues, as its high individual contribution originates in its alkyl side-chain forming strong C–H … π interactions with the available aromatic moieties, the quinoline unit in **29** and the harmine core in **32** (Fig. 3). This is followed by the ATP binding site residues, Asn37 in particular (−2.29 kcal mol^{-1} for **29**, and –1.63 kcal mol^{-1} for **32**), which uses its side-chain amide to form analogous N–H … π contacts with the same aromatic units in both derivatives. It is also worth pointing to an exceedingly favourable contribution from Lys44, being, for example, the second most dominant residue in binding **32**, which facilitates its activity through the N–H•••O=C hydrogen bonding with its oxygen atom within the amide linker. This agrees with the already demonstrated significance of Lys44 in binding various druggable ligands within the ATP binding site of the eukaryotic Hsp90 protein [53]. Lastly, Met84 also turned out as an important residue, established through its side-chain methyl group engaging in a range of C–H … π contacts with aromatic units in both **29** and **32**. Interestingly, although three of the ATP binding site residues, Asn37, Phe124 and Arg98, are strongly promoting the interactions with the most potent ligands, the other residue belonging to this structural fragment within the P*f*Hsp90 pocket, Asp79, is significantly disfavouring the binding. For **32**, its individual contribution is +1.19 kcal mol^{-1}, while for **29** it even reaches +1.41 kcal mol^{-1}. In the most potent **32**, this is brought about through an unfavourable pairing between anionic carboxylate in Asp79 and the methoxy group on its harmine core (Fig. 3), while, in **29**, this similarly occurs with the methyl group attached to the pyridine part of its harmine core. This insight opens up an interesting perspective and suggests guidelines for the further derivatization of both **29** and, especially, **32** towards even more potent ligands. Replacing the indicated methyl group in **29** and the methoxy group in **32** with, for example, the hydroxyl moiety, or any group able to donate hydrogen bonding to Asp79, seems like a good strategy in that direction, which will be inspected in our subsequent synthetic efforts.

In concluding this section, let us mention that data in Table 4 also offer some indication as to why other considered derivatives exhibit reduced affinities relative to **32**. Namely, increasing the length of the alkyl linker, as in **27**, certainly improves its flexibility, which might allow it a more optimal position within the binding pocket. Contrary to that, this results in a further distancing between harmine and chloroquine fragments, which disallows the latter to engage in favourable interactions with Ile82, demonstrated as crucial in **32** (Fig. 3), thereby making **27** a weaker binder. In other words, the binding position of **27** reduces the contribution from Ile82, from −2.60 kcal mol^{-1} in **32** to −0.78 kcal mol^{-1} in **27**. This difference of 1.82 kcal mol^{-1} is already responsible for 59% of the total reduction in the binding affinity, in this case assuming $\Delta\Delta G_{BIND}$ = 3.1 kcal mol^{-1}, which is significant. In addition, twisting the geometry of the amide bond also reduces the favourable contribution from Lys44, from −2.25 kcal mol^{-1} in **32** to −0.23 kcal mol^{-1} in **27**, which illustrates the inability of the Lys44 sidechain to engage in the hydrogen bonding contact with such oriented amide moiety. On the other hand, given the differences in the

Table 4
Total binding free energies (ΔG_{BIND}) towards P*f*Hsp90 and their decomposition on a *per-residue* basis following the MM-GBSA analysis of the obtained molecular dynamics trajectories.[a]

Ligand	27	28	29	30	31	32	harmine	CQ[b]
Total ΔG_{BIND}	−35.1	−36.8	−37.2	−35.5	−31.8	−38.2	−7.5	−21.2
Ile82	−0.78	−0.62	−2.44	−0.90	−0.85	−2.60	0.00	−0.51
Lys44	−0.23	−0.87	−0.98	−1.32	−1.76	−2.25	0.00	−0.12
Met84	−2.17	−1.29	−2.27	−1.83	−1.44	−2.07	0.00	−1.46
Asn37	**−2.26**	**−1.20**	**−2.29**	**−3.35**	**−2.98**	**−1.63**	**0.00**	**−0.75**
Asn91	−2.39	−2.54	−0.68	−1.13	−0.71	−1.45	0.00	−1.55
Phe124	**−0.93**	**−1.92**	**−0.82**	**−0.51**	**−0.79**	**−1.43**	0.00	**−0.58**
Leu93	−0.80	−0.78	−0.67	−0.38	−0.61	−1.25	0.00	−0.54
Ala41	−1.17	−0.83	−1.38	−1.77	−1.22	−1.22	0.00	−0.93
Thr171	−0.43	−0.20	−2.40	−1.63	−0.26	−0.73	0.00	−0.35
Ile173	−0.47	−0.20	−0.89	−0.15	−0.17	−0.71	−0.01	−0.29
Ala38	−0.32	−0.17	−1.34	−0.51	−0.15	−0.58	0.00	−0.16
Asn140	0.02	0.01	0.00	0.02	0.01	−0.51	0.00	0.03
Val136	−0.36	−0.08	−0.19	−0.08	−0.07	−0.40	−0.02	−0.12
Arg98	**−0.28**	**−5.25**	**0.01**	**−1.84**	**−2.40**	**−0.30**	**0.00**	**−0.34**
Thr85	−0.14	−0.03	−0.15	−0.08	−0.02	−0.27	0.00	−0.04
Leu43	−0.18	−0.12	−1.09	−0.09	−0.10	−0.24	0.00	−0.19
Tyr125	−0.04	−0.29	−0.05	−0.04	−0.04	−0.24	0.00	−0.03
Ile96	−1.64	−0.47	−0.03	−0.23	−0.36	−0.22	0.00	−0.49
Glu48	0.04	0.04	0.06	0.06	0.05	−0.21	0.00	−0.01
Asp40	−0.37	−0.18	−0.50	−1.04	−1.89	0.06	0.00	−0.31
Arg169	0.05	0.04	0.01	0.05	0.05	0.07	0.00	0.08
Asp142	0.04	0.01	0.04	0.02	0.03	0.11	0.00	−0.01
Asp88	−0.13	−0.17	0.24	−0.15	−0.06	0.21	0.00	−0.20
Asp79	**0.35**	**0.18**	**1.41**	**0.70**	**0.17**	**1.19**	0.00	**0.18**

[a] Residues are selected to list those belonging to the ATP binding pocket (Asn37, Asp79, Arg98, Phe124, in bold) and all of those with contributions higher than −0.20 and lower than 0.06 kcal mol^{-1} for **32**. All values are in kcal mol^{-1}.
[b] CQ, chloroquine.

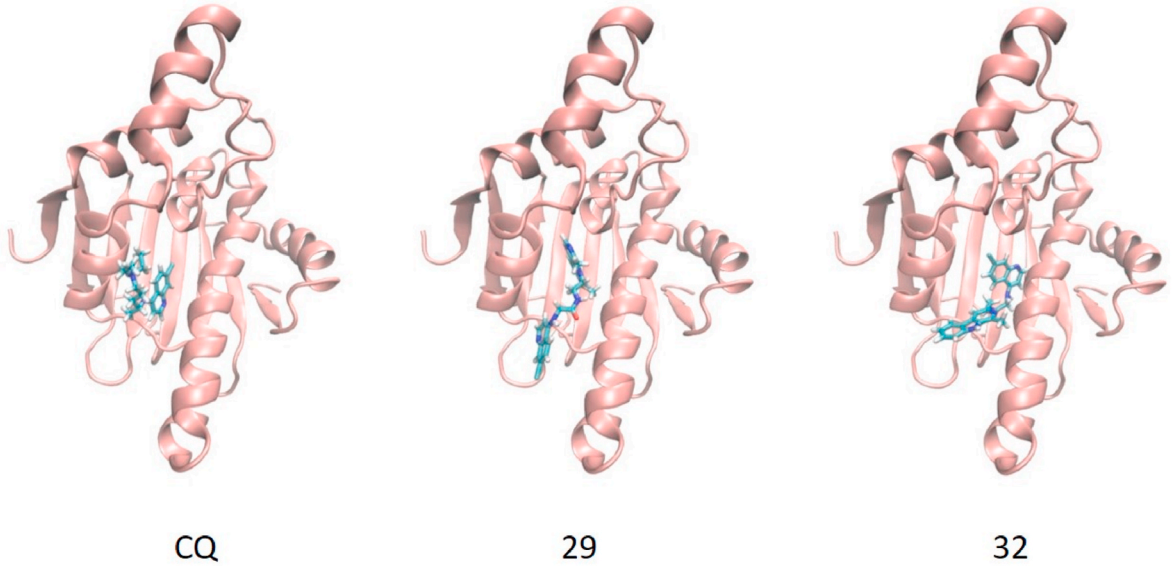

Fig. 2. Position of CQ and the investigated harmiquins **29** and **32**, within the ATP binding site of the P*f*Hsp90, as revealed through the MD simulations.

substitution patterns in **28**, **30** and **31**, it is not surprising that these derivatives consistently show a reduction in the contribution from residues most dominant for the binding of **32**, which ultimately reduces their affinities. This confirms the suitability of the N-9 derivatization of the harmine fragment as most optimal for increasing the potency of such-like derivatives against the P*f*Hsp90, in line with experiments presented here and in some of our earlier reports [21–23].

3. Conclusions

In this paper, we demonstrated the application of the molecular hybridisation approach in the design and synthesis of two types of novel harmine and CQ hybrids, AT, and TT harmiquins. The evaluation of their antiplasmodial activity against the erythrocytic stage of *P. falciparum* revealed their remarkable activity against CQ-sensitive, as well as CQ-resistant *Plasmodium* strains. Notably, the most active compound, AT harmiquine **32**, displayed a 5.5-fold higher activity against *Pf*3D7 than CQ ($IC_{50} = 2 \pm 0.3$ nM), and at least 15.9-fold higher activity than CQ against *P. falciparum* CQ-resistant strains. Based on the structure of harmiquins, we investigated two possible mechanisms of action, inhibition of heme polymerization and binding to *Pf*Hsp90. Our experiments show that both might play a role in the inhibition of intraerythrocytic development of *Plasmodium*. Our future work will focus on the enrichment of the harmiquins library and the establishment of a reliable SAR,

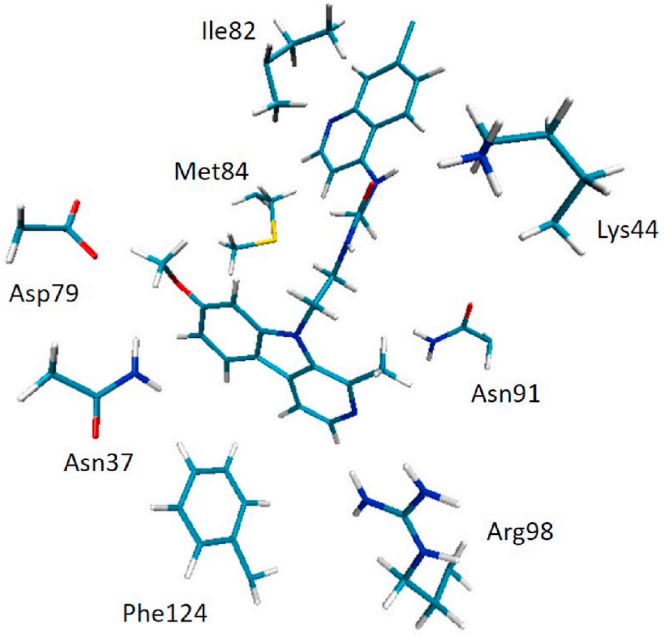

Fig. 3. Specific interactions governing the binding of the most potent **32** within the ATP binding site of the P*f*Hsp90 protein.

towards more potent antimalarial compounds.

4. Materials and Methods

4.1. Chemistry

4.1.1. General information

Melting points were determined on a Stuart Melting Point Apparatus (Barloworld Scientific, UK) in open capillaries and were uncorrected. FTIR-ATR spectra were recorded using a Fourier-Transform Infrared Attenuated Total Reflection UATR Two spectrometer (PerkinElmer, Waltham, MA, USA) in the range from 450 to 4000 cm^{-1}.^{1}H and ^{13}C NMR spectra were recorded on a Bruker Avance III HD operating at 300, 400 or 600 MHz for the ^{1}H and 75, 101 or 151 MHz for the ^{13}C nuclei (Bruker, Billerica, MA, USA). Samples were measured in DMSO-d_6 solutions at 20 °C in 5 mm NMR tubes. Chemical shifts (δ) are reported in parts per million (ppm) using tetramethylsilane (TMS) as a reference in the ^{1}H and DMSO residual peak as a reference in the ^{13}C spectra (39.52 ppm). Coupling constants (J) are reported in hertz (Hz). Mass spectra were recorded on Agilent 1200 Series HPLC coupled with Agilent 6410 Triple Quad, (Agilent Technologies, St. Clara, CA, USA). The mobile phase consisted of Milli Q water as component A and MeOH (HPLC grade, J. T. Baker) as component B, and as the stationary phase Zorbax XDC C18 column (4.6 × 75 mm, 3.5 μm) was used. Gradient elution was used at a flow rate of 0.5 mL/min, and 5 μL of analyte solution was injected per analysis. The starting conditions and gradient steepness were adjusted according to the analyte polarity. A diode array detector was utilized, while the data were presented as a total wavelength chromatogram (TWC). Mass spectrometry conditions were as follows: electrospray ionization (ESI) in positive and negative mode was used. Capillary voltage and current were set to 4.0 kV and 20 nA, respectively. Nebulizer pressure was set to 15 psi, while the drying gas (nitrogen) temperature and flow were 300 °C and 11 L/min. For the MS data analysis Agilent MassHunter software (Agilent Technologies, St. Clara, CA, USA) was used. Elemental analyses were performed on a CHNS LECO analyzer (LECO Corporation, St. Joseph, MI, USA). Analyses indicated by the symbols of the elements were within ±0.4% of their theoretical values. Microwave-assisted reactions were performed in a microwave reactor CEM Discover (CEM, USA) in a glass reaction vessel. All compounds were routinely checked by TLC with silica gel 60F-254 glass plates (Merck, Germany) using DCM/MeOH or cyclohexane/EtOAc/MeOH as the solvent system. Spots were visualized by UV light (λ = 254 nm; 365 nm) and iodine vapor. Column chromatography was performed on silica gel 0.063–0.200 mm (Sigma-Aldrich, USA) with the same eluents used for TLC. All chemicals and solvents were of analytical grade and purchased from commercial sources.

β-carbolines-based azides **7**, **9**, alkynes **11**, **13**, **15**, carboxylic acid **17** and amines **8**, **10**, **12**, **14**, **16** were prepared according to procedures published by us or others [21–23,44]. 7-Chloroquinoline-based azide **2**, amines **4**, **5** and carboxylic acid **6** were synthesized as described earlier [38–40]. Alkyne **1** was prepared by a different procedure than the one described in the literature [54]. Azide **3** was prepared according to the modified literature procedure from the corresponding alcohol, using ADMP/DBU [18,37].

*4.1.1.1. Synthesis of 7-chloro-4-(prop-2-yn-1-yloxy)quinoline (**1**).* 7-chloroquinolin-4-ol (0.2 g, 1.114 mmol) [55] was suspended in dry DMF (4 mL). Under argon atmosphere cesium carbonate (0.508 g, 1.56 mmol) was added, followed by dropwise addition of 80% solution of propargyl bromide in toluene (0.143 mL, 1.337 mmol). The reaction was stirred at rt and under argon atmosphere for 1.5 h. Upon completion, the reaction mixture was poured into 40 mL of water. Product was extracted with EtOAc (3 × 40 mL). Organic layers were collected and washed with water (2 × 100 mL), dried over anhydrous sodium sulfate and evaporated under reduced pressure. After purification by column chromatography (DCM/methanol = 9:1) and trituration with diethyl ether 0.143 g (59%) of **1** was obtained.

*4.1.1.2. General procedure for the synthesis of TT harmiquins **18–25**.* To a solution of an alkyne (0.230 mmol) and the corresponding azide (0.253 mmol) in MeOH (5 mL), catalytic amount of $Cu(OAc)_2$ was added. The reaction mixture was stirred at rt for 24 h. Upon completion of the reaction, the solvent was removed under the reduced pressure. The residue was purified by column chromatography (with an additional Al_2O_3 layer in order to remove Cu-salts) with DCM/MeOH or cyclohexane/EtOAc/MeOH as a mobile phase. The crude product was triturated with diethyl ether/petroleum ether.

*4.1.1.3. 1-((4-(((7-Chloroquinolin-4-yl)oxy)methyl)-1H-1,2,3-triazol-1-yl)methyl)-9H-pyrido [3,4-b]indole (**18**).* Alkyne **1**: 0.050 g; azide **7**: 0.056 g, mobile phase: cyclohexane/EtOAc/MeOH 1:1:0.5; yield: 0.046 g, (45%); mp 170–172 °C; IR (ATR, ν/cm^{-1}) 3235, 3058, 1619, 1604, 1566, 1541, 1488, 1454, 1432, 1374, 1322, 1299, 1228, 1136, 1100, 1054, 945, 856, 806, 755, 724, 656, 587, 541, 493, 478; ^{1}H NMR (DMSO-d_6) δ 11.93 (s, 1H), 8.30 (s, 1H), 8.28-8.24 (m, 2H), 8.19 (d, 1H, J = 7.8 Hz), 8.14 (d, 1H, J = 8.6 Hz), 8.11 (d, 1H, J = 5.1 Hz), 8.00 (d, 1H, J = 1.9 Hz), 7.65 (dt, 1H, J = 8.2, 0.9 Hz), 7.60-7.58 (m, 1H), 7.38 (dd, 1H, J = 8.6, 1.9 Hz), 7.29-7.27 (m, 1H), 6.13 (d, 1H, J = 7.8 Hz), 6.06 (s, 2H), 5.55 (s, 2H); ^{13}C NMR (DMSO-d_6) δ 175.78, 145.22, 141.86, 140.68, 140.57, 137.85, 137.84, 136.92, 133.82, 128.72, 128.56, 127.86, 125.26, 124.62, 123.75, 121.91, 120.72, 119.65, 116.69, 114.85, 112.05, 109.78, 51.25, 46.88; ESI-MS: m/z 441.0 $(M+1)^+$. Anal. Calcd. for $C_{24}H_{17}ClN_6O$: C, 65.38; H, 3.89; N, 19.06; found: C, 65.57; H, 3.95; N, 19.25.

*4.1.1.4. 3-((4-(((7-Chloroquinolin-4-yl)oxy)methyl)-1H-1,2,3-triazol-1-yl)methyl)-1-methyl-9H-pyrido [3,4-b]indole (**19**).* Alkyne **1**: 0.050 g; azide **9**: 0.060 g, mobile phase: DCM/MeOH 9:1; yield: 0.042 g, (40%); mp 172–174.5 °C; IR (ATR, ν/cm^{-1}) 3617, 3130, 3057, 2888, 2787, 1623, 1603, 1568, 1507, 1486, 1468, 1446, 1398, 1376, 1357, 1340, 1254, 1224, 1140, 1103, 1058, 1055, 1027, 971, 860, 812, 800, 749, 646, 589, 543, 479; ^{1}H NMR (DMSO-d_6) δ 11.66 (s, 1H), 8.25 (s, 1H), 8.19 (d, 1H, J = 7.8 Hz), 8.14 (d, 1H, J = 8.6 Hz), 8.11 (d, 1H, J = 7.9 Hz), 8.00 (d, 1H, J = 1.8 Hz), 7.90 (s, 1H), 7.59 (d, 1H, J = 8.16 Hz),

7.56-7.52 (m, 1H), 7.38 (dd, 1H, J = 8.6, 1.8 Hz), 7.27-7.22 (m, 1H), 6.13 (d, 1H, J = 7.8 Hz), 5.73 (s, 2H), 5.55 (s, 2H), 2.71 (s, 3H); ^{13}C NMR (DMSO-d_6) δ 175.79, 145.24, 142.44, 142.14, 141.95, 140.75, 140.55, 136.90, 133.95, 128.09, 127.87, 127.55, 125.28, 124.08, 123.73, 121.62, 120.87, 119.43, 116.65, 112.09, 111.81, 109.77, 55.19, 46.97, 20.34; ESI-MS: m/z 455.4 $(M+1)^+$. Anal. Calcd. for $C_{25}H_{19}ClN_6O$: C, 66.01; H, 4.21; N, 18.47; found: C, 66.34; H, 4.37; N, 18.75.

*4.1.1.5. 6-((1-(7-Chloroquinolin-4-yl)-1H-1,2,3-triazol-4-yl)methoxy)-1-methyl-9H-pyrido [3,4-b]indole (**20**).* Alkyne **11**: 0.054 g; azide **2**: 0.052 g, mobile phase: cyclohexane/EtOAc/MeOH 1:1:0.5; yield: 0.043 g, (42%); mp 281.5–283 °C; IR (ATR, ν/cm^{-1}) 3247, 3076, 3030, 2901, 1588, 1567, 1497, 1477, 1458, 1441, 1414, 1372, 1350, 1265, 1253, 1208, 1174, 1116, 1076, 1039, 1030, 1008, 987, 968, 878, 849, 829, 816, 803, 770, 736, 700, 672, 655, 621, 543, 500; ^{1}H NMR (DMSO-d_6) δ 11.42 (s, 1H), 9.17 (d, 1H, J = 4.6 Hz), 9.01 (s, 1H), 8.30 (d, 1H, J = 2.2 Hz), 8.18 (d, 1H, J = 5.3 Hz), 8.00-7.98 (m, 2H), 7.93 (d, 1H, J = 5.3 Hz), 7.89 (d, 1H, J = 4.6 Hz), 7.75 (dd, 1H, J = 9.1, 2.2 Hz), 7.55 (d, 1H, J = 8.8 Hz), 7.31 (dd, 1H, J = 8.8, 2.5 Hz), 5.42 (s, 2H), 2.75 (s, 3H); ^{13}C NMR (DMSO-d_6) δ 152.38, 151.88, 149.38, 143.96, 142.25, 140.38, 137.00, 135.56, 135.36, 135.10, 128.98, 128.14, 126.85, 126.69, 125.35, 121.39, 120.34, 118.44, 117.15, 112.82, 112.69, 105.40, 61.80, 20.40; ESI-MS: m/z 441.4 $(M+1)^+$. Anal. Calcd. for $C_{24}H_{17}ClN_6O$: C, 65.38; H, 3.89; N, 19.06; found: C, 65.23; H, 3.99; N, 19.37.

*4.1.1.6. 7-((1-(7-Chloroquinolin-4-yl)-1H-1,2,3-triazol-4-yl)methoxy)-1-methyl-9H-pyrido [3,4-b]indole (**21**).* Alkyne **13**: 0.054 g; azide **2**: 0.052 g, mobile phase: DCM/MeOH 95:5; yield: 0.051 g, (50%); mp 236–239.5 °C; IR (ATR, ν/cm^{-1}) 3049, 1629, 1610, 1564, 1505, 1486, 1440, 1321, 1295, 1278, 1253, 1233, 1215, 1106, 1071, 1036, 996, 953, 920, 872, 822, 812, 801, 767, 629, 572; ^{1}H NMR (DMSO-d_6) δ 11.51 (s, 1H), 9.17 (d, 1H, J = 4.7 Hz), 9.02 (s, 1H), 8.30 (d, 1H, J = 2.1 Hz), 8.17 (d, 1H, J = 5.3 Hz), 8.11 (d, 1H, J = 8.6 Hz), 8.01 (d, 1H, J = 9.1 Hz), 7.90 (d, 1H, J = 4.7 Hz), 7.83 (d, 1H, J = 5.3 Hz), 7.79 (dd, 1H, J = 9.1, 2.2 Hz), 7.27 (d, 1H, J = 2.2 Hz), 6.99 (dd, 1H, J = 8.6, 2.2 Hz), 5.47 (s, 2H), 2.74 (s, 3H); ^{13}C NMR (DMSO-d_6) δ 158.72, 152.39, 149.39, 143.72, 141.79, 141.37, 140.36, 137.74, 135.39, 134.62, 129.03, 128.17, 127.14, 127.00, 125.35, 122.73, 120.34, 117.17, 115.31, 111.99, 109.45, 96.03, 61.29, 20.32; ESI-MS: m/z 441.3 $(M+1)^+$. Anal. Calcd. for $C_{24}H_{17}ClN_6O$: C, 65.38; H, 3.89; N, 19.06; found: C, 65.15; H, 4.11; N, 19.33.

*4.1.1.7. 9-((1-(7-Chloroquinolin-4-yl)-1H-1,2,3-triazol-4-yl)methyl)-7-methoxy-1-methyl-9H-pyrido [3,4-b]indole (**22**).* Alkyne **15**: 0.058 g; azide **2**: 0.052 g, mobile phase: cyclohexane/EtOAc/MeOH 1:1:0.5, DCM/MeOH 95:5; yield: 0.040 g, (38%); mp 235–237 °C; IR (ATR, ν/cm^{-1}) 3143, 1621, 1561, 1499, 1442, 1406, 1372, 1345, 1255, 1223, 1194, 1171, 1138, 1115, 1036, 931, 925, 876, 813, 722, 623, 554; ^{1}H NMR (DMSO-d_6) δ 9.09 (d, 1H, J = 4.7 Hz), 8.83 (s, 1H), 8.26 (d, 1H, J = 2.2 Hz), 8.20 (d, 1H, J = 5.2 Hz), 8.11 (d, 1H, J = 8.6 Hz), 7.95-7.88 (m, 2H), 7.78 (d, 1H, J = 4.7 Hz), 7.74 (dd, 1H, J = 9.1, 2.2 Hz), 7.42 (d, 1H, J = 2.2 Hz), 6.90 (dd, 1H, J = 8.6, 2.1 Hz), 6.05 (s, 2H), 3.92 (s, 3H), 3.13 (s, 3H); ^{13}C NMR (DMSO-d_6) δ 160.62, 152.29, 149.31, 144.79, 142.74, 141.17, 140.22, 138.15, 135.28, 134.75, 128.91, 128.62, 128.10, 125.34, 122.40, 120.31, 117.20, 114.51, 112.29, 109.48, 94.13, 55.66, 23.31; ESI-MS: m/z 455.3 $(M+1)^+$. Anal. Calcd. for $C_{25}H_{19}ClN_6O$: C, 66.01; H, 4.21; N, 18.47; found: C, 65.82; H, 4.37; N, 18.13.

*4.1.1.8. 7-Chloro-N-(2-(4-(((1-methyl-9H-pyrido [3,4-b]indol-6-yl)oxy)methyl)-1H-1,2,3-triazol-1-yl)ethyl)quinolin-4-amine (**23**).* Alkyne **11**: 0.054 g; azide **3**: 0.063 g, mobile phase: DCM/MeOH 7.5:2.5; yield: 0.048 g, (43%); mp 272–273 °C; IR (ATR, ν/cm^{-1}) 3201, 1608, 1583, 1544, 1498, 1456, 1429, 1383, 1365, 1352, 1330, 1248, 1207, 1170, 1061, 1139, 1050, 1026, 990, 909, 872, 845, 808, 765, 624, 492; ^{1}H NMR (DMSO-d_6) δ 11.43 (s, 1H), 8.41 (d, 1H, J = 5.4 Hz), 8.32 (s, 1H), 8.20 (d, 1H, J = 9.1 Hz), 8.16 (d, 1H, J = 5.3 Hz), 7.92-7.85 (m, 2H), 7.81 (d, 1H, J = 2.2 Hz), 7.54 (t, 1H, J = 5.8 Hz), 7.50 (d, 1H, J = 8.8 Hz), 7.44 (dd, 1H, J = 9.0, 2.3 Hz), 7.20 (dd, 1H, J = 8.8, 2.5 Hz), 6.57 (d, 1H, J = 5.5 Hz), 5.21 (s, 2H), 4.70 (t, 2H, J = 6.1 Hz), 3.82 (q, 2H, J = 5.9 Hz), 2.75 (s, 3H); ^{13}C NMR (DMSO-d_6) δ 151.99, 151.87, 149.76, 148.95, 142.97, 142.22, 136.93, 135.43, 135.09, 133.53, 127.47, 126.70, 124.96, 124.35, 124.00, 121.35, 118.28, 117.47, 112.76, 112.66, 105.00, 98.90, 61.91, 47.86, 42.46, 20.41; ESI-MS: m/z 484.1 $(M+1)^+$. Anal. Calcd. for $C_{26}H_{22}ClN_7O$: C, 64.53; H, 4.58; N, 20.26; found: C, 64.82; H, 4.32; N, 20.58.

*4.1.1.9. 7-Chloro-N-(2-(4-(((1-methyl-9H-pyrido [3,4-b]indol-7-yl)oxy)methyl)-1H-1,2,3-triazol-1-yl)ethyl)quinolin-4-amine (**24**).* Alkyne **13**: 0.054 g; azide **3**: 0.063 g, mobile phase: cyclohexane/EtOAc/MeOH 1:1:0.5; yield: 0.060 g, (54%); mp 238–241 °C; IR (ATR, ν/cm^{-1}) 3340, 3158, 3065, 2957, 1638, 1584, 1543, 1485, 1450, 1428, 1371, 1338, 1251, 1235, 1155, 1110, 1056, 874, 851, 813, 800, 761, 648, 858, 531; ^{1}H NMR (DMSO-d_6) δ 11.48 (s, 1H), 8.41 (d, 1H, J = 5.4 Hz), 8.32 (s, 1H), 8.19-8.15 (m, 2H), 8.05 (d, 1H, J = 8.6 Hz), 7.82-7.80 (m, 2H), 7.54 (t, 1H, J = 5.2 Hz), 7.45 (dd, 1H, J = 9.0, 2.3 Hz), 7.17 (d, 1H, J = 2.2 Hz), 6.88 (dd, 1H, J = 8.7, 2.3 Hz), 6.57 (d, 1H, J = 5.5 Hz), 5.25 (s, 2H), 4.70 (t, 2H, J = 5.8 Hz), 3.82 (q, 2H, J = 6.0 Hz), 2.73 (s, 3H); ^{13}C NMR (DMSO-d_6) δ 158.79, 151.77, 149.82, 148.82, 142.70, 141.82, 141.30, 137.65, 134.59, 133.60, 127.38, 127.18, 125.08, 124.40, 124.00, 122.64, 117.44, 115.10, 111.98, 109.42, 98.91, 95.82, 61.45, 47.90, 42.43, 20.29; ESI-MS: m/z 482.1 $(M-1)^-$. Anal. Calcd. for $C_{26}H_{22}ClN_7O$: C, 64.53; H, 4.58; N, 20.26; found: C, 64.75; H, 4.63; N, 19.98.

*4.1.1.10. 7-Chloro-N-(2-(4-((7-methoxy-1-methyl-9H-pyrido [3,4-b]indol-9-yl)methyl)-1H-1,2,3-triazol-1-yl)ethyl)quinolin-4-amine (**25**).* Alkyne **15**: 0.058 g; azide **3**: 0.063 g, mobile phase: DCM/MeOH 85:15, 8:2; yield: 0.076 g, (66%); mp 244–245.5 °C; IR (ATR, ν/cm^{-1}) 2957, 1619, 1578, 1495, 1441, 1428, 1403, 1369, 1355, 1324, 1252, 1224, 1193, 1171, 1082, 973, 926, 910, 875, 814, 764, 732, 641, 593, 462; ^{1}H NMR (DMSO-d_6) δ 8.31 (d, 1H, J = 5.4 Hz), 8.17 (d, 1H, J = 5.2 Hz), 8.08 (d, 1H, J = 8.6 Hz), 8.05 (d, 1H, J = 9.1 Hz), 7.98 (s, 1H), 7.87 (d, 1H, J = 5.2 Hz), 7.79 (d, 1H, J = 2.2 Hz), 7.44-7.37 (m, 2H), 7.26 (d, 1H, J = 2.1 Hz), 6.87 (dd, 1H, J = 8.6, 2.1 Hz), 6.45 (d, 1H, J = 5.5 Hz), 5.83 (s, 2H), 4.57 (t, 2H, J = 6.0 Hz), 3.83 (s, 3H), 3.70 (q, 2H, J = 5.9 Hz), 2.98 (s, 3H); ^{13}C NMR (DMSO-d_6) δ 160.52, 151.63, 149.73, 148.74, 143.88, 142.65, 141.07, 137.98, 134.60, 133.56, 128.49, 127.34, 124.35, 123.78, 123.47, 122.34, 117.33, 114.39, 112.23, 109.36, 98.77, 93.95, 55.53, 47.86, 42.34, 23.11; ESI-MS: m/z 496.1 $(M-1)^-$. Anal. Calcd. for $C_{27}H_{24}ClN_7O$: C, 65.12; H, 4.86; N, 19.69; found: C, 64.87; H, 4.92; N, 19.93.

General procedure for the synthesis of AT harmiquins **26** and **27**.

A solution of a harmine-based carboxylic acid **17** (0.050 g, 0.176 mmol), DIEA (0.061 mL, 0.352 mmol) and HATU (0.067 g, 0.176 mmol) in DCM (4 mL) was stirred at rt for 20 min, followed by the addition of amine **4** or **5** (0.160 mmol). The resulting solution was stirred at rt for 18 h. The formed precipitate was filtered off. After purification by column chromatography (DCM/MeOH 75:25) and trituration with diethyl ether compounds **26**, **27** were obtained.

*4.1.1.11. N-(2-((7-chloroquinolin-4-yl)amino)ethyl)-3-(7-methoxy-1-methyl-9H-pyrido [3,4-b]indol-9-yl)propanamide (**26**).* Amine **4**: 0.035 g; yield: 0.027 g, (35%); mp 224–227 °C; IR (ATR, ν/cm^{-1}) 3226, 3060, 2967, 1645, 1624, 1582, 1547, 1503, 1449, 1409, 1342, 1300, 1284, 1267, 1231, 1167, 1140, 1120, 1083, 1042, 1017, 976, 946, 872, 853, 827, 814, 801, 764, 636, 595, 567, 546, 474; ^{1}H NMR (DMSO-d_6) δ 8.40 (d, 1H, J = 5.4 Hz), 8.23 (t, 1H, J = 5.8 Hz), 8.20-8.12 (m, 2H), 8.05 (d, 1H, J = 8.6 Hz), 7.85 (d, 1H, J = 5.1 Hz), 7.79 (d, 1H, J = 2.2 Hz), 7.44 (dd, 1H, J = 9.0, 2.3 Hz), 7.31 (t, 1H, J = 5.5 Hz), 7.22 (d, 1H, J = 2.2 Hz), 6.85 (dd, 1H, J = 8.6, 2.2 Hz), 6.47 (d, 1H, J = 5.5 Hz), 4.82 (t, 2H, J = 7.2 Hz), 3.90 (s, 3H), 3.27 (q, 2H, J = 6.3 Hz), 3.17 (q, 2H, J = 5.9

Hz), 2.97 (s, 3H), 2.63 (t, 2H, $J = 7.2$ Hz); ^{13}C NMR (DMSO-d_6) δ 170.35, 160.43, 151.89, 149.97, 149.07, 142.51, 140.75, 137.90, 134.49, 133.40, 128.56, 127.52, 124.10, 123.94, 122.29, 117.42, 114.32, 112.21, 109.20, 98.57, 93.88, 55.52, 41.76, 40.87, 37.23, 36.34, 23.11; ESI-MS: *m/z* 488.1 $(M+1)^+$. Anal. Calcd. for $C_{27}H_{26}ClN_5O_2$: C, 66.46; H, 5.37; N, 14.35; found: C, 66.52; H, 5.25; N, 14.58.

*4.1.1.12. N-(4-((7-chloroquinolin-4-yl)amino)butyl)-3-(7-methoxy-1-methyl-9H-pyrido [3,4-b]indol-9-yl)propanamide (**27**).* Amine **5**: 0.040 g; yield: 0.036 g, (43%); mp 230–233 °C; IR (ATR, ν/cm^{-1}) 3306, 2936, 1642, 1624, 1577, 1499, 1448, 1408, 1366, 1330, 1305, 1227, 1205, 1166, 1187, 1119, 1046, 883, 849, 810, 546; ^{1}H NMR (DMSO-d_6) δ 8.39 (d, 1H, $J = 5.6$ Hz), 8.31 (d, 1H, $J = 9.0$ Hz), 8.16 (d, 1H, $J = 5.2$ Hz), 8.06 (d, 1H, $J = 8.6$ Hz), 7.96 (t, 1H, $J = 5.6$ Hz), 7.86 (d, 1H, $J = 5.2$ Hz), 7.79 (d, 1H, $J = 2.3$ Hz), 7.54-7.40 (m, 2H), 7.20 (d, 1H, $J = 2.2$ Hz), 6.85 (dd, 1H, $J = 8.6$, 2.1 Hz), 6.43 (d, 1H, $J = 5.6$ Hz), 4.79 (t, 2H, $J = 7.1$ Hz), 3.90 (s, 3H), 3.23-3.13 (m, 2H), 3.04 (q, 2H, $J = 6.5$ Hz), 2.97 (s, 3H), 2.60 (t, 2H, $J = 7.0$ Hz), 1.53-1.43 (m, 2H), 1.36 (q, 2H, $J = 7.2$ Hz); ^{13}C NMR (DMSO-d_6) δ 169.59, 160.42, 151.10, 150.48, 148.19, 142.54, 140.71, 137.75, 134.48, 133.71, 128.57, 126.73, 124.28, 124.17, 122.26, 117.27, 114.26, 112.22, 109.21, 98.57, 93.91, 55.50, 42.01, 40.96, 38.17, 36.37, 26.49, 24.98, 23.04; ESI-MS: *m/z* 516.4 $(M+1)^+$. Anal. Calcd. for $C_{29}H_{30}ClN_5O_2$: C, 67.50; H, 5.86; N, 13.57; found: C, 67.38; H, 5.71; N, 13.25.

*4.1.1.13. General procedure for the synthesis of AT harmiquins **28**–**32**.* A suspension of a 7-chloroquinoline-based carboxylic acid **22** (0.050 g, 0.211 mmol), amine **8**, **10**, **12**, **14**, **16** (0.192 mmol) and TEA (0.059 mL, 0.422 mmol) in DMF (2 mL) was stirred at rt for 10 min, followed by the dropwise addition of T3P (≥50% in ethyl acetate, 0.126 mL, 0.211 mmol). The reaction mixture was stirred at rt for 18 h. Afterwards, the reaction mixture was placed in an ultrasonic bath and 5% NaOH was added dropwise until the formation of white precipitate was completed. The formed precipitate was filtered off and the crude product purified by column chromatography (DCM/MeOH 85:15). After trituration with diethyl ether, compounds **28**–**32** were obtained.

*4.1.1.14. N-((9H-pyrido [3,4-b]indol-1-yl)methyl)-2-((7-chloroquinolin-4-yl)amino)acetamide (**28**).* Amine **8**: 0.038 g; yield: 0.034 g, (42%); mp 244–247 °C; IR (ATR, ν/cm^{-1}) 3267, 1651, 1627, 1585, 1451, 1431, 1323, 1284, 1235, 1151, 1126, 1082, 1023, 986, 902, 871, 853, 742, 578, 563, 519; ^{1}H NMR (DMSO-d_6) δ 11.54 (s, 1H), 8.79 (t, 1H, $J = 5.5$ Hz), 8.34 (d, 1H, $J = 5.4$ Hz), 8.28-8.25 (m, 2H), 8.22 (d, 1H, $J = 7.9$ Hz), 8.03 (d, 1H, $J = 5.2$ Hz), 7.83 (t, 1H, $J = 6.5$ Hz), 7.81 (d, 1H, $J = 2.3$ Hz), 7.59 (d, 1H, $J = 8.2$ Hz), 7.56-7.53 (m, 1H), 7.50 (dd, 1H, $J = 9.0$, 2.3 Hz), 7.26-7.23 (m, 1H), 6.40 (d, 1H, $J = 5.4$ Hz), 4.81 (d, 2H, $J = 5.4$ Hz), 4.07 (d, 2H, $J = 6.0$ Hz); ^{13}C NMR (DMSO-d_6) δ 169.38, 151.63, 150.35, 148.74, 141.33, 140.40, 137.30, 133.56, 133.36, 128.14, 127.74, 127.36, 124.41, 124.23, 121.76, 120.83, 119.42, 117.56, 113.89, 112.03, 99.44, 45.81, 41.48; ESI-MS: *m/z* 416.1 $(M+1)^+$. Anal. Calcd. for $C_{23}H_{18}ClN_5O$: C, 66.43; H, 4.36; N, 16.84; found: C, 66.55; H, 4.58; N, 16.51.

*4.1.1.15. 2-((7-Chloroquinolin-4-yl)amino)-N-((1-methyl-9H-pyrido [3,4-b]indol-3-yl)methyl)acetamide (**29**).* Amine **10**: 0.041 g; yield: 0.023 g, (28%); mp 274.5–277 °C; IR (ATR, ν/cm^{-1}) 3616, 3285, 1662, 1629, 1587, 1502, 1453, 1431, 1375, 1328, 1234, 1150, 1083, 1014, 901, 851, 801, 737; ^{1}H NMR (DMSO-d_6) δ 11.48 (s, 1H), 8.71 (t, 1H, $J = 5.9$ Hz), 8.44 (d, 1H, $J = 5.4$ Hz), 8.29 (d, 1H, $J = 9.0$ Hz), 8.05 (d, 1H, $J = 7.8$ Hz), 7.90-7.79 (m, 2H), 7.71 (s, 1H), 7.60-7.46 (m, 3H), 7.26-7.19 (m, 1H), 6.47 (d, 1H, $J = 5.4$ Hz), 4.52 (d, 2H, $J = 5.8$ Hz), 4.07 (d, 2H, $J = 6.0$ Hz), 2.70 (s, 3H); ^{13}C NMR (DMSO-d_6) δ 168.98, 151.79, 150.26, 148.97, 146.08, 141.11, 140.73, 133.51, 133.45, 127.82, 127.65, 127.46, 124.32, 121.46, 120.94, 119.13, 117.63, 111.95, 109.34, 99.28, 46.01, 44.21, 20.24; ESI-MS: *m/z* 430.1 $(M+1)^+$. Anal. Calcd. for $C_{24}H_{20}ClN_5O$: C, 67.05; H, 4.69; N, 16.29; found: C, 66.85; H, 4.84; N, 16.08.

*4.1.1.16. 2-((7-Chloroquinolin-4-yl)amino)-N-(2-((1-methyl-9H-pyrido [3,4-b]indol-6-yl)oxy)ethyl)acetamide (**30**).* Amine **12**: 0.046 g; yield: 0.023 g, (26%); mp 304–307 °C; IR (ATR, ν/cm^{-1}) 3525, 3369, 3219, 3145, 3054, 2874, 1679, 1581, 1530, 1505, 1485, 1452, 1372, 1334, 1287, 1240, 1213, 1116, 1075, 990, 877, 854, 810, 793, 629, 614, 488, 467; ^{1}H NMR (DMSO-d_6) δ 11.41 (s, 1H), 8.41 (t, 1H, $J = 5.7$ Hz), 8.29 (d, 1H, $J = 5.4$ Hz), 8.27 (d, 1H, $J = 9.1$ Hz), 8.15 (d, 1H, $J = 5.3$ Hz), 7.88 (d, 1H, $J = 5.3$ Hz), 7.82 (t, 1H, $J = 6.4$ Hz), 7.81 (d, 1H, $J = 2.3$ Hz), 7.73 (d, 1H, $J = 2.5$ Hz), 7.52-7.48 (m, 2H), 7.15 (dd, 1H, $J = 8.8$, 2.5 Hz), 6.31 (d, 1H, $J = 5.4$ Hz), 4.10 (t, 2H, $J = 5.6$ Hz), 3.98 (d, 2H, $J = 5.9$ Hz), 3.54 (q, 2H, $J = 5.6$ Hz), 2.74 (s, 3H); ^{13}C NMR (DMSO-d_6) δ 169.14, 152.30, 151.54, 150.39, 148.64, 142.18, 136.88, 135.36, 135.08, 133.57, 127.24, 126.70, 124.36, 124.26, 121.37, 118.23, 117.52, 112.73, 112.69, 104.77, 99.15, 66.99, 45.80, 38.50, 20.39; ESI-MS: *m/z* 460.0 $(M+1)^+$. Anal. Calcd. for $C_{25}H_{22}ClN_5O_2$: C, 65.29; H, 4.82; N, 15.23; found: C, 65.02; H, 4.73; N, 15.53.

*4.1.1.17. 2-((7-Chloroquinolin-4-yl)amino)-N-(2-((1-methyl-9H-pyrido [3,4-b]indol-7-yl)oxy)ethyl)acetamide (**31**).* Amine **14**: 0.046 g; yield: 0.026 g, (30%); mp 275–277.5 °C; IR (ATR, ν/cm^{-1}) 3641, 3284, 3093, 1659, 1631, 1612, 1587, 1487, 1431, 1376, 1328, 1274, 1232, 1178, 1148, 1109, 1056, 974, 903, 878, 852, 801, 569; ^{1}H NMR (DMSO-d_6) δ 11.54 (s, 1H), 8.46 (t, 1H, $J = 5.7$ Hz), 8.30-8.28 (m, 2H), 8.16 (d, 1H, $J = 5.3$ Hz), 8.06 (d, 1H, $J = 8.6$ Hz), 7.92 (t, 1H, $J = 6.1$ Hz), 7.82 (d, 1H, $J = 5.3$ Hz), 7.81 (d, 1H, $J = 2.3$ Hz), 7.50 (dd, 1H, $J = 9.0$, 2.3 Hz), 7.02 (d, 1H, $J = 2.2$ Hz), 6.83 (dd, 1H, $J = 8.6$, 2.2 Hz), 6.32 (d, 1H, $J = 5.5$ Hz), 4.12 (t, 2H, $J = 5.6$ Hz), 3.99 (d, 2H, $J = 5.9$ Hz), 3.55 (q, 2H, $J = 5.6$ Hz), 2.74 (s, 3H); ^{13}C NMR (DMSO-d_6) δ 169.16, 159.20, 151.28, 150.57, 148.37, 141.96, 141.23, 137.51, 134.57, 133.69, 127.28, 127.01, 124.42, 124.35, 122.68, 117.48, 114.98, 112.00, 109.35, 99.13, 95.41, 66.42, 45.78, 38.38, 20.27; ESI-MS: *m/z* 460.1 $(M+1)^+$. Anal. Calcd. for $C_{25}H_{22}ClN_5O_2$: C, 65.29; H, 4.82; N, 15.23; found: C, 65.45; H, 4.75; N, 14.98.

*4.1.1.18. 2-((7-Chloroquinolin-4-yl)amino)-N-(2-(7-methoxy-1-methyl-9H-pyrido [3,4-b]indol-9-yl)ethyl)acetamide (**32**).* Amine **16**: 0.049 g; yield: 0.032 g, (35%); mp 252.5–255 °C; IR (ATR, ν/cm^{-1}) 3268, 3063, 1656, 1625, 1582, 1445, 1408, 1375, 1343, 1280, 1251, 1198, 1174, 1140, 1081, 1047, 1025, 976, 809, 639, 597, 569; ^{1}H NMR (DMSO-d_6) δ 8.37 (t, 1H, $J = 6.0$ Hz), 8.31 (d, 1H, $J = 5.3$ Hz), 8.24 (d, 1H, $J = 9.0$ Hz), 8.16 (d, 1H, $J = 5.2$ Hz), 8.10 (d, 1H, $J = 8.6$ Hz), 7.87 (d, 1H, $J = 5.1$ Hz), 7.81 (d, 1H, $J = 2.3$ Hz), 7.74 (t, 1H, $J = 6.1$ Hz), 7.49 (dd, 1H, $J = 9.0$, 2.3 Hz), 7.28 (d, 1H, $J = 2.2$ Hz), 6.89 (dd, 1H, $J = 8.6$, 2.2 Hz), 6.07 (d, 1H, $J = 5.4$ Hz), 4.58 (t, 2H, $J = 7.1$ Hz), 3.90 (s, 3H), 3.85 (d, 2H, $J = 6.0$ Hz), 3.52 (q, 2H, $J = 6.8$ Hz), 2.96 (s, 3H); ^{13}C NMR (DMSO-d_6) δ 169.63, 160.57, 151.91, 150.13, 148.95, 142.90, 140.62, 137.87, 134.64, 133.50, 128.43, 127.53, 124.36, 124.22, 122.48, 117.56, 114.31, 112.30, 109.25, 98.97, 93.63, 55.57, 45.97, 43.29, 38.84, 23.14; ESI-MS: *m/z* 474.1 $(M+1)^+$. Anal. Calcd. for $C_{26}H_{24}ClN_5O_2$: C, 65.89; H, 5.10; N, 14.78; found: C, 65.76; H, 4.99; N, 15.01.

4.2. In vitro drug sensitivity assay against erythrocytic stages of P. Falciparum

Antiplasmodial activity of harmiquins **18**–**32** was evaluated against four laboratory *P. falciparum* strains (3D7 – CQ-sensitive, Dd2 and K1 – multidrug-resistant, 7G8 – CQ-resistant), as previously described, using the histidine-rich protein 2 (HRP2) assay [46,47]. Briefly, 96-well plates were pre-coated with the tested compounds in a three-fold dilution before ring-stage parasites were added to the complete culture medium at a hematocrit of 1.5% and a parasitaemia of 0.05%. After three days of

incubation at 37 °C, 5% CO_2 and 5% oxygen, plates were frozen until analyzed by HRP2-ELISA. All compounds were evaluated in duplicate in at least two independent experiments. The IC_{50} was determined by nonlinear regression analysis of log concentration-response curves using the drc-package v0.9.0 of R v2.6.1 [48].

4.3. In vitro cytotoxicity assay

Cytotoxicity against a human cell line (HepG2) was evaluated using the neutral red assay [56] with minor modifications [57]. In brief, human cells were seeded to a 96 well plate in a complete culture medium; on the following day, a serial dilution of the respective compound was added. After one day of incubation, cytotoxicity was evaluated by the addition of Neutral Red, subsequent lysis of cells and measurement of absorbance (540 nm) in a plate reader (CLARIOstar, BMG Labtech). The IC_{50} was determined similarly to the *in vitro* drug assay against *P. falciparum*. To assess the safety of a compound, SI was calculated as the fractional ratio between the IC_{50}s for HepG2 and *P. falciparum* 3D7 strain.

4.4. Inhibition of heme polymerization

The inhibition assay of heme polymerization was performed as previously described [49]. 50 μL solution of hemin chloride in DMSO (5.2 mg/mL) was added per well in a standard 96-well microtiter plate, followed by the addition of test compounds dissolved in DMSO (50 μL) at different concentration levels (0.1–4 mM). Chloroquine diphosphate was used as the positive control, whereas the negative control was DMSO. β-hematin formation was initiated by the addition of acetate buffer 0.2 M (100 μL, pH 4.4). Plates were incubated at 37 °C for 48 h, then centrifuged at 1500 rcf (Eppendorf® Centrifuge 5804/5804R) for 20 min. The supernatant was removed, and the precipitate was washed three times with DMSO (200 μL) and once with distilled water (200 μL). Each washing was followed by centrifugation at 1500 rcf for 20 min and removal of the supernatant. Finally, the obtained precipitate was dissolved in 0.2 M aq. NaOH (200 mL), and solubilized aggregates were further diluted 1:6 with 0.1 M aq NaOH. Absorbance was recorded at 405 nm with a microplate reader (VICTOR3, PerkinElmer).

4.5. Computational details

The starting point of our molecular dynamics simulations was a P*f*Hsp90 *N*-terminal domain structure obtained from the Protein Data Bank (accession code 3K60). Ligands (ADP and SO_4^{2-}) and original crystal waters were removed from the structure and selected compounds were placed within the protein binding pocket with the help of molecular docking simulations. For that purpose, we used SwissDock [58], a web server for docking small molecules on the target proteins based on the EADock DSS engine, while taking into account the entire protein surface as potential binding sites for the investigated ligands. Following the docking analysis, the identified best binding positions were utilized as a starting point for the subsequent molecular dynamics simulations.

In order to parameterise the investigated ligands, geometry optimization and RESP charge calculations were performed with the Gaussian 16 program [59] at the HF/6–31G(d) level to be consistent with the employed GAFF force field, while the P*f*Hsp90 protein was modelled using the AMBER ff14SB force field. Such protein complexes were solvated in a truncated octahedral box of TIP3P water molecules spanning a 10 Å-thick buffer, neutralized by Na^+ ions and submitted to geometry optimization in the AMBER 16 program [60] by employing periodic boundary conditions in all directions. Optimized systems were gradually heated from 0 to 300 K and equilibrated during 30 ps using NVT conditions, followed by productive and unconstrained MD simulations of 300 ns by employing a time step of 2 fs at constant pressure (1 atm) and temperature (300 K), with the latter held constant using a Langevin thermostat with a collision frequency of 1 ps^{-1}. Bonds involving hydrogen atoms were constrained using the SHAKE algorithm, while the long-range electrostatic interactions were calculated employing the Particle Mesh Ewald method. The nonbonded interactions were truncated at 10.0 Å.

The binding free energies, ΔG_{BIND}, of each ligand were calculated using the established MM-GBSA protocol [61,62] available in AmberTools16 [59], and in line with our earlier reports [21–23]. For that purpose, 1.000 snapshots collected from the last 30 ns of the corresponding MD trajectories were utilized. The calculated MM-GBSA binding free energies were decomposed into specific residue contributions on a *per-residue* basis according to the established procedure [63,64]. This protocol calculates contributions to ΔG_{BIND} arising from each amino acid residue and identifies the nature of the energy change in terms of interaction and solvation energies or entropic contributions.

Declaration of competing interest

The authors declare that they have no known competing financial interests or personal relationships that could have appeared to influence the work reported in this paper.

Acknowledgement

The authors acknowledge the financial support by the Croatian Science Foundation (research project UIP-2017-05-5160), University of Zagreb (support for 2020), and Fundação para a Ciência e Tecnologia (grant 02/SAICT/2017/29550). This work has been supported in part by project Strengthening the scientific research and innovation capacities of the Faculty of Pharmacy and Biochemistry, University of Zagreb (FarmInova; project number KK.01.1.1.02.0021), financed from the European Regional Development Fund, Operational Program Competitiveness and Cohesion for the period 2014–2020. T.T. and R.V. would like to thank the Zagreb University Computing Centre (SRCE) for granting computational resources on the ISABELLA cluster. T.T. and R. V. would like to thank the Zagreb University Computing Centre (SRCE) for granting computational resources on the ISABELLA cluster.

Abbreviations

ADMP	2-azido-1,3-dimethyl-imidazolinium hexafluorophosphate
AT	amide-type
ATR	attenuated total reflection
Boc	*tert*-butyloxycarbonyl
CQ	chloroquine
DBU	1,8-diazabicyclo(5.4.0)undec-7-ene
DCM	dichloromethane
DIEA	*N,N*-diisopropylethylamine
DMF	*N,N*-dimethylformamide
ESI	electrospray ionization
ΔG_{BIND}	binding free energies
HAR	harmine
HATU	1-[bis(dimethylamino)methylene]-1*H*-1,2,3-triazolo[4,5-*b*] pyridinium-3-oxidhexafluorophosphate
HEPES	2-(4-(2-hydroxyethyl)piperazin-1-yl)ethanesulfonic acid
HepG2	human liver hepatocellular carcinoma cell line
hpi	hours post infection
HRP2	histidine-rich protein 2
IC_{50}	the concentration of the tested compound necessary for 50% growth inhibition
MD	molecular dynamics
*Pf*3D7	chloroquine-sensitive strain of *P. falciparum*
*Pf*Dd2 and *Pf*K1	multidrug resistant strains of *P. falciparum*
*Pf*7G8	chloroquine-resistant strain of *P. falciparum*
*Pf*Hsp90	*P. falciparum* heat shock protein 90
SI	selectivity index
TEA	triethylamine

T3P	propylphosphonic anhydride
TMS	tetramethylsilane
TT	triazole-type
TWC	total wavelength chromatogram

Appendix A. Supplementary data

Supplementary data to this article can be found online at https://doi.org/10.1016/j.ejmech.2022.114408.

References

[1] World Malaria Report 2021, World Health Organisation, 2021.
[2] M. Mishra, V.K. Mishra, V. Kashaw, A.K. Iyer, S.K. Kashaw, Comprehensive review on various strategies for antimalarial drug discovery, Eur. J. Med. Chem. 125 (2017) 1300–1320, https://doi.org/10.1016/j.ejmech.2016.11.025.
[3] E. Fernández-Álvaro, W.D. Hong, G.L. Nixon, P.M. O'Neill, F. Calderón, Antimalarial chemotherapy: natural product inspired development of preclinical and clinical candidates with diverse mechanisms of action, J. Med. Chem. 59 (2016) 5587–5603, https://doi.org/10.1021/acs.jmedchem.5b01485.
[4] X.-Z. Su, K.D. Lane, L. Xia, J.M. Sá, T.E. Wellems, *Plasmodium* genomics and genetics: new insights into malaria pathogenesis, drug resistance, epidemiology, and evolution, Clin. Microbiol. Rev. 32 (2019), e00019, https://doi.org/10.1128/CMR.00019-19, 19.
[5] E.M. Guantai, K. Ncokazi, T.J. Egan, J. Gut, P.J. Rosenthal, P.J. Smith, K. Chibale, Design, synthesis and *in vitro* antimalarial evaluation of triazole-linked chalcone and dienone hybrid compounds, Bioorg. Med. Chem. 18 (2010) 8243–8256, https://doi.org/10.1016/j.bmc.2010.10.009.
[6] S. Kapishnikov, T. Staals, Y. Yang, J. Lee, A.J. Pérez-Berná, E. Pereiro, Y. Yang, S. Werner, P. Guttmann, L. Leiserowitz, J. Als-Nielsen, Mode of action of quinoline antimalarial drugs in red blood cells infected by *Plasmodium falciparum* revealed *in vivo*, Proc. Natl. Acad. Sci. U.S.A. 116 (2019) 22946–22952, https://doi.org/10.1073/pnas.1910123116.
[7] A.F.G. Slater, Chloroquine: mechanism of drug action and resistance in *Plasmodium falciparum*, Pharmacol. Ther. 57 (1993) 203–235, https://doi.org/10.1016/0163-7258(93)90056-J.
[8] D. Shahinas, A. Folefoc, D.R. Pillai, Targeting *Plasmodium falciparum* Hsp90: towards reversing antimalarial resistance, Pathogens 2 (2013) 33–54, https://doi.org/10.3390/pathogens2010033.
[9] J. Kim, Y.Z. Tan, K.J. Wicht, S.K. Erramilli, S.K. Dhingra, J. Okombo, J. Vendome, L.M. Hagenah, S.I. Giacometti, A.L. Warren, K. Nosol, P.D. Roepe, C.S. Potter, B. Carragher, A.A. Kossiakoff, M. Quick, D.A. Fidock, F. Mancia, Structure and drug resistance of the *Plasmodium falciparum* transporter *Pf*CRT, Nature 576 (2019) 315–320, https://doi.org/10.1038/s41586-019-1795-x.
[10] J.F. Trape, The public health impact of chloroquine resistance in Africa, Am. J. Trop. Med. Hyg. 64 (2001) 12–17, https://doi.org/10.4269/ajtmh.2001.64.12.
[11] S. Agrawal, K.A. Moser, L. Morton, M.P. Cummings, A. Parihar, A. Dwivedi, A. C. Shetty, E.F. Drabek, C.G. Jacob, P.P. Henrich, C.M. Parobek, K. Jongsakul, R. Huy, M.D. Spring, C.A. Lanteri, S. Chaorattanakawee, C. Lon, M.M. Fukuda, D. L. Saunders, D.A. Fidock, J.T. Lin, J. Juliano, C.V. Plowe, J.C. Silva, S. Takala-Harrison, Association of a novel mutation in the *Plasmodium falciparum* chloroquine resistance transporter with decreased piperaquine sensitivity, J. Infect. Dis. 216 (2017) 468–476, https://doi.org/10.1093/infdis/jix334.
[12] H. Ledford, Malaria vaccine shows promise — now come tougher trials, Nature 593 (2021), https://doi.org/10.1038/d41586-021-01096-7, 17–17.
[13] K. Kaur, M. Jain, R.P. Reddy, R. Jain, Quinolines and structurally related heterocycles as antimalarials, Eur. J. Med. Chem. 45 (2010) 3245–3264, https://doi.org/10.1016/j.ejmech.2010.04.011.
[14] P.N. Kalaria, S.C. Karad, D.K. Raval, A review on diverse heterocyclic compounds as the privileged scaffolds in antimalarial drug discovery, Eur. J. Med. Chem. 158 (2018) 917–936, https://doi.org/10.1016/j.ejmech.2018.08.040.
[15] V. Srivastava, H. Lee, Chloroquine-based hybrid molecules as promising novel chemotherapeutic agents, Eur. J. Pharmacol. 762 (2015) 472–486, https://doi.org/10.1016/j.ejphar.2015.04.048.
[16] Y.Q. Hu, C. Gao, S. Zhang, L. Xu, Z. Xu, L.S. Feng, X. Wu, F. Zhao, Quinoline hybrids and their antiplasmodial and antimalarial activities, Eur. J. Med. Chem. 139 (2017) 22–47, https://doi.org/10.1016/j.ejmech.2017.07.061.
[17] P.M. Njogu, J. Gut, P.J. Rosenthal, K. Chibale, Design, synthesis, and antiplasmodial activity of hybrid compounds based on (2*R*,3*S*)-*N*-Benzoyl-3-phenylisoserine, ACS Med. Chem. Lett. 4 (2013) 637–641, https://doi.org/10.1021/ml400164t.
[18] S. Kumar, A. Saini, J. Gut, P.J. Rosenthal, R. Raj, V. Kumar, 4-Aminoquinoline-chalcone-*N*-acetylpyrazoline conjugates: synthesis and antiplasmodial evaluation, Eur. J. Med. Chem. 138 (2017) 993–1001, https://doi.org/10.1016/j.ejmech.2017.07.041.
[19] X. Nqoro, N. Tobeka, B.A. Aderibigbe, Quinoline-based hybrid compounds with antimalarial activity, Molecules 22 (2017) 2268, https://doi.org/10.3390/molecules22122268.
[20] A. Uddin, M. Chawla, I. Irfan, S. Mahajan, S. Singhb, M. Abid, Medicinal chemistry updates on quinoline- and endoperoxide-based hybrids with potent antimalarial activity, RSC Med. Chem. 12 (2021) 24–42, https://doi.org/10.1039/D0MD00244E.
[21] I. Perković, S. Raić-Malić, D. Fontinha, M. Prudêncio, L. Pessanha de Carvalho, J. Held, T. Tandarić, R. Vianello, B. Zorc, Z. Rajić, Harmicines - harmine and cinnamic acid hybrids as novel antiplasmodial hits, Eur. J. Med. Chem. 187 (2020), 111927, https://doi.org/10.1016/j.ejmech.2019.111927.
[22] M. Marinović, I. Perković, D. Fontinha, M. Prudencio, J. Held, L.P. de Carvalho, T. Tandarić, R. Vianello, B. Zorc, Z. Rajić, Novel harmicines with improved potency against *Plasmodium*, Molecules 25 (2020) 4376, https://doi.org/10.3390/molecules25194376.
[23] M. Marinović, G. Poje, I. Perković, D. Fontinha, M. Prudêncio, J. Held, L. Pessanha de Carvalho, T. Tandarić, R. Vianello, Z. Rajić, Further investigation of harmicines as novel antiplasmodial agents: synthesis, structure-activity relationship and insight into the mechanism of action, Eur. J. Med. Chem. 224 (2021), 113687, https://doi.org/10.1016/j.ejmech.2021.113687.
[24] A. Kamboj, B. Sihag, D.S. Brar, A. Kaur, D.B. Salunke, Structure activity relationship in β-carboline derived anti-malarial agents, Eur. J. Med. Chem. 221 (2021), 113536, https://doi.org/10.1016/j.ejmech.2021.113536.
[25] S.T.S. Chan, A. Norrie Pearce, M.J. Page, M. Kaiser, B.R. Copp, Antimalarial β-carbolines from the New Zealand Ascidian *Pseudodistoma opacum*, Nat. Prod. 74 (2011) 1972–1979, https://doi.org/10.1021/np200509g.
[26] D. Shahinas, G. Macmullin, C. Benedict, I. Crandall, D.R. Pillai, Harmine is a potent antimalarial targeting Hsp90 and synergises with chloroquine and artemisinin, Antimicrob. Agents Chemother. 56 (2012) 4207–4213, https://doi.org/10.1128/AAC.00328-12.
[27] D. Shahinas, M. Liang, A. Datti, D.R. Pillai, A repurposing strategy identifies novel synergistic inhibitors of *Plasmodium falciparum* heat shock protein 90, J. Med. Chem. 53 (2010) 3552–3557, https://doi.org/10.1021/jm901796s.
[28] T. Wang, P. Maser, D. Picard, Inhibition of *Plasmodium falciparum* Hsp90 contributes to the antimalarial activities of aminoalcohol-carbazoles, J. Med. Chem. 59 (2016) 6344–6352, https://doi.org/10.1021/acs.jmedchem.6b00591.
[29] A.G. Bayih, A. Folefoc, A.N. Mohon, S. Eagon, M. Anderson, D.R. Pillai, *In vitro* and *in vivo* anti-malarial activity of novel harmine-analog heat shock protein 90 inhibitors: a possible partner for artemisinin, Malar. J. 15 (2016) 579, https://doi.org/10.1186/s12936-016-1625-7.
[30] M.L. Stofberg, C. Caillet, M. de Villiers, T. Zininga, Inhibitors of the *Plasmodium falciparum* Hsp90 towards selective antimalarial drug design: the past, present and future, Cells 10 (2021) 2849, https://doi.org/10.3390/cells10112849.
[31] S. Raić-Malić, A. Meščić, Recent trends in 1,2,3-triazolo-nucleosides as promising anti-infective and anticancer agents, Curr. Med. Chem. 22 (2015) 1462–1499. https://doi:10.2174/0929867322666150227150127.
[32] G.C. Tron, T. Pirali, R.A. Billington, P.L. Canonico, G. Sorba, A.A. Genazzani, Click chemistry reactions in medicinal chemistry: applications of the 1,3-dipolar cycloaddition between azides and alkynes, Med. Res. Rev. 28 (2008) 278–308, https://doi.org/10.1002/med.20107.
[33] S.G. Agalave, S.R. Maujan, V.S. Pore, Click chemistry: 1,2,3-triazoles as pharmacophores, Chem. Asian J. 6 (2011) 2696–2718, https://doi.org/10.1002/asia.201100432.
[34] X.M. Chu, C. Wang, W.L. Wang, L.L. Liang, W. Liu, K.K. Gong, K.L. Sun, Triazole derivatives and their antiplasmodial and antimalarial activities, Eur. J. Med. Chem. 166 (2019) 206–223, https://doi.org/10.1016/j.ejmech.2019.01.047.
[35] E. Bonandi, M.S. Christodoulou, G. Fumagalli, D. Perdicchia, G. Rastelli, D. Passarella, The 1,2,3-triazole ring as a bioisostere in medicinal chemistry, Drug Discov. Today 22 (2017) 1572–1581, https://doi.org/10.1016/j.drudis.2017.05.014.
[36] P. Thirumurugan, D. Matosiuk, K. Jozwiak, Click Chemistry for drug development and diverse chemical–biology applications, Chem. Rev. 113 (2013) 4905–4979, https://doi.org/10.1021/cr200409f.
[37] M.V. de Souza, K.C. Pais, C.R. Kaiser, M.A. Peralta, M. de Ferreira, M.C. Lourenço, Synthesis and *in vitro* antitubercular activity of a series of quinoline derivatives, Bioorg. Med. Chem. 17 (2009) 1474–1480, https://doi.org/10.1016/j.bmc.2009.01.013.
[38] P. Coghi, J.P.L. Ng, A.A. Nasim, V.K.W. Wong, *N*-[7-Chloro-4-[4-(phenoxymethyl)-1*H*-1,2,3-triazol-1-yl]quinoline]-acetamide, Molbank 2021 (2021) M1213, https://doi.org/10.3390/M1213.
[39] M. Beus, D. Fontinha, J. Held, Z. Rajić, L. Uzelac, M. Kralj, M. Prudêncio, B. Zorc, Primaquine and chloroquine fumardiamides as promising antiplasmodial agents, Molecules 24 (2019) 2812, https://doi.org/10.3390/molecules24152812.
[40] K. Starčević, D. Pešić, A. Toplak, G. Landek, S. Alihodžić, E. Herreros, S. Ferrer, R. Spaventi, M. Perić, Novel hybrid molecules based on 15-membered azalide as potential antimalarial agents, Eur. J. Med. Chem. 49 (2012) 365–378, https://doi.org/10.1016/j.ejmech.2012.01.039.
[41] S. Eagon, M.O. Anderson, Microwave-assisted synthesis of tetrahydro-β-carbolines and β-carbolines, Eur. J. Org Chem. (2014) 1653–1665, https://doi.org/10.1002/ejoc.201301580, 2014.
[42] N. Devi, D. Singh, Honey, S. Mor, S. Chaudhary, R.K. Rawal, V. Kumar, A. K. Chowdhury, V. Singh, In(OTf)$_3$ catalysed an expeditious synthesis of β-carboline-imidazo[1,2-*a*] pyridine and imidazo[1,2-*a*] pyrazine conjugates, RSC Adv. 6 (2016) 43881–43891, https://doi.org/10.1039/c6ra04841b.
[43] D. Singh, C.K. Hazra, C.C. Malakar, S.K. Pandey, B.S. Kaith, V. Singh, Indium-mediated domino allylation-lactonisation approach: Diastereoselective synthesis of β-carboline C-3 tethered α-methylene γ-butyrolactones, ChemistrySelect 3 (2018) 4859–4864, https://doi.org/10.1002/slct.201800006.
[44] B. Bálint, C. Wéber, F. Cruzalegui, M. Burbridge, A. Kotschy, Structure-based design and synthesis of harmine derivatives with different selectivity profiles in kinase versus monoamine oxidase inhibition, ChemMedChem 12 (2017) 932–939, https://doi.org/10.1002/cmdc.201600539.

[45] Chemicalize ChemAxon. https://chemicalize.com/, 2018. (Accessed 30 July 2021).
[46] J. Held, T. Gebru, M. Kalesse, R. Jansen, K. Gerth, R. Müller, B. Mordmüller, Antimalarial activity of the myxobacterial macrolide chlorotonil A, Antimicrob. Agents Chemother. 58 (2014) 6378–6384, https://doi.org/10.1128/AAC.03326-14.
[47] H. Noedl, J. Bronnert, K. Yingyuen, B. Attlmayr, H. Kollaritsch, M. Fukuda, Simple histidine-rich protein 2 double-site sandwich enzyme-linked immunosorbent assay for use in malaria drug sensitivity testing, Antimicrob, Agents Chemother 49 (2005) 3575–3577, https://doi.org/10.1128/AAC.49.8.3575-3577.2005.
[48] R Core Team, A Language and Environment for Statistical Computing, R foundation for statistical computing, Vienna, Austria, 20 December 2021 available from: https://www.R-project.org/.
[49] K.N. Olafson, M.A. Ketchum, J.D. Rimer, P.G. Vekilov, Mechanisms of hematin crystallization and inhibition by the antimalarial drug chloroquine, Proc. Natl. Acad. Sci. U.S.A. 112 (2015) 4946–4951, https://doi.org/10.1073/pnas.1501023112.
[50] B.C. Pérez, C. Teixeira, M. Figueiras, J. Gut, P.J. Rosenthal, J.R. Gomes, P. Gomes, Novel cinnamic acid/4-aminoquinoline conjugates bearing non-proteinogenic amino acids: towards the development of potential dual action antimalarials, Eur. J. Med. Chem. 54 (2012) 887–899, https://doi.org/10.1016/j.ejmech.2012.05.022.
[51] K.D. Corbett, J.M. Berger, Structure of the ATP-binding domain of *Plasmodium falciparum* Hsp90, Proteins 78 (2010) 2738–2744, https://doi.org/10.1002/prot.22799.
[52] S.M. Roe, C. Prodromou, R. O'Brien, J.E. Ladbury, P.W. Piper, L.H. Pearl, Structural basis for inhibition of the Hsp90 molecular chaperone by the antitumor antibiotics radicicol and geldanamycin, J. Med. Chem. 42 (1999) 260–266, https://doi.org/10.1021/jm980403y.
[53] S.H. Millson, C.S. Chua, S.M. Roe, S. Polier, S. Solovieva, L.H. Pearl, T.S. Sim, C. Prodromou, P.W. Piper, Features of the Streptomyces hygroscopicus HtpG reveal how partial geldanamycin resistance can arise with mutation to the ATP binding pocket of a eukaryotic Hsp90, Faseb. J. 25 (2011), https://doi.org/10.1096/fj.11-188821, 3828-3737.
[54] M.M.S. Andrade, L.C. Martins, G.V.L. Marques, C.A. Silva, G. Faria, S. Caldas, J.S. C. dos Santos, S.Y. Leclercq, V.G. Maltarollo, R.S. Ferreira, R.B. Oliveira, Synthesis of quinoline derivatives as potential cysteine protease inhibitors, Future Med. Chem. 12 (2020) 571–581, https://doi.org/10.4155/fmc-2019-0201.
[55] N. Terzic, J. Konstantinovic, M. Tot, J. Burojevic, O. Djurkovic-Djakovic, J. Srbljanovic, T. Stajner, T. Verbic, M. Zlatovic, M. Machado, I.S. Albuquerque, M. Prudêncio, R.J. Sciotti, S. Pecic, S. D'Alessandro, D. Taramelli, B.A. Šolaja, Reinvestigating old pharmacophores: are 4-aminoquinolines and tetraoxanes potential two-stage antimalarials? J. Med. Chem. 59 (2016) 264–281, https://doi.org/10.1021/acs.jmedchem.5b01374.
[56] E. Borenfreund, J.A. Puerner, A simple quantitative procedure using monolayer cultures for cytotoxicity assays (HTD/NR-90), J. Tissue Cult, Methods 9 (1985) 7–9, https://doi.org/10.1007/BF01666038.
[57] L.P. de Carvalho, S. Groeger-Otero, A. Kreidenweiss, P.G. Kremsner, B. Mordmüller, J. Held, Boromycin has rapid-onset antibiotic activity against asexual and sexual blood stages of *Plasmodium falciparum*, Front. Cell. Infect. Microbiol. 11 (2022) 802294, https://doi.org/10.3389/fcimb.2021.802294.
[58] A. Grosdidier, V. Zoete, O. Michielin, SwissDock, a protein-small molecule docking web service based on EADock DSS, Nucleic Acids Res. 39 (2011) W270–W277, https://doi.org/10.1093/nar/gkr366.
[59] Gaussian 16, Revision C. 01, M.J. Frisch, G.W. Trucks, H.B. Schlegel, G.E. Scuseria, M.A. Robb, J.R. Cheeseman, G. Scalmani, V. Barone, G.A. Petersson, H. Nakatsuji, X. Li, M. Caricato, A.V. Marenich, J. Bloino, B.G. Janesko, R. Gomperts, B. Mennucci, H.P. Hratchian, J.V. Ortiz, A.F. Izmaylov, J.L. Sonnenberg, D. Williams-Young, F. Ding, F. Lipparini, F. Egidi, J. Goings, B. Peng, A. Petrone, T. Henderson, D. Ranasinghe, V.G. Zakrzewski, J. Gao, N. Rega, G. Zheng, W. Liang, M. Hada, M. Ehara, K. Toyota, R. Fukuda, J. Hasegawa, M. Ishida, T. Nakajima, Y. Honda, O. Kitao, H. Nakai, T. Vreven, K. Throssell, J. A. Montgomery Jr., J.E. Peralta, F. Ogliaro, M.J. Bearpark, J.J. Heyd, E. N. Brothers, K.N. Kudin, V.N. Staroverov, T.A. Keith, R. Kobayashi, J. Normand, K. Raghavachari, A.P. Rendell, J.C. Burant, S.S. Iyengar, J. Tomasi, M. Cossi, J. M. Millam, M. Klene, C. Adamo, R. Cammi, J.W. Ochterski, R.L. Martin, K. Morokuma, O. Farkas, J.B. Foresman, D.J. Fox, Gaussian, Inc., Wallingford CT, 2016.
[60] D.A. Case, R.M. Betz, D.S. Cerutti, T.E. Cheatham, T.A. Darden, R.E. Duke, T. J. Giese, H. Gohlke, A.W. Goetz, N. Homeyer, S. Izadi, P. Janowski, J. Kaus, A. Kovalenko, T.S. Lee, S. LeGrand, P. Li, C. Lin, T. Luchko, R. Luo, B. Madej, D. Mermelstein, K.M. Merz, G. Monard, H. Nguyen, H.T. Nguyen, I. Omelyan, A. Onufriev, D.R. Roe, A. Roitberg, C. Sagui, C.L. Simmerling, W.M. Botello-Smith, J. Swails, R.C. Walker, J. Wang, R.M. Wolf, X. Wu, L. Xiao, P.A. Kollman, Amber 16 (2016).
[61] T. Hou, J. Wang, Y. Li, W. Wang, Assessing the performance of the MM/PBSA and MM/GBSA methods. 1. The accuracy of binding free energy calculations based on molecular dynamics simulations, J. Chem. Inf. Model. 51 (2011) 69–82, https://doi.org/10.1021/ci100275a.
[62] S. Genheden, U. Ryde, The MM/PBSA and MM/GBSA methods to estimate ligand-binding affinities, Expet Opin. Drug Discov. 10 (2015) 449–461, https://doi.org/10.1517/17460441.2015.1032936.
[63] G. Rastelli, A. Del Rio, G. Degliesposti, M. Sgobba, Fast and accurate predictions of binding free energies using MM-PBSA and MM-GBSA, J. Comput. Chem. 31 (2010) 797–810, https://doi.org/10.1002/jcc.21372.
[64] H. Gohlke, C. Kiel, D.A. Case, Insights into protein-protein binding by binding free energy calculation and free energy decomposition for the Ras-Raf and Ras-RalGDS complexes, J. Mol. Biol. 330 (2003) 891–913, https://doi.org/10.1016/S0022-2836(03)00610-7.

International Journal of
Molecular Sciences

MDPI

Article

Harmicens, Novel Harmine and Ferrocene Hybrids: Design, Synthesis and Biological Activity

Goran Poje [1,†], Marina Marinović [1,†], Kristina Pavić [1], Marija Mioč [2], Marijeta Kralj [2], Lais Pessanha de Carvalho [3], Jana Held [3,4], Ivana Perković [1] and Zrinka Rajić [1,*]

1 Faculty of Pharmacy and Biochemistry, University of Zagreb, 10 000 Zagreb, Croatia
2 Laboratory of Experimental Therapy, Division of Molecular Medicine, Ruder Boškovic Institute, 10 000 Zagreb, Croatia
3 Institute of Tropical Medicine, University of Tübingen, 72074 Tübingen, Germany
4 German Center for Infection Research (DZIF), Partner Site Tübingen, 72074 Tübingen, Germany
* Correspondence: zrajic@pharma.hr
† These authors contributed equally to this work.

Abstract: Cancer and malaria are both global health threats. Due to the increase in the resistance to the known drugs, research on new active substances is a priority. Here, we present the design, synthesis, and evaluation of the biological activity of harmicens, hybrids composed of covalently bound harmine/β-carboline and ferrocene scaffolds. Structural diversity was achieved by varying the type and length of the linker between the β-carboline ring and ferrocene, as well as its position on the β-carboline ring. Triazole-type harmicens were prepared using Cu(I)-catalyzed azide-alkyne cycloaddition, while the synthesis of amide-type harmicens was carried out by applying a standard coupling reaction. The results of in vitro biological assays showed that the harmicens exerted moderate antiplasmodial activity against the erythrocytic stage of *P. falciparum* (IC_{50} in submicromolar and low micromolar range) and significant and selective antiproliferative activity against the MCF-7 and HCT116 cell lines (IC_{50} in the single-digit micromolar range, SI > 5.9). Cell localization experiments showed different localizations of nonselective harmicene **36** and HCT116-selective compound **28**, which clearly entered the nucleus. A cell cycle analysis revealed that selective harmicene **28** had already induced G1 cell cycle arrest after 24 h, followed by G2/M arrest with a concomitant drastic reduction in the percentage of cells in the S phase, whereas the effect of nonselective compound **36** on the cell cycle was much less pronounced, which agreed with their different localizations within the cell.

Keywords: β-carboline; harmine; ferrocene; hybrid; amide; triazole; synthesis; antiplasmodial; antiproliferative

Citation: Poje, G.; Marinović, M.; Pavić, K.; Mioč, M.; Kralj, M.; de Carvalho, L.P.; Held, J.; Perković, I.; Rajić, Z. Harmicens, Novel Harmine and Ferrocene Hybrids: Design, Synthesis and Biological Activity. *Int. J. Mol. Sci.* **2022**, *23*, 9315. https://doi.org/10.3390/ijms23169315

Academic Editors: Po-Lin Liao and Tsung-Yun Liu

Received: 29 July 2022
Accepted: 16 August 2022
Published: 18 August 2022

1. Introduction

Cancer remains one of the leading causes of mortality worldwide, as it was responsible for nearly 10 million deaths in 2020 [1]. Unfortunately, these numbers are expected to rise in the future [2,3]. Current cancer treatment still faces many challenges, such as low specificity and high toxicity of the available drugs, drug resistance, and high cost of the targeted therapy [4]. Malaria, an infectious disease caused by a protozoan parasite of the genus *Plasmodium*, is another serious global health threat [5]. The deadliest form of the disease is caused by the most prevalent and drug-resistant species, *P. falciparum* [6]. Unfortunately, the COVID-19 outbreak interrupted the steady decline in both malaria cases and deaths since 2000, resulting in an increase of 13 million malaria cases and 69,000 deaths in 2020 compared to 2019 [7]. Therefore, the discovery of new anticancer and antimalarial agents is a top priority.

Due to the complexity of cancer pathophysiology and the complex life cycle of the malaria parasite, a combination of drugs is a standard treatment option and could provide

protection against drug resistance. However, complications such as drug–drug interactions and lower treatment adherence may also occur. On the other hand, the molecular hybridization approach is a rational strategy for the synthesis of new bioactive compounds. In this approach, a covalent bond is established between two or more pharmacophores to obtain hybrid compounds that have the potential to bridge the shortcomings of combination therapy [8–10].

β-carbolines, which are naturally occurring or synthetic compounds with a tricyclic pyrido[3,4-*b*]indole ring in their structure, have been extensively studied and have shown a wide range of biological activities, such as anticancer, antimalarial, antiviral, antibacterial, neuropharmacological, and antithrombotic activities [11]. Harmine, isolated from *Peganum harmala*, and its numerous analogues have shown significant cytotoxic activity against human cancer cell lines in the low micromolar and sub-micromolar range [12–16]. Several reviews addressed the anticancer activity of β-carboline derivatives and proposed different modes of action [9,15,17]. Similarly, the antimalarial activity of harmine and other β-carboline derivatives is also well-documented [18–20]. On the other hand, ferrocene is an important compound in bioinorganometallic chemistry due to its high stability, favorable redox properties, and low toxicity [21]. Furthermore, extensive research has shown that the incorporation of ferrocene in the structure of known anticancer or antimalarial agents improved activity [4,22–27]. The best-known examples are ferrocifen and ferroquine, ferrocene–tamoxifen or chloroquine hybrids [4]. Ferroquine, the first organometallic drug candidate, showed potent and significant antiplasmodial activity against CQ-resistant strains of *P. falciparum* and is in the clinical trials for the treatment of malaria [28,29]. Interestingly, ferroquine also demonstrated potential as an anticancer drug [30].

Our previous work on harmine hybrids, i.e., harmicines, harmirins, and harmiquins, demonstrated that the development of hybrids is indeed a valid strategy for obtaining biologically active compounds that exhibit more pronounced activity than the parent compounds [31–35]. Encouraged by the literature data, which clearly show the potential of organometallic compounds as anticancer and antimalarial therapeutics [36–41], we set out to prepare harmicens—hybrids in which ferrocene is covalently bound to harmine/β-carboline (Figure 1), and to investigate their antiproliferative and antiplasmodial activities.

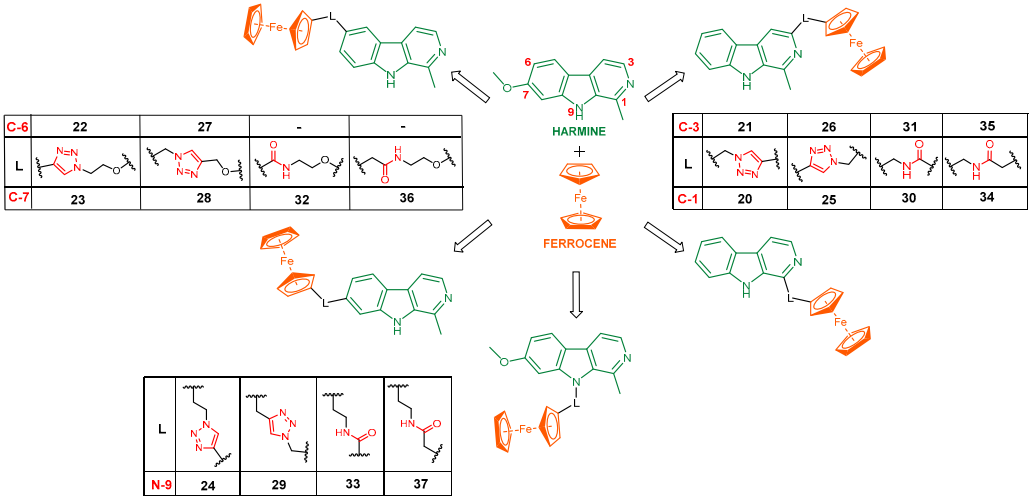

Figure 1. Harmicens—new harmine–ferrocene hybrids (harmine/β-carboline is marked in green and ferrocene is marked in red).

2. Results and Discussion

2.1. Chemistry

In this paper, we report the synthesis of hybrid compounds composed of harmine/β-carboline and ferrocene covalently bound via a triazole ring or an amide bond, leading to the triazole- (TT, **20**–**24** and **25**–**29**) or amide-type (AT, **30**–**33** and **34**–**37**) harmicens,

respectively. Additional structural diversity was achieved by changing the position and length of the linker between the β-carboline ring and ferrocene. Thus, harmicens were prepared at five positions of the β-carboline ring, namely C-1, C-3, O-6, O-7, and N-9. Within both series of harmicens, compounds **20**–**24** and **30**–**33** contain either a triazole or an amide bond directly linked to ferrocene, in contrast to compounds **25**–**29** and **34**–**37**, which have a methylene bridge between the triazole/amide and ferrocene (Figure 1).

TT harmicens were prepared using Cu(I)-catalyzed azide-alkyne cycloaddition (CuAAC), known as "click" chemistry, while the synthesis of AT harmicens was performed using a standard coupling reaction. Since both methods required starting building blocks based on harmine and ferrocene motifs, i.e., azides and alkynes or amines and carboxylic acids, extensive synthetic work was performed prior to the synthesis of the title compounds. In our previous work, we synthesized azides at the C-1 and C-3 (**3** and **6**), alkynes at the O-6, O-7, and N-9 (**10**, **13**, and **16**), and amines at the C-1, C-3, O-6, O-7, and N-9 positions of the β-carboline ring (**4**, **7**, **11**, **14**, and **17**) [31–33,35]. Here, we present the synthesis of alkynes at the C-1 and C-3 (**2**, **9**) and azides at the O-6, O-7, and N-9 (**12**, **15,** and **18**) positions of the β-carboline ring. We also prepared the required azide-based ferrocene **19**. Scheme 1 shows the simplified synthetic routes to the aforementioned intermediates.

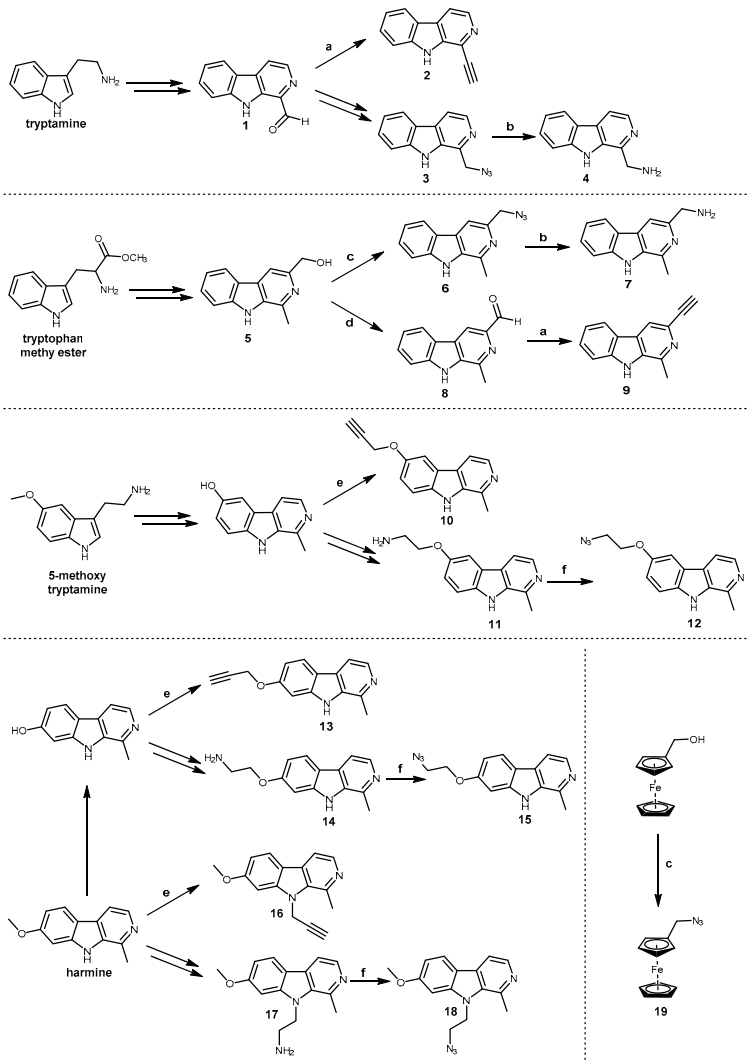

Scheme 1. Synthesis of β-carboline and ferrocene intermediates **1**–**19**. Reagents and conditions: (a) Bestmann–Ohira reagent, K_2CO_3, MeOH, rt; (b) H_2/Pd/C, MeOH, rt; (c) ADMP, DBU, THF, 0 °C; (d) MnO_2, THF, rt; (e) $HC{\equiv}CCH_2Br$, Cs_2CO_3, DMF, rt; (f) ISA × HCl, K_2CO_3, $CuSO_4 \times 5H_2O$, MeOH, rt.

The synthesis of alkynes **2** and **9** proved to be the most challenging. We tried several synthetic approaches, as shown in Scheme 2, for the synthesis of alkyne at the position C-1. The selective alkylation of the corresponding alcohol with propargyl bromide in the presence of Cs_2CO_3 resulted in a complete alkylation of β-carboline at position N-9.

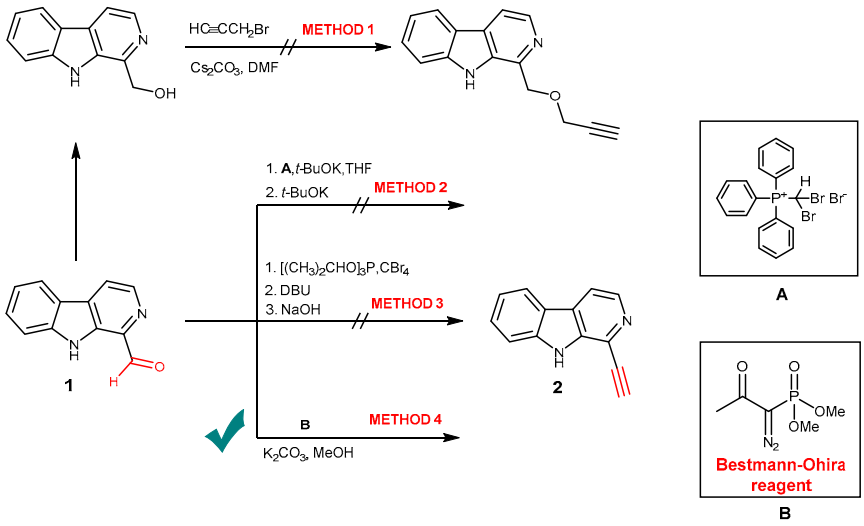

Scheme 2. Optimization of the alkyne **2** synthesis.

The second attempt was made using aldehyde-to-alkyne homologation (Methods 2–4). Methods 2 and 3 implied the use of strong bases (t-BuOK, DBU, and NaOH), required complex work-up [42], and the reactions resulted in a mixture of products. Method 4 represents the Bestmann–Ohira modification of the Seyferth–Gilbert reaction. Classical Seyferth–Gilbert homologation is a one-pot reaction in which aldehyde is converted to the corresponding alkyne in the presence of dimethyl (diazomethyl)phosphonate (DAMP, the Seyferth–Gilbert reagent). This reagent is not commercially available due to its instability, and requires preparation before the reaction is carried out. The Bestmann–Ohira procedure uses a more stable dimethyl (1-diazo-2-oxopropyl)phosphonate (Bestmann–Ohira reagent (BOR); reagent B, Scheme 2) that is converted to DAMP in situ. This reaction can be successfully employed for the preparation of a wide range of terminal alkynes with good to excellent yields under mild reaction conditions (strong bases, low temperatures, and inert gas techniques are not necessary) following a simple work-up [42]. To our delight and after careful optimization of the reaction conditions, **2** and **9** were successfully prepared from the corresponding aldehydes **1** and **8** by applying Method 4.

On the other hand, amines **11**, **14**, and **17** were easily and effectively converted to azides **12**, **15**, and **18**, respectively, with imidazole-1-sulfonyl azide hydrochloride (ISA × HCl), a diazotransfer reagent, in the presence of K_2CO_3 and $CuSO_4 \times 5H_2O$. ISA × HCl is an efficient, shelf-stable crystalline crude reagent that can be prepared in a one-pot reaction from inexpensive materials (imidazole, NaN_3, and SO_2Cl_2) [43].

TT harmicens **20**–**24** were prepared from ethynylferrocene and β-carboline azides **3**, **6**, **12**, **15**, and **18**, whereas the synthesis of TT harmicens **25**–**29** was carried out via a "click" reaction between (azidomethyl)ferrocene **19** and β-carboline alkynes **2**, **9**, **10**, **13**, and **16** (Scheme 3). The use of copper(II) acetate in methanol at room temperature resulted in a poor reaction performance and a large number of side products. Since we were not satisfied with the reaction outcome, we decided to investigate whether changing the reaction conditions would increase the reaction yield, decrease the number of side products, and simplify the work-up. Heating the reaction mixture in a microwave reactor (50 °C, 1 h) had no positive effect on the progress of the reaction or the purity of the products. Reactions carried out in the presence of sodium ascorbate and $CuSO_4 \times 5H_2O$ in a mixture of tert-butanol and water (1:1 ratio) at room temperature progressed well, but the selectivity was low again. Changing the solvent to DMF and water (2:1 ratio) significantly reduced the number of

side products and increased the reaction yield. Work-up included filtration of the crude product from the reaction mixture or solvent extraction and column chromatography with the addition of Al_2O_3 to remove the residual copper salts.

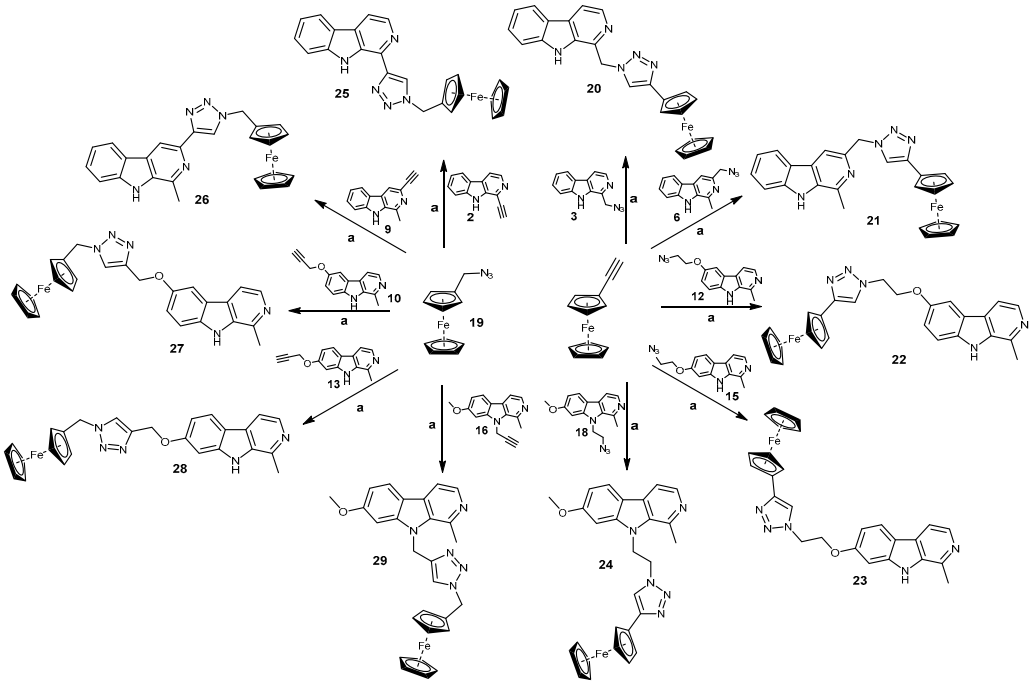

Scheme 3. Synthesis of TT harmicens **20**–**29**. Reagents and conditions: (a) Na ascorbate, $CuSO_4 \times 5H_2O$, DMF/H_2O, rt.

The synthesis of harmicens **30**–**33** and **34**–**37** at positions C-1, C-3, O-7, and N-9 was successfully carried out via a standard coupling reaction (HATU, DIEA) using amines **4**, **7**, **14**, and **17** and ferrocenecarboxylic or ferroceneacetic acid (Scheme 4). The carboxylic acids were added in small excess (1.1 equivalents) to increase the reaction yield. Unfortunately, the preparation of AT harmicene at position 6 of the β-carboline ring was not successful. Attempts to optimize the reaction conditions and to carry out the synthesis via other intermediates did not afford the desired results.

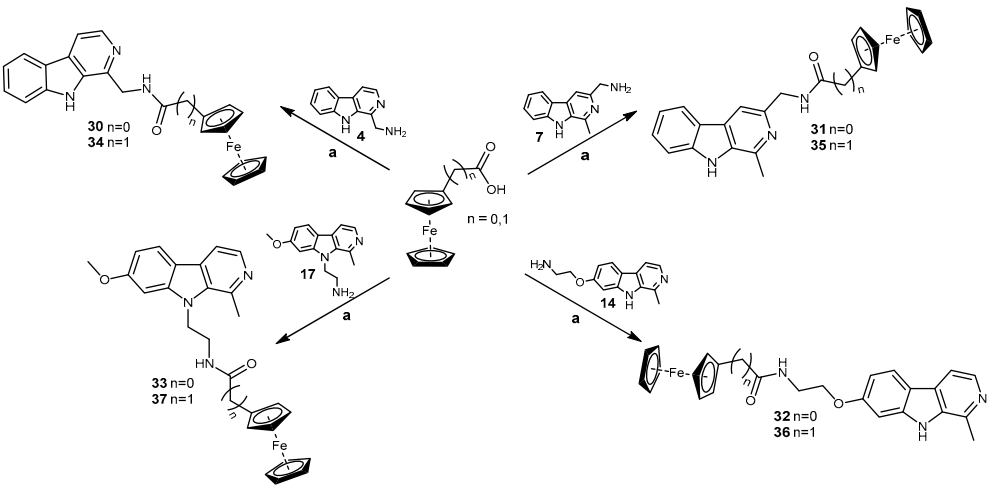

Scheme 4. Synthesis of AT harmicens **30**–**37**. Reagents and conditions: (a) HATU, DIEA, CH_2Cl_2, rt.

Harmicens were characterized by standard methods (MS, IR, ^{1}H and ^{13}C NMR), whereas their purity was checked by elemental analysis and HPLC. The data obtained are given in the Materials and Methods section and in the Supplementary Material (Tables S1–S11).

2.2. Biological Activity

Our further work was focused on the evaluation of harmicens' antiplasmodial and antiproliferative activities against the erythrocytic stages of the *Plasmodium* life cycle and a panel of human cell lines, respectively.

2.2.1. In Vitro Antiplasmodial Activity

The in vitro activity of harmicens **20**–**37** against the erythrocytic stages of CQ-sensitive (*Pf*3D7) and multidrug-resistant (*Pf*Dd2) *P. falciparum* strains was evaluated following a previously described method (Table 1) [44–46]. The results showed that the antiplasmodial activity of the prepared harmicens was moderate (IC_{50} in submicromolar and micromolar range). A detailed analysis revealed that most of the TT and AT harmicens exhibited improved antiplasmodial activity over the parent compound harmine against *Pf*3D7. Notably, 7/18 compounds exerted activity that was an order of magnitude stronger. All harmicens had markedly better antiplasmodial activity against *Pf*Dd2 than harmine, which was not active at all. Unfortunately, their activity against both strains was lower than the activity of the reference drug, chloroquine.

Table 1. In vitro antiplasmodial activity of harmicens **20**–**37** against the erythrocytic stages of *P. falciparum* (*Pf*3D7 and *Pf*Dd2 strains).

Compd.	IC_{50} [a] (μM)				
	***Pf*3D7**	***Pf*Dd2**		***Pf*3D7**	***Pf*Dd2**
20	9.23 ± 1.96	11.20 ± 2.23	**30**	>56 [b]	14.01 ± 1.95 [c]
21	7.14 ± 0.38	6.06 ± 1.36	**31**	13.24 ± 8.54	8.03 ± 0.19
22	0.35 ± 0.19	0.89 ± 0.01	**32**	0.30 ± 0.09	0.66 ± 0.01
23	0.15 ± 0.05	1.02 ± 0.52	**33**	0.40 ± 0.18	2.04 ± 0.29
24	1.35 ± 0.28	2.31 ± 0.29	**34**	1.34 ± 0.09	1.11 ± 0.01
25	3.62 ± 1.08	4.37 ± 1.79	**35**	7.85 ± 2.18	12.99 ± 5.90
26	2.63 ± 0.27	4.02 ± 0.61	**36**	0.42 ± 0.02	1.53 ± 0.06
27	0.31 ± 0.01	1.09 ± 0.01	**37**	0.83 ± 0.23	1.80 ± 0.35
28	>56	>56	HAR [d]	8.25 ± 2.83	>27.7
29	2.12 ± 0.81	2.91 ± 0.05	CQ [e]	0.004 ± 0.002	0.29 ± 0.10

[a] IC_{50}, the concentration of the tested compound necessary for 50% growth inhibition. [b] The exact IC_{50} could not be obtained, as activity could only be detected at the highest tested concentration. [c] Results represent mean ± SD, n > 2. [d] HAR, harmine; [e] CQ, chloroquine.

A comparison of the harmicens' activity against two *P. falciparum* strains showed that *Pf*3D7 was generally more sensitive than *Pf*Dd2, as 7/18 compounds were active at submicromolar concentrations, whereas only 2/18 harmicens had submicromolar activity against *Pf*Dd2. Among TT harmicens, hybrids in which the β-carboline ring was substituted at O-6 and O-7 showed activity at submicromolar concentrations. On the other hand, AT harmicens substituted at O-7 and N-9 showed better activity. The length of the linker also influenced the activity. Interestingly, the highest activity against *Pf*3D7 was exerted by TT harmicene **23**, bearing a triazole directly linked to ferrocene (IC_{50} = 0.15 ± 0.05 μM), whereas its counterpart, harmicene **28**, which had a methylene bridge between triazole and ferrocene, was inactive at the highest concentration tested, resulting in a 370-fold decrease in antiplasmodial activity. On the contrary, AT harmicens with a shorter amide linker generally showed stronger antiplasmodial activity against *Pf*Dd2 than their counterparts with a longer linker. The most active compound against *Pf*Dd2 was AT harmicene **32** (IC_{50} = 0.66 ± 0.01 μM). The effect of the linker remains a potentially useful parameter that should be further investigated.

2.2.2. In Vitro Antiproliferative Activity

The antiproliferative activity of harmicens **20**–**37** was evaluated against a panel of human tumor cell lines (hepatocellular carcinoma—HepG2, colorectal adenocarcinoma, Dukes' type C—SW620, colorectal carcinoma—HCT116, and breast adenocarcinoma—MCF-7) and

a noncancer cell line (embryonic kidney—Hek293T) in vitro; the obtained results are shown in Table 2. The parent compound harmine, as well as the reference drug 5-fluorouracil, were used as positive controls. Initially, a prescreening was performed, and only the compounds that resulted in more than a 50% reduction in the mitochondrial metabolic activity at a concentration of 50 μM were selected for IC_{50} determination. Since the MCF-7 and HCT116 cell lines were the most sensitive to harmicens, we decided to calculate the selectivity index (SI) for each harmicene as the fractional ratio between the IC_{50} values for Hek293T and the tumor cell line MCF-7 or HCT116.

Table 2. In vitro antiproliferative activity of harmicens **20**–**37** against human cell lines and calculated selectivity indices.

Compd.	IC_{50} [a] (μM)					SI [b] (HCT116)	SI (MCF-7)
	HepG2	SW620	HCT116	MCF-7	Hek293T		
20	43.9 ± 1.1	>50	29.4 ± 4.6	39.4 ± 7.9	>50	>1.7	>1.3
21	>50	19.7 ± 1.9	8.3 ± 1.4	17.7 ± 0.6	>50	>6	>2.8
22	8.4 ± 0.9	6.5 ± 0.7	9 ± 0.7	6.9 ± 0.5	7.3 ± 2.8	0.8	1.1
23	9.5 ± 0.5	7.6 ± 0.1	38.6 ± 2.8	8.0 ± 0.2	17.1 ± 1.8	0.4	2.1
24	>50	>50	>50	>50	>50	>1	>1
25	>50	23.1 ± 6.4	7.6 ± 0.5	>50	>50	>6.6	>1
26	12.3 ± 5	3.8 ± 0.4	35.2 ± 4.7	3.7 ± 0.2	46.5 ± 1	1.3	12.6
27	17 ± 0.3	8.1 ± 0.2	>50	6.8 ± 0.2	43 ± 8.6	< 0.9	6.3
28	>50	>50	7.4 ± 0.4	>50	>50	>6.8	>1
29	>50	>50	14.6 ± 3.7	>50	>50	>3.4	>1
30	>50	45.1 ± 3.7	16.8 ± 0.9	8.5 ± 1.5	>50	>3	>5.9
31	>50	>50	>50	19.9 ± 1.1	>50	>1	>2.51
32	15.6 ± 0.3	9.9 ± 4	6.6 ± 0.8	9.1 ± 1.4	18.6 ± 0.2	2.8	2
33	>50	>50	16.3 ± 3.2	30.5 ± 13.2	>50	>1	>1.7
34	>50	>50	>50	>50	>50	>1	>1
35	>50	25 ± 8.1	20.9 ± 1.5	36.9 ± 6.8	>50	>2.4	>1.4
36	7.4 ± 0.5	4.2 ± 0.3	5.9 ± 1.3	4.5 ± 0.3	8.4 ± 0.3	1.4	1.9
37	28 ± 2.5	9.9 ± 1.1	7.5 ± 0.4	13.2 ± 0.5	30.8 ± 2.4	4.1	2.3
HAR [c]	18.7 ± 0.8	4.7 ± 0.6	4.0 ± 0.8	13.5 ± 1.1	12.6 ± 0.8	3.2	0.9
5-FU [d]	5.5 ± 0.6	9.4 ± 0.3	5.2 ± 2.8	23.9 ± 5.7	8.1 ± 0.8	1.6	0.3

[a] IC_{50}, the concentration that causes 50% growth inhibition; [b] SI, selectivity index; [c] HAR, harmine; [d] 5-FU, 5-fluorouracil.

The results showed that harmicens exhibited significant antiproliferative activity against the tested tumor cell lines, especially against MCF-7, HCT116, and SW620 (7/18 compounds displayed activity in the low micromolar range), whereas HepG2 was the least sensitive cell line (3/18 compounds displayed a single-digit micromolar IC_{50}). Remarkably, their activity against noncancer cell line Hek293T was much lower. Only the most active and nonselective compounds significantly affected Hek293T (**22** and **36**). Thus, the bridging of harmine and ferrocene led to selective compounds, which is a very important result.

TT harmicens showed stronger and more selective activity against the tumor cell lines than the AT harmicens. In particular, TT harmicens containing a methylene group between the triazole and ferrocene moieties, i.e., compounds **25**–**29**, showed the least activity against Hek293T and the strongest against the tumor cell lines. A more detailed analysis revealed that TT harmicens **21**, **25,** and **28** exhibited selective activity against HCT116 (SIs > 6), and AT harmicene **30** against MCF-7 (SI > 5.9). In addition, TT harmicens **26** and **27** displayed selective antiproliferative activity against SW620 and MCF-7, but not against HCT116. Remarkably, the activity of harmicens selective against MCF-7, **26**, **27**, and **30**, was ~3–6.5-fold stronger than the activity of 5-FU. The most active harmicene against MCF-7 was compound **26** (IC_{50} = 3.7 ± 0.2 μM, SI = 12.6). On the other hand, the activity of harmicens against HCT116 was similar to the activity of 5-FU, but, as mentioned earlier, was much more selective (IC_{50} (**28**) = 7.4 ± 0.4 μM, SI > 6.8).

A comparison of compounds prepared at the same position of the β-carboline ring revealed the following:

(1) C-1: Harmicens were either selective against HCT116 (TT harmicene **25**) or MCF-7 (AT harmicene **30**), or exerted very low activity/were inactive.
(2) C-3: Harmicens were mostly selective, especially TT harmicens **21** and **26**. Although AT harmicens had lower activity, a similar trend was observed.
(3) O-6: Harmicens exerted very strong activity against the tumor cell lines. Harmicene **27** was also selective against MCF-7 and SW620. Unfortunately, only TT harmicens were prepared, so comparison with AT harmicens was not possible.
(4) O-7: Harmicens showed pronounced and nonselective activity against all cell lines tested, with the exception of TT harmicene **28**.
(5) N-9: The activity of harmicens was moderate to low, and some degree of selectivity was observed against the HCT116 and MCF-7 cell lines.

2.2.3. Cell Localization

To gain insight into the destiny of the compounds within the cell, we decided to investigate the cell localization of two compounds with low micromolar IC_{50} values: (1) compound **28,** which was cytotoxic only against HCT116; and (2) compound **36,** which showed cytotoxicity toward all tested cell lines. The aforementioned compounds were selected particularly to investigate whether there was a difference in the potential mode of action between the HCT116-selective and generally less selective compounds.

To examine the intracellular localization of compounds **28** and **36**, we took advantage of their intrinsic fluorescence properties. We incubated MCF-7 cells with compound **28** at two concentrations (10 and 50 μM), or with compound **36** at a 5 μM concentration for 30 min and 1 h and analyzed their distribution using fluorescence microscopy. We chose different concentrations and incubation periods to determine the optimal treatment protocol that would not cause cell damage and would result in high-contrast images. No autofluorescence was detected by examining untreated cells under typical imaging conditions.

Harmicene **28** showed punctate, bright staining within the cytoplasm at a 10 μM concentration after 30 min, while nuclei also fluoresced, suggesting that compound **28** did enter the nucleus. Thus, compound **28** possibly targeted both nuclear DNA and cytoplasmic targets (Figure 2). This was contrary to our previous finding that harmine derivatives did not enter the cell nuclei [34]. A longer incubation period did not improve the fluorescence signal, while the 5-fold higher concentration disrupted the cell morphology (data not shown). On the other hand, compound **36** clearly showed different distribution within the cell in comparison with **28**. The staining within the cytoplasm appeared less bright, while the fluorescence of the nuclei was not as apparent. However, due to the technical limitations and spectral characteristics of the compound, we could not draw a definite conclusion on the cell distribution of **36** based on the obtained photographs (data shown in Figure S1 of the Supplementary Materials).

2.2.4. Cell Cycle Analysis

As cell localization experiments showed different distributions of compounds **28** and **36** within the cell, we decided to assess their influences on the cell cycle. To that end, the cells were treated for 24 and 48 h with 3 μM and 6 μM concentrations of each compound, which corresponded to 0.5 × IC_{50} and IC_{50} values obtained in the MTT assay after 72 h, respectively. Afterward, the DNA was stained with propidium iodide and subjected to flow cytometry analysis. The cell cycle distribution is shown in Figure 3.

The treatment of cells with compound **28** resulted in a statistically significant increase in cells in the G1 phase at both tested concentrations already after 24 h, while compound **36** caused G1 phase arrest only at a higher concentration. Furthermore, our data showed a pronounced G2/M cell cycle arrest following the 48 h treatment with **28**, with a simultaneous drastic reduction in the percentage of cells in the S phase. Precisely, the ability of compound **28** to enter the nucleus may be a reason for its pronounced effect on the cell

cycle. Conversely, the influence of **36** on the cell cycle of HCT116 was significantly less pronounced, indicating that its pronounced cytotoxicity was mediated through a different mechanism. This finding was consistent with their different localizations within the cell.

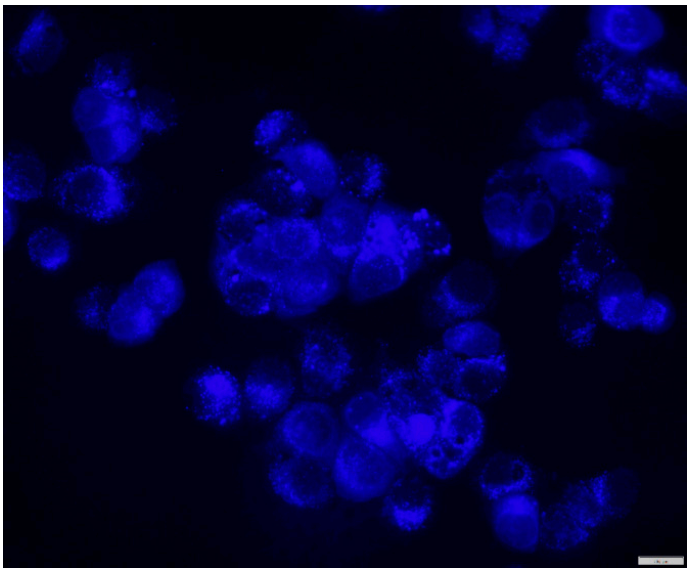

Figure 2. A fluorescence microscopy image (400× magnification) of MCF-7 cells incubated with 10 μM of compound **28** for 30 min showing both cytoplasmic and nuclear localization. The scale bar is 20 μm.

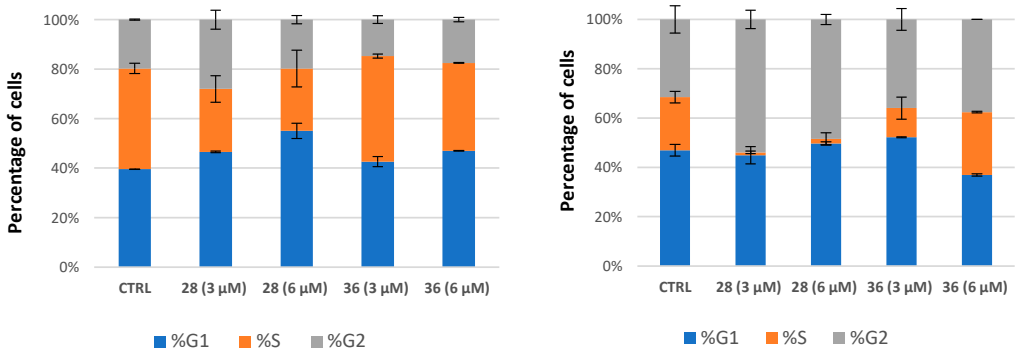

Figure 3. The effect of **28** and **36** on the cell cycle distribution of HCT116 cells. Cells were treated with 3 μM and 6 μM of each compound for 24 h (**A**) and 48 h (**B**), and then the cell cycle was analyzed using flow cytometry. The histograms represent the percentage of cells in the respective cell cycle phase (G1, S, and G2/M). Average values from duplicates from one representative experiment ± SD are presented.

Numerous studies have shown that harmine significantly influences the cell cycle of various cancer cell lines, including HCT116, via induction of G2/M cell cycle arrest, intercalation into DNA and induction of DNA fragmentation; upregulation of p53 and p21 expression; and downregulation of cyclin B1, p-cdc2, cdc2, cdc25, and p-cdc25 expression necessary for G2/M transition [47–49]. In our previous paper, we also confirmed that the parent compound harmine induced arrest in the G1 phase of MCF-7 cells already after 24 h, along with a reduction in cells in the S phase and an additional accumulation of cells in the G2/M phase after 48 h. The O-7-substituted TT harmine–coumarin derivative, which was synthesized by our research group, caused even more prominent G1 arrest than harmine, accompanied by a drastic reduction in the percentage of cells in the S phase, which also

persisted after 48 h [34]. Harmicene **28**, also an O-7-substituted TT-harmine derivative, had an even more pronounced effect on the HCT116 cell cycle. Furthermore, it is known that ferrocene derivatives also inhibit the proliferation of various cancer cells through the induction of G0/G1 cell cycle arrest, downregulation of cyclin D1, CDK4 [50], and CDK6 and concomitant increases in p27 and p21 expression [51].

Considering all the facts mentioned above, harmicene **28** might significantly influence the cell cycle of the colorectal cancer cell line HCT116 as a result of its hybrid nature. However, we must stress the importance of a spacer type—a triazole ring—since the less selective compound **36**, differing only in the spacer type, did not show such an effect on the cell cycle. This finding indicates that their molecular targets are probably different and should be determined in future studies.

3. Materials and Methods

3.1. Chemistry

3.1.1. General Information

Melting points were determined on a Stuart Melting Point Apparatus (Barloworld Scientific, Stone, UK) in open capillaries and were uncorrected. FTIR-ATR spectra were recorded using a Fourier-Transform Infrared Attenuated Total Reflection UATR Two spectrometer (PerkinElmer, Waltham, MA, USA) in the range of 450 to 4000 cm^{-1}. ^{1}H and ^{13}C NMR spectra were recorded on a Bruker Avance III HD operating at 400 or 600 MHz for the ^{1}H and 100, 101, or 151 MHz for the ^{13}C nuclei (Bruker, Billerica, MA, USA). Samples were measured in DMSO-d_6 solutions at 20 °C in 5 mm NMR tubes. Chemical shifts are reported in parts per million (ppm) using tetramethylsilane (TMS) as a reference in the ^{1}H and the DMSO residual peak as a reference in the ^{13}C spectra (39.52 ppm). Coupling constants (J) are reported in hertz (Hz). Mass spectra were recorded on an Agilent 1200 Series HPLC coupled with an Agilent 6410 Triple Quad (Agilent Technologies, Santa Clara, CA, USA). The mobile phase consisted of Milli-Q water as component A and MeOH (HPLC grade, J. T. Baker) as component B, and a Zorbax XDC C18 column (4.6 × 75 mm, 3.5 µm) was used as the stationary phase. Gradient elution was used at a flow rate of 0.5 mL/min, and 5 µL of analyte solution was injected per analysis. The starting conditions and gradient steepness were adjusted according to the analyte polarity. A diode array detector was utilized, and the data are presented as a total wavelength chromatogram (TWC). Mass spectrometry conditions were as follows: electrospray ionization (ESI) in positive and negative mode was used; the capillary voltage and current were set to 4.0 kV and 20 nA, respectively; the nebulizer pressure was set to 15 psi; and the drying gas (nitrogen) temperature and flow were 300 °C and 11 L/min, respectively. For the MS data analysis, Agilent MassHunter software (Agilent Technologies, Santa Clara, CA, USA) was used. Elemental analyses were performed on a CHNS LECO analyzer (LECO Corporation, St. Joseph, MI, USA). Analyses indicated by the symbols of the elements were within ±0.4% of their theoretical values. Microwave-assisted reactions were performed in a CEM Discover microwave reactor (CEM, Matthews, NC, USA) in a glass reaction vessel.

All compounds were routinely checked using TLC with silica gel 60F-254 glass plates (Merck KGaA, Darmstadt, Germany) using DCM/MeOH 8:1, 9:1, 97:3, cyclohexane/EtOAc/MeOH 1:1:0.5, 1:1:0.1, and acetone/DCM 1:1, 9:1, 3:2 as the solvent system. Spots were visualized using UV light (λ = 254 nm; 365 nm) and iodine vapor. Column chromatography was performed on silica gel 0.063–0.200 mm (Sigma-Aldrich, Waltham, MA, USA) with the same eluents used for TLC. All chemicals and solvents were of analytical grade and purchased from commercial sources.

ISA × HCl, alcohol **5**, and aldehydes **1** and **8** were prepared according to the procedures found in the literature [42,52,53]. Amines **4**, **7**, **11**, **14**, and **17**, azides **3** and **6**, and alkynes **10**, **13**, and **16** were prepared according to our published procedures [31–33].

3.1.2. General Procedure for the Synthesis of Alkynes **2** and **9**

A corresponding aldehyde **1** or **8** (0.476 mmol) and K_2CO_3 (0.132 g, 0.952 mmol) were suspended in anhydrous MeOH (7.186 mL). Under a nitrogen atmosphere, Bestmann–Ohira reagent was added (0.857 mL, 5.712 mmol), and the reaction was stirred at room temperature for 3 h (alkyne **2**) or 48 h (alkyne **9**). Upon completion, MeOH was evaporated and 5% $NaHCO_3$ was added dropwise until the precipitate formation was complete. The resulting precipitate was filtered off, purified using column chromatography with DCM/MeOH 9:1 (**2**) or cyclohexane/EtOAc/MeOH 1:1:0.1 (**9**) as a mobile phase, and triturated with a diethyl ether/petroleum ether mixture.

1-Ethynyl-9*H*-pyrido[3,4-*b*]indole (**2**)

Aldehyde **1**: 0.093 g; yield: 0.068 g (74%); IR (ATR, ν/cm^{-1}) 3289, 3154, 3061, 2111, 1626, 1562, 1498, 1452, 1424, 1387, 1321, 1273, 1246, 1151, 1081, 1066, 939, 874, 856, 837, 783, 748, 684, 631, 569, 513; ^{1}H NMR (DMSO-d_6) δ 11.79 (s, 1H), 8.34 (d, 1H, J = 5.2 Hz), 8.26 (d, 1H, J = 7.9 Hz), 8.17 (d, 1H, J = 5.2 Hz), 7.64 (d, 1H, J = 8.2 Hz), 7.60–7.56 (m, 1H), 7.32–7.24 (m, 1H), 4.77 (s, 1H); ^{13}C NMR (DMSO-d_6) δ 140.83, 138.66, 137.67, 128.67, 128.14, 125.42, 122.02, 120.69, 119.81, 115.32, 112.33, 84.94, 30.68; ESI-MS: m/z 193.1 $(M + 1)^+$.

3-Ethynyl-1-methyl-9*H*-pyrido[3,4-*b*]indole (**9**)

Aldehyde **8**: 0.100 g; yield: 0.060 g (61%); mp 230–235 °C; IR (ATR, ν/cm^{-1}) 3306, 3143, 2104, 1622, 1597, 1563, 1499, 1446, 1375, 1338, 1315, 1281, 1247, 1178, 1147, 1014, 961, 899, 877, 776, 740, 654, 625, 587, 504, 457; ^{1}H NMR (DMSO-d_6) δ 11.83 (s, 1H), 8.25–8.22 (m, 1H), 8.21 (s, 1H), 7.62–7.59 (m, 1H), 7.57–7.53 (m, 1H), 7.27–7.23 (m, 1H), 4.03 (s, 1H), 2.74 (s, 3H); ^{13}C NMR (DMSO-d_6) δ 142.83, 140.70, 134.06, 129.54, 128.30, 127.01, 122.05, 120.72, 119.78, 117.22, 112.15, 84.85, 76.72, 20.33; ESI-MS: m/z 207.6 $(M + 1)^+$.

3.1.3. General Procedure for the Synthesis of Azides **12**, **15**, **18**

An appropriate amine **11**, **14**, or **17** (0.746 mmol); K_2CO_3 (0.258 g, 1.865 mmol); $CuSO_4 \times 5H_2O$ (q.s.); and ISA × HCl (0.188 g, 0.895 mmol) were suspended in anhydrous MeOH (2 mL). The mixture was stirred at room temperature for 2 h, the organic solvent was evaporated, and the residue was dissolved in H_2O (15 mL) and extracted with EtOAc (2 × 40 mL). The collected organic layers were dried over anhydrous sodium sulfate, filtered, and evaporated under the reduced pressure. The crude product (oil) was purified using column chromatography (cyclohexane/EtOAc/MeOH 1:1:0.5).

6-(2-Azidoethoxy)-1-methyl-9*H*-pyrido[3,4-*b*]indole (**12**)

Amine **11**: 0.180 g; yield: 0.185 g (93%).

7-(2-Azidoethoxy)-1-methyl-9*H*-pyrido[3,4-*b*]indole (**15**)

Amine **14**: 0.180 g; yield: 0.158 g (79%); ^{1}H NMR (DMSO-d_6) δ 11.44 (s, 1H), 8.16 (d, 1H, J = 5.3 Hz), 8.08 (d, 1H, J = 8.6 Hz), 7.82 (d, 1H, J = 5.2 Hz), 7.04 (d, 1H, J = 2.2 Hz), 6.87 (dd, 1H, J = 8.6, 2.2 Hz), 4.30 (t, 2H, J = 4.8 Hz), 3.72 (t, 2H, J = 4.8 Hz), 2.73 (s, 3H); ^{13}C NMR (DMSO-d_6) δ 158.70, 141.77, 141.35, 137.78, 134.60, 127.12, 122.75, 115.26, 111.99, 109.14, 95.62, 67.14, 49.64, 20.33.

9-(2-Azidoethyl)-7-methoxy-1-methyl-9*H*-pyrido[3,4-*b*]indole (**18**)

Amine **17**: 0.190 g; yield: 0.111 g (53%).

3.1.4. (Azidomethyl)ferrocene (**19**)

To a suspension of ferrocenemethanol (0.100 g, 0.463 mmol) in dry THF (5 mL), ADMP (0.330 g, 1.158 mmol) and DBU (0.187 mL, 1.250 mmol) were added at 0 °C. The reaction was stirred at 0 °C for 1 h, diluted with saturated NH_4Cl solution (40 mL), and extracted with DCM (2 × 30 mL). Organic layers were collected and washed with brine (2 × 30 mL) and H_2O (1 × 20 mL), filtered, dried over anhydrous sodium sulfate, and the solvent

evaporated under the reduced pressure. The crude product was purified using column chromatography (cyclohexane/EtOAc/MeOH 1:1:0.5); yield: 0.080 g (72%); oil; ^{1}H NMR (DMSO-d_6) δ 4.29 (t, 2H, J = 1.8 Hz), 4.21 (t, 2H, J = 1.9 Hz), 4.20 (s, 2H), 4.20 (s, 5H); ^{13}C NMR (DMSO-d_6) δ 81.78, 68.62, 68.58, 68.44, 50.02.

3.1.5. General Procedure for the Synthesis of TT Harmicens **20**–**24**

An appropriate azide **3**, **6**, **12**, **15,** or **18** (0.209 mmol) and ethynylferrocene (0.040 g, 0.190 mmol) were dissolved in dry DMF (2 mL), followed by the addition of sodium ascorbate (0.202 mmol, 1 mL of freshly prepared 0.2 M solution in H_2O) and $CuSO_4 \times 5H_2O$ (0.02 mmol, 20 µL of 1 M solution in H_2O). The reaction mixture was stirred overnight at room temperature. After completion of the reaction, purification was performed using either Method A or Method B.

Method A: Ice-cold H_2O (5 mL) was added to the reaction mixture and the resulting precipitate was filtered off, purified using column chromatography (with an additional Al_2O_3 layer to remove Cu salts, mobile phase cyclohexane/EtOAc/MeOH 1:1:0.5), and triturated with diethyl ether/petroleum ether mixture.

Method B: The reaction mixture was diluted with H_2O (20 mL) and the product was extracted with EtOAc (2 × 30 mL). Organic layers were dried over anhydrous sodium sulfate, filtered, and the solvent evaporated under the reduced pressure. The crude product was purified using column chromatography (with an additional Al_2O_3 layer to remove Cu salts, mobile phase cyclohexane/EtOAc/MeOH) and triturated with a diethyl ether/petroleum ether mixture.

1-((4-Ferrocenyl-1*H*-1,2,3-triazol-1-yl)methyl)-9*H*-pyrido[3,4-*b*]indole (**20**)

Azide **3**: 0.047 g; purification: Method A; yield: 0.064 g (78%); mp 252–255.5 °C; IR (ATR, ν/cm^{-1}) 3249, 3138, 3094, 2987, 2953, 1625, 1585, 1567, 1497, 1455, 1430, 1389, 1321, 1236, 1212, 1189, 1094, 1058, 998, 875, 816, 794, 750, 730, 622, 592, 500; ^{1}H NMR (DMSO-d_6) δ 11.95 (s, 1H), 8.31 (d, 1H, J = 5.2 Hz), 8.28–8.26 (m, 2H), 8.13 (d, 1H, J = 5.1 Hz), 7.70–7.68 (m, 1H), 7.60 (ddd, 1H, J = 8.2, 7.1, 1.2 Hz), 7.28 (ddd, 1H, J = 8.0, 7.0, 1.0 Hz), 6.08 (s, 2H), 4.73 (t, 2H, J = 1.9 Hz), 4.28 (t, 2H, J = 1.8 Hz), 4.03 (s, 5H); ^{13}C NMR (DMSO-d_6) δ 145.22, 140.71, 138.17, 137.86, 133.85, 128.71, 128.54, 121.91, 121.57, 120.76, 119.64, 114.82, 112.09, 76.04, 69.23, 68.21, 66.34, 51.24; ESI-MS: *m*/*z* 434.9 $(M + 1)^+$. HPLC purity > 99%. Anal. Calcd. for $C_{24}H_{19}FeN_5$: C, 66.53; H, 4.42; N, 16.16; found: C, 66.87; H, 4.09; N, 16.54.

1-Methyl-3-((4-ferrocenyl-1*H*-1,2,3-triazol-1-yl)methyl)-9*H*-pyrido[3,4-*b*]indole (**21**)

Azide **6**: 0.050 g; purification: Method B; cyclohexane/EtOAc/MeOH 1:1:0.1; yield: 0.053 g (62%); mp 242.5–244 °C; IR (ATR, ν/cm^{-1}) 3148, 3101, 2993, 2891, 1737, 1627, 1566, 1506, 1456, 1443, 1351, 1328, 1251, 1219, 1086, 1057, 1019, 1000, 874, 815, 729, 680, 587, 506, 487; ^{1}H NMR (DMSO-d_6) δ 11.66 (s, 1H), 8.23 (s, 1H), 8.16 (d, 1H, J = 7.9 Hz), 7.90 (s, 1H), 7.60−7.59 (m, 1H), 7.55−7.52 (m, 1H), 7.24−7.21 (m, 1H), 5.76 (s, 2H), 4.74 (t, 2H, J = 1.9 Hz), 4.29 (t, 2H, J = 1.9 Hz), 4.03 (s, 5H), 2.76 (s, 3H); ^{13}C NMR (DMSO-d_6) δ 145.37, 142.95, 142.05, 140.77, 133.94, 128.08, 127.63, 121.64, 121.06, 120.91, 119.44, 112.09, 111.42, 76.09, 69.26, 68.21, 66.32, 55.10, 20.38; ESI-MS: *m*/*z* 448.9 $(M + 1)^+$. Anal. Calcd. for $C_{25}H_{21}FeN_5$: C, 67.13; H, 4.73; N, 15.66; found: C, 67.38; H, 4.54; N, 15.39.

1-Methyl-6-(2-(4-ferrocenyl-1*H*-1,2,3-triazol-1-yl)ethoxy)-9*H*-pyrido[3,4-*b*]indole (**22**)

Azide **12**: 0.056 g; purification: Method B; mobile phase: cyclohexane/EtOAc/MeOH 1:1:0.5; yield: 0.034 g (37%); mp 201.5–204.0 °C; IR (ATR, ν/cm^{-1}) 3133, 2949, 2872, 1583, 1568, 1497, 1458, 1286,1210, 1105, 1041, 988, 878, 818, 705, 621, 504; ^{1}H NMR (DMSO-d_6) δ 11.39 (s, 1H), 8.29 (s, 1H), 8.15 (d, 1H, J = 5.3 Hz), 7.87 (d, 1H, J = 5.3 Hz), 7.78 (d, 1H, J = 2.5 Hz), 7.48 (d, 1H, J = 8.8 Hz), 7.16 (dd, 1H, J = 8.8, 2.5 Hz), 4.82 (t, 2H, J = 5.1 Hz), 4.73 (t, 2H, J = 1.9 Hz), 4.53 (t, 2H, J = 5.2 Hz), 4.30 (t, 2H, J = 1.8 Hz), 4.01 (s, 5H), 2.72 (s, 3H); ^{13}C NMR (DMSO-d_6) δ 151.85, 145.24, 142.24, 136.98, 135.52, 135.10, 126.63, 121.35, 121.28, 118.14, 112.77, 112.64, 105.13, 76.05, 69.22, 68.21, 67.14, 66.34, 49.24, 20.40; ESI-MS: *m*/*z* 477.9

$(M + 1)^+$. HPLC purity > 98%. Anal. Calcd. for $C_{26}H_{23}FeN_5O$: C, 65.42; H, 4.86; N, 14.67; found: C, 65.69; H, 4.98; N, 14.37.

1-Methyl-7-(2-(4-ferrocenyl-1*H*-1,2,3-triazol-1-yl)ethoxy)-9*H*-pyrido[3,4-*b*]indole (**23**)

Azide **15**: 0.056 g; purification: Method A; yield: 0.070 g, (77%); mp 228–229.5 °C; IR (ATR, ν/cm^{-1}) 3125, 3077, 2959, 2850, 2772, 1623, 1566, 1443, 1426, 1301, 1278, 1240, 1185, 1108, 1053, 1042, 977, 874, 822, 810, 743, 720, 693, 638, 587, 570, 522, 513, 495, 483; ^{1}H NMR (DMSO-d_6) δ 11.44 (s, 1H), 8.30 (s, 1H), 8.14 (d, 1H, J = 5.3 Hz), 8.05 (d, 1H, J = 8.6 Hz), 7.79 (d, 1H, J = 5.3 Hz), 7.03 (d, 1H, J = 2.2 Hz), 6.85 (dd, 1H, J = 8.6, 2.2 Hz), 4.83 (t, 2H, J = 5.1 Hz), 4.73 (t, 2H, J = 1.9 Hz), 4.55 (t, 2H, J = 5.1 Hz), 4.30 (t, 2H, J = 1.8 Hz), 4.01 (s, 5H), 2.72 (s, 3H); ^{13}C NMR (DMSO-d_6) δ 158.62, 145.25, 141.72, 141.35, 137.76, 134.59, 127.07, 122.71, 121.34, 115.33, 111.98, 109.17, 95.73, 76.01, 69.23, 68.22, 66.57, 66.35, 49.09, 20.36; ESI-MS: *m*/*z* 477.9 $(M + 1)^+$. HPLC purity > 99.5%. Anal. Calcd. for $C_{26}H_{23}FeN_5O$: C, 65.42; H, 4.86; N, 14.67; found: C, 65.77; H, 4.56; N, 14.44.

7-Methoxy-1-methyl-9-(2-(4-ferrocenyl-1*H*-1,2,3-triazol-1-yl)ethyl)-9*H*-pyrido[3,4-*b*]indole (**24**)

Azide **18**: 0.059 g; purification: Method A; yield: 0.059 g, (63%); mp 218–220 °C; IR (ATR, ν/cm^{-1}) 2968, 1621, 1565, 1445, 1404, 1339, 1253, 1222, 1158, 1182, 1136, 1096, 1041, 1021, 970, 929, 877, 821, 807, 641, 590, 545, 501, 475; ^{1}H NMR (DMSO-d_6) δ 8.17 (d, 1H, J = 5.2 Hz), 8.04 (d, 1H, J = 8.5 Hz), 7.88 (d, 1H, J = 5.2 Hz), 7.80 (s, 1H), 6.84−6.78 (m, 2H), 5.08 (t, 2H, J = 5.6 Hz), 4.88 (t, 2H, J = 5.6 Hz), 4.49 (t, 2H, J = 1.9 Hz), 4.22 (t, 2H, J = 1.9 Hz), 3.86−3.85 (m, 8H), 2.90 (s, 3H); ^{13}C NMR (DMSO-d_6) δ 160.51, 145.15, 142.76, 140.67, 138.12, 134.68, 128.73, 122.23, 121.79, 114.10, 112.26, 109.81, 92.93, 75.78, 68.09, 68.06, 66.26, 55.37, 49.71, 44.47, 23.18; ESI-MS: *m*/*z* 491.9 $(M + 1)^+$. HPLC purity > 99.5%. Anal. Calcd. for $C_{27}H_{25}FeN_5O$: C, 66.00; H, 5.13; N, 14.25; found: C, 65.94; H, 4.89; N, 14.38.

3.1.6. General Procedure for the Synthesis of TT Harmicens **25**–**29**

An appropriate alkyne **2**, **9**, **20**, **13**, or **16** (0.169 mmol) and (azidomethyl)ferrocene (**19**) (0.045 g, 0.186 mmol) were dissolved in dry DMF (2 mL), followed by the addition of sodium ascorbate (0.202 mmol, 1 mL of freshly prepared 0.2 M solution in H_2O) and $CuSO_4 \times 5\ H_2O$ (0.02 mmol, 20 µL of 1 M solution in H_2O). The reaction mixture was stirred overnight at room temperature. After completion of the reaction, 5 mL of H_2O was added and the precipitate was filtered off. Purification was performed using column chromatography (with an additional Al_2O_3 layer to remove Cu salts, mobile phase cyclohexane/EtOAc/MeOH 1:1:0.5 or DCM/MeOH 97:3) and triturated with a diethyl ether/petroleum ether mixture.

1-(1-(Ferrocenylmethyl)-1*H*-1,2,3-triazol-4-yl)-9*H*-pyrido[3,4-*b*]indole (**25**)

Alkyne **2**: 0.032 g; yield: 0.037 g, (51%); mp 229–230 °C; IR (ATR, ν/cm^{-1}) 3385, 3172, 3105, 3065, 2991, 1625, 1576, 1489, 1452, 1437, 1419, 1351, 1314, 1282, 1254, 1239, 1152, 1103, 1000, 829, 807, 749, 629, 591, 548, 499, 479; ^{1}H NMR (DMSO-d_6) δ 11.53 (s, 1H), 8.78 (s, 1H), 8.38 (d, 1H, J = 5.2 Hz), 8.26−8.24 (m, 1H), 8.11 (d, 1H, J = 5.1 Hz), 7.91−7.90 (m, 1H), 7.57−7.54 (m, 1H), 7.27−7.25 (m, 1H), 5.49 (s, 2H), 4.46 (t, 2H, J = 1.9 Hz), 4.24 (s, 5H), 4.22 (t, 2H, J = 1.9 Hz); ^{13}C NMR (DMSO-d_6) δ 147.60, 141.15, 137.83, 133.68, 131.74, 129.05, 128.18, 122.94, 121.47, 120.40, 119.51, 114.11, 113.23, 82.36, 68.74, 68.69, 68.48, 49.33; ESI-MS: *m*/*z* 434.1 $(M + 1)^+$. HPLC purity > 99.5%. Anal. Calcd. for $C_{24}H_{19}FeN_5$: C, 66.53; H, 4.42; N, 16.16; found: C, 66.38; H, 4.27; N, 16.32.

3-(1-(Ferrocenylmethyl)-1*H*-1,2,3-triazol-4-yl)-1-methyl-9*H*-pyrido[3,4-*b*]indole (**26**)

Alkyne **9**: 0.035 g; yield: 0.036 g, (45%); mp 183–186 °C; IR (ATR, ν/cm^{-1}) 3361, 2920, 2851, 1734, 1626, 1574, 1496, 1455, 1431, 1373, 1338, 1303, 1277, 1234, 1172, 1104, 1049, 1024, 1000, 924, 889, 818, 788, 775, 704, 631, 558, 584, 503, 478; ^{1}H NMR (DMSO-d_6) δ 11.69 (s, 1H), 8.58 (s, 1H), 8.41 (s, 1H), 8.29 (d, 1H, J = 7.9 Hz), 7.60 (d, 1H, J = 8.1 Hz), 7.54 (t, 1H, J = 7.6 Hz), 7.24 (t, 1H, J = 7.4 Hz), 5.39 (s, 2H), 4.45 (t, 2H, J = 1.9 Hz), 4.23 (s, 5H), 4.21 (t,

2H, J = 1.9 Hz), 2.80 (s, 3H); ^{13}C NMR (DMSO-d_6) δ 148.61, 141.93, 140.82, 139.95, 133.96, 128.02, 127.73, 121.97, 121.27, 121.25, 119.36, 112.01, 108.31, 82.45, 68.86, 68.68, 68.44, 49.05, 20.48; ESI-MS: *m*/*z* 447.9 (M + 1)$^+$. HPLC purity > 97.5%. Anal. Calcd. for $C_{25}H_{21}FeN_5$: C, 67.13; H, 4.73; N, 15.66; found: C, 67.41; H, 4.91; N, 15.36.

6-((1-(Ferrocenylmethyl)-1*H*-1,2,3-triazol-4-yl)methoxy)-1-methyl-9*H*-pyrido[3,4-*b*]indole (**27**)

Alkyne **10**: 0.040 g; yield: 0.055 g, (68%); mp 245–248 °C; IR (ATR, ν/cm^{-1}) 3631, 3137, 3081, 2950, 1637, 1603, 1583, 1567, 1499, 1480, 1451, 1411, 1283, 1211, 1107, 1069, 1054, 1040, 1027, 849, 821, 765, 620, 504; ^{1}H NMR (DMSO-d_6) δ 11.37 (s, 1H), 8.24 (s, 1H), 8.16 (d, 1H, J = 5.3 Hz), 7.89–7.88 (m, 2H), 7.49 (d, 1H, J = 8.8 Hz), 7.21 (dd, 1H, J = 8.9, 2.5 Hz), 5.32 (s, 2H), 5.21 (s, 2H), 4.32 (t, 2H, J = 1.8 Hz), 4.16–4.14 (m, 7H), 2.73 (s, 3H); ^{13}C NMR (DMSO-d_6) δ 151.88, 142.95, 142.19, 136.96, 135.42, 135.08, 126.69, 124.09, 121.34, 118.39, 112.73, 112.67, 105.20, 82.49, 68.62, 68.31, 61.88, 48.92, 20.40; ESI-MS: *m*/*z* 478.1 (M + 1)$^+$. HPLC purity > 97%. Anal. Calcd. for $C_{26}H_{23}FeN_5O$: C, 65.42; H, 4.86; N, 14.67; found: C, 65.25; H, 4.63; N, 14.42.

7-((1-(Ferrocenylmethyl)-1*H*-1,2,3-triazol-4-yl)methoxy)-1-methyl-9*H*-pyrido[3,4-*b*]indole (**28**)

Alkyne **13**: 0.040 g; yield: 0.048 g, (60%); mp 242–244 °C; IR (ATR, ν/cm^{-1}) 3344, 3072, 2869, 2785, 1738, 1626, 1567, 1488, 1444, 1377, 1325, 1305, 1290, 1278, 1177, 1142, 1110, 1058, 1142, 1011, 965, 828, 813, 781, 661, 639, 598, 572, 505, 480; ^{1}H NMR (DMSO-d_6) δ 11.45 (s, 1H), 8.23 (s, 1H), 8.15 (d, 1H, J = 5.2 Hz), 8.05 (d, 1H, J = 8.6 Hz), 7.80 (d, 1H, J = 5.3 Hz), 7.16 (d, 1H, J = 2.2 Hz), 6.89 (dd, 1H, J = 8.7, 2.3 Hz), 5.33 (s, 2H), 5.25 (s, 2H), 4.34 (t, 2H, J = 1.9 Hz), 4.18–4.16 (m, 7H), 2.72 (s, 3H); ^{13}C NMR (DMSO-d_6) δ 158.74, 142.71, 141.76, 141.33, 137.74, 134.58, 127.13, 124.15, 122.63, 115.11, 111.95, 109.46, 95.86, 82.41, 68.66, 68.64, 68.36, 61.45, 48.98, 20.32; ESI-MS: *m*/*z* 478.1 (M + 1)$^+$. HPLC purity > 97%. Anal. Calcd. for $C_{26}H_{23}FeN_5O$: C, 65.42; H, 4.86; N, 14.67; found: C, 65.71; H, 4.59; N, 14.82.

9-((1-(Ferocenylmethyl)-1*H*-1,2,3-triazol-4-yl)methyl)-7-methoxy-1-methyl-9*H*-pyrido [3,4-*b*]indole (**29**)

Alkyne **16**: 0.042 g; yield: 0.025 g, (30%); mp 187–190 °C; IR (ATR, ν/cm^{-1}) 3135, 3090, 2929, 1709, 1623, 1564, 1499, 1449, 1408, 1325, 1252, 1227, 1193, 1174, 1106, 1042, 1000, 913, 815, 764, 732, 638, 596, 550, 481;^{1}H NMR (DMSO-d_6) δ 8.16 (d, 1H, J = 5.2 Hz), 8.07 (d, 1H, J = 8.5 Hz), 7.98 (s, 1H), 7.86 (d, 1H, J = 5.2 Hz), 7.32 (d, 1H, J = 2.2 Hz), 6.87 (dd, 1H, J = 8.5, 2.2 Hz), 5.86 (s, 2H), 5.21 (s, 2H), 4.23 (t, 2H, J = 1.8 Hz), 4.12 (t, 2H, J = 1.8 Hz), 4.06 (s, 5H), 3.88 (s, 3H), 3.03 (s, 3H); ^{13}C NMR (DMSO-d_6) δ 160.55, 143.81, 142.67, 141.13, 138.05, 134.66, 128.54, 122.55, 122.38, 114.46, 112.26, 109.46, 94.05, 82.59, 68.54, 68.44, 68.21, 55.62, 48.77, 23.24; ESI-MS: *m*/*z* 492.1 (M + 1)$^+$. HPLC purity > 99.5%. Anal. Calcd. for $C_{27}H_{25}FeN_5O$ C, 66.00; H, 5.13; N, 14.25; found: C, 66.23; H, 5.32; N, 14.59.

3.1.7. General Procedure for the Synthesis of AT Harmicens **30**–**33**

A solution of a ferrocenecarboxylic acid (0.050 g, 0.217 mmol), DIEA (0.075 mL, 0.434 mmol), and HATU (0.083 g, 0.217 mmol) in DCM (4 mL) was stirred at room temperature for 20 min, followed by the addition of the corresponding amine **4**, **7**, **11**, or **17** (0.197 mmol). The resulting solution was stirred overnight at room temperature. Purification was performed using either Method A or Method B.

Method A: After completion of the reaction, the solvent was evaporated, and the residue was dissolved in EtOAc (20 mL) and washed with brine (2 × 20 mL) and water (1 × 20 mL). The organic layer was dried over anhydrous sodium sulfate, filtered, and evaporated under the reduced pressure. The crude product was purified using column chromatography with acetone/DCM as a mobile phase and triturated with diethyl ether/petroleum ether mixture.

Method B: The resulting precipitate was filtered off, purified using column chromatography (acetone/DCM 9:1), and triturated with diethyl ether/petroleum ether mixture.

N-((9*H*-Pyrido[3,4-*b*]indol-1-yl)methyl)ferrocenecarboxamide (**30**)

Amine **4**: 0.039 g; purification: Method A; mobile phase: acetone/DCM 1:1; yield: 0.039 g, (48%); mp 210–213 °C; IR (ATR, ν/cm^{-1}) 3623, 3467, 3085, 3050, 2962, 2928, 1711, 1649, 1622, 1531, 1503, 1444, 1408, 1375, 1340, 1300, 1249, 1229, 1195, 138, 1123, 1106, 1041, 1017, 914, 819, 801, 634, 598, 558; ^{1}H NMR (DMSO-d$_6$) δ 11.49 (s, 1H), 8.58 (t, 1H, J = 6.0 Hz), 8.31 (d, 1H, J = 5.2 Hz), 8.23 (d, 1H, J = 7.8 Hz), 8.05 (d, 1H, J = 5.2 Hz), 7.68 (d, 1H, J = 8.2 Hz), 7.56 (t, 1H, J = 7.6 Hz), 7.25 (t, 1H, J = 7.5 Hz), 4.88–4.87 (m, 4H), 4.35 (t, 2H, J = 1.9 Hz), 4.07 (s, 5H); ^{13}C NMR (DMSO-d$_6$) δ 169.83, 142.64, 140.17, 137.35, 133.55, 128.10, 127.74, 121.74, 120.93, 119.37, 113.86, 111.99, 76.11, 70.10, 69.31, 68.30, 41.73; ESI-MS: *m*/*z* 410.0 (M + 1)$^+$. Anal. Calcd. for $C_{23}H_{19}FeN_3O$: C, 67.50; H, 4.68; N, 10.27; found: C, 67.78; H, 4.59; N, 10.62.

N-((1-Methyl-9*H*-pyrido[3,4-*b*]indol-3-yl)methyl)ferrocenecarboxamide (**31**)

Amine **7**: 0.042 g; purification: Method A; mobile phase: acetone/DCM 1:1; yield: 0.033 g, (39%); mp 240.5–243 °C; IR (ATR, ν/cm^{-1}) 3324, 3226, 1634, 1574, 1532, 1498, 1447, 1380, 1348, 1297, 1248, 1104, 1026, 901, 814, 755, 738, 629, 528, 482; ^{1}H NMR (DMSO-d$_6$) δ 11.51 (s, 1H), 8.47 (t, 1H, J = 6.1 Hz), 8.12 (d, 1H, J = 7.9 Hz), 7.89 (s, 1H), 7.57 (d, 1H, J = 8.2 Hz), 7.52–7.48 (m, 1H), 7.21–7.17 (m, 1H), 4.90 (t, 2H, J = 1.9 Hz), 4.60 (d, 2H, J = 6.0 Hz), 4.37 (t, 2H, J = 1.9 Hz), 4.20 (s, 5H), 2.78 (s, 3H); ^{13}C NMR (DMSO-d$_6$) δ 168.94, 147.17, 141.14, 140.76, 133.49, 127.78, 127.66, 121.35, 120.95, 119.16, 111.98, 109.47, 76.73, 69.96, 69.25, 68.28, 44.31, 20.27; ESI-MS: *m*/*z* 424.0 (M + 1)$^+$. Anal. Calcd. for $C_{24}H_{21}FeN_3O$: C, 68.10; H, 5.00; N, 9.93; found: C, 68.28; H, 4.69; N, 9.62.

N-(2-((1-Methyl-9*H*-pyrido[3,4-*b*]indol-7-yl)oxy)ethyl)ferrocenecarboxamide (**32**)

Amine **11**: 0.048 g; purification: Method B; yield: 0.038 g, (42%); mp 243–245.5 °C; IR (ATR, ν/cm^{-1}) 3216, 1716, 1622, 1551, 1451, 1422, 1376, 1312, 1278, 1236, 1217, 1105, 960, 842, 801, 741, 641, 605, 505,476; ^{1}H NMR (DMSO-d$_6$) δ 11.41 (s, 1H), 8.14 (d, 1H, J = 5.3 Hz), 8.07–8.05 (m, 2), 7.79 (d, 1H, J = 5.3 Hz), 7.07 (d, 1H, J = 2.4 Hz), 6.90 (dd, 1H, J = 8.7, 2.2 Hz), 4.83 (t, 2H, J = 2.0 Hz), 4.35 (t, 2H, J = 1.9 Hz), 4.23 (t, 2H, J = 5.7 Hz), 4.13 (s, 5H), 3.63 (q, 2H, J = 5.7 Hz), 2.71 (s, 3H); ^{13}C NMR (DMSO-d$_6$) δ 169.36, 159.31, 141.89, 141.28, 137.74, 134.55, 127.17, 122.69, 114.98, 111.93, 109.22 95.38, 76.31, 70.01, 69.40, 68.22, 66.40, 38.49, 20.33; ESI-MS: *m*/*z* 454.0 (M + 1)$^+$. Anal. Calcd. for $C_{25}H_{23}FeN_3O_2$: C, 66.24; H, 5.11; N, 9.27; found: C, 65.99; H, 5.21; N, 9.54.

N-(2-(7-Methoxy-1-methyl-9*H*-pyrido[3,4-*b*]indol-9-yl)ethyl)ferrocenecarboxamide (**33**)

Amine **17**: 0.050 g; purification: Method A; mobile phase: acetone/DCM 3:2; yield: 0.046 g, (50%); mp 225–227 °C; IR (ATR, ν/cm^{-1}) 3623, 3467, 3085, 3050, 2962, 2928, 1711, 1649, 1622, 1531, 1503, 1444, 1408, 1375, 1340, 1300, 1249, 1229, 1195, 1177, 1138, 1123, 1107, 1041, 1016, 914, 819, 801, 634, 598, 558; ^{1}H NMR (DMSO-d$_6$) δ 8.17 (d, 1H, J = 5.1 Hz), 8.10–8.07 (m, 2H), 7.88 (d, 1H, J = 5.1 Hz), 7.32 (d, 1H, J = 2.2 Hz), 6.88 (dd, 1H, J = 8.5, 2.1 Hz), 4.69 (t, 2H, J = 1.9 Hz), 4.66 (t, 2H, J = 7.1 Hz), 4.34 (t, 2H, J = 1.9 Hz), 4.07 (s, 5H), 3.91 (s, 3H), 3.60 (q, 2H, J = 6.7 Hz), 3.04 (s, 3H); ^{13}C NMR (DMSO-d$_6$) δ 169.75, 160.52, 143.00, 140.66, 137.82, 134.67, 128.43, 122.39, 114.28, 112.26, 109.20, 93.78, 76.40, 69.93, 69.32, 68.08, 55.50, 43.56, 39.1, 23.14; ESI-MS: *m*/*z* 468.1 (M + 1)$^+$. Anal. Calcd. for $C_{26}H_{25}FeN_3O_2$: C, 66.82; H, 5.39; N, 8.99; found: C, 66.78; H, 5.52; N, 9.15.

3.1.8. General Procedure for the Synthesis of AT Harmicens **34**–**37**

A solution of a ferroceneacetic acid (0.050 g, 0.205 mmol), DIEA (0.071 mL, 0.410 mmol), and HATU (0.078 g, 0.205 mmol) in DCM (4 mL) was stirred at room temperature for 20 min, followed by the addition of the corresponding amine **4**, **7**, **11**, or **17** (0.186 mmol). The resulting solution was stirred at room temperature for 1 h and purified using either Method A or Method B.

Method A: The resulting precipitate was filtered off and recrystallized from EtOH.

Method B: The reaction mixture was extracted with brine (2 × 20 mL) and water (1 × 20 mL). The organic layer was dried over anhydrous sodium sulfate, filtered, and evaporated under the reduced pressure. The crude product was triturated with a diethyl ether/petroleum ether mixture.

N-((9*H*-Pyrido[3,4-*b*]indol-1-yl)methyl)-2-ferrocenylacetamide (**34**)

Amine **4**: 0.037 g; purification: Method A; yield: 0.027 g, (34%); mp 222.0–224.5 °C; IR (ATR, ν/cm^{-1}) 3333, 3219, 3168, 3099, 2995, 2898, 1651, 1568, 1521, 1502, 1445, 1436, 1413, 1361, 1321, 1285, 1248, 1151, 1106, 1045, 1026, 999, 878, 820, 740, 677, 595, 564, 504; ^{1}H NMR (DMSO-d$_6$) δ 11.50 (s, 1H), 8.55 (t, 1H, J = 5.4 Hz), 8.29 (d, 1H, J = 5.2 Hz), 8.22 (d, 1H, J = 7.8 Hz), 8.04 (d, 1H, J = 5.2 Hz), 7.63 (d, 1H, J = 8.2 Hz), 7.55 (t, 1H, J = 7.6 Hz), 7.25 (t, 1H, J = 7.4 Hz), 4.76 (d, 2H, J = 5.4 Hz), 4.22 (t, 2H, J = 1.9 Hz), 4.05 (m, 7H), 3.26 (s, 2H); ^{13}C NMR (DMSO-d$_6$) δ 170.47, 141.60, 140.36, 137.36, 133.50, 128.12, 127.74, 121.73, 120.87, 119.39, 113.89, 112.05, 82.66, 68.58, 68.41, 67.11, 41.52, 36.33; ESI-MS: *m*/*z* 424.1 (M + 1)$^{+}$; HPLC purity > 99.5%. Anal. Calcd. for $C_{24}H_{21}FeN_3O$: C, 68.10; H, 5.00; N, 9.93; found: C, 68.48; H, 4.79; N, 9.63.

N-((1-Methyl-9*H*-pyrido[3,4-*b*]indol-3-yl)methyl)-2-ferrocenylacetamide (**35**)

Amine **7**: 0.039 g; purification: Method A; yield: 0.032 g, (39%); mp 247.5–250.0 °C; IR (ATR, ν/cm^{-1}) 3404, 3191, 3081, 2944, 1649, 1621, 1570, 1522, 1471, 1455, 1421, 1312, 1247, 1267, 1136, 1103, 1038, 1023, 997, 925, 826, 803, 753, 741, 693, 621, 584, 543, 500, 482; ^{1}H NMR (DMSO-d$_6$) δ 11.48 (s, 1H), 8.42 (t, 1H, J = 5.9 Hz), 8.10 (d, 1H, J = 7.8 Hz), 7.73 (s, 1H), 7.56 (d, 1H, J = 8.2 Hz), 7.52–7.50 (m, 1H), 7.21 (t, 1H, J = 7.4 Hz), 4.46 (d, 2H, J = 5.8 Hz), 4.27 (t, 2H, J = 1.9 Hz), 4.12 (s, 5H), 4.10 (t, 2H, J = 1.9 Hz), 3.24 (s, 2H), 2.73 (s, 3H); ^{13}C NMR (DMSO-d$_6$) δ 169.93, 146.33, 141.16, 140.71, 133.44, 127.78, 127.66, 121.49, 120.98, 119.11, 111.94, 109.54, 83.05, 68.63, 68.45, 67.15, 44.28, 36.72, 20.28; ESI-MS: *m*/*z* 438.0 (M + 1)$^{+}$; HPLC purity > 99.5%. Anal. Calcd. for $C_{25}H_{23}FeN_3O$: C, 68.66; H, 5.30; N, 9.61; found: C, 68.75; H, 5.47; N, 9.32.

N-(2-((1-Methyl-9*H*-pyrido[3,4-*b*]indol-7-yl)oxy)ethyl)-2-ferrocenylacetamide (**36**)

Amine **11**: 0.045 g; purification: Method B; yield: 0.050 g, (58%); mp 176.0–177.5 °C; IR (ATR, ν/cm^{-1}) 3222, 3055, 2875, 1656, 1630, 1539, 1484, 1434, 1378, 1324, 1299, 1273, 1238, 1174, 1134, 1106, 1073, 1037, 1023, 1002, 961, 924, 871, 814, 776, 738, 661, 634, 590, 567, 484; ^{1}H NMR (DMSO-d$_6$) δ 11.40 (s, 1H), 8.19 (t, 1H, J = 5.5 Hz), 8.14 (d, 1H, J = 5.3 Hz), 8.05 (d, 1H, J = 8.6 Hz), 7.80 (d, 1H, J = 5.3 Hz), 7.02 (d, 1H, J = 2.2 Hz), 6.85 (dd, 1H, J = 8.6, 2.2 Hz), 4.20 (t, 2H, J = 1.9 Hz), 4.13 (t, 2H, J = 5.5 Hz), 4.11 (s, 5H), 4.05 (t, 2H, J = 1.9 Hz), 3.51 (q, 2H, J = 5.6 Hz), 3.16 (s, 2H), 2.72 (s, 3H); ^{13}C NMR (DMSO-d$_6$) δ 170.25, 159.17, 141.84, 141.29, 137.75, 134.56, 127.16, 122.63, 115.00, 111.93, 109.30, 95.40, 82.72, 68.50, 68.43, 67.08, 66.55, 38.40, 36.37, 20.35; ESI-MS: *m*/*z* 468.1 (M + 1)$^{+}$; HPLC purity > 99.5%. Anal. Calcd. For $C_{26}H_{25}FeN_3O_2$: C, 66.82; H, 5.39; N, 8.99; found: C, 66.53; H, 5.67; N, 9.12.

N-(2-(7-Methoxy-1-methyl-9*H*-pyrido[3,4-*b*]indol-9-yl)ethyl)-2-ferrocenylacetamide (**37**)

Amine **17**: 0.047 g; purification: Method B; yield: 0.062 g, (69%); mp 170.5–172.0 °C; IR (ATR, ν/cm^{-1}) 3341, 2931, 1655, 1624, 1566, 1503, 1451, 1439, 1410, 1347, 1330, 1300, 1251, 1195, 1172, 1141, 1104, 1048, 1024, 929, 835, 813, 794, 639, 567, 496, 482; ^{1}H NMR (DMSO-d$_6$) δ 8.17 (d, 1H, J = 5.1 Hz), 8.09 (d, 1H, J = 8.6 Hz), 8.01 (t, 1H, J = 6.0 Hz), 7.88 (d, 1H, J = 5.1 Hz), 7.27 (d, 1H, J = 2.2 Hz), 6.89 (dd, 1H, J = 8.6, 2.2 Hz), 4.57 (t, 2H, J = 7.1 Hz), 4.13 (t, 2H, J = 1.9 Hz), 4.11 (s, 5H), 4.05 (t, 2H, J = 1.8 Hz), 3.92 (s, 3H), 3.45 (q, 2H, J = 6.7 Hz), 3.07 (s, 2H), 2.95 (s, 3H); ^{13}C NMR (DMSO-d$_6$) δ 170.58, 160.52, 142.86, 140.61, 137.80, 134.64, 128.43, 122.40, 114.31, 112.25, 109.24, 93.64, 82.12, 68.72, 68.46, 67.21, 55.52, 43.37, 38.73, 36.65, 23.08; ESI-MS: *m*/*z* 482.2 (M + 1)$^{+}$. Anal. Calcd. For $C_{27}H_{27}FeN_3O_2$: C, 67.37; H, 5.65; N, 8.73; found: C, 67.16; H, 5.84; N, 8.89.

3.2. Biological Evaluation

3.2.1. In Vitro Drug Sensitivity Assay against Erythrocytic Stages of *P. falciparum*

The antiplasmodial activity of harmicens **20**–**37** was evaluated against two strains of *P. falciparum* (3D7—CQ-sensitive, Dd2—multidrug-resistant) as previously described using the histidine-rich protein 2 (HRP2) assay [44,45]. Briefly, 96-well plates were pre-coated with the tested compounds in a three-fold dilution before ring-stage parasites were added to complete the culture medium at a hematocrit of 1.5% and parasitemia of 0.05%. After three days of incubation at 37 °C, 5% CO_2, and 5% oxygen, plates were frozen until HRP2-ELISA analysis. All compounds were evaluated in duplicate in at least two independent experiments. The IC_{50} was determined using a nonlinear regression analysis of log concentration–response curves using the drc-package v0.9.0 of R v2.6.1 (R Foundation, Vienna, Austria) [46].

3.2.2. Cytotoxicity Assay in Human Cell Lines

The experiments were carried out on five human cell lines purchased from American Type Culture Collection (ATCC): HepG2 (hepatocellular carcinoma; ATCC® HB-8065™), SW620 (colorectal adenocarcinoma; ATCC® CCL-227™), HCT116 (colorectal carcinoma; ATCC® CCL-247™), MCF-7 (breast adenocarcinoma; ATCC® HTB-22™), and Hek293T (embryonic kidney cells; ATCC® CRL-3216™). All cell lines were cultured as monolayers and maintained in Dulbecco's Modified Eagle Medium (DMEM) (Capricorn Scientific, Ebsdorfergrund, Germany) supplemented with 10% fetal bovine serum (FBS) (Capricorn Scientific, Ebsdorfergrund, Germany), 100 U/mL penicillin, and 100 µg/mL streptomycin (Capricorn Scientific, Ebsdorfergrund, Germany) in a humidified atmosphere with 5% CO_2 at 37 °C. Cells were seeded in 96-well plates (Corning, Durham, NC, USA) at 5000–7000 cells per well (depending on the cell-doubling time of a specific cell line) in 0.1 mL media and cultured for 24 h. The next day, the medium was aspirated, and cells were treated for 72 h. Only the compounds that led to more than a 50% reduction in mitochondrial metabolic activity at a concentration of 50 µM were selected for further analysis. The following concentrations of selected compounds were used: 25, 10, 5, and 1 µM. Working dilutions were freshly prepared on the day of the testing. A fresh growth medium was added to untreated control cells, which were defined as 100% viable. DMSO (0.13%) in DMEM was considered a negative control. 5-Fluorouracil (5-FU) and harmine were used as positive controls. At the end of treatment, the medium was removed, and cells were incubated for 1 h with 0.5 mg/mL MTT (Abcam, Cambridge, MA, USA) dissolved in serum-deprived DMEM. The MTT-containing medium was then removed, and 0.1 mL isopropanol was added per well to lyse cells and dissolve formazan. The optical density was measured at 570 nm using a microplate reader (VICTOR3, PerkinElmer, Waltham, MA, USA). Each test point was performed in triplicate. The absorbance was directly proportional to the cell viability. The IC_{50} values (concentration required to decrease viability by 50%) were calculated by using nonlinear regression on the sigmoidal dose–response plots and are expressed as mean ± SD.

3.2.3. Cell Localization

The MCF-7 cells were seeded onto round microscopic glass coverslips placed in 24-well plates at a density of 5×10^4 cells per well and grown at 37 °C and 5% CO_2 for 24 h in DMEM supplemented with FBS, penicillin, and streptomycin, as described above. On the next day, the growth medium was replaced with compound **28** at 10 and 50 µM concentrations or compound **36** at a 5 µM concentration in a complete cell culture medium and incubated for 30 min and 1 h. Afterward, the medium was discarded and the coverslips were rinsed twice with PBS, placed on the microscopic slides, and immediately analyzed. The uptake and intracellular distribution of the tested derivative were analyzed under a fluorescence microscope (Olympus BX51, Tokyo, Japan) at 400× magnification using a DAPI filter. Images were captured with an Olympus DP70 digital camera.

3.2.4. Cell Cycle Analysis

HCT116 cells were seeded onto 6-well plates (2×10^5 cells per well). After 24 h, the tested compounds **28** and **36** were added at two concentrations—3 μM and 6 μM. After 24 h and 48 h, the attached cells were trypsinized, combined with floating cells, washed with phosphate buffer saline (PBS), fixed with 70% ethanol, and stored at −20 °C. Immediately before analysis, the cells were washed two times with PBS, treated with 0.1 μg/μL of RNAse A, and stained for 1 h on ice with 50 μg/mL of propidium iodide. The stained cells were then analyzed using a BD FACScalibur flow cytometer (20,000 counts were measured). The percentage of cells in each cell cycle phase was determined using FlowJo software (TreeStar Inc., San Francisco, CA, USA). The tests were performed in duplicate and repeated in two separate experiments. The average values from duplicates from one representative experiment ± SD are presented.

3.2.5. Statistical Analysis

Data are presented as mean ± SD for the indicated number of independent experiments. Statistical significance ($p < 0.05$) was determined via one-way ANOVA using the Microsoft Excel Analysis ToolPak add-in (Microsoft 365 MSO, v.2206 build 16.0.15330.20216, Redmond, WA, USA).

4. Conclusions

We synthesized 18 harmicens—new hybrids combining harmine/β-carboline and ferrocene motifs. The compounds obtained differed in the type and length of the linker between the β-carboline ring and ferrocene, as well as its position at the β-carboline ring. Evaluation of their antiplasmodial activity in vitro against the erythrocytic stages of *P. falciparum* showed that the hybrids had moderate antiplasmodial activity in the submicromolar/low micromolar range. On the other hand, their antiproliferative activity in vitro was significant. Several compounds exhibited selective activity against tumor cells (MCF-7 and HCT116) compared to a nontumor cell line (Hek293T) (IC_{50} in the single-digit micromolar range, SI > 5.9). We further demonstrated that cell localization and its effect on the cell cycle were markedly different for HCT116-selective **28** and nonselective **36**. The experiments revealed that **28** penetrated the nucleus and induced G2/M cell cycle arrest with a concomitant drastic reduction in the percentage of cells in the S phase, whereas the effect of the nonselective compound **36** on the cell cycle was much less pronounced. We believe that our study clearly demonstrated the potential of harmicens as valuable anticancer hits. In future experiments, we will focus on the enrichment of the harmicene library to establish a reliable structure–activity relationship and the elucidation of their mechanism of action.

Supplementary Materials: The supporting information can be downloaded at: https://www.mdpi.com/article/10.3390/ijms23169315/s1.

Author Contributions: Conceptualization, Z.R.; methodology, G.P., M.M. (Marina Marinović), K.P., M.M. (Marija Mioč), M.K., J.H. and L.P.d.C.; writing—original draft preparation, Z.R., K.P. and I.P.; supervision—Z.R.; writing—review and editing, Z.R.; funding acquisition, Z.R. All authors have read and agreed to the published version of the manuscript.

Funding: This research was funded by the Croatian Science Foundation under grant number UIP-2017-05-5160. The work of M.M. was fully supported by the Croatian Science Foundation's Young Researcher's Career Development Project—Training of Doctoral Students (funded by the European Union from the European Social Fund).

Data Availability Statement: The data presented in this study are available in this article and in the Supplementary Materials.

Conflicts of Interest: The authors declare no conflict of interest. The funders had no role in the design of the study; in the collection, analyses, or interpretation of data; in the writing of the manuscript; or in the decision to publish the results.

References

1. World Health Organization. Available online: https://www.who.int/news-room/fact-sheets/detail/cancer (accessed on 20 July 2022).
2. Ferlay, J.; Colombet, M.; Soerjomataram, I.; Parkin, D.M.; Piñeros, M.; Znaor, A.; Freddie, B. Cancer statistics for the year 2020: An overview. *Int. J. Cancer.* **2021**, *149*, 778–789. [CrossRef] [PubMed]
3. World Health Organization. International Agency for Research on Cancer. Available online: https://gco.iarc.fr/today (accessed on 18 February 2022).
4. Wang, R.; Chen, H.; Yan, W.; Zheng, M.; Zhang, T.; Zhang, Y. Ferrocene-containing hybrids as potential anticancer agents: Current developments, mechanisms of action and structure-activity relationships. *Eur. J. Med. Chem.* **2020**, *190*, 112019. [CrossRef] [PubMed]
5. Sato, S. *Plasmodium*—A brief introduction to the parasites causing human malaria and their basic biology. *J. Physiol. Anthropol.* **2021**, *40*, 1. [CrossRef] [PubMed]
6. Yeung, S. Malaria-Update on Antimalarial Resistance and Treatment Approaches. *Pediatr. Infect. Dis. J.* **2018**, *37*, 367–369. [CrossRef]
7. World Health Organization. World Malaria Report 2021. Available online: https://www.who.int/publications/i/item/9789240040496 (accessed on 15 July 2022).
8. Nepali, K.; Sharma, S.; Sharma, M.; Bedi, P.M.; Dhar, K.L. Rational approaches, design strategies, structure activity relationship and mechanistic insights for anticancer hybrids. *Eur. J. Med. Chem.* **2014**, *77*, 422–487. [CrossRef]
9. Soni, J.P.; Yeole, Y.; Shankaraiah, N. β-Carboline-based molecular hybrids as anticancer agents: A brief sketch. *RSC Med. Chem.* **2021**, *12*, 730–750. [CrossRef]
10. Walsh, J.J.; Bell, A. Hybrid drugs for malaria. *Curr. Pharm. Des.* **2009**, *15*, 2970–2985. [CrossRef]
11. Cao, R.; Peng, W.; Wang, Z.; Xu, A. beta-Carboline alkaloids: Biochemical and pharmacological functions. *Curr. Med. Chem.* **2007**, *14*, 479–500. [CrossRef]
12. Ishida, J.; Wang, H.K.; Bastow, K.F.; Hu, C.Q.; Lee, K.H. Antitumor agents 201. Cytotoxicity of harmine and β-carboline analogs. *Bioorg. Med. Chem. Lett.* **1999**, *9*, 3319–3324. [CrossRef]
13. Guan, H.; Chen, H.; Peng, W.; Ma, Y.; Cao, R.; Liu, X.; Xu, A. Design of beta-carboline derivatives as DNA-targeting antitumor agents. *Eur. J. Med. Chem.* **2006**, *41*, 1167–1179. [CrossRef]
14. Xu, Q.B.; Chen, X.F.; Feng, J.; Miao, J.F.; Liu, J.; Liu, F.T.; Niu, B.X.; Cai, J.Y.; Huang, C.; Zhang, Y.; et al. Design, synthesis and biological evaluation of hybrids of β-carboline and salicylic acid as potential anticancer and apoptosis inducing agents. *Sci. Rep.* **2016**, *6*, 36238. [CrossRef]
15. Aaghaz, S.; Sharma, K.; Jain, R.; Kamal, A. β-Carbolines as potential anticancer agents. *Eur. J. Med. Chem.* **2021**, *216*, 113321. [CrossRef]
16. Meinguet, C.; Bruyère, C.; Frédérick, R.; Mathieu, V.; Vancraeynest, C.; Pochet, L.; Laloy, J.; Mortier, J.; Wolber, G.; Kiss, R.; et al. 3D-QSAR, design, synthesis and characterization of trisubstituted harmine derivatives with *in vitro* antiproliferative properties. *Eur. J. Med. Chem.* **2015**, *94*, 45–55. [CrossRef]
17. Kumar, S.; Singh, A.; Kumar, K.; Kumar, V. Recent insights into synthetic β-carbolines with anti-cancer activities. *Eur. J. Med. Chem.* **2017**, *142*, 48–73. [CrossRef]
18. Shahinas, D.; Macmullin, G.; Benedict, C.; Crandall, I.; Pillai, D.R. Harmine is a potent antimalarial targeting Hsp90 and synergizes with chloroquine and artemisinin. *Antimicrob. Agents Chemother.* **2012**, *56*, 4207–4213. [CrossRef]
19. Gorki, V.; Walter, N.S.; Singh, R.; Chauhan, M.; Dhingra, N.; Salunke, D.B.; Kaur, S. β-Carboline Derivatives Tackling Malaria: Biological Evaluation and Docking Analysis. *ACS Omega* **2020**, *5*, 17993–18006. [CrossRef]
20. Kamboj, A.; Sihag, B.; Brar, D.S.; Kaur, A.; Salunke, D.B. Structure activity relationship in β-carboline derived anti-malarial agents. *Eur. J. Med. Chem.* **2021**, *221*, 113536. [CrossRef]
21. Heinze, K.; Lang, H. Ferrocene—Beauty and Function. *Organometallics* **2013**, *32*, 5623–5625. [CrossRef]
22. Sharma, B.; Kumar, V. Has Ferrocene Really Delivered Its Role in Accentuating the Bioactivity of Organic Scaffolds? *J. Med. Chem.* **2021**, *64*, 16865–16921. [CrossRef]
23. Roux, C.; Biot, C. Ferrocene-based antimalarials. *Future Med. Chem.* **2012**, *4*, 783–797. [CrossRef]
24. Peter, S.; Aderibigbe, B.A. Ferrocene-Based Compounds with Antimalaria/Anticancer Activity. *Molecules* **2019**, *24*, 3604. [CrossRef]
25. Ren, S.Z.; Wang, Z.C.; Zhu, D.; Zhu, X.H.; Shen, F.Q.; Wu, S.Y.; Chen, J.J.; Xu, C.; Zhu, H.L. Design, synthesis and biological evaluation of novel ferrocene-pyrazole derivatives containing nitric oxide donors as COX-2 inhibitors for cancer therapy. *Eur. J. Med. Chem.* **2018**, *157*, 909–924. [CrossRef]
26. Chellan, P.; Sadler, P.J. Enhancing the Activity of Drugs by Conjugation to Organometallic Fragments. *Chem. Eur. J.* **2020**, *26*, 8676–8688. [CrossRef]
27. Nguyen, A.; Top, S.; Pigeon, P.; Vessières, A.; Hillard, E.A.; Plamont, M.A.; Huché, M.; Rigamonti, C.; Jaouen, G. Synthesis and structure-activity relationships of ferrocenyl tamoxifen derivatives with modified side chains. *Chem. Eur. J.* **2009**, *15*, 684–696. [CrossRef]
28. Dubar, F.; Khalife, J.; Brocard, J.; Dive, D.; Biot, C. Ferroquine, an ingenious antimalarial drug: Thoughts on the mechanism of action. *Molecules* **2008**, *13*, 2900–2907. [CrossRef]

29. Adoke, Y.; Zoleko-Manego, R.; Ouoba, S.; Tiono, A.B.; Kaguthi, G.; Bonzela, J.E.; Duong, T.T.; Nahum, A.; Bouyou-Akotet, M.; Ogutu, B.; et al. A randomized, double-blind, phase 2b study to investigate the efficacy, safety, tolerability and pharmacokinetics of a single-dose regimen of ferroquine with artefenomel in adults and children with uncomplicated *Plasmodium falciparum* malaria. *Malar. J.* **2021**, *20*, 222. [CrossRef]
30. Kondratskyi, A.; Kondratska, K.; Vanden Abeele, F.; Gordienko, D.; Dubois, C.; Toillon, R.A.; Slomianny, C.; Lemière, S.; Delcourt, P.; Dewailly, E.; et al. Ferroquine, the next generation antimalarial drug, has antitumor activity. *Sci. Rep.* **2017**, *7*, 15896. [CrossRef]
31. Perković, I.; Raić-Malić, S.; Fontinha, D.; Prudêncio, M.; Pessanha de Carvalho, L.; Held, J.; Tandarić, T.; Vianello, R.; Zorc, B.; Rajić, Z. Harmicines-harmine and cinnamic acid hybrids as novel antiplasmodial hits. *Eur. J. Med. Chem.* **2020**, *187*, 111927. [CrossRef]
32. Marinović, M.; Perković, I.; Fontinha, D.; Prudêncio, M.; Held, J.; Pessanha de Carvalho, L.; Tandarić, T.; Vianello, R.; Zorc, B.; Rajić, Z. Novel Harmicines with Improved Potency against *Plasmodium*. *Molecules* **2020**, *25*, 4376. [CrossRef]
33. Marinović, M.; Poje, G.; Perković, I.; Fontinha, D.; Prudêncio, M.; Held, J.; Pessanha de Carvalho, L.; Tandarić, T.; Vianello, R.; Rajić, Z. Further investigation of harmicines as novel antiplasmodial agents: Synthesis, structure-activity relationship and insight into the mechanism of action. *Eur. J. Med. Chem.* **2021**, *15*, 113687. [CrossRef] [PubMed]
34. Pavić, K.; Beus, M.; Poje, G.; Uzelac, L.; Kralj, M.; Rajić, Z. Synthesis and Biological Evaluation of Harmirins, Novel Harmine-Coumarin Hybrids as Potential Anticancer Agents. *Molecules* **2021**, *26*, 6490. [CrossRef] [PubMed]
35. Poje, G.; Pessanha de Carvalho, L.; Held, J.; Moita, D.; Prudêncio, M.; Perković, I.; Tandarić, T.; Vianello, R.; Rajić, Z. Design and synthesis of harmiquins, harmine and chloroquine hybrids as potent antiplasmodial agents. *Eur. J. Med. Chem.* **2022**, *238*, 114408. [CrossRef] [PubMed]
36. Allardyce, C.S.; Dorcier, A.; Scolaro, C.; Dyson, P.J. Development of organometallic (organo-transitionmetal) pharmaceuticals. *Appl. Organometal. Chem.* **2005**, *19*, 1–10. [CrossRef]
37. Hartinger, C.G.; Dyson, P.J. Bioorganometallic chemistry–from teaching paradigms to medicinal applications. *Chem. Soc. Rev.* **2009**, *38*, 391–401. [CrossRef]
38. Matos, J.; da Cruz, F.P.; Cabrita, É.; Gut, J.; Nogueira, F.; do Rosário, V.E.; Moreira, R.; Rosenthal, P.J.; Prudêncio, M.; Gomes, P. Novel potent metallocenes against liver stage malaria. *Antimicrob. Agents Chemother.* **2012**, *56*, 1564–1570. [CrossRef]
39. Patra, M.; Gasser, G. The medicinal chemistry of ferrocene and its derivatives. *Nat. Rev. Chem.* **2017**, *1*, 66. [CrossRef]
40. Wani, W.A.; Jameel, E.; Baig, U.; Mumtazuddin, S.; Hun, L.T. Ferroquine and its derivatives: New generation of antimalarial agents. *Eur. J. Med. Chem.* **2015**, *101*, 534–551. [CrossRef]
41. Ludwig, B.S.; Correia, J.D.G.; Kühn, F.E. Ferrocene derivatives as anti-infective agents. *Coord. Chem. Rev.* **2019**, *396*, 22–48. [CrossRef]
42. Habrant, D.; Rauhala, V.; Koskinen, A.M. Conversion of carbonyl compounds to alkynes: General overview and recent developments. *Chem. Soc. Rev.* **2010**, *39*, 2007–2017. [CrossRef]
43. Goddard-Borger, E.D.; Stick, R.V. An efficient, inexpensive, and shelf-stable diazotransfer reagent: Imidazole-1-sulfonyl azide hydrochloride. *Org. Lett.* **2007**, *9*, 3797–3800. [CrossRef]
44. Held, J.; Gebru, T.; Kalesse, M.; Jansen, R.; Gerth, K.; Müller, R.; Mordmüller, B. Antimalarial activity of the myxobacterial macrolide chlorotonil a. *Antimicrob. Agents Chemother.* **2014**, *58*, 6378–6384. [CrossRef]
45. Noedl, H.; Bronnert, J.; Yingyuen, K.; Attlmayr, B.; Kollaritsch, H.; Fukuda, M. Simple histidine-rich protein 2 double-site sandwich enzyme-linked immunosorbent assay for use in malaria drug sensitivity testing. *Antimicrob. Agents Chemother.* **2005**, *49*, 3575–3577. [CrossRef]
46. The R Project for Statistical Computing. Available online: https://www.R-project.org/ (accessed on 20 December 2021).
47. Kim, G.D. Harmine Hydrochloride Triggers G2/M Cell Cycle Arrest and Apoptosis in HCT116 Cells through ERK and PI3K/AKT/mTOR Signaling Pathways. *Prev. Nutr. Food Sci.* **2021**, *26*, 445–452. [CrossRef]
48. Ock, C.W.; Kim, G.D. Harmine Hydrochloride Mediates the Induction of G2/M Cell Cycle Arrest in Breast Cancer Cells by Regulating the MAPKs and AKT/FOXO3a Signaling Pathways. *Molecules* **2021**, *26*, 6714. [CrossRef]
49. Mota, N.S.R.S.; Kviecinski, M.R.; Felipe, K.B.; Grinevicius, V.M.A.S.; Siminski, T.; Almeida, G.M.; Zeferino, R.C.; Pich, C.T.; Filho, D.W.; Pedrosa, R.C.; et al. β-carboline alkaloid harmine induces DNA damage and triggers apoptosis by a mitochondrial pathway: Study in silico, in vitro and in vivo. *Int. J. Funct. Nutr.* **2020**, *1*, 1.
50. Zheng, J.; Zeng, L.; Tang, M.; Lin, H.; Pi, C.; Xu, R.; Cui, X. Novel Ferrocene Derivatives Induce G0/G1 Cell Cycle Arrest and Apoptosis through the Mitochondrial Pathway in Human Hepatocellular Carcinoma. *Int. J. Mol. Sci.* **2021**, *22*, 3097. [CrossRef]
51. Zeng, L.; Tang, M.; Pi, C.; Zheng, J.; Gao, S.; Chabanne, T.; Chauvin, R.; Cheng, W.; Lin, H.; Xu, R.; et al. Novel Ferrocene Derivatives Induce Apoptosis through Mitochondria-Dependent and Cell Cycle Arrest via PI3K/Akt/mTOR Signaling Pathway in T Cell Acute Lymphoblastic Leukemia. *Cancers* **2021**, *13*, 4677. [CrossRef]
52. Singh, D.; Hazra, C.K.; Malakar, C.C.; Pandey, S.K.; Kaith, B.S.; Singh, V. Indium-Mediated Domino Allylation-Lactonisation Approach: Diastereoselective Synthesis of β-Carboline C-3 Tethered α-Methylene γ-Butyrolactones. *ChemistrySelect* **2018**, *3*, 4859–4864. [CrossRef]
53. Szabó, T.; Hazai, V.; Volk, B.; Simig, G.; Milen, M. First total synthesis of the β-carboline alkaloids trigonostemine A, trigonostemine B and a new synthesis of pityriacitrin and hyrtiosulawesine. *Tetrahedron Lett.* **2019**, *60*, 1471–1475. [CrossRef]

TEMELJNA DOKUMENTACIJSKA KARTICA

Temeljna dokumentacijska kartica

Sveučilište u Zagrebu
Farmaceutsko-biokemijski fakultet
Zavod za farmaceutsku kemiju
A. Kovačića 1, 10000 Zagreb, Hrvatska

Doktorski rad

SINTEZA, KARAKTERIZACIJA I BIOLOŠKO DJELOVANJE HARMICINA, HARMIKINA I HARMICENA

Goran Poje

SAŽETAK

Rak i malarija su smrtonosne bolesti koje predstavljaju značajan globalni javnozdravstveni problem. Učinkovitost postojećih citostatika i antimalarika opada uslijed pojave rezistencije, zbog čega je potrebno kontinuirano istraživati nove potencijalne lijekove. Popularan pristup u razvoju novih lijekova je molekulska hibridizacija, odnosno kovalentno povezivanje dva bioaktivna spoja s ciljem poboljšanja njihovog djelovanja. U okviru ovog doktorskog rada sintetizirani su hibridni spojevi harmina, β-karbolinskog alkaloida s izraženim antimalarijskim i protutumorskim djelovanjem, i: 1) derivata cimetne kiseline (harmicini), 2) klorokina (harmikini), 3) ferocena (harmiceni). U pripravi harmicina korištena je bakrom(I) katalizirana azid-alkin cikloadicija, odnosno klik-reakcija koja je rezultirala harmicinima triazolskog tipa. Harmikini i harmiceni pripravljeni su korištenjem klik-reakcije te reakcije povezivanja amina i karboksilnih kiselina, dajući harmikine i harmicene triazolskog i amidnog tipa. Za potrebe klik-reakcija sintetizirani su odgovarajući alkini i azidi β-karbolina, derivata cimetne kiseline, 7-klorkinolina te ferocena, dok su amini i karboksilna kiselina harmina te karboksilna kiselina i amini 7-klorkinolina pripravljeni za potrebe reakcija povezivanja. Novi spojevi karakterizirani su uobičajenim analitičkim i spektroskopskim metodama te je ispitano njihovo antiproliferativno i antimalarijsko djelovanje *in vitro*. U seriji harmicina najjače antiproliferativno djelovanje ostvarili su triazoli **49a-e**, dok su u seriji harmikina najcitotoksičniji bili triazoli **54** i **57**. Najsnažnije antiproliferativno djelovanje među harmicenima prema svim ispitivanim staničnim linijama pokazao je amid **82**, dok su harmiceni triazolskog tipa **67**, odnosno **66** i **69** pokazali značajno i selektivno djelovanje prema MCF-7 i HCT116. Najbolje antimalarijsko djelovanje na eritrocitnu fazu životnog ciklusa svih ispitanih sojeva *P. falciparum*, u nanomolarnim koncentracijama, pokazali su harmikini. Spoj **63** ispoljio je 5,5 puta snažniji učinak u odnosu na klorokin (CQ) (IC_{50} = 2 ± 0,3 nM), dok je spoj **65** bio najučinkovitiji prema sojevima plazmodija rezistentnima na postojeće antimalarike. Temeljem dobivenih rezultata može se zaključiti da harmikini predstavljaju spojeve uzore za razvoj novih potencijalnih antimalarika, dok je harmicine i harmicene potrebno razvijati kao potencijalne protutumorske lijekove.

Rad je pohranjen u Centralnoj knjižnici Farmaceutsko-biokemijskog fakulteta Sveučilišta u Zagrebu.

Rad sadrži: 236 stranica, 65 slika, 47 tablica, 26 shema i 222 literaturna navoda. Izvornik je na hrvatskom jeziku.

Ključne riječi: harmin, derivati cimetne kiseline, klorokin, ferocen, hibridni spojevi, klik-reakcija, reakcija povezivanja, antimalarijsko djelovanje, antiproliferativno djelovanje.

Mentor: **Dr. sc. Zrinka Rajić**, *redovita profesorica, Farmaceutsko-biokemijski fakultet Sveučilišta u Zagrebu.*

Ocjenjivači: **Dr. sc. Branka Zorc**, *profesorica emerita, Farmaceutsko-biokemijski fakultet Sveučilišta u Zagrebu*
Dr. sc. Ivana Perković, *izvanredna profesorica, Farmaceutsko-biokemijski fakultet Sveučilišta u Zagrebu*
Dr. sc. Marijeta Kralj, *znanstvena savjetnica u trajnom zvanju, Institut Ruđer Bošković*

Rad prihvaćen: rujan 2022.

Basic documentation card

University of Zagreb
Faculty of Pharmacy and Biochemistry
Department of Medicinal Chemistry
A. Kovacica , 10000 Zagreb, Croatia

Doctoral dissertation

SYNTHESIS, CHARACTERIZATION AND BIOLOGICAL ACTIVITY OF HARMICINES, HARMIQUINS AND HARMICENES

Goran Poje

SUMMARY

Cancer and malaria are life-threatening diseases that pose a permanent public health problem. Existing cytostatic and antimalarial drugs are progressively losing their efficacy due to the development of drug resistance. Thus, there is a constant need for the development of novel and effective drugs. One of the possible approaches is molecular hybridization, *i.e.* covalent linking of two bioactive moieties into a single molecule with improved properties. In this dissertation, hybrids comprising harmin, a β-carboline alkaloid with pronounced antimalarial and antitumor activity, and: 1) cinnamic acid derivatives (harmicines), 2) chloroquine (harmiquins), 3) ferrocene (harmicenes) were prepared. The harmicines were synthesized by a copper(I)-catalyzed azide-alkyne cycloaddition ("click" reaction) leading to triazole-type hybrids. On the other hand, harmiquins and harmicenes were prepared by both "click" and coupling reactions, giving triazole- and amide-type harmiquins and harmicenes. To obtain the required starting compounds for the "click" reaction, synthetic routes to β-carboline-, cinnamic acid derivative-, 7-chloroquinoline-, and ferrocene-based alkynes and azides were developed. For the purpose of coupling reactions, 7-chloroquinoline- and harmine-based amines and acids were prepared. The novel compounds were characterized by standard methods (^{1}H and ^{13}C NMR, IR, MS). The antimalarial activity of the prepared compounds was evaluated *in vitro* against the erythrocytic and hepatic stages of the *Plasmodium* life cycle, as well as the antiproliferative activity against a panel of human tumor cell lines. Among the harmicines, triazoles **49a-e** exhibited the strongest antiproliferative activity, whereas in the harmiquins series, triazoles **54** and **57** were the most cytotoxic compounds. Among the harmicenes, amide **82** showed the strongest cytotoxic activity against all tested cell lines (IC_{50} < 10 μM), whereas triazole-type harmicenes **67**, **66**, and **69** displayed significant and selective activity against MCF-7 and HCT116. Harmiquins have shown the best antimalarial activity against the erythrocytic phase of chloroquine-sensitive and -resistant *P. falciparum* strains (IC_{50} in low nanomolar concentrations). Compound **63** showed a 5.5-fold stronger effect than chloroquine (IC_{50} = 2 ± 0.3 nM), while compound **65** was the most effective against resistant *Plasmodium* strains. The results suggest that harmiquins represent novel antimalarial hits, whereas further studies including harmicines and harmicenes should focus on their anticancer properties.

The disertation is deposited in the Central Library of Faculty of Pharmacy and Biochemistry.

Dissertation includes: 236 pages, 65 figures, 47 tables, 26 schemes and 222 references. Original is in Croatian language.

Keywords: harmine, cinnamic acid derivatives, chloroquine, ferrocene, hybrid compounds, „click“ chemistry, coupling reaction, antimalarial activity, antiproliferative activity.

Menthor: **Zrinka Rajić, Ph.D.**, *Full Professor, Faculty of Pharmacy and Biochemistry, University of Zagreb.*

Reviewers: **Branka Zorc, Ph.D.**, *Professor Emeritus, Faculty of Pharmacy and Biochemistry, University of Zagreb*
Ivana Perković, Ph.D., *Associate Professor, Faculty of Pharmacy and Biochemistry, University of Zagreb*
Marijeta Kralj, Ph.D., *Senior Scientist, tenured, Ruđer Bošković Institute*

Dissertation accepted: September 2022